Master Thesis, Department of Geosciences

Geochemical Comparison of Oils and Source Rocks from Barents Sea

Correlation between crude oils and source rock core samples from the western Barents Sea by GC-FID and GC-MS techniques

Dimitrios Rallakis

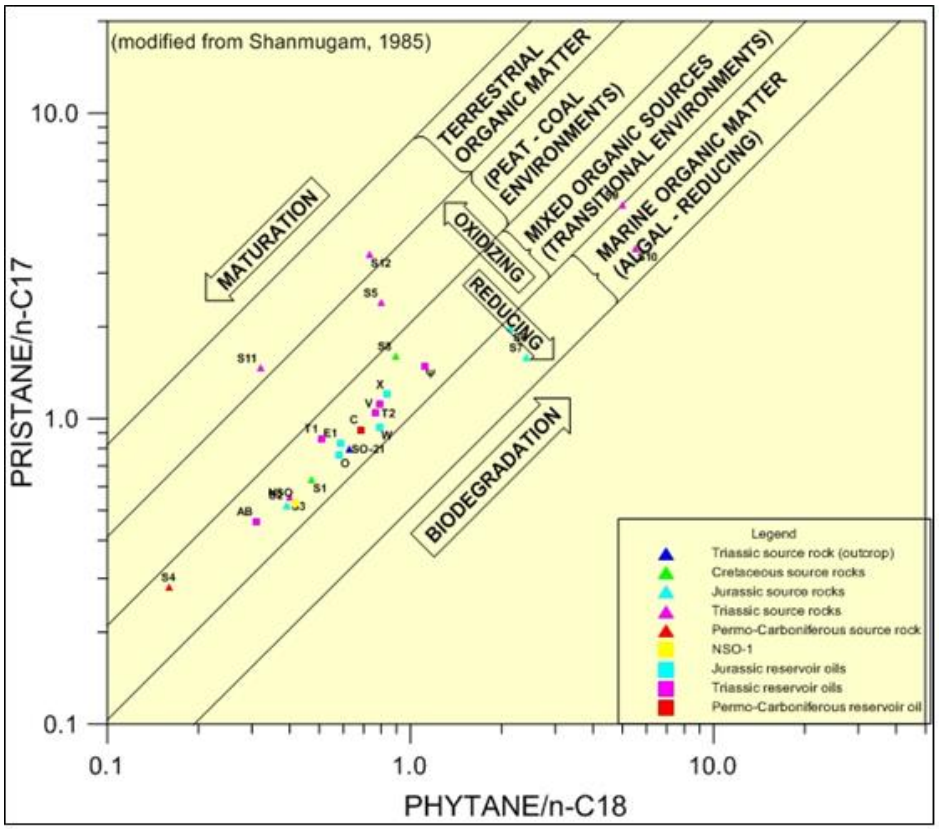

UNIVERSITY OF OSLO

FACULTY OF MATHEMATICS AND NATURAL SCIENCES

Geochemical Comparison of Oils and Source Rocks from Barents Sea

Correlation between crude oils and source rock core samples from the western Barents Sea by GC-FID and GC-MS techniques

Dimitrios Rallakis

Master Thesis in Geosciences

Discipline: Petroleum Geology and Petroleum Geophysics

Department of Geosciences

Faculty of Mathematics and Natural Sciences

University of Oslo

June, 2015

“Patience is bitter, but its fruit is sweet.”

Aristotle (384–322 B.C.E.)

Abstract

This project is part of the qualification for M.Sc. at Department of Geosciences, University of Oslo, in the direction of "Petroleum Geology and Petroleum Geophysics".

The initial notion that the Barents Sea was a dry gas region proved to be incorrect since commercially valuable oil fields were also discovered. Examples of such fields include the wells 7125/4-1 (Nucula discovery), 7122/7-1 (Goliat field), 7222/6-1 S, and the most recent Lundin discovery in well 7220/11-1 (Gotha and Alta fields), NW of 7121/4-1 (Snøhvit field). The Barents Sea exploration campaign has had, and continues to have a high drilling success rate since most of the exploration wells of the 68 in total, until 2008, discovered sedimentary strata containing in some cases petroleum. However, most of the reservoirs discovered contain gaseous hydrocarbons and/or thin oil legs or residual oils i.e "shows" and this seems to be related mainly to uplift and remigration (Ohm *et al.,* 2008).

The main objective of this study is to attempt to correlate twelve (12) core and (1) one outcrop source rock samples, recovered from the Hammerfest Basin, the Nyslepp/Måsøy Fault Complex, the Finnmark Platform, the Nordkapp Basin, the Svalis Dome, the Bjarmeland Platform and the outcrop sample from the Trehøgdene on Svalbard, with ten (10) oil samples from the Hammerfest Basin, the Nyslepp/Måsøy Fault Complex, the Bjarmeland Platform, the Loppa High and the Nordkapp Basin in western Barents Sea, for the purpose of understanding better the source and maturity aspects of the petroleums.

The oil samples represent liquid hydrocarbons from exploration oil wells. Eight of them were produced from reservoir rocks that are of Triassic-Jurassic age i.e. from the Kapp Toscana Group, one is from the Middle Triassic of the Sassendalen Group, and one is of Permo-Carboniferous age and from the Gipsdalen Group.

This study aims to evaluate if the source rock (SR) samples are reasonable analogues for the SR of any of the oils and also as a help in overviewing the maturity of the oils.

Furthermore, it attempts to address the aspects of secondary processes like biodegradation, organofacies or in-reservoir mixing.

As a matter of fact it is not easy to address the potential source of petroleum accumulations in the Barents Sea due to dysmigration, tilting and spill phenomena, as a result of several uplift episodes. Furthermore, the fact that Barents Sea is a multi-SR basin (Ohm *et al*., 2008; Faleide *et al.,* 2010) means that oils may have mixed in the reservoirs.

Acknowledgements

I would like to express my sincere gratitude to my supervisor Dr. Dag Arild Karlsen for giving me the opportunity of walking together with this thesis. I am grateful to Dr. Karlsen for assigning to me the topic that was my first priority and for guiding me with his fruitful comments and observations that led to the completion of the present study.

Additionally, I am truly indebted to the PhD candidates Tesfamariam Berhane Abay and Benedikt Lerch for trusting me with their gas chromatogram database, part of their PhDs. I also thank the PhD candidate Zagros Matapour for his feedback and recommendations on previous studies.

I take this opportunity to acknowledge all the Professors of the Petroleum Geology and Petroleum Geophysics master program for pursuing to transform us into professionals. These two years notably enriched my knowledge as I obtained various new skills.

In the long run I would like to thank my family Athanasios, Vasiliki, Stavros, Artemis, and Lydia who supported and encouraged me all these years.

Dimitrios Rallakis

Oslo, 2015

Table of Contents

Chapter 1

Introduction

What exactly is Petroleum Geochemistry? The definition is best expressed by Hunt (1996) as *"the application of chemical principles to the study of the origin, migration, accumulation and alteration of the petroleum (oil and gas) and the use of this knowledge in exploring for and recovering petroleum"*.

Petroleum derives almost totally from organic matter which was synthesized by living organisms and affected through the stages of organic diagenesis, catagenesis and metagenesis. For this reason it inherits and maintains, in some organic components (biomarkers) the same biochemical structure (carbon skeleton) with the living organisms, so that tracing and correlation with the source becomes possible. In other words, the organic compounds that are directly linked to the living organisms are also present in source rocks and in sediments that may later form source rocks. These organic compounds are notated as "biomarkers" (Hunt, 1996). Another definition proposes that the molecules which inherited their primary or base structure (carbon skeleton) from the living organisms and were not significantly altered (despite having functional groups) after deposition could be defined as biomarkers (Tissot and Welte, 1984).

Oil exploration in Barents Sea started already in the beginning of the 1980's. The discoveries were mainly dry gas containing, with or without thin oil legs. The western Barents Sea province is overfilled and is highly affected by uplift and erosion cycles (Ohm *et al.,* 2008). There are numerous publications describing the petroleum potential of the region: Rasmussen *et al.* (1995); Stewart *et al.* (1995); Knutsen *et al.* (2000), to name but a few.

The western Barents Sea (Figure 1), is almost twice the size compared to the northern North Sea, with the main source rock formation in the latter being the Draupne black shales of Upper Jurassic that is isochronous to the Kimmeridge shale; both of them being equivalent to the Upper Jurassic Hekkingen Formation in Barents

Sea (Figure 2.3). However, despite the large petroleum reserves in the North Sea with both oil and gas, early exploration in Barents Sea (1980's) verified mainly gas discoveries.

Today this picture is more complex and the assumptions that the region was a gas province have been proved to be incorrect since commercially valuable oil fields have also been discovered. Examples of such fields include Nucula, Goliat, Well 7222/6-1 and the most recent Lundin's finding in well 7220/11-1 (Gotha and Alta) NW of Snøhvit (N.P.D website).

The aim of this study is to attempt to correlate source rocks with migrated oils in order to better understand the source rock to oil relationships in the region; hence 11 Mesozoic (e.g Kapp Toscana-Adventalen-Sassendalen Groups) organic rich shales and siltstones, as well as 1 from Upper Paleozoic (Tempelfjorden Group) are attempted to be correlated with 9 Mesozoic oil samples (e.g Kapp Toscana-Sassendalen Groups) and 1 oil sample from the Upper Paleozoic (Gipsdalen Group), all being extracted from wells operated in western Barents Sea. The 10 oil samples have a more limited stratigraphic range, from Carboniferous to Jurassic compared to the source rock samples that range from Permo-Carboniferous to Cretaceous. The outcrop sample, namely SO-21, from the De Geerdalen Formation from onshore Svalbard was also analyzed due to its special, almost standard type, chromatogram. In both cases the samples were annotated and calibrated based on the standard sample NSO-1 (North Sea Oil) from Oseberg field, one of the most widespread world-wide used standards, introduced by the Norwegian petroleum industry and NPD.

The common analytical technique for organic correlation studies is gas chromatography (GC) of biomarkers. Among other applications, e.g environmental studies this matches also in the petroleum exploration to identify thermal maturity, biodegradation, source rock depositional environment and the type of organic input that defines the kerogen type (organic facies). Biomarkers from hydrocarbon seepages or oil in traps can make source rock quality analysis possible when the latter is not recoverable (Peters *et al.,* 2005). Oil to source rock correlation is best achieved with the help of gas chromatography. More specifically this study includes

analytical methodologies of GC-FID and GC-MS for biomarkers. The ultimate results can lead to safe decisions when planning the next exploration step, as most of the samples used in this study were obtained from wildcat wells.

Therefore, gas chromatography coupled with mass spectrometry (GC-MS) technique was applied to get the m/z (mass to ion ratios), namely 191, 217, 218, 231, 253, 178, 198 and 192 in order to obtain information about a series of biomarkers and associated parameters (27 in total, see Table 5.3). The gas chromatography coupled with flame ionization detector (GC-FID) technique was used to obtain chromatograms, mainly from C_{15} to C_{40} in order to calculate the ratios of the isoprenoids, pristane and phytane (Pr/Ph) and isoprenoids with *n*-alkanes, Pr/n-C_{17} and Ph/n-C_{18}. The CPI (carbon preference index) was computed for both datasets and the OEP (odd to even predominance) only for the oil dataset (Table 5.1). Geochemical correlation was used to evaluate if there is any genetic relationship between the source rocks and the oils. The results obtained from the gas chromatography analyses were used to make conventional plots according to previous studies and to obtain information about the depositional environment, the biodegradation, the maturity and the type of kerogen. These methodologies were used to evaluate the potential source for the migrated oil. Some of the oil samples are medium biodegraded, meaning the composition of the organic matter is affected by microbial alteration, thus there was an attempt to use as many parameters as possible, in order to reach safe conclusions, following also an evaluation of the levels of biodegradation.

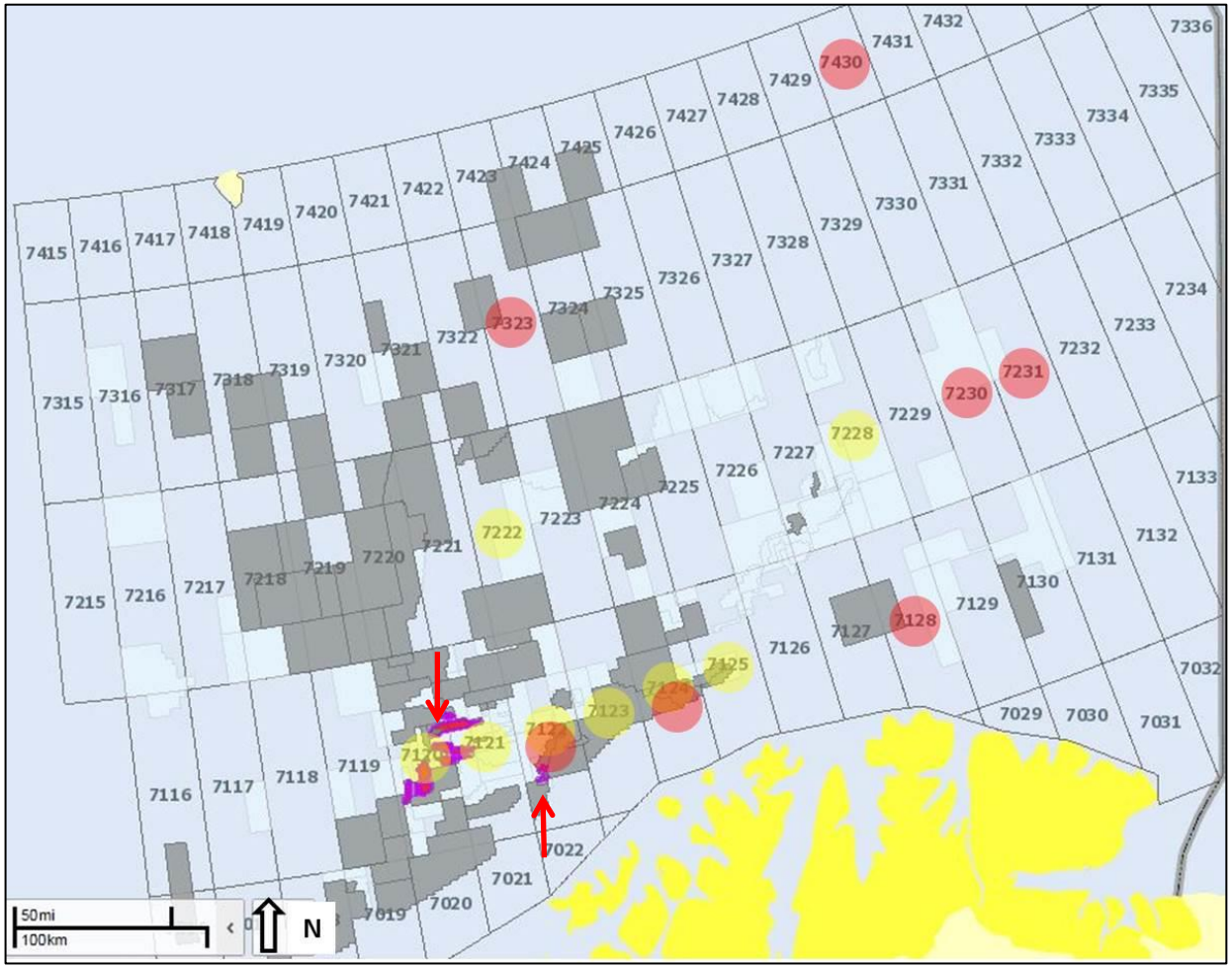

Figure 1: Overview of the Norwegian continental shelf in the western Barents Sea region including the fields and crucial discoveries. Marked in red transparent circles are the wells from which the source rock samples were recovered. Marked in yellow are the crude oil samples. The upper red arrow depicts Snøhvit gas field and the lower red arrow Goliat oil field (from N.P.D website)

Chapter 2

Geological Setting

Chapter 2 is dedicated to the geological evolution of the south-western Barents Sea. It contains the following four subchapters:

2.1 Architectural Elements of the Geology

2.2 Structure

2.3 Stratigraphy and Geological Evolution

2.3.1 Upper Paleozoic

2.3.2 Mesozoic

2.3.3 Cenozoic

2.4 The Western Barents Sea petroleum system

2.1 Architectural Elements of the Geology

The area of study is the south-western Barents Sea that is part of the northern offshore regions of Norway, and as such includes the following elements: the Hammerfest Basin, the Tromsø Basin, the Bjørnøya Basin, the Nordkapp Basin, the Loppa High, the Stappen High and the Finnmark and Bjarmeland Platforms as shown in Figure 2.1, (Rodrigues Duran *et al.,* 2013). The western Barents Sea covers a total area of 1.2×10^6 km^2 (Vorren *et al.,* 1991).

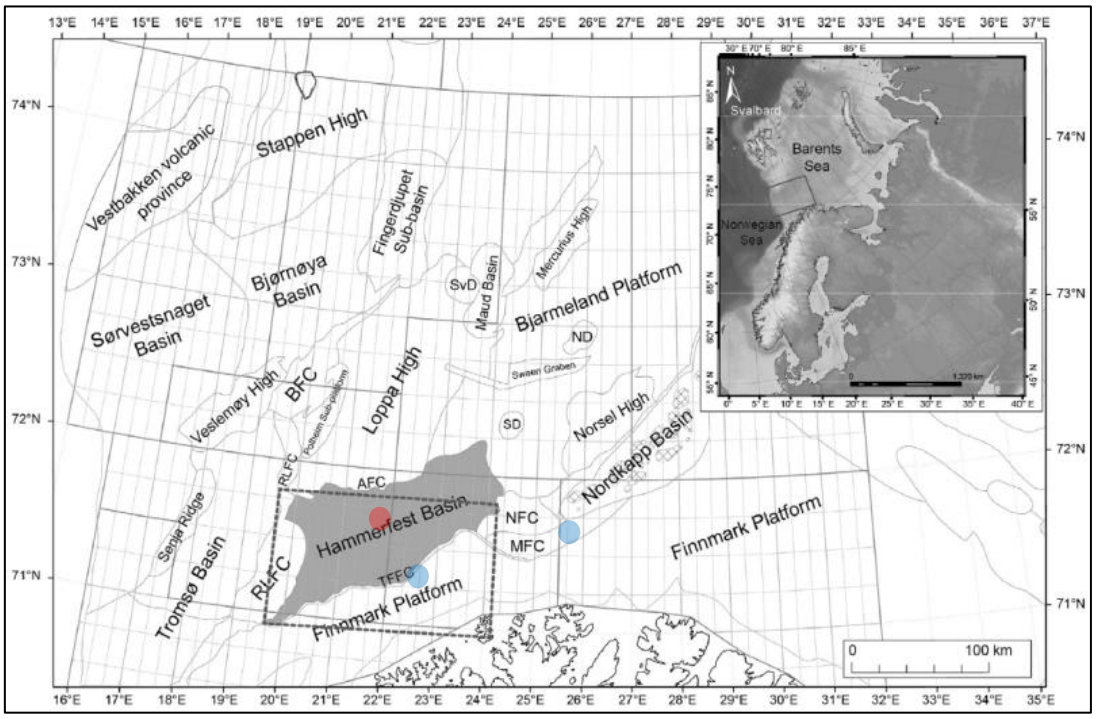

Figure 2.1: General aspects of the south-western Barents Sea with the associated basins, platforms and highs. AFC: Asterias Fault Complex; BFC: Bjørnøyrenna Fault Complex; MFC: Måsøy Fault Complex; ND: Nordvarg Dome; NFC: Nyslepp Fault Complex; RLFC: Ringvassøy–Loppa Fault Complex; SD: Samson Dome; SvD: Svalis Dome; SLHFC: Southern Loppa High Fault Complex; TFFC: Troms–Finnmark Fault Complex. Marked by the red dot the Snøhvit gas field and in blue the Goliat (West) and Nucula (East) oil fields (Rodrigues Duran et al., 2013).

The lithostratigraphical column of south-western Barents Sea is presented in figure 2.3. The base of the stratigraphy consists of Mississippian (Early Carboniferous) sandstones and alluvial shales with the latter having an average source potential. During Pennsylvanian times (Late Carboniferous) the depositional environment was gradually changing, leading to the deposition of dolostones and limestones up to Late Permian. This is expressed very well in the Nordkapp basin (Figure 2.1) which is characterized by thick salt deposits. The age from Upper Permian into the Triassic is

characterized by marine and alluvial shales and to a lesser extent by sandstone beds, as a result of multiple sea level fluctuations (regression-transgression cycles). The Late Triassic-Middle Jurassic period is marked by the high influx of sand that reached the basin, reflecting high energy environment. The important interval of Upper Jurassic-Cretaceous is characterized by the deposition of deep marine shales in the more remote areas. Late Cretaceous and Tertiary sediments have been affected by three different episodes of uplift and erosion (Figure 2.2). These episodes occurred respectively during the Paleocene (60), the Oligocene (33) and the Pliocene-Pleistocene (5 Ma), with the latter two being more intensive (Ohm *et al.,* 2008). The potential source rocks exist at many stratigraphic intervals, and this should make the Barents Sea more prolific than the North Sea. In other words, the source rocks extend from Upper Paleozoic to Late Mesozoic. It is a clear possibility that the high number of source rocks at medium and greater depths resulted in this basin being classified as an overfilled petroleum province (Ohm *et al.,* 2008).

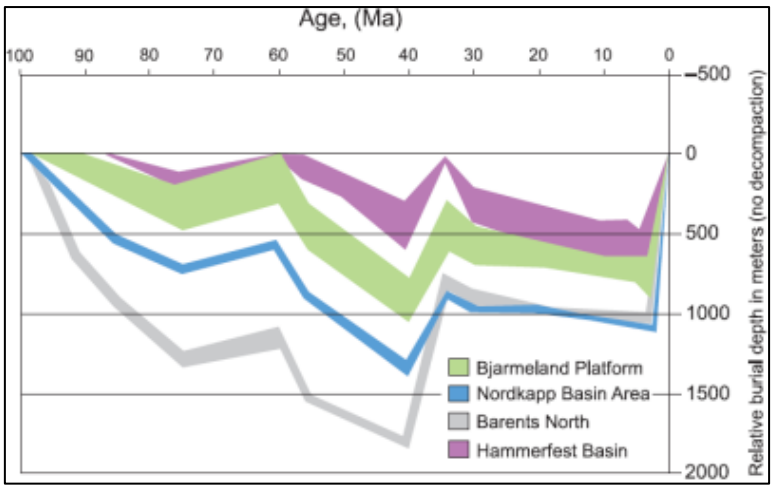

Figure 2.2: Time cross-plotted with subsidence. Mark the uplift peaks at Paleocene (60), Oligocene (33) and Pliocene-Pleistocene (5 Ma), with the latter two being more extensive (Ohm et al., 2008). Glacial rebound is also likely.

In terms of structural geology, the Barents Sea is characterized as an intracratonic epicontinental setting that has been modified by a number of tectonic phases in post-Caledonian, Early Devonian times. The faults in the area could mainly be separated into two categories, one of ENE-WSW to NE-SW trending and another set of faults which trends NNE-SSW.

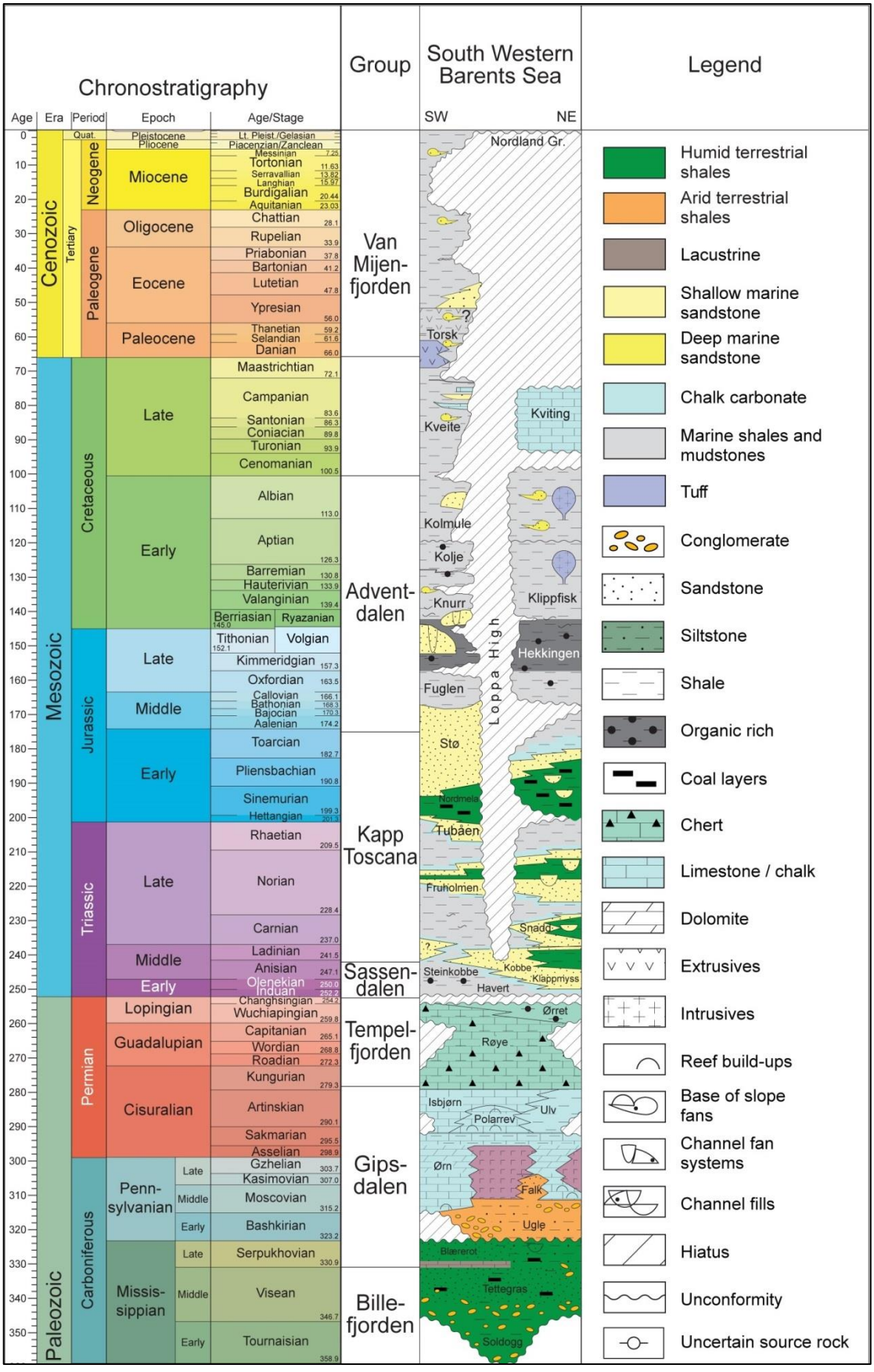

Figure 2.3: Lithostratigraphical column of the south-western Barents Sea. Group names are originally referring to Svalbardian lithologies (modified from Norlex website).

The Hammerfest and Nordkapp Basins are influenced by ENE-WSW fault complexes. The western part of the Barents Sea is affected by N-S faulting and became active later in Mesozoic-Cenozoic times. The eastern part, on the other hand was active in the Upper Paleozoic (Gabrielsen *et al.,* 1990). The western margin in the Barents Sea did not experience the same degree of uplift as the rest of the area. This is marked by the deposition of thick sedimentary packages as a response to the accommodation space which was created due to the differential uplift. The maximum uplift is estimated to be around 3000 m at the NW and S margins of Barents Sea (Reemst & Cloetingh, 1993; Vorren *et al.,* 1991). The degree of uplift is minor in the axial areas of Tromsø and Hammerfest basins and decreases southwards. Due to the uplift, oil accumulations are expected to be spilled from the initial traps (Doré and Jensen, 1996; Ohm *et al.,* 2008).

2.2 Structure

The Barents shelf is located in the north-western corner of the Eurasian plate/shelf. It is characterized as an epicontinental sea (shallow marine platform) that is bounded by passive continental margins (tectonically not active) in the North, South and West as a response to the opening between the Eurasia basin and the Norwegian-Greenland Sea in the Cenozoic (Gudlaugsson *et al.,* 1997; Faleide *et al.,* 2010). The main architectural elements of the western Barents Sea are namely: the Stappen High, the Nordkapp Basin, the Hammerfest Basin, the Loppa High, the Bjørnøya Basin, the Svalbard Platform, the Hopen High and the Sørkapp Basin (Faleide *et al.,* 1984).

The Barents shelf is mainly subdivided into two geological provinces that together cover the area from the shores of northern Norway and Russia to the Arctic Ocean and from Novaya Zemlya to the Norwegian and Greenland Sea (Worsley, 2008) (Figure 2.1). Earlier studies (Faleide *et al.,* 1984) suggest Barents shelf to be subdivided into three provinces: 1) an area of EW trend that lies between 74^{o}N and the northern coast of Norway, 2) an uplifted platform towards Svalbard and 3) the area of the western continental margin. The average sedimentary succession is estimated to be thicker than 10 km and sits on the Pre-Caledonian basement

(Faleide *et al.,* 1984) which was consolidated during the Caledonian Orogeny, influencing the later structural development (Gudlaugsson *et al.,* 1997).

The sedimentary record has been modified by three discrete post-Caledonian movements, namely:

- The Svalbardian phase that started in the Late Devonian-Early Carboniferous transition
- The Middle Jurassic-Early Cretaceous which is known as the Kimmerian phase and
- The gradual opening of the Norwegian-Greenland Sea that resulted in Cenozoic tectonism

As already mentioned, the post-Caledonian sedimentary sequence from Late Paleozoic to Quaternary exceeds 10 km. In general the sedimentary input is described to be of clastic origin with an exemption during Paleozoic in Middle Carboniferous-Lower Permian times, which is marked by carbonates and evaporites of high thicknesses. These salt diapirs are better expressed in the Nordkapp basin as they penetrate more than 7 km of the overlying sediments in the form of salt walls (Faleide *et al.,* 1984).

2.3 Stratigraphy and Geological Evolution

The Precambrian Fennoscandian-Baltic and Laurentian-Greenland shields in south-western Barents Sea are intersected by numerous thrust and fold belts, typical for compressional tectonics, namely:

- The Eocambrian-Early Cambrian Timanides
- The Late Silurian-Early Devonian Caledonides
- The fold belt formed in Late Devonian-Early Carboniferous known as the Innuitian-North Greenland belt, and
- The Ural-Novaya Zemlya as moving towards the end of Paleozoic, more specifically during the Hercynian Orogeny in Late Permian-Early Triassic times

All the above shields and fold belts compose the crystalline basement (Siedlecka, 1975; Faleide *et al.,* 1984). Onshore expressions (outcrops) of the Upper Paleozoic sedimentary record are also present on Svalbard.

The Caledonides, which were formed in Late Silurian, started to get gradually eroded by Early Devonian time creating "molassic" sediments that are deposited around Svalbard and eastern Greenland. The climate at that time was arid, typical for continental conditions. However, the compressional tectonic regime during the end of the Caledonian mountain built-up, changed to a left-lateral shear regime that caused strike-slip movements (Svalbardian) to take place in the Arctic and North Atlantic region (area) which in turn caused folding, leading to horst-graben formation on Spitsbergen.

In Lower Carboniferous, continental sediment input prevailed. Thus, coal deposits started to form to the north and west from Franz Josef Land and to the Svedrup Basin. On the other hand, carbonates were deposited in the Pechora Basin and Novaya Zemlya. In Early to Middle Carboniferous time tectonic movement in the Barents Sea was reactivated. There is a high possibility that the faults incision cut as deep as Devonian formations in Bjørnøya, Novaya Zemlya and Svalbard. In the Upper Carboniferous (Pennsylvanian) the sedimentation record was affected by marine transgression in the whole area. Carbonate and evaporite deposits of great thickness accompanied by clastic sediments were accumulated in the Sverdrup Basin, in Svalbard and in the Wandel Sea.

During Lower Permian (Cisuralian), Svalbard and Bjørnøya started to become less tectonically active. The shelf area of the Svedrup Basin and the Pechora Basin was dominated by carbonates and evaporites. During the end of Permian, East Greenland was already connected with the North Sea. The dominant clastic deposition is typical for Late Permian. Finally, the area was affected by the Hercynian Orogeny that occurred during the Permo-Triassic boundary. This is best expressed in Novaya Zemlya as a mountain range built up.

During the beginning of the Mesozoic and in Triassic times the seaway connection between East Greenland and North Sea was closed. At that time the areas of Svalbard and Bjørnøya continued to be tectonically passive and clastic sedimentation dominated between the area of Sverdrup Basin and Pechora Basin. However, the Jurassic rifting between Norway and Greenland was discontinuous and occurred in several pulses.

The Kimmerian phase is divided into three segments, the Early in the Rhaetian (Upper Triassic), the Mid in Aalenian-Bajocian (Middle Jurassic) times and the Late in the Valanginian (Early Cretaceous), with the latter being the most crucial. Nevertheless, all three segments are not directly discernible on Svalbard. During the Middle Jurassic, in Bathonian-Callovian times, the sea level increased abruptly; hence sediment lag (starvation) appears on the sedimentary record as a hiatus.

Due to the latter Kimmerian rifting phase, the area between Norway and Greenland was rapidly subsided. Additionally, the igneous activity that started in the Svedrup Basin in Jurassic time spread across the northern part of Barents shelf. It reached a peak on Svalbard and Franz Josef Land in Early Cretaceous which in turn resulted in dolerite intrusions and basaltic lava flows. Finally, moving towards Late Cretaceous, the area around Svalbard was uplifted.

Following the opening between the Norwegian-Greenland Sea and the Eurasian Basin, the western Barents Sea transformed into a shear margin. In Upper Paleocene times western Spitsbergen was affected by compressive tectonics as a result of folding and reverse-faulting at the time that the same area was mainly receiving clastics. In Middle Oligocene this area was developed as a passive margin. In the Tertiary, most of the Barents Sea experienced differential uplift. Finally, the prolonged erosion in the eastern Barents Sea resulted in extended deposition of clastics in the western margin which experienced uplift in a lesser degree (Faleide *et al.,* 1984).

2.3.1 Upper Paleozoic

The Late Paleozoic tectonic history of western Barents Sea includes four distinct events, which are summarized below.

1) The pre-Devonian basement was consolidated during the Caledonian Orogeny.

2) The whole Svalbard area was affected by both compressional and extensional tectonics in Devonian.

3) The Permo-Carboniferous era was marked by excessive rifting and crustal extension between Norway and Greenland.

4) The western Barents Sea continued to subside for non-regional tectonic reasons, i.e. Uralian Orogeny (Gudlaugsson *et al.,* 1997).

The depositional strata in the Lower Carboniferous is mainly made of clastics. This changed towards the Late Carboniferous-Permian to dolomites, evaporites and massive limestones, and again during the Late Permian when shales and cherty limestones were deposited into the subsiding sag basin in the western Barents Sea depocenter (Faleide *et al.,* 2010).

2.3.2 Mesozoic

According to Faleide *et al.* (1992), the Mesozoic geological evolution could be concluded into three different stages.

1) The Middle-Late Jurassic (Bathonian-Callovian) rifting that is isochronous to the continental breakup and the extensive rifting in the Arctic and North Atlantic regions. Therefore mudstones were deposited between the tilted fault-blocks in the Upper Jurassic as synrift sediments.

2) In Early Cretaceous the Harstad, the Bjørnøya and the Tromsø Basins transformed into depocenters isochronous with the opening of the Amerasia Basin and the North Atlantic where rifting prolonged into Aptian-Albian times. The same three basins

underwent fast subsidence until lower Late Cretaceous (Cenomanian), leading to extensive sediment infill (circa 5-6 km).

3) Late Cretaceous is marked by seafloor spreading in Labrador Sea, faulting in the Harstad and Sørrestsnaget Basins as well as rifting in North Atlantic and pull-appart basins in NE Greenland.

2.3.3 Cenozoic

The Cenozoic geological evolution is inferred by Vorren *et al.* (1991) as five main stages:

1) In the Late Paleocene the sedimentation was centered in the intraratonic basins and in the beginning of Eocene, the Stappen High and the Loppa High acted as sediment sources.

2) During the period from Early Eocene to Mid-Miocene the sedimentation was focused into the western continental margin by the time when the Stappen High was severely eroded.

3) During the interval from Mid-Miocene to Early Pliocene, the southern Barents Sea shelf prograded by an average of 30 km/Ma. Stappen High was exposed and was as a result eroded again due to the sea level lowstand. On the other hand, sediments were accumulated on the shelf during the highstand periods.

4) From Late Pliocene to Early Pleistocene the whole Barents Sea experienced differential uplift that resulted in fluvial and glacifluvial erosion. The erosion was more extented in the southern Barents Sea and the adjacent coastal areas.

5) Holocene is marked by a number of glaciations. The shelf at that time was prograding faster than the previous periods by up to of 34 km/Ma. The relief decreased by an average of 150 m, meaning high erosion in glacial troughs whereas there was limited to none in bank areas.

2.4 The western Barents Sea petroleum system

A characteristic hydrocarbon bearing formation in the Barents Sea is mainly consisting of gas associated with residual oil where commercial production is not possible. Other common type of traps would be partially filled with gas close to the spill point with only thin oil legs. The formations below these traps often contain residual oil. This indicates that oil was in place inside the trap which today is filled with gas. After tilting occurred, during the several uplift episodes, the oil spilled to another trap or reached the surface, leaving back traces of residual saturation (Ohm *et al.,* 2008).

According to the same authors and references therein, the uplift and erosion episodes affected the basin as follows:

- Pressure was reduced as the source rock moved to shallower depths due to uplift, thus gas was exsolved out of the liquid mixture. This gas accumulated in the top of the structures. Expansion of gas forced oil below the spill point to the adjacent traps.
- The non-uniform (flexural) uplift caused tilting that in turn led to oil spill.
- Petroleum might be leaked from the fractured caprock due to the respective tectonic movements.
- The source rock's maturation (cooking) was halted due to uplift as it reentered lower P-T regimes.
- The final reservoir quality was poor as the reservoir rocks, which were initially deeply buried and highly compacted, were subjected to uplift which made them brittle.

The shales of the Hekkingen Formation of the Upper Jurassic are the most prolific source rocks in the Barents Sea and this is indicated by the quantity of total organic carbon (TOC), the high hydrocarbon potential (S2) and the world class hydrogen index (HI). The Jurassic era is in general characterized by high potential in each shale interval. The Triassic, Permian and the Carboniferous shales also have remarkable source rock potential. Older Paleozoic formations are possibly post-mature in the

deeper part of the basins and would in the later part of their genetic period have expelled mainly gas. Nevertheless, it is important to remember that oil could have been expelled earlier, e.g from the coal intervals of the Billefjorden Group on Svalbard (Figure 4) which have potential also for liquid hydrocarbons. Due to the deeper occurrences of the Late Paleozoic source rocks, this would have resulted in early migration and possibly oil filled traps. Thus, the migration avenues might have been saturated with respect to hydrocarbons, a fact that would later enhance the migration efficiency of the oil from the Mesozoic source rocks. Furthermore, the early charging of traps led to overpressure that does not favor compaction so that porosity was better maintained (Ohm *et al.,* 2008).

As discussed earlier, most of the traps in the south-western Barents Sea contain gas. The Tertiary uplift episodes caused reduced pressure and gas expansion. On the other hand the Nucula and Goliat discoveries contain oil with associated gas. Diphasic separation could be prevented if the carrier beds were deeply buried so that pressure was maintained. The most important element which will result in low GOR petroleum in traps is leaking caprocks as discussed by e.g. Sales (1997); Karlsen and Skeie (2006). Another significant process that could take place during uplift is trap recharging. By setting the source rocks to shallower depths (uplift) they are forced to re-release petroleum quantities from their source rock-lattice. These could migrate to trap formations where the caprock is not leaking, thus refeeding them to the spill point (Ohm *et al.,* 2008). Finally, dysmigration (remigration) due to fill to spill phenomena could charge other proximal and shallower traps, also resulting in a high and a low fractionated petroleum phase (Silverman, 1965). Due to trap recharging, oil-spill phenomena and several source rocks that accrue over the stratigraphic intervals, most of the Barents Sea oils that are analyzed in Ohm *et al.* (2008) appear to be mixtures from more than one source. For instance oil from the most prolific source rock, the Hekkingen Formation of Upper Jurassic can have mixed with older petroleum which was derived from the Upper Paleozoic sequence. The same scenario might be expected to occur in the oil samples that are analyzed in the present study. In other words it is expected to find multiple sources for some of the oil samples.

Chapter 3

Sample database

3.1 Oil dataset

Ten oil samples were studied in total. Nine of them come from the Mesozoic sequence, eight from the Kapp Toscana Group and one from the Sassendalen Group. Only one sample comes from the Upper Paleozoic Gipsdalen Group (Table 3.1). The standard oil that was used for calibrating the GC instruments is the NSO-1 and is discussed in sub-chapter 3.1.10. For simplicity reasons the samples were given different ID letters.

All of the oil samples were recovered from exploration wells in the western Barents Sea. All the Mesozoic oils come from sandstone reservoirs whereas the one from the Paleozoic was contained within a carbonate lithology. The information discussed below originates from the Norwegian Petroleum Directorate website (www.npd.no) unless otherwise stated.

Chapter 3.1 is divided in ten sub-chapters in order to provide some information on the individual wells, namely:

3.1.1 Well 7120/2-1 (1944 m)

3.1.2 Well 7120/6-1 (2432 m)

3.1.3 Well 7121/5-2 (2328 m)

3.1.4 Well 7122/7-3 (1195.6 m & 1812)

3.1.5 Well 7123/4-1 A (2165.9 m)

3.1.6 Well 7124/3-1 (1298 m)

3.1.7 Well 7125/1-1 (1403.8 m)

3.1.8 Well 7222/6-1 S (1633.8 m)

3.1.9 Well 7228/7-1 A (2091.1 m)

3.1.10 NSO-1 standard

Table 3.1: Summary of the oil samples used in the GC-FID and GC-MS analyses. Age and spatial assessment according to Dahl and Speers (1985); Dalland et al. (1988); Vigran et al. (2014); and N.P.D website.

No.	Sample ID	Well	Group	Reservoir	Reservoir age	Area/Basin
1.	C	7120/2-1	GIPSDALEN	ØRN	LATE CARBONIFEROUS-EARLY PERMIAN	LOPPA HIGH
2.	E1	7120/6-1	KAPP TOSCANA	STØ	EARLY JURASSIC	HAMMERFEST BASIN
3.	O	7121/5-2	KAPP TOSCANA	STØ	MIDDLE JURASSIC	HAMMERFEST BASIN
4.	T1	7122/7-3	KAPP TOSCANA	SNADD	LATE TRIASSIC	HAMMERFEST BASIN
5.	T2	7122/7-3	SASSENDALEN	KOBBE	MIDDLE TRIASSIC	HAMMERFEST BASIN
6.	V	7123/4-1 A	KAPP TOSCANA	FRUHOLMEN	LATE TRIASSIC/EARLY JURASSIC	HAMMERFEST BASIN
7.	W	7124/3-1	KAPP TOSCANA	TUBÅEN	EARLY JURASSIC	NYSLEPP/MÅSØY FAULT COMPLEX
8.	X	7125/1-1	KAPP TOSCANA	STØ	JURASSIC	NYSLEPP/MÅSØY FAULT COMPLEX
9.	Ø	7222/6-1 S	KAPP TOSCANA	SNADD	MIDDLE TRIASSIC	BJARMELAND PLATFORM
10.	AB	7228/7-1 A	KAPP TOSCANA	SNADD	LATE TRIASSIC	NORDKAPP BASIN
11.	NSO-1	30/6-1	VIKING	DRAUPNE	UPPER JURASSIC	OSEBERG FIELD (N. NORTH SEA)

3.1.1 Well 7120/2-1 (1944 m)

The wildcat well 7120/2-1 (Table 3.1.1) was drilled on the Loppa High (Figure 3.1.1) and reached a total depth of 3502 m, penetrating a dolerite sequence of Early-Middle Carboniferous age. The first evidence for gas came already from shallow depths (618-620 m) but is of biogenic origin; hence this gas is characterized as a shallow gas pocket justifying the strong seismic reflector. A very important observation in well 7120/2-1 is the great unconformity (613 m) that exists between the Late Triassic and the Early Eocene. There is also a second unconformity as the Middle Triassic sedimentary strata lies on sediments of Early Permian age (base Ladinian unconformity).

Table 3.1.1: Table summarizing the main aspects for the Well 7120/2-1 (www.npd.no).

Well	7120/2-1
NPD ID Wellbore	473
Date of completion	29.10.1985
Water Depth (m)	387.0
UTM coordinates	NS 7987305.65, EW 481923.84
UTM zone	34
Deepest Formation Age	Early-Middle Carboniferous
Area	Barents Sea
Field	Loppa High
Total Depth (MD), m	3502.0
Kelly Bushing (KB), m	23.0
Sample data	
Sample ID notation	C
Sample depth, m	1944.0
Sample formation	Ørn
Group	Gipsdalen
Age	Moscovian (Middle Pennsylvanian)
Hydrocarbon shows, m	1937-2196, m, migrated oil and gas
Lithology	limestone

The Ørn Formation lies at 1945 m depth and is easily recognizable as a limestone with extremely high Gamma Ray index. Below 2140 m there is a variation in lithology that could be described as a dolomitic limestone with thin sand and slate layers. The main shows are found between 1960-2218 m and were recorded as "oil bleeding from fractures and vugs" meaning that there are open fractures and secondary

porosity in the carbonate reservoir. The section from 1937-2196 m contains free petroleum with migrated oil and gas, from which (1944 m) sample "C" was taken. Despite the shows, the well was not productive. The TOC (total organic carbon) is high but the source rock potential is low. The kerogen is of type III, thus the organic matter has terrestrial source and is gas prone. Sample "C" contains more mature petroleum than expected due to a maturity "jump" of 613 m justified by the Triassic unconformity. Samples shallower than 1600 m are immature and those below 3270 m have reached the post-maturation stage.

The Ørn Formation pinches out and is only 79 m thick in well 7120/2-1 near the crest of the Loppa High and has suffered severe erosion due to its crest geometry. It is dominated by shallow marine carbonate facies deposited on platform areas and by interbedded evaporites and carbonates in the more deep-distal areas. The carbonate is composed of foraminifers, fusulinids and calcareous algae with Palaeoaplysina fragments forming wackestones and packstones. Siliciclastic input, on the other hand is rare. The age of the Ørn Formation in well 7120/2-1, based on the fusulinids, was estimated to be Late Moscovian (Late Carboniferous) (Larsen *et al.,* 2002).

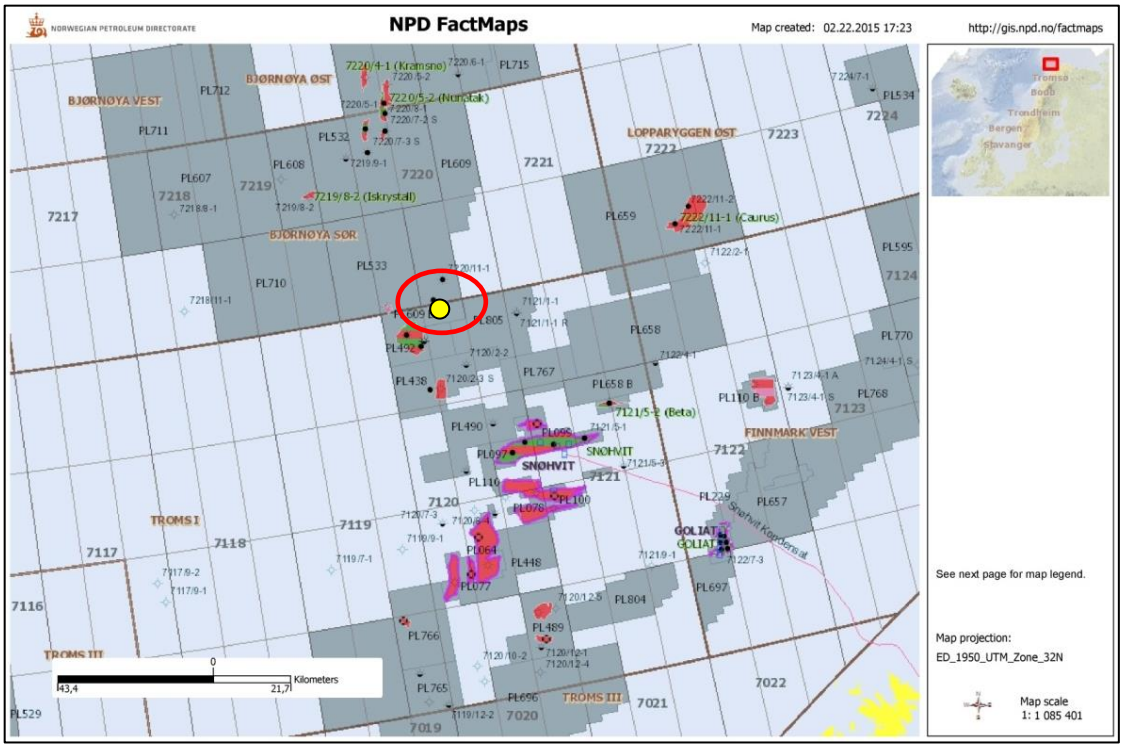

Figure 3.1.1: Fact map depicting Well 7120/2-1. The well is marked by the yellow dot encircled in red (www.npd.no).

3.1.2 Well 7120/6-1 (2432 m)

The wildcat well 7120/6-1 (Table 3.1.2) is located in the northern central part of the Hammerfest Basin (Figure 3.1.2). The well penetrated through an East-West horst block of Middle Jurassic age. It reached a final depth of 2820 m, cutting Late Triassic rocks (Tubåen Formation). The first level with shows was the Cretaceous claystones at 2176 m depth, but the most important level was the Early-Middle Jurassic Stø reservoir sandstone that lies between 2385.5-2469.5 m depth where sample "E1" (2432 m) belongs. In more detail the intervals from 2385.5-2427 m contained gas and from 2427-2443 m oil; hence "E1" (see Appendix I, Figure 1). The Tubåen Formation lies between the Jurassic-Triassic boundary and is in this well composed of mature source rocks of good potential. Gaseous hydrocarbons were also located deeper between 2559-2800 m inside the same formation. The Tubåen Formation is found interbedded with coal at depths exceeding 2660 m.

Table 3.1.2: Table summarizing the main aspects for the Well 7120/6-1 (www.npd.no).

Well	7120/6-1
NPD ID Wellbore	456
Date of completion	02.05.1985
Water Depth (m)	314.0
UTM coordinates	NS 7946756.85, EW 497650.92
UTM zone	34
Deepest Formation Age	Late Triassic
Area	Barents Sea
Field	Hammerfest Basin-Snøhvit
Total Depth (MD), m	2820.0
Kelly Bushing (KB), m	23.0
Sample data	
Sample ID notation	E1
Sample depth, m	2432.0
Sample formation	Stø
Group	Kapp Toscana
Age	Early Jurassic
Hydrocarbon shows, m	2385.5-2469.5 m, oil and gas
Lithology	sandstone

Geochemically, the Tertiary and Cretaceous intervals have low source potential. The sediments above 2300 m have controversial potential, but below and until 2335 m

there is high potential for oil and gas hydrocarbons. The Stø and the Nordmela sandstones contain waxy crude between the 2420-2540 m interval. Geochemical analyses suggest this oil to be associated with the source rock facies of the Tubåen and the base of Nordmela Formations (Figure 4).

The Stø Formation has a total thickness of 84 m in well 7120/6-1. It is mainly composed of moderate to well sorted homogenous sandstones. Laminas of shale and siltstone are present, whereas phosphatic conglomerates appear in adjacent wells. The whole Stø Formation could be sub-divided based on three transgressive sequences. The oldest sequence is only present in the western Hammerfest Basin whereas the middle Toarcian/Aalenian age marks a maximum transgression. The youngest Bajocian sequence has a syn-depositional character with the uplift.

The Stø Formation has a late Pliensbachian to Bajocian age (Early-Middle Jurassic) and becomes younger when moving east towards the Hammerfest Basin. The sandstones were deposited in prograding coastal environments, witnessed by the variation in clastic coast lithofacies (Dalland *et al.,* 1988).

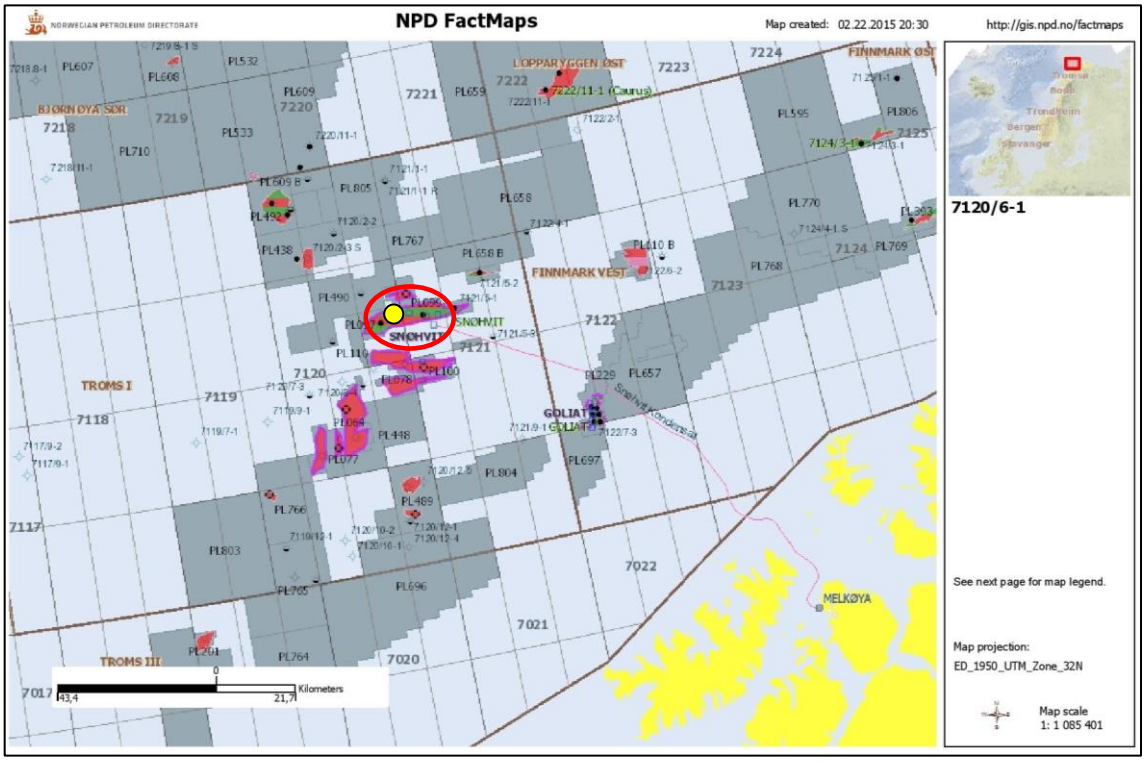

Figure 3.1.2: Fact map depicting Well 7120/6-1. The well is marked by the yellow dot encircled in red (www.npd.no).

3.1.3 Well 7121/5-2 (2328 m)

The wildcat well 7121/5-2 (Table 3.1.3) is located around 10 km NE of Snøhvit in the Hammerfest Basin (Figure 3.1.3). The first layer with petroleum shows was encountered in 2323 m depth in Middle Jurassic sandstone reservoirs of the Stø Formation. The shows contained gas and extended until 2346 m. The interval between 2352.0-2358.5 m contained oil and was separated from the upper gas zone with 6 m of shale. Since the well contained hydrogen sulphide (H_2S) it did not undergo further testing. The Stø Formation in well 7121/5-2 was found in the interval from 2323-2400 m having a thickness of 77 m. The depositional environment of Stø Formation is discussed in subchapter 3.1.2. The well reached 2328.0 m penetrating the Fruholmen Formation (Figure 2.3).

Table 3.1.3: Table summarizing the main aspects for the Well 7121/5-2 (www.npd.no).

Well	7121/5-2
NPD ID Wellbore	907
Date of completion	06.07.1986
Water Depth (m)	328.0
UTM coordinates (m)	NS 7952737.91, EW 523051.48
UTM zone	34
Deepest Formation Age	Late Triassic
Area	Barents Sea
Field	Hammerfest Basin NE of Snøhvit
Total Depth (MD), m	2543.0
Kelly Bushing (KB), m	22.0
Sample data	
Sample ID notation	O
Sample depth, m	2328.0
Sample formation	Stø
Group	Kapp Toscana
Age	Early Jurassic
Hydrocarbon shows, m	2323.5-2400.0 m, oil and gas
Lithology	sandstone

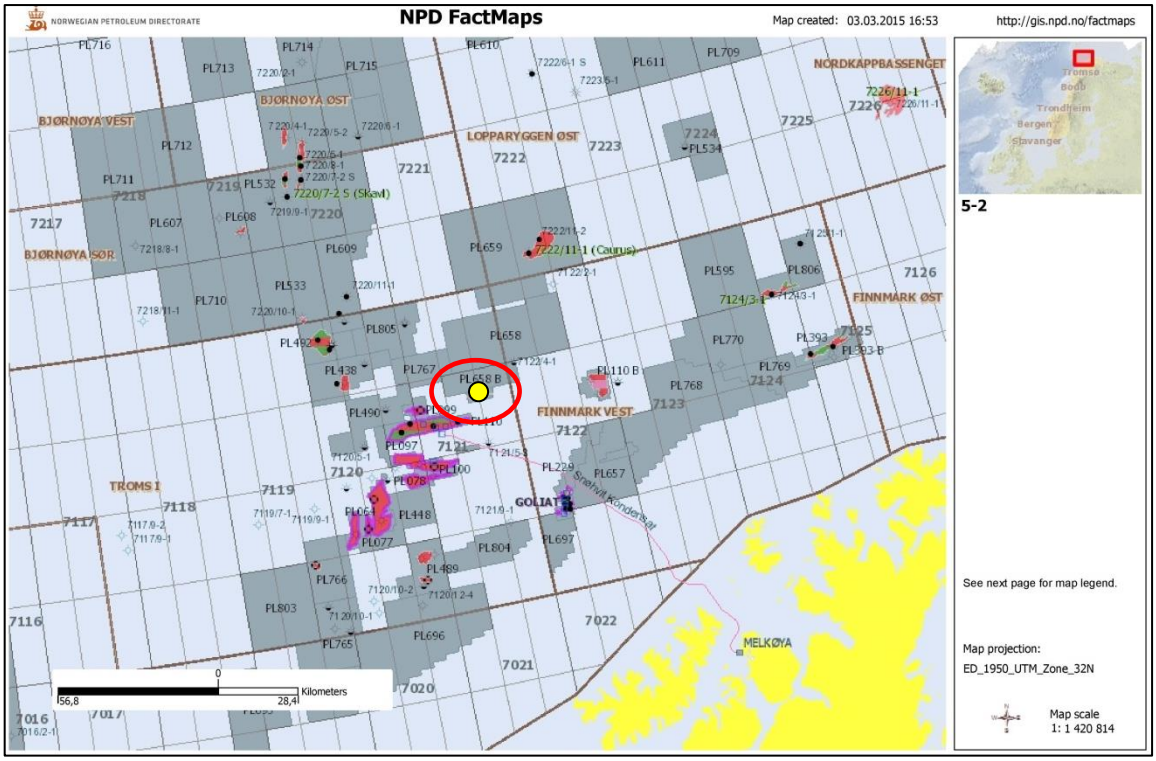

Figure 3.1.3: Fact map depicting Well 7121/5-2. The well is marked by the yellow dot encircled in red (www.npd.no).

3.1.4 Well 7122/7-3 (1195.6 m & 1812)

The wildcat well 7122/7-3 (Table 3.1.4) is located circa 55 km NE of Snøhvit (Figure 3.1.4). It was drilled on Goliat oil field on the crest of a rollover anticlinal structure of NE-SW orientation, located in the north-eastern part of the Hammerfest Basin along the Troms-Finnmark Fault.

The Tubåen Formation (Late Triassic) was encountered in 1087 m. The reservoir part of the Tubåen Formation had the GOC located in 1145.6 m while the OWC was not observable. The Snadd Formation was encountered in 1180 m, contained oil and had an OWC in 1199.5 m; hence the oil sample "T1" from 1087 m. The pressure regime in the latter reservoir was different than the first. The third reservoir of Kobbe Formation in 1808 m was also oil bearing; hence "T2" from 1812 m. The OWC was approximated at 1878 m. The Kobbe oil has geochemical differences from those of Snadd and Tubåen Formations which appear to have the same composition. For instance, the Kobbe oil is not biodegraded (no removal of *n*-alkanes lighter than C_{15}) and has very light stable carbon isotope composition in contrast to the other two,

Tubåen and Snadd Formations. These geochemical differences indicate that Kobbe oil from the Sassendalen Group and the upper oils of Snadd and Tubåen Formations from the Kapp Toscana Group were expelled from different source rocks.

Table 3.1.4: Table summarizing the main aspects for the Well 7122/7-3 (www.npd.no).

Well	7122/7-3
NPD ID Wellbore	5214
Date of completion	08.01.2006
Water Depth (m)	343.0
UTM coordinates (m)	NS 7906512.67, EW 545476.82
UTM zone	34
Deepest Formation Age	Permian
Area	Barents Sea
Field	Hammerfest Basin-Goliat
Total Depth (MD), m	2726.0
Kelly Bushing (KB), m	25.0
Sample data	
Sample ID notation	T1 & T2
Sample depth, m	1195.6 & 1812.0
Sample formation	Snadd & Kobbe
Group	Kapp Toscana & Sassendalen
Age	Late & Middle Triassic
Hydrocarbon shows, m	1087.0-1878.0, oil and gas
Lithology	sandstone

The Snadd Formation is forming an upward coarsening sequence. It starts with basal grey shales that grow into siltstones and finally sandstones. It has a total thickness of 628 m in well 7122/7-3. The limestones are found interbedded in the lower and middle part of the shale interval. On the other hand coal lenses develop higher in the sequence, of which the top part is marked again by red-brown shales. The Snadd Formation was developed during Middle to Upper Triassic (Ladinian-Norian). The Ladinian sequence contains deep sea sediments as a result of a prior extensive sea level transgression event, while storm deposits from the shallower southern parts of the basin are also indicated. The transition period between Ladinian-Norian (Carnian) is characterized by deltaic progradation and deposition of clastics in the central part of the Hammerfest Basin (Dalland *et al.,* 1988).

The Kobbe Formation is found in 236 m depth in well 7122/7-3 and is composed of basal shales that are upward coarsening and liming until they transform into carbonate cemented sandstones. The basal shales deposition is linked to a transgressive event. The sedimentary facies of the Kobbe Formation are characterized in general as proximal, coarser in the southern margin and finer in the axial area of the Hammerfest Basin. The Kobbe Formation age is of Middle Jurassic (Anisian). The Botheheia Member of Barentsøya Formation located in eastern and central Svalbard has somehow the same facies development with Kobbe but has yet to be encountered in the Hammerfest Basin. However the Bravaisberget Formation in western Spitsbergen has more similarities with the Kobbe Formation (Dalland *et al.,* 1988).

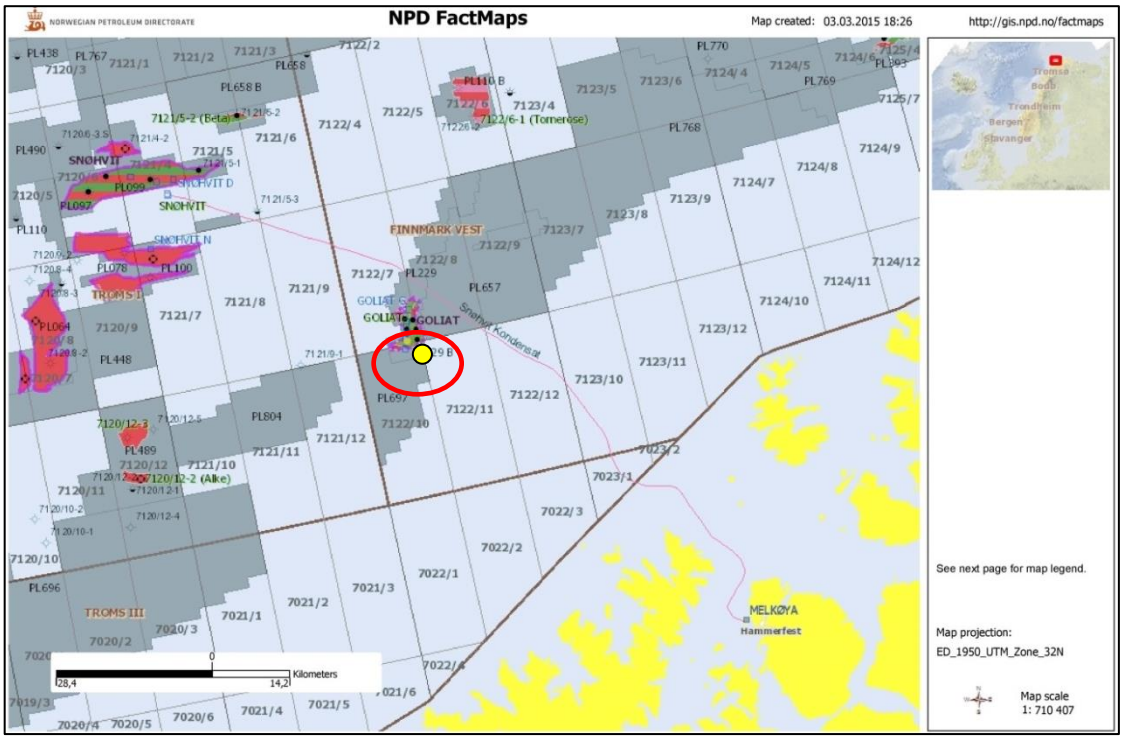

Figure 3.1.4: Fact map depicting Well 7122/7-3. The well is marked by the yellow dot encircled in red (www.npd.no).

3.1.5 Well 7123/4-1 A (2165.9 m)

The appraisal well 7123/4-1 A (Table 3.1.5) lies close to the Tornerose field which is located 50 km East of the Snøhvit field in the Hammerfest Basin (Figure 3.1.5). The development is unlikely as it was found to contain only gaseous hydrocarbons. The Fruholmen Formation of Kapp Toscana Group has Late Triassic to Early Jurassic age.

Table 3.1.5: Table summarizing the main aspects for the Well 7123/4-1 A (www.npd.no).

Well	7123/4-1 A
NPD ID Wellbore	5808
Date of completion	14.05.2008
Water Depth (m)	413.0
UTM coordinates (m)	NS 7947301.07, EW 572637.44
UTM zone	34
Deepest Formation Age	Late Triassic
Area	Barents Sea
Field	Hammerfest Basin-Tornerose
Total Depth (MD), m	2855.0
Kelly Bushing (KB), m	23.0
Sample data	
Sample ID notation	V
Sample depth, m	2165.9
Sample formation	Fruholmen
Group	Kapp Toscana
Age	Late Triassic/Early Jurassic
Hydrocarbon shows, m	2165.9-2551.5, residual oil
Lithology	sandstone

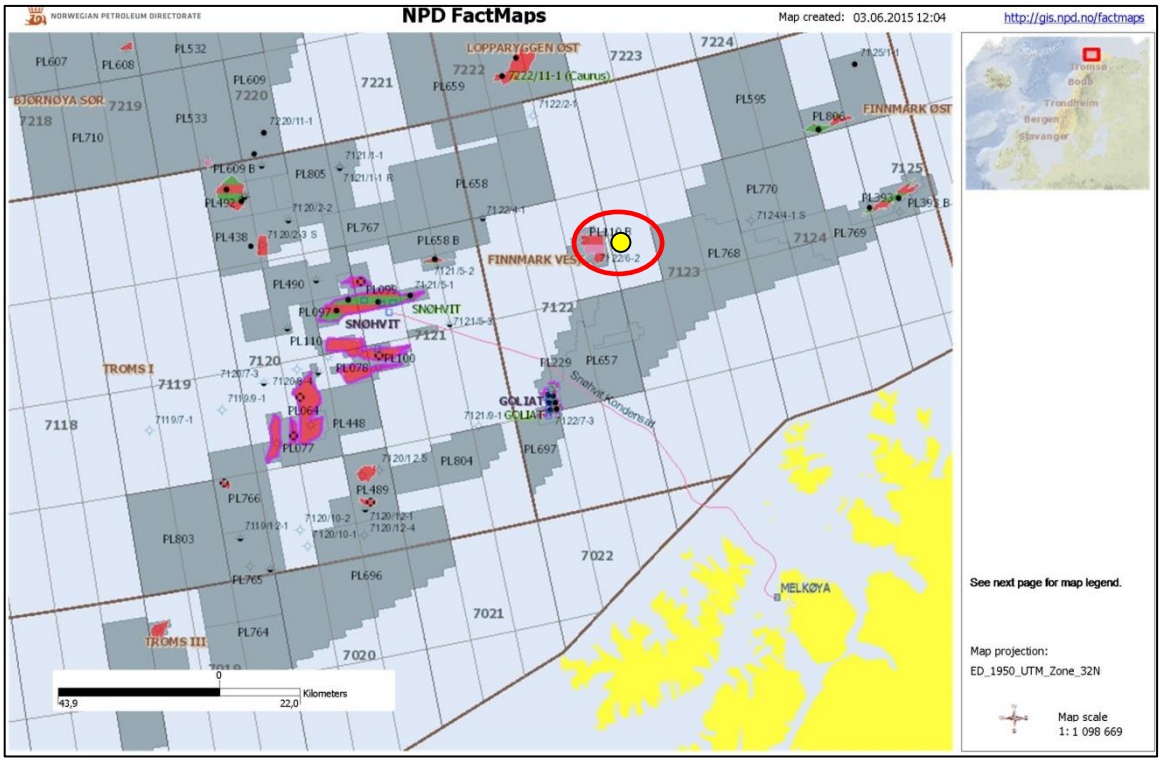

Figure 3.1.5: Fact map depicting Well 7123/4-1 A. The well is marked by the yellow dot encircled in red (www.npd.no).

The Fruholmen Formation was encountered between 2141-2259 m in well 7123/4-1 A and had a thickness of 118 m. Sample "V" belongs to this interval as it was recovered from 2165.9 m. The Fruholmen sequence consists of basal dark grey shales that transform upwards into interbedded sandstones, shales and coals. These lithological variations subdivide the formation in three different divisions, the basal "Akkar", the sandy mid "Reke" and the shaly top "Krabbe". The latter is a physical transition to the overlying Tubåen Formation (Figure 2.3). As already mentioned the basal Akkar has Early Norian age (Middle Triassic) while the top Akkar marks the Triassic-Jurassic transition. The Akkar Member consists of open marine shales and the Reke of coastal and fluvial sequences (Dalland *et al.,* 1988).

3.1.6 Well 7124/3-1 (1298 m)

The wildcat well 7124/3-1 (Table 3.1.6) is located in the eastern part of the Hammefest Basin along the Nyslepp Fault Complex (Figure 3.1.6). The first interval with hydrocarbons was engaged in 1284.5 m, penetrating the Early Jurassic Tubåen Formation of Kapp Toscana Group. In this well it lies from 1285-1305 m and has 20 m thickness. From 1284.5 m until 1297.5 m it contained gas with an oil leg until 1304 m from where sample "W" was recovered (see Appendix I, Figure 2). The Carboniferous sequence was encountered in 3900 m and was composed of sandstone units interbedded with limestone.

The Tubåen Formation is mainly composed of sandstones and in a lesser extent of shales and coals with the latter being more abundant in the south-eastern basinal margins. Due to lithological variations it is subdivided in three divisions, the lower and upper sand units, separated from an intermediate shaly unit. The clay content decreases (shales out) towards the north-west. The sand units were deposited in high energy marginal marine settings (e.g tidal inlet, barrier complex or estuarine). On the other hand the marine shales found in the north-west, were deposited in deep marine environment while the coals and shales in the south-east were deposited in protected back-barrier lagoonal settings. Finally, the Tubåen Formation generally extends from Late Rhaetian to Early Hettangian (Triassic-Jurassic transition) (Dalland *et al.,* 1988).

Table 3.1.6: Table summarizing the main aspects for the Well 7124/3-1 (www.npd.no).

Well	7124/3-1
NPD ID Wellbore	1066
Date of completion	20.10.1987
Water Depth (m)	273.0
UTM coordinates (m)	NS 7963806.28, EW 422476.34
UTM zone	35
Deepest Formation Age	Late Carboniferous
Area	Barents Sea
Field	Hammerfest Basin, Nyslepp/Måsøy F.C
Total Depth (MD), m	4730.0
Kelly Bushing (KB), m	23.0
Sample data	
Sample ID notation	W
Sample depth, m	1298.0
Sample formation	Tubåen
Group	Kapp Toscana
Age	Early Jurassic
Hydrocarbon shows, m	1284.5, gas-oil leg
Lithology	sandstone

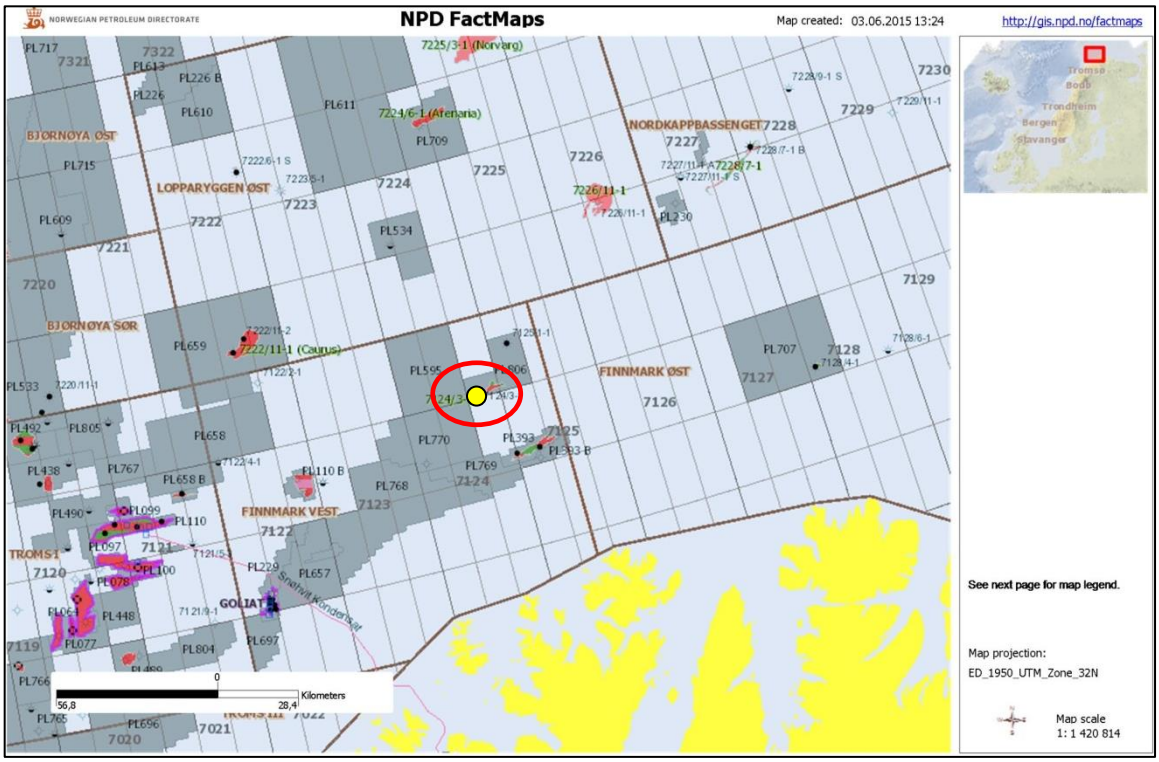

Figure 3.1.6: Fact map depicting Well 7124/3-1 A. The well is marked by the yellow dot encircled in red (www.npd.no).

3.1.7 Well 7125/1-1 (1403.8 m)

The wildcat well 7125/1-1 (Table 3.1.7) was drilled on the southern margin of the Bjarmeland Platform towards the Nyslepp Fault Complex in the eastern Lopparyggen area (Figure 3.1.7).

The Stø Formation of Kapp Toscana Group is 130 m thick in the present well and has good reservoir properties. It was encountered between 1399-1521 m, having a thickness of 122 m. Oil was contained between the 1402.5-1435 m interval from which sample "X" was recovered.

The Triassic Kobbe Formation of Sassendalen was encountered at 2104.5 m, the top part of which contained gas in two sand intervals.

Further details regarding Stø Formation are discussed in subchapters 3.1.2 & 3.1.3.

Table 3.1.7: Table summarizing the main aspects for the Well 7125/1-1 (www.npd.no).

Well	7125/1-1
NPD ID Wellbore	1350
Date of completion	30.12.1988
Water Depth (m)	252.2
UTM coordinates (m)	NS 7977833.23, EW 437126.92
UTM zone	35
Deepest Formation Age	Middle Triassic
Area	Barents Sea
Field	Bjarmeland Platform, Nyslepp/Måsøy F.C
Total Depth (MD), m	2200.0
Kelly Bushing (KB), m	23.5
Sample data	
Sample ID notation	X
Sample depth, m	1403.8
Sample formation	Stø
Group	Kapp Toscana
Age	Early Jurassic
Hydrocarbon shows, m	1402.5-1435, oil
Lithology	sandstone

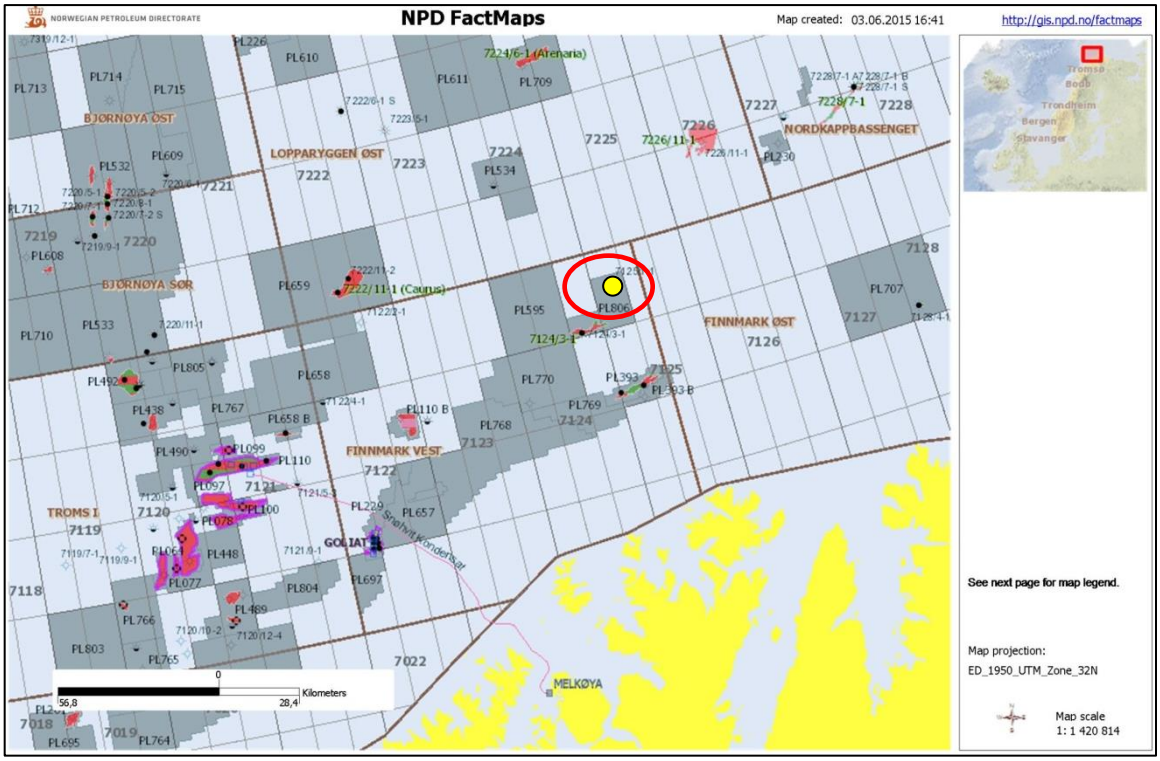

Figure 3.1.7: Fact map depicting Well 7125/1-1 A. The well is marked by the yellow dot encircled in red (www.npd.no).

3.1.8 Well 7222/6-1 S (1633.8 m)

The wildcat well 7222/6-1 S (Table 3.1.8) is located in the Bjarmeland Platform (Figure 3.1.8) specifically east of the Loppa High and south of Swaen (Figure 2.1).

The well drilled through Quaternary sediments and then Triassic, meaning that the Tertiary, Cretaceous and Jurassic sedimentary record was missing. Therefore the reservoir sands of the Snadd Formation from Kapp Toscana Group were encountered very shallow in 484 m. Next, Kobbe Formation of Sassendalen Group was penetrated in 1890 m. The same formation contained hydrocarbons inside channelized sandstones of Middle Triassic age (Ladinian). On the other hand the Kobbe Formation contained petroleum inside sandstone stringers.

Migrated oil was contained between 1617-1648 m inside Snadd Formation, from which sample "Ø" was recovered. Deeper between 1920-2067 m inside Kobbe Formation the saturation was found to be more patchy. Short migrated hydrocarbons were recorded also deeper inside the Klappmyss Formation, originating from adjacent carbonaceous claystones.

Table 3.1.8: Table summarizing the main aspects for the Well 7222/6-1 S (www.npd.no).

Well	7222/6-1 S
NPD ID Wellbore	5755
Date of completion	10.03.2008
Water Depth (m)	364.0
UTM coordinates (m)	NS 8063310.53, EW 364449.65
UTM zone	35
Deepest Formation Age	Early Triassic
Area	Barents Sea
Field	Bjarmeland Platform-Obesum
Total Depth (MD), m	2895.0
Kelly Bushing (KB), m	23.0
Sample data	
Sample ID notation	Ø
Sample depth, m	1633.8
Sample formation	Snadd
Group	Kapp Toscana
Age	Middle Triassic
Hydrocarbon shows, m	1617-1648, oil
Lithology	sandstone

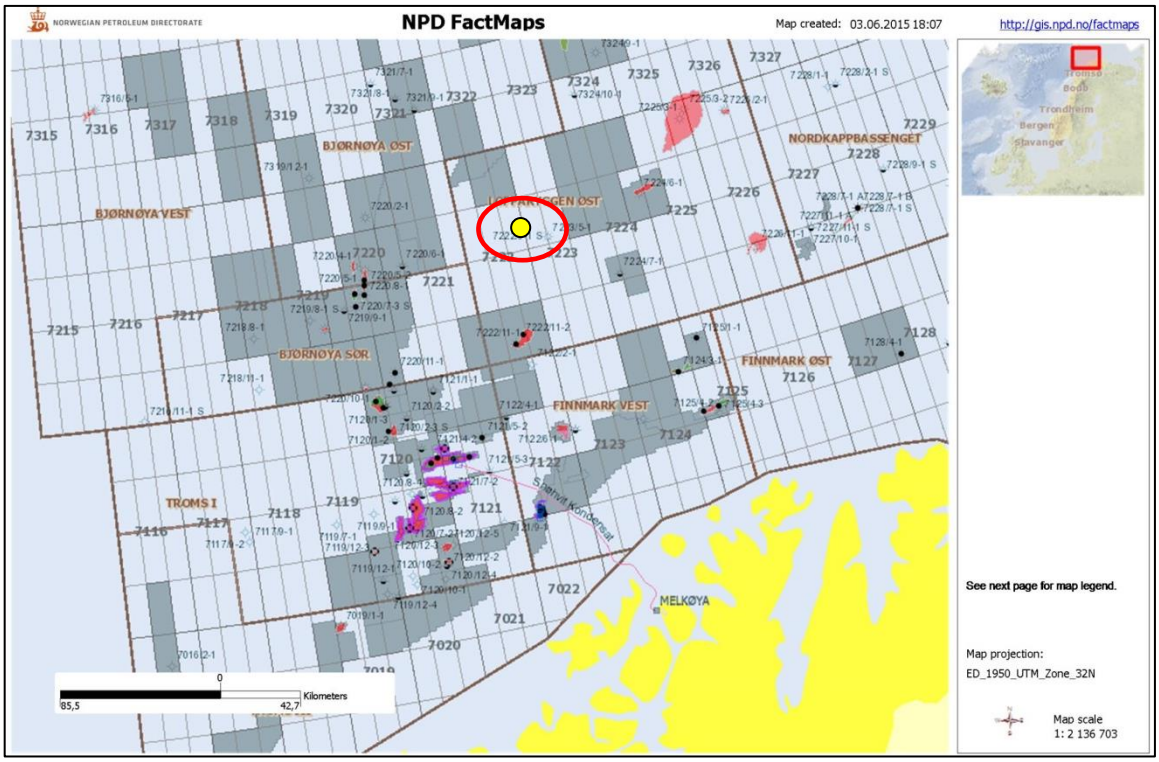

Figure 3.1.8: Fact map depicting Well 7222/6-1 S. The well is marked by the yellow dot encircled in red (www.npd.no).

Therefore the source rocks in this well could be summarized into three intervals: a gas prone in Klappmyss Formation from 2579-2675 m, another being oil prone in Kobbe Formation from 2447-2465 m and a very thin but oil prone at the top of Kobbe Formation at 1887 m. The latter was proven to be immature from Rock-eval and vitrinite reflectance data while the two other deeper intervals were proven to be at the onset of the oil window and therefore immature.

The Snadd Formation is thoroughly discussed in the previous sub-chapter 3.1.4.

3.1.9 Well 7228/7-1 A (2091.1 m)

The wildcat well 7228/7-1 A (Table 3.1.9) is located in the Nordkapp Basin (Figure 3.1.9) East of the Loppa High (Figure 2.1) with a NE-SW oriented basinal-axis. As discussed in Chapter 2, the Nordkapp Basin is highly affected by salt tectonics. Therefore the sediments from Cretaceous and below are affected by the salt diapirs located SE of the present well.

Table 3.1.9: Table summarizing the main aspects for the Well 7228/7-1 A (www.npd.no).

Well	7228/7-1 A
NPD ID Wellbore	4257
Date of completion	02.02.2001
Water Depth (m)	288.0
UTM coordinates (m)	NS 8018306.53, EW 539111.27
UTM zone	35
Deepest Formation Age	Early Triassic
Area	Barents Sea
Field	Nordkapp Basin
Total Depth (MD), m	2881.0
Kelly Bushing (KB), m	23.0
Sample data	
Sample ID notation	AB
Sample depth, m	2091.1
Sample formation	Snadd
Group	Kapp Toscana
Age	Late Triassic
Hydrocarbon shows, m	1617-1648, oil
Lithology	sandstone

The Middle-Late Triassic sandstones of the Snadd Formation were encountered between 1642-2255 m. The Lower Carnian sandstones of the same formation were found to contain both oil and gas. The deeper Klappmyss Formation contained only gas. The oil sample "AB" was recovered from 2091.1 m and therefore belongs to the Snadd Formation (see Appendix I, Figure 3).

Details about Snadd Formation are discussed in sub-chapter 3.1.4.

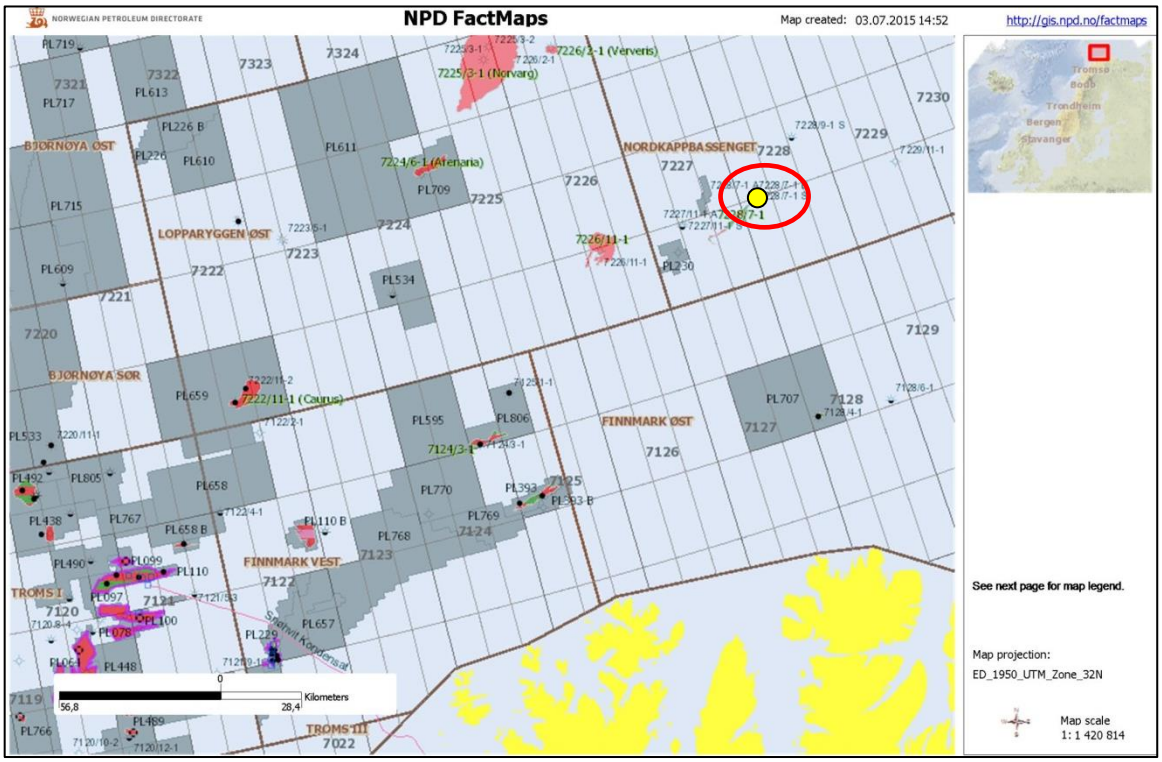

Figure 3.1.9: Fact map depicting Well 7228/7-1 A. The well is marked by the yellow dot encircled in red (www.npd.no).

3.1.10 NSO-1 standard

The NSO notation stands for "North Sea oil". It is an oil sample from the Kimmeridge clay Formation from the Oseberg field, well 30/6-1 (Dahl and Speers, 1985), located in the northern part of the North Sea. It is widely used as an organic geochemical standard by the Norwegian Petroleum Directorate (NPD) in order to calibrate laboratory instruments before running certain geochemical analyses (Weiss *et al.*, 2000; Abay *et al*., 2014). Above that, it was used in the present study for comparing between different samples. The NSO sample used here is referred as NSO-1.

3.2 Source rock dataset

The source rock dataset consists of thirteen core samples, eleven of which come from the Mesozoic sequence: four from the Sassendalen Group, three from the Kapp Toscana Group and the last four from the Adventdalen Group. Only one sample comes from the Tempelfjorden Group of the Upper Paleozoic sequence. Finally, there is a unique outcrop sample from onshore Svalbard, also from the Kapp Toscana Group. For simplicity reasons, the samples were given different ID letters (Table 3.2).

Among the twelve core samples there are seven that were recovered from shallow stratigraphic cores, which comprise regions such as the Nordkapp Basin, the Svalis Dome, the Bjarmeland Platform and the Nordkapp Basin (Figure 3.2).

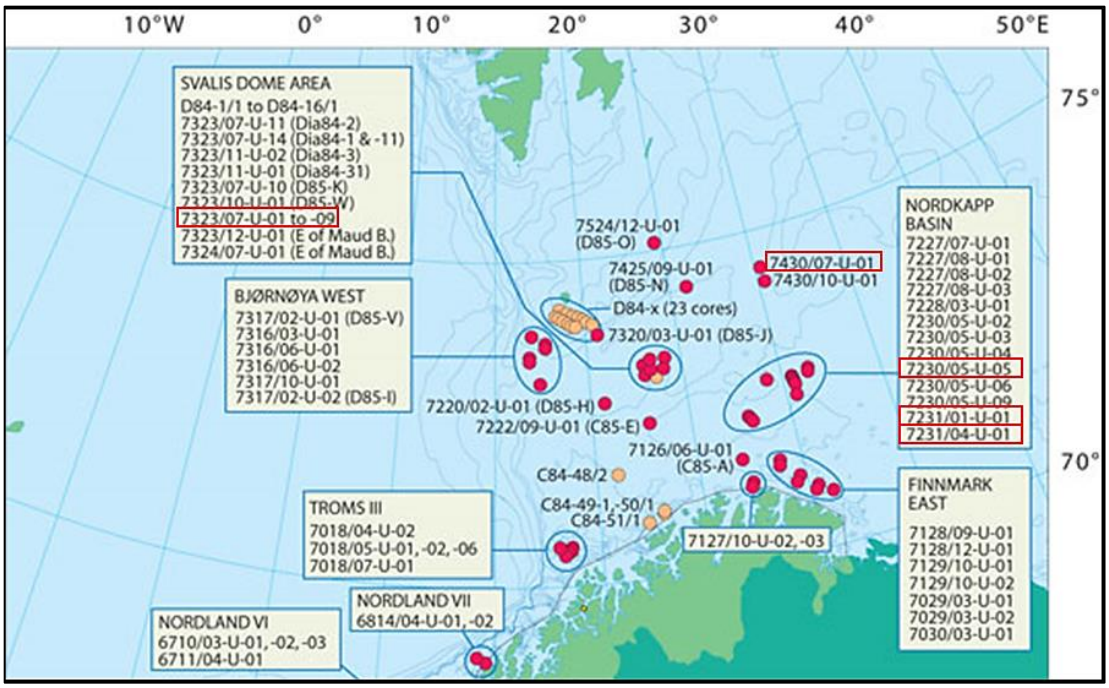

Figure 3.2: Fact map depicting the shallow stratigraphic cores, namely: well 7230/5-U-5, 7231/1-U1 and 7231/4-U-1 in Nordkapp Basin, well 7323/7-U-3 and 7323/7-U9 in the Svalis Dome area and well 7430/7-U-1 in Bjarmeland Platform in northern Barents Sea (IKU-SINTEF Petroleum Research, 1982-1993).

Therefore, Chapter 3.2 contains ten sub-chapters in order to provide some information on the individual wells, namely:

3.2.1 Well 7122/6-1 (1156.60 & 2061.50 m)

3.2.2 Well 7124/3-1 (1367.50 m)

3.2.3 Well 7128/6-1 (1738.50 m)

3.2.4 Well 7230/5-U-5 (43.85)

3.2.5 Well 7231/1-U-1 (70.90 & 76.20 m)

3.2.6 Well 7231/4-U-1 (84.70 m)

3.2.7 Well 7323/7-U-3 (100.30 m)

3.2.8 Well 7323/7-U-9 (106.00 m)

3.2.9 Well 7430/7-U-1 (38.80 & 64.70 m)

3.2.10 De Geerdalen/Svalbard (outcrop)

The information discussed below originates from the Norwegian Petroleum Directorate website (www.npd.no) unless otherwise stated.

Table 3.2: Summary of the source rock samples used in the GC-FID and GC-MS analyses. Age assessment according to Bugge *et al.* (2002); I.K.U-SINTEF and N.P.D websites.

Sample ID	Well	Group	Source rock Formation	Source rock age	Area/Basin
S1	7122/6-1	ADVENTDALEN	KOLMULE	CRETACEOUS	HAMMERFEST BASIN
S2	7122/6-1	KAPP TOSCANA	TUBÅEN	LATE TRIASSIC-EARLY JURASSIC	HAMMERFEST BASIN
S3	7124/3-1	KAPP TOSCANA	FRUHOLMEN	LATE TRIASSIC-EARLY JURASSIC	NYSLEPP/MÅSØY FAULT COMPLEX
S4	7128/6-1	TEMPELFJORDEN	RØYE	PERMIAN	FINNMARK PLATFORM
S5	7230/5-U-5	SASSENDALEN	KOBBE	EARLY-MIDDLE TRIASSIC	NORDKAPP BASIN
S6	7231/1-U-1	ADVENTDALEN	HEKKINGEN	LATE JURASSIC-EARLY CRETACEOUS	NORDKAPP BASIN
S7	7231/1-U-1	ADVENTDALEN	HEKKINGEN	LATE JURASSIC-EARLY CRETACEOUS	NORDKAPP BASIN
S8	7231/4-U-1	ADVENTDALEN	KOLJE	EARLY CRETACEOUS	NORDKAPP BASIN
S9	7323/7-U-3	SASSENDALEN	STEINKOBBE	EARLY TRIASSIC	SVALIS DOME
S10	7323/7-U-9	SASSENDALEN	STEINKOBBE	MIDDLE TRIASSIC	SVALIS DOME
S11	7430/7-U-1	KAPP TOSCANA	SNADD	LATE TRIASSIC	BJARMELAND PLATFORM
S12	7430/7-U-1	SASSENDALEN	SNADD	LATE TRIASSIC	BJARMELAND PLATFORM
SO-21	OUTCROP	KAPP TOSCANA	DE GEERDALEN	UPPER TRIASSIC	TREHØGDENE-SVALBARD

3.2.1 Well 7122/6-1 (1156.60 & 2061.50 m)

The wildcat well 7122/6-1 (Table 3.2.1) is located in the Tornerose field, 50 km north-east of Snøhvit (Figure 3.2.1). The well was drilled on a large tilted fault-block dipping southwards. The northern part of the structure is transected by a WNW-ESE fault. The well reached a final depth of 2707 m, penetrating the Snadd Formation in the Middle-Late Triassic.

Table 3.2.1: Table summarizing the main aspects for the Well 7122/6-1 (www.npd.no).

Well	7122/6-1
NPD ID Wellbore	1140
Date of completion	11.11.1987
Water Depth (m)	401.0
UTM coordinates (m)	NS 7949804.84, EW 563698.43
UTM zone	34
Deepest Formation Age	Middle Triassic
Area	Barents Sea
Field	Hammerfest Basin-Tornerose
Total Depth (MD), m	2707.0
Kelly Bushing (KB), m	23.0
Sample data	
Sample ID notation	S1 & S2
Sample depth, m	1156.6 & 2061.5
Sample formation	Kolmule & Tubåen
Group	Adventalen & Kapp Toscana
Age	Cretaceous & Early Jurassic
Oil window, m	≈2050.0
Lithology	shale

The Jurassic reservoir formations were found to be water-bearing (e.g Stø Formation) with only minor shows. The Snadd Formation of the Late Triassic has 71.5 m gross thickness and contains both gas and condensate. The Hekkingen shales in the present well have only weak oil shows. However, deeper within the Stø Formation the shows became stronger, but they were again weaker in the Nordmela, Tubåen and Fruholmen Formations. The Triassic reservoirs have in general weak oil shows.

The source rocks above 1340 m contain less than 1% of total organic carbon (TOC), meaning that sample "S1" (1156.6 m) from the Kolmule Formation of Adventalen

Group has an average source potential. However, deeper between the section from 1340 to 1931 m, the TOC is higher than 1% and in the interval from 1750 to 1900 m it even reach 3% at the same time that the hydrogen index (HI) does not surpass 100 mgHC/gTOC, meaning that the organic matter is inert.

The next interval of the Hekkingen Formation between 1931-2015 m has very high TOC values that ranged between 10-15% as well as the high HI values of 280-350 mgHC/gTOC. Also the high TOC values between 2040-2099 m were related to coal that is interbedded in the organic shales of the Nordmela and the Tubåen Formations, with sample "S2" deriving from the latter. Finally, from 2100-2710 m the TOC values are low but there are some intervals (e.g 2100-2150 m) which reached 3%. In addition, the HI is in general lower than 100 mg/g with again minor exemptions.

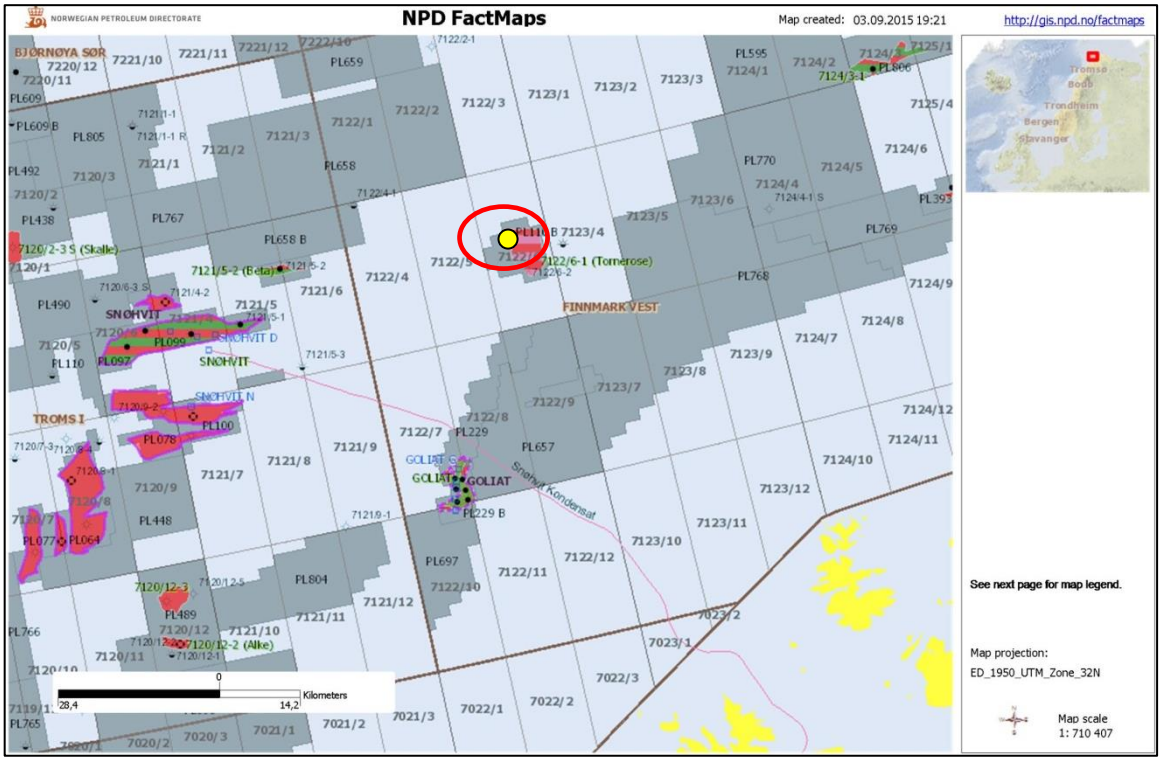

Figure 3.2.1: Fact map depicting Well 7122/6-1. The well is marked by the yellow dot encircled in red (www.npd.no).

According to vitrinite reflectance and T_{MAX} data, well 7122/6-1 enters the oil window at around 2050 m. The Hekkingen shales lie at that depth and have a maturity of 0.6%R_o and a Tmax of 435°C. The sample "S1" comes from shallower depths, hence it

should be immature. The deeper sample "S2" (2061.5 m) is also in the beginning of the oil window. The Kolmule Formation belongs to the Adventalen Group and is of Aptian to Mid-Cenomanian age (Cretaceous). In the present well (7122/6-1) it has a total thickness of 733 m (916-1649 m). The Kolmule Formation is mainly composed of dark shales interbedded with siltstones, limestones and dolomites. There are also some traces of pyrite and glauconite, typical for anoxia that favor organic matter preservation. The thickness increases towards the east part of the Hammerfest Basin. The lower part of the formation was deposited in a prodeltaic environment and clearly depicts a transgressive pulse. Finally, the top of the basal part was eroded in response to the Cretaceous uplift. (Dalland *et al.,* 1988).

3.2.2 Well 7124/3-1 (1367.50 m)

The well 7124/3-1 (Figure 3.1.6) has already been discussed in sub-chapter 3.1.6. The present sample "S3" (see Appendix I, Figure 4) belongs to the Fruholmen Formation of Kapp Toscana Group (Table 3.2.2), which was deposited during the Jurassic-Triassic transition and in well 7124/3-1 has a thickness of 133 m (1305-1438 m).

Table 3.2.2: Table summarizing the main aspects for the Well 7124/3-1 (www.npd.no).

Well	7124/3-1
NPD ID Wellbore	1066
Date of completion	20.10.1987
Water Depth (m)	273.0
UTM coordinates (m)	NS 7963806.28, EW 422476.34
UTM zone	35
Deepest Formation Age	Late Carboniferous
Area	Barents Sea
Field	Hammerfest Basin, Nyslepp/Måsøy F.C
Total Depth (MD), m	4730.0
Kelly Bushing (KB), m	23.0
Sample data	
Sample ID notation	S3
Sample depth, m	1367.5
Sample formation	Fruholmen
Group	Kapp Toscana
Age	Late Triassic-Early Jurassic
Lithology	shale

Additional information for Fruholmen Formation is found in sub-chapter 3.1.5.

3.2.3 Well 7128/6-1 (1738.50 m)

The wildcat well 7128/6-1 (Table 3.2.3) was drilled in the eastern part of the Finnmark Platform (Figure 3.2.3), circa 226 km ENE of the Hammerfest Basin. Top Røye Formation of Kungurian (Early Permian) age was encountered at 1623 m and continued until 1745 m; hence sample "S4" (see Appendix I, Figure 5). An Artinskian to Gzhelian age (Early Permian) limestone succession was penetrated, between 1745.4-2102 m. The next interval, before the basement at 2533.5 m, consists of an Early Carboniferous thick sandstone sequence, namely the Soldogg Formation.

Table 3.2.3: Table summarizing the main aspects for the Well 7128/6-1 (www.npd.no).

Well	7128/6-1
NPD ID Wellbore	1836
Date of completion	08.11.1991
Water Depth (m)	336.0
UTM coordinates (m)	NS 7936359.06, EW 564304.64
UTM zone	35
Deepest Formation Age	Pre-Devonian
Area	Barents Sea
Field	East Finnmark Platform
Total Depth (MD), m	2543.0
Kelly Bushing (KB), m	23.5
Sample data	
Sample ID notation	S4
Sample depth, m	1738.5
Sample formation	Røye
Group	Tempelfjorden
Age	(?) Lower-Middle Permian
Oil shows, m	1630-2076
Lithology	silicified calcareous claystone

The Røye Formation is 122 m thick in well 7128/6-1 on the central Finnmark Platform. In general it is dominated by silicified sediments originated from the abundance of silica spicules (sponges). The lower part in well 7128/6-1 consists of dark silicified calcareous claystone with traces of pyrite and organic matter, affected by secondary dissolution processes. The depositional environment of the lower part reflects a low energy and distal marine regime. The Loppa High and the Finnmark Platform areas

were dominated by bryozoan that grew on low relief carbonate platforms. The middle and upper parts of the Røye Formation depict again distal marine environment where sediments were affected by episodic storms which reworked the sediments composed of siliceous sponge fauna (Larssen *et al.,* 2002).

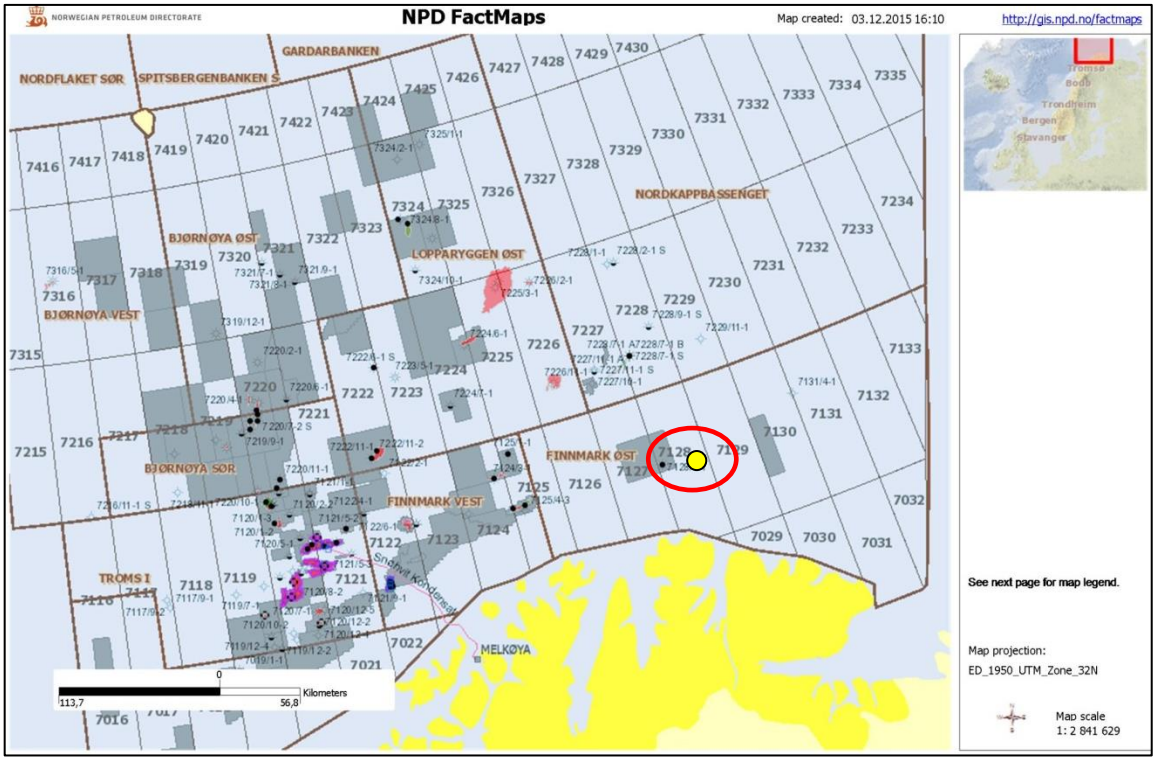

Figure 3.2.3: Fact map depicting Well 7128/6-1. The well is marked by the yellow dot encircled in red (www.npd.no).

3.2.4 Well 7230/5-U-5 (43.85 m)

The shallow stratigraphic core 7230/5-U-5 (Table 3.2.4) was drilled in the central-east Nordkapp Basin (Figure 3.2). It mainly penetrated the Middle-Late Triassic (Anisian-Ladinian to Carnian) strata of the Snadd Formation belonging to the Kapp Toscana Group (Bugge *et al.,* 2002; Vigran *et al.,* 2014) but it penetrated also 26.4 m deeper inside the Kobbe Formation of Sassendalen Group (Bugge *et al.,* 2002; Lundschien *et al.,* 2014).

The sample "S5" was recovered from 43.85 m. In the present well the interval from 24.42-49.22 m belongs to the Snadd Formation and has Middle Triassic (Anisian-Ladinian) age (Vigran *et al.,* 2014). Other authors suggest that the same interval is

equivalent to the adjacent Kobbe Formation of the Sassendalen Group (see Appendix II, Figure 2). However, since the Snadd Formation is mainly composed of sandstone units and sample "S5" is closer to being shale (sandy claystone), it is safer to suggest that it belongs to the Kobbe Formation that mainly contains shales. The depositional environment of the latter is characterized as a shelf to inner paralic setting (Bugge *et al.,* 2002).

Table 3.2.4: Table summarizing the main aspects for the shallow stratigraphic core 7230/5-U-5 (www.npd.no; Bugge *et al.,* 2002; Lundschien *et al.,* 2014; Vigran *et al.,* 2014).

Well	7230/5-U-5
NPD ID Wellbore	1151
Date of completion	09.09.1987
Water Depth (m)	286.0
UTM coordinates (m)	NS 8070572.18, EW 611979.53
UTM zone	35
Deepest Formation Age	Middle Triassic
Area	Barents Sea
Field	Nordkapp Basin
Total Depth (MD), m	335.7
Kelly Bushing (KB), m	2.9
Sample data	
Sample ID notation	S5
Sample depth, m	43.85
Sample formation	? Snadd/Kobbe
Group	? Kapp Toscana/Sassendalen
Age	Early-Middle Triassic
Lithology	sandy claystones

3.2.5 Well 7231/1-U-1 (70.90 & 76.20 m)

The shallow stratigraphic core 7231/1-U-1 (Table 3.2.5) was drilled on the central-west Nordkapp Basin (Figure 3.2). It mainly comprises the upper part of the Hekkingen Formation of Adventdalen Group. As already discussed the Hekkingen shales are of Upper Jurassic-Early Cretaceous age and have excellent source rock potential. The Lower Cretaceous limestones of the Knurr Formation and the Klippfisk Formation, as well as the siltstones of the Kolje Formation were found overlying the Hekkingen Formation shales, see Figure 2.3 and Bugge *et al.* (2002).

The samples "S6" and "S7" were recovered from 70.90 m and 76.20 m, both belonging to the Hekkingen Formation (see Appendix II, Figure 3). According to Bugge *et al.* (2002), both contain kerogen type II and III with only minor content of type IV (inert); hence they are oil and gas prone. The Hekkingen shales typically have high TOC content of 4.0 to 21.0% (weight) but at the same time appear to be immature, with mean vitrinite reflectance values fluctuating between 0.25-0.32% (Bugge *et al.,* 2002).

Table 3.2.5 Table summarizing the main aspects for the shallow stratigraphic core 7231/1-U-1 (www.npd.no; Bugge *et al.,* 2002; Lundschien *et al.,* 2014; Vigran *et al.,* 2014).

Well	7231/1-U-1
NPD ID Wellbore	1153
Date of completion	28.08.1987
Water Depth (m)	278.0
UTM coordinates (m)	NS 8077891.78, EW 636418.11
UTM zone	35
Deepest Formation Age	Upper Jurassic
Area	Barents Sea
Field	Nordkapp Basin
Total Depth (MD), m	371.0
Kelly Bushing (KB), m	2.9
Sample data	
Sample ID notation	S6 & S7
Sample depth, m	70.90 & 76.20
Sample formation	Hekkingen
Group	Adventdalen
Age	Late Jurassic-Early Cretaceous
Lithology	organic rich black shale

3.2.6 Well 7231/4-U-1 (84.70 m)

The shallow stratigraphic core 7231/1-U-1 (Table 3.2.6) was drilled on the central-west Nordkapp Basin (Figure 3.2). It mainly comprises the Kolmule and the Kolje Formations of the Adventdalen Group that are composed of dark brown-grey claystones. In contrast to the underlying Hekkingen Formation, they show only average source potential as their organic matter is low in hydrogen (type III) and is mainly inert, i.e. type IV (see Appendix II, Figure 4) The Kolje Formation was encountered at 62.5 m, the sample "S8" was recovered from 84.70 and belongs to

the Kolje Formation which represents a sedimentary wedge that prograded towards the NE part of the Nordkapp Basin. The wedge was drowned during a sea transgression episode that occurred during Aptian times (Early Cretaceous). The result was the deposition of the dark brown-grey claystones that formed the Kolje Formation (Bugge *et al*., 2002).

Table 3.2.6: Table summarizing the main aspects for the shallow stratigraphic core 7231/4-U-1 (www.npd.no; Bugge *et al.,* 2002; Lundschien *et al.,* 2014; Vigran *et al.,* 2014).

Well	7231/4-U-1
NPD ID Wellbore	1154
Date of completion	28.08.1987
Water Depth (m)	280.0
UTM coordinates (m)	NS 8076155.04, EW 636526.01
UTM zone	35
Deepest Formation Age	Upper Cretaceous
Area	Barents Sea
Field	Nordkapp Basin
Total Depth (MD), m	378.0
Kelly Bushing (KB), m	2.9
Sample data	
Sample ID notation	S8
Sample depth, m	84.70
Sample formation	Kolje
Group	Adventdalen
Age	Early Cretaceous
Lithology	dark brown-grey claystone

3.2.7 Well 7323/7-U-3 (100.30 m)

The shallow stratigraphic core 7323/7-U-3 (Table 3.2.7) is located at the Svalis Dome area (Figure 3.2). It penetrated through the Steinkobbe Formation of Anisian (Middle Jurassic) and the Klappmyss Formation of Olenekian (Early Jurassic) and reached a final depth at 551 m. The sample "S9" was revovered from 100.3 m and belongs to the Steinkobbe Formation (Lundschien *et al.,* 2014).

The Steinkobbe Formation is an organic rich mudstone with some siltstone interbeds (see Appendix II, Figure 5). The TOC ranges between 1.5% to 9.0%. The upper part of the formation (sample "S9") is bioturbated, but the lower is finely laminated.

Phosphate and pyrite nodules are abundant in the whole succession. Thin carbonate and cemented siltstone beds are also present (Dallmann, 1999)

Finally, it must be stressed that the Steinkobbe Formation represents restricted open marine environment and is facies equivalent to the Botneheia Formation from Svalbard. It is further discussed later in sub-chapter 3.2.11 (Lundschien *et al.,* 2014).

Table 3.2.7: Table summarizing the main aspects for the shallow stratigraphic core 7323/7-U-3 (www.npd.no; Lundschien *et al.,* 2014).

Well	7323/7-U-3
NPD ID Wellbore	984
Date of completion	29.07.1986
Water Depth (m)	419.0
UTM coordinates (m)	NS 8135668.70, EW 373441.02
UTM zone	35
Deepest Formation Age	Early Triassic
Area	Barents Sea
Field	Bjørnøya East-Svalis Dome
Total Depth (MD), m	551.0
Kelly Bushing (KB), m	0.0
Sample data	
Sample ID notation	S9
Sample depth, m	100.30
Sample formation	Steinkobbe
Group	Sassendalen
Age	Early Triassic
Lithology	organic rich mudstone

3.2.8 Well 7323/7-U-9 (106.00 m)

The shallow stratigraphic core 7323/7-U-3 (Table 3.2.8) is located in the East Bjørnøya basin at the Svalis Dome (Figure 3.2). It penetrated through the Anisian (Middle Triassic) Steinkobbe Formation of Sassendalen Group and reached a final depth of 543 m.

The sample "S10" was recovered from 106.0 m and belongs to the Steinkobbe Formation (Lundschien *et al.,* 2014). The sample "S10" consists of organic rich mudstone (see Appendix II, Figure 6).

The Steinkobbe Formation is characterized as an organic rich dark shale with thickness ranging between 118-250 m, at the Svalis Dome area. Furthermore, the TOC ranges between 2-6% and in certain intervals it reaches 8%. The kerogen type is II/III. It is therefore capable of forming both liquid and gaseous hydrocarbons. As already stressed, the Steinkobbe Formation is equivalent to the Botneheia Formation in Svalbard, although the deposition of the first started earlier, which reflects that the necessary conditions for source rock generation and preservation started earlier in the central part of the Barents Sea (Lundschien *et al.,* 2014).

Table 3.2.8: Table summarizing the main aspects for the shallow stratigraphic core 7323/7-U-9 (www.npd.no; Lundschien *et al.,* 2014).

Well	7323/7-U-9
NPD ID Wellbore	990
Date of completion	29.07.1986
Water Depth (m)	420.0
UTM coordinates (m)	NS 8136264.98, EW 372556.84
UTM zone	35
Deepest Formation Age	Middle Triassic
Area	Barents Sea
Field	Bjørnøya East-Svalis Dome
Total Depth (MD), m	543.0
Kelly Bushing (KB), m	0.0
Sample data	
Sample ID notation	S10
Sample depth, m	100.60
Sample formation	Steinkobbe
Group	Sassendalen
Age	Middle Triassic
Lithology	organic rich mudstone

3.2.9 Well 7430/7-U-1 (38.80 & 64.70 m)

The shallow stratigraphic core 7430/7-U-1 (Table 3.2.9) is located on the Bjarmeland Platform in the northern Barents Sea (Figure 3.2). It penetrated through the Early to Middle Carnian (Late Triassic) Snadd Formation of the Kapp Toscana Group and reached a final depth of 109.88 m.

Both "S11" and "S12" were recovered from the Snadd Formation. According to Auset (2012), the shallow core 7430/7-U-1 is composed of shale, siltstone and sandstone

coarsening upward units, often overlaid by coal beds (Figure 2.3; see also Appendix II, Figures 7 and 8).

The succession of the Snadd Formation starts with prodelta to distal marine shales, deposited during the Ladinian. However, the depositional pattern changed into massive prograding deltaic systems during the Ladinian-Norian transition, in response to the sea regression that occurred towards the end of the Early Ladinian (Lundschien *et al.,* 2014 and references therein).

Table 3.2.9: Table summarizing the main aspects for the shallow stratigraphic core 7430/7-U-1 (www.npd.no; Lundschien *et al.,* 2014).

Well	7430/7-U-1
NPD ID Wellbore	1326
Date of completion	28.08.1988
Water Depth (m)	343.0
UTM coordinates (m)	NS 8264346.19, EW 597223.05
UTM zone	35
Deepest Formation Age	Middle Triassic
Area	Barents Sea
Field	Bjarmeland Platform
Total Depth (MD), m	460.0
Kelly Bushing (KB), m	0.0
Sample data	
Sample ID notation	S11 & S12
Sample depth, m	38.80 & 64.70
Sample formation	Snadd
Group	Kapp Toscana
Age	Late Triassic
Lithology	sandy shale

3.2.10 De Geerdalen/Svalbard (outcrop)

The De Geerdalen Formation of the Kapp Toscana Group as well as the underlying Tschermakfjellet Formation are the most typical formations for the Carnian-Norian (Late Triassic) sedimentary succession on Svalbard. The De Geerdalen Formation is mainly composed of sandstones that were sourced from the SE, probably from the northern Uralides, also with contribution from the Timanides. The succession is formed of continuous upward coarsening units from shale to sand. The sandstones are separated in two categories. The first is defined by an upward coarsening

massive unit and the second by an upward fining unit with mud conglomerate and gravelstones. Both contain ripple lamination and cross bedding, therefore they are interpreted to be deposited in shallow shelf or deltaic environments (Lundschien *et al.,* 2014). Sample "SO-21" belongs to the De Geerdalen Formation but from the shales that are interbedded inside the two main sandstone units (Table 3.2.10, Figure 3.3).

Table 3.2.10: Table summarizing the main aspects for the outcrop sample from De Geerdalen Fm. (www.npd.no; Lundschien *et al.,* 2014).

Outcrop	De Geerdalen/Svalbard
UTM coordinates (m)	N 78° 13’ 48.0", E 17° 04' 14.2"
UTM zone	33
Area	Trehøgdene-Svalbard
Sample data	
Sample ID notation	SO-21
Sample depth, m	outcrop
Sample formation	De Geerdalen
Group	Kapp Toscana
Age	Late Triassic
Lithology	black shale

Figure 3.3: Geographical map depicting the location of the outcrop sample on Svalbard.

Another important potential source rock for Svalbard is the Botneheia Formation of the Sassendalen Group that is mainly composed of organic rich shale and has Anisian to Ladinian age (Middle Triassic). It is used to describe the Middle Triassic formation in eastern Svalbard, as the notation Bravaisberget is used for the western Svalbard equivalent. It is proposed that it is equivalent with the Steinkobbe and Snadd Formations from the Barents Sea that were also sampled for the present study. The Botneheia Formation itself is sub-divided into the lower Muen Member and the upper Blanknuten Member (Lundschien *et al*., 2014).

Chapter 4

Analytical techniques

The oil and source rock databases discussed in the present study are part of prior academic research elaborated by the PhD candidates Mr. Benedikt Lerch and Mr. Tesfamariam Abay, respectively. With respect to the oils, both the chromatograms and their parameters were processed by APT Kjelle Norge. The source rock sample preparation and the laboratory gas chromatography assessment were done by Mr. Tesfamariam Abay. On the other hand the source rock chromatogram interpretation and the calculation of their parameters were part of the present study. In any case the procedure followed for processing both datasets is very similar to the methodology described in Abay *et al*. (2014) and is discussed below.

Therefore Chapter 4 is dedicated to the analytical techniques of gas chromatography and contains the following five subchapters:

4.1 Sample preparation

4.2 GC-FID (Gas Chromatography-Flame Ionization Detector)

4.3 Molecular sieving

4.4 GC-MS (Gas Chromatography-Mass Spectrometry)

4.5 Introduction to Oil-Source Rock Correlation

4.1 Sample preparation

A specific step to step procedure was followed to prepare the 13 source rock samples for the gas chromatography analysis following the methodology discussed in Abay *et al*. (2014) and detailed here as a reference.

First the core samples (and one outcrop) were thoroughly cleansed by water and then dried at room temperature. They were then crushed down to powder by using a steel mill. A conventional Soxtec System HT 1043 Extraction Unit, manufactured by Tecator, was used to extract the bitumens from the powder fraction. Then 3.1 g of each of the extracted samples were mounted on pre-extracted cellulose cartridges and then covered with glass-wool. The solvent used for the dilution of the samples was a mixture of 45 ml of 93% (volume) dichloromethane and 7% (volume) methanol. After mixing, the solvent was heated up to 90^{o}C. Six samples at a time were put in the solvent and boiled for one hour. The samples were then rinsed for two hours. In order to concentrate the extract, the valve responsible for the back-flux of the solvent was closed. Beads of activated copper were used to remove elemental sulphur. The concentrated extracted residue was then transferred into a 15 ml volume glass vial. There were filled up with dichloromethane until 5 ml in order to standardize the concentration. Finally the vials were sealed with teflon plastic corks. The organic solvent was concentrated before GC-FID and GC-MS analyses.

4.2 GC-FID (Gas Chromatography-Flame Ionization Detector)

The GC-FID technique is used to identify and quantify the *n*-alkanes up to C_{40} with special focus on the C_{15+} components (Fig. 5.2). In other words it identifies and quantifies the major petroleum components (e.g *n*-alkanes, isoprenoids, xylene, toluene, hexane and others). The distribution of the *n*-alkanes as well as the isoprenoid ratios (pristane/phytane, pristane/n-C_{17}, and phytane/n-C_{18}) can provide with useful information regarding the maturity, biodegradation, depositional environment, organic facies and for general fingerprinting of the samples. The methodology followed in the present study is based on Abay (2010).

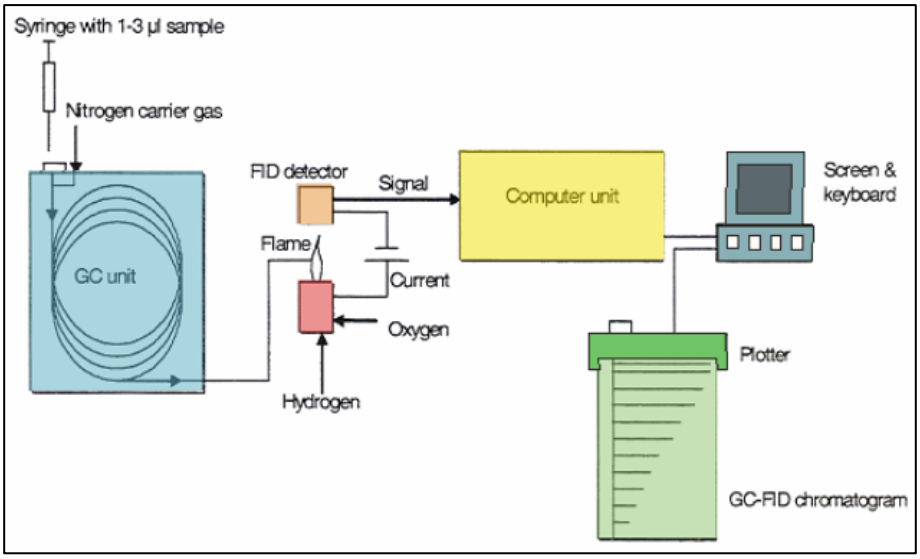

Figure 4.1: Schematic overview of the GC-FID set-up used in the present study (Abay, 2010; originally from Pedersen, 2002)

For the GC-FID analysis, the sample is initially injected and vaporized before entering the chromatographic column (GC-unit), where it is separated into different molecular groups. A film layer inside the column acts a stationary phase. The molecules with short-chains that have high vapor pressure and low boiling points travel faster inside the column compared to the longer and branched molecules that need more time to travel through the column. The carrier gas which is the mobile phase must be inert to avoid interaction with the sample; hence nitrogen (N_2) for GC-FID and helium (He) for GC-MS, are used. A program increases the temperature from the initial 40^{o}C to 325^{o}C in 75 minutes with a temperature gradient of 4^{o}C/min. When the temperature reaches 325^{o}C it is maintained for 20 minutes, so that a full run lasts 95 minutes. The high temperature helps to mobilize the longer and branched molecules that have low vapor pressure and high boiling points at ambient temperature. When the molecules exit the chromatographic column they enter the flame ionization detector chamber (Fig. 4.1). Then a computer receives the signal from the FID sensor and the final gas chromatogram is plotted by using certain software.

In the present study the extracts and the oil samples were analyzed using a Varian Capillary Gas Chromatography-Flame Ionization Detector (GC-FID) Model 3800, featuring a 25 m long Hewlett Packard Ultra II that was cross-linked to a methyl

silicone gum column with 0.2 mm inner diameter and 0.33 µm film thickness. The target injector temperature was set to 330^{o}C, had a hold time of 2^{o}C min^{-1} and a temperature gradient of 4^{o}C. Nitrogen was used as the carrier gas. As described above it took 75 minutes for the temperature to reach 330^{o}C from the initial 40^{o}C and then it was held for 20 minutes.

4.3 Molecular sieving

Molecular sieving is a fractionation technique that can be applied on crude oil samples and source rock extracts before running the GC-MS analysis in order to remove the *n*-alkanes which may cause interference with biomarkers during GC-MS analysis. In more detail it is used to remove the *n*-alkanes (straight-chain saturated hydrocarbons) as well as the polar compounds (e.g resins and asphaltenes) from the organic solvent (Pedersen *et al.,* 2006; Abay *et al*., 2014), so there would be no interference from signals that are not coming from the biomarkers. Asphaltenes are composed of cross-linked polycondensed aliphatic, aromatic and NSO (nitrogen-sulphur-oxygen) moieties that with increasing maturity tend to break down into aromatic and aliphatic hydrocarbons of lower molecular weight (Jones *et al.,* 1987).

Each of the sieve-pores has an opening of 5 Å. Therefore the long-chain *n*-alkanes are hold back and remain inside the sample solution. On the contrary, the biomarkers and aromatics remain in solution, while asphaltenes and resins remain onto the molecular sieve. The procedure must be repeated twice for light oils and condensates which have higher concentration of *n*-alkanes compare to biomarkers (Pedersen *et al*., 2006).

The procedure followed in the present study is discussed in Pedersen *et al*., 2006. About 0.20 g of silicalite (Union Carbide) molecular sieve (UOP MHS2-4120LC silica) with 5 Å molecular diameter was transferred into a 15 ml glass vial. Then three to five drops of sample were mixed with the powdered molecular sieve in the glass vial by using a pipete. The mixture was diluted with 2.5 ml of cyclohexane and stirred thoroughly. It was then centrifuged for 4 minutes at 2000 rpm to settle the sieve in a Heraeus Sepatech Labofuge H. Following this, the sample was decanted into another

15 ml glass vial. About 75% of the sample was evaporated using a warming plate and nitrogen flow in order to concentrate the sample. The whole procedure was repeated to achieve higher enrichment in biomarkers and aromatics.

Finally, the cyclohexane residue was removed and the samples were decanted to glass vials with a pipete and sealed with teflon-lined caps.

4.4 GC-MS (Gas Chromatography-Mass Spectrometry)

The GC-MS technique is used for identification of the biomarkers. It combines a gas chromatograph (GC) with a mass spectrometer and is hence capable for both compound separation and identification. The molecular groups that have different chemical properties appear as discrete peaks on the final chromatogram as each of the molecules requires different travel time (retention time, X axis on the chromatogram, Fig. 5.2) to travel through the gas chromatograph column (GC-unit, Fig. 4.2). Since each molecular group requires different time to travel through the gas chromatograph column, the mass spectrometer in the MS-chamber is able to capture each ionized molecular group separately. There, every molecule is broken down to a series of ionized fragments which are then detected by the MS according to their m/z ratio (mass to charge), which is characteristic for specific carbon molecules. Some molecules can produce abundant characteristic ions i.e. the terpane biomarker compounds have m/z ratio equal to 191. The detector's task is to register their relative abundance marked as peak height (Y axis on the chromatogram, Fig. 5.2). The GC-MS instrument is connected to a PC during the procedure that records the data and constructs the chromatograms by using the appropriate software. The final chromatograms are actually the retention time (X axis) cross-plotted with the relative abundance (Y axis) (Fig. 5.2.1 for the m/z=191) (Abay, 2010).

As discussed in Chapter 4.3, all the samples underwent molecular sieving before running the GC-MS analysis. Doing so enhances the biomarker signal as it removes the *n*-alkanes. In the present study a Fisons Instruments MD800 GC-MS system in SIM-mode (selected ion monitoring) with a 50 m long Chromopak CP-SIL 5CB-MS FS

50X.32 (40) WCOT fused silica-type column with an inner diameter of 0.32 mm that contained a CP-SIL5CB Low bleed/MS stationary phase was used. The starting temperature of the column was 80°C and it was gradually raised primary up to 180°C with a 10°C/min gradient and secondly up to 310°C with a 1.7°C/min gradient where it was maintained stable for 30 minutes. The m/z ratios which were monitored in the present study are 178, 191, 192, 217, 218, 231 and 253. Their chromatograms allow the measurment of a variety of parameters that can indicate the organic facies, maturity and source of the studied samples (Table 5.3).

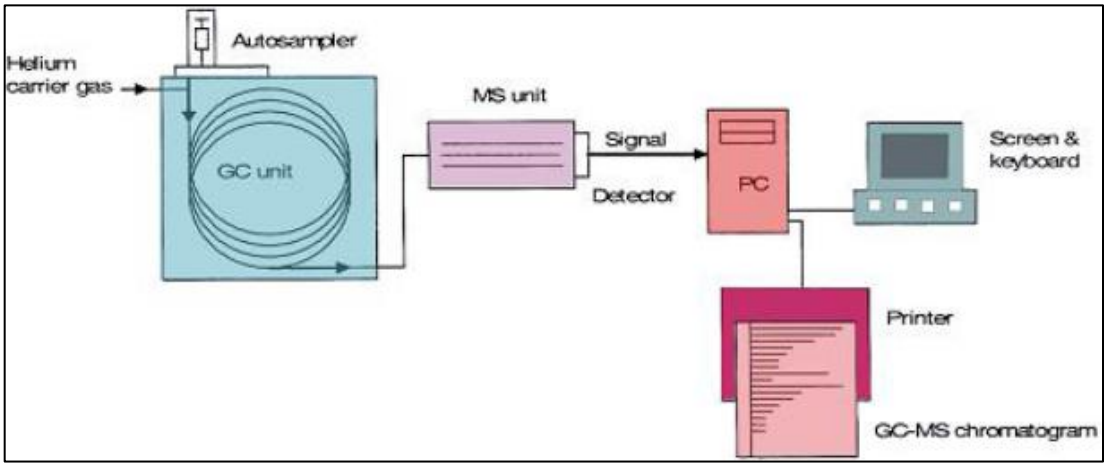

Figure 4.2: Schematic overview of the GC-MS set-up used in the present study (Abay, 2010; originally from Pedersen, 2002)

4.5 Introduction to Oil-Source Rock Correlation

Correlating source rock extracts (bitumens) with crude or seepage oils allows the detection of potential genetic relationships between source rocks and oils, since the entrapped migrated oil will contain the same biomarkers as do the source rocks. These properties can include isotopic composition ($\delta^{13}C$) to even more complex indexes such as the pristane/phytane ratio. For instance, the ratio "$C_{27}/C_{27}+C_{28}+C_{29}$" of steranes does not change its value significantly throughout the maturation stage making this ratio a good facies indicator. Oil-source rock correlation is important to determine the origin and the potential migration pathways of oils. This will help to identify potential new prospects (Peters *et al*., 2005).

Even if the samples demonstrate between them positive correlation they may not be associated, as various source rocks could have the same geochemical composition. Nevertheless, a negative correlation leaves no possibility for samples to be associated. Potential factors that could influence the biomarkers and cause problems to the interpretations are the following with decreasing order of significance (Peters *et al*., 2005):

1. The amount of the indigenous bitumens in the source rock might be contaminated with hydrocarbons expelled from adjacent source rocks.
2. For oil-bitumen correlation to be possible, the thermal maturation stage for all the samples must be nearly equal or at least comparatively similar so that differences arising due to maturity may be fully explained.
3. The bitumen samples should ideally be obtained from thick representative source rock intervals to include the whole vertical compositional in-situ variation from the selected sites.
4. Petroleum in traps is often associated with expulsion of oil and gas over a considerable time and maturity interval, and often may more than one source rocks have contributed to the charge in the trap (Karlsen *et al.,* 1993). In most of the cases, only few source rock samples are available, and this must be considered in terms of correlations studies.
5. During migration and expulsion, the properties of petroleum such as polarity, molecular weight distribution and adsorptivity change, in addition to bulk properties like API and GOR. A good example is the depletion of the migrated hydrocarbons in NSO (nitrogen, sulfur, oxygen) compounds and asphaltenes while the oil in a trap is enriched in saturated and aromatic hydrocarbons (Tissot and Welte, 1984). Migration through clays can alter the expected stereochemistry or polarity of the oil as significant quantities of hydrocarbons are adsorbed.
6. The petroleum in a trap might have an organic composition that deviates compared to that which is currently expelled from the source rocks. With progressive thermal maturation, different compounds are forming so that

each petroleum charge in a given reservoir may end up with different chemical composition.

Thus, oil to source rock correlation must include analytical data for triterpenoid and steroid hydrocarbons that do not change their physicochemical parameters during migration. Other correlation parameters that should be used include medium range maturity parameters i.e. H/C parameters in the molecular weight of C_{13}-C_{20} range that is typical for aromatics and saturates and C_{27+} range of cyclic hydrocarbons (Peters *et al*., 2005). Another way to identify potential contamination from another source is to correlate the immobile kerogen (reflectance of vitrinite macerals) with the maturity of the contained bitumen after the latter has been estimated by the methyl-phenanthrene index (MPI.1) (Tissot and Welte, 1984).

Chapter 5

Petroleum Geochemical Parameters of Gas Chromatography

Chapter 5 is dedicated to the analytical techniques of gas chromatography and the organic compounds they possess. It contains the following subchapters:

5.1 GC-FID Geochemical Parameters

5.1.1 *n*-alkane patterns and biodegradation

5.1.2 Pristane/Phytane

5.1.3 Pristane/n-C17 & Phytane/n-C18

5.1.4 *n*-alkane ratios

5.2 GC-MS Geochemical Parameters

5.2.1 Terpanes

5.2.2 Steranes

5.2.3 Triaromatic Steroids

5.2.4 Monoaromatic Steroids

5.2.5 Phenanthrene

5.2.6 Methyl-phenanthrene & Methyl-dibenzothiophene

5.1 GC-FID Geochemical Parameters

The gas chromatography coupled with flame ionization detector is mainly used to identify the *n*-alkanes with carbon atoms between the C_{15}-C_{40} ranges. The dominant compounds identified in the GC-FID chromatograms are the *n*-alkanes and the isoprenoids, pristane and phytane (Figure 5.1 & 5.2). The X-axis represents increase in time (retention) and the Y-axis the signal intensity (abundance). The GC-FID technique is deployed for the quantitative analysis of the non-polar hydrocarbons that are extracted by organic solvents (acetone/*n*-heptane or dichloromethane/*n*-hexane), Beškoski *et al.* (2012). The ratios of several *n*-alkanes and isoprenoids provide with important information regarding the organic facies, the maturity and the biodegradation of the studied samples.

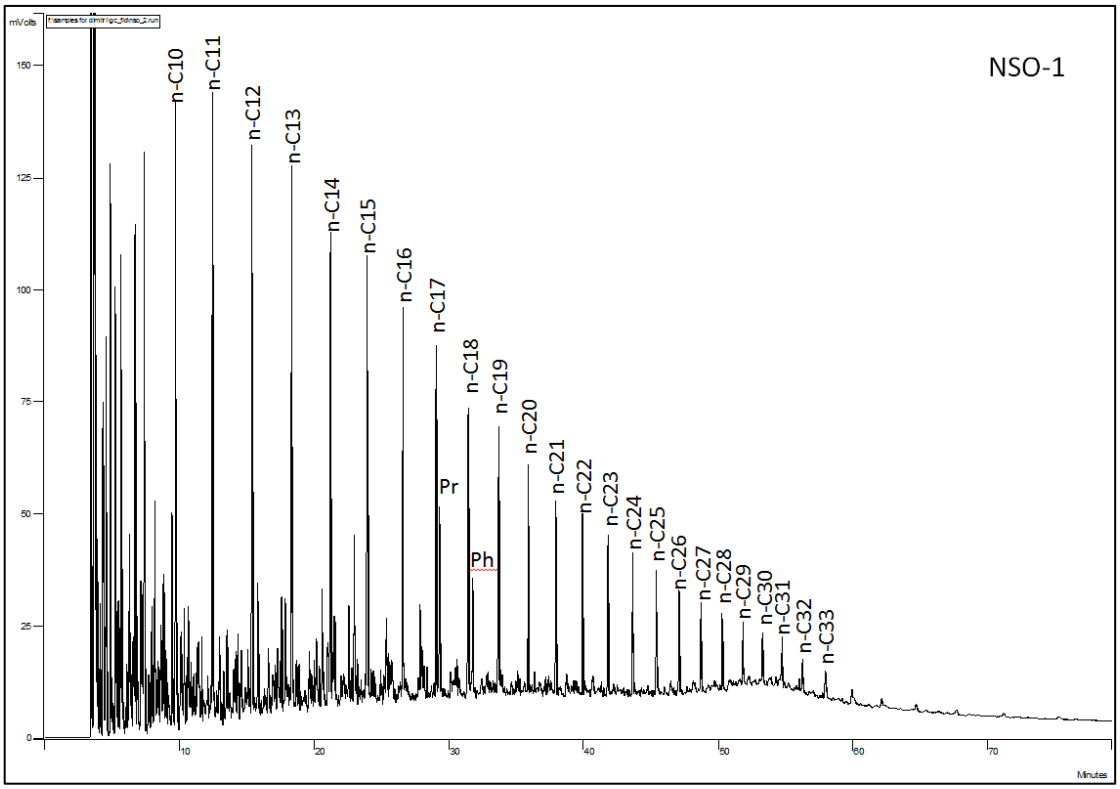

Figure 5.1: The GC-FID *n*-alkane asymptotic envelope pattern for the NSO-1 standard oil from Oseberg field. The X axis is retention time (minutes) and the Y axis is the abundance (counts). The pristane (Pr) and phytane (Ph) peaks are easily discriminated, here at each sides of 30' minutes retention time.

The isoprenoid peaks, pristane and phytane, are always traced near the $C_{17}H_{36}$ and $C_{18}H_{38}$ *n*-alkanes respectfully (Fig. 5.2). As shown in the same figure, the major peaks represent *n*-alkanes. The minor peaks between the *n*-alkanes, which are not

considered here are in fact isoalkanes, cycloalkanes and aromatic hydrocarbons. Generally a "hump" on the baseline of a chromatogram is considered to be a UCM (Unresolved Complex Mixture) or hump of hydrocarbons. The UCM is very common in crude oils when they are biodegraded and in sediment extracts when they are polluted by oil. The peaks of *n*-alkanes can be very weak or absent from the chromatogram if the UCM is too high as often encountered in biodegraded petroleum products (Beškoski *et al*., 2012).

Therefore, gas chromatography coupled with flame ionization detector (GC-FID) was used to identify the non-biomarker maturity parameters depicted on Table 5.1.

Table 5.1: Parameters calculated from the GC-FID chromatogram peaks

No	Parameters and References
1	Pristane/Phytane
2	Pristane/n-C_{17}
3	Phytane/n-C_{18}
4	CPI 1 (Carbon Preference Index) (*Bray and Evans, 1961*)
5	OEP 1,2 (Odd-to-Even Predominance) (*Scalan and Smith, 1970*)

5.1.1 *n*-alkane patterns and biodegradation

Petroleum is a complex mixture that contains thousands of hydrocarbon compounds. However these hydrocarbons can be grouped into four main categories according to (Tissot and Welte, 1984; Beškoski *et al*., 2012).

- The saturated hydrocarbons or aliphatics that include normal alkanes (*n*-alkanes), branched alkanes or isoalkanes and cycloalkanes.
- The aromatic hydrocarbons that include pure aromatics, cycloalkanoaromatic or naphthenoaromatic molecules and cyclic sulfur compounds.
- The resins and asphaltenes that include the high molecular weight nitrogen-oxygen-sulphur (NSO) compounds. The asphaltenes are solvent insoluble in light alkanes (e.g they precipitate in *n*-hexane). On the other hand the resins are more soluble but at the same time very polar.

The saturated hydrocarbons are commonly the dominant components in oils compared to the NSO's. The above hydrocarbons do, however, not have the same resistance to biodegradation. The microbes attack the oil components with the following order of increasing biodegradation resistance: *n*-alkanes-> branched alkanes-> branched alkenes-> *n*-alkylaromates of small molecular mass-> monoaromates-> cyclic alkanes-> polycyclic aromates-> asphaltenes (Beškoski *et al*., 2012).

Biodegradation is accomplished by aerobic bacteria that require molecular oxygen to degrade the organic matter. This is ensured by water washing that removes light hydrocarbons (aromatics) and the sediment provides a substrate for bacteria growth. In the long run, the biodegraded petroleum would be depleted in *n*-alkanes and enriched in NSO compounds (polars and asphaltenes). In addition to these effects the oil will get decreased API gravity (making it more viscous) and it would be richer in sulfur, resins/asphaltenes and metals (Ni & V), Karlsen *et al*. (1995). Biodegradation is easily recognizable as the UCM or hump becomes larger and the baseline of the chromatogram is shifted upwards. The first *n*-alkanes to suffer biodegradation are the C_6-C_{12} range and then the reaction proceeds selectively to remove other saturated hydrocarbon compounds. The UCM area consists mainly of branched and cyclic saturated, aromatic, napthoaromatic and polar compounds plus also partly oxidized species by the acids . The hump on the chromatogram is notated "UCM", unresolved-complex-mixture. exactly because these compounds are not detectable by the usual gas chromatography techniques (Peters *et al*., 2005).

Therefore the *n*-alkane pattern can provide with significant information regarding the maturation, organic facies and biodegradation of the samples. For instance the typical *n*-alkane pattern of normal North Sea oils would be asymptotic (see the NSO-1 standard in Figure 5.1). This means that the peak height of the n-alkanes on the chromatogram decreases more or less exponentially rather than linear as the carbon number increases. That criterion could be enough for an initial screening and classification of the chromatograms (Peters and Moldowan, 1993).

5.1.2 Pristane/Phytane ratios

The main source of pristane (C_{19}) or 2, 6, 10, 14-tetramethylpentadecane and phytane (C_{20}) or 2, 6, 10, 14-tetramethylhexadecane (Tissot and Welte, 1984) is phytol, the phytyl side chain of chlorophyll (Fig. 5.2). The presence or absence of oxygen inside the sediments during diagenesis determines the relative amounts of pristane and phytane that will be formed, respectively (Peters *et al*., 2005).

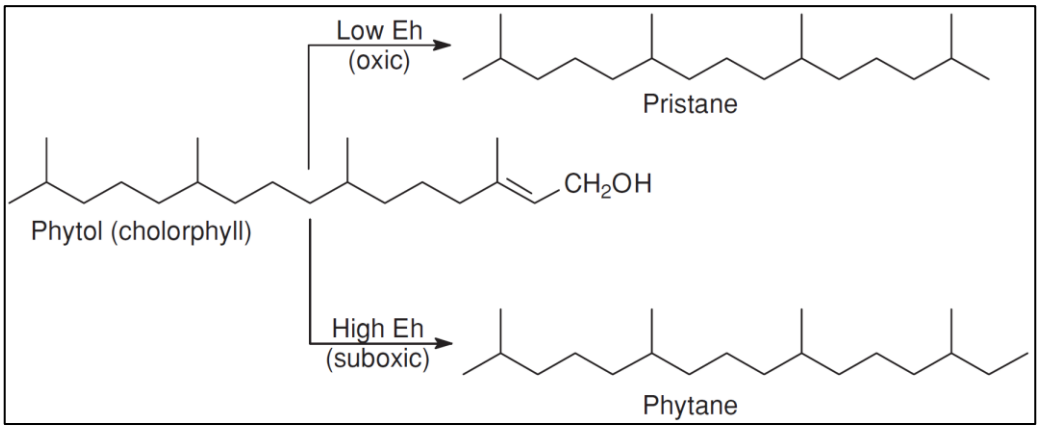

Figure 5.2: The redox potential effect on phytol and the diagenetic transformation to pristane and phytane (Peters et al., 2005).

In more detail, reducing or anoxic conditions will promote the cleavage of the phytyl side chain to yield phytol which in turn will undergo further reduction to form dihydrophytol and finally phytane. On the other hand, oxic conditions will promote the competing conversion of phytol to form pristane. The oxidation of phytol produces phytenic acid that is decarboxylized to pristine and finally to pristane (Fig. 5.2). The pristane/phytane ratio is a valuable index for thermal maturity and source input. In crude oils if Pr/Ph <1 then the source rock was deposited under anoxic conditions, in carbonate or lacustrine environment, which could be also verified by the increased porphyrin and sulphur contents. It thus follows logically that if Pr/Ph >1 the conditions were oxic or hypersaline. Crude oils that originate from coal/resin or paralic shales will cause high Pr/Ph values (3.0 and higher than 10.0) due to high terrestrial input. On the other hand low values (<0.8) are typical for anoxic hypersaline or carbonate environments. Nevertheless most of the crude oils are expected to fall inside the range 0.8-3.0, as the redox depositional conditions can also affect other parameters like the sulphur content and the C_{35} homohopane index.

Furthermore, values between 1.3-1.7 indicate marine oil and at about 2.5 indicate marine environment that is significantly affected by terrestrial input (Peters and Molodwan 1993). The oxicity and the clay activity (acidity) inside the sediments during deposition but also in the water column, can affect the Pr/Ph ratio. Caution must be applied when interpreting the depositional environment for mature samples by using the Pr/Ph index as thermal maturation will result in higher Pr/Ph values. Lab experiments proved artificial generation of pristane from low maturity kerogen with the help of flash pyrolysis (Peters *et al*., 2005). According to the same authors the Pr/Ph ratio must not be used alone to describe the redox condition of the paleoenvironment due to the following factors:

- Variable source input: Besides chlorophyll, other factors may also give rise to pristane or phytane, e.g. phytane will originate from bacteria.
- Different rates of early generation: Phytane content is always higher than pristane in oils and source rock extracts with low maturity; hence when studying samples of higher maturity the result can be misleading.
- Variations at higher maturity: In general, the Pr/Ph ratio increases with progressive thermal maturity while the Pr/*n*-C_{17} and Ph/*n*-C_{18} decrease (see sub-chapter 5.1.3). However this trend is not systematic. Pristane is a smaller molecule than phytane and will hence always have higher survivability with higher temperature.
- Analytical uncertainty: Other isoprenoid hydrocarbons can co-elute with pristane due to technical reasons and perturb the Pr/Ph ratio.

To sum up, Pr/Ph >3.0 is typical for terrigenous plant input deposited in oxic to suboxic environments, while Pr/Ph <0.8 is typical for anoxic to dysoxic depositional environments or for hypersaline to saline conditions, associated with carbonate and evaporite deposition (Peters *et al*., 2005; Justwan *et al*., 2006).

5.1.3 Pristane/n-C17 & Phytane/n-C18

As discussed in subchapter 5.1.2, the ratios of pristane/*n*-C_{17} and phytane/*n*-C_{18} decrease their values as thermal maturation progresses and further *n*-alkanes are

liberated from the from kerogen. Therefore these acyclic-isoprenoids/*n*-alkanes ratios are mostly appropriate for defining thermal maturity, but also for source correlation and for measuring the relative biodegradation of the oil and bitumen samples. For instance oils which have experienced low to moderate biodegradation show higher values for the pristane/*n*-C_{17} and phytane/*n*-C_{18} than non-biodegraded oils. Therefore special caution is required when analyzing samples that are affected by secondary processes like biodegradation and allochthonous organic matter input as they are capable of leading to confusing results (*Peters et al*., 2005).

5.1.4 *n*-Alkane ratios

The carbon preference index (CPI) (Bray and Evans, 1961) and the improved odd-to-even predominance/preference (OEP) (Scalan and Smith 1970) are two of the most widely used *n*-alkane ratios to determine maturity, though they are influenced by the organic matter input and level of biodegradation. The immature source rocks that contain land-plant organic matter have odd-carbon number predominance especially for the *n*-C_{27}, *n*-C_{29} and *n*-$C_{31.}$ The *n*-C_{24} to *n*-C_{34} alkanes originate from marine organic matter and show very little carbon-number preference for even-number *n*-alkanes if they originate from hypersaline carbonate and evaporite source rocks. Therefore, the abundance of odd versus even carbon-numbered *n*-alkanes can determine the maturity of petroleum (Peters *et al*., 2005). The CPI and OEP formulas that were used in the present study are given by the equations below, as is discussed in Peters *et al*., (2005):

$$\mathbf{CPI(1)} = \frac{2(C_{23} + C_{25} + C_{27} + C_{29})}{[C_{22} + 2(C_{24} + C_{26} + C_{28}) + C_{30}]}$$

$$\mathbf{OEP(1)} = \frac{(C_{21} + 6C_{23} + C_{25})}{(4C_{22} + 4C_{24})}, \mathbf{OEP(2)} = \frac{(C_{25} + 6C_{27} + C_{29})}{(4C_{26} + 4C_{28})}$$

The CPI and OEP values that are remarkably below (even preference) or above (odd preference) 1.0 are typical for low thermal maturity. Bitumens or oils with values close to the unity are possibly mature. Values below 1.0 are rare and are related to extracts and oils that were formed in hypersaline or carbonate environments (Peters *et* al., 2005). In more specific, CPI<1 is linked to predominance of phytane over

pristane and reducing environments whereas CPI>1 is linked to predominance of pristane over phytane and less reducing environments (Tissot and Welte, 1984).

5.2 GC-MS Geochemical Parameters

The gas chromatography-mass spectrometry technique is used to identify certain ions that have the following mass/charge ratios (m/z): 191, 217, 218, 231, 253, 178, 192 and 198 (Table 5.2; Figure 5.2). After the peak identification on each of the chromatograms, peak ratios are constructed and used to provide information regarding the relevant depositional environment, the biodegradation, the maturity and the type of kerogen (for the full list of parameters see Table 5.3).

Table 5.2: The mass/charge ratios (m/z) and the contained compounds used in the GC-MS analysis.

m/z	Compounds	Fraction	Type
191	Terpanes	Saturates	Biomarkers
217	Steranes		
218	Steranes		
231	Triaromatic steroids	Aromatics	
253	Monoaromatic steroids		
178	Phenanthrene		Non-biomarkers
192	Methylphenanthrene		
198	Methyl-dibenzothiophenes		

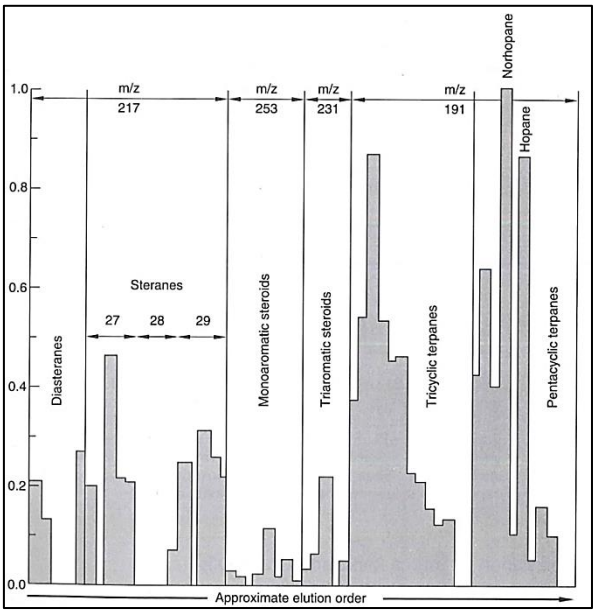

Figure 5.2: Histogram showing the different compound classes in order of elution from left to right (Hunt, 1996).

Table 5.3: Calculated geochemical parameters obtained from the GC-MS chromatogram peaks.

No	m/z	Parameters and References
1	191	Ts/(Ts + Tm) (Seifert and Moldowan, 1978)
2		Diahopane/(diahopane + normoretane) (Cornford *et al.,* 1986)
3		22S/(22S+22R) of C_{31}17α(H), 21ß(H)-hopanes (Mackenzie *et al.,* 1980)
4		C_{30}-hopane/(C_{30}-hopane + C_{30}-moretane) (Mackenzie *et al.,* 1985)
5		29Ts/(29Ts + norhopane) (Moldowan *et al*., 1991)
6		Bisnorhopane/(bisnorhopane + norhopane) (Wilhelms and Larter, 1994)
7		C_{23}-C_{29} tricyclic terpanes/C_{30} αß-hopane (*modified from* Mello *et al.,* 1988)
8		C_{24} tetracyclic terpanes/C_{30} αß-hopane (Mello *et al.,* 1988)
9		Hopane/sterane of C_{30} αß-hopane and regular C_{29} sterane (Mackenzie *et al.,* 1984)
10	217	ßß/(ßß+αα) of C_{29} (20R+20S) sterane isomer (Mackenzie *et al.,* 1980)
11		20S/(20S+20R) of C_{29} 5α(H), 14α(H), 17α(H) steranes (Mackenzie, 1980)
12		Diasterane/(diasterane + regular sterane) (Mackenzie *et al*., 1985)
13	218	% C_{27} of C_{27}+C_{28}+C_{29} ßß-steranes (Mackenzie *et al*., 1985)
14		% C_{28} of C_{27}+C_{28}+C_{29} ßß-steranes (Mackenzie *et al*., 1985)
15		% C_{29} of C_{27}+C_{28}+C_{29} ßß-steranes (Mackenzie *et al*., 1985)
16	231, 253	C_{20}/(C_{20}+C_{28}) triaromatic steroids (TA) (Mackenzie *et al*., 1985)
17		C_{28} TA/(C_{28}TA + C_{29}MA) (Peters and Moldowan, 1991)
18	178, 192, 198	Methylphenanthrene ratio, MPR (Radke *et al*., 1982b)
19		Methylphenanthrene index 1, MPI 1 (Radke *et al*., 1982a)
20		Methylphenanthrene distribution fraction 1, MPDF (F1) (Kvalheim *et al.,* 1987)
21		Methyldibenzothiophene ratio, MDR (Radke, 1988)
22		Calculated vitrinite reflectivity, R_c = 1.1*log10 MPR + 0.95 (Radke, 1988)
23		Calculated vitrinite reflectivity, %R_c = 0.60*MPI1 + 0.40 (Radke and Welte, 1983)
24		Calculated vitrinite reflectivity, %R_o = 2.242*F1 - 0.166 (Kvalheim *et al*., 1987)
25		Calculated vitrinite reflectivity, R_c = 0.073*MDR + 0.51 (Radke, 1988)
26		3-methyl phenanthrene/4-methyl dibenzothiophene (Radke *et al*., 2000)
27		MDBTs/MPs (Radke *et al*., 2000).

5.2.1 Terpanes

Terpanes are saturated hydrocarbons and are identified on the m/z=191 chromatogram (Table 5.2.1 and Fig. 5.2.1).

Table 5.2.1: The triterpanes identified on the chromatograms with m/z=191.

Peak	Stereochemistry	Type	Composition
P		Tricyclic terpane	$C_{23}H_{42}$
Q		Tricyclic terpane	$C_{24}C_{44}$
R	(17R+17S)	Tricyclic terpane	$C_{25}H_46$
S		Tetracyclic terpane	$C_{24}H_{42}$
U		Tricyclic terpane	$C_{28}H_{48}$
V		Tricyclic terpane	$C_{29}H_{50}$
A		18α (H)-trisnorneohopane	C_{27}
B		17α (H)-trisnorhopane	C_{27}
Z		17α (H)-trisnorhopane	$C_{28}H_{48}$
C		17α (H), 21β(H)-norhopane	$C_{29}H_{50}$
29Ts		18α (H)-30-norneohopane	C_{29}
X		17α (H), 15α-methyl-27-norhopane	$C_{30}H_{52}$
D		17β (H), 21α (H)-30-normoretane	$C_{29}H_{50}$
E		17α (H), 21β (H)-hopane	$C_{30}H_{52}$
F		17β (H), 21α (H)-moretane	$C_{30}H_{52}$
G	22S	17α (H), 21β (H)-22-homohopane	$C_{31}H_{54}$
H	22R	17α (H), 21β (H)-22-homohopane	$C_{31}H_{54}$

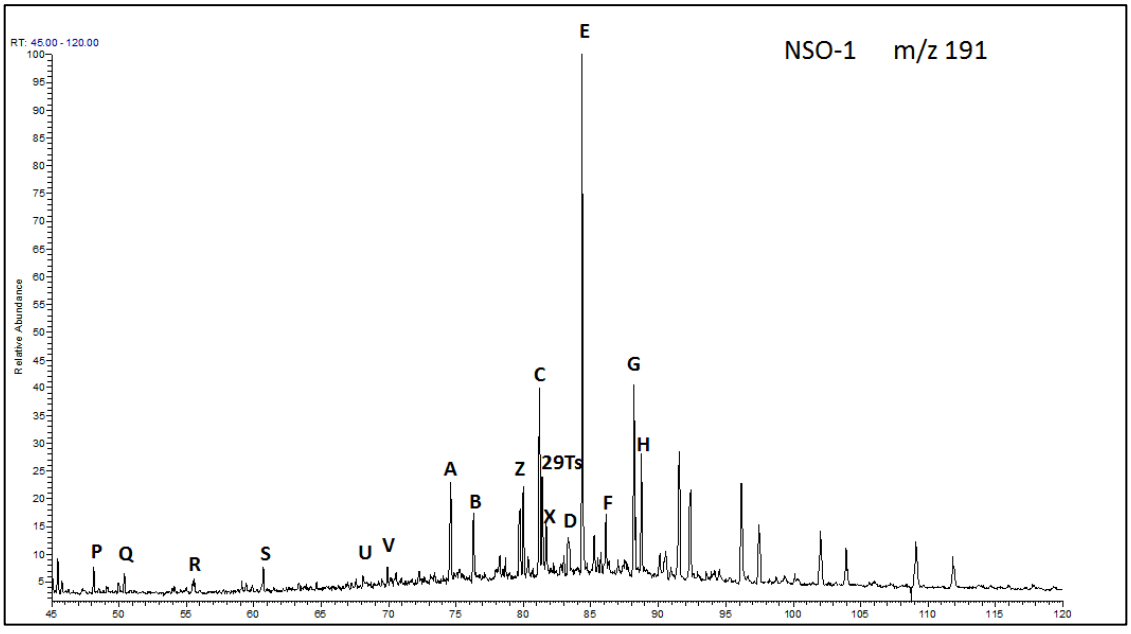

Figure 5.2.1: The peaks identified on GC-MS chromatogram with m/z=191 based on peak identification accrording to Table 5.2.1 for the NSO-1.

Parameters from m/z=191

Parameter 1: Ts/(Ts + Tm) or Ts/Tm (Seifert and Moldowan, 1978) i.e. maturity parameter, peaks A & B.

This is a thermal parameter that is dependent on the relative stability of the C_{27} hopanes, first used by Seifer and Moldowan (1978). It is applicable throughout all maturation stages that can range from immature to post-mature. Its value is highly affected by the source. It is measured in the m/z=191 chromatogram. Parameter 1 represents the ratio of two C_{27} hopanes, the Ts (or 18α-22, 29, 30-trisnorneohopane) and the Tm (or C_{27} 17α-22, 29, 30-trisnorhopane). The Ts notation stands for "terpane stable" and Tm for "terpane maturable". The latter (Tm) becomes less stable with high maturation during catagenesis (Peters *et al*., 2005). In more detail the Ts is more stable than Tm by 4.4 kcal/mol. According to Waples and Machinara (1991) the Tm represents the biological structure whereas the Ts is formed later inside the rocks or sediments due to diagenetic and thermal processes. It thus follows logically that the amount of Tm decreases compared with Ts with increasing maturation, therefore the ratio Ts/Tm or Ts/(Ts+Tm) increases with maturation. The parameter is therefore mainly used for maturity and source identification/correlation. The advantage of the parameter is that it can be used in early to medium late maturations (Fig. 5.3) and i.e. is very resistant to biodegradation (Moldowan *et al*., 1991).

Parameter 2: Diahopane/(diahopane + normoretane), Cornford *et al.* (1986) i.e. maturity parameter, peaks X & D.

Diahopanes (17α (H), 15α-methyl-27-norhopane) are hopanes where the methyl group that was prior attached to C_{14} has been rearranged to C_{15} (Dasgupta *et al*., 1995; Peters *et al*., 2004). The normoretanes are pentacyclic triterpanes, stereoisomers of hopanes found at the C_{27}-C_{35} range that decrease their relative concentratios with respect to hopanes with increasing thermal maturity (Fig. 5.3). Thus, as maturation progresses the normoretane's value decreases and as a result the total ratio's value increases (Peters *et al*., 2004).

Parameter 3: 22S/(22S + 22R) of C_{31} 17α (H), 21β (H)-22-homohopane, Mackenzie *et al.* (1980), maturity parameter, peaks G & H.

The homohopane isomerization ratio [22S/(22S+22R)] is a biomarker maturity ratio that describes the conversion of the biological 22R to the geological 22S configuration of the homohopane molecules. It is thus very useful for studying immature to marginally mature samples. The 22R and 22S doublets (peaks H and G in Fig. 5.2.1 respectively) are found in the C_{31}-C_{35} range and they are called homohopanes. However, the C_{31}-C_{32} compounds are more commonly used to determine the ratio. The ratio is affected by biodegradation and interference, as other peaks may co-elute with the 22R and 22S doublets. Ratios between 0.50-0.54 indicate early oil generation whereas between 0.57-0.62 indicate that the oil generation has been reached or surpassed. There are also some occasions that the ratios can fall below 0.50 and that indicates interference from heterogenic sources, e.g leaching (Peters *et al*., 2004).

Parameter 4: C_{30}-hopane/(C_{30}-hopane + C_{30}-moretane), Mackenzie *et al.* (1985), maturity parameter, peaks E & F.

The C_{30}-hopane is more stable than the C_{30}-moretane. Therefore the ratio increases with increasing maturation. Since C_{30}-moretane is lost with increasing maturation the ratio is limited only to immature oils and extracts (Mackenzie *et al.,* 1985).

Parameter 5: 29Ts/(29Ts + norhopane), Moldowan *et al*. (1991), maturity parameter, peaks 29Ts & C.

The ratio of C_{29}Ts (18α-30-Norneohopane) and 17α-hopane is related to thermal maturity. The 29Ts is more stable than 17α-30-norhopane by 3.5 kcal/mol, therefore thermal maturation affects 29Ts to a lesser degree. Parameter 5 follows the same pattern as parameter 1, so that both increase their values with thermal maturation (Peters *et al*., 2004).

Parameter 6: Bisnorhopane/(bisnorhopane + norhopane), Wilhelms and Larter (1994); Justwan *et al.* (2006), facies parameter, peaks Z & C.

The ratio of bisnorhopane (peak Z) and norhopane (peak C). Bisnorhopane (BNH) is related to bacterial markers that are associated with anoxic depositional

environments. BNH is depleted rapidly with increasing maturation on contraire to the 17α-hopane (norhopane) whose value will increase. As a result the ratio of bisnorhopane/(bisnorhopane + norhopane) will decrease very fast as source rock maturation progresses (Peters *et al*., 2004). In the North Sea bisnorhopane seems to be present in the Upper Jurassic "Hot Shale" but can also occur in the Lower Draupne sequence, probably due to anoxic depositional settings (Justwan *et al*., 2005). However, the ratio of the relative abundance of bisnorhopane is affected by thermal maturation and must be used with care (Justwan *et al*., 2006).

Parameter 7: (C_{23}-C_{29} tricyclic terpanes)/(C_{30} αß-hopane), modified from Mello *et al.* (1988), maturity parameter, peaks P, Q, R, T, U, V & E.

The amount of the tricyclic terpanes (C_{23}-C_{29}) will increase compared to the C_{30} αß-hopane with progressive thermal maturity. The advantage of the parameter is that it can be applied to the whole oil window but at the same time it is strongly affected by the phase and evaporative fractionation (Karlsen *et al*., 1995).

Parameter 8: C_{24} tetracyclic terpane/C_{30} aß-hopane, Mello *et al.* (1988)**,** maturity parameter, peaks S & E.

The amount of the C_{24} tetracyclic terpanes will increase compared to the C_{30} αß-hopane with progressive thermal maturity (Peters and Moldowan, 1993). As a result their ratio will also increase. The C_{24} tetracyclic terpanes are more stable/resistant to biodegradation than hopanes. Additionally, the abundance of the C_{24} tetracyclic terpanes indicates carbonate and evaporite source rock settings but on some occasions also terrestrial input (Peters *et al*., 2004).

Parameter 9: hopane/sterane, Mackenzie *et al.* (1984), facies parameter, peaks E from the m/z=191 and q, r, s, t from m/z=217 chromatograms.

It is calculated from both m/z=191 (Fig. 5.2.1) and m/z=217 (Fig. 5.2.2.1) chromatograms. The steranes are derived from algae and higher plants whereas the hopanes originate from bacteria. As a result high hopane/sterane ratio indicates bacterial source or bacteria reworked organic matter. The steranes are also influenced by thermal maturation so the ratio can be affected by non-facies factors (Peters and Moldowan, 1993).

5.2.2 Steranes

Steranes are in fact tetracyclic saturated hydrocarbons, meaning that their side chain is composed of one 5-ring and three 6-ring structures. They are identified on the m/z=217 (Figure 5.2.2.1) and m/z=218 chromatograms (Figure 5.2.2.2).

As followed, the tables 5.2.2.1 and 5.2.2.2 contain information about the peaks that are identified on the m/z=217 and m/z=218 chromatograms.

Table 5.2.2.1: The steranes identified on the m/z=217 chromatograms (Weiss *et al.*, 2000)

Peak	Stereochemistry	Name	Composition
a	20S	13β(H), 17α(H), 20(S)-cholestane (diasterane)	$C_{27}H_{12}$
b	20R	13β(H), 17α(H), 20(R)-cholestane (diasterane)	$C_{27}H_{48}$
q	20S	24-ethyl-5α(H), 14α(H), 17α(H), 20(S)-cholestane	$C_{29}H_{52}$
r	20R	24-ethyl-5α(H), 14β(H), 17β(H), 20(R)-cholestane	$C_{29}H_{52}$
s	20S	24-ethyl-5α(H), 14β(H), 17β(H), 20(S)-cholestane	$C_{29}H_{52}$
t	20R	24-ethyl-5α(H), 14α (H), 17α(H), 20(R)-cholestane	$C_{29}H_{52}$

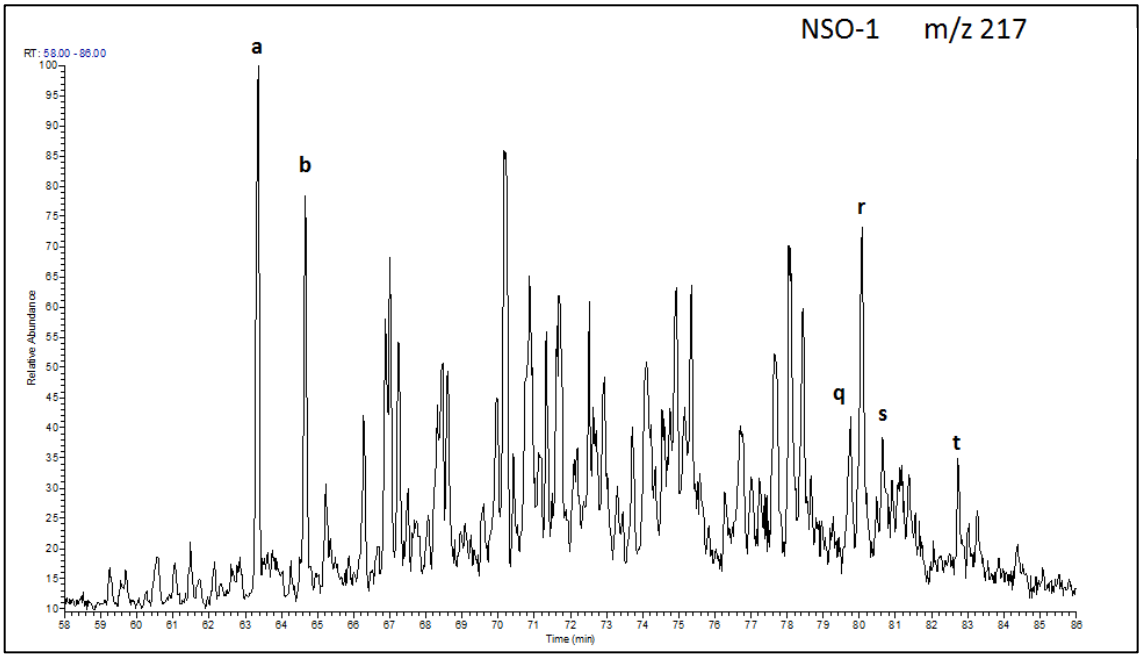

Figure 5.2.2.1: The m/z=217 chromatogram for the NSO-1 standard oil with the relative identified peaks, according to Table 5.2.2.1.

Parameters from m/z=217

Parameter 10: ββ/(ββ + αα) of the C_{29} (20R + 20S) sterane isomers, Mackenzie *et al. (*1980), maturity parameter, peaks q, r, s and t.

The ββ/(ββ+αα) sterane isomerization ratio applies to a very wide range from immature to mature. Isomerization at the C-14 and C-17 in the C_{29} (20S + 20R) causes the ββ/(ββ+αα) ratio to increase from near-zero to about 0.7 (equilibrium) with progressive thermal maturity. The main advantage of this parameter is that it is independent of source, except hypersaline rocks. It is very effective when cross-plotted with 20S/(20S+20R), as both will indicate the maturity of a sample and any disagreements will immediately uncover systematic or other irrelevant to maturity errors, such as different heating rates or clay catalysis (Peters *et al*., 2005).

Parameter 11: 20S/(20S + 20R) of the C_{29} 5α (H), 14α (H), 17α (H), Mackenzie (1980), maturity parameters, peaks q, r, s, and t.

The 20R isomer converts gradually to the 20S isomer with progressive maturation. The equilibrium is reached at the mid of the oil window, 0.52-0.55 (Seifert and Moldowan, 1986) and the maximum value is 0.55. The parameter is affected by biodegradation facies and weathering (Peters and Moldowan, 1993).

Table 5.2.2.2: The steranes identified on the m/z=218 chromatograms (Weiss *et al.,* 2000).

Peak	Name
i	C_{27} regular sterane (5α(H), 14β(H), 17β(H), 20(S)-cholestane)
o	C_{28} regular sterane (24-methyl-5α(H), 14β(H), 17β(H), 20(S)-cholestane)
s	C_{29} regular sterane (24-ethyl-5α(H), 14β(H), 17β(H), 20(S)-cholestane)

Parameter 12: Diasteranes/(diasteranes + regular steranes), Mackenzie *et al*. (1985), facies and maturity parameter, peaks a, b, q, r, s and t.

This parameter is called diasterane index and it is the ratio of the rearranged steranes (diasteranes) to regular steranes. The concentration of the rearranged steranes depends on Eh, pH, depositional settings, clay content and the thermal maturation level of the source rock. The amount of rearranged steranes increases relative to the regular steranes with thermal maturation. The maximum ratio is 1.0.

Oils or extracts from carbonate source rocks are possible to have lower ratios than those from clastic source rocks. The main advantage of the parameter is that it is applicable through the whole oil window (Peters *et al*., 2005) but can be affected by thermal maturity (Justwan *et al*., 2006).

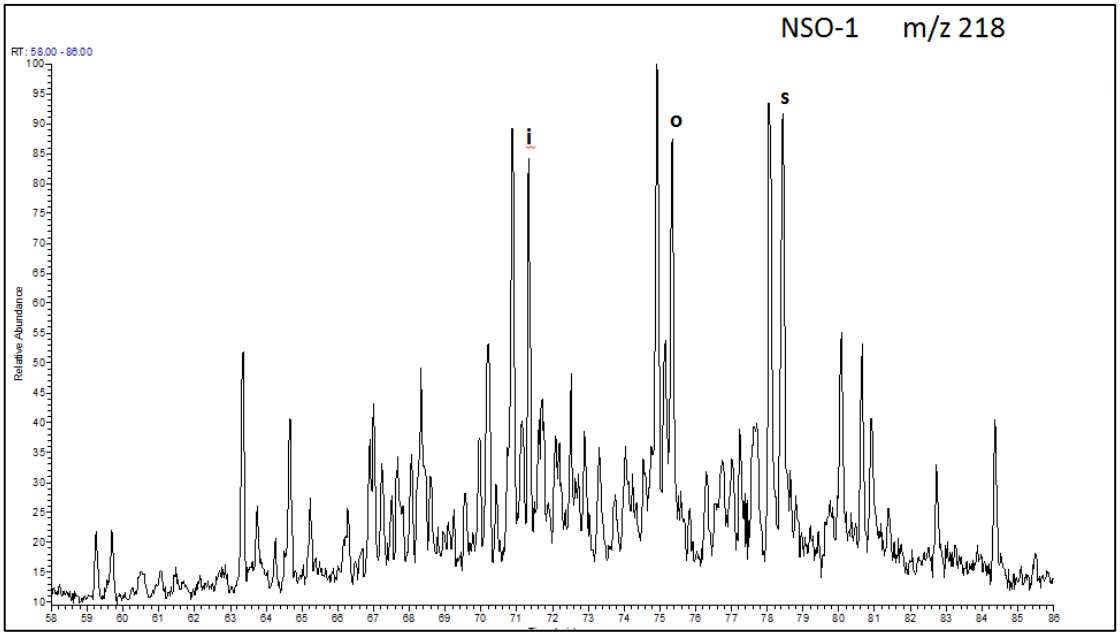

Figure 5.2.2.2: The m/z=218 chromatogram for the NSO-1 standard oil with the relative identified peaks, according to Table 5.2.2.2.

Parameters from m/z=218

Parameters 13, 14 & 15: (peaks i, o & s respectively), Mackenzie *et al*. (1985)

The peaks i, o and s correspond to the relative percentages of the C_{27}, C_{28} and C_{29} of ββ steranes. The distribution of these regular steranes on a ternary diagram can be used to differentiate organic facies (marine or terrigenous organic matter). Therefore the principal use is oil-source rock correlation, by plotting crude oils with source rock extracts (Peters *et al*., 2005).

5.2.3 Triaromatic steroids

Triaromatic Steroids are aromatic hydrocarbons that are useful for maturity assessment. They are identified on the m/z=231 chromatogram (Figure 5.2.3). The relevant peaks are presented in Table 5.1.3.

Table 5.2.3: The triaromatic steroids identified on the m/z=231 chromatograms.

Peak	Name
a1	C_{20} triaromatic steroid (TA)
g1	C_{28} triaromatic steroid (TA)

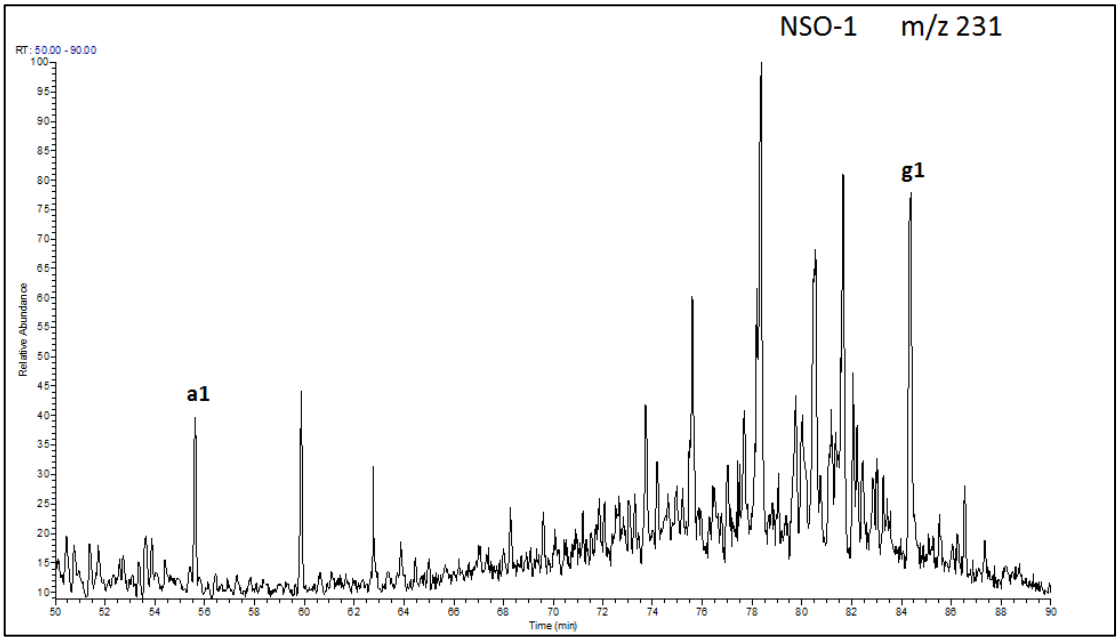

Figure 5.2.3: The m/z=231 chromatogram for the NSO-1 standard oil with the relative identified peaks, according to Table 5.2.3.

Parameters from m/z=231

Parameter 16: $C_{20}/(C_{20} + C_{28})$, Mackenzie *et al*. (1985), maturity parameter, peaks a1 & g1.

The abundance of the triaromatic steroids (TA) serves as maturity parameter as the amount of C_{20} increases relative to C_{28}. The maximum ratio is 1.0. The parameter is valid through the whole oil window (Peters and Moldowan, 1993).

5.2.4 Monoaromatic steroids

Monoaromatic steroids are aromatic hydrocarbons which are identified on the m/z=253 chromatogram (Figure 5.2.4). They are precursors for the triaromatic steroids. They are useful for maturity assessment, correlation (fingerprinting) and for comparing the ratio of triaromatic to monoaromatic steroids. Table 5.2.4 presents the unique peak notation for the monoaromatic steroids.

Table 5.2.4: The triaromatic steroids identified on the m/z=231 chromatograms.

Peak	Name
H1	C_{29} monoaromatic steroid (MA)

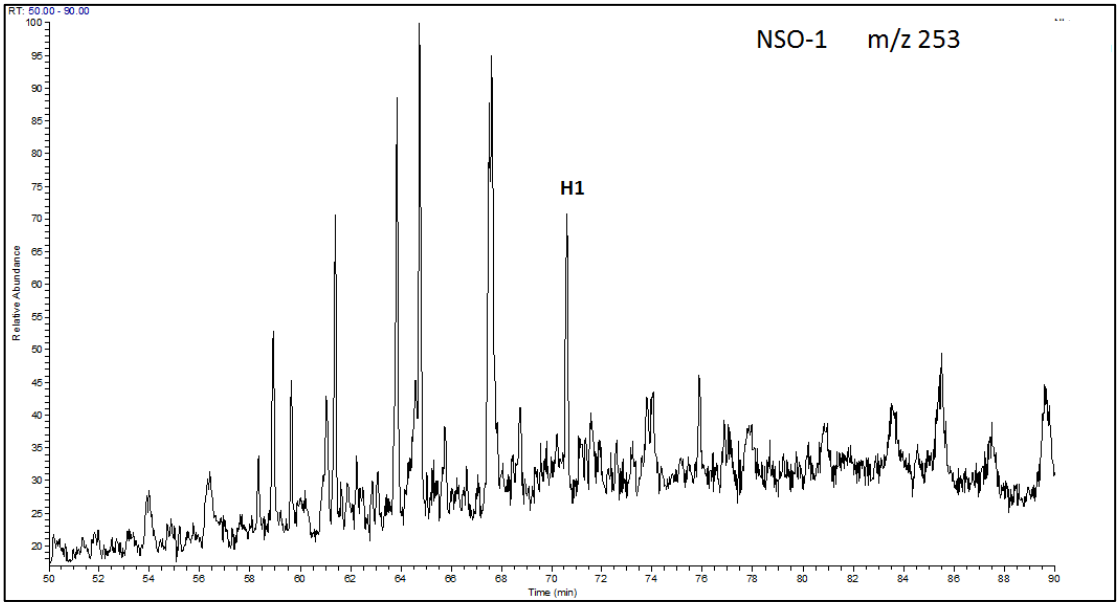

Figure 5.2.4: The m/z=253 chromatogram for the NSO-1 standard oil with the relative identified peaks, according to Table 5.2.4.

Parameters from m/z=253

Parameter 17: $C_{28}TA/(C_{28}TA + C_{29}MA)$, Peters and Moldowan, (1991), maturity parameter, peaks g1 from m/z=231 & H1 from m/z=253 chromatograms.

This parameter combines data from the m/z=231 and m/z=253 chromatograms. The monoaromatic steroids (MA) are rearranged to triaromatic steroids (TA) with thermal maturation and as a result their ratio holds information about maturity but also for phase fractionation. The maximum value of the ratio is 1.0 (Peters and Moldowan, 1993).

5.2.5 Phenanthrene

The phenanthrene organic compound is an aromatic hydrocarbon. The peak is clearly identified on the m/z=178 chromatogram (Figure 5.2.5). It is as well useful for maturity assessment. Table 5.2.5 presents the relevant peak identified on Figure 5.2.5.

Table 5.2.5: The phenanthrene identified on the m/z=178 chromatograms.

Peak	Name
P	Phenanthrene

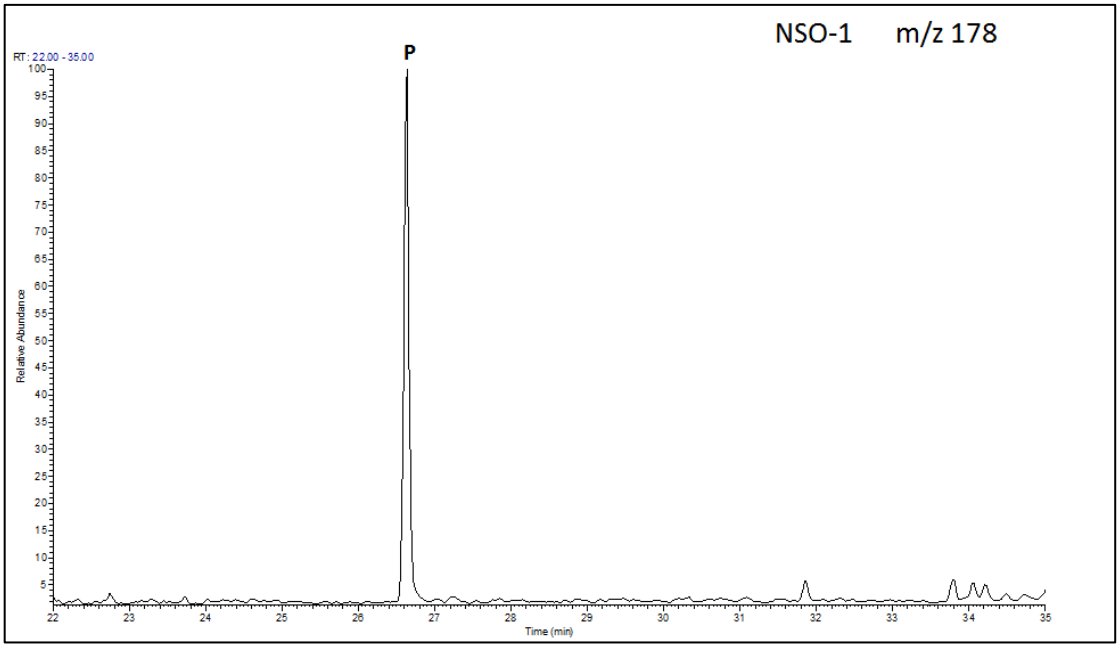

Figure 5.2.5: The m/z=178 chromatogram for the NSO-1 standard oil with the relative identified peaks, according to Table 5.2.5.

5.2.6 Methyl-phenanthrene & Methyl-dibenzothiophene

The methyl-phenanthrene organic compounds belong also to the aromatic hydrocarbons. The peak are clearly identified on m/z=192 chromatogram (Figure 5.2.6). It is very useful for maturity assessment. Table 5.2.6.1 presents the relevant peaks identified on Figure 5.2.6, top.

The methyl-dibenzothiophene organic compounds are sulphur rich aromatic hydrocarbons. They are identified on the m/z=198 chromatogram (Figure 5.2.6, bottom). They are mainly used for maturity assessment and they can provide better results than the phenanthrenes when analyzing medium to low maturity samples. The difference between the 4-MDBT and 1-MDBT is directly proportional to the maturity (Peters *et al.,* 2005). Table 5.2.6.2 shows the peaks identified on the m/z=192 chromatogram.

Table 5.2.6.1: The methylphenanthrenes identified on the m/z=192 chromatograms.

Peak	Name
3-MP	3-methylphenanthrene
2-MP	2-methylphenanthrene
9-MP	9-methylphenanthrene
1-MP	1-methylphenanthrene

Table 5.2.6.2: The methyldibenzothiophene identified on the m/z=198 chromatograms (Weiss *et al.,* 2000).

Peak	Name
4-MDBT	4-methyldibenzothiophene
1-MDBT	1-methyldibenzothiophene

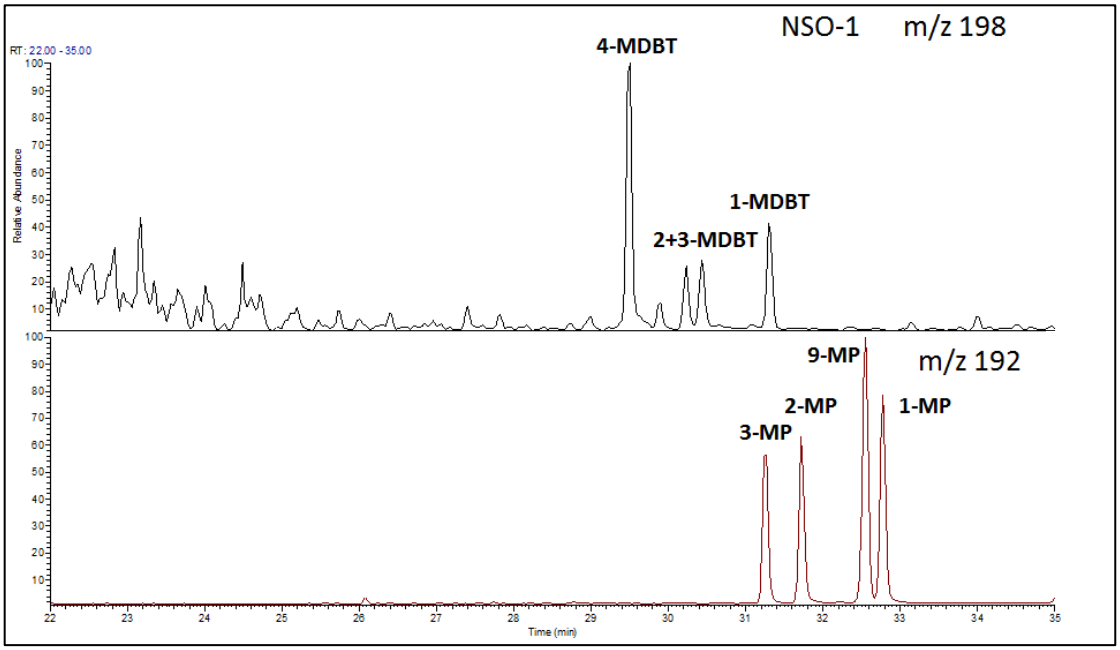

Figure 5.2.6: The m/z=198 and m/z=192 chromatograms for the NSO-1 standard oil with the relative identified peaks, according to Tables 5.2.6.1-2.

Parameters from m/z=178, 192 & 198

The parameters 18-27 contain tricyclic hydrocarbons that are identified on the m/z=178, 192 and 198 chromatograms. Phenanthrene is measured on m/z=178 (Fig. 5.2.5) and the four isomers of methyl-phenanthrene on m/z=192 (Fig. 5.2.6). The number in front of the abbreviation MP indicates the respective position of the methyl group (-CH_3) on the Phenanthrene chain. The isomers 3-MP and 2-MP are

thermally more stable compared to the 1-MP and 9-MP isomers that decay faster during maturation.

Parameter 18: Methyl-phenanthrene ratio: MPR, Radke *et al*. (1982b), maturity parameter, peaks 1-MP & 2-MP.
MPR = 2-MP/(1-MP)

Parameter 19: Methyl-phenanthrene index 1: MPI 1, Radke *et al*. (1982a), maturity parameter, peaks P from m/z=178 and 1-MP, 2-MP, 3-MP, 9-MP from m/z=192 chromatograms.
MPI.1=1.5(3-MP + 2-MP)/(P + 9-MP + 1-MP)

Parameter 20: Methyl-phenanthrene distribution factor: F1 or MPDF, Kvalheim *et al.* (1987), maturity parameter, peaks 1-MP, 2-MP, 3-MP, 9-MP.
MPDF = (3-MP + 2-MP)/(3-MP + 2-MP + 1-MP + 9-MP)

Parameter 21: Methyl-dibenzothiophene ratio: MDR, Radke (1988), facies and maturity parameter, peaks 1-MP-1 & 4-MP.
MDR=4-MDBT/1-MDBT
The ratio makes use of the two isomers of methyl-dibenzothiophene, 4-MDBT and 1-MDBT with the first being thermally more stable. A sulphur atom is contained inside the methyl-dibenzothiophene molecule, so the quantity of MDBT discloses the amount of sulphur contained in crude oils or source rock extracts.

Vitrinite reflectivity (%R) was calculated from the henanthrene (P), methyl-phenanthrenes (MP) and methyl-dibenzothiophenes (MDBT) according to the equations below:

Parameter 22: Calculated vitrinite reflection: R_c (Radke, 1988), maturity parameter, MPR from parameter 18)
R_c = 1.1*log10MPR + 0.95

Parameter 23: Calculated vitrinite reflection: $\%R_c$ (Radke and Welte, 1983), maturity parameter, MPI from parameter 19.

$\%R_c = 0.60*MPI1 + 0.40$

Parameter 24: Calculated vitrinite reflection: $\%R_c$ (Kvalheim *et al*., 1987), maturity parameter, MPDF from parameter 20.

$\%R_c = 2.242*MPDF - 0.166$

Parameter 25: Calculated vitrinite reflection: $\%R_c$ (Radke, 1988), maturity parameter, MDR from parameter 21.

$\%R_c = 0.073*MDR + 0.51$

Parameter 26: 3-MP/4-MDBT (Radke *et al*., 2000), facies parameter, peaks 3-MP from m/z=192 and 4-MDBT from m/z=198 chromatograms.
Parameter 26 can be cross-plotted with Pr/Ph to identify organic facies and the relative amount of sulphur in source rocks.

Parameter 27: MDBTs /MPs (Radke *et al*., 2000), facies parameter, peaks 1+2, 3, 4-MDBT from m/z=198 and 1, 2, 3, 4-MP from m/z=192 chromatograms.
Ratios above 1 indicate carbonate facies and ratios below 1 shale facies.

The biomarker maturation parameters respond unlikely during the different maturation stages. Figure 5.3 shows how these parameters are affected by thermal maturation and how they link to vitrinite reflectance and oil generation.

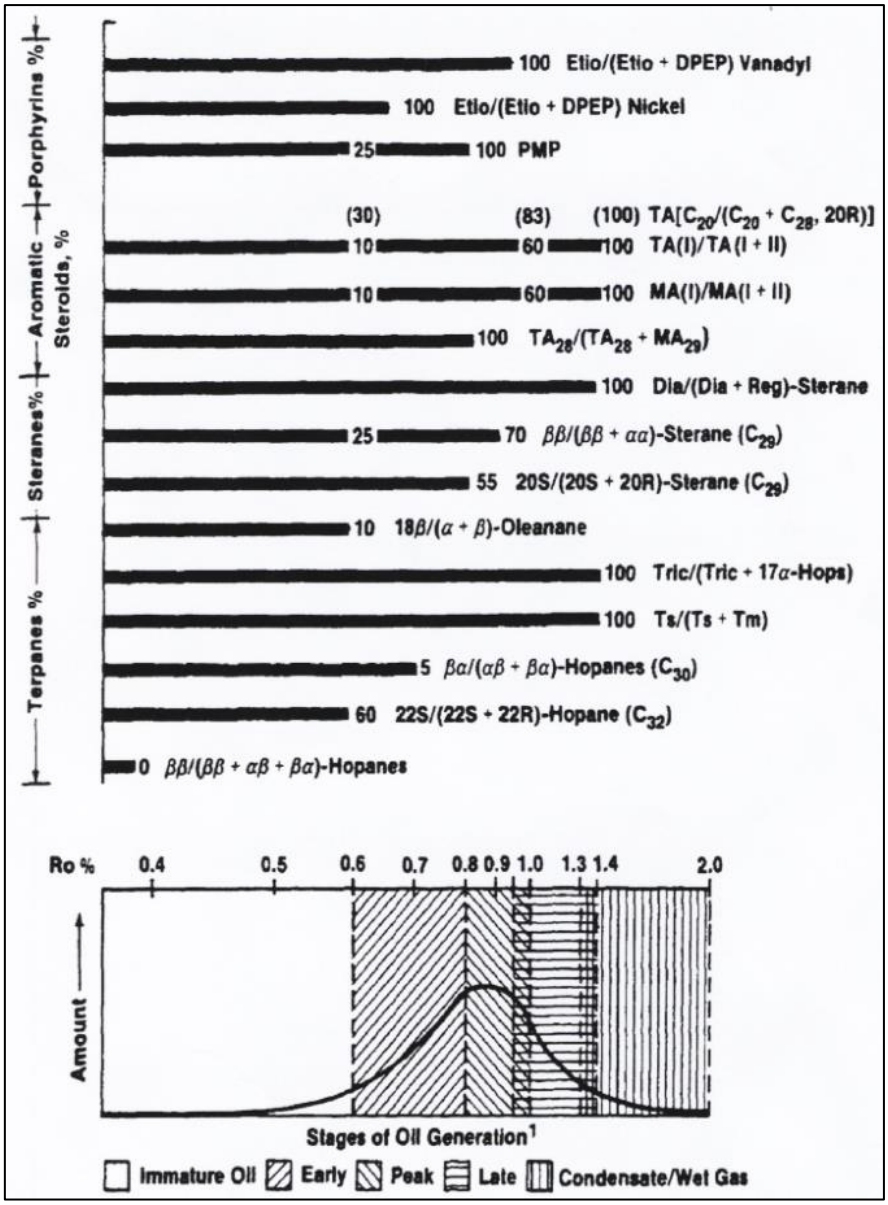

Figure 5.3: The effect of thermal maturation on the validity of the biomarker parameters (Peters *et al.*, 2005; originally from Mackenzie, 1984). Note that parameters are not internally linear, and they are also not comparable between the individual parameters. MA: Mono-aromatics, TA: Three-aromatics.

Chapter 6

Results

Chapter 6 contains the results from the GC-FID and GC-MS analyses that were performed in the laboratory. These results are organized as follows:

6.1 GC-FID Results

6.2 GC-MS Results

6.3 Summary of results

6.4 Presentation of chromatograms

6.1 GC-FID Results

Results for the GC-FID are found in Table 6.1. All chromatograms are found in Appendix III.

The source rocks and oil core extracts, described in Chapter 3, were analyzed by means of GC-FID as discussed in Chapters 4 and 5, to identify the *n*-alkane and isoprenoid distributions which provide with information about the maturity and the source rock facies of the samples (Peters and Moldowan, 1993). The GC-FID technique was mainly deployed to calculate the pristane/phytane (Pr/Ph), pristane/*n*-C_{17} (Pr/n-C_{17}) and phytane/*n*-C_{18} (Ph/n-C_{18}) ratios. The CPI values were calculated for both the oil and source rock samples. The formula for the oils is described in sub-chapter 5.1.4, but it was modified for the source rocks to $C_{25}/C_{24}+C_{26}$, as it was not possible to identify the *n*-alkane peaks required on the GC-FID chromatograms. The OEP values were calculated only for the oil samples.

Table 6.1: The isoprenoid and *n*-alkane ratios results age coloured. Red for Permo-Carboniferous, purple for Triassic, teal for Jurassic, green for Cretaceous. NSO-1 sample is coloured in yellow.

Sample	Formation	Pr/Ph	Pr/n-C17	Ph/n-C18	CPI (1)	OEP (1)	OEP (2)
C	ØRN	1.51	0.92	0.69	1.17	1.01	1.08
T1	SNADD	1.85	0.86	0.51	1.12	1,00	1.08
T2	KOBBE	1.63	1.11	0.79	1.09	0.99	1.10
V	FRUHOLMEN	1.44	1.04	0.77	1.14	1.00	1.09
Ø	SNADD	1.50	1.49	1.11	1.21	1.01	1.10
AB	SNADD	1.50	0.46	0.31	1.13	1.02	1.13
E1	STØ	1.40	0.83	0.59	1.15	0.99	1.11
O	STØ	1.46	0.76	0.58	1.10	0.97	1.06
X	STØ	2.00	1.20	0.84	1.27	1.01	1.15
W	TUBÅEN	1.38	0.94	0.79	1.11	0.95	1.07
NSO-1	NSO-1	1.67	0.53	0.39	0.50	-	-
S4	RØYE	2.01	0.28	0.16	0.53	-	-
S9	STEINKOBBE	1.00	5.00	5.00	0.54	-	-
S10	STEINKOBBE	0.81	3.60	5.54	0.52	-	-
S11	SNADD	4.30	1.46	0.32	0.86	-	-
S12	SNADD	3.88	3.44	0.73	0.89	-	-
S5	KOBBE	3.04	2.38	0.80	0.80	-	-
S3	FRUHOLMEN	2.56	0.55	0.42	1.33	-	-
S2	TUBÅEN	1.85	0.52	0.39	0.56	-	-
S6	HEKKINGEN	1.08	1.96	2.15	0.80	-	-
S7	HEKKINGEN	0.94	1.58	2.41	0.78	-	-
S8	KOLJE	1.63	1.60	0.89	0.55		
S1	KOLMULE	1.82	0.63	0.47	0.47	-	-
SO-21	DE GEERDALEN	1.64	0.79	0.63	0.50	-	-

The qualitative levels of biodegradation and maturation were also estimated from the unresolved complex mixture (UCM) compounds and the *n*-alkane envelope patterns, respectively. Table 6.1 presents the results obtained from the GC-FID analyses that are discussed below. The NSO-1 standard sample was used as a reference to help with the analysis of the studied samples and for calibrating the GC-FID apparatus and to assist in peak identification.

6.1.1 Oil dataset

The GC-FID results for the oils which were introduced in section 3.1 are given below.

C (7120/2-1, 1944.0 m): On the GC-FID chromatogram for the oil sample **"C"** (see Table 6.1, Fig. 6.1 and Appendix III) the Pr/Ph ratio is 1.51, while the ratios of Pr/*n*-C_{17} and Ph/*n*-C_{18} are 0.92 and 0.69 respectively. The reservoir is of Permo-Carboniferous age and the oil was recovered from carbonate lithology (Ørn Formation). The Pr/Ph ratio suggests that the source rock was deposited under less reducing conditions favoring the formation of pristane. The CPI value (1.17) suggests also an oxic depositional source rock environment and this is in accordance with the Pr/Ph result. The OEP values, which range from 1.01-1.08, verify that the oil sample is mature. The chromatogram shows *n*-alkanes in the range of C_3-C_{36}. The highest peak values are found in the n-C_{13}-n-C_{17} range. The normal alkanes decrease their peak heights asymptotically after n-C_{19}. The hump in the biomarker range, after *n*-C_{25}, is not due to biodegradation but due to column-bleed, an artificial phenomenon caused by high temperature. The chromatogram is heavy-end-biased which is typical for waxy oils, coal sourced. The high peaks in the n-C_6-n-C_8 range are isomers. The medium range compounds in the n-C_{13}-n-C_{18} range have experienced incipient biodegradation.

T1 (7122/7-3, 1195.6 m): Sample **"T1"** (see Table 6.1, Fig. 6.2 and Appendix III) returns a Pr/Ph ratio of 1.85, while the ratios of Pr/*n*-C_{17} and Ph/*n*-C_{18} are 0.86 and 0.51 respectively. The sample contains *n*-alkanes in the range of C_3-C_{36}. The oil sample **"T1"** was recovered from a sandstone lithology, namely from the Triassic Snadd Formation. The Pr/Ph ratio suggests that the source rock was deposited under

"oxic" (less reducing) conditions, a fact that is also verified by the CPI value (1.12). The OEP values, range from 1.00-1.08 and suggest that the oil sample is mature as the values approach the unity. The hump with the appex in *n*-C_{30} is again due to column-bleed. The peak *n*-C_{15} has the highest value. The *n*-alkane envelope becomes assymptotic after *n*-C_{15} and greatly resembles NSO-1 standard. The *n*-alkanes with low carbon-number in the medium range show very low values, thus the chromatogram is dominated by higher carbon-number compounds that make it waxier. Apparently, the oil sample has experienced incipient biodegradation. The high peaks in the beginning of the chromatogram belong to isomer compounds.

T2 (7122/7-3, 1812.0 m): The GC-FID chromatogram for the sample **"T2"** (see Table 6.1, Fig. 6.3 and Appendix III) returns a Pr/Ph ratio of 1.63, while the Pr/*n*-C_{17} and Ph/*n*-C_{18} ratios are 1.11 and 0.79 respectively. The sample contains *n*-alkanes in the range of C_3-C_{36}. The oil sample **"T2"** was recovered from a sandstone lithology, namely from the Middle Triassic Kobbe Formation. The Pr/Ph ratio suggests that the source rock was deposited under "oxic" (less reducing) conditions. The CPI value is 1.12 and suggests a more oxic depositional environment for the source rock. The OEP values that range from 1.00-1.08 indicate that the oil sample is mature. The sample is unbiodegraded. The peaks *n*-C_4 and *n*-C_5 have the highest values. The *n*-alkane envelope is highly asymptotic after *n*-C_{15} and resembles the NSO-1 standard. The *n*-alkanes with low carbon-number dominate the chromatogram although higher carbon number compounds have also high concentrations. Therefore the petroleum sample might be blended with different oils.

V (7123/4-1 A, 2165.9 m): Sample **"V"** (see Table 6.1, Fig. 6.4 and Appendix III) returns a Pr/Ph ratio of 1.44, while the Pr/*n*-C_{17} and Ph/*n*-C_{18} ratios are 1.04 and 0.77 respectively. The sample contains *n*-alkanes in the range of C_3-C_{36}. It was recovered from a sandstone lithology, namely the Fruholmen Formation from the Triassic-Jurassic transition. The Pr/Ph ratio suggests that the source rock was deposited under "oxic" (less reducing) conditions. The CPI value is 1.14 and suggests source rock deposition under sub-oxic conditions. The OEP values range from 1.00-1.09 suggest that the oil sample has reached a certain level of maturation. The

chromatogram has a unimodal distribution of *n*-alkanes with maxima at *n*-C_{15}. After *n*-C_{15} the *n*-alkane envelope resembles the NSO's pattern where the *n*-alkanes values decrease asymptotically from *n*-C_{10} to *n*-C_{33} (Fig. 5.1).

Ø (7222/6-1 S, 1633.8 m): On the GC-FID chromatogram for the oil sample **"Ø"** (see Table 6.1, Fig. 6.5 and Appendix III) the Pr/Ph ratio is 1.50, while the Pr/*n*-C_{17} and Ph/*n*-C_{18} ratios are 1.49 and 1.11 respectively. The reservoir has Middle Triassic age and the oil was recovered from the sandstone of Snadd Formation). The Pr/Ph ratio suggests that the source rock was deposited under oxic conditions. The CPI value is 1.21 and indicates source rock deposition under oxic conditions. The OEP values range from 1.01-1.08 and the low isoprenoid peaks suggest that the oil sample is mature. The chromatogram shows *n*-alkanes in the C_3-C_{36} range. The highest peak value is from the n-C_7. The *n*-alkane envelope is generally assympotic with a peak increase around the *n*-C_{13}-*n*-C_{19} range and the whole chromatogram has unimodal distribution of the *n*-alkanes. The sample seems to be unbiodegraded.

AB (7228/7-1 A, 2091.1 m): On the GC-FID chromatogram for the sample **"AB"** (see Table 6.1, Fig. 6.6 and Appendix III) the Pr/Ph ratio is 1.50 and the isoprenoid-normal alkanes ratios Pr/*n*-C_{17} and Ph/*n*-C_{18} are 0.46 and 0.31 respectively. Sample **"AB"** was recovered from the Triassic sandstone of the Snadd Formation. The Pr/Ph ratio suggests oxic depositional conditions. The chromatogram contains normal alkanes in the range of C_3-C_{36} and the *n*-alkanes show unimodal distribution with maxima at *n*-C_{17}. The CPI value is 1.13 and the OEP values 1.02 and 1.13, meaning that the oil is mature. The sample has experienced only incipient biodegradation that lowered the medium range compound peaks. The chromatogram is heavy-end-biased which denotes terrestrial organic input.

E1 (7120/6-1, 2432.0 m): The GC-FID chromatogram for the sample **"E1"** (see Table 6.1, Fig. 6.7 and Appendix III) gives Pr/Ph ratio of 1.40 and Pr/*n*-C_{17} and Ph/*n*-C_{18} ratios of 0.83 and 0.59 respectively. The sample contains *n*-alkanes in the range of C_3-C_{36}. The oil was recovered from a sandstone reservoir that belongs to the Early Jurassic Stø Formation. The Pr/Ph ratio suggests that the source rock was deposited under "oxic" (less reducing) conditions. The CPI value is 1.15 and suggests less

reducing environment which is in accordance with the Pr/Ph result. Furthermore the OEP values which range from 0.99-1.11 verify that the oil sample is mature as the values approximate the unity. The chromatogram is affected by the column-bleed phenomenon. The high carbon-number normal alkanes dominate the chromatogram but as there are also significant quantities of medium range compounds. Thus, the depositional environment of the source rock could be characterized as paralic.

O (7121/5-2, 2328.0 m): The GC-FID chromatogram for the sample **"O"** (see Table 6.1, Fig. 6.8 and Appendix III) gives Pr/Ph ratio of 1.46 and Pr/*n*-C_{17} and Ph/*n*-C_{18} ratios 0.76 and 0.58, respectively. The sample contains *n*-alkanes in the range of C_3-C_{36}. The oil sample **"O"** was recovered from a sandstone lithology, namely from the Middle Jurassic Stø Formation. The Pr/Ph ratio suggests that the source rock was deposited under "oxic" (less reducing) conditions. The CPI value is 1.10 and suggests also oxic depositional enviroment. The OEP values range from 0.97-1.06 show that the oil sample is mature. The chromatogram shows a slight UCM-hump with an appex underneath the Pr, Ph peaks. The peaks in the range of *n*-C_{15}-*n*-C_{17} have the highest values. The *n*-alkane envelope becomes assymptotic after *n*-C_{15} and it does not follow any particular pattern prior to that, probably due to the incipient biodegradation which lowered the concentration of the medium range compounds in the *n*-C_{13}-*n*-C_{18} range.

X (7125/1-1, 1403.8 m): The GC-FID chromatogram for the sample **"X"** (see Table 6.1, Fig. 6.9 and Appendix III) returns Pr/Ph ratio of 2.00, while the Pr/*n*-C_{17} and Ph/*n*-C_{18} are 1.20 and 0.84 respectively. The sample contains *n*-alkanes in the range of C_3-C_{36}. The oil sample **"X"** was recovered from a sandstone lithology, namely from the Jurassic Stø Formation. The Pr/Ph ratio suggests that the source rock was deposited under oxic conditions. The CPI value is 1.27 and suggests as well source rock deposition under less reducing conditions. The OEP values range from 1.01-1.15 and indicate mature sample. There is no evidence for biodegradation. The peaks in the range of *n*-C_{14}-*n*-C_{18} have the highest values. The *n*-alkane envelope is asymptotic and resembles the NSO-1.

W (7124/3-1, 1298.0 m): The GC-FID chromatogram for the sample **"W"** (see Table 6.1, Fig. 6.10 and Appendix III) gives Pr/Ph ratio of 1.38, while the Pr/*n*-C_{17} and Ph/*n*-C_{18} ratios are 0.94 and 0.79, respectively. The sample contains *n*-alkanes in the range of C_3-C_{36}. The oil was recovered from a sandstone reservoir that belongs to the Tubåen Formation of Early Jurassic. The Pr/Ph ratio suggests that the source rock was deposited under "oxic" (less reducing) conditions. The CPI value is 1.11, typical for "oxic" conditions. Furthermore the OEP values range from 1.01-1.15 and suggest maturation. From the whole GC-FID chromatogram oil database, sample **"W"** has the best fit to the NSO sample, which indicates almost zero level of biodegradation and high maturation.

NSO-1 (reference): Figure 5.1 depicts the normal *n*-alkane pattern with the typical asymptotic profile of an oil sample with medium to high maturation and low to zero biodegradation. All the studied samples were interpreted with NSO-1 as a reference.

6.1.2 Source rock dataset

The GC-FID results for the source rocks which were introduced in section 3.2, are given below.

S4 (7128/6-1, 1738.5 m): The GC-FID chromatogram for sample **"S4"** (see Table 6.1, Fig. 6.11 and Appendix III) returned Pr/Ph ratio of 2.01, while the Pr/*n*-C_{17} and Ph/*n*-C_{18} ratios were calculated 0.28 and 0.16 respectively. Sample **"S4"** is a silicified calcareous claystone recovered from the Permian Røye Formation. The sample contains *n*-alkanes in the range of C_8-C_{34} and is biased by the medium range compounds. The Pr/Ph ratio suggests that the source rock was deposited under "oxic" conditions. The low isoprenoid amounts denote significant maturation level.

S9 (7323/7-U-3, 100.30 m): The GC-FID chromatogram for sample **"S9"** (see Table 6.1, Fig. 6.13 and Appendix III) returned a Pr/Ph ratio of 1.09, while the Pr/*n*-C_{17} and Ph/*n*-C_{18} ratios are both 5.00. Sample **"S9"** is an organic rich mudstone recovered from the Triassic Steinkobbe Formation. Generally the sample is heavily biodegraded and also very immature. These are easily recognized by the excessive UCM and the

very high pristane and phytane peaks that dominate the chromatogram. The sample was probably deposited under oxic conditions.

S10 (7323/7-U-9, 100.60 m): On the GC-FID chromatogram for sample **"S10"** (see Table 6.1, Fig. 6.14 and Appendix III) the Pr/Ph ratio is 0.81, while the Pr/*n*-C_{17} and Ph/*n*-C_{18} ratios are 3.60 and 5.54, respectively. Sample **"S10"** is an organic rich mudstone recovered from the Triassic Steinkobbe Formation. Generally the sample is heavily biodegraded and also immature but in a lesser degree than the shallower **"S9"** sample. The main difference between them is that sample **"S10"** shows higher phytane amount; hence the sample was deposited under anoxic conditions.

S11 (7430/7-U-1, 38.80 m): The GC-FID chromatogram for sample **"S11"** (see Table 6.1, Fig. 6.15 and Appendix III) gives Pr/Ph ratio of 4.30, while the Pr/*n*-C_{17} and Ph/*n*-C_{18} ratios are 1.46 and 0.32 respectively. Sample **"S11"** has sandy shale lithology and is recovered from the Triassic Snadd Formation. The sample has experienced slight to moderate biodegradation. As a result the medium range compound peaks were decreased. Furthermrore the sample is early mature as there are normal alkane peaks that are higher than the isoprenoid peaks. The excess of pristane indicates terrestrial organic matter input (coal, resin).

S12 (7430/7-U-1, 64.70 m): The GC-FID chromatogram for sample **"S12"** (see Table 6.1, Fig. 6.16 and Appendix III) gives Pr/Ph ratio of 3.88, while the Pr/*n*-C_{17} and Ph/*n*-C_{18} ratios are 3.44 and 0.73, respectively. Sample **"S12"** has sandy shale lithology and is recovered from the Triassic Snadd Formation. The sample shows almost the same properties as sample **"S11"** but at the same time it appears to be more immature.

S5 (7230/5-U-5, 43.85 m): On the GC-FID chromatogram for sample **"S5"** (see Table 6.1, Fig. 6.17 and Appendix III) the Pr/Ph ratio is 3.04, while the Pr/*n*-C_{17} and Ph/*n*-C_{18} ratios are 2.38 and 0.80 respectively. Sample **"S5"** has sandy shale lithology and is recovered from the Triassic Kobbe Formation. The sample is slightly biodegraded. The high isoprenoid peaks show early maturation. The high peak at 18' is probably due to contamination. The normal alkanes at the range of medium biomarkers have been biodegraded. On the other hand the isoprenoids and the biomarker range

compounds were more resilient. The Pr/Ph ratio suggests terrestrial organic matter input.

S3 (7124/3-U-1, 1367.50 m): On the GC-FID chromatogram for sample **"S3"** (see Table 6.1, Fig. 6.18 and Appendix III) the Pr/Ph value is 2.56, while the Pr/*n*-C_{17} and Ph/*n*-C_{18} values are 0.55 and 0.42 respectively. Sample **"S3"** has shaly lithology and is recovered from the Triassic Fruholmen Formation. The high peak at 54' is probably due to contamination. There appears to be slight to moderate biodegradation in the medium range normal alkanes that also dominate the chromatogram. The Pr/Ph ratio suggests marine depositional environment but with significant terrestrial input. Apparently the sample has reached early to medium maturation.

S2 (7122/6- 1, 2061.50 m): The GC-FID chromatogram for sample **"S2"** (see Table 6.1, Fig. 6.19 and Appendix III) returned Pr/Ph value of 1.85 and 0.52 and 0.39 for the Pr/*n*-C_{17} and Ph/*n*-C_{18} ratios, respectively. Sample **"S2"** has shaly lithology and is recovered from the Jurassic Tubåen Formation. In general the sample is unbiodegraded and contains normal alkanes in the range C_7-C_{34} with particular low values. The most abundant compounds are the *n*-C_{13} (methyl-naphthalenes), *n*-C_{14} (dimethyl-naphthalenes) and *n*-C_{14} (trimethyl-napthalenes). The discrete high peak between the two isoprenoids is phenanthrene. Finally the Pr/Ph ratio suggests marine depositional environment.

S6 (7231/1-U-1, 70.90 m): On the GC-FID chromatogram for sample **"S6"** (see Table 6.1, Fig. 6.20 and Appendix III) the Pr/Ph value is 1.08, while the Pr/*n*-C_{17} and Ph/*n*-C_{18} were calculated 1.96 and 2.15 respectively. The source rock has been recovered from the Jurassic Hekkingen black shale. The chromatograph contains *n*-alkanes in the range of C_7-C_{34}. The sample has experienced slight to moderate biodegradation and is early mature. Thus, the isoprenoid peaks are higher than the adjacent *n*-alkanes. The Pr/Ph ratio suggests slightly oxic depositional environment.

S7 (7231/1-U-1, 76.20m): The GC-FID chromatogram for sample **"S7"** (see Table 6.1, Fig. 6.21 and Appendix III) gives Pr/Ph value equal to 0.94 and 1.58 and 2.41 for the Pr/*n*-C_{17} and Ph/*n*-C_{18} ratios, respectively. Sample **"S7"** belongs also to the Hekkingen

Formation. The Pr/Ph ratio suggests that the source rock was deposited under anoxic conditions. The sample is heavy biodegraded; therefore the ratios calculated might be unreliable.

S8 (7231/4-U-1, 84.70 m): On the GC-FID chromatogram for sample **"S8"** (see Table 6.1, Fig. 6.22 and Appendix III) the Pr/Ph value is 1.63, while the Pr/*n*-C_{17} and Ph/*n*-C_{18} ratios were calculated 1.60 and 0.89, respectively. Sample **"S8"** is a dark brown claystone recovered from the Cretaceous Kolje Formation. The Pr/Ph value suggests that the source rock was deposited under oxic conditions. The sample is heavily biodegraded and as a result the isoprenoid and normal alkane ratios are not reliable. The appex of the UCM is located around the *n*-C_{31} range but affects the whole chromatogram.

S1 (7122/6-1, 1156.60 m): The GC-FID chromatogram for sample **"S1"** (see Table 6.1, Fig. 6.22 and Appendix III) gives Pr/Ph value of 1.82 and 0.79 and 0.63 for the Pr/*n*-C_{17} and Ph/*n*-C_{18} ratios respectively. The source rock sample **"S1"** has shaly lithology and is recovered from the Cretaceous Kolmule Formation. The Pr/Ph ratio suggests deposition under oxic conditions. The sample is early mature and the *n*-alkane envelope is asymptotic and resembles perfectly the NSO-1 sample. Finally the sample is only slightly biodegraded.

SO-21 (outcrop): The **SO-21** outcrop source rock sample has shaly lithology and is recovered from the Triassic De Geerdalen Formation (see Table 6.1, Fig. 23 and Appendix III). The Pr/Ph value is 1.64 that is typical for marine oxic deposition. The Pr/*n*-C_{17} and Ph/*n*-C_{18} ratios are 0.79 and 0.63 respectively. The chromatogram contains normal alkane in the range of C_8-C_{33} with predominance of the medium range compounds. The sample clearly resembles the NSO-1 standard.

6.2 GC-MS Results

The source rocks and oil core extracts, described in Chapter 3, were also analyzed by means of GC-MS in order to identify the compounds called biomarkers in the range of C_{27}-C_{35}.

The GC-MS technique is used to trace the biomarker compounds (m/z=191, 217, 218, 231, 253) that are present only in minute quantities. The aromatic compounds from m/z=178, 192 and 198 namely, phenanthrene, methyl-phenanthrenes and methyl-dibenzothiophenes were also analyzed by GC-MS though are not biomarkers. A total of 27 parameters as presented on Table 5.3 were calculated by measuring the relevant peaks on the chromatograms. Their properties are discussed in sub-chapter 5.2. The results were then used to address the depositional system (lacustrine, marine or mixed) and the level of maturity (gas, condensate or oil).

6.2.1 Oil dataset

The GC-MS results for the oil samples which were introduced in section 3.1, are given below.

C (7120/2-1, 1944.0 m): On the MS chromatograms for the oil sample **"C"** (see Table 6.2, Fig. 6.1 and Appendix III) the Ts/(Ts + Tm) ratio (Par. 1) is 0.85 which is the highest for both datasets. The diahopane/(diahopane+normoretane) ratio is 0.91 (Par. 2) and is the second highest. It is obvious from these two parameters that sample **"C"** is mature. The 22S/(22S+22R) (Par. 3) value is 0.58 and indicates oil generation as it is expected for crude oils. Parameter 4 may be unreliable due to thermal maturation. The 29Ts/(29Ts + norhopane) (Par. 5) value is 0.52, the highest in the database and indicates high maturation. On the contrary the bisnorhopane/(bisnorhopane + norhopane) value (Par. 6) is very low, 0.09, as it is expected for a mature sample. The ratio of C_{23}-C_{29} tricyclic terpanes/C_{30} αβ-hopane (Par. 7) is 0.73 which is also very high value. Parameter 7 increases with thermal maturity and can be applied in the whole oil window. The hopane/sterane of C_{30} αβ-hopane and regular C_{29} sterane (Par. 9) value is 3.36 and indicates non-bacterial source (possibly algal or higher plant). The MDBT ratio (Par. 21) is 9.30 which is two times higher than the second highest value and indicates late maturation (MDBT-4 dominates over MDBT-1). The calculated vitrinite reflectivities are respectively R_c=0.94% (Par. 22 after Radke, 1988), R_c=0.84% (Par. 23 after Radke and Welte, 1983), R_c=0.85% (Par. 24 after Kvalheim *et al*., 1987) and R_c=1.19% (Par. 25 after Radke, 1988), meaning that the oil window (~1.3) has not been surpassed as is of

course expected for oil samples. Finally the ratio MDBT/MPs (Par. 27) is 0.40 and indicates that the oil was expelled from a shale lithology.

T1 (7122/7-3, 1195.6 m): On the GC-MS chromatograms for the oil sample **"T1"** (see Table 6.2, Fig. 6.2 and Appendix III) the Ts/(Ts + Tm) ratio (Par. 1) is 0.47 which indicates medium maturation. The diahopane/(diahopane+normoretane) (Par. 2) ratio is 0.63, indicating medium to medium-high maturation. The 22S/(22S+22R) (Par. 3) value is 0.58 and indicates oil generation as for all the oil samples; hence it will not be further discussed. Parameter 4 is 0.91 and may be unreliable due to the excessive thermal maturation. However, the value confirms high maturation as well. The 29Ts/(29Ts + norhopane) (Par. 5) value is 0.23 and shows moderate maturation. Parameter 6, bisnorhopane/(bisnorhopane + norhopane) is 0.10, typical for high maturation. The ratio of C_{23}-C_{29} tricyclic terpanes/C_{30} αβ-hopane (Par. 7) is only 0.14 and though the parameter is applicable through the whole oil window, its value is particularly low and indicates low maturation. The hopane/sterane of C_{30} αβ-hopane and regular C_{29} sterane (Par. 9) value is 3.61 and indicates algae or higher-plant source. The MDBT ratio (Par. 21) is 4.12 and indicates high maturation as MDBT-4 dominates MDBT-1. The calculated vitrinite reflectivities are respectively R_c=0.95% (Par. 22 after Radke, 1988), R_c=0.79% (Par. 23 after Radke and Welte, 1983), R_c=0.86% (Par. 24 after Kvalheim *et al.*, 1987) and R_c=0.81% (Par. 25 after Radke, 1988); all of them falling inside the oil window. Finally the ratio MDBT/MPs (Par. 27) is 0.92 and indicates shaly source rock lithology.

T2 (7122/7-3, 1812.0 m): On the GC-MS chromatogram for sample **"T2"** (see Table 6.2, Fig. 6.3 and Appendix III) the Ts/(Ts + Tm) ratio (Par. 1) is 0.83, the second highest and indicates late maturation. The diahopane/(diahopane+normoretane) ratio (Par. 2) is 0.92, the highest in the database and indicates late maturation as well. Parameter 4 is 0.90 and may be unreliable due to thermal maturation. The 29Ts/(29Ts + norhopane) ratio (Par. 5) is 0.51, the second highest and shows high maturation. The bisnorhopane/(bisnorhopane + norhopane) ratio (Par. 6) is 0.09, again typical for high maturation. The ratio of C_{23}-C_{29} tricyclic terpanes/C_{30} αβ-hopane (Par. 7) is 0.45 which is medium maturity value. The hopane/sterane of C_{30}

Table 6.2: The GC-MS results obtained from the parameters described on Table 5.3 age coloured. Red for Permo-Carboniferous, purple for Triassic, teal for Jurassic, green for Cretaceous. NSO-1 sample is coloured in yellow.

Sample	Formation	1	2	3	4	5	6	7	8	9
C	ØRN	0.85	0.91	0.58	0.91	0.52	0.09	0.73	0.04	3.36
T1	SNADD	0.47	0.63	0.58	0.91	0.23	0.10	0.14	0.06	3.61
T2	KOBBE	0.83	0.92	0.57	0.90	0.51	0.09	0.45	0.04	3.15
V	FRUHOLMEN	0.38	0.64	0.59	0.91	0.23	0.12	0.16	0.05	5.15
Ø	SNADD	0.69	0.75	0.59	0.92	0.32	0.04	0.47	0.03	5.96
AB	SNADD	0.36	0.53	0.59	0.84	0.19	0.06	0.54	0.07	4.19
E1	STØ	0.52	0.70	0.59	0.92	0.26	0.13	0.12	0.06	2.71
O	STØ	0.66	0.89	0.58	0.89	0.44	0.13	0.29	0.10	3.22
X	STØ	0.69	0.76	0.58	0.92	0.35	0.09	0.50	0.03	5.67
W	TUBÅEN	0.47	0.66	0.60	0.92	0.27	0.12	0.19	0.05	4.50
NSO-1	NSO-1	0.60	0.56	0.61	0.90	0.34	0.27	0.20	0.02	2.97
S4	RØYE	0.37	0.15	0.61	0.80	0.27	0.03	0.89	0.07	0.86
S9	STEINKOBBE	0.41	0.44	0.39	0.78	0.24	0.22	0.25	0.02	2.33
S10	STEINKOBBE	0.48	0.28	0.28	0.87	0.35	0.38	0.15	0.02	0.89
S11	SNADD	0.73	0.20	0.48	0.74	0.10	0.08	0.08	0.01	10.15
S12	SNADD	0.71	0.22	0.52	0.74	0.06	0.52	0.10	0.02	6.59
S5	KOBBE	0.45	0.05	0.35	0.56	0.17	0.09	0.24	0.02	6.17
S3	FRUHOLMEN	0.33	0.31	0.55	0.86	0.17	0.20	0.30	0.03	4.48
S2	TUBÅEN	0.20	0.51	0.59	0.82	0.13	0.08	1.20	0.08	6.09
S6	HEKKINGEN	0.51	0.17	0.27	0.72	0.17	0.41	0.30	0.01	2.10
S7	HEKKINGEN	0.53	0.10	0.26	0.72	0.14	0.27	0.40	0.05	1.85
S8	KOLJE	0.22	0.37	0.17	0.66	0.33	0.10	0.41	0.04	2.79
S1	KOLMULE	0.49	0.53	0.60	0.92	0.25	0.06	0.45	0.06	4.73
SO-21	DE GEERDALEN	0.66	0.29	0.62	0.89	0.31	0.13	0.79	0.06	4.54

Table 6.2 (continued): The GC-MS results obtained from the parameters described on Table 5.3 age coloured. Red for Permo-Carboniferous, purple for Triassic, teal for Jurassic, green for Cretaceous. NSO-1 sample is coloured in yellow.

Sample	Formation	10	11	12	13	14	15	16	17	18
C	ØRN	0.62	0.49	0.54	29.90	28.06	42.04	0.58	0.88	0.97
T1	SNADD	0.56	0.49	0.38	30.27	28.23	41.50	0.34	0.91	1.00
T2	KOBBE	0.58	0.46	0.47	28.59	26.98	44.43	0.51	0.83	1.06
V	FRUHOLMEN	0.61	0.51	0.50	31.98	27.36	40.66	0.34	0.96	0.91
Ø	SNADD	0.63	0.49	0.42	29.34	28.37	42.29	0.46	0.88	0.81
AB	SNADD	0.50	0.51	0.50	27.31	27.04	45.65	0.46	0.91	1.00
E1	STØ	0.61	0.51	0.35	29.48	28.17	42.35	0.55	0.95	0.95
O	STØ	0.61	0.53	0.58	33.88	28.09	38.02	0.79	0.83	0.97
X	STØ	0.57	0.46	0.42	31.39	25.34	43.27	0.32	0.85	1.04
W	TUBÅEN	0.58	0.52	0.49	35.15	27.29	37.56	0.45	0.95	0.90
NSO-1	NSO-1	0.51	0.37	0.46	30.81	33.42	35.77	0.32	0.82	0.81
S4	RØYE	0.24	0.26	0.18	35.71	26.19	38.10	0.28	0.70	1.34
S9	STEINKOBBE	0.33	0.14	0.45	20.69	37.93	41.38	0.19	0.11	0.37
S10	STEINKOBBE	0.21	0.05	0.10	25.64	28.21	46.15	0.30	0.14	0.53
S11	SNADD	0.33	0.17	0.06	22.06	29.41	48.53	0.15	0.44	0.70
S12	SNADD	0.39	0.12	0.07	25.00	20.83	54.17	0.45	0.14	0.71
S5	KOBBE	0.47	0.14	0.16	13.60	32.89	53.51	0.45	0.12	0.67
S3	FRUHOLMEN	0.42	0.23	0.37	27.73	28.15	44.12	0.39	0.33	0.65
S2	TUBÅEN	0.36	0.32	0.28	25.97	31.17	42.86	0.62	0.39	0.95
S6	HEKKINGEN	0.43	0.13	0.20	31.55	24.76	43.69	0.30	0.10	0.56
S7	HEKKINGEN	0.49	0.17	0.27	30.08	31.20	38.72	0.26	0.11	0.49
S8	KOLJE	0.43	0.12	0.09	16.67	11.90	71.43	0.44	0.18	0.60
S1	KOLMULE	0.54	0.41	0.41	31.75	28.57	39.68	0.73	0.60	0.97
SO-21	DE GEERDALEN	0.57	0.41	0.32	31.83	24.23	43.94	0.52	0.92	0.72

Table 6.2 (continued): The GC-MS results obtained from the parameters described on Table 5.3 age coloured. Red for Permo-Carboniferous, purple for Triassic, teal for Jurassic, green for Cretaceous. NSO-1 sample is coloured in yellow. (b.d.l = below detection limit)

Sample	Formation	19	20	21	22	23	24	25	26	27
C	ØRN	0.74	0.46	9.30	0.94	0.84	0.85	1.19	1.79	0.40
T1	SNADD	0.65	0.46	4.12	0.95	0.79	0.86	0.81	0.94	0.92
T2	KOBBE	0.55	0.43	4.62	0.98	0.73	0.81	0.85	3.00	0.28
V	FRUHOLMEN	0.61	0.43	2.24	0.90	0.77	0.80	0.67	1.71	0.58
Ø	SNADD	0.64	0.43	4.73	0.85	0.79	0.80	0.86	5.06	0.16
AB	SNADD	0.57	0.45	4.14	0.95	0.74	0.84	0.81	3.23	0.28
E1	STØ	0.68	0.43	3.83	0.93	0.81	0.80	0.79	1.06	0.76
O	STØ	0.66	0.43	4.79	0.93	0.79	0.80	0.86	0.46	1.60
X	STØ	0.43	0.41	1.81	0.97	0.66	0.75	0.64	1.87	0.48
W	TUBÅEN	0.58	0.42	3.36	0.90	0.75	0.78	0.76	0.53	1.57
NSO-1	NSO-1	b.d.l	0.40	2.48	0.85	0.40	0.73	0.69	1.92	0.40
S4	RØYE	0.68	0.55	2.50	1.09	0.81	1.06	0.69	5.50	0.24
S9	STEINKOBBE	0.01	0.39	0.75	0.47	0.41	0.70	0.56	2.02	0.78
S10	STEINKOBBE	b.d.l	0.34	1.64	0.65	0.40	0.59	0.63	3.34	0.24
S11	SNADD	0.01	0.33	3.20	0.78	0.40	0.56	0.74	5.54	0.11
S12	SNADD	0.03	0.35	4.71	0.78	0.42	0.61	0.85	5.52	0.10
S5	KOBBE	b.d.l	0.31	3.80	0.76	0.40	0.52	0.79	4.41	0.11
S3	FRUHOLMEN	b.d.l	0.36	2.83	0.75	0.40	0.64	0.72	1.42	0.52
S2	TUBÅEN	0.01	0.45	1.61	0.93	0.41	0.85	0.63	0.91	1.61
S6	HEKKINGEN	b.d.l	0.33	0.63	0.68	0.40	0.57	0.56	1.10	1.08
S7	HEKKINGEN	0.01	0.31	0.34	0.61	0.41	0.54	0.53	0.94	1.88
S8	KOLJE	0.01	0.27	2.54	0.71	0.40	0.45	0.70	5.09	0.09
S1	KOLMULE	1.27	0.46	3.46	0.94	1.16	0.86	0.76	0.92	0.92
SO-21	DE GEERDALEN	0.01	0.37	2.52	0.79	0.40	0.65	0.69	1.03	0.69

αβ-hopane and regular C_{29} sterane (Par. 9) value is 3.15 and indicates algae or higher-plant source. The MDBT ratio (Par. 21) is 4.62 and indicates high maturation as MDBT-4 dominates MDBT-1. The calculated vitrinite reflectivities are respectively R_c=0.98% (Par. 22 after Radke, 1988), R_c=0.73% (Par. 23 after Radke and Welte, 1983), R_c=0.81% (Par. 24 after Kvalheim *et al*., 1987) and R_c=0.85% (Par. 25 after Radke, 1988); all of them falling inside the oil window. Finally the ratio MDBT/MPs (Par. 27) is 0.28 and clearly indicates shaly source rock lithology.

V (7123/4-1 A, 2165.9 m): On the GC-MS chromatograms for the oil sample **"V"** (see Table 6.2, Fig. 6.4 and Appendix III) the Ts/(Ts + Tm) ratio (Par. 1) is 0.38 which indicates medium level of maturation. The same rule applies for the diahopane/ (diahopane+normoretane) ratio (Par. 2) which is 0.64. The 29Ts/(29Ts + norhopane) ratio (Par. 5) is 0.23 which shows medium-low maturity. The bisnorhopane/(bisnorhopane + norhopane) ratio (Par. 6) is 0.12 that is typical for medium mature samples. The ratio of C_{23}-C_{29} tricyclic terpanes/C_{30} αβ-hopane (Par. 7) is 0.16 which is particularly low and shows immature sample. The hopane/sterane of C_{30} αβ-hopane and regular C_{29} sterane (Par. 9) value is 5.15 and indicates mixed organic matter. The MDBT ratio (Par. 21) is 2.24 and indicates medium maturation. The calculated vitrinite reflectivities are respectively R_c=0.90% (Par. 22 after Radke, 1988), R_c=0.77% (Par. 23 after Radke and Welte, 1983), R_c=0.80% (Par. 24 after Kvalheim *et al*., 1987) and R_c=0.67% (Par. 25 after Radke, 1988); all of them falling inside the oil window. Finally the ratio MDBT/MPs (Par. 27) is 0.58 and clearly indicates shaly source rock lithology.

Ø (7222/6-1 S, 1633.8 m): The GC-MS chromatograms for the oil sample **"Ø"** (see Table 6.2, Fig. 6.5 and Appendix III) gives Ts/(Ts + Tm) ratio (Par. 1) of 0.69 indicating high maturation. The diahopane/(diahopane + norhopane) ratio (Par. 5) is 0.32 and shows medium maturity. On the other hand the bisnorhopane/(bisnorhopane + norhopane) ratio (Par. 6) is 0.04 which is particularly low and highlights late maturation. The ratio of C_{23}-C_{29} tricyclic terpanes/C_{30} αβ-hopane (Par. 7) is 0.47 and shows medium maturity. The hopane/sterane of C_{30} αβ-hopane and regular C_{29} sterane (Par. 9) value is 5.96 and indicates mixed organic matter. The MDBT ratio

(Par. 21) is 4.73 and indicates high maturation. The calculated vitrinite reflectivities are respectively R_c=0.85% (Par. 22 after Radke, 1988), R_c=0.79% (Par. 23 after Radke and Welte, 1983), R_c=0.80% (Par. 24 after Kvalheim *et al*., 1987) and R_c=0.86% (Par. 25 after Radke, 1988); all of them falling inside the oil window. Finally the ratio MDBT/MPs (Par. 27) is 0.16, outmarking shaly source rock lithology.

AB (7228/7-1 A, 2091.1 m): The GC-MS chromatograms for the oil sample **"AB"** (see Table 6.2, Fig. 6.6 and Appendix III) gives Ts/(Ts + Tm) ratio (Par. 1) of 0.36 which is the lowest among the oil dataset and indicates low maturation. The diahopane/(diahopane + norhopane) ratio (Par. 5) is 0.19, denoting low maturation. On the contrary, the bisnorhopane/(bisnorhopane + norhopane) ratio (Par. 6) is 0.06 and indicates high maturation. The ratio of C_{23}-C_{29} tricyclic terpanes/C_{30} αβ-hopane (Par. 7) is 0.54 and shows medium to high maturity. The hopane/sterane of C_{30} αβ-hopane and regular C_{29} sterane (Par. 9) value is 4.19 and indicates algae or higher-plant source. The MDBT ratio (Par. 21) is 4.14 and indicates high maturation. The calculated vitrinite reflectivities are respectively R_c=0.95% (Par. 22 after Radke, 1988), R_c=0.74% (Par. 23 after Radke and Welte, 1983), R_c=0.84% (Par. 24 after Kvalheim *et al*., 1987) and R_c=0.81% (Par. 25 after Radke, 1988); all of them falling inside the oil window. Finally the ratio MDBT/MPs (Par. 27) is 0.28, outmarking shaly source rock lithology.

E1 (7120/6-1, 2432.0 m): The GC-MS chromatograms for the oil sample **"E1"** (see Table 6.2, Fig. 6.7 and Appendix III) gives Ts/(Ts + Tm) ratio (Par. 1) of 0.52 indicating medium maturation. The diahopane/(diahopane + norhopane) ratio (Par. 5) is 0.26 and shows medium-low maturity. The bisnorhopane/ (bisnorhopane + norhopane) ratio (Par. 6) is 0.13 which is high for an oil sample. The ratio of C_{23}-C_{29} tricyclic terpanes/C_{30} αβ-hopane (Par. 7) is 0.12 and shows early maturation. The hopane/sterane of C_{30} αβ-hopane and regular C_{29} sterane (Par. 9) value is 2.71 and indicates non-bacterial organic matter. The MDBT ratio (Par. 21) is 3.83 and indicates medium maturation. The calculated vitrinite reflectivities are respectively R_c=0.93% (Par. 22 after Radke, 1988), R_c=0.81% (Par. 23 after Radke and Welte, 1983), R_c=0.80% (Par. 24 after Kvalheim *et al*., 1987) and R_c=0.79% (Par. 25 after Radke,

1988); all of them falling inside the oil window. Finally the ratio MDBT/MPs (Par. 27) is 0.76, indicating shaly source rock lithology.

O (7121/5-2, 2328.0 m): The GC-MS chromatograms for the oil sample **"O"** (see Table 6.2, Fig. 6.8 and Appendix III) gives Ts/(Ts + Tm) ratio (Par. 1) of 0.66 indicating medium to late maturation. The diahopane/(diahopane + norhopane) ratio (Par. 5) is 0.44 and shows medium maturity. The bisnorhopane/ (bisnorhopane + norhopane) ratio (Par. 6) is 0.13 which again is high for an oil sample. The ratio of C_{23}-C_{29} tricyclic terpanes/C_{30} αβ-hopane (Par. 7) is 0.29 and shows medium maturation. The hopane/sterane of C_{30} αβ-hopane and regular C_{29} sterane (Par. 9) value is 3.22 and indicates non-bacterial organic matter. The MDBT ratio (Par. 21) is 4.79, the second higher and indicates late maturation. The calculated vitrinite reflectivities are respectively R_c=0.93% (Par. 22 after Radke, 1988), R_c=0.79% (Par. 23 after Radke and Welte, 1983), R_c=0.80% (Par. 24 after Kvalheim *et al*., 1987) and R_c=0.86% (Par. 25 after Radke, 1988); all of them falling inside the oil window. Finally the ratio MDBT/MPs (Par. 27) is 1.60, outmarking carbonate source rock facies.

X (7125/1-1, 1403.8 m): The GC-MS chromatograms for the oil sample **"X"** (see Table 6.2, Fig. 6.9 and Appendix III) gives Ts/(Ts + Tm) ratio (Par. 1) of 0.69, indicating high maturation. The diahopane/(diahopane + norhopane) ratio (Par. 5) is 0.35 and shows medium maturity. The bisnorhopane/ (bisnorhopane + norhopane) ratio (Par. 6) is 0.09 and shows medium-high maturity. The ratio of C_{23}-C_{29} tricyclic terpanes/C_{30} αβ-hopane (Par. 7) is 0.50 and shows medium-high maturation. The hopane/sterane of C_{30} αβ-hopane and regular C_{29} sterane (Par. 9) value is 5.67 and indicates non-bacterial organic matter. The MDBT ratio (Par. 21) is 1.81 and indicates early maturation. The calculated vitrinite reflectivities are respectively R_c=0.97% (Par. 22 after Radke, 1988), R_c=0.66% (Par. 23 after Radke and Welte, 1983), R_c=0.75% (Par. 24 after Kvalheim *et al*., 1987) and R_c=0.64% (Par. 25 after Radke, 1988); all of them falling inside the oil window. Finally the ratio MDBT/MPs (Par. 27) is 0.48 and shows shale source rock facies.

W (7124/3-1, 1298.0 m): The GC-MS chromatograms for the oil sample **"W"** (see Table 6.2, Fig. 6.10 and Appendix III) gives Ts/(Ts + Tm) ratio (Par. 1) of 0.47

indicating medium maturation. The diahopane/(diahopane + norhopane) ratio (Par. 5) is 0.27 and shows medium-low maturity. The bisnorhopane/(bisnorhopane + norhopane) ratio (Par. 6) is 0.12, among the highest in the database. The ratio of C_{23}-C_{29} tricyclic terpanes/C_{30} αβ-hopane (Par. 7) is 0.19 and shows low maturity. The hopane/sterane of C_{30} αβ-hopane and regular C_{29} sterane (Par. 9) value is 4.50 and indicates mixed organic matter. The MDBT ratio (Par. 21) is 3.36 and indicates medium maturation. The calculated vitrinite reflectivities are respectively R_c=0.90% (Par. 22 after Radke, 1988), R_c=0.75% (Par. 23 after Radke and Welte, 1983), R_c=0.78% (Par. 24 after Kvalheim *et al*., 1987) and R_c=0.76% (Par. 25 after Radke, 1988); all of them falling inside the oil window. Finally the ratio MDBT/MPs (Par. 27) is 1.57 which indicates carbonate source rock facies.

NSO-1 (reference): The GC-MS chromatograms for the standard oil sample **"NSO-1"** (see Table 6.2, Figures in chapter 5.2 and Appendix III) gives Ts/(Ts + Tm) ratio (Par. 1) of 0.60 indicating medium-high maturation. The diahopane/(diahopane + norhopane) ratio (Par. 5) is 0.34 and shows medium maturity. The bisnorhopane/ (bisnorhopane + norhopane) ratio (Par. 6) is 0.27, indicating medium maturity. The ratio of C_{23}-C_{29} tricyclic terpanes/C_{30} αβ-hopane (Par. 7) is 0.20 and shows low maturity. The hopane/sterane of C_{30} αβ-hopane and regular C_{29} sterane (Par. 9) value is 2.97 and indicates non-bacterial organic matter. The MDBT ratio (Par. 21) is 2.48 and indicates medium maturation. The calculated vitrinite reflectivities are respectively R_c=0.85% (Par. 22 after Radke, 1988), R_c=0.40% (Par. 23 after Radke and Welte, 1983), R_c=0.73% (Par. 24 after Kvalheim *et al*., 1987) and R_c=0.69% (Par. 25 after Radke, 1988); all of them falling inside the oil window except for Parameter 23 that is lower than 0.5 in terms of vitrinite reflectivity. Finally the ratio MDBT/MPs (Par. 27) is 0.40 which indicates shale source rock facies.

6.2.2 Source rock dataset

The GC-MS results for the source rock samples which were introduced in section 3.2 are given below.

S4 (7128/6-1, 1738.5 m): The GC-MS chromatograms for the source rock sample **"S4"** (see Table 6.2, Fig. 6.10 and Appendix III) gives Ts/(Ts + Tm) ratio (Par. 1) of 0.37, indicating medium maturation. On the other hand the 22S/(22S+22R) ratio (Par. 3) is 0.61, close to peak-oil generation. The diahopane/(diahopane + norhopane) ratio (Par. 5) is 0.27, showing medium maturation. The bisnorhopane/(bisnorhopane + norhopane) ratio (Par. 6) is only 0.03, the lowest in both the oil and source rock databases, meaning that the organic matter extracted from the source rock is very mature. The ratio of C_{23}-C_{29} tricyclic terpanes/C_{30} αβ-hopane (Par. 7) is 0.89 and shows high maturity. The hopane/sterane of C_{30} αβ-hopane and regular C_{29} sterane (Par. 9) value is 0.86 and clearly indicates that the organic matter derives from non-bacterial source. The MDBT ratio (Par. 21) is 2.50 and indicates medium maturation. The calculated vitrinite reflectivities are respectively R_c=1.09% (Par. 22 after Radke, 1988), R_c=0.81% (Par. 23 after Radke and Welte, 1983), R_c=1.06% (Par. 24 after Kvalheim *et al.*, 1987) and R_c=0.69% (Par. 25 after Radke, 1988); all of them falling inside the oil window. Finally the ratio MDBT/MPs (Par. 27) is 0.24 which indicates shale source rock facies.

S9 (7323/7-U-3, 100.30 m): The GC-MS chromatograms for the source rock sample **"S9"** (see Table 6.2, Fig. 6.11 and Appendix III) gives Ts/(Ts + Tm) ratio (Par. 1) of 0.41, indicating medium maturation. The 22S/(22S+22R) ratio (Par. 3) is 0.39 and is known that values below 0.50 indicate interference from heterogenic sources. The diahopane/(diahopane + norhopane) ratio (Par. 5) is 0.24, showing medium maturation. The bisnorhopane/(bisnorhopane + norhopane) ratio (Par. 6) is 0.22, meaning that the organic matter is medium mature. The ratio of C_{23}-C_{29} tricyclic terpanes/C_{30} αβ-hopane (Par. 7) is 0.25 and shows low maturity. The hopane/sterane of C_{30} αβ-hopane and regular C_{29} sterane (Par. 9) value is 2.33 and clearly indicates that the organic matter derives from non-bacterial source. The MDBT ratio (Par. 21) is 0.75 and indicates very low maturation. The calculated vitrinite reflectivities are respectively R_c=0.47% (Par. 22 after Radke, 1988), R_c=0.41% (Par. 23 after Radke and Welte, 1983), R_c=0.70% (Par. 24 after Kvalheim *et al.*, 1987) and R_c=0.56% (Par. 25 after Radke, 1988). The general trend based on synthetic vitrinite reflectivites is that

the sample is immature. Finally the ratio MDBT/MPs (Par. 27) is 0.78 which indicates shale source rock facies.

S10 (7323/7-U-9, 100.60 m): The GC-MS chromatograms for the source rock sample **"S10"** (see Table 6.2, Fig. 6.12 and Appendix III) gives Ts/(Ts + Tm) ratio (Par. 1) of 0.48, indicating medium maturation. The 22S/(22S+22R) ratio (Par. 3) is 0.28, indicating interference from heterogenic source. The diahopane/(diahopane + norhopane) ratio (Par. 5) is 0.35, showing medium maturation. The bisnorhopane/(bisnorhopane + norhopane) ratio (Par. 6) is 0.38, meaning that the organic matter is medium-high mature. The ratio of C_{23}-C_{29} tricyclic terpanes/C_{30} αβ-hopane (Par. 7) is 0.15 that also denotes medium-high maturation. The hopane/sterane of C_{30} αβ-hopane and regular C_{29} sterane (Par. 9) value is 0.89, indicating non-bacterial organic matter source. The MDBT ratio (Par. 21) is 1.64 and indicates low maturation. The calculated vitrinite reflectivities are respectively R_c=0.65% (Par. 22 after Radke, 1988), R_c=0.40% (Par. 23 after Radke and Welte, 1983), R_c=0.59% (Par. 24 after Kvalheim *et al*., 1987) and R_c=0.63% (Par. 25 after Radke, 1988); all of them falling outside the oil window. Finally the ratio MDBT/MPs (Par. 27) is 0.24 which indicates shale source rock facies.

S11 (7430/7-U-1, 38.80 m): The GC-MS chromatograms for the source rock sample **"S11"** (see Table 6.2, Fig. 6.13 and Appendix III) gives Ts/(Ts + Tm) ratio (Par. 1) of 0.73, indicating high maturation. The 22S/(22S+22R) ratio (Par. 3) is 0.48 that could possibly be due to heterogenic source mixing. The bisnorhopane/(bisnorhopane + norhopane) ratio (Par. 6) is 0.08, meaning that the organic matter is late mature. The hopane/sterane of C_{30} αβ-hopane and regular C_{29} sterane (Par. 9) value is 10.15 that may indicate bacterial reworked organic matter. The MDBT ratio (Par. 21) is 3.20 and indicates medium maturation. The calculated vitrinite reflectivities are respectively R_c=0.78% (Par. 22 after Radke, 1988), R_c=0.40% (Par. 23 after Radke and Welte, 1983), R_c=0.56% (Par. 24 after Kvalheim *et al*., 1987) and R_c=0.74% (Par. 25 after Radke, 1988), values that possibly describe immature sample. Finally the ratio MDBT/MPs (Par. 27) is 0.11 which indicates shale source rock facies.

S12 (7430/7-U-1, 64.70 m): On the GC-MS chromatograms for the source rock sample **"S12"** (see Table 6.2, Fig. 6.14 and Appendix III) gives Ts/(Ts + Tm) ratio (Par. 1) of 0.71, indicating high maturation. The 22S/(22S+22R) ratio (Par. 3) is 0.52 that could indicate early oil generation. The bisnorhopane/(bisnorhopane + norhopane) ratio (Par. 6) is 0.52 meaning that the organic matter is very immature. The hopane/sterane of C_{30} αβ-hopane and regular C_{29} sterane (Par. 9) value is 6.59 which indicates mixed organic matter source. The MDBT ratio (Par. 21) is 4.71 and indicates medium-high maturation. The calculated vitrinite reflectivities are respectively R_c=0.78% (Par. 22 after Radke, 1988), R_c=0.42% (Par. 23 after Radke and Welte, 1983), R_c=0.61% (Par. 24 after Kvalheim *et al.*, 1987) and R_c=0.85% (Par. 25 after Radke, 1988), values that may indicate early oil generation. Finally the ratio MDBT/MPs (Par. 27) is 0.10 which indicates shale source rock facies.

S5 (7230/5-U-5, 43.85 m): On the GC-MS chromatograms for the source rock sample **"S5"** (see Table 6.2, Fig. 6.15 and Appendix III) gives Ts/(Ts + Tm) ratio (Par. 1) of 0.45, indicating medium-high maturation. The 22S/(22S+22R) ratio (Par. 3) is 0.35 indicating interference from heterogenic sources. The bisnorhopane/(bisnorhopane + norhopane) ratio (Par. 6) is 0.09 meaning that the organic matter is mature. The hopane/sterane of C_{30} αβ-hopane and regular C_{29} sterane (Par. 9) value is 6.17 that indicates mixed organic matter source. The MDBT ratio (Par. 21) is 3.80 and indicates medium-high maturation. The calculated vitrinite reflectivities are respectively R_c=0.76% (Par. 22 after Radke, 1988), R_c=0.40% (Par. 23 after Radke and Welte, 1983), R_c=0.52% (Par. 24 after Kvalheim *et al.*, 1987) and R_c=0.79% (Par. 25 after Radke, 1988), values that may indicate early oil generation. Finally the ratio MDBT/MPs (Par. 27) is 0.11 which indicates shale source rock facies.

S3 (7124/3-U-1, 1367.50 m): On the GC-MS chromatograms for the source rock sample **"S3"** (see Table 6.2, Fig. 6.16 and Appendix III) gives Ts/(Ts + Tm) ratio (Par. 1) of 0.33, indicating medium-high maturation. The 22S/(22S+22R) ratio (Par. 3) is 0.55 indicating as well medium-high oil generation. The bisnorhopane/ (bisnorhopane + norhopane) ratio (Par. 6) is 0.20 meaning that the organic matter is medium mature. The hopane/sterane of C_{30} αβ-hopane and regular C_{29} sterane (Par.

9) value is 4.48 which indicates no-bacterial organic matter reworking. The MDBT ratio (Par. 21) is 2.83 and indicates medium maturation. The calculated vitrinite reflectivities are respectively R_c=0.75% (Par. 22 after Radke, 1988), R_c=0.40% (Par. 23 after Radke and Welte, 1983), R_c=0.64% (Par. 24 after Kvalheim *et al*., 1987) and R_c=0.72% (Par. 25 after Radke, 1988), values that may indicate early oil generation. Finally the ratio MDBT/MPs (Par. 27) is 0.52 which indicates shale source rock facies.

S2 (7122/6- 1, 2061.50 m): On the GC-MS chromatograms for the source rock sample **"S2"** (see Table 6.2, Fig. 6.17 and Appendix III) gives Ts/(Ts + Tm) ratio (Par. 1) of 0.20 which is the lowest value in the dataset. The 22S/(22S+22R) ratio (Par. 3) is 0.35 indicating mixing with oil from non-authigenic sources. On the other hand the bisnorhopane/(bisnorhopane + norhopane) ratio (Par. 6) is 0.08 meaning that the organic matter is mature. The hopane/sterane of C_{30} αβ-hopane and regular C_{29} sterane (Par. 9) value is 6.09 that indicates mixed organic matter source. The MDBT ratio (Par. 21) is 1.61 which is low and shows early maturation. The calculated vitrinite reflectivities are respectively R_c=0.93% (Par. 22 after Radke, 1988), R_c=0.41% (Par. 23 after Radke and Welte, 1983), R_c=0.85% (Par. 24 after Kvalheim *et al*., 1987) and R_c=0.63% (Par. 25 after Radke, 1988), values that may indicate early oil generation. Finally the ratio MDBT/MPs (Par. 27) is 1.61 which indicates carbonate source rock facies.

S6 (7231/1-U-1, 70.90 m): On the GC-MS chromatograms for the source rock sample **"S6"** (see Table 6.2, Fig. 6.18 and Appendix III) gives Ts/(Ts + Tm) ratio (Par. 1) of 0.51, indicating medium-high maturation. The 22S/(22S+22R) ratio (Par. 3) is 0.27 indicating interference from heterogenic sources. The bisnorhopane/(bisnorhopane + norhopane) ratio (Par. 6) is 0.41 which is a very high value but is probably affected by biodegradation. The hopane/sterane of C_{30} αβ-hopane and regular C_{29} sterane (Par. 9) value is 2.10 and indicates algal or higher-plant organic matter. The MDBT ratio (Par. 21) is 0.63 and indicates immature organic matter. The calculated vitrinite reflectivities are respectively R_c=0.68% (Par. 22 after Radke, 1988), R_c=0.40% (Par. 23 after Radke and Welte, 1983), R_c=0.57% (Par. 24 after Kvalheim *et al*., 1987) and R_c=0.56% (Par. 25 after Radke, 1988), values that fall outside oil window. However

sincethe Hekkingen Formation is very prolific it is most likely that sample S6 has expelled early oil quantities. Finally the ratio MDBT/MPs (Par. 27) is 1.08, indicating carbonate source rock facies which are often contained inside the Hekkingen shale.

S7 (7231/1-U-1, 76.20m): On the GC-MS chromatograms for the source rock sample **"S7"** (see Table 6.2, Fig. 6.18 and Appendix III) gives Ts/(Ts + Tm) ratio (Par. 1) of 0.53, indicating medium-high maturation. The 22S/(22S+22R) ratio (Par. 3) is 0.26 indicating interference from heterogenic sources. The bisnorhopane/(bisnorhopane + norhopane) ratio (Par. 6) is 0.27 meaning that the organic matter is early mature. The hopane/sterane of C_{30} αβ-hopane and regular C_{29} sterane (Par. 9) value is 1.85 and indicates algal or higher-plant organic matter. The MDBT ratio (Par. 21) is 0.34 and indicates very immature organic matter. The calculated vitrinite reflectivities are respectively R_c=0.61% (Par. 22 after Radke, 1988), R_c=0.41% (Par. 23 after Radke and Welte, 1983), R_c=0.54% (Par. 24 after Kvalheim *et al*., 1987) and R_c=0.53% (Par. 25 after Radke, 1988), values that fall outside the oil window. Finally, the ratio MDBT/MPs (Par. 27) is 1.88, indicating carbonate source rock facies which are often contained inside the Hekkingen shale, same as sample **"S7"**.

S8 (7231/4-U-1, 84.70 m): On the GC-MS chromatograms for the source rock sample **"S8"** (see Table 6.2, Fig. 6.19 and Appendix III) gives Ts/(Ts + Tm) ratio (Par. 1) of 0.22, indicating low maturation. The 22S/(22S+22R) ratio (Par. 3) is 0.17 indicating heterogenic source mixing. The bisnorhopane/(bisnorhopane + norhopane) ratio (Par. 6) is 0.10 meaning that the organic matter is mature. The hopane/sterane of C_{30} αβ-hopane and regular C_{29} sterane (Par. 9) value is 2.79 that indicates non-bacterial organic matter source. The MDBT ratio (Par. 21) is 2.54 and indicates medium maturation. The calculated vitrinite reflectivities are respectively R_c=0.71% (Par. 22 after Radke, 1988), R_c=0.40% (Par. 23 after Radke and Welte, 1983), R_c=0.45% (Par. 24 after Kvalheim *et al*., 1987) and R_c=0.70% (Par. 25 after Radke, 1988), values that may indicate early oil generation. Finally, the ratio MDBT/MPs (Par. 27) is 0.09 which clearly indicates shale source rock facies.

S1 (7122/6-1, 1156.60 m): On the GC-MS chromatograms for the source rock sample **"S1"** (see Table 6.2, Fig. 6.20 and Appendix III) gives Ts/(Ts + Tm) ratio (Par. 1) of

0.49, indicating medium maturation. The 22S/(22S+22R) ratio (Par. 3) is 0.60 and indicates peak-oil generation. The bisnorhopane/(bisnorhopane + norhopane) ratio (Par. 6) is 0.06 meaning that the organic matter is very mature. The hopane/sterane of C_{30} αβ-hopane and regular C_{29} sterane (Par. 9) value is 4.73 which indicates no-bacterial reworking. The MDBT ratio (Par. 21) is 3.46 and indicates medium maturation. The calculated vitrinite reflectivities are respectively R_c=0.94% (Par. 22 after Radke, 1988), R_c=1.16% (Par. 23 after Radke and Welte, 1983), R_c=0.86% (Par. 24 after Kvalheim *et al*., 1987) and R_c=0.76% (Par. 25 after Radke, 1988), values that fall inside the oil window. Finally the ratio MDBT/MPs (Par. 27) is 0.92 which indicates shale source rock facies.

SO-21 (outcrop): On the GC-MS chromatograms for the source rock sample **"SO-21"** (see Table 6.2, Fig. 6.21 and Appendix III) gives Ts/(Ts + Tm) ratio (Par. 1) of 0.66, indicating high maturation. The 22S/(22S+22R) ration (Par. 3) is 0.62 indicating peak-oil generation. The bisnorhopane/(bisnorhopane + norhopane) ratio (Par. 6) is 0.13 meaning that the organic matter is mature. The hopane/sterane of C_{30} αβ-hopane and regular C_{29} sterane (Par. 9) value is 4.54 that indicates non-bacterial organic matter source. The MDBT ratio (Par. 21) is 3.80 and indicates medium-high maturation. The calculated vitrinite reflectivities are respectively R_c=0.79% (Par. 22 after Radke, 1988), R_c=0.40% (Par. 23 after Radke and Welte, 1983), R_c=0.65% (Par. 24 after Kvalheim *et al*., 1987) and R_c=0.69% (Par. 25 after Radke, 1988), values that in general indicate oil generation. Finally the ratio MDBT/MPs (Par. 27) is 0.69 which indicates shale source rock facies.

6.3 Summary of results

Table 5.3 is summarizes the most important results and observations from the GC-FID and GC-MS analyses and includes biodegradation, maturity, mean vitrinite reflectance and lithofacies data. It is obvious that it would be very unsafe to correlate the mature oils with the low mature source rocks based solely on these data. Still most facies parameters will allow a correlation to be effectivelly made; hence the results will be better understood when illustrated on several plots that are discussed in Chapter 7.

Table 6.3: Summarizing the main aspects of the studied samples, age coloured. Red for Permo-Carboniferous, purple for Triassic, teal for Jurassic, green for Cretaceous. NSO-1 sample is coloured in yellow. Mean V.R for average vitrinite reflectance, calculated from parameters 22-25.

Sample	Type	Biodegradation	Maturity	Mean V.R	Lithofacies
C	OILS	slight	very high	1.0	shale
T1		slight	high	0.8	shale
T2		zero	very high	0.8	shale
V		zero	medium	0.9	shale
Ø		zero	high	0.8	shale
AB		slight	medium	0.8	shale
E1		slight	medium-high	0.8	shale
O		zero	high	0.8	carbonate
X		zero	high	0.8	shale
W		zero	medium	0.8	carbonate
NSO-1		zero	high	0.9	shale
S4	SOURCE ROCKS	slight	medium	0.7	shale
S9		medium	medium	0.6	shale
S10		medium	medium	0.9	shale
S11		medium	very high	0.6	shale
S12		slight	very high	0.6	shale
S5		slight	medium	0.5	shale
S3		high	medium	0.6	shale
S2		zero	low	0.5	carbonate
S6		high	medium	0.6	carbonate
S7		high	medium	0.6	carbonate
S8		high	low	0.7	shale
S1		zero	medium	0.7	shale
SO-21		zero	high	0.6	shale

6.4 Presentation of chromatograms

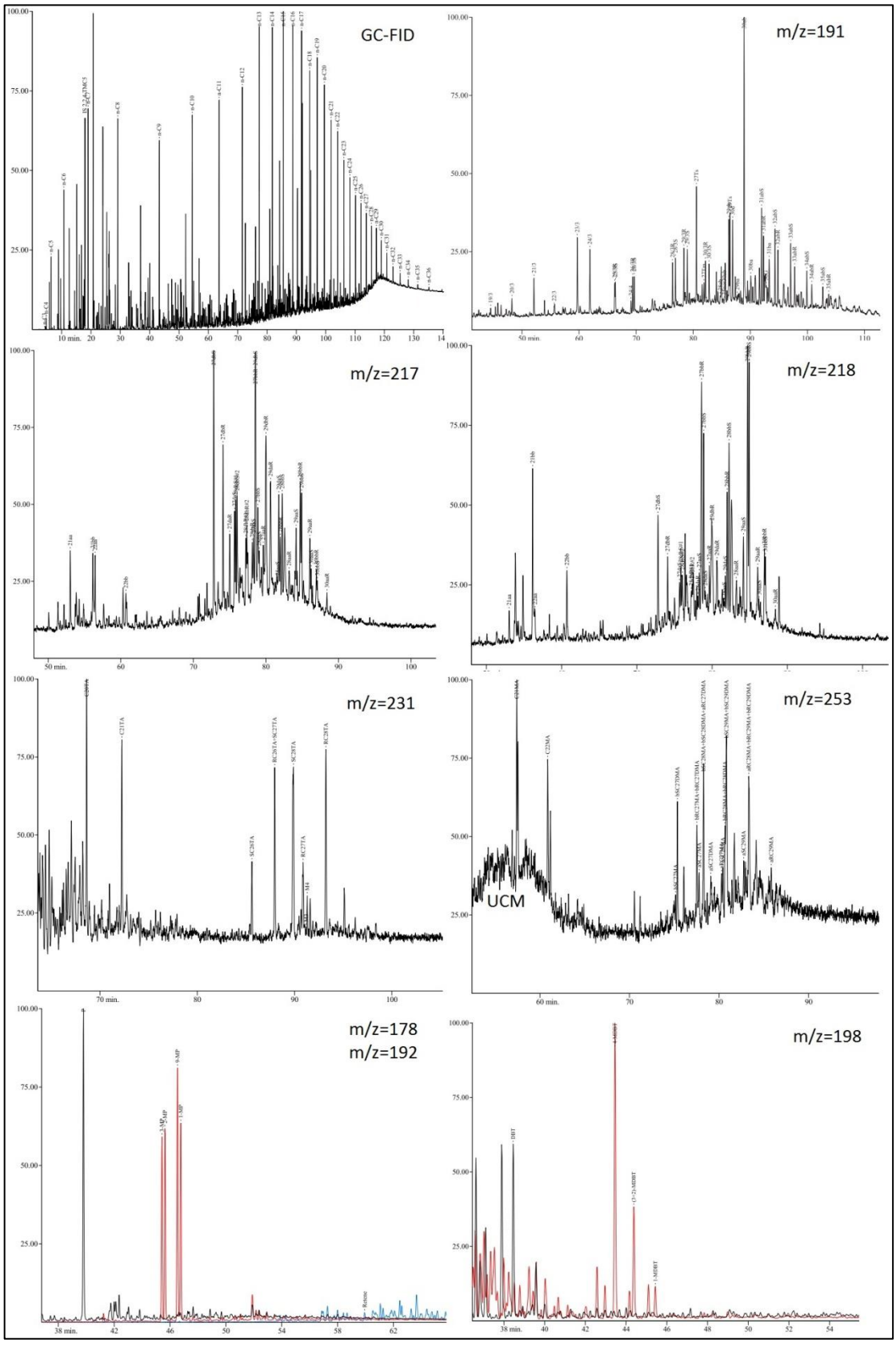

Figure 6.1: Overview of GC-FID and GC-MS chromatograms for oil sample "C" from well 7120/2-1.

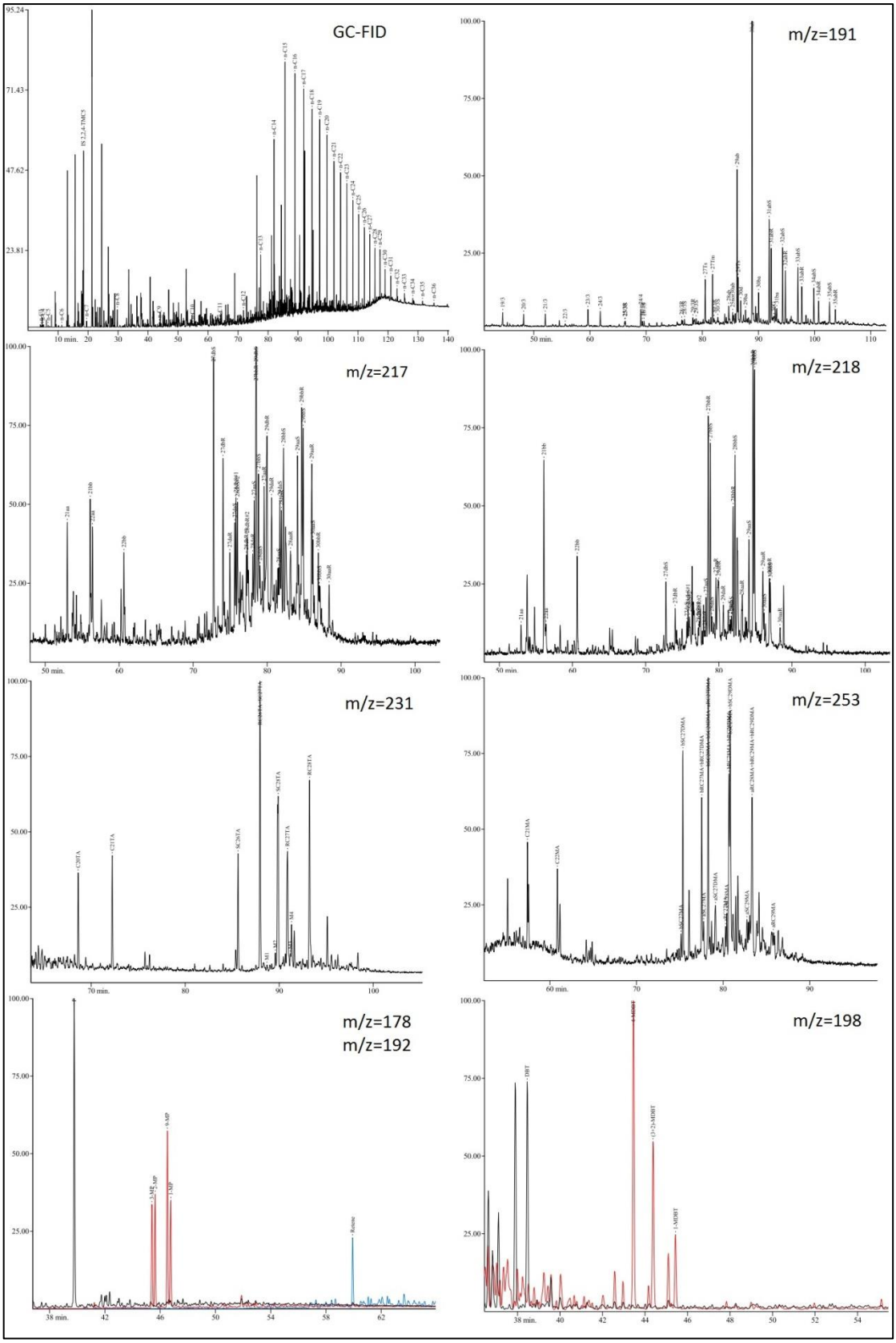

Figure 6.2: Overview of GC-FID and GC-MS chromatograms for oil sample "T1" from well 7122/7-3.

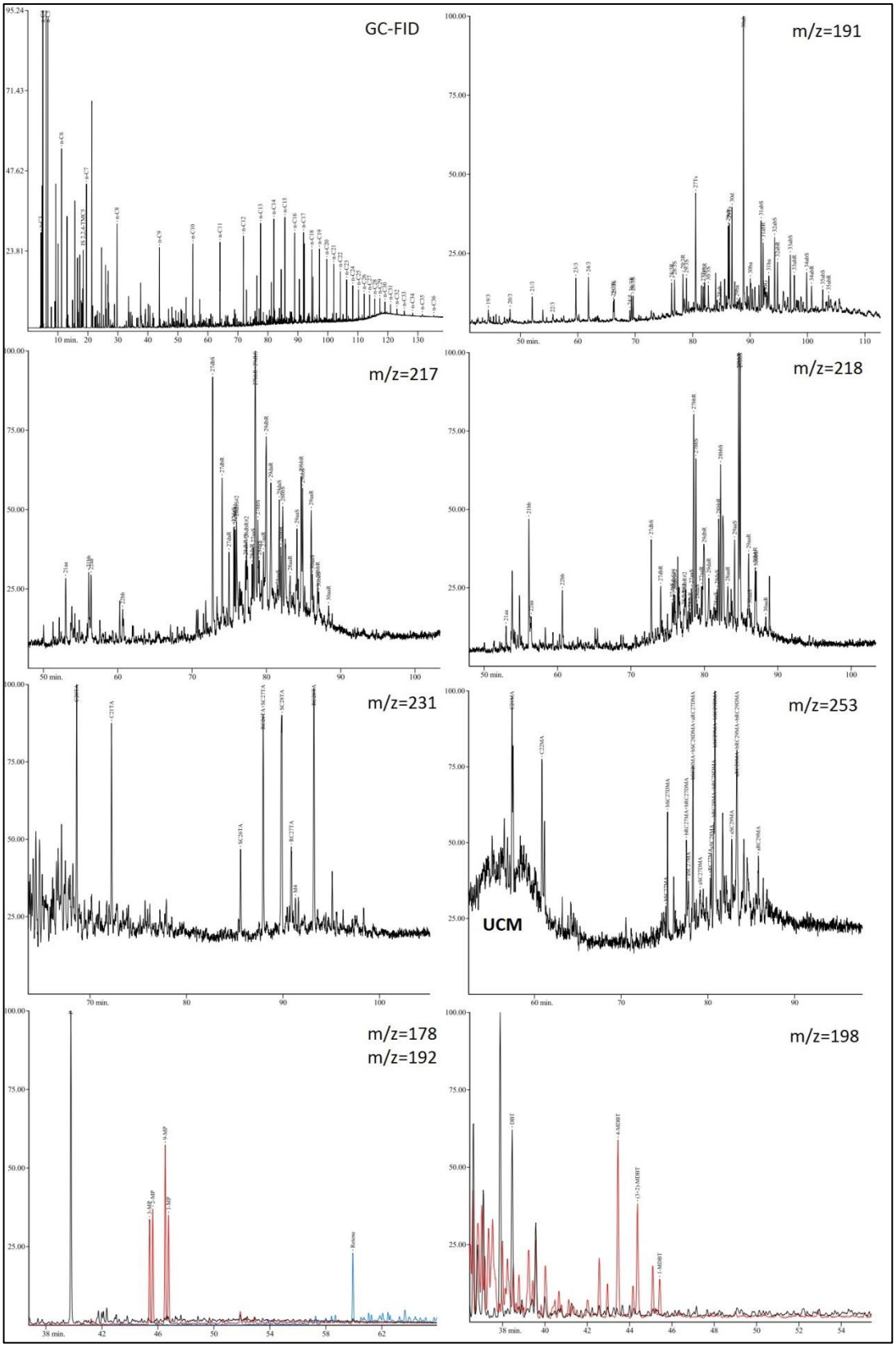

Figure 6.3: Overview of GC-FID and GC-MS chromatograms for oil sample "T2" from well 7122/7-3.

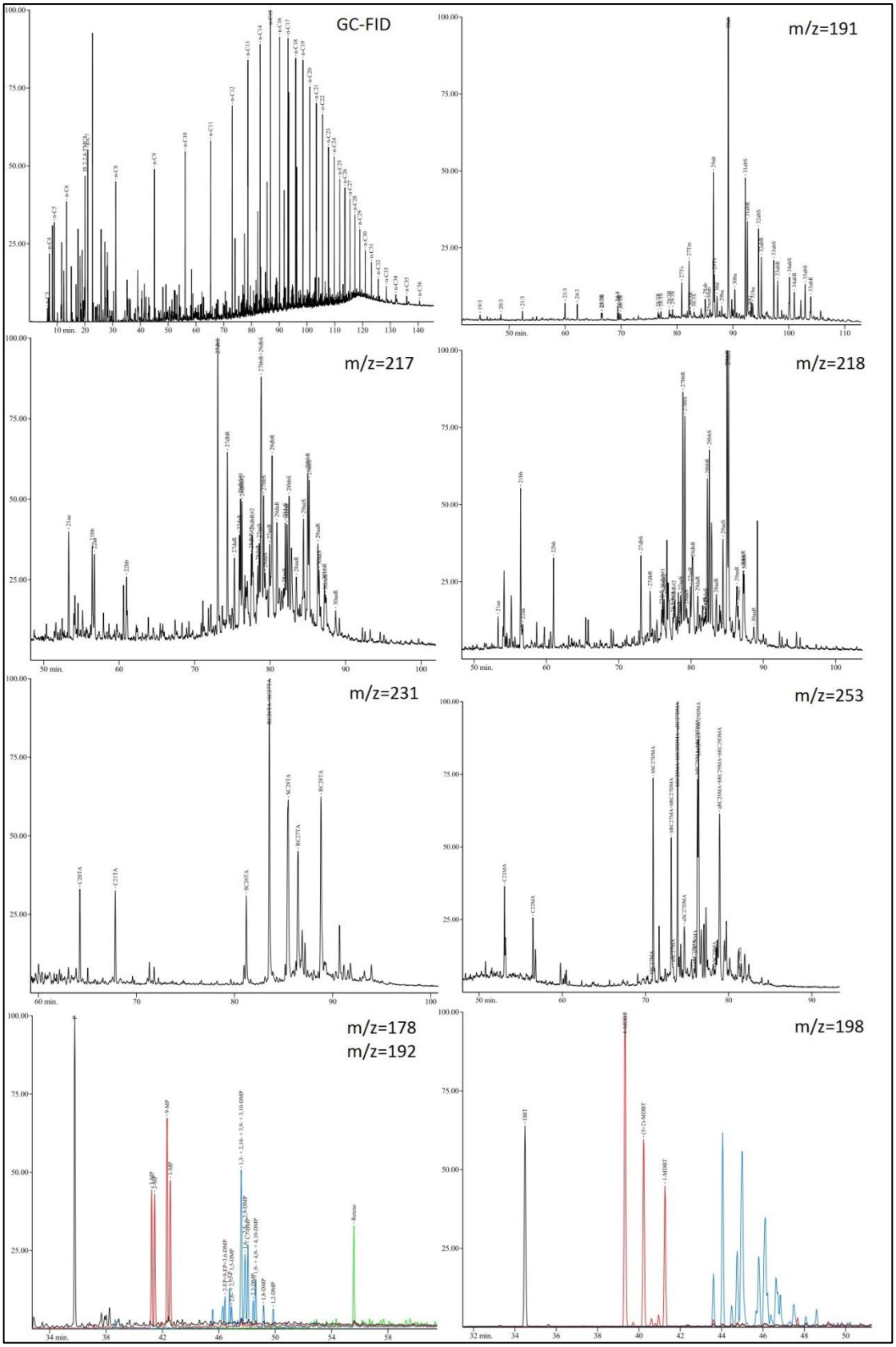

Figure 6.4: Overview of GC-FID and GC-MS chromatograms for oil sample "V" from well 7123/4-1 A.

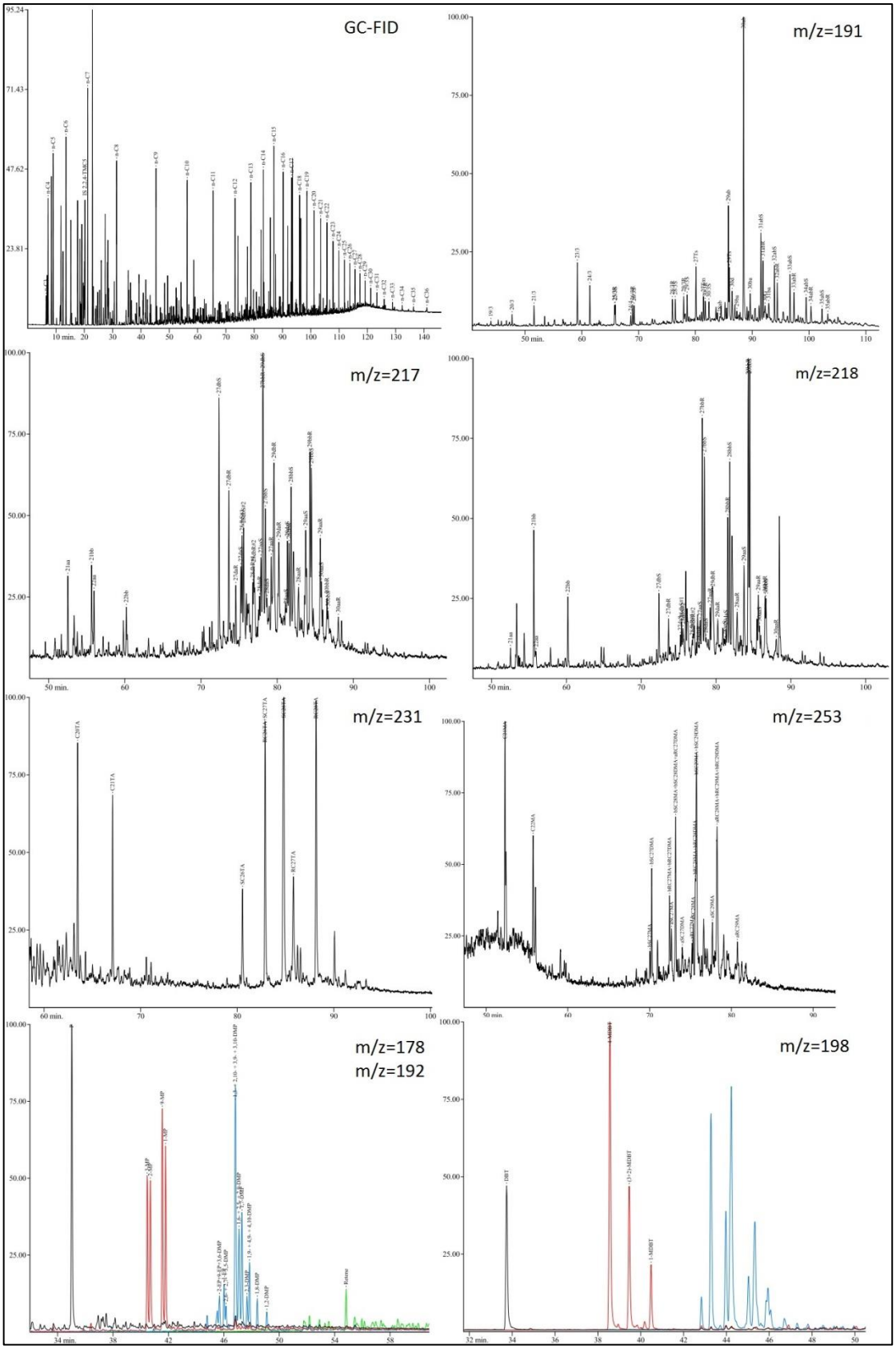

Figure 6.5: Overview of GC-FID and GC-MS chromatograms for oil sample "Ø" from well 7222/6-1 S.

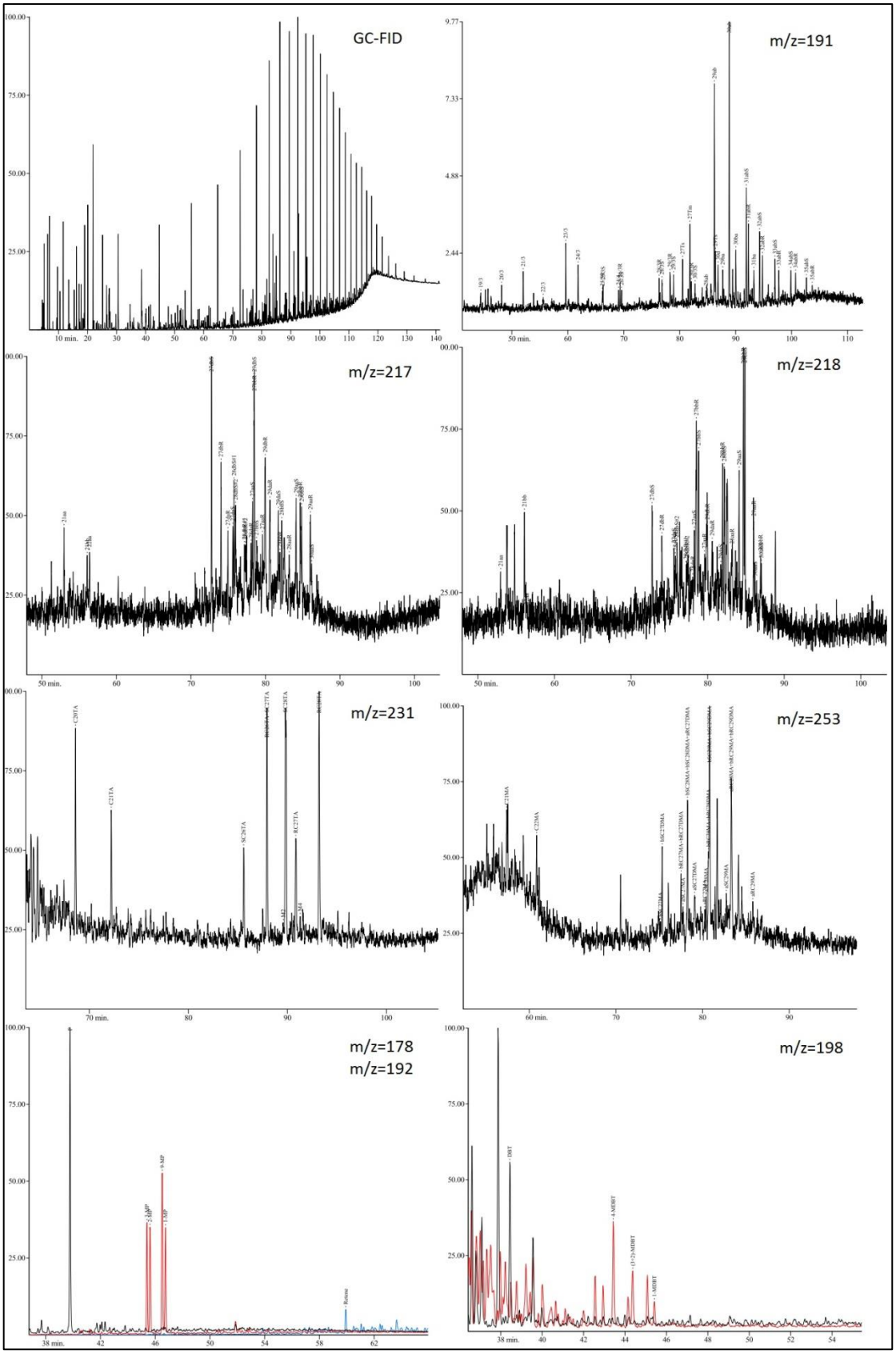

Figure 6.6: Overview of GC-FID and GC-MS chromatograms for oil sample "AB" from well 7228/7-1 A.

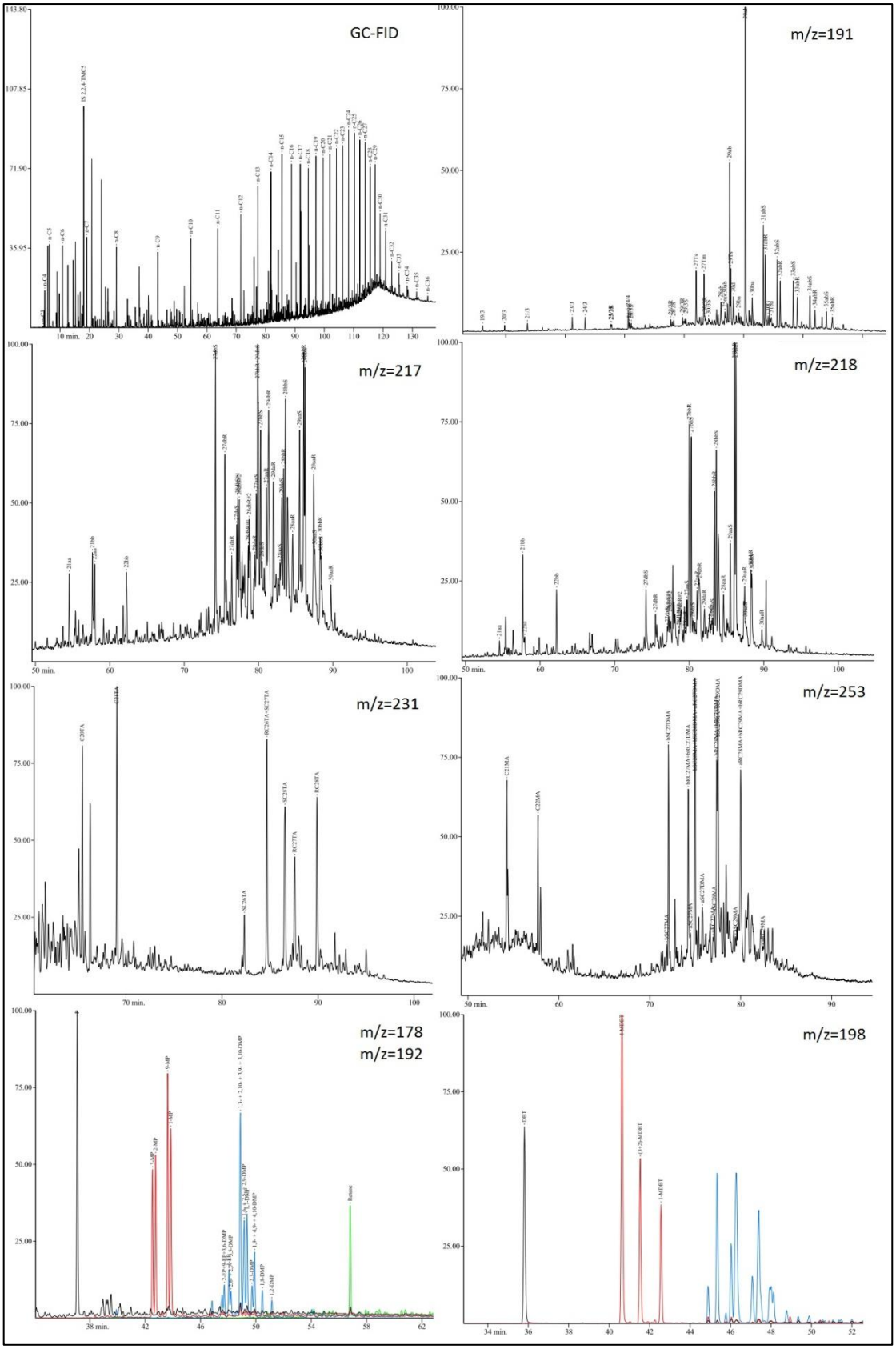

Figure 6.7: Overview of GC-FID and GC-MS chromatograms for oil sample "E1" from well 7120/6-1.

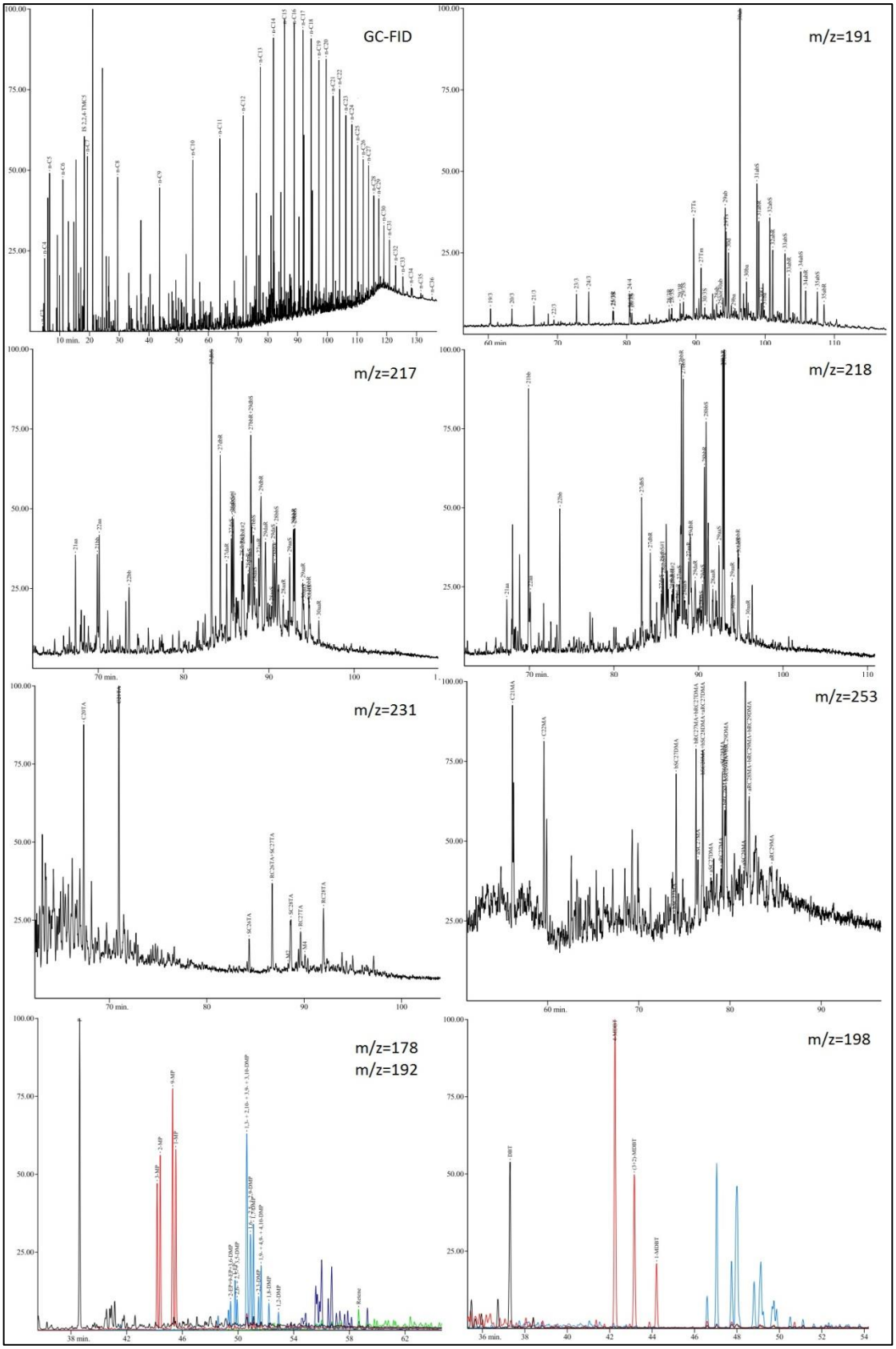

Figure 6.8: Overview of GC-FID and GC-MS chromatograms for oil sample "O" from well 7121/5-2.

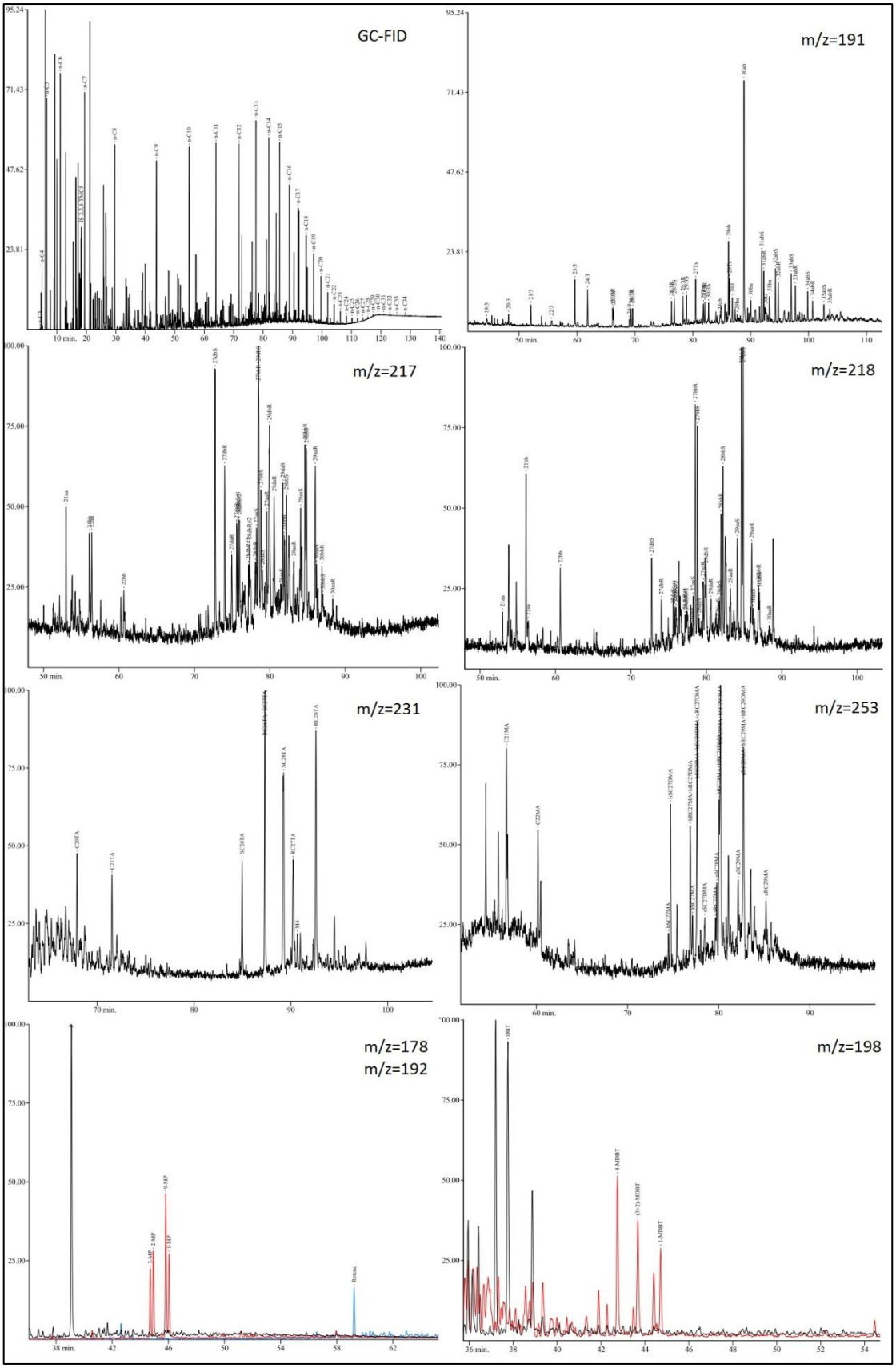

Figure 6.9: Overview of GC-FID and GC-MS chromatograms for oil sample "X" from well 7125/1-1.

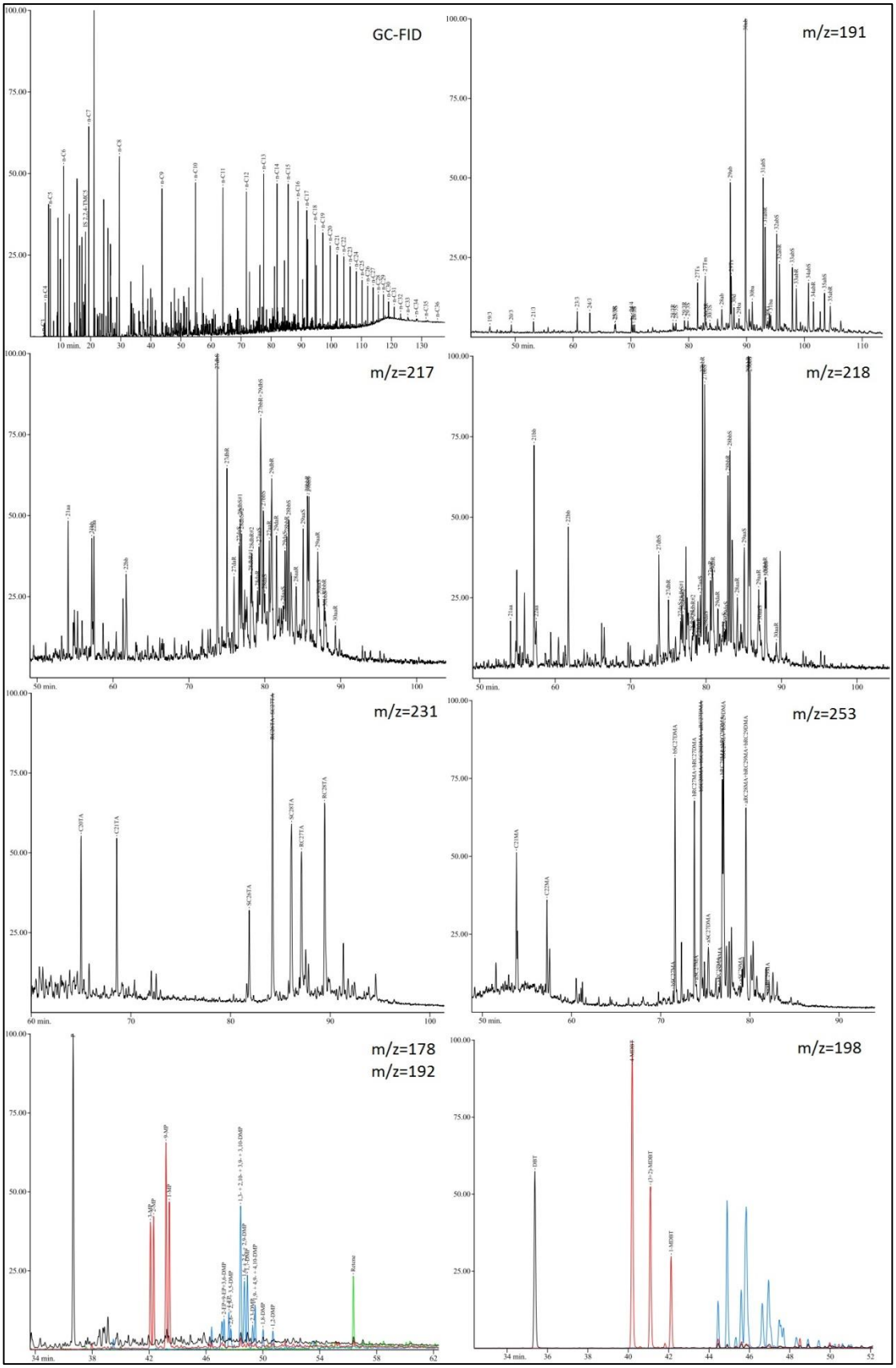

Figure 6.10: Overview of GC-FID and GC-MS chromatograms for oil sample "W" from well 7124/3-1.

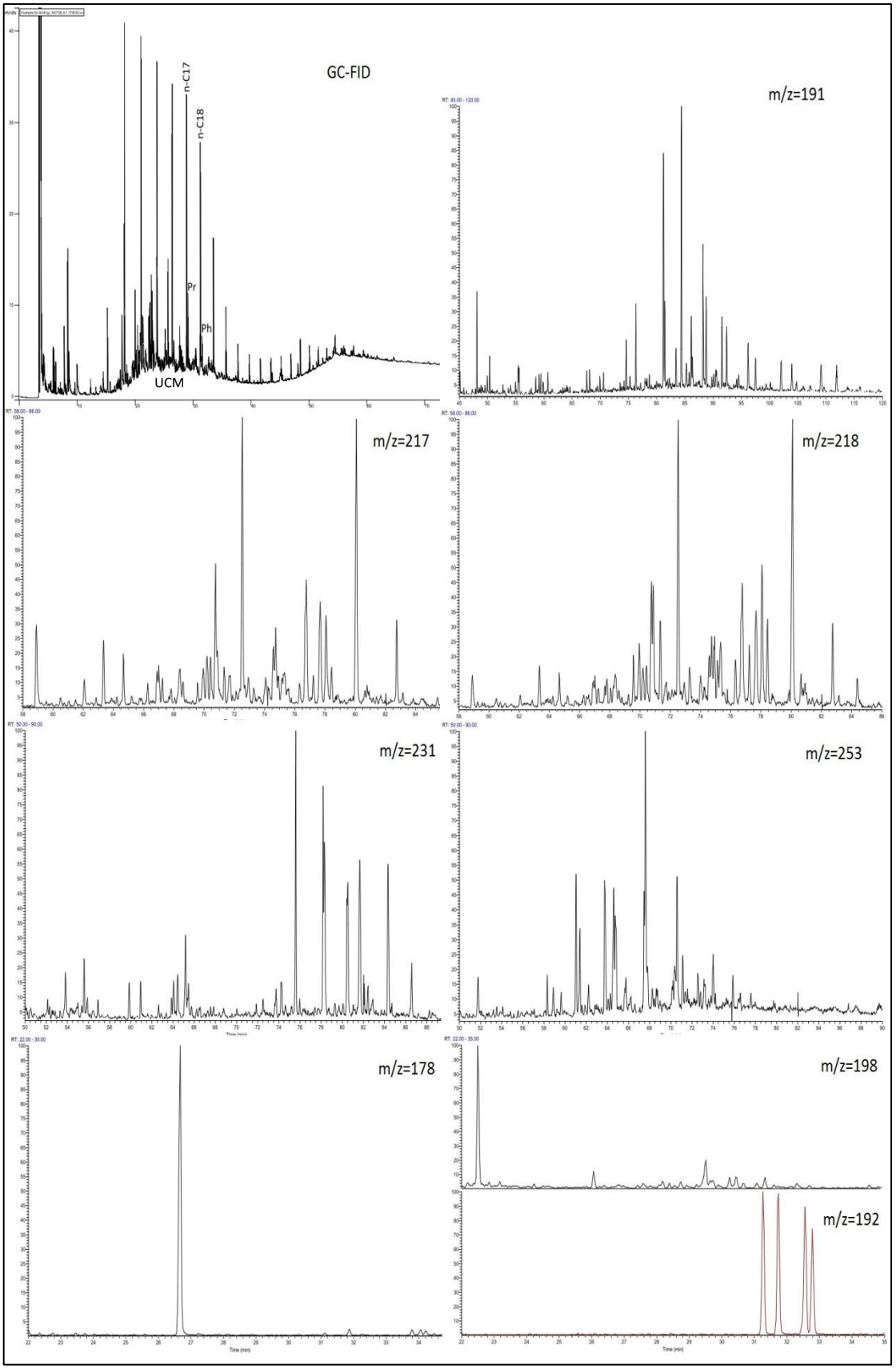

Figure 6.11: Overview of GC-FID and GC-MS chromatograms for source rock sample "S4" from well 7128/6-1.

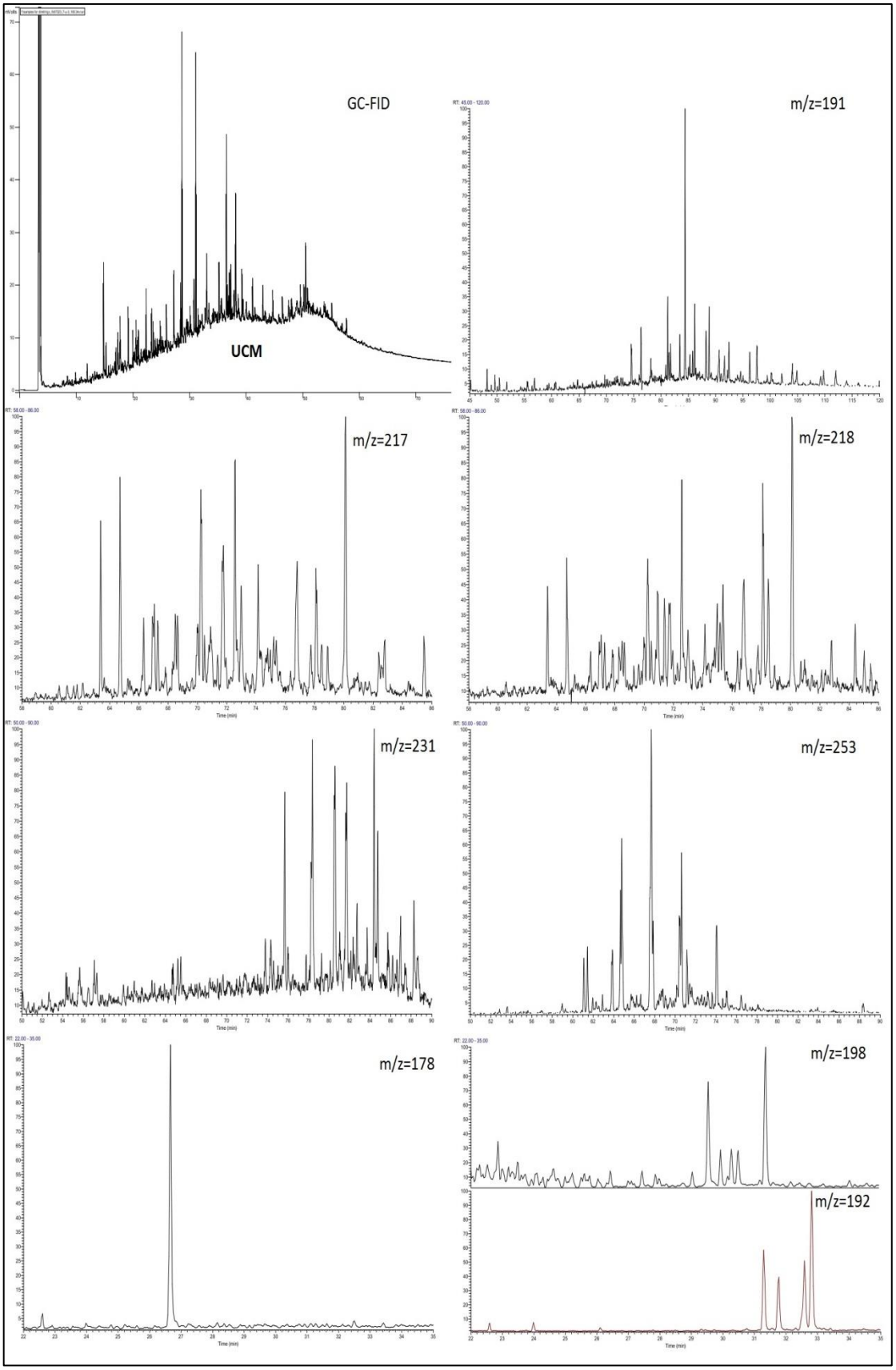

Figure 6.13: Overview of GC-FID and GC-MS chromatograms for source rock sample "S9" from well 7323/7-U-3.

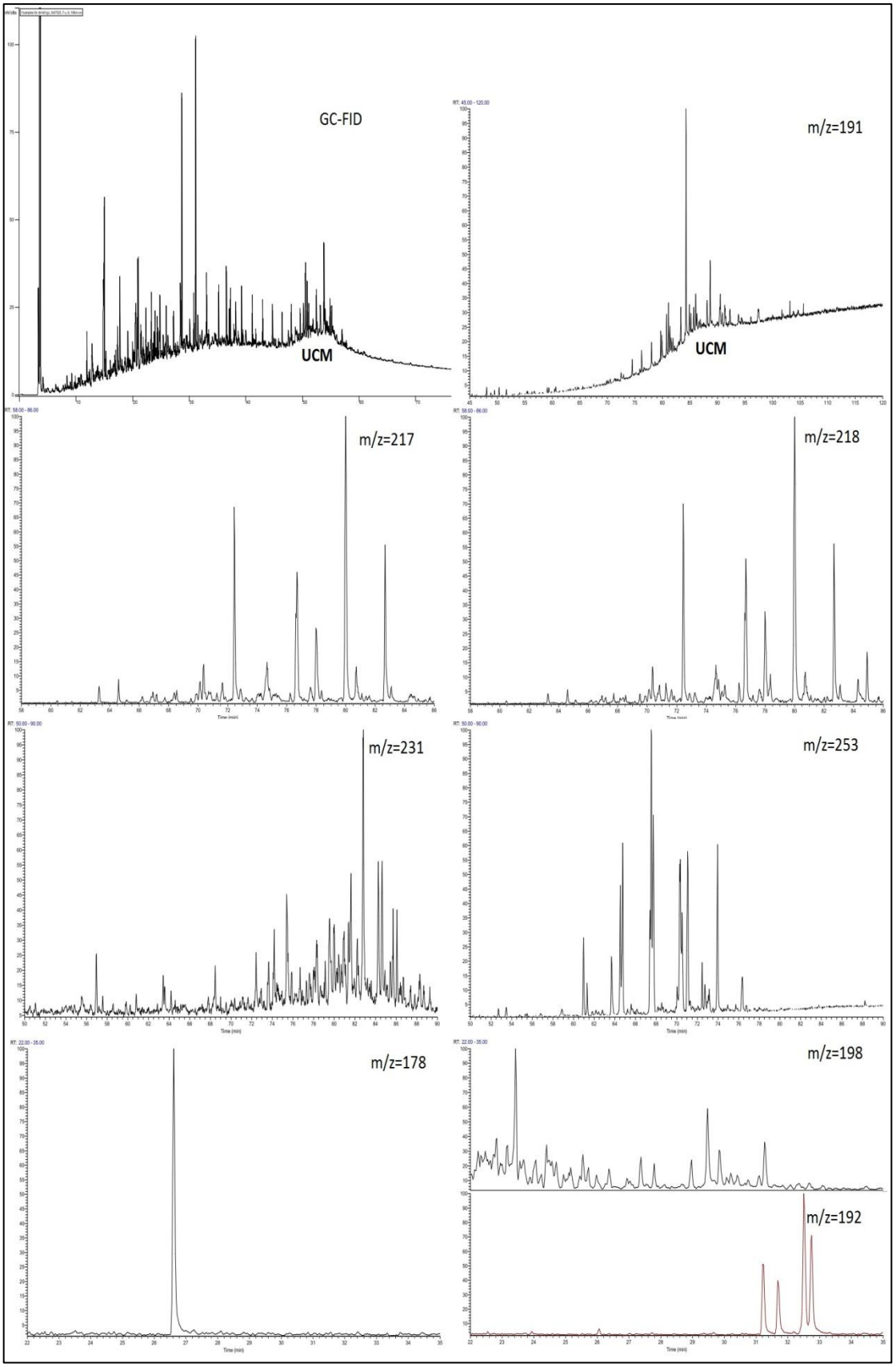

Figure 6.14: Overview of GC-FID & GC-MS chromatograms for source rock sample "S10" from well 7323/7-U-9.

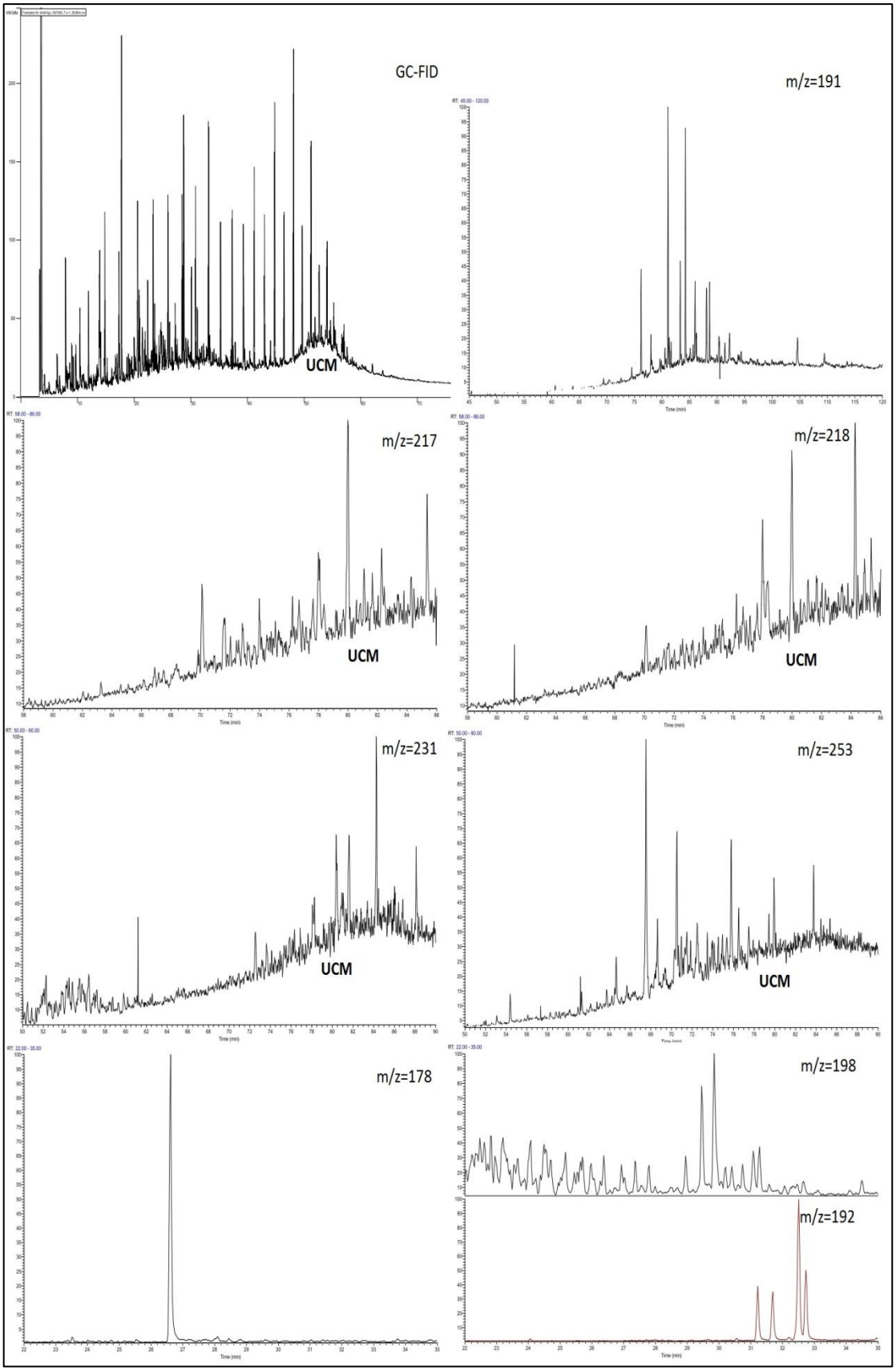

Figure 6.15: Overview of GC-FID & GC-MS chromatograms for source rock sample "S11" from well 7430/7-U-1.

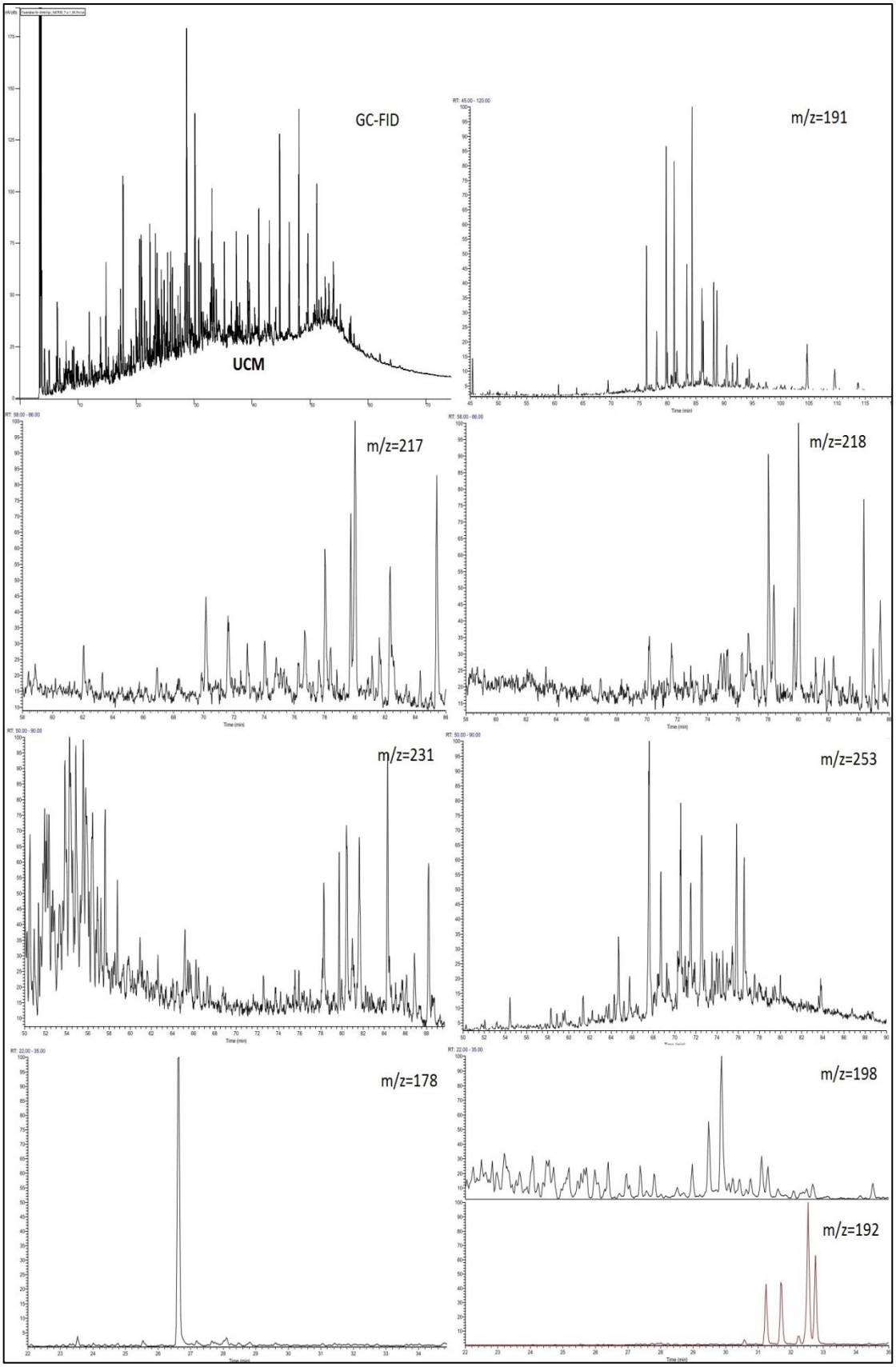

Figure 6.16: Overview of GC-FID & GC-MS chromatograms for source rock sample "S12" from well 7430/7-U-1.

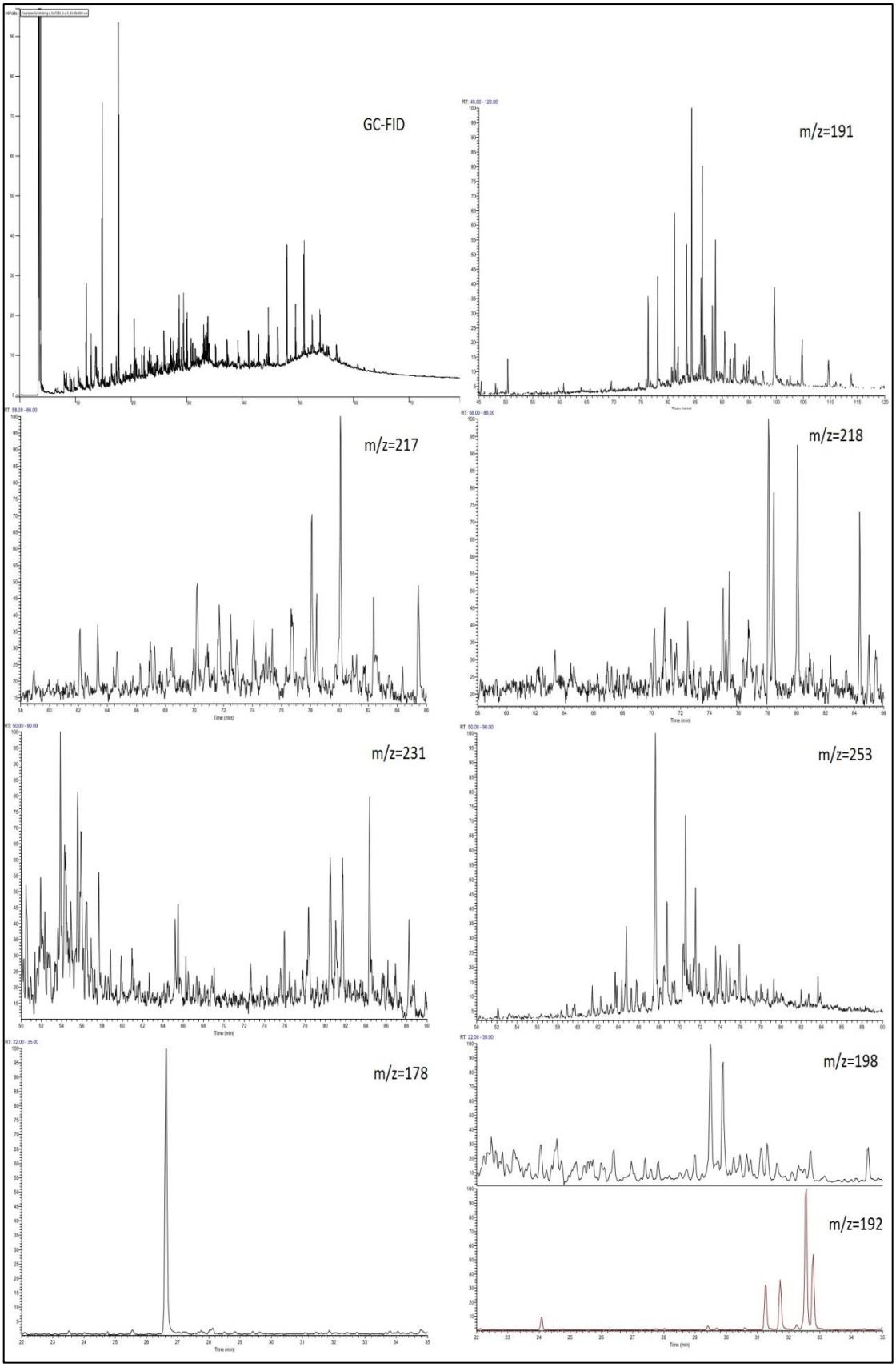

Figure 6.17: Overview of GC-FID & GC-MS chromatograms for source rock sample "S5" from well 7230/5-U-5.

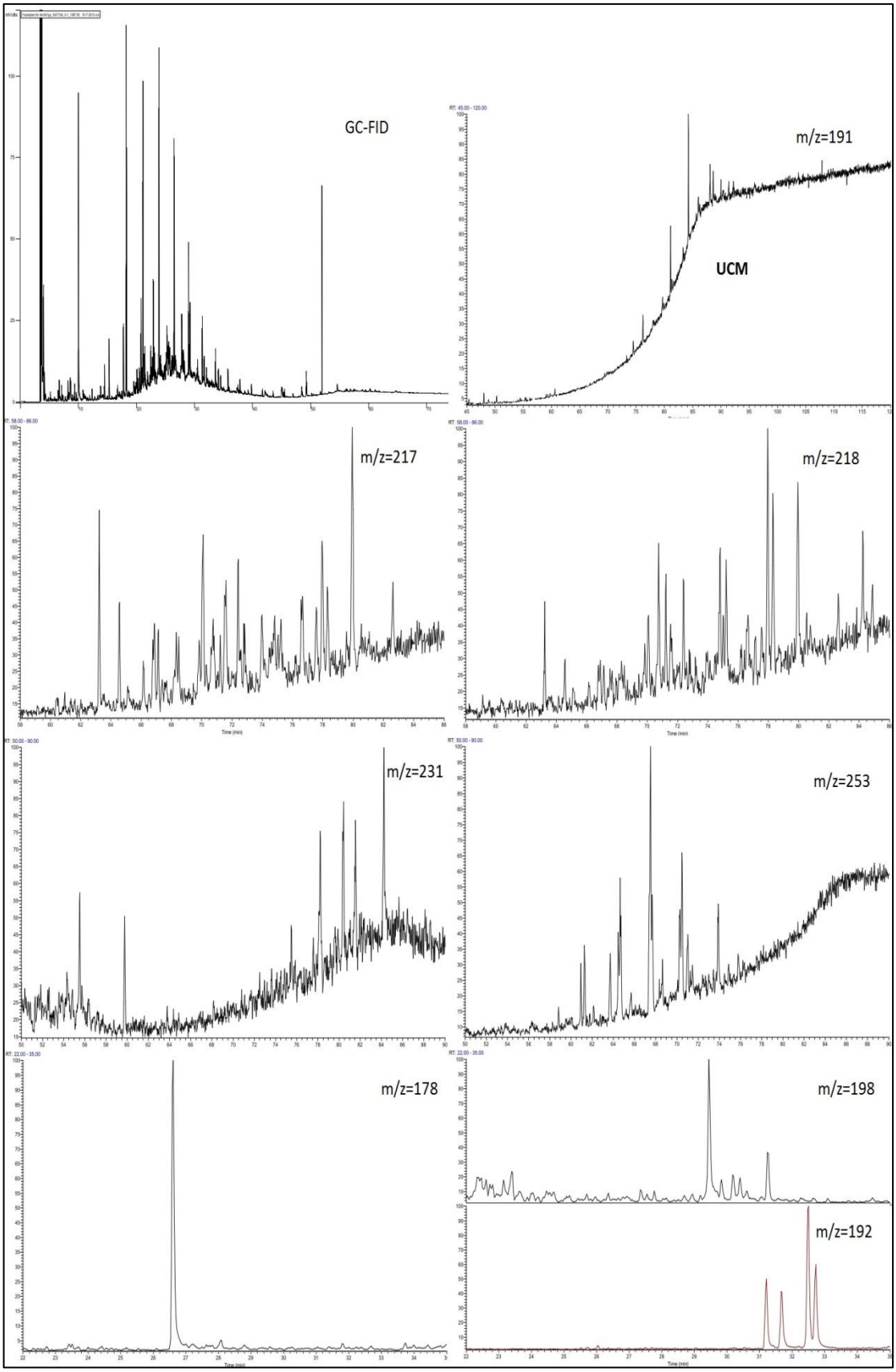

Figure 6.18: Overview of GC-FID & GC-MS chromatograms for source rock sample "S3" from well 7124/3-1.

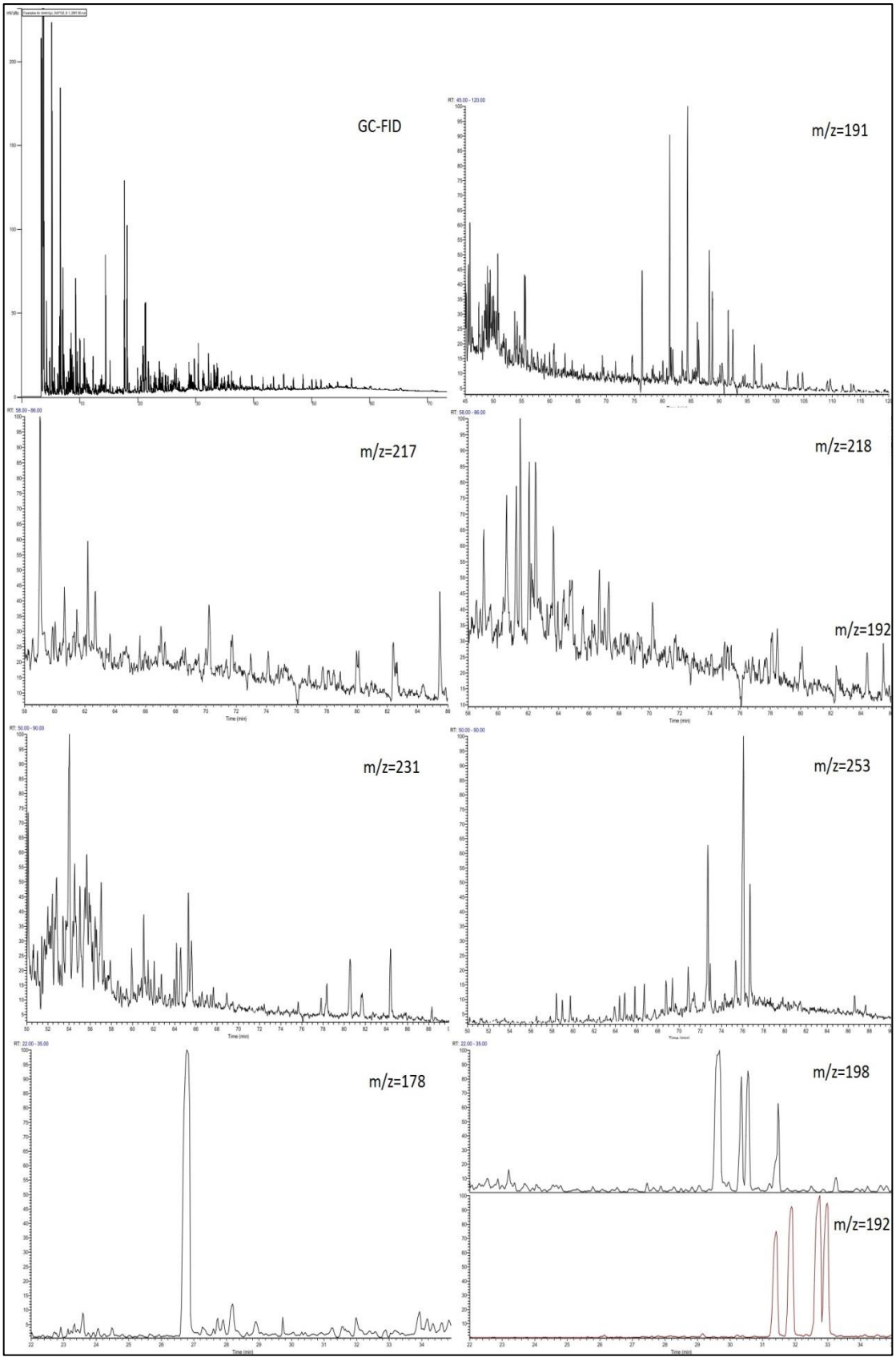

Figure 6.19: Overview of GC-FID & GC-MS chromatograms for source rock sample "S2" from well 7122/6-1.

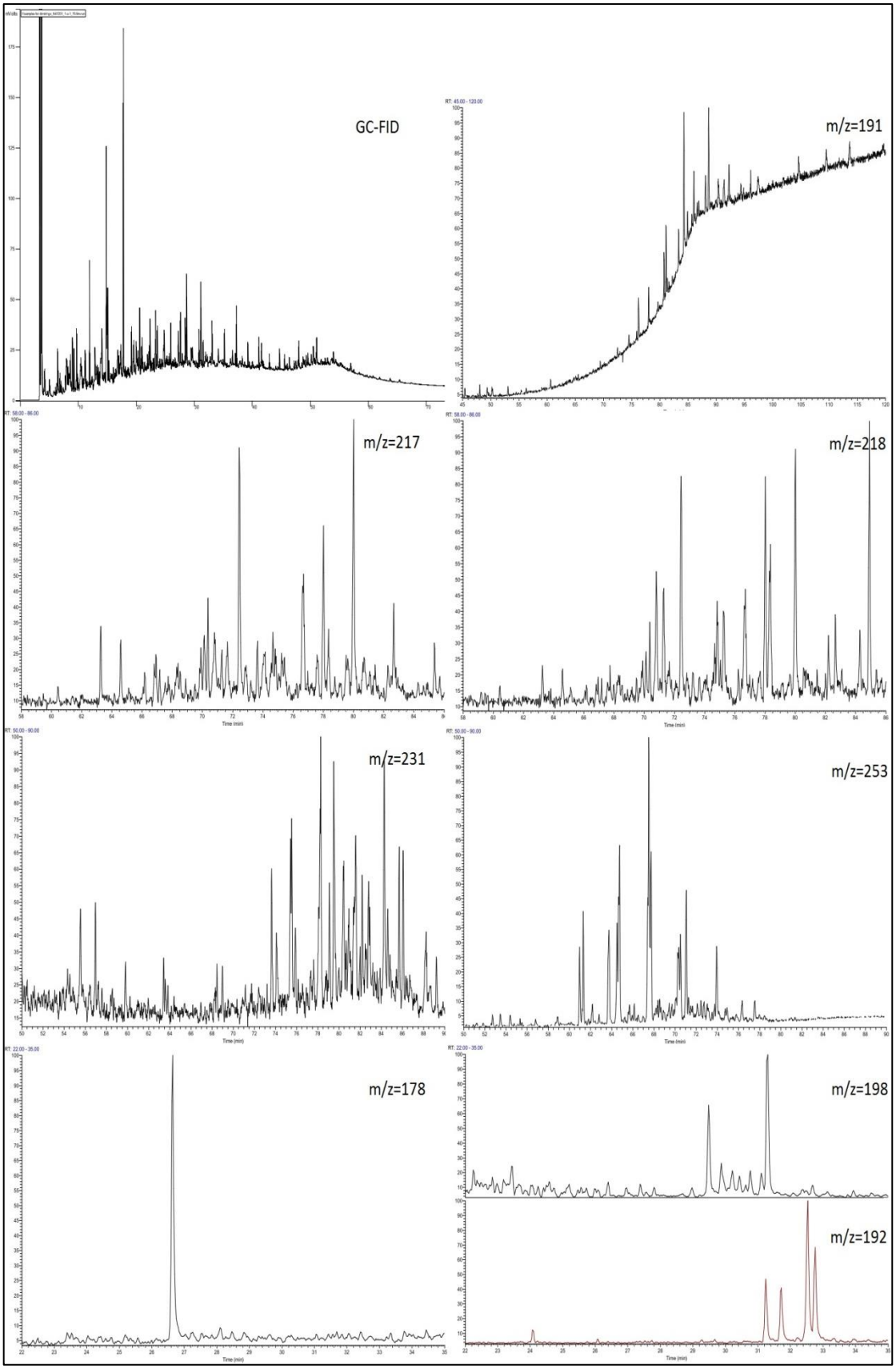

Figure 6.20: Overview of GC-FID & GC-MS chromatograms for source rock sample "S6" from well 7231/1-U-1.

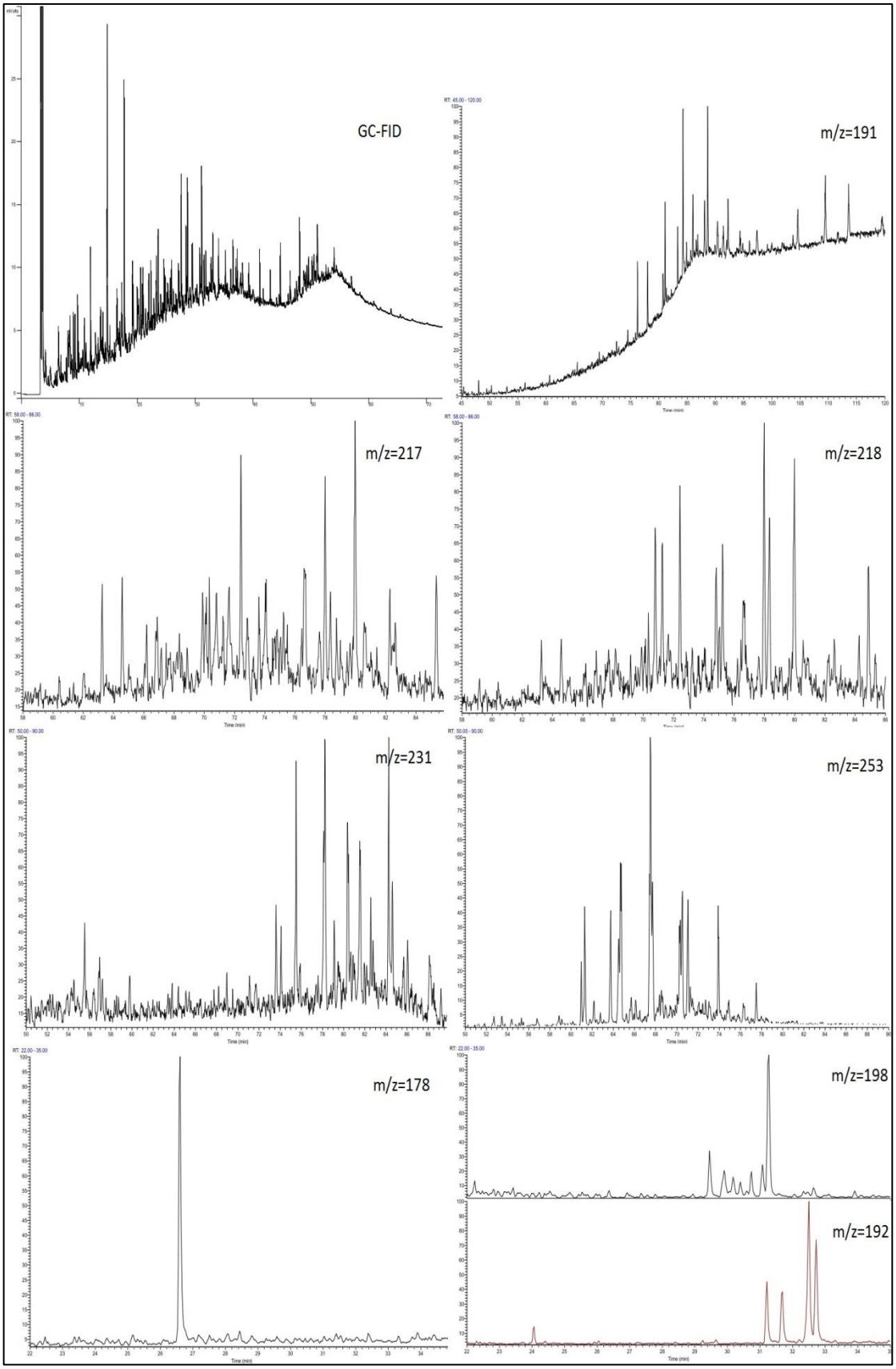

Figure 6.21: Overview of GC-FID & GC-MS chromatograms for source rock sample "S7" from well 7231/1-U-1.

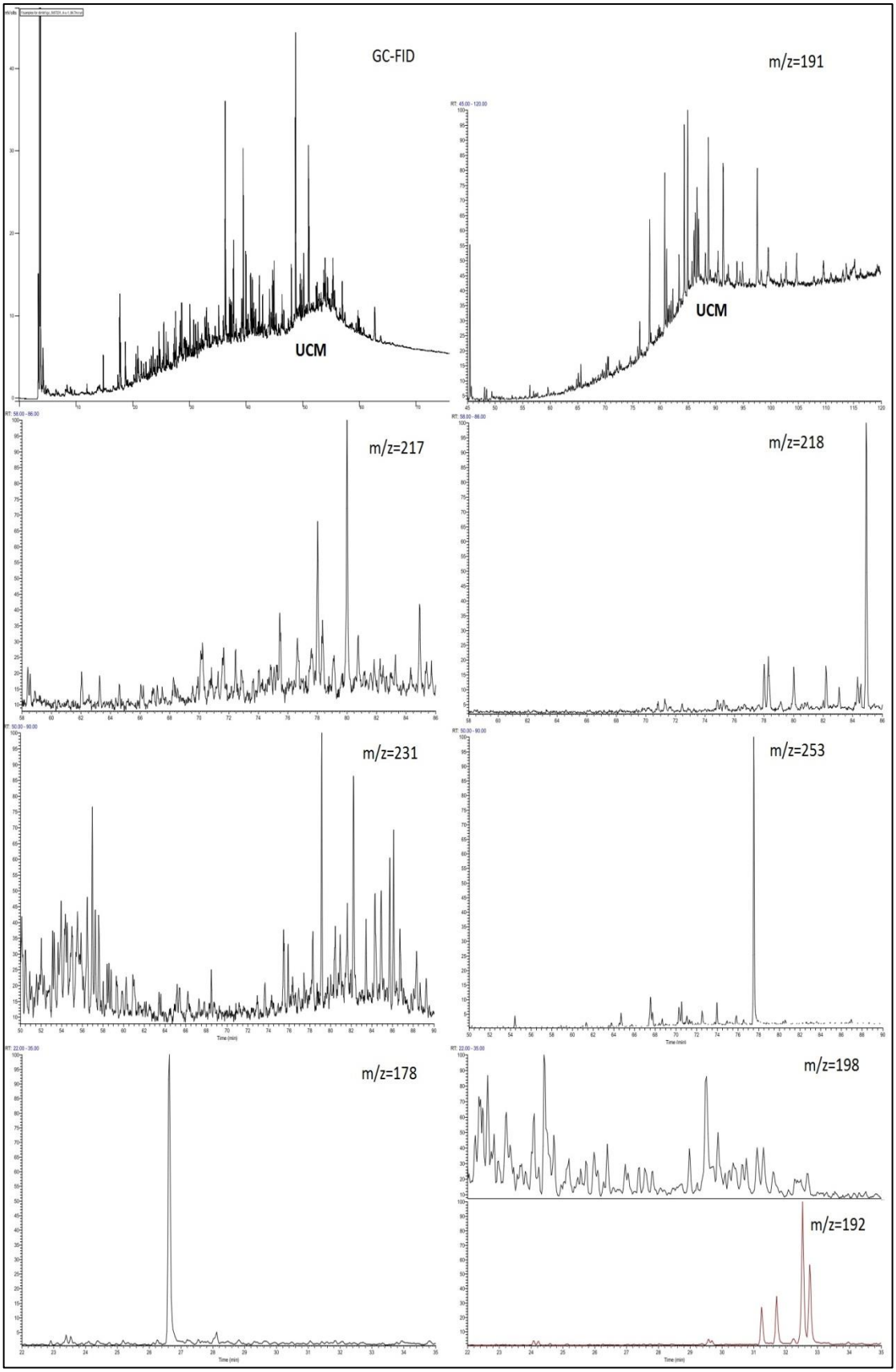

Figure 6.12: Overview of GC-FID and GC-MS chromatograms for source rock sample "S8" from well 7231/4-U-1.

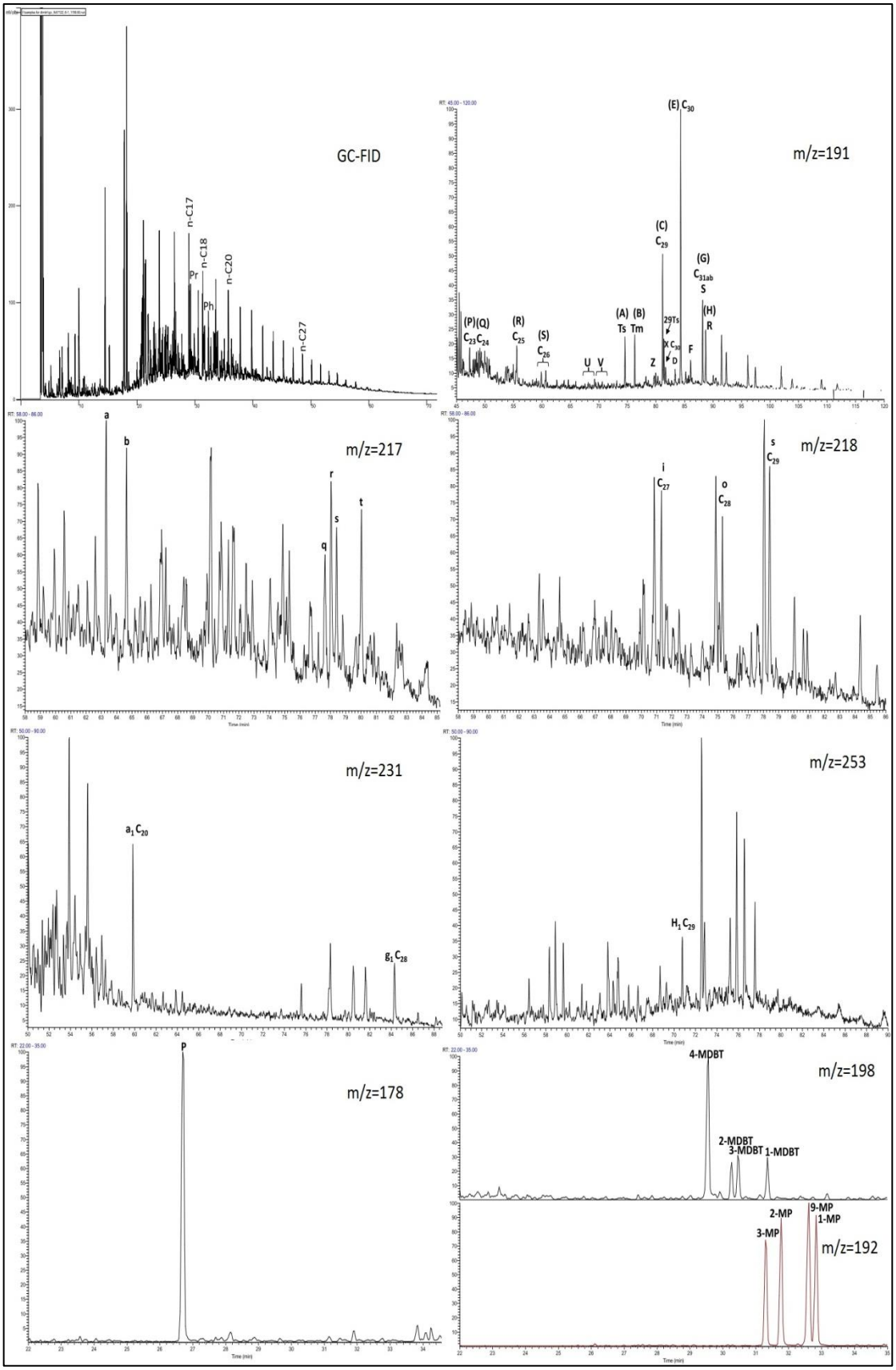

Figure 6.12: Overview of GC-FID and GC-MS chromatograms for source rock sample "S1" from well 7122/6-1.

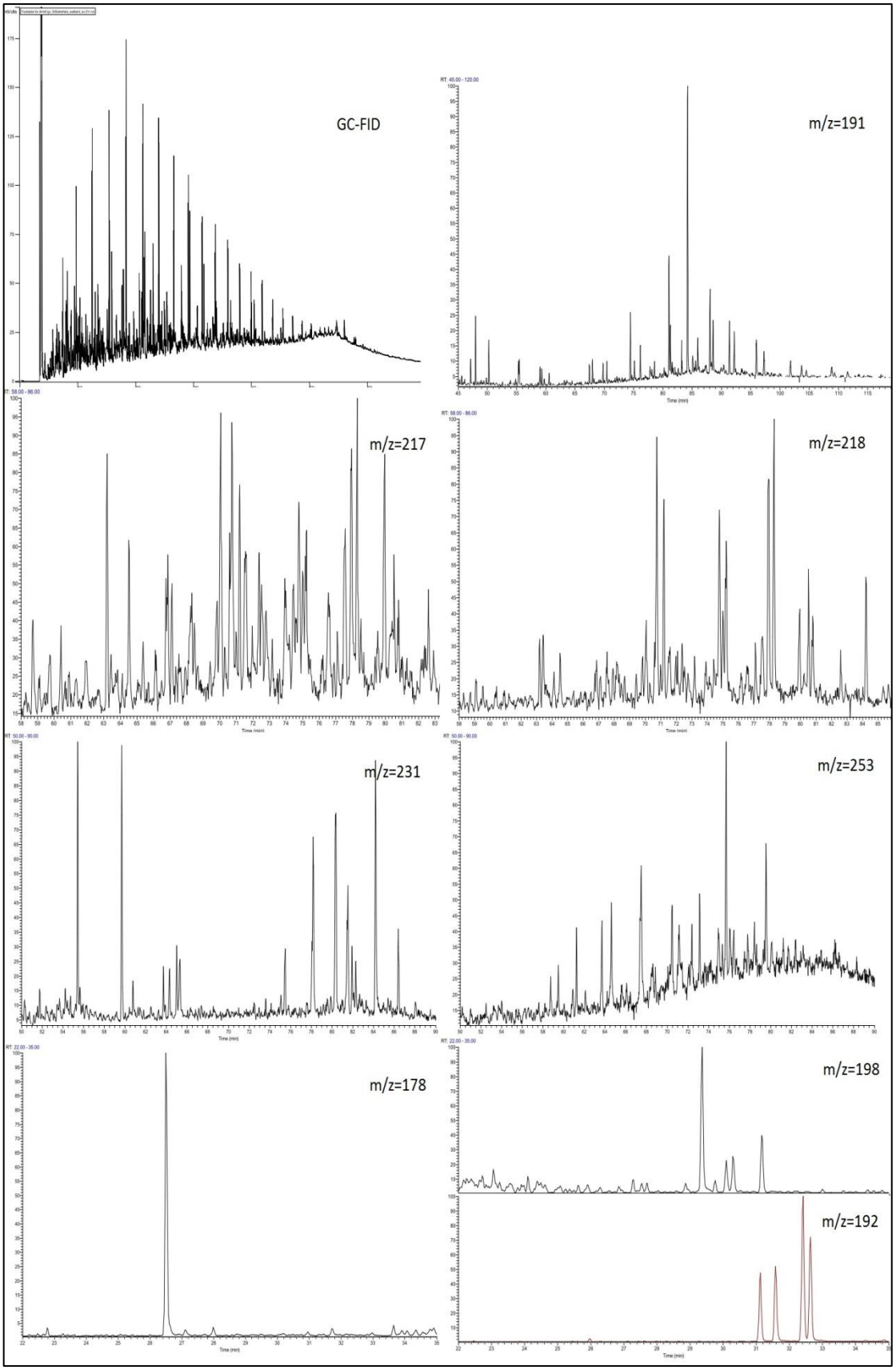

Figure 6.12: Overview of GC-FID and GC-MS chromatograms for the outcrop sample "SO-21" from Svalbard.

Chapter 7

Discussion

The results from the previous chapter are discussed in Chapter 7. Several cross-plots have been generated to identify the maturity sequence, organofacies and to find evidence for biodegradation in order to correlate the source rocks with the crude oils.

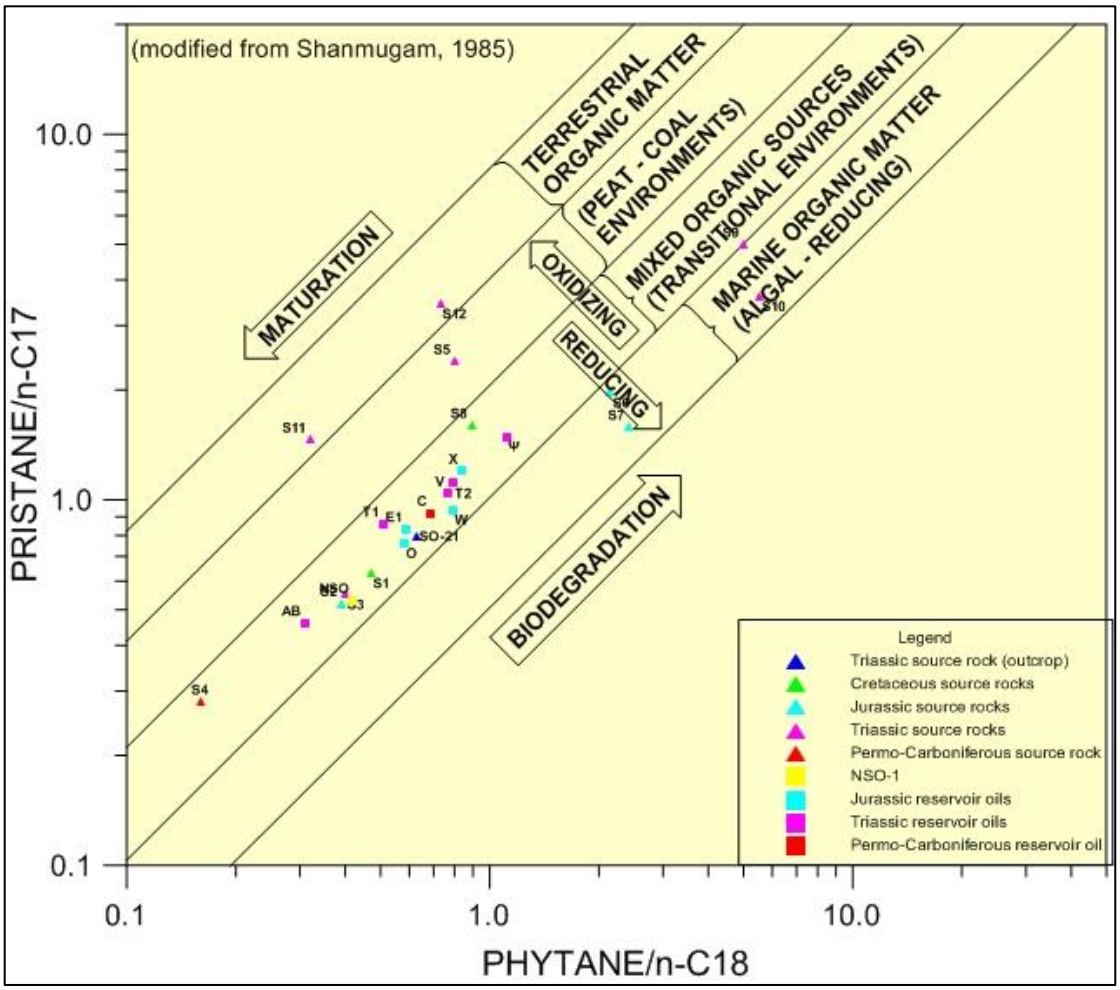

Figure 7.1: Crossplot of phytane/n-C_{18} with pristane/n-C_{17}, showing maturity, biodegradation and depositional environment variations among the studied datasets, after Shanmugam (1985). Oil sample (Ψ) is sample (Ø).

Figure 7.1 illustrates the crossplot between the isoprenoids and *n*-alkane ratios as proposed by Shanmugam (1985). This cross-plot is very important because it summarizes the data regarding biodegradation, maturation and organofacies. The ratios pristane/n-C_{17} and phytane/n-C_{18} decrease their values with maturity as the *n*-alkanes dominate over isoprenoids. Most of the samples plot in the "mixed organic

sources" area which is typical for paralic-transitional environments and they also appear to be medium to low biodegraded. As in figure 7.11 samples S12, S5 and S11 show high terrestrial organic matter input and samples S9 and S10 are probably derived from algal-marine environment, though they are highly biodegraded. The Hekkingen shales S6 and S7 fall also under the pure marine organic matter area and seem to have suffered medium biodegradation.

According to Hunt (1996) oil to source rock correlation could be much trickier compared to oil to oil correlation. The problems addressed are mainly caused by the sampling methods and the laboratory analytical techniques. For instance, extracting oils from source rocks decreases the quantity of the volatile hydrocarbons in the C_{12}-C_{15} range. Consequently, the reservoir oil samples must be heated at certain temperature to remove the same amount of volatile compounds. Another technical issue is contamination of the core samples from well-cuts during the drilling operations. Additionally, there are geological problems which include bacterial degradation, uplift and erosion cycles as well as differential thermal maturity between given source rocks and oil bearing reservoir rocks. Oils extracted from one particular source rock interval can vary in geochemical composition from reservoir oils which were expelled from the bulk formation of the source rock. Another limitation is phase fractionation which takes place during secondary migration and results into loss of light hydrocarons. It must also be stressed that the source rocks expel oils of varied geochemical composition during their generation history, since the organic matter is progressively subjected to higher temperatures in greater depths. Finally, the bitumens that are in vivo extracted from the source rocks can have different composition than the previously expelled oil from the bedding planes and microfractures of the source rocks in nature (Hunt, 1996).

However, there are certain biomarker parameters that do not change their properties significantly with thermal maturation and can be safely used for oil to source rock correlation. The discussion of these geochemical parameters is subdivided into the medium range (e.g Pr/Ph, Pr/*n*-C_{17}, Ph/*n*-C_{18}, CPI and aromatics) and biomarker range parameters.

The aromatics, methyldibenzothiophenes and methylphenanthrenes are made by components having carbon numbers in the C_{14}-C_{18} range. The methyldibenzothiophenes contain sulphur into their aromatic structure which makes the molecules less stable; hence methyldibenzothiophene molecules are sensitive and respond even to minute maturity increase in the early part of the oil window, in contrast to the methylphenanthrene molecules which respond much better to higher maturities towards the condensates. It was concluded that the sulphur incorporated into the aromatics makes the parameter $\%R_c$=0.073*MDR+0.51 (Radke, 1988) in figure 7.9 to be more sensitive than the parameter $\%R_c$=2.242*F1-0.166 (Kvalheim *et al*., 1987) in figure 7.8.

These will be further discussed in the following sub-chapters:

7.1 Biomarker maturity parameters

7.2 Medium-range (aromatics) maturity parameters

7.3 Organic Facies signatures and Biodegradation

7.4 Comparison of Medium-range parameters and Biomarkers

7.1 Biomarker maturity parameters

One of the best biomarker maturity indicator is the crossplot of ββ/(ββ+αα) of C_{29} (20R+20S) sterane isomers with the 20S(20S+20R) of C29 5α, 14α, 17α(H) sterane (Fig. 7.2). All values plot from near-zero to circa 0.7 (equilibrium) on X axis and from near-zero to circa 0.53 on Y axis. The ββ/(ββ + αα) ratio (X axis) is independent of source organic matter input and reaches equilibrium much slower than the 20S/(20S +20R) ratio (Y axis) (Seifert & Moldowan, 1986; Peters *et al.,* 2005).

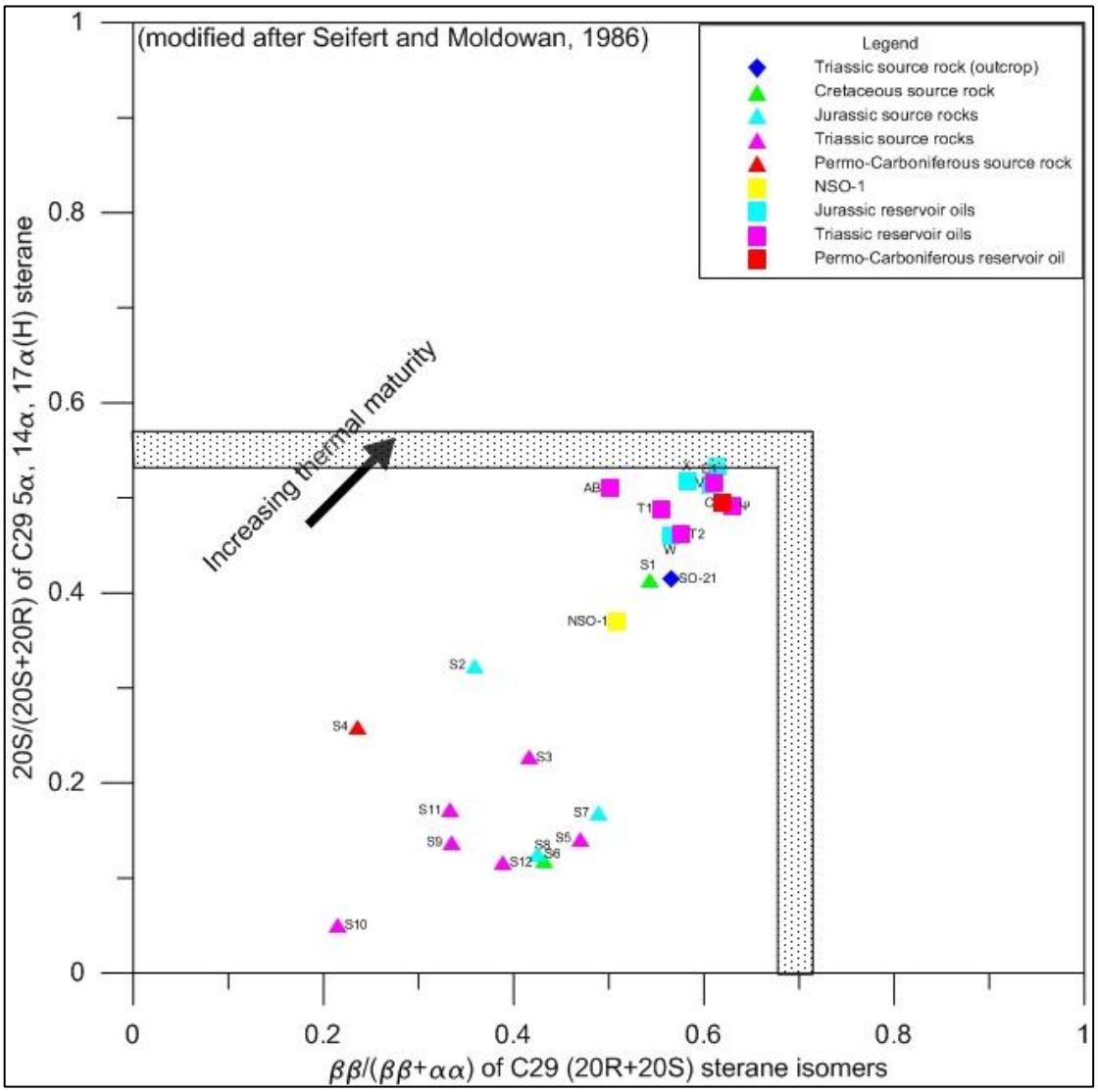

Figure 7.2: Crossplot of ββ/(ββ+αα) of C_{29} (20R+20S) sterane isomers with 20S(20S+20R) of C_{29} 5α, 14α, 17α(H) sterane. The stripled area marks the endpoints for the reactions. Oil sample (Ψ) is sample (Ø). Modified after Seifert and Moldowan (1986).

The crossplot of ββ/(ββ+αα) versus 20S(20S+20R) can effectively determine the maturity for both source rocks and oils. All the oil samples show high maturation and plot at the far right corner of the crossplot. This trend is expected for old oils from the Mesozoic and Paleozoic. Only two of the source rocks, namely the Cretaceous shale from the Kolmule Formation (S1) and the Upper Triassic black shale outcrop sample from the De Geerdalen Formation (SO-21) plot at the mature range area. Most of the Triassic and Jurassic (S6 and S7 from the Hekkingen Formation) source rocks plot around the range 0.3-0.5 on X axis and 0.1-0.2 on Y axis. However, it is very important to bear in mind that other factors such as biodegradation, weathering as well as differences in organofacies, heating rates and clay catalysis can affect the (20S/20S + 20R) ratio. The Jurassic S2 sample plots in the middle of the diagram. The Triassic S10 sample should theoretically plot near S9 since their depth difference is only 30 cm and were sampled from the same formation. From the GC-FID analysis it was found that these two mudstone samples are immature and medium biodegraded. This explains why they plot as immature samples in figure 7.2. Although the S4 Paleozoic source rock was concluded to be very mature in the previous chapter, it plots at the area of low maturity in figure 7.2. This disagreement could be explainded due to poor sample quality, analytical errors or very high maturation that reversed the steranes ratios (Peters *et al*., 2005).

To sum up all the oil samples are highly mature and follow the same trend since they plot in the upper right corner of figure 7.2. On the other hand the source rocks show medium maturation and plot in the middle of the diagram. Samples S4 and S10 plot in the immature area, whereas samples S1 and SO-21 plot near the oils. The NSO-1 standard sample plots in between the source rocks and oils indicating medium-high maturity.

Figure 7.3 is a crossplot between (diasteranes/diasteranes + regular steranes) and synthetic vitrinite reflectance according to parameter 23 (Table 5.3). The diasteranes/steranes ratio is very effective when comparing oils and bitumens from the same source rock facies. In general diasteranes can survive heating in

postmature ranges where other biomarkers are destroyed (Peters *et al*., 2005). The diasteranes can also be used to identify certain source lithologies (Fig. 7.5).

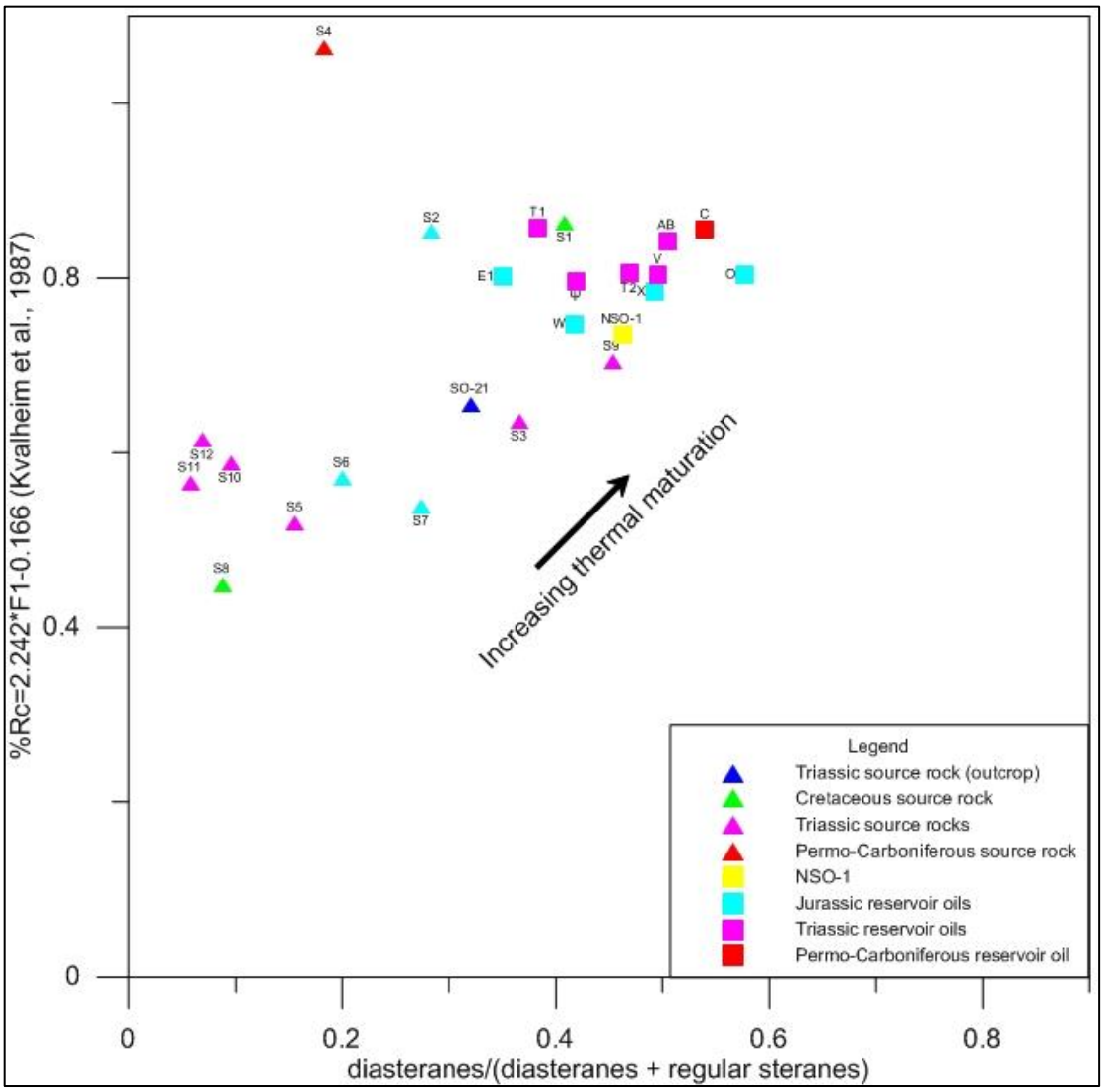

Figure 7.3: Crossplot of diasteranes/(diasteranes + regular steranes) with the calculated vitrinite reflectivity %R_c = 2.242*F1-0.166 (after Kvalheim *et al*. 1987). Oil sample (Ψ) is sample (Ø).

The vitrinite reflectance values for the oil samples fluctuate at the R_c=0.8% range and between R_c=0.5-0.63% for the source rock samples. Sample S8 falls out of the oil window. Sample S4 has the highest reflectance value. Samples S1, S2 and S9 are very mature and plot close to the oil group. Samples SO-21 and S3 plot in the middle of the diagram. Oils and bitumens which are sourced from carbonate lithologies are low in diasteranes and steranes since these lithofacies are poor in clay content which favors hydrogen-exchange reactions that in turn help steranes to rearrange to

diasteranes (Rullkötter *et al*., 1985). Although oil sample "C" was contained inside a carbonate reservoir, the high diasteranes value indicates that it was probably sourced from a shale lithology. Initially the high MDBT/MPH ratio of sample "O" was interpreted to be due to carbonate source facies but the high diasteranes value in the present diagram indicates shale source facies.

To conclude, samples S1, S2 and S9 are highly mature and seem to be closely linked to the oils of the studied dataset. It is worth noting that the Hekkingen shale samples S6 and S7 which in Ohm *et al*. (2008) are discussed as the most prolific source rocks in the western Barents Sea, fall below R_c=0.6% and do not seem to be genetically linked to the studied oils.

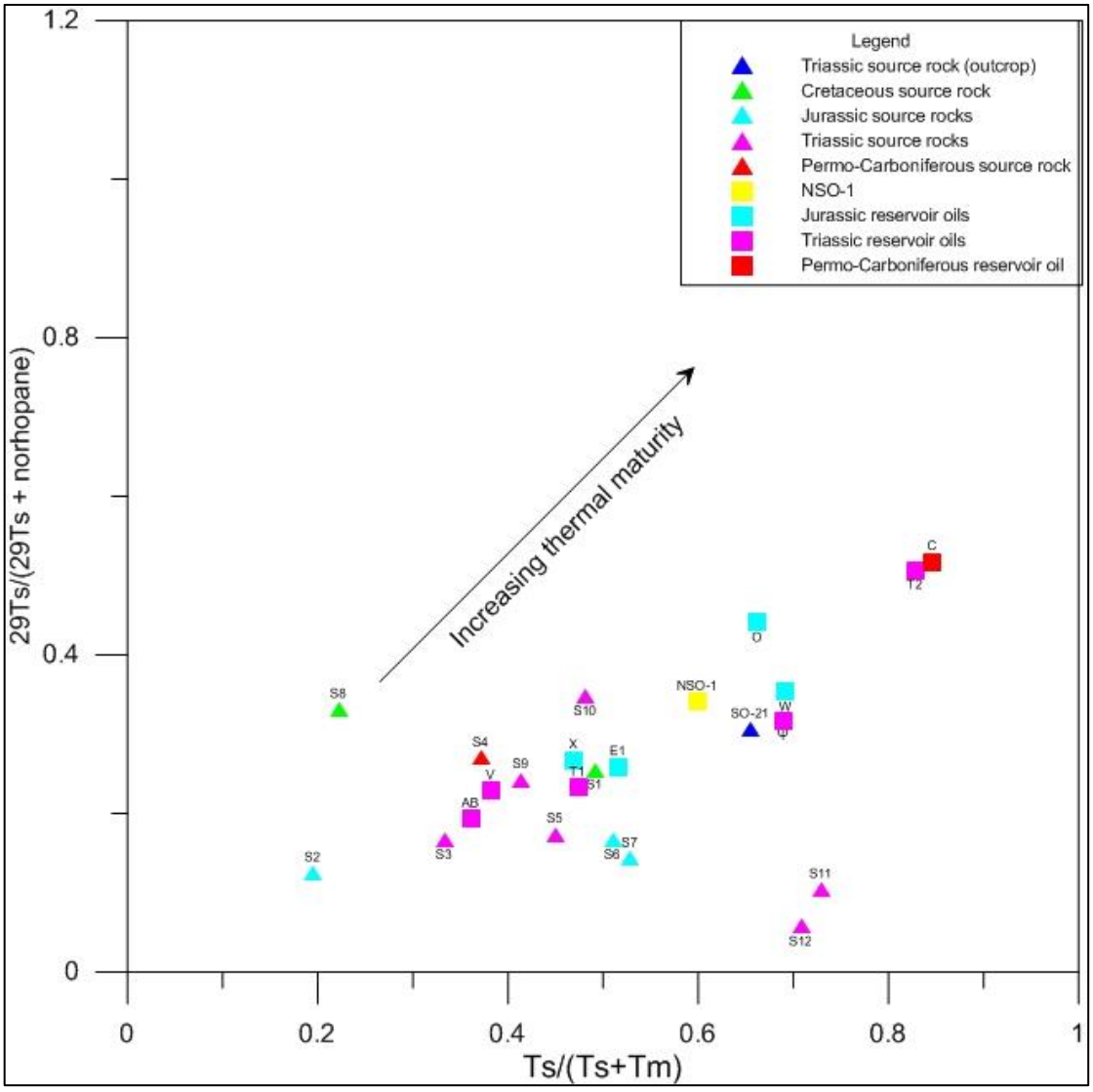

Figure 7.4: Crossplot of Ts/(Ts + Tm) with the 29Ts/(29Ts + norhopane). Oil sample (Ψ) is sample (Ø).

Figure 7.4 is a crossplot of Ts/(Ts + Tm) with 29Ts/(29Ts + norhopane), both measured on the m/z = 191 chromatogram. It is valiable for immature to post-mature samples.

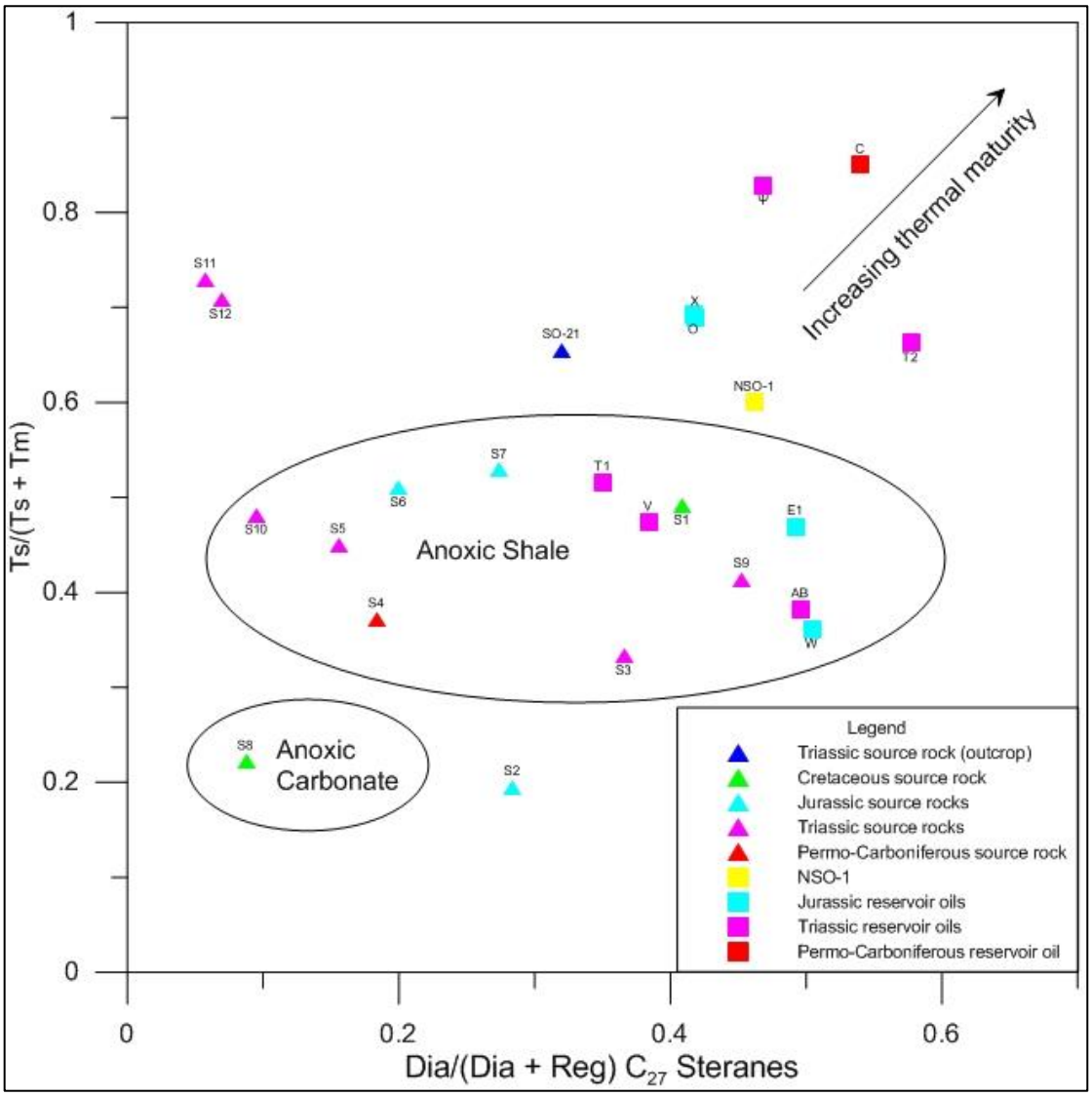

Figure 7.5: Crossplot of diasteranes/(diasteranes + regular steranes) of C_{27} steranes with the Ts/(Ts + Tm). Oil sample (Ψ) is sample (Ø). The present crossplot serves as both maturity and facies indicator.

The Ts/(Ts + Tm) parameter is strongly influenced by the source. For example oils from carbonate sources have unusually low Ts/(Ts + Tm) values compared to oils of similar maturity which are sourced from shales. On the other hand bitumen extracts sourced from hypersaline facies show abnormal high Ts/(Ts + Tm) ratios. The ratio is also affected by the Eh and pH conditions of the depositional environment. Caution must be applied when measuring the Ts, Tm peaks as other compounds (e.g

tetracyclic terpanes) may also co-elute. Finally the C_{29}Ts/(C_{29} hopane + C_{29}Ts) ratio increases with thermal maturity but slower than the Ts/(Ts + Tm) ratio (Peters *et al.*, 2005).

In figures 7.2 and 7.3 the oil and source rock values plot in totally different areas. On the other hand they plot very closely in figure 7.4. For instance the samples S3, S4, S1, S5 and S9 plot close to AB, V, T1, X and E1, all having medium to high maturity. Also the SO-21 plots near W and Ø. This fact might indicate genetic relationships between those samples.

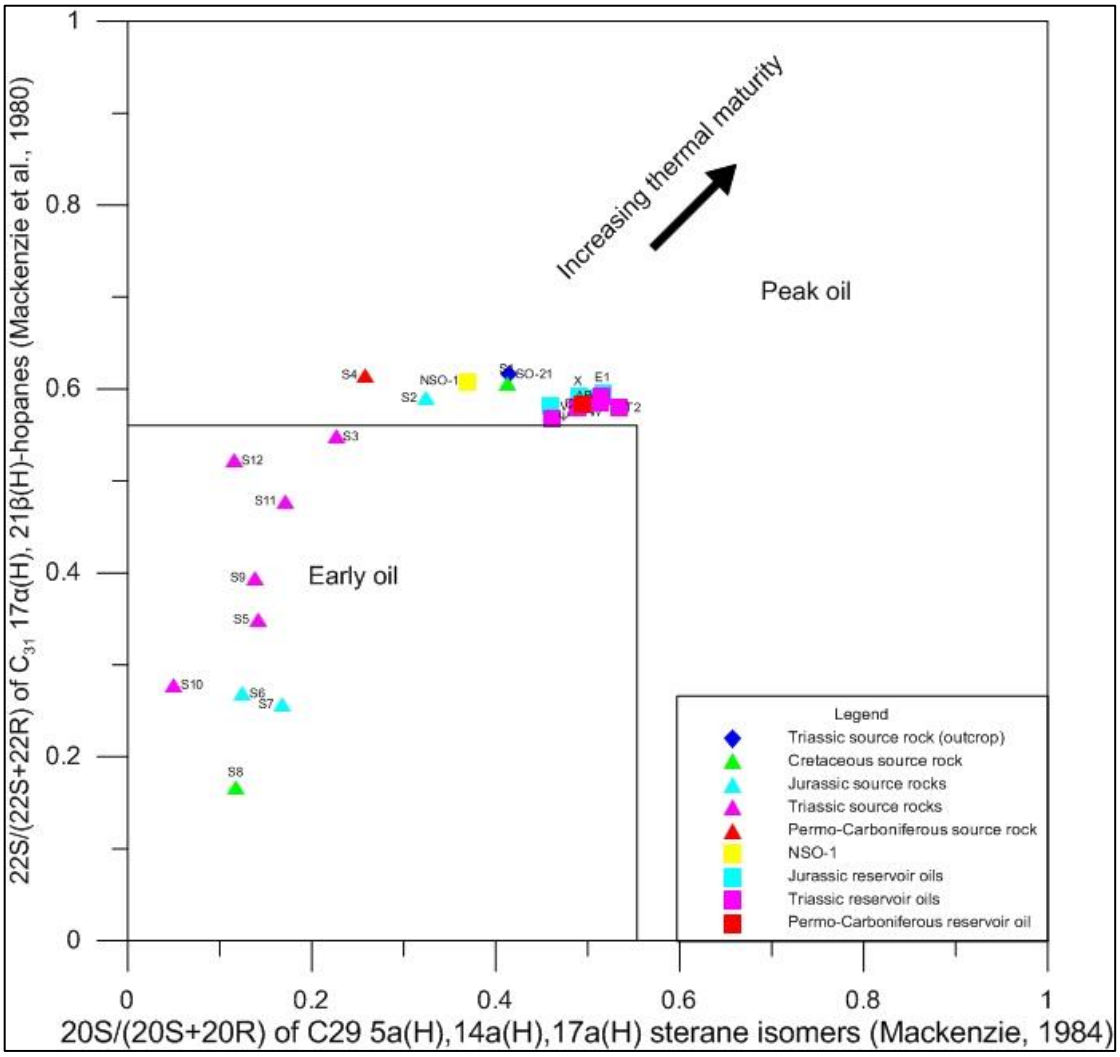

Figure 7.6: Crossplot of 20S/(20S+20R) of C_{29}5α,14α,17α(H)-sterane (after Mackenzie, 1984) with 22S(22S+22R) of C_{31} 17α(H), 21β(H)-hopanes (after Mackenzie *et al*. 1980). Oil sample (Ψ) is sample (Ø).

Figure 7.5 serves as both maturity and facies indicator as the diasteranes/steranes ratio is partly affected by the depositional environment. Even in post-mature ranges

when all other biomarkers are lost, diasteranes can survive. The samples that have medium level of maturity plot in the middle part which is typical for anoxic shales. Samples that have high Ts/(Ts + Tm) ratio and are hence mature, may show low diasteranes/steranes ratios if they are sourced from carbonates (Peters et al., 2005).

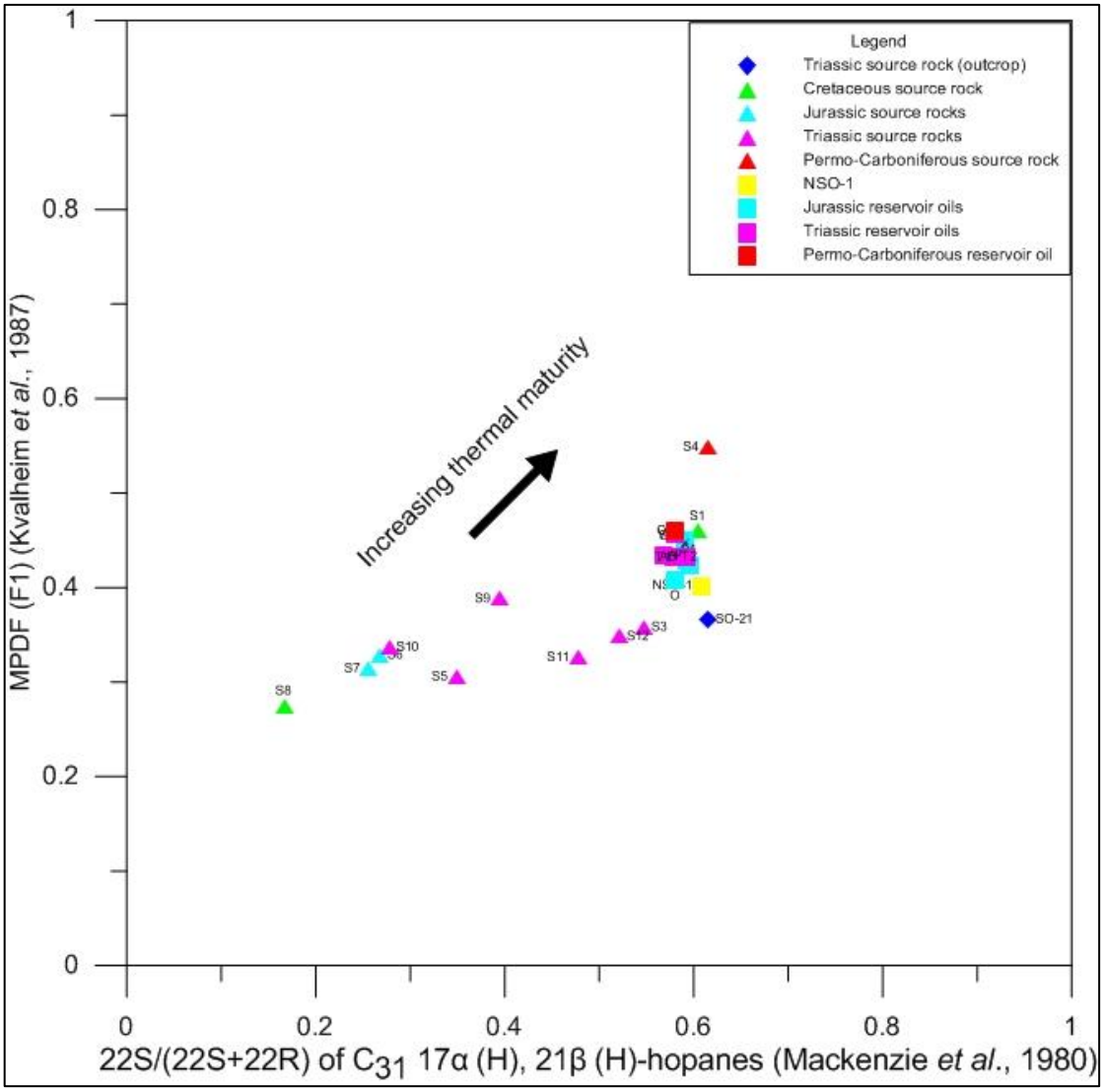

Figure 7.7: Crossplot of 22S/(22S+22R) of C_{31} 17α(H), 21β(H)-hopanes (after Mackenzie *et al*. 1980) with MPDF (F1) (after Kvalheim *et* al. 1987). Oil sample (Ψ) is sample (Ø).

Figure 7.6 is a crossplot of 20S(20S+20R) of C_{29}5α,14α,17α(H)-sterane (after Mackenzie, 1984) with 22S(22S+22R) of C_{31}17α(H),21β(H)-hopanes (after Mackenzie *et al*. 1980). These parameters are measured on m/z=217 and m/z=191 respectively. As mentioned earlier the first parameter reaches equilibrium, for values ranging between 0.52-0.55, with increasing thermal maturity and is strongly influenced by

biodegradation and organic facies. The homohopanes reach average equilibrium around 0.55 as well. All of the studied oil samples fall under these equilibriums, except for NSO-1 which is sourced from the North Sea.

All source rock samples fall under the early oil area except for four, SO-21, S4, S2 and S1 that fall in the peak oil range, probably due to high maturation (Figure 7.6).

The final plot for biomarker maturity assessment is the 22S/(22S+22R) of C_{31} 17α(H), 21β(H)-hopanes (after Mackenzie *et al*. 1980) with the methylphenanthrene distribution factor MPDF (F1) (after Kvalheim *et al*. 1987) that is calculated from the four isomers of the methylphenanthrene group (1, 2, 3, 4-MP) on m/z=192 (Figure 7.7). All samples show MPDF values in the 0.30-0.52 range, except for the S4 Paleozoic sample. The oil group plots very tightly. The source rocks range from immature to post mature. Only two of the source rock samples, S1 and S2 fall near the oil area.

To conclude the six plots (Figure 7.2-7) suggest that the source rocks range from immature to post-mature. In figure 7.6, the lowest and more immature plot at the area where the values of 20S/(20S+20R) range from 0.05-0.20 and the values of 22S(22S+22R) from 0.15-0.20. The highest and more mature plot at the 0.20-0.42 and 0.50-0.65 range, respectively. Based on the biomarker range parameters the source rocks form the following maturity sequence, from the lowest to highest: S8, S7, S6, S10, S5, S9, S11, S12, S3, SO-21, S2, S1 and S4.

On the other hand all the oil samples appear to have high maturities and tend to plot very closely to each other. Their values, in figure 7.6, show narrow distribution and range from 0.42-0.55 for the 20S/(20S+20R) ratio and from 0.55-0.61 for the 22S(22S+22R) ratio. Therefore based on the biomarker range parameters, the following oil maturity sequence is suggested, from the lowest to highest: NSO-1, O, Ø, V, X, W, T1, AB, E1, T2 and C.

It is yet difficult to address if any genetic relationships exist between the two datasets from the maturity assessment based on the biomarker range parameters.

7.2 Medium-range (aromatics) maturity parameters

The parameters 18-27 presented in Table 5.3 and Table 5.1 belong to the medium range compounds and are not considered biomarkers; for example the methyl-phenanthrene compounds are not clearly linked to any biological precursors (Radke *et al.*, 1982).

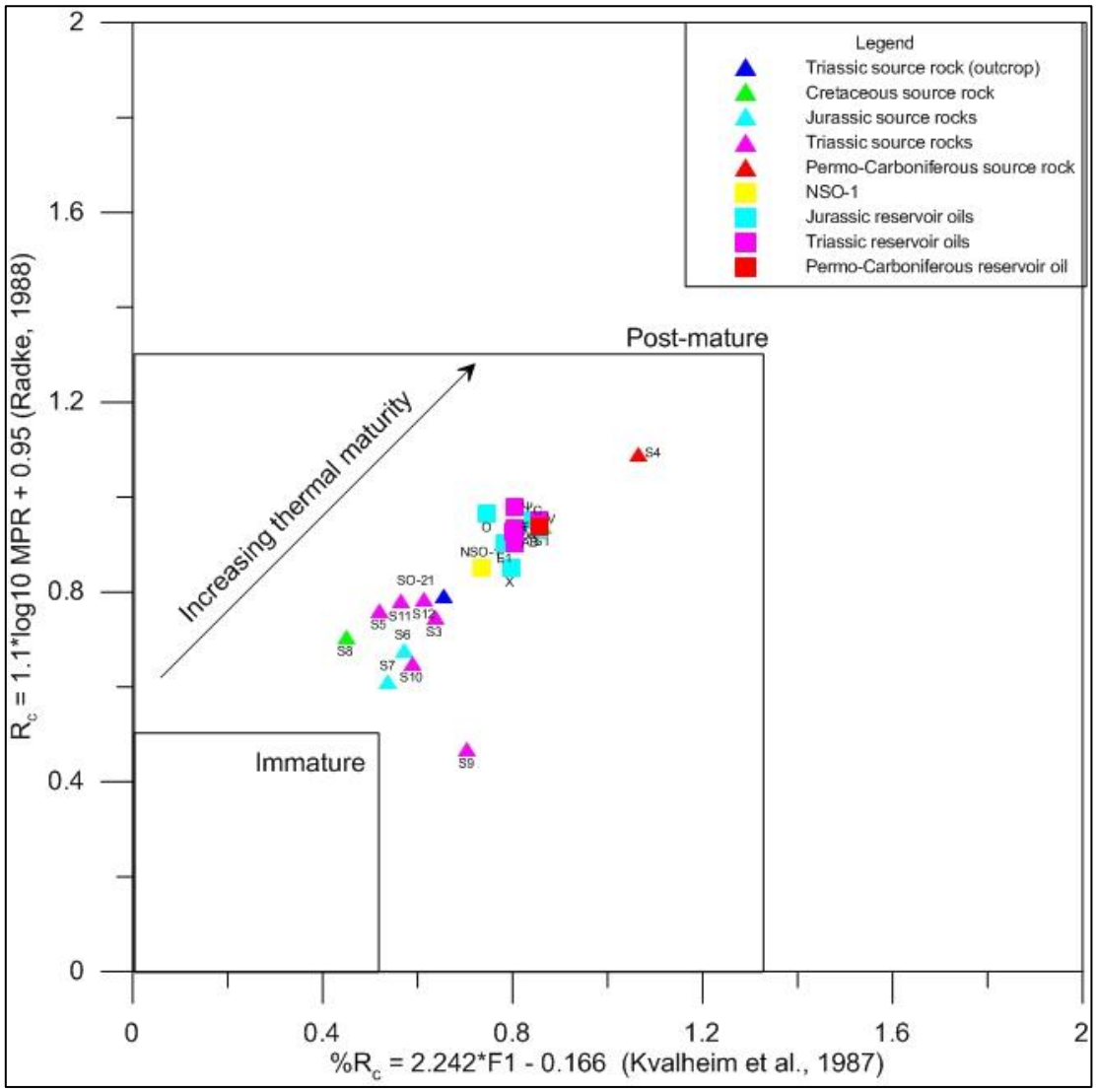

Figure 7.8: Crossplot of calculated vitrinite reflectivity, $\%R_c$=2.242*F1-0.166 (Kvalheim *et al.*, 1987) with calculated vitrinite reflectivity, R_c=1.1*log10 MPR+0.95 (Radke, 1988). Oil sample (Ψ) is sample (Ø).

Excessive thermal maturation causes the concentration of biomarkers to decrease as they crack to lighter compounds (Rullkötter *et al.*, 1984); hence the aromatic maturity parameters, both the phenanthrene and dibenzothiophene aromatic hydrocarbons which are resistant to biodegradation, especially during the early

stages of maturity (Connan, 1984) become very useful. Phenanthrenes in petroleums are originally derived from triterpenoids and steroids contained in the living organisms. Dealkylation and methylation of phenanthrenes result into the formation of methylphenanthrenes. With progressive maturation the amount of 2, 3-methylphenanthrenes increases relative to phenanthrene and 1, 9-methylphenanthrenes (Figure 7.10), therefore the ratio MPI.1 (parameter 19) increases (Radke *et al*., 1982a; Tissot and Welte, 1984). Vitrinite reflectivities were calculated (parameters 22-25, Table 5.3) using a set of formulas based on the abundances of methylphenanthrenes and methyldibenzothiophenes (Figures 7.8-13).

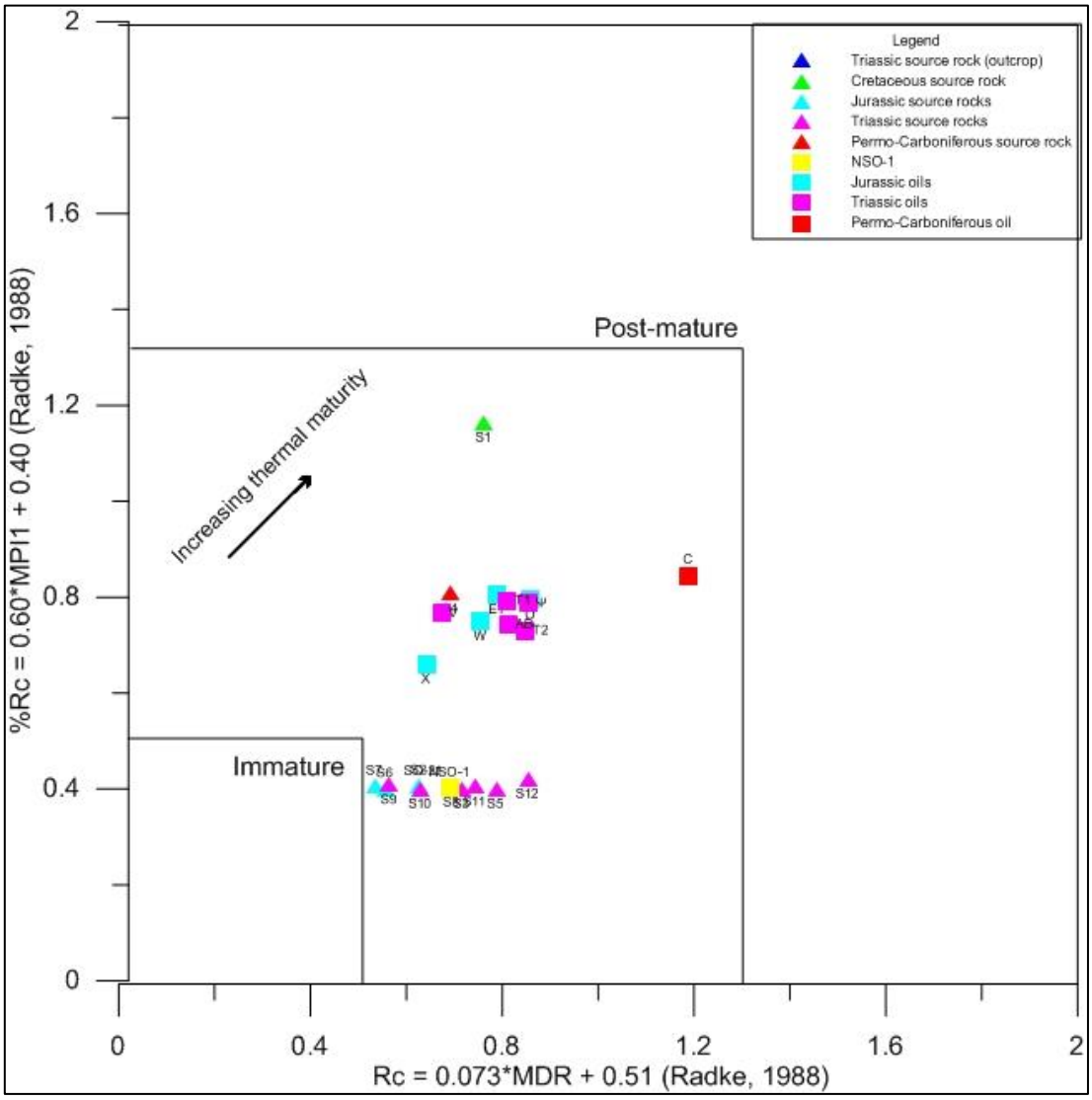

Figure 7.9: Crossplot of calculated vitrinite reflectivity, $\%R_c$ = 0.073*MDR + 0.51 with calculated vitrinite reflectivity, $\%R_c$ = 0.60*MPI1 + 0.40, both formulas from Radke (1988). Oil sample (Ψ) is sample (Ø).

Figure 7.8 illustrates the results of two different synthetic vitrinite reflectance data after Kvalheim *et al*. (1987) and Radke (1988). The oils show vitrinite reflectivities higher than 0.80% for both formulas. The source rocks range from R_c=0.40-0.80% except for S4 and S1 that move towards the post-mature zone. It must be stressed that all source rocks fall inside the oil generation zone have reflectances ranging from 0.5-1.3%. The next plot (Fig. 7.9) is probably the best for maturity assessment.

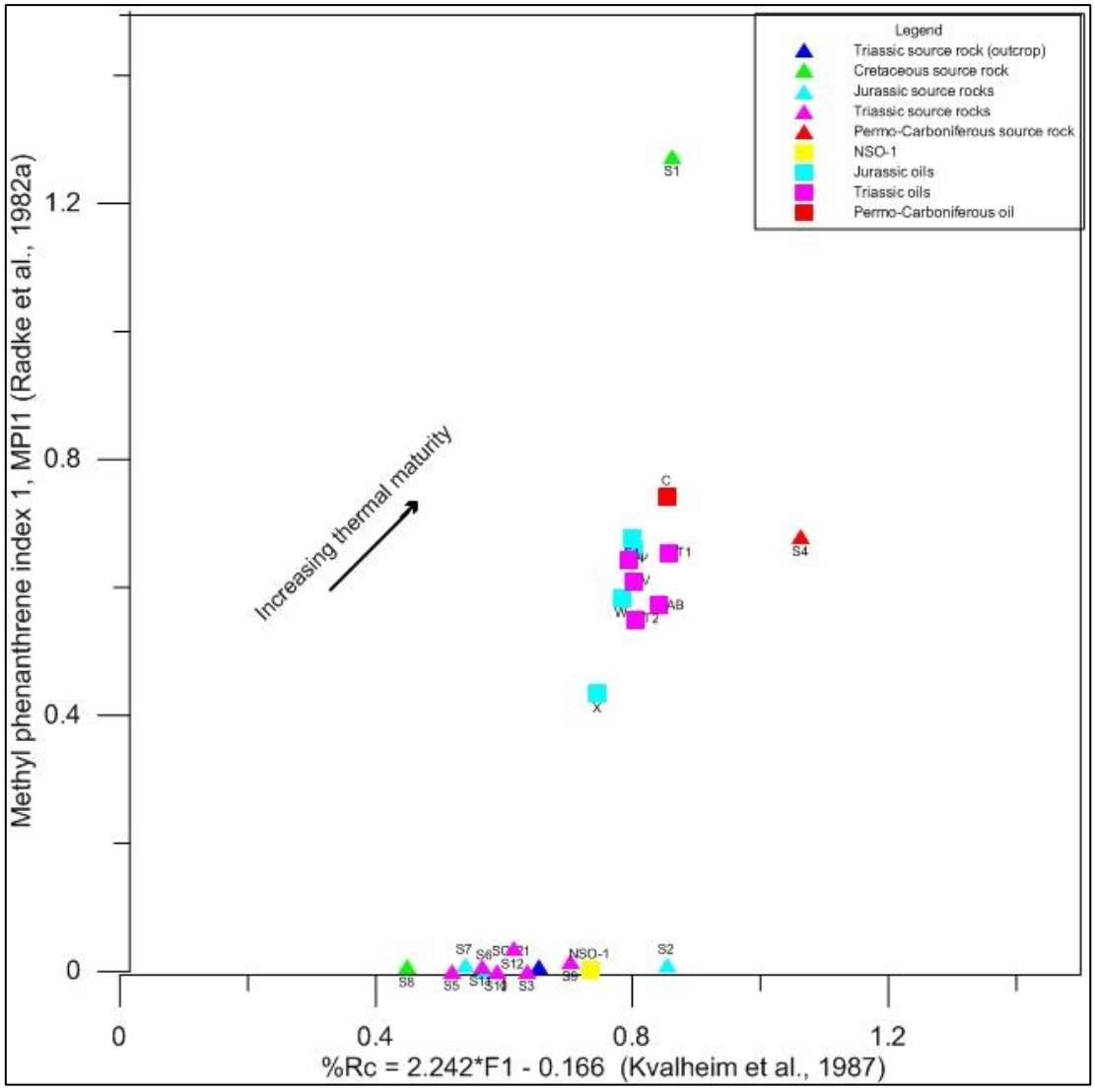

Figure 7.10: Crossplot of calculated vitrinite reflection, %R_o = 2.242*F1 - 0.166 (Kvalheim et al., 1987) with methyl-phenanthrene index 1, MPI 1 (Radke et al., 1982a). Oil sample (Ψ) is sample (Ø).

Figure 7.9 follows the same pattern as the previous plot but makes use of two different parameters of calculated vitrinite reflectance as discussed in Radke (1988). Regarding the oil dataset, the two plots (Figures 7.8 and 7.9) show similarities with

the oils plotting in the R_c=0.80% range. On the other hand there are not any relationships between the source rocks. The source rocks show linear increase for the R_c=0.073*MDR+0.51 formula but there is hardly any distinction between them when deploying the R_c=0.60*MPI1+0.40 formula. However sample S4 plots close to the oils and sample S1 plots very high, near the post-mature area.

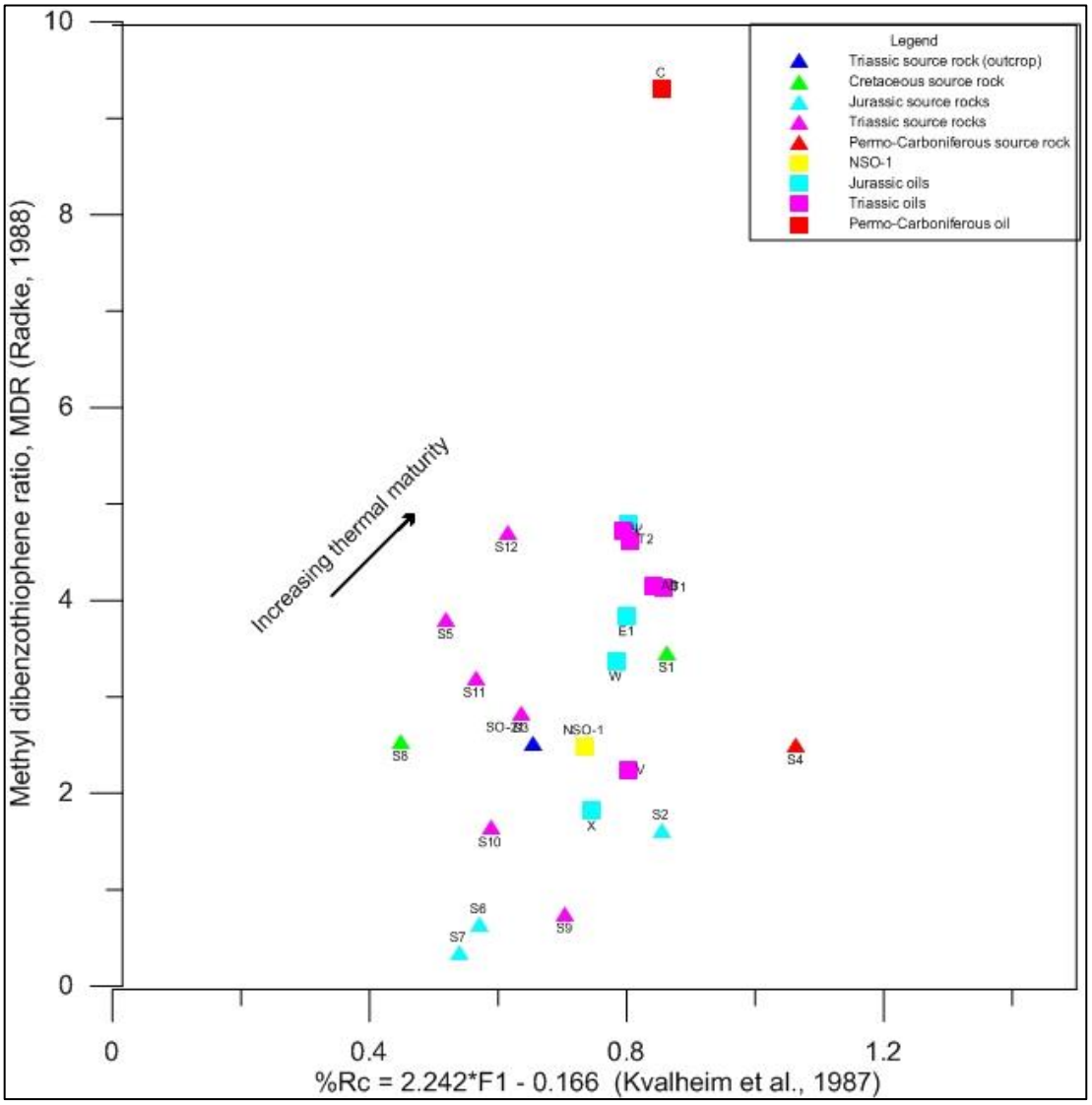

Figure 7.11: Crossplot of calculated vitrinite reflection, R_c=2.242*F1-0.166 (Kvalheim et al., 1987) with methyl-dibenzothiophene ratio, MDR (Radke, 1988). Oil sample (Ψ) is sample (Ø).

Due to disagreements between the formulas discussed in Radke (1988), the calculated vitrinite reflectance from Kvalheim *et al*. (1987) was selected to plot against the methylphenanthrene index 1, MPI.1, in figure 7.10 (Radke *et al*., 1982a). Again the oils plot in the middle part of the diagram and source rock samples S1 and

S4 show a tendency to plot far off their dataset. The rest source rocks have very low methylphenanthrene values and plot close to zero. These source rocks are probably low mature so that the methylphenanthrene ratio was not yet differentiated. On the other hand the methyldibenzothiophenes change their values more rappidly than methylphenanthrenes and are hence more useful (Figure 7.11). The samples in figure 7.11 appear mixed. The lowest maturity comes from the Hekkingen shales S6, S7 and the Steinkobbe shale S9. The Triassic and Jurassic oils seem to have the exact maturation degree. However it is not easy to address genetic relationships between the two datasets from figure 7.11, as the samples plot in a mixed trend.

To sum up, the source rock samples appear to be early mature, close to the onset of the oil window. The oil samples have medium to high maturities with values around R_c=0.80%. The paradox of source rocks having lower vitrinite reflectance values than oils which were ideally sourced from them could be explained by the sampling methodology. Almost all the source rocks were "cut" from structural highs in western Barents Sea, from the same and occassionally shallower depth than oils. The original source rock kitchen may belong to the same geological formations as the source rocks of the present dataset, but they are located in the deeper parts of the basin. These generated and expelled petroleum, probably during Mesozoic and continued subsiding. Therefore maturity assessment is not very efficient when comparing so many different samples with such a limited number of samples. Nevertheless, organic facies analysis indicates better potential genetic relationships since the type of organic input serves as a better correlation tool.

Figures 7.12 and 7.13 are crossplots of facies parameters and aromatic maturity data. The oil samples plot at the same area and source rock samples S6 and SO-21 plot close to them. Based on both figures, samples S10, S11 and S5 are either biodegraded or very immature, since the pristane dominates over *n*-C_{17}. This occurs because the pristane (also phytane, depending on the redox conditions) that is inherited directly from the living organisms is contained in high amounts inside the immature samples and decreases with maturation as the *n*-alkane peaks pop-up.

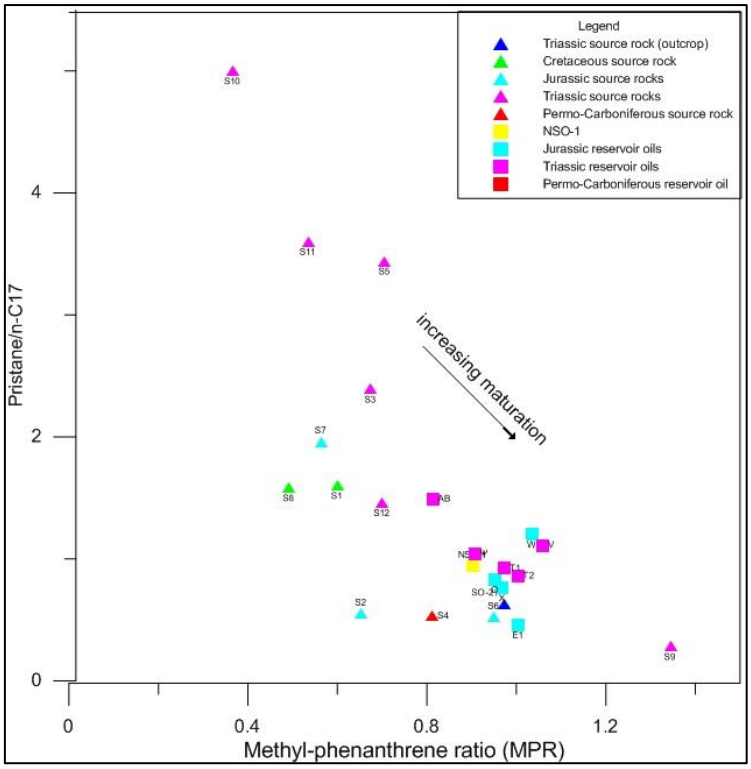

Figure 7.12: Crossplot of methylphenanthrene ratio (MPR) (Radke *et al.*, 1982a) with pristane/n-C_{17}. Oil sample (Ψ) is sample (Ø).

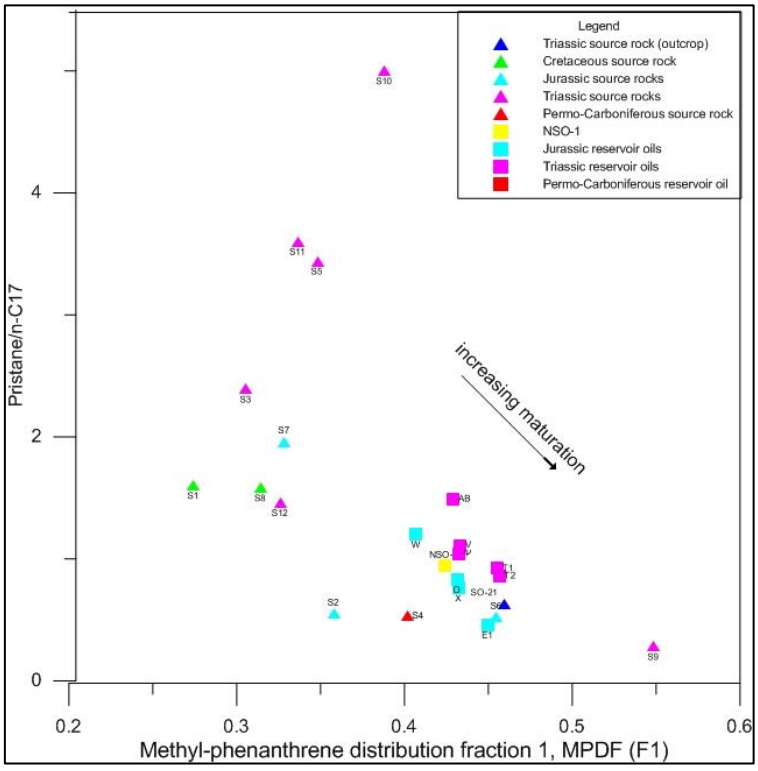

Figure 7.13: Crossplot of methylphenanthrene distribution fraction 1, MPDF (F1) (Kvalheim *et al.*, 1987) with pristane/n-C_{17}. Oil sample (Ψ) is sample (Ø).

When hydrocarbons are microbically attacked, the first organic compounds to experience biodegradation are the normal alkanes, like *n*-C_{17} and *n*-C_{18}. The pristane and phytane are isoprenoids that are more difficult to biodegrade; hence bacteria prefer to attack the chain of the *n*-alkanes, especially during incipient biodegradation. However, knowing that it is more difficult for source rocks to get biodegraded than oils, the Triassic samples S10, S11 and S5 are more likely to be immature rather than biodegraded.

To conclude the six plots (Figure 7.8-13) suggest that the source rocks range from immature to late mature. In figure 7.9, the lowest and more immature plot at the area where the values of R_c=0.0.73*MDR+0.51 range from 0.50-0.85% and the values of R_c=0.60*MPI1+0.40 are constant at 0.40%. The highest and more mature plot at the 0.63-0.80% and 0.80-1.20% ranges, respectively. Based on the medium range parameters the source rocks have the following maturity sequence, from the lowest to highest: S8, S5, S7, S11, S6, S10, S12, S3, SO-21, S9, S2, S1 and S4. This sequence does not differ greatly from the one suggested based on the biomarker range parameters. On the other hand all the oil samples appear to have high maturities and tend to plot again very closely to each other. They are narrow distributed in figure 7.9 and range from 0.52-0.85% for the R_c=0.0.73*MDR+0.51 (sample C reaches 1.2%) and from 0.60-0.81% for the R_c=0.60*MPI1+0.40. Therefore based on the medium range parameters, the following oil maturity sequence is suggested, from the lowest to highest: NSO-1, X, T2, W, AB, V, Ø, O, E1, T1 and C. This sequence shows a limited match with the maturity sequence based on biomarkers.

7.3 Organic Facies signatures and Biodegradation

Certain biomarker and non-biomarker parameters were used to construct plots that can indicate the organic facies and biodegradation level of the samples. Oils that are derived from lacustrine source rocks will have a predominance to contain little sulphur except if they come from hypersaline lacustrine environments (Peters *et al*., 2005). Therefore, the 3-methylphenanthrene/4-methyldibenzonthiophene ratio can indicate if the depositional environment is marine or lacustrine (Figure 7.16), since the methyldibenzothiophene structure is rich in sulhpur. Source rocks that were

generated under anoxic marine settings have predominance for 28, 30-bisnorhopane (Figure 7.17).

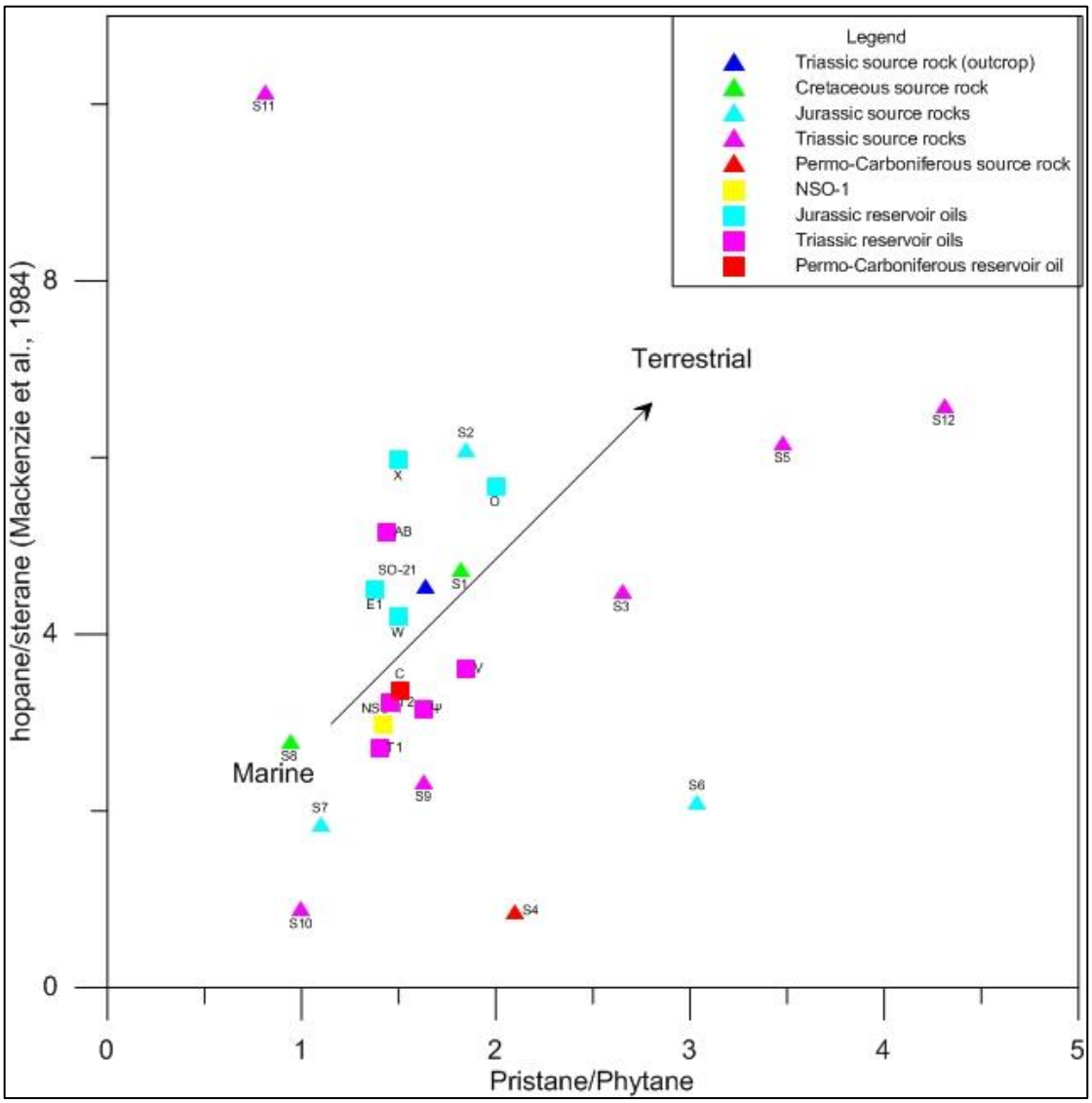

Figure 7.14: Crossplot of pristane/phytane with hopane/sterane ratio (Mackenzie *et al.*, 1984). Oil sample (Ψ) is sample (Ø).

However high maturation can alter significantly the biomarker components of oils or bitumen extracts and hence lead to false interpretations (Peters *et al.*, 2005).

Oils or bitumens which are derived from marine source rocks tend to have high sterane concentrations, therefore the hopane/sterane ratio in figure 7.14 (Mackenzie *et al.*, 1984) decreases (Moldowan *et al.*, 1985). High pristane concentrations or pristane/phytane (Pr/Ph) ratios indicate terrestrial input (Philp,

1994) but progressively higher maturities will also increase the ratio (ten Haven *et al*., 1987). Finally very high pristane/phytane ratios (>3) indicate coaly source rocks (Peters *et al*., 2005).

Figure 7.14 makes use of both pristane/phytane and hopane/sterane ratios. All the oils appear to have mixed sources, although Triassic oils have a preference for marine organic matter and Jurassic oils for more terrestrial. The source rock samples S10, S8 and S7 appear to be purely marine. Samples S2, S1, S9, S3 and SO-21 have mixed sources. Samples S5 and S12 seem to be strongly influenced by terrestrial sources.

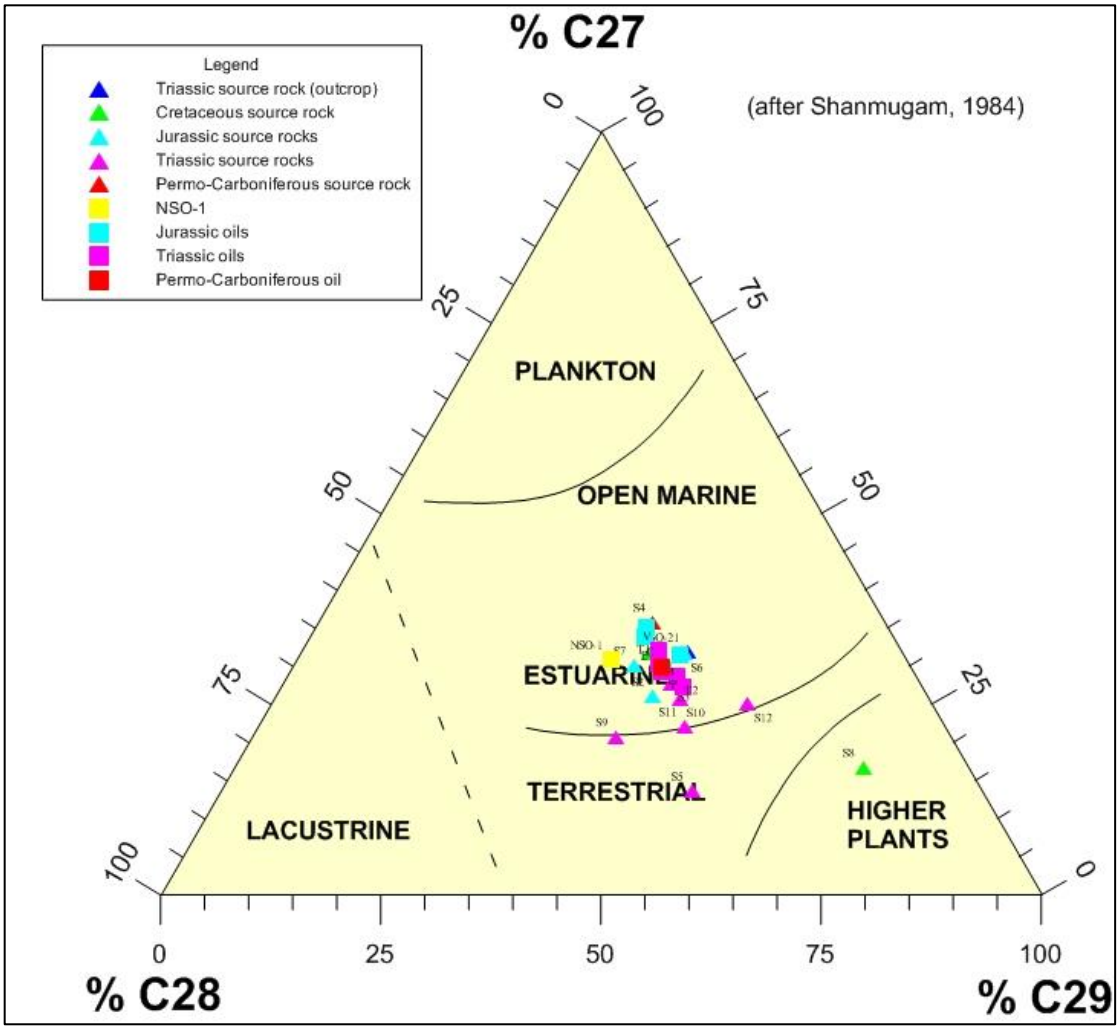

Figure 7.15: The sterane distribution ternary diagram, after Shanmugam (1984). Most of the source rocks and all the oil samples show a predominance for estuarine environments. Sample S5 is terrestrial sourced and S8 is derived from higher plants. Oil sample (Ψ) is sample (Ø).

Figure 7.15 shows the sterane distribution of C_{27}-C_{28}-C_{29} steranes as discussed in Shanmugam (1984). There are many similarities with figure 7.1. For instance the majority of the samples fall under the estuarine area which describes transitional environments with mixed organic sources. The samples S11, S12 and S5 appear to be affected by terrestrial input. Sample S8 plots in the higher-plants area. Details as such would not be identified from figure 7.1.

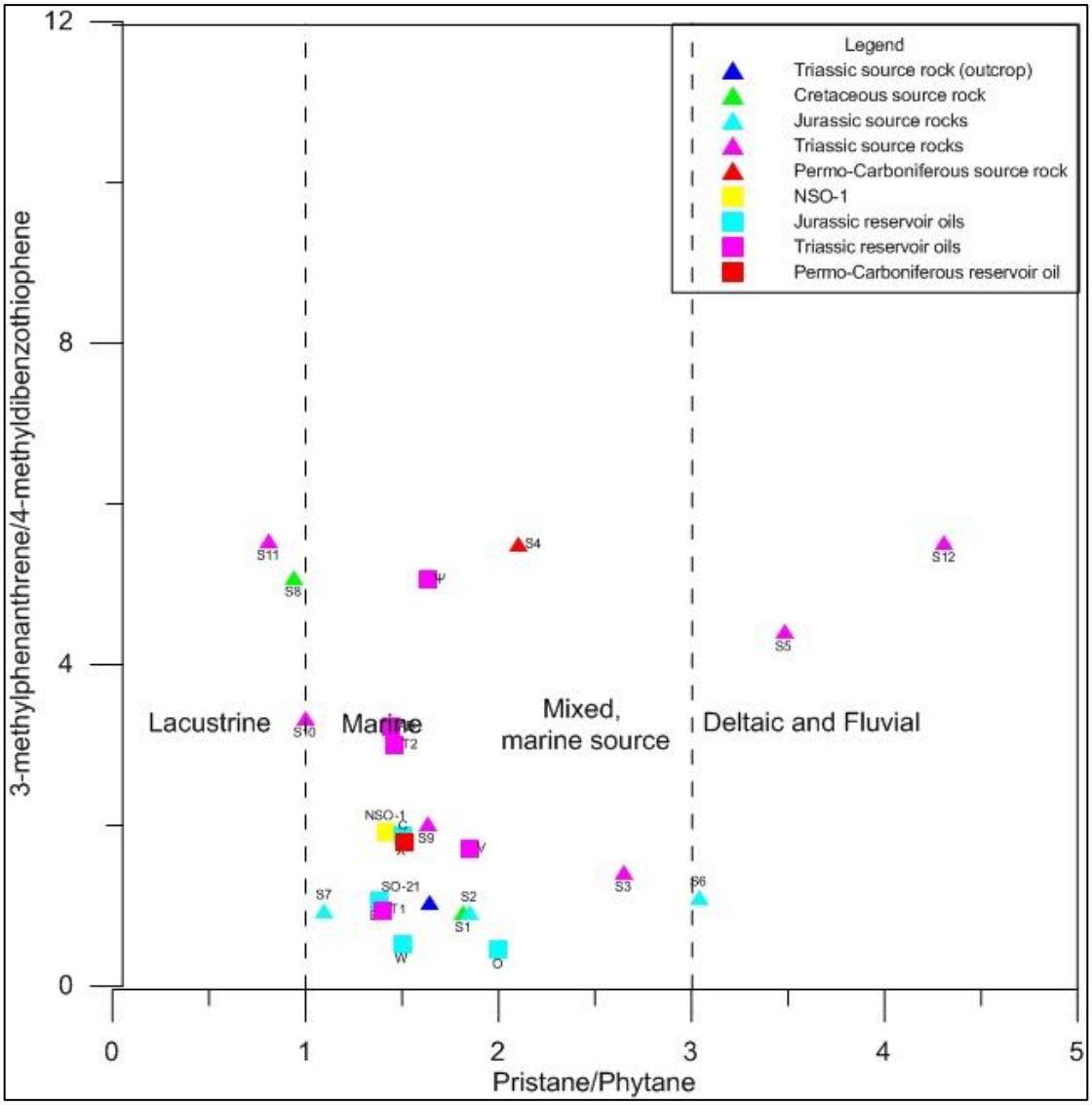

Figure 7.16: Crossplot of pristane/phytane with 3-methylphenanthrene/4-methyldibenzothiophene (Radke *et al*., 2000). Oil sample (Ψ) is sample (Ø). (Modified from Hughes *et al*. 1995).

Figure 7.16 is a crossplot between pristane/phytane and 3-methylphenanthrene/4-methyldibenzothiophene (Radke *et al*., 2000) ratios. The pristane/phytane ratios that are lower than 1.0 indicate lacustrine settings. Between 1.0-2.0 indicate pure marine

settings and between 2.0-3.0 indicate mixed marine sources. Finally those that are higher than 3.0 indicate deltaic-fluvial environments. As described earlier, low sulphur content returns low 3-methylphenanthrene/4-methyldibenzothiophene ratios. This is typical in lacustrine settings. On the contrary, high sulphur amount indicates marine settings. However, since dibenzothiophenes are durable against biodegradation, they may concentrate against other compounds and lead to high sulphur contents, causing wrong interpretations (Tissot and Welte, 1984).

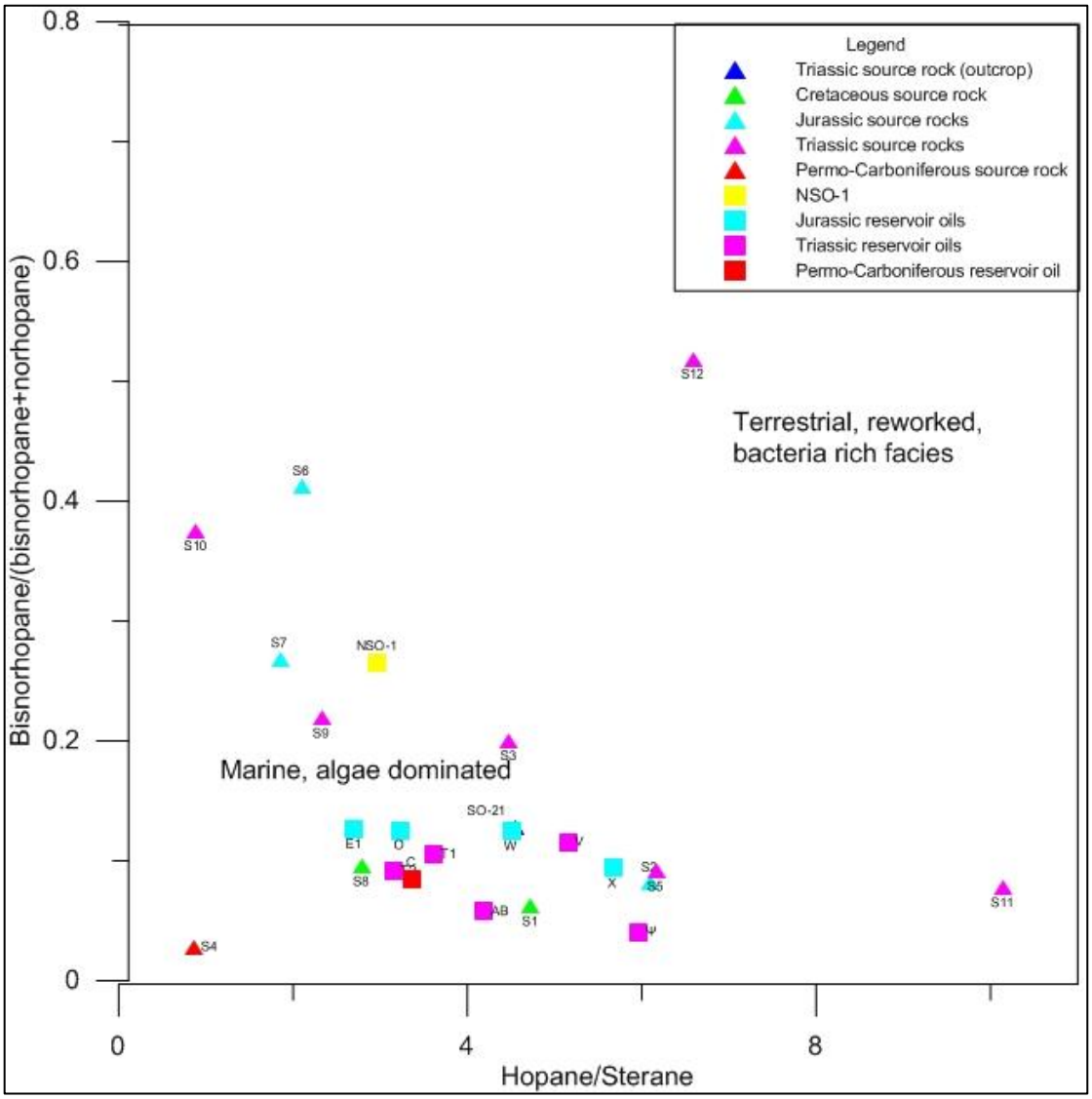

Figure 7.17: Crossplot of hopane/sterane ratio with bisnorhopane/bisnorhopane+norhopane) ratio. Oil sample (Ψ) is sample (Ø).

This time most of the samples concentrate towards the marine area (Figure 7.16). This is important because previous figures suggested mixed marine sources. Figure

7.16 also suggests that the samples S8 and S11 plot at the lacustrine area. Samples S3 and S4 plot in the mixed, marine source area and finally samples S5 and S12 plot clearly inside the deltaic-fluvial area.

Figure 7.17 is a crossplot between the hopane/sterane (Mackenzie *et al.,* 1984) and the bisnorhopane/bisnorhopane+norhopane (Wilhelms and Larter, 1994) ratios. Marine algae dominated source rocks tend to have low hopane/sterane ratios, whereas bacteria reworked or terrestrial facies tend to have high ratios (Peters *et al*., 2005). High quantity of bisnorhopane indicates anoxic settings and algal organic matter input (blue algae) but not always since the Middle Jurassic coal intervals in the North Sea have very high bisnorhopane ratios (Justwan *et al*., 2006). The 17α(H),21β(H)-28,30-bisnorhopane is depleted with maturation; hence its use is limited to low-middle maturities. In addition, bisnorhopane originates from chemoautotrophic bacteria that thrive between the oxic-anoxic boundary. Bisnorophane will eventually become depleted with increasing maturatity compared to the 17α-hopane (norhopane) which will increase. Therefore the ratio of bisnorhopane/bisnorhopane+norhopane will decrease very fast (Peters *et al*., 2004; Justwan *et al*., 2006).

Most of the samples plotted in figure 7.17 show a preference for the marine, algal dominated area. Samples S10, S6 and S7 have high bisnorhopane/ bisnorhopane+norhopane ratio values, which could mainly be due to low maturity. The S6 and S7 source rock samples come from the Upper Jurassic Hekkingen Formation which is the reasonable analogue of the Upper Jurassic Draupne Formation in the North Sea. The relative abundance of bisnorhopane in the Upper Draupne shales ranges between 0.2-0.3 (Justwan *et* al., 2006). Sample S7 falls inside that range. On the other hand sample S6 is more enriched in bisnorhopane (>0.4), close to the Kimmeridge Clay (0.5) from Oseberg Field that is discussed in Dahl and Speers (1985) and is considered to be immature. In both cases the S6 and S7 samples show similarities with the Upper Draupne shales. However, the S6 and S7 samples may not ideally represent the Hekkingen Formation since they are sourced from sturtural highs and they are probably immature. Their high UCM has also a negative

effect. Samples S11 and S12 plot alone in the terrestrial facies, bacteria reworked area. The latter might be also very immature, indicated by the high bisnorhopane content.

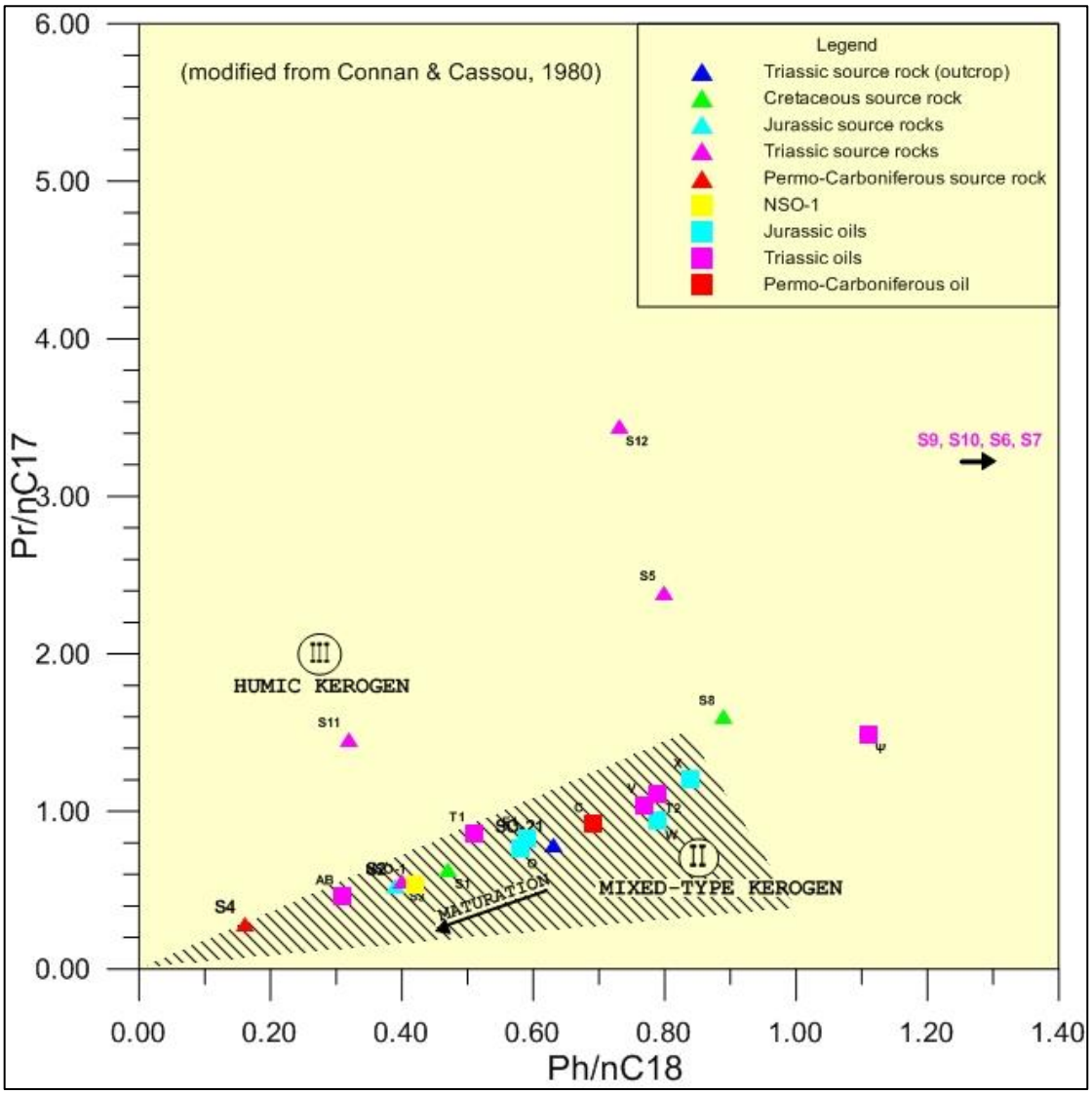

Figure 7.18: Crossplot of the phytane/n-C_{18} with pristane/n-C_{17}. Oil sample (Ψ) is sample (Ø). Modified from Connan and Cassou (1980). Note that samples S9, S10, S6 and S7 fall very far outside the present crossplot.

Figure 7.18 shows the type of kerogen contained inside the source rocks as well as the type of organic matter contained in the source rock analogues of the oils (modified after Connan and Cassou, 1980). Almost all the oils fall inside the type II mixed-type kerogen, which is in accordance to all previously discussed figures 7.1 and 7.14-17. Sample S11 contains type III humic kerogen and samples S8, S5 and oil sample Ø probably contain mixed type kerogen. The samples S9, S10, S6 and S7 take

very high values for the Ph/*n*-C_{18} ratio. High phytane could indicate biodegradation or very low maturity, as it was previously discussed in figures 7.16 and 7.17.

To identify the degree of biodegradation more crossplots were made, out of new modified parameters (Figures 7.19-7.22 and Table 7.1). Table 7.1 contains the values for the *n*-C_{15}/*n*-C_{20} and *n*-C_{25}/*n*-C_{30} ratios. For instance the *n*-C_{15}/*n*-C_{20} ratio is expected to become low with incipient biodegradation, since the low carbon number normal alkanes are the first to get attacked by the bacteria. Samples that are maturing properly are expected to follow the trendline as the *n*-alkane concentrations raise almost evenly. On the other hand biodegradation will interfere and decrease the *n*-alkane peaks.

Table 7.1: Numerical results for the *n*-C_{15}/*n*-C_{20} and *n*-C_{25}/*n*-C_{30} ratios. The *n*-C_{15}/*n*-C_{20} result for sample S3 is given with an asterisk because the value is too high compared to the other samples. That is probably a systematic error caused by wrong peak identification as the source rock S3 GC-FID chromatogram contains high peaks due caused by polymers.

Oils	C	T1	T2	V	Ø	AB	E1	O	X	W
n-C_{15}/*n*-C_{20}	1.37	1.44	1.70	1.37	1.64	1.15	1.07	1.18	3.92	1.63
n-C_{25}/*n*-C_{30}	2.61	3.00	2.43	2.56	2.33	3.20	2.18	2.51	3.00	3.00
Sour.rocks	**S4**	**S9**	**S10**	**S11**	**S12**	**S5**	**S3**	**S2**	**S6**	**S7**
n-C_{15}/*n*-C_{20}	4.21	0.83	0.83	1.19	1.02	1.33	14.11*	1.20	1.64	0.96
n-C_{25}/*n*-C_{30}	2.00	3.25	0.89	3.25	4.26	1.53	1.33	1.67	0.80	1.62
Sour.rocks	**S8**	**S1**	**SO-21**				**NSO-1**			
n-C_{15}/*n*-C_{20}	0.73	1.68	2.18				1.92			
n-C_{25}/*n*-C_{30}	0.21	3.20	3.75				2.58			

From figure 7.19, it becomes clear that the source rock signatures of S4, S3, S9, S11, S12 samples are biodegraded, immature or have experienced interference from heterogenic sources, meaning that the hydrocarbons inside the source rocks are not clearly indigenous. The oils plot near the trendline but not entirely as NSO-1 does. This could mean that the oils are actually blended (Ohm et al., 2008). The oil samples X and AB plot far off the trendline. Sample X is clearly non-biodegraded but the high peaks at the medium range compounds could mean that it is blended and therefore its signature is modified. Sample AB suffers from the column-bleed phenomenon and for this reason the ratio of n-C_{25}/n-C_{30} is very likely to be miscalculated.

Figure 7.20 is a crossplot between synthetic vitrinite reflectivity and the inverse ratio of n-alkane/isoprenoid which value increases with maturation.

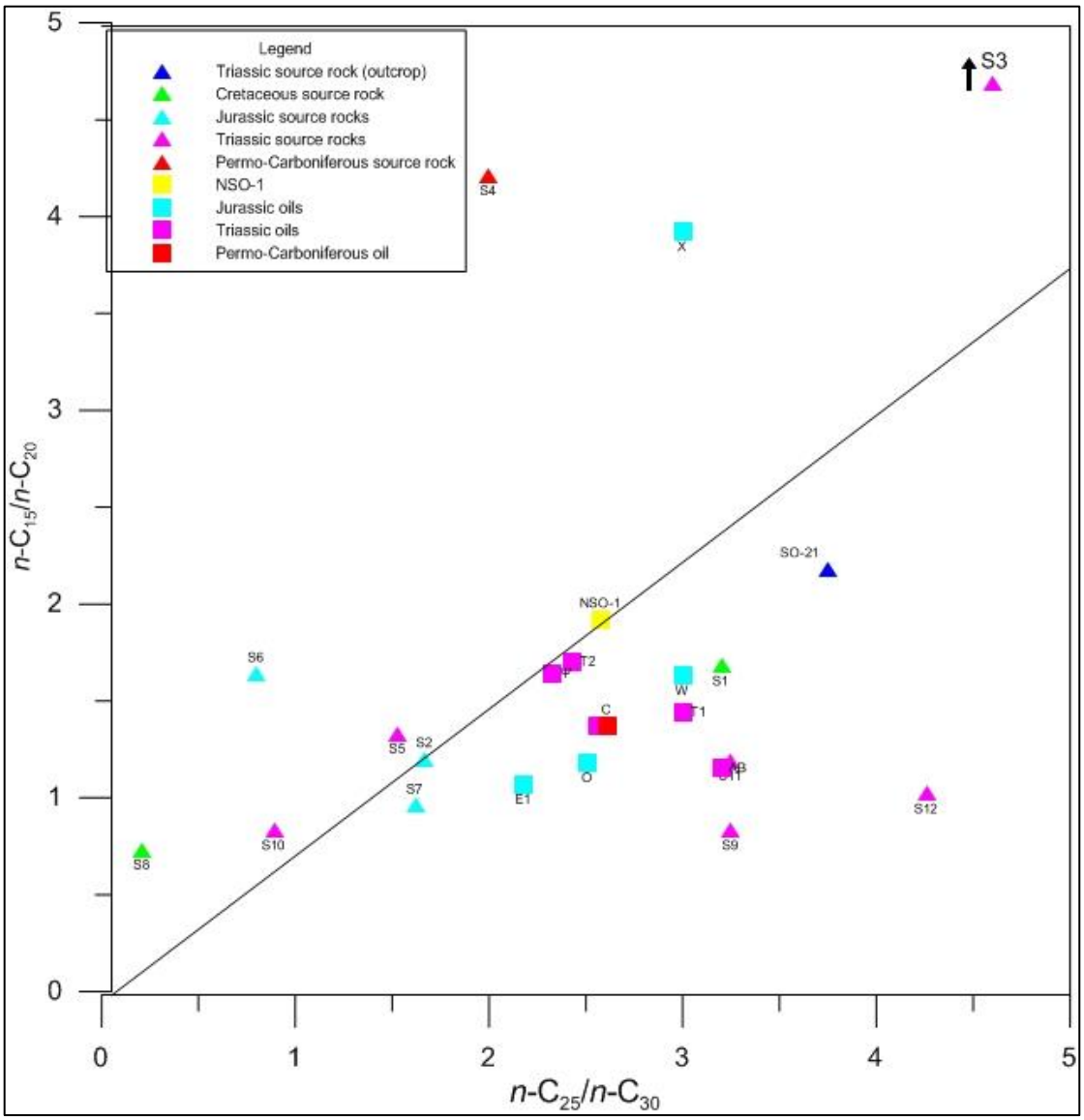

Figure 7.19: The crossplot of the *n*-C_{25}/*n*-C_{30} ratio with the *n*-C_{15}/*n*-C_{20} ratio serves as biodegradation parameter. Oil sample (Ψ) is sample (Ø). Note that sample S3 falls outside the area due to biodegradation. In general samples that plot far off the trendline are candidates for biodegedation.

Again, properly mature samples tend to plot across the trendline whereas those that are biodegraded or their signature is interefered by heterogenic sources plot far off. Here, source rock samples S11, S5 and S12 are again candidates for biodegradation, same as the oil samples Ø and T2. The chromatograms of the source rocks contain large UCMs which justify their tendency to plot off the trendline. The indications for UCM in the oil chromatograms are minor but their signature is probably source

dependent, since the reflectivity is calculated with the help of the methyldibenzothiophene ratio. Finally, both the S4 and C from Paleozoic are highly mature but they tend to plot in different parts of the crossplot.

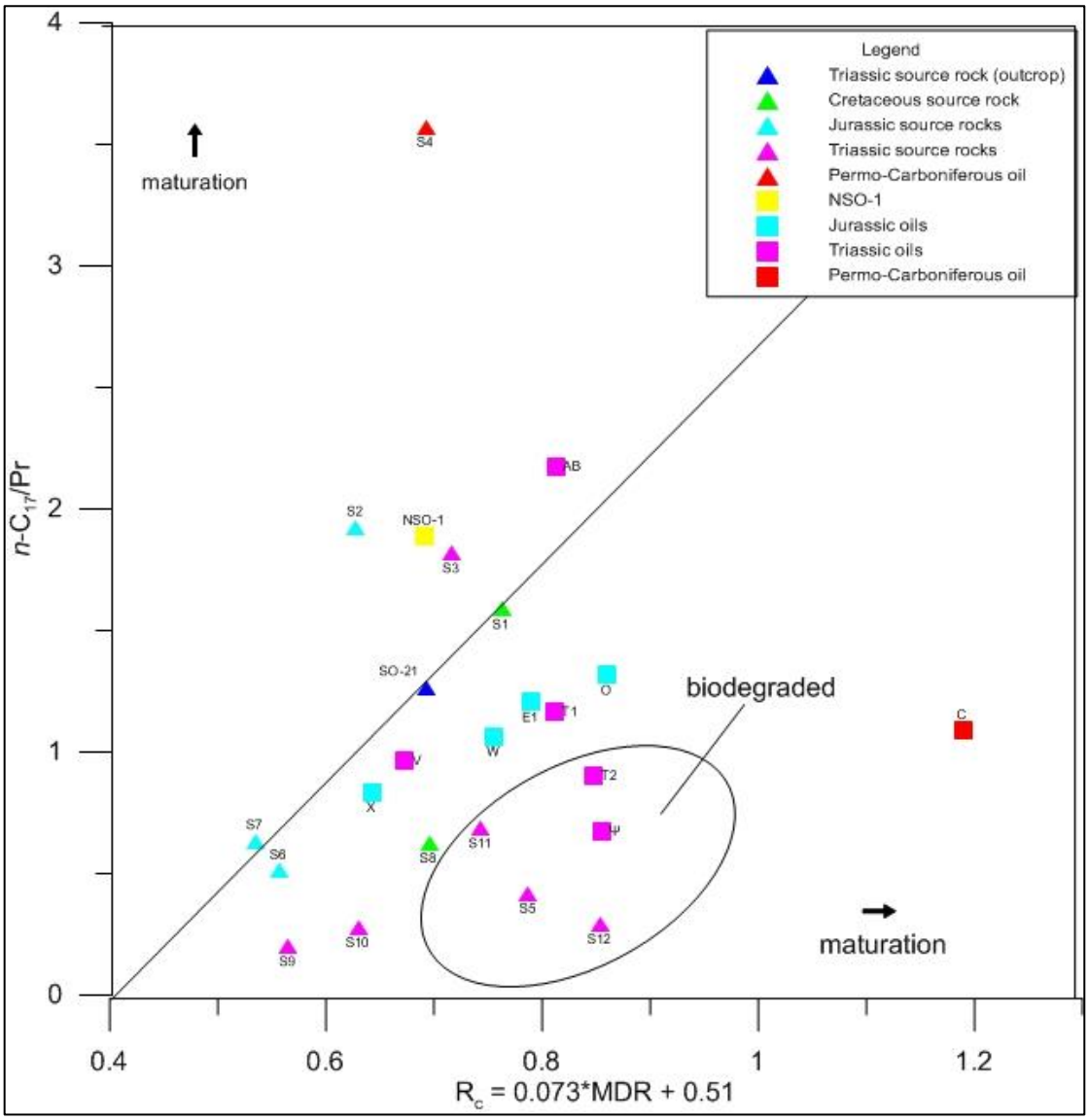

Figure 7.20: Crossplot of the %R_c = 0.073*MDR + 0.51 (Radke, 1988) with *n*-C_{17}/Pr, reversed ratio of Pr/*n*-C_{17}, which increases with maturation. Oil sample (Ψ) is sample (Ø). Samples that fall off the trendline are candidates for biodegradation.

The final figure (7.22) is a crossplot between the CPI (Carbon Preference Index) and the synthetic vitrinite reflectivity from the methyldibenzothiophene ratio. The results of the present plot may be not very accurate because different formulas were used to calculate the CPI for the oils and for the source rocks, as mentioned in Chapter 6.

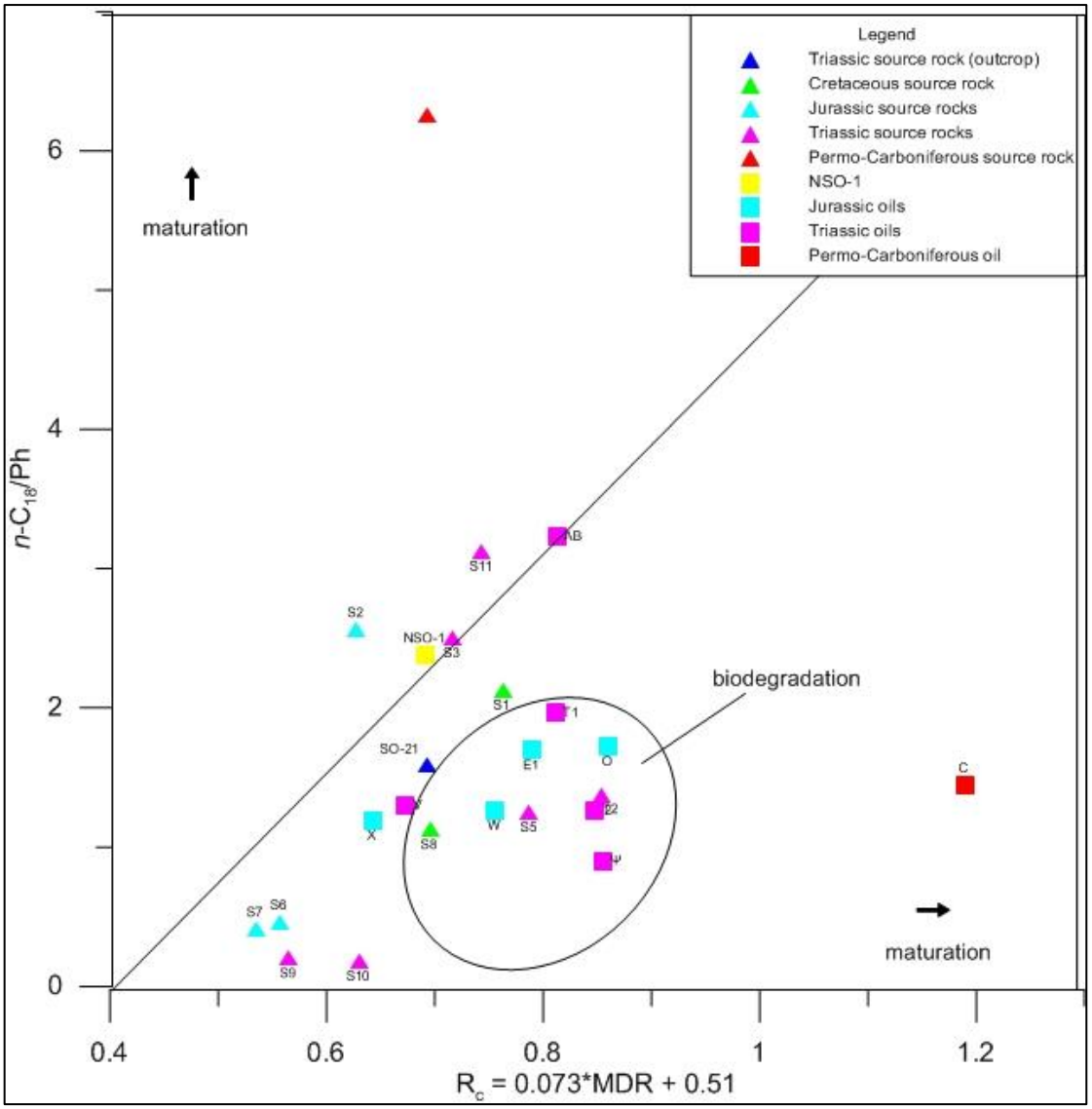

Figure 7.21: Crossplot of the %R_c = 0.073*MDR + 0.51 (Radke, 1988) with *n*-C_{18}/Ph, reversed ratio of Ph/*n*-C_{18}, which increases with maturation. Oil sample (Ψ) is sample (Ø). Samples that fall off the trendline are candidates for biodegradation.

However it is clear that the samples group together in different areas of the diagram (Figure 7.22). The CPI values that range between 0.80-1.20, in other words fluctuate near the unity, are typical for high maturity. All the oils except for sample X and source rock samples S5, S11 and S5 plot in that range and are hence mature. The samples that have values below 0.8 show even predominance of normal alkanes, are immature and were deposited in reducing hypersaline or carbonate environments. This range includes the samples S9, S10, S2, SO-21, S4, S8, S1 and NSO-1. On the other hand samples that have CPI values higher than 1.2 show preference for odd normal alkanes, are as well immature and were deposited in oxic (less reducing

environments). Samples S3 and X plot in that range. Biodegradation and interference from heterogenic sources can significantly alter the CPI ratios. For instance the S5, S11 and S12 source rock samples are biodegraded but plot in the mature area in figure 7.22.

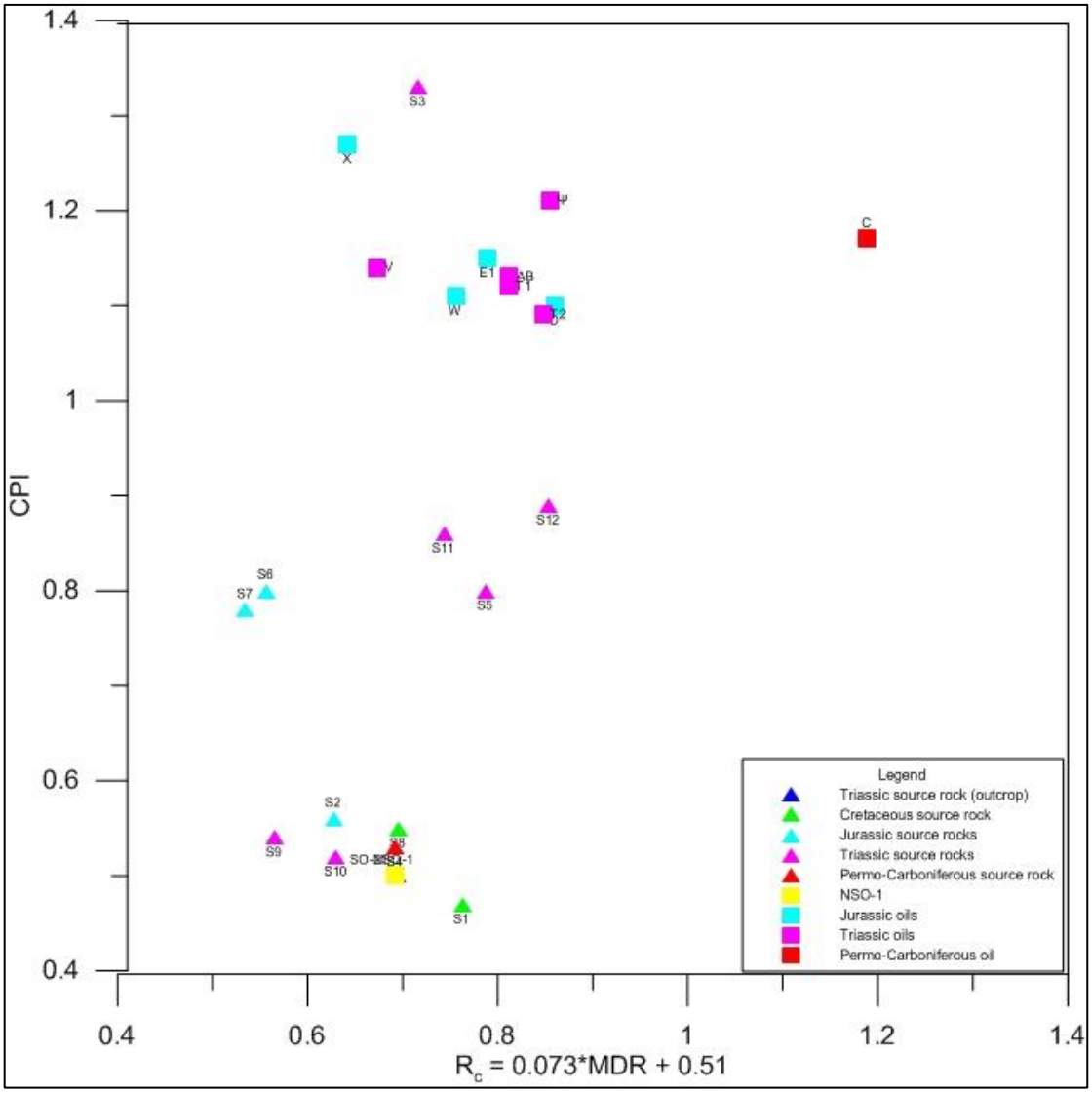

Figure 7.22: Crossplot of the %R_c = 0.073*MDR + 0.51 (Radke, 1988) with the CPI index which increases with maturation. Oil sample (Ψ) is sample (Ø).

To conclude on the facies, the source rock samples S1, S2, S3, S4, S6, S7 and SO-21 were apparently deposited in transitional (marine to estuarine/lagoonal) paleodepositional settings and contain mixed, type II kerogen. Sample S8 was deposited in lacustrine or marine setting that was influenced by higher plant organic matter input. However, The samples S5, S9, S10, S11 and S12 were deposited in

deltaic-fluvial settings that were affected by terrestrial organic matter input (type III humic kerogen). However there is a certain degree of uncertainty for the source rock samples S3, S6, S7 and S8 that are obviously affected by secondary processes (Figure 7.1).

All the oil samples are derived from transitional organic facies (marine to estuarine/lagoonal) with preferance for marine and were deposited under reducing conditions with kerogen type II organic matter input.

To sum up, it is difficult and potentially risky to address if any genetic relationships exist between the studied datasets, since the source rocks demonstrate variations in organofacies whereas the oils do not and also because there are indications that the oils are blended (two or more oils are mixed in the reservoir). However, if a correlation attempt was to be made that would include only the source rocks S1, S2, S3, S4, S6, S7 and SO-21 which have the same type of organofacies with the oils (transitional marine-estuarine with kerogen type II).

To conclude, it is suggested that the Jurassic oil samples E1, O and X from the Stø Formation as well as the oil sample W from the Tubåen Formation are probably genetically linked to the Jurassic source rock sample S2 from the Tubåen Formation. The Triassic oil samples T1, AB and Ø from Snadd Formation, T2 from Kobbe Formation and V from Fruholmen Formation seem to be correlated to the Triassic source rock S3 from the Fruholmen Formation. The Permo-Carboniferous oil sample C from Ørn Formation could be linked to source rock sample S4 from the Permian Røye Formation. The Hekkingen shales of the present dataset, samples S6 and S7 from the Nordkapp Basin, were concluded to be immature and biodegraded. Therefore it would be too risky to correlate them with the oil samples despite the fact that previous studies (Ohm *et al.,* 2008) suggest that Hekkingen Formation has very high source rock potential. The Triassic outcrop source rock sample SO-21 from the De Geerdalen Formation from Svalbard is very mature and could act as potential source rock for the studied Mesozoic oils. Finally it must be stressed that the Cretaceous source rock sample S1 does not seem to fit well with any of the oils despite the very high maturation level.

7.4 Comparison of Medium-range parameters and Biomarkers

The maturities of the samples were determined by using both the medium-range parameters and biomarkers, although they were compared mostly based on the depositional environment and organic matter input (kerogen type) (Table 7.2). The source rock maturities estimated from the medium range compounds and from biomarkers are not very contrasting. Thus, the source rocks maturation pattern for both approaches (medium-range parameters and biomarkers) is almost ideal. On the other hand the oils show highly contrasting maturities. However this fact is of minor importance since all of them plot together in every figure discussed in Chapter 7. The oils ranking variation was hence limited to subjective observations.

As already stressed, the oil to source rock correlation was mostly based on the organofacies signatures and secondly on their maturation. The final correlation results are presented in Table 7.2.

Table 7.2: Ranking of source rocks and oils based on their maturity. Mark that only the source rock samples with marine to estuarine-lagoonal organofacies, S2, S3 and S4 were attempted to be correlated with the oils whose source rock analogues were as well deposited under marine to estuarine-lagoonal settings and contained mixed type II kerogen.

MATURITY RANK OF SOURCE ROCKS													
Type/No	**1**	**2**	**3**	**4**	**5**	**6**	**7**	**8**	**9**	**10**	**11**	**12**	**13**
Biomarkers	S8	S7	S6	S10	S5	S9	S11	S12	S3	S0-21	S2	S1	S4
Medium range par.	S8	S5	S7	S11	S6	S10	S12	S3	S0-21	S9	S2	S1	S4

MATURITY RANK OF OILS											
Type/No	**1**	**2**	**3**	**4**	**5**	**6**	**7**	**8**	**9**	**10**	**11**
Biomarkers	NSO-1	O	Ø	V	X	W	T1	AB	E1	T2	C
Medium range par.	NSO-1	X	T2	W	AB	V	Ø	O	E1	T1	C

ORGANOFACIES & OIL TO SOURCE ROCK CORRELATION			
Marine to estuarine-lagoonal (kerogen type II)			
E1, O, X	Stø Fm	**S2**	Tubåen Fm
W	Tubåen Fm		
T1, AB, Ø	Snadd Fm	**S3**	Fruholmen Fm
T2	Kobbe Fm		
V	Fruholmen Fm		
C	Ørn Fm	**S4**	Røye Fm

Chapter 8

Conclusion

A total of 23 samples, 10 oils and 13 source rocks ranging from Permo-Carboniferous to Cretaceous, were studied by means of gas chromatography, GC-MS and GC-FID, to address potential genetic relationships. A set of 35 parameters was calculated out of the chromatograms and then the samples were plotted together to indicate the maturity, organic facies and biodegradation.

The initial aim was to evaluate if the oils are genetically linked to the Jurassic shales of the Hekkingen Formation as this is the most prolific source rock in the western Barents Sea (Ohm *et al*., 2008). In addition Permo-Carboniferous, Jurassic, Triassic and Cretaceous source rocks were available to address source rock relationships of the oil to other units, despite these source rocks being often at low maturity. Thus, since the source rock samples were recovered from wells drilled on structural highs, in addition to the low maturity and on several cases severe biodegradation, it was concluded that with the present dataset it would be too risky to reach a final outcome. However the analysis of the results leads to certain conclusions:

- Based on the biomarker range parameters the source rocks have the following maturity sequence, from the lowest to highest: **S8** (Cretaceous/Kolje Fm), **S7** (Late Jurassic/Hekkingen Fm), **S6** (Late Jurassic/Hekkingen Fm), **S10** (Middle Triassic/Steinkobbe Fm), **S5** (Middle Triassic/Kobbe Fm), **S9** (Early Triassic/Steinkobbe Fm), **S11** (Late Triassic/Snadd Fm), **S12** (Late Triassic/Snadd Fm), **S3** (Late Triassic/Fruholmen Fm), **SO-21** (Upper Triassic/De Geerdalen Fm), **S2** (Early Jurassic/Tubåen), **S1** (Cretaceous/Kolmule Fm) and **S4** (Permian/Røye Fm), whereas the oil sequence is defined as **NSO-1**, **O** (Middle Jurassic/Stø Fm), **Ø** (Middle Triassic/Snadd Fm), **V** (Late Triassic/Fruholmen Fm), **X** (Jurassic/Stø Fm), **W** (Early Jurassic/Tubåen Fm), **T1** (Triassic/Snadd Fm), **AB** (Late Triassic/Snadd Fm), **E1** (Early Jurassic/Stø Fm), **T2** (Middle Triassic/Kobbe Fm) and **C** (Permo-Carboniferous/Ørn Fm).

- The maturity sequence of the source rocks based on the medium-range parameters, from the lowest to highest, is defined as: **S8** (Cretaceous/Kolje Fm), **S5** (Middle Triassic/Kobbe Fm), **S7** (Late Jurassic/Hekkingen Fm), **S11** (Late Triassic/Snadd Fm), **S6** (Late Jurassic/Hekkingen Fm), **S10** (Middle Triassic/Steinkobbe Fm), **S12** (Late Triassic/Snadd Fm), **S3** (Late Triassic/Fruholmen Fm), **SO-21** (Upper Triassic/De Geerdalen Fm), **S9** (Early Triassic/Steinkobbe Fm), **S2** (Early Jurassic/Tubåen), **S1** (Cretaceous/Kolmule Fm) and **S4** (Permian/Røye Fm) and for the oils: NSO-1, **X** (Jurassic/Stø Fm), **T2** (Middle Triassic/Kobbe Fm), **W** (Early Jurassic/Tubåen Fm), **AB** (Late Triassic/Snadd Fm), **V** (Late Triassic/Fruholmen Fm), **Ø** (Middle Triassic/Snadd Fm), **O** (Middle Jurassic/Stø Fm), **E1** (Early Jurassic/Stø Fm), **T1** (Triassic/Snadd Fm) and **C** (Permo-Carboniferous/Ørn Fm).
- The maturity assessment based on both the biomarker and the medium-range parameters suggests that the studied source rocks range from immature to post-mature, whereas the studied oils have about the same degree of maturity and are late mature. This homogeneity could also be due to in-reservoir mixing processes (blended oils).
- The source rocks S1, S2, S3, S4, S6, S7, SO-21 and all of the oils source rock analogues were deposited in transitional, marine to estuarine environments, which favored mixed, kerogen type II, organic matter input.
- The source rock samples S5, S9, S10, S11 and S12 were deposited in deltaic-fluvial settings that were affected by terrestrial organic matter input (type III humic kerogen) and sample S8 was probably deposited in transitional settings, also with high terrestrial input.
- The source rock samples S3, S6, S7 and S8 are highly biodegraded and the samples S9, S10 and S11 have experienced incipient biodegradation.
- The Triassic oil samples E1, O and X (Stø Fm) and W (Tubåen Fm) are probably linked to the Triassic source rock sample S2 (Tubåen Fm).
- The Jurassic oil samples T1, AB and Ø (Snadd Fm), T2 (Kobbe Fm) and V (Fruholmen Fm) are probably linked to the Jurassic source rock sample S3 (Fruholmen Fm).

- The Permo-Carboniferous oil sample C (Ørn Fm) is probably linked to the Permian source rock sample S4 (Røye Fm)
- The Jurassic source rock sample S2, located in Hammerfest Basin (Field 7122), was concluded to be genetically linked to the Jurassic oil samples E1 (Field 7120), O (Field 7121), W (Field 7124) and X (Field 7125). The Triassic source rock sample S3 (Field 7124), located in the Nyslepp/Måsøy Fault Complex, was also concluded to be linked to the Triassic oils T1, T2 (Field 7122), V (Field 7123), AB (Field 7228) and Ø (Field 7222). Obviously there is a certain filling pattern forming a ENE-WSW regional trend. This trend could be explained by the regional geology. For example the Hammerfest Basin is transected by the Troms-Finnmark Fault Complex which is ENE-WSW oriented. Furthermore, the Nyslepp/Måsøy Fault Complex is oriented in the same ENE-WSW trend. Therefore it could be suggested that the the bedding planes of these two structural elements, Troms-Finnmark and Nyslepp/Måsøy Fault Complexes, served as efficient migration pathways.

References

ABAY, T.B., 2010. Vertical variation in reservoir core geochemistry:Bitumen samples from a well in the deep and hot Devonian age Embla Oil Field, Offshore Norway. Master Thesis in Geology, Department of Geology, University of Oslo, June 2010, 296 pp.

ABAY, T. B., KARLSEN, D. A., & OHM, S. E., 2014. Vertical variations in reservoir geochemistry in a palaeozoic trap, Embla field, offshore Norway. Journal of Petroleum Geology, Vol. 37 (4), October 2014, pp. 349-372.

AUSET, M., 2012. Sedimentology and Diagenesis of Upper Triassic Sandstones, with Emphasis on the Snadd-Fruholmen Transition, Barents Sea, (Master thesis), Department of Geology and Mineral Resources Engineering, NTNU, 73 pp.

BEŠKOSKI, V.P.,GOJGIĆ-CVIJOVIĆ, G., JOVANČIĆEVIĆ, B., & VRVIĆ, M, M., (2012). Gas Chromatography in Environmental Sciences and Evaluation of Bioremediation, in: Gas Chromatography - Biochemicals, Narcotics and Essential Oils, Dr. Bekir Salih (Ed.), ISBN: 978-953-51-0295-3, InTech, DOI: 10.5772/33955. Available from:http://www.intechopen.com/books/gas-chromatography-biochemicals-narcotics-and-essential-oils/gas-chromatography-in-environmental-sciences-and-evaluation-of-bioremediation.

BRAY, E.E., & EVANS, E.D., 1961. Distribution of n-paraffins as a clue to recognition of source beds. Geochimica et Cosmochimica Acta, 22, 2-15.

BUGGE, T., ELVEBAKK, G., FARAVOLL, S., MANGERUD, G., SMELROR, M., WEISS, H. M., GJELBERG, J., KRISTENSEN, S. E., KÅRE, N., 2002. Shallow stratigraphic drilling applied in hydrocarbon exploration of the Nordakapp Basin, Barents Sea. Marine and Petroleum Geology 19, Elsevier Science B.V., Amsterdam, 13-37.

CONNAN, J. AND CASSOU, A. M., 1980: Properties of gases and petroleum liquids derived from terrestrial kerogen at various maturation levels. Geochimica et Cosmochimica Acta, 44, 1-23.

CONNAN, J., 1984: Biodegradation of crude oils in reservoirs. In: Brooks. J. & Welte, D. (eds) Advances in Petroleum Geochemistry, volume 1. Academic Press. London. 299-335.

CORNFORD, C., MORROW, J.A., TURRINGTON, A., MILES, J.A., AND BROOKS, J., 1983, Some geological controls on oil composition in the U.K. North Sea. Petroleum geochemistry and exploration of Europe; International congress., Brooks, J., Ed.: Geological Society of London, 175-194.

DAHL, B. AND SPEERS, G. C., 1985: Organic geochemistry of the Oseberg field. Petroleum geochemistry in exploration of the Norwegian Continental shelf, Thomas Bruce, M. E. A., Ed., Graham and Trotman, 185-195.

DALLAND, A., WORSLEY, D. & OFSTAD, K., 1988: A lithostratigraphic scheme for the Mesozoic and Cenozoic succession offshore mid- and northern Norway. NPD-Bulletin No. 4, 65 pp.

DALLMANN, W. K. (ed.) 1999: Lithostratigraphic lexicon of Svalbard. Review and recommendations for nomenclature use. Upper Paleozoic to Quaternary Bedrock. Norwegian Polar Institute, 318 pp.

DORÉ, A. G. & JENSEN, L. N. 1996. The impact of late Cenozoic uplift and erosion on hydrocarbon exploration: offshore Norway and some other uplifted basins. Global and Planetary Change, 12, pp. 415-436.

DASGUPTA, S., TANG, Y., MOLDOWAN, J. M., CARLSON, R. M. K. AND GODDARD, W. A., III (1995) Stabilizing the boat conformation of cyclohexane rings. Journal of the American Chemical Society, 117, 6532-4.

FALEIDE, J. I., GUDHAUGSSON, S. T., JACQUART, G., 1984. Evolution of the western Barents Sea. Marine and Petroleum Geology 1, pp. 123-150.

FALEIDE, J.I., VÅGNES, E., GUDLAUGSSON, S. T., 1992. Late Mesozoic-Cenozoic evolution of the south-western Barents Sea in a regional rift-shear tectonic setting. Marine and Petroleum Geology, Vol. 10. pp. 186-214.

FALEIDE, J. I., BJØRLYKKE, K. & GABRIELSEN, R. H., 2010: Geology of the Norwegian Continental Shelf. In: BJØRLYKKE, K.: Petroleum Geoscience: From Sedimentary Environments to Rock Physics. Springer-Verlag, Berlin Heidelberg, pp. 467-499.

GABRIELSEN, R. H., FÆRSETH, R. B., JENSEN, L. N., KALHEIM, J. E. & RISS, F. 1990. Structural elements of the Norwegian continental shelf : Part I : The Barents sea region, Stavanger, Oljedirektoratet.

GUDLAUGSSON, S.T., FALEIDE, J. I., JOHANSEN, S. E., BREIVIK, A.J., 1997. Late Paleozoic structural development of the South-Western Barents Sea. Marine and Petroleum Geology 15, pp. 73-102.

JONES, D. M., DOUGLAS., A. G. & CONNAN J., 1987: Hydrous pyrolysis of asphaltenes and polar fractions of biodegraded oils. In: MATTAVELLI, L. & NOVELLI, L.: Advances in Organic Geochemistry 1987. Org. Geochem. Vol. 13, Nos 4-6, pp. 981-993.

JUSTWAN, H., DAHL, B., ISAKSEN, G. H. & MEISINGSET, I., 2005. Late to Middle Jurassic soure facies variations, south Viking Graben, North Sea. Journal of Petroleum Geology, Vol. 28 (3), July 2005, pp. 241-268.

JUSTWAN, H., DAHL, B., ISAKSEN, G.H., 2006. Geochemical characterization and genetic origin of oils and condensates in the South Viking Graben, Norway. Marine and Petroleum Geology 23, pp. 213-239.

HUGHES, W.B., HOLBA, A.G., AND DZOU, L.I.P., 1995. The ratios of dibenzothiophene to phenanthrene and pristane to phytane as indicators of depositional environment and lithology of petroleum source rocks: Geochimica et Cosmochimica Acta, v. 59, p. 3581-3598.

HUNT, J. M. 1996. Petroleum geochemistry and geology, New York, W. H. Freeman, 743 pp.

KARLSEN, D. A., NEDKVITNE, T., LARTER, S. R. & BJØRLYKKE, K. 1993. Hydrocarbon composition of authigenic inclusions: application to elucidation of petroleum reservoir filling history. Geochimica et Cosmochimica Acta, 57, 3641-3659.

KARLSEN, D.A., NYLAND, B., FLOOD, B., OHM, S.E., BREKKE, T., OLSEN, S. & BACKER-OWE, K. 1995. Petroleum geochemistry of the Haltenbanken, Norwegian continental shelf. In: Cubitt, J.M. & England, W.A. (eds) The Geochemistry of Reservoirs. Geological Society, London, Special Publications, 86, 203–256.

KARLSEN, D. A., NEDKVITNE, T., LARTER, S., AND BJORLYKKE, K., 1995: The best paper award in organic geochemistry - hydrocarbon composition of authigenic inclusions - application to elucidation of petroleum reservoir filling history: Geochimica et Cosmochimica Acta, v. 59, p. 1439-1439.

KARLSEN, D. A., J. E. SKEIE, K. BACKER-OWE, K. BJØRLYKKE, R. OLSTAD, K. BERGE, M. CECCHI, E. VIK, & R. G. SCHAEFER, 2004, Petroleum migration, faults and

overpressure: II. Case history: The Haltenbanken Petroleum Province, offshore Norway, in J.M. Cubitt, W.A. ENGLAND, & S. LARTER, eds., Understanding petroleum reservoirs: Toward and intergrated reservoir engineering and geochemical approach: Geological Society (London) Special Publications 237, pp. 305-372.

KNUTSEN, S. M., AUGUSTSON, J. H. & HAREMO, P., 2000. Exploring the Norwegian part of the Barents Sea-Norsk Hydro's lessons from nearly 20 years of experience. In: OFSTAD, K., KITTILSEN, J.E., ALEXANDER-MARRACK, P., Improving the Exploration Process by Learning from the Past. NPF Special Publication 9, Elsevier Science B.V., Amsterdam. pp. 99-112.

KVALHEIM, O. M., TELNAES, N., BJORSETH, A. AND CHRISTY, A. A., 1987: Interpretation of multivariate data; relationship between phenanthrenes in crude oils. Multivariate statistical workshop for geologists and geochemists., Kvalheim, O. M., Ed., Elsevier, 149-153.

LARSSEN, G. B., ELVEBAKK, G., HENRIKSEN, L. B., KRISTENSEN, S. E., NILSSON, I., SAMUELSBERG, T. J., SVÅNÅ, T. A., STEMMERIK, L. AND WORSLEY, D. 2002: Upper Paleozoic lithostratigraphy of the Southern Norwegian Barents Sea. NPD-Bulletin No. 9, 69 pp.

LUNDSCHIEN, B.A., HØY, T. & MØRK, A., 2014: Triassic hydrocarbon potential in the Northern Barents Sea; integrating Svalbard and stratigraphic core data. Norwegian Petroleum Directorate Bulletin, No. 11, 168 pp. Stavanger 2014, ISSN Online 1894 7670, ISBN 978-82-7257-117-6.

MACKENZIE, A.S., PATIENCE R.L., MAXWELL, J.R., VANDENBROUCKE, M., DURAND B., 1980: Molecular parameters of maturation in the Toarcian shales, Paris Basin, France—I. Changes in the configurations of acyclic isoprenoid alkanes, steranes and triterpanes, Geochimica et Cosmochimica Acta, Volume 44, Issue 11, November 1980, Pages 1709-1721, ISSN 0016-7037

MACKENZIE, A.S, AND MAXWELL, J.R, 1981. Assessment of thermal maturation of sedimentary rocks by molecular measurement. In: J. Brooks, Editor, Organic Maturation Studies and Fossil Fuel Exploration, Academic Press, London (1981), pp. 239-254.

MACKENZIE, A. S., 1984: Applications of biological markers in petroleum geochemistry. Advances in petroleum geochemistry; Volume 1., Welte, D. H., Ed., Acad. Press, 115-214.

MACKENZIE, A.S., MAXWELL, J.R., COLEMAN, M.L. AND DEEGAN, C.E., 1984: Biological marker and isotope studies of North Sea crude oils and sediments. Proceedings – World Petroleum Congress = Actes et Documents – Congres Mondial du Petrole, 11, 45-56.

MACKENZIE, A.S., RULLKOETTER, J., WELTE, D.H., AND MANKIEWICZ, P., 1985, Reconstruction of oil formation and accumulation in North Slope, Alaska, using quantitative gas chromatography-mass spectrometry. Alaska North Slope oil-rock correlation study; analysis of North Slope crude, American Association of Petroleum Geologists, p. 319-377.

MELLO, M.R., GAGLIANONE, P.C., BRASSELL, S.C., MAXWELL, J.R., 1988: Geochemical and biological marker assessment of depositional environments using Brazilian offshore oils, Marine and Petroleum Geology, Volume 5, Issue 3, August 1988, Pages 205-223.

MOLDOWAN, J. M., SEIFERT, W. K. and GALLEGOS, E. J. (1985): Relationship between petroleum composition and depositional environment of petroleum source rocks. American Association of Petroleum Geologists Bulletin, 69, 1255-68.

MOLDOWAN, J. M., FAGO, F. J., CARLSON, R. M. K., YOUNG, D. C., VAN, D. G., CLARDY, J., SCHOELL, M., PILLINGER, C. T. AND WATT, D. S., 1991: Rearranged hopanes in sediments and petroleum. Geochimica et Cosmochimica Acta, 55, p. 3333 – 3353.

NORWEGIAN INTERACTIVE OFFSHORE STRATIGRAPHIC LEXICON, (NORLEX). Naturhistorisk Museum, Universitetet i Oslo. Available from: http://nhm2.uio.no/norges/litho/barentsealithotable.php

OHM, S. E., KARLSEN, D. A. & AUSTIN, T. J. F. 2008. Geochemically driven exploration models in uplifted areas: Examples from the Norwegian Barents Sea. AAPG Bull., 92, 1191-1223.

PEDERSEN, J.H., 2002: Atypical oils, unusual condensates and bitumens of the Norwegian Continental Shelf: an organic geochemical study, Cand. Scient. Thesis in Geology, Department of Geology, University of Oslo.

PEDERSEN, J.H., KARLSEN, D.A., BACKER-OWE, K., LIE, J.E., AND BRUNSTAD, H., 2006, The geochemistry of two unusual oils from the Norwegian North Sea: implications for new source rock and play scenario: Petroleum Geoscience, v. 12, p. 85-96.

PEDERSEN, J.H., KARLSEN, D.A., BACKER-OWE, K., LIE, J.E., AND BRUNSTAD, H., 2006, The geochemistry of two unusual oils from the Norwegian North Sea: implications for new source rock and play scenario: Petroleum Geoscience, v. 12, p. 85-96.

PETERS, K.E. AND MOLDOWAN, J.M., 1991: Effects of source, thermal maturity, and biodegradation on the distribution and isomerization of homohopanes in petroleum . Organic Geochemistry, 17, 47-61. (1993) The Biomarker Guide. Interpreting Molecular Fossils in Petroleum and Ancient Sediments. Prentice-Hall, Englewood Cliffs, NJ.

PETERS, K.E., AND MOLDOWAN, J.M., 1993: The biomarker guide: interpreting molecular fossils in petroleum and ancient sediments: Englewood Cliffs, N.J., Prentice Hall, XVI, 363 s. p.

PETERS, K.E., WALTERS, C.C. AND MOLDOWAN, J.M. 2004. The Biomarker Guide, Volume 1: Biomarkers and Isotopes in the Environment and Human history. 2nd edition, Cambridge University Press. 471 pp.

PETERS, K.E., WALTERS, C.C. AND MOLDOWAN, J.M. 2005. The Biomarker Guide, Volume 2 : Biomarkers and isotopes in petroleum systems and earth history, Cambridge, Cambridge University Press, 704 pp.

PHILP, R.P. (1994). Geochemical characteristics of oils derived predominantly from terrigenous source materials. In: Coal and Coal-bearing Strata as Oil-prone Source Rocks? Geol. Soc. Special Publication No. 77 , Geological Society pp. 71-92, ISBN: 0-903317-99-0.

RADKE, M. AND WELTE, D. H., 1983: The methylphenanthrene index (MPI); a maturity parameter based on aromatic hydrocarbons. Advances in organic geochemistry 1981., Speers, G., Ed., Wiley & Sons, 504-512.

RADKE, M., WELTE, D. H. AND WILLSCH, H., (1982a): Geochemical study on a well in the western Canada Basin; relation of the aromatic distribution pattern to maturity of organic matter. Geochimica et Cosmochimica Acta, 46, 1-10.

RADKE, M., WILLSCH, H. AND LEYTHAEUSER, D., (1982b): Geochemical study on a well in the Western Canada Basin: relation of the aromatic distribution pattern to maturity of organic matter. Geochimica et Cosmochimica Acta, 46, 1-10.

RADKE, M., 1988, Application of aromatic compounds as maturity indicators in source rocks and crude oils: Marine and Petroleum Geology, v. 5, pp. 224-236.

RADKE, M., VRIEND, S.P., RAMANAMPISOA L.R., 2000: Alkyldibenzofurans in terrestrial rocks: influence of organic facies and maturation, Geochimica et Cosmochimica Acta, Volume 64, Issue 2, January 2000, Pages 275-286,

RASMUSSEN, E., SKOTT, P. H. & LARSEN, K. J., 1995. Hydrocarbon potential of the Bjorneya West Province, western Barents Sea Margin. In: HANSHEN, S., Petroleum Exploration and Exploitation in Norway. NPF Special Publication 4, Elsevier, Amsterdam, pp. 277-286.

REEMST, P., & CLOETINGH, S., 1994. Tectonostratigraphic modeling of Cenozoic uplift and erosion in the southwestern Barents Sea: Marine and Petroleum Geology, v. 11, pp. 478–490.

RODRIGUES DURAN, E., DI PRIMIO, R., ANKA, Z., STODDART, D. & HORSFIELD, B. 2013. Petroleum system analysis of the Hammerfest Basin (southwestern Barents Sea): Comparison of basin modelling and geochemical data. Organic Geochemistry, 63, pp. 105-121.

RULLKÖTTER, J., AIZENSHTAT, Z. AND SPIRO, B. 1984: Biological markers in bitumens and pyrolyzates of Upper Cretaceous bituminous chalks from the Ghareb Formation (Israel). Geochimica et Cosmochimica Acta, 48, 151-7.

SALES, J. K., 1993, Closure vs. seal capacity—A fundamental control on the distribution of oil and gas, in A. G. DORE´, J. H. AUGUSTSON, C. HERMANRUD, D. J. STEWARD, and Ø. SYLTA, eds., Basin modeling: Advances and application: Norwegian Petroleum Society (NPF) Special Publication 3, pp. 399-414.

SCALAN, R.S., & SMITH, J.E., 1970. An improved measure of the odd-to-even predominance in the normal alkanes of sediment extracts and petroleum. Geochimica et Cosmochimica Act, 34, 611-620.

SEIFERT, W.K., & MOLDOWAN, J.M., 1986, Use of biological markers in petroleum exploration. In: Johns, R. B. (Editor): Methods in Geochemistry and Geophysics, v.24, p. 261-290.

SHANMUGAM, G., 1984: Significance of terrestrial environments and related organic matter in generating commercial quantities of oil, Gippsland Basin, Australia. Society of Economic Paleontologists and Mineralogists First annual midyear meeting. Society of Economic Paleontologists and Mineralogists, 73.

SIEDLECKA, A., 1975. Late Precambrian stratigraphy and structure of the north-eastern margin of the Fennoscandian Shield (East Finnmark-Timan region), Norges Geol. Undersøkelse (Skr.) 316, pp. 313-348.

SILVERMAN, S. R., 1965: Investigations of Petroleum Origin and Evolution Mechanisms by Carbon Isotope studies. In: Isotopic and Cosmic Chemistry, North-Holland Publishing Co., Amsterdam. pp. 92-102.

SINTEF., Shallow Stratigraphic Drilling projects 1982-1993., www.sintef.no.

STEWART, D. J., BERGE, K. & BOWLIN, B., 1995. Exploration trends in the Southern Barents Sea. In: HANSHEN, S., Petroleum Exploration and Exploitation in Norway. NPF Special Publication 4, Elsevier, Amsterdam, pp. 253-276.

TEN HAVEN, H.L., DE LEEUW, J.W., RULLKÖTTER, J. & SINNINGHE-DAMSTÉ, J. (1987). Restricted utility of the pristane/phytane ratio as a palaeoenvironmental indicator. In: Nature vol. 330 pp. 641-643.

TISSOT, B. P., WELTE, D. H., 1984, Petroleum formation and occurrence, (2nd edition) Springer-Verlag, 699 pp.

VIGRAN, J. O., MANGERUD, G., MØRK, A., WORSLEY, D., HOCHULI, P. A., 2014. Palynology and Geology of the Triassic succession of Svalbard and the Barents Sea. Geological survey of Norway Special Publication, 14, 270 pp.

VORREN, T. O., RICHARDSEN, G., KNUTSEN, S. M., HENRIKSEN, E., 1990. Cenozoic erosion and sedimentation in the western Barents Sea. Marine and Petroleum Geology, Vol. 8, pp. 317-340.

WAPLES, D. W. AND MACHIHARA, T., 1991: Biomarkers for geologists – A practical guide to the application of steranes and triterpanes in petroleum geology. Vol. 9, AAPG Methods in Exploration, AAPG, 91 pp.

WEISS, H. M., WILHELMS, A., MILLS, N., SCOTCHMER, J., HALL, P. B., LIND, K. & BREKKE, T., 2000: NIGOGA – The Norwedian Industry Guide to Organic Geochemical Analyses [online]. Norsk Hydro, Statoil, Geolab Nor, SINTEF Petroleum Research and the Norwegian Petroleum Directorate. Available from World Wide Web: http://www.npd.no/ 4.0, 1-102

WILHELMS, A., LARTER, S. R., 1994: Origin of tar mats in petroleum reservoirs. Part I: introduction and case studies, Marine and Petroleum Geology, Volume 11, Issue 4, August 1994, pp 418-441,.

WORSLEY, D., 2008. The post-Caledonian development of Svalbard and the western Barents Sea. Polar research 27, pp. 298-317.

APPENDIX I (Core photographs)

Core photographs for Wells 7120/2-1, 7121/5-2, 7122/7-3, 7123/4-1 A and 7125/1-1, 7222/6-1 S for crude oils and 7122/6-1 for source rock are not available.

Table 1: Summarizing the contents from Appendix I.

Figure	Well	Sample	Sample type
1	7120/6-1	E1	Crude oil
2	7124/3-1	W	Crude oil
3	7228/7-1 A	AB	Crude oil
4	7124/3-1	S3	Source rock
5	7128/6-1	S4	Source rock

Figure 1: Core photograph for Well 7120/6-1 for the interval between 2428.50-2433.50 m. Mark the depth 2432.0 m encircled in red from where sample "E1" was recovered (Norsk Hydro, www.npd.no)

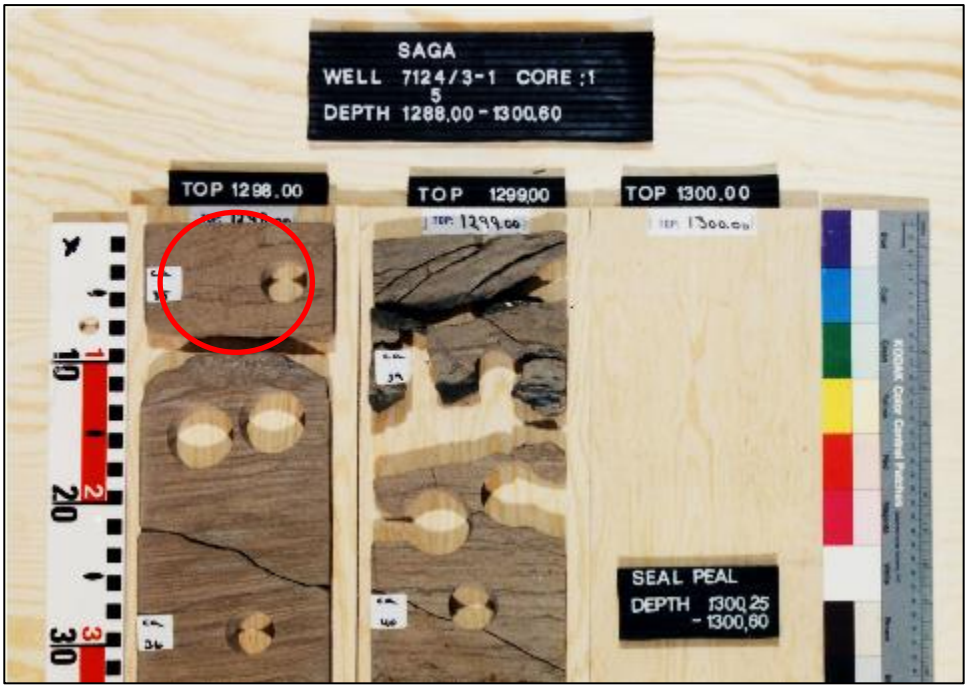

Figure 2: Core photograph for Well 7124/3-1 for the interval between 1298.0-1299.70 m. Mark the depth 1298.0 m encircled in red from where sample "W" was recovered (Saga Petroleum, www.npd.no)

Figure 3: Core photograph for Well 7228/7-1 A for the interval between 2089.0-2094.0 m. Mark the depth 2091.10 m encircled in red from where sample "AB" was recovered (Statoil, www.npd.no)

Figure 4: Core photograph for Well 7124/3-1 for the interval between 1364.0-1386.80 m. Mark the depth 1367.50 m encircled in red from where sample "S3" was recovered (Saga Petroleum, www.npd.no)

Figure 5: Core photograph for Well 7128/6-1 for the interval between 1738.0-1743.00 m. Mark the depth 1738.50 m encircled in red from where sample "S4" was recovered (Conoco, www.npd.no)

APPENDIX II (Shallow stratigraphic core photographs and logs)

Appendix II contains core photographs and sedimentological logs with respect to facies interpretations, namely: gamma, sound velocity and kerogen type/TOC, based on core measurements (IKU-SINTEF Petroleum Research & Bugge *et al.,* 2002).

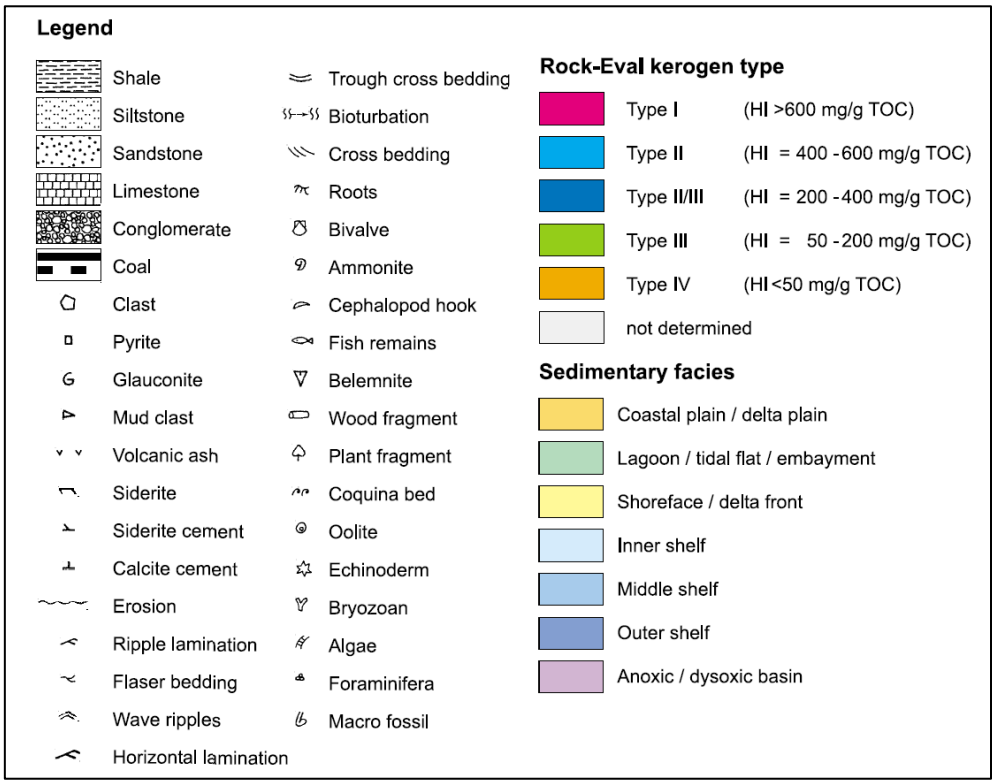

Figure 1: Legend of the shallow stratigraphic core logs (from Bugge *et al.,* 2002).

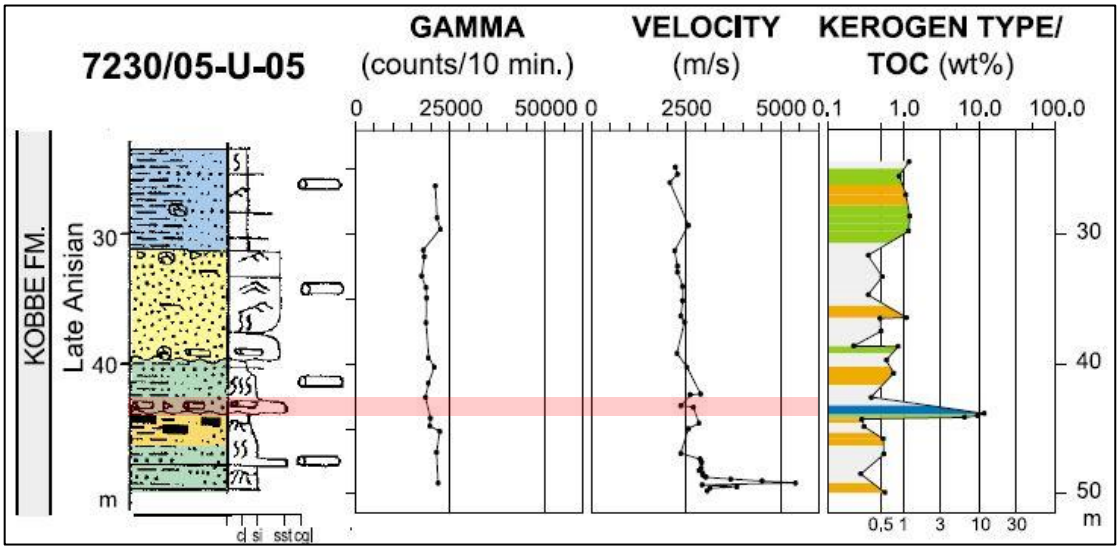

Figure 2: The shallow stratigraphic core logs of 7230/5-U-5. Mark the TOC peak at 43.85 m in red transparent color which provided sample "S5". Mark also that the formation here is the Kobbe and not Snadd as discussed in chapter 6.2.4 (Bugge *et al.,* 2002).

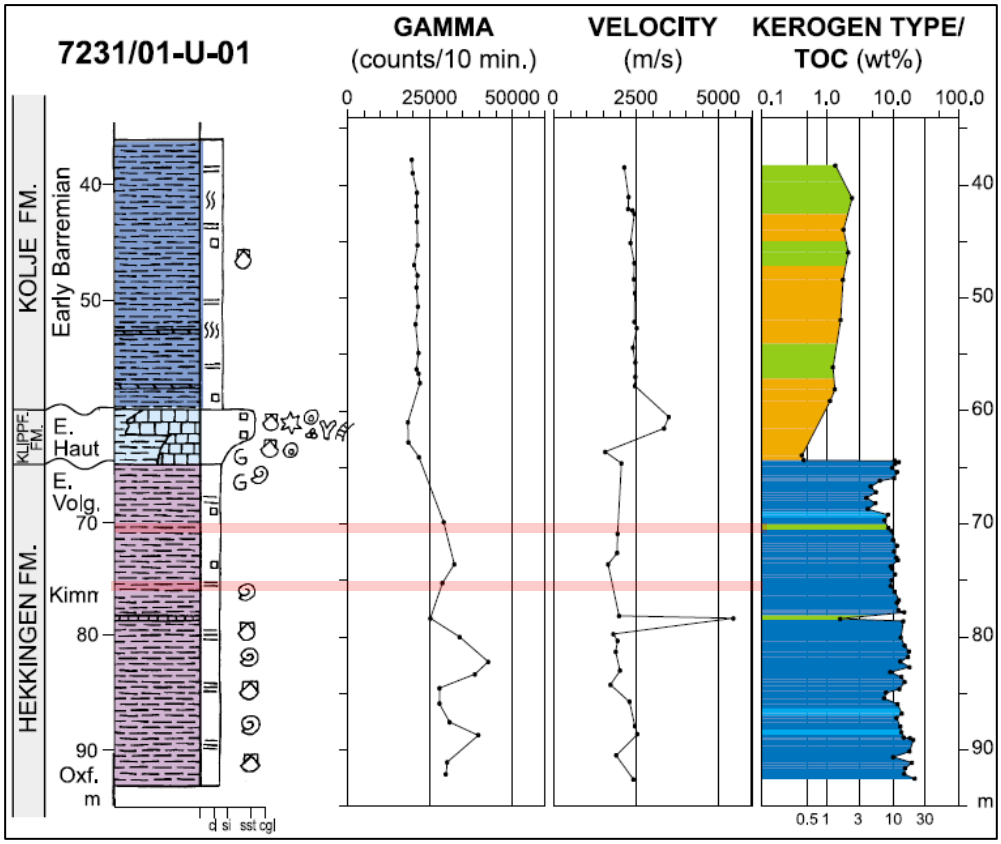

Figure 3: The shallow stratigraphic core logs of 7231/1-U-1. Mark the depths 70.90 m and 76.20 m in red transparent color which provided "S6" and "S7" respectively (Bugge *et al.,* 2002).

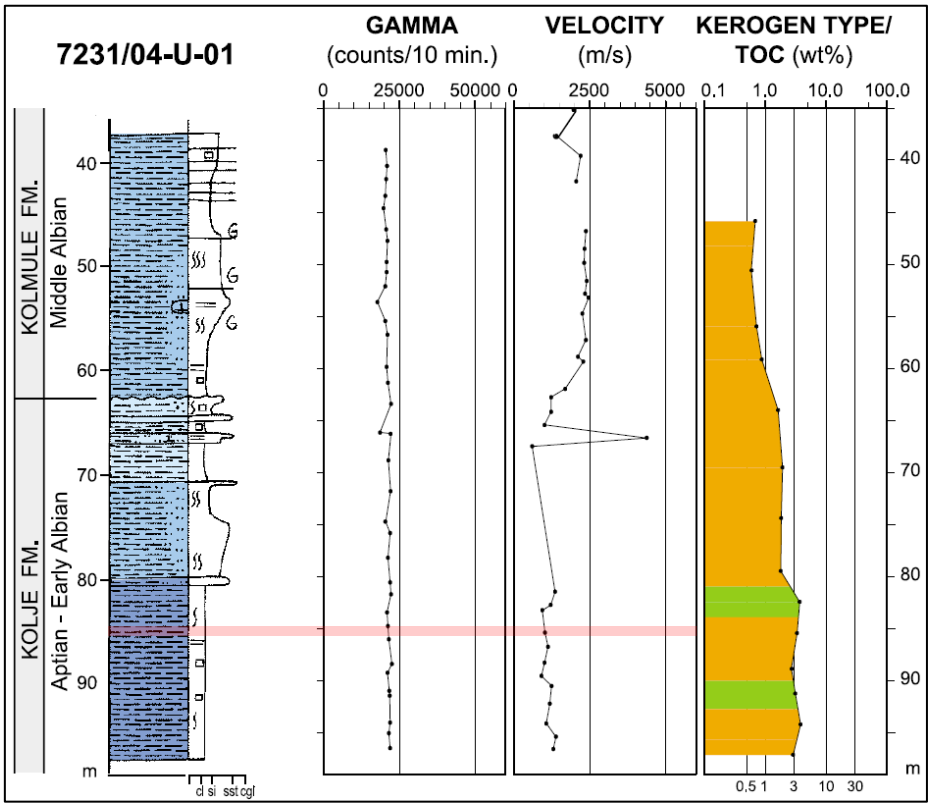

Figure 4: The shallow stratigraphic core logs of 7231/4-U-1. Mark the depth 84.70 m from which sample "S8" was recovered (Bugge *et al.,* 2002).

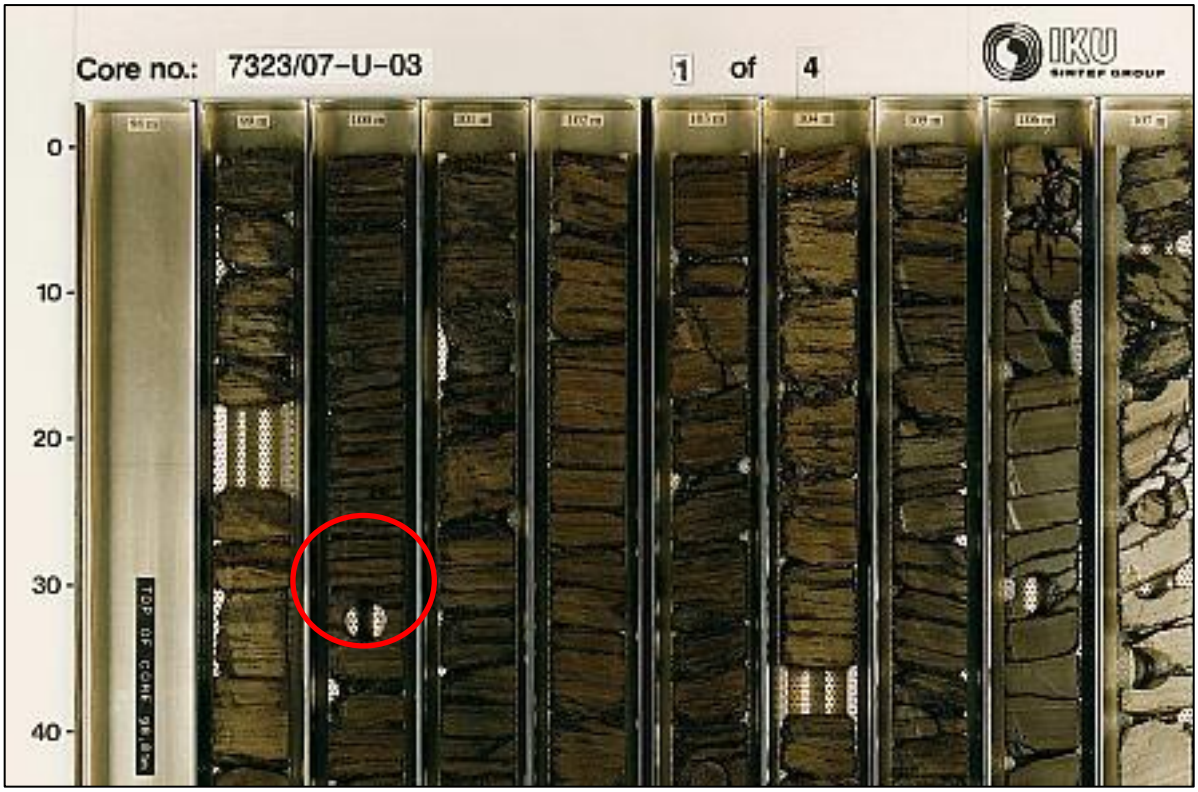

Figure 5: IKU stratigraphic drilling core photograph for the shallow core 7323/7-U-3 for the interval between 98.81-108.00 m. Mark the depth 100.30 m encircled in red that provided sample "S9" (www.sintef.no)

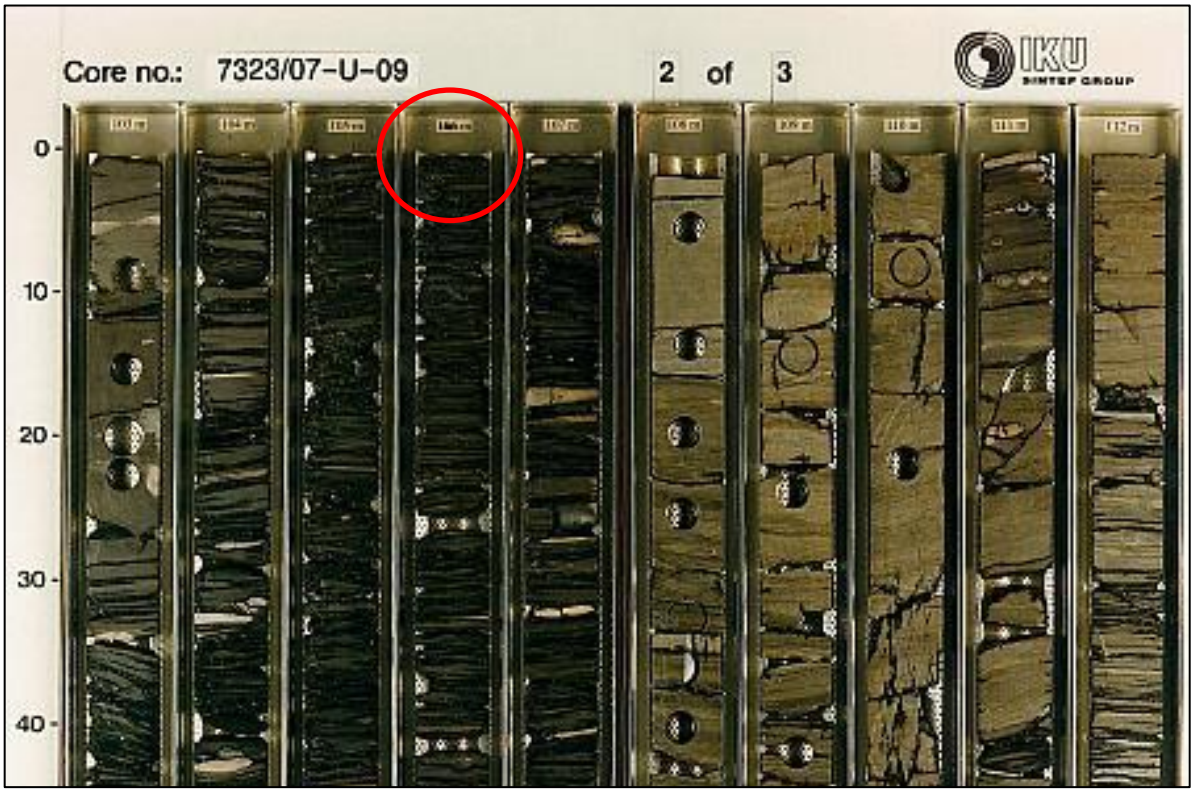

Figure 6: IKU stratigraphic drilling core photograph for the shallow core 7323/7-U-9 for the interval between 103.00-113.00 m. Mark the depth 106.00 m encircled in red that provided sample "S10" (www.sintef.no)

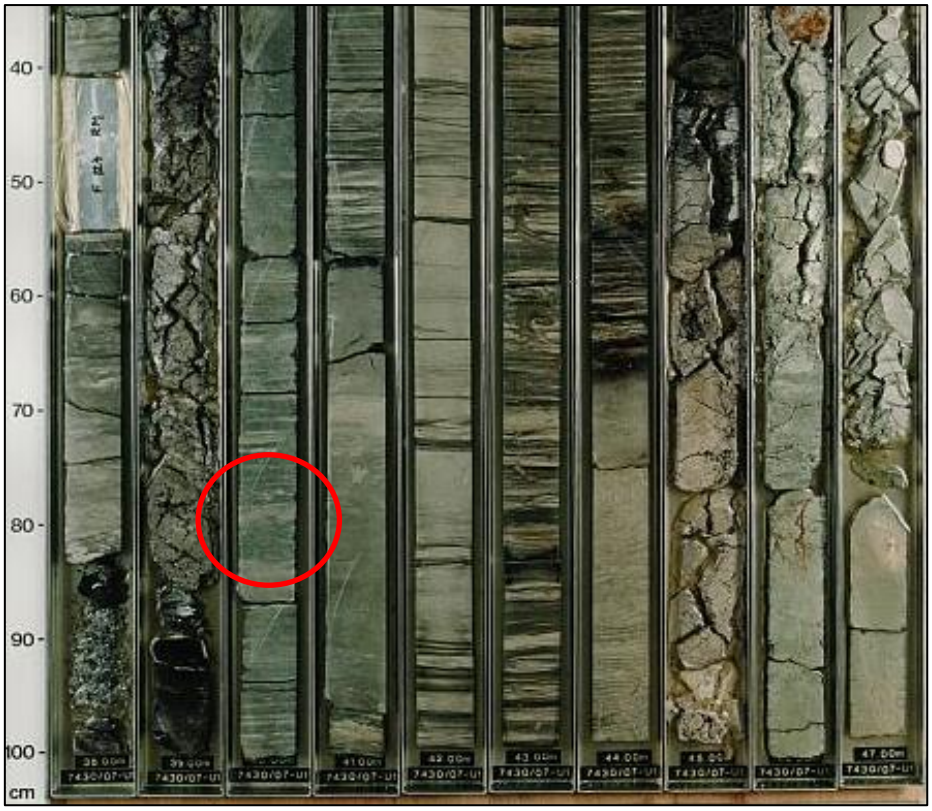

Figure 7: IKU stratigraphic drilling core photograph for the shallow core 7430/7-U-1 for the interval between 37.00-47.00 m. Mark the depth 38.80 m encircled in red that provided sample "S11" (www.sintef.no)

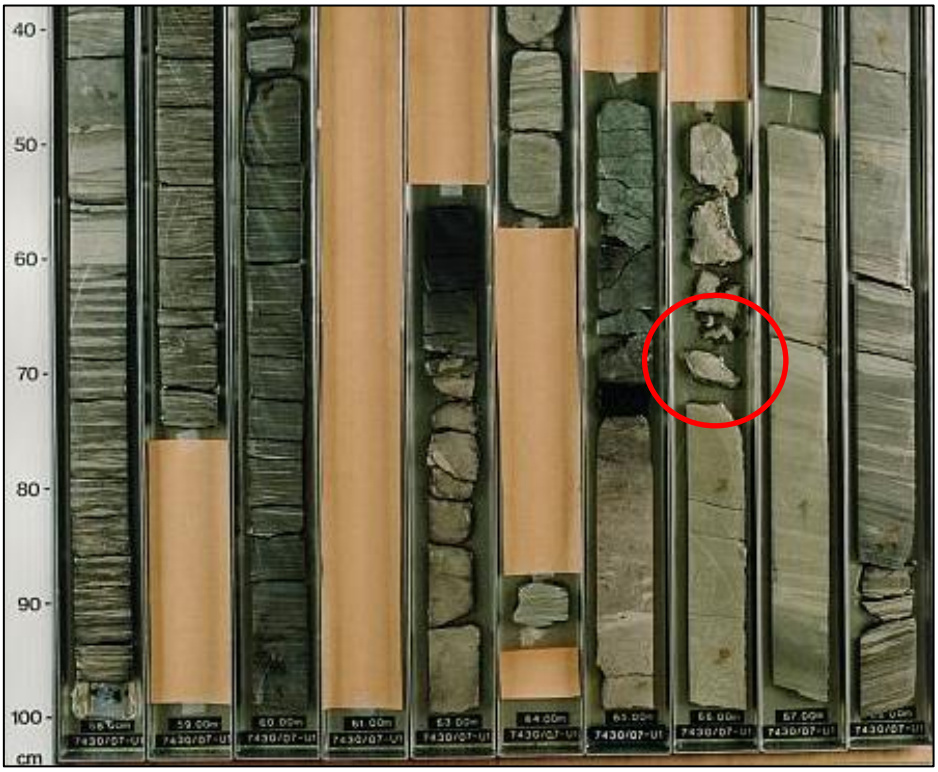

Figure 8: IKU stratigraphic drilling core photograph for the shallow core 7430/7-U-1 for the interval between 57.00-67.00 m. Mark the depth 64.70 m encircled in red that provided sample "S12" (www.sintef.no)

APPENDIX III (Chromatograph database)

GC-FID Chromatogram for standard oil sample NSO-1

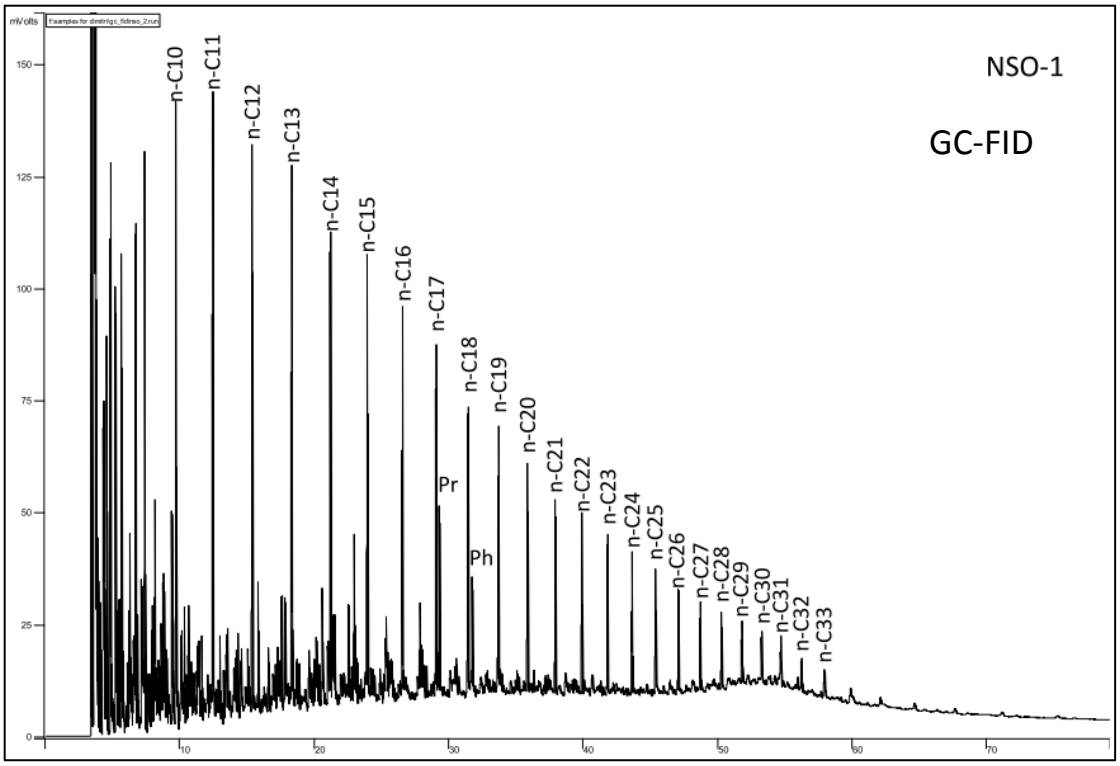

GC-MS Chromatograms for standard oil sample NSO-1

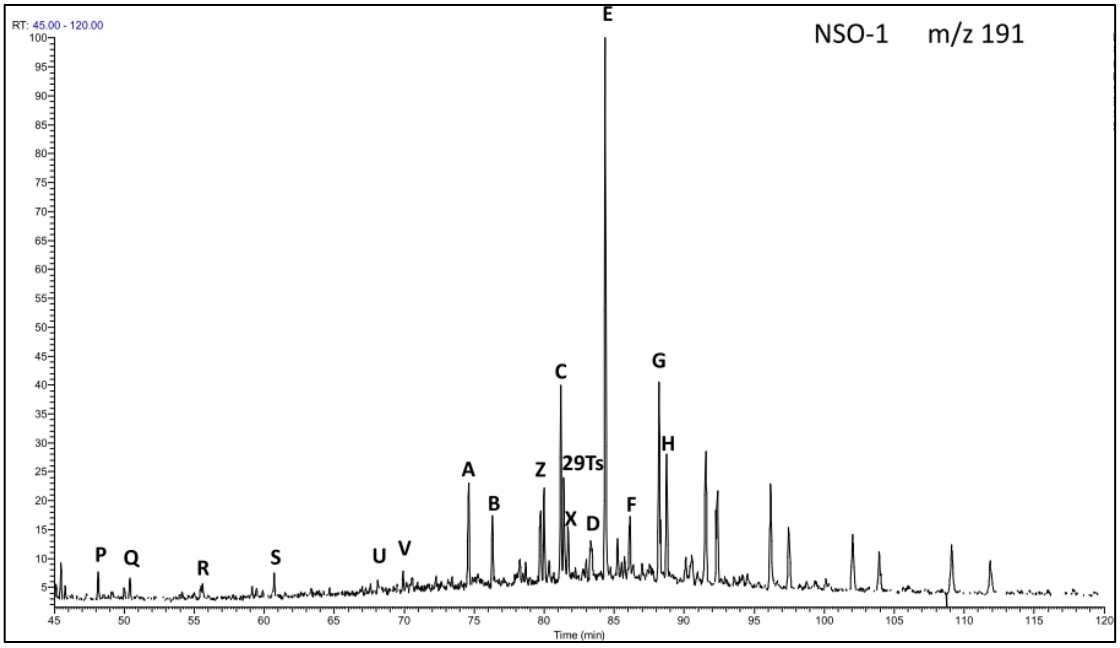

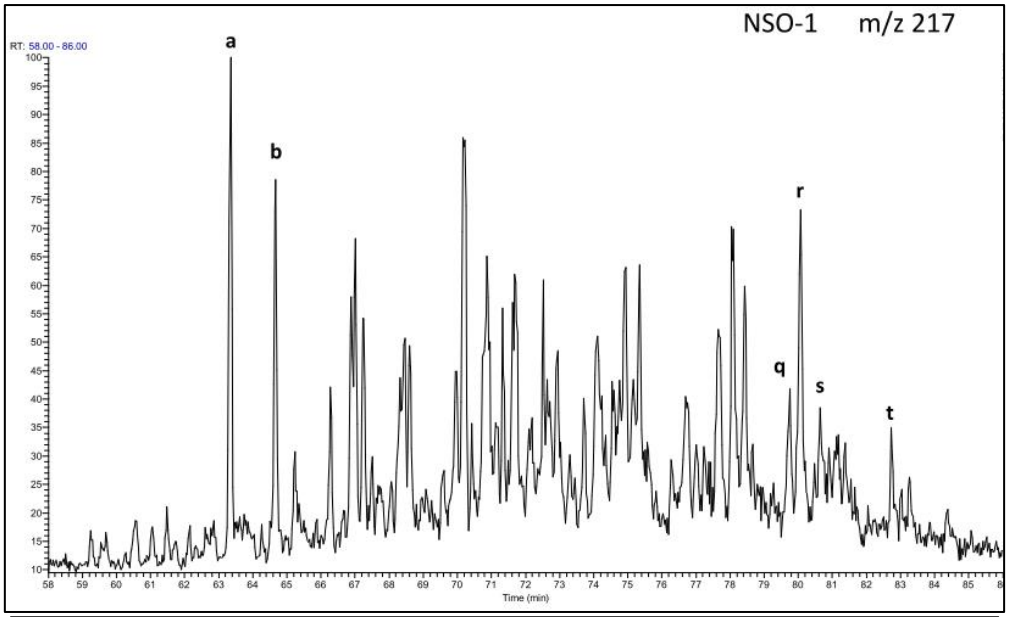
NSO-1 m/z 217
RT: 58.00 - 86.00
a
b
r
q
s
t
Time (min)

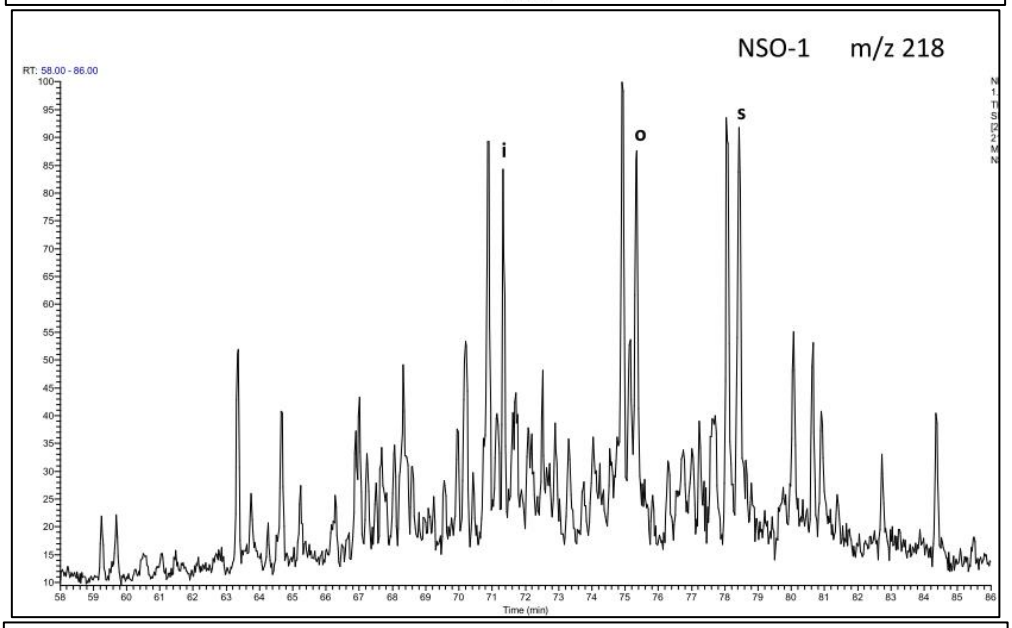
NSO-1 m/z 218
RT: 58.00 - 86.00
i
o
s
Time (min)

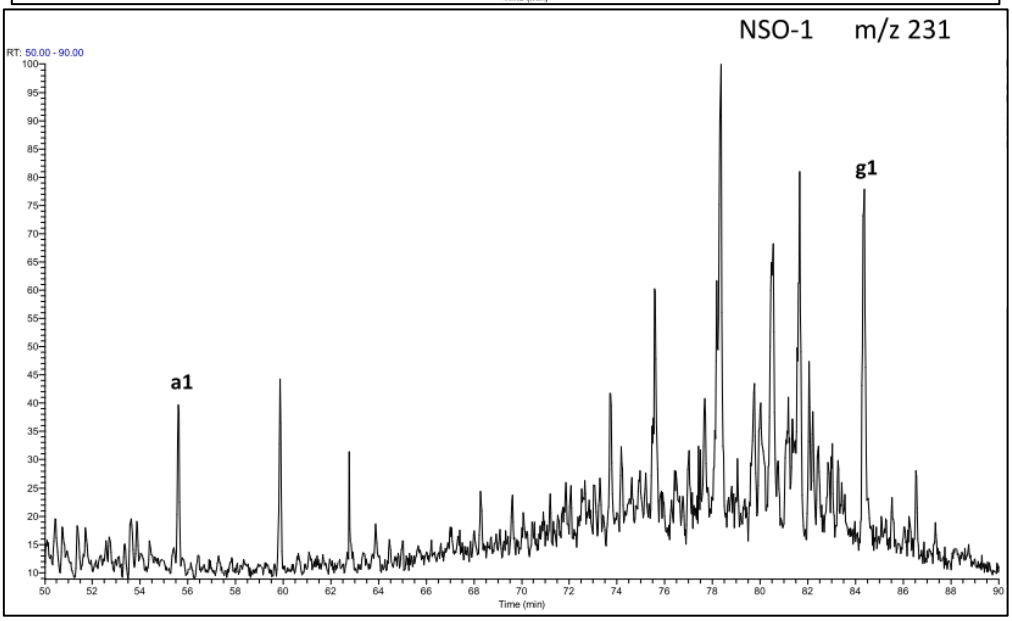
NSO-1 m/z 231
RT: 50.00 - 90.00
a1
g1
Time (min)

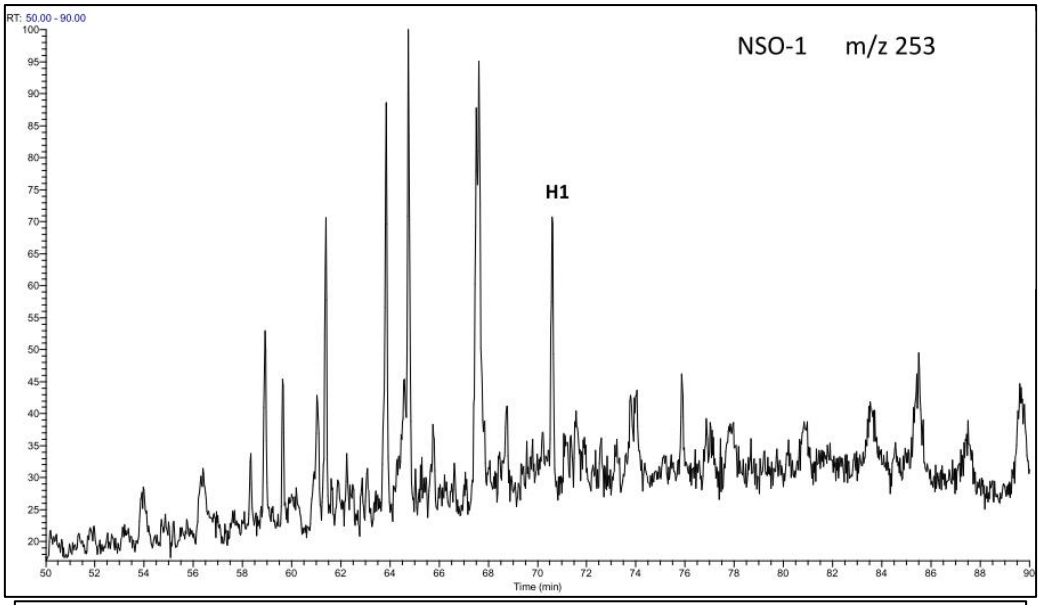
RT: 50.00 - 90.00
NSO-1 m/z 253
H1
Time (min)

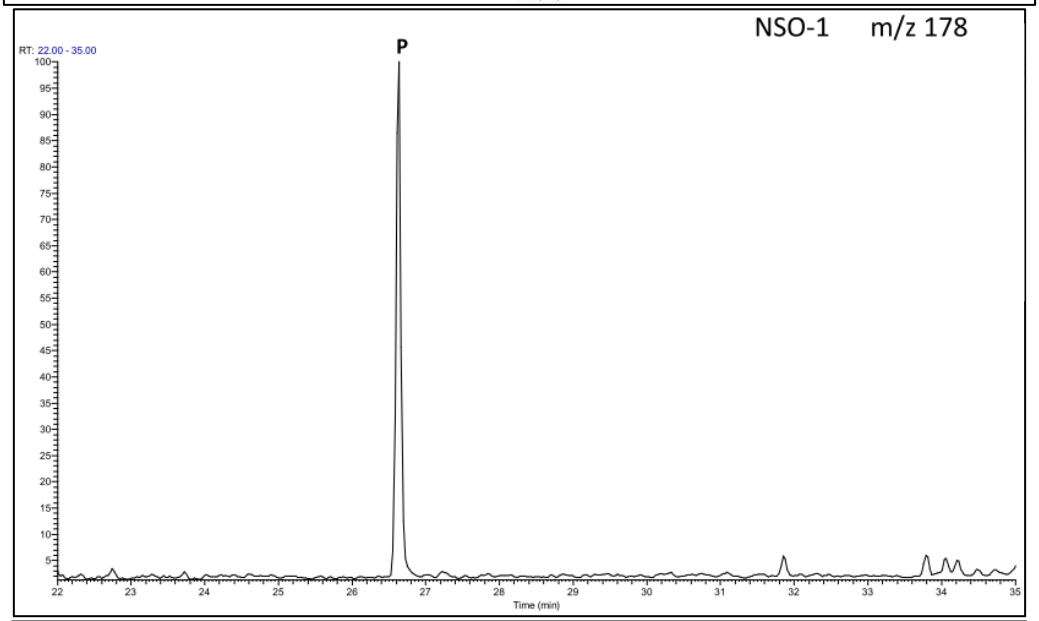
RT: 22.00 - 35.00
NSO-1 m/z 178
P
Time (min)

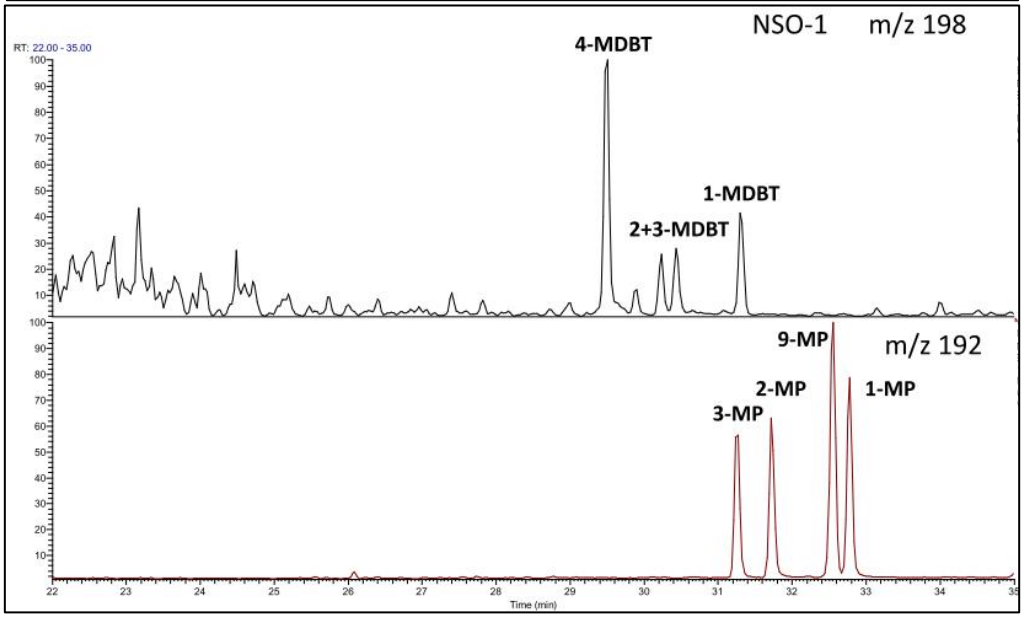
RT: 22.00 - 35.00
NSO-1 m/z 198
4-MDBT
1-MDBT
2+3-MDBT
m/z 192
9-MP
2-MP
1-MP
3-MP
Time (min)

GC-FID Chromatogram for oil sample "C" from well 7120/2-1

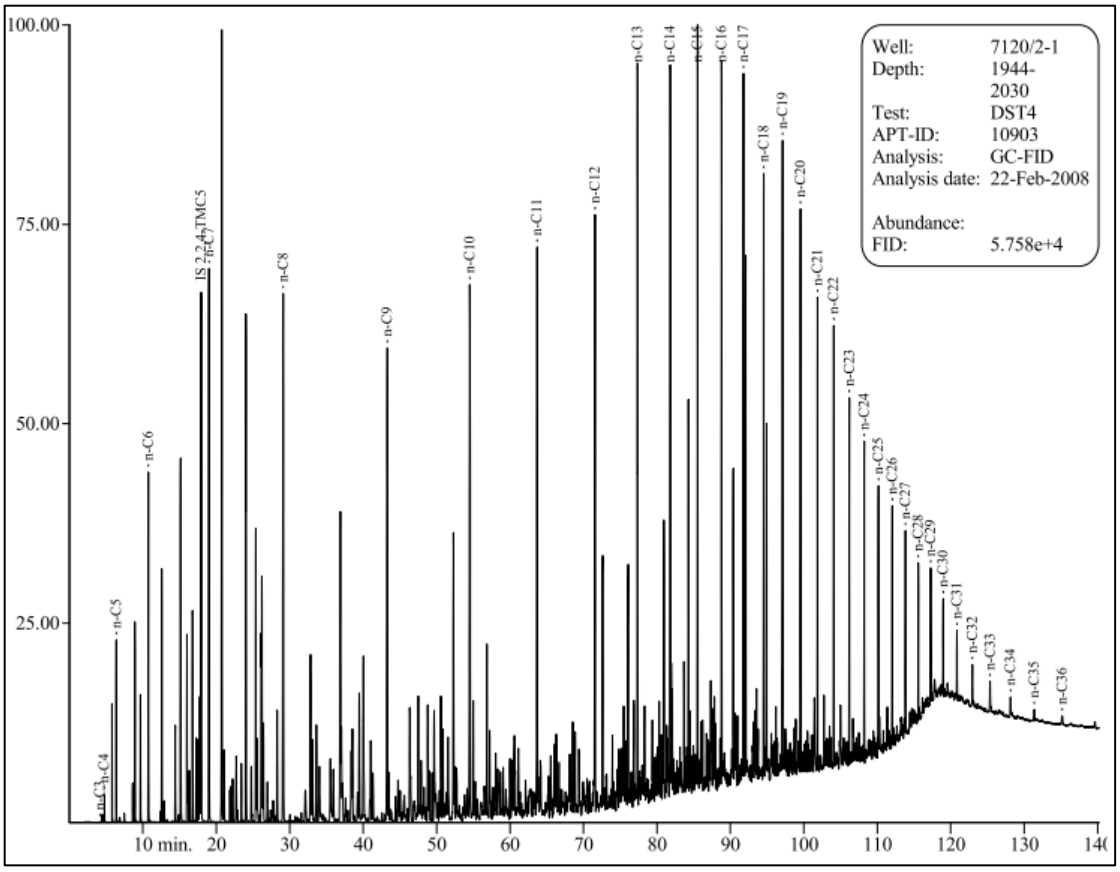

GC-MS Chromatograms for oil sample "C" from well 7120/2-1

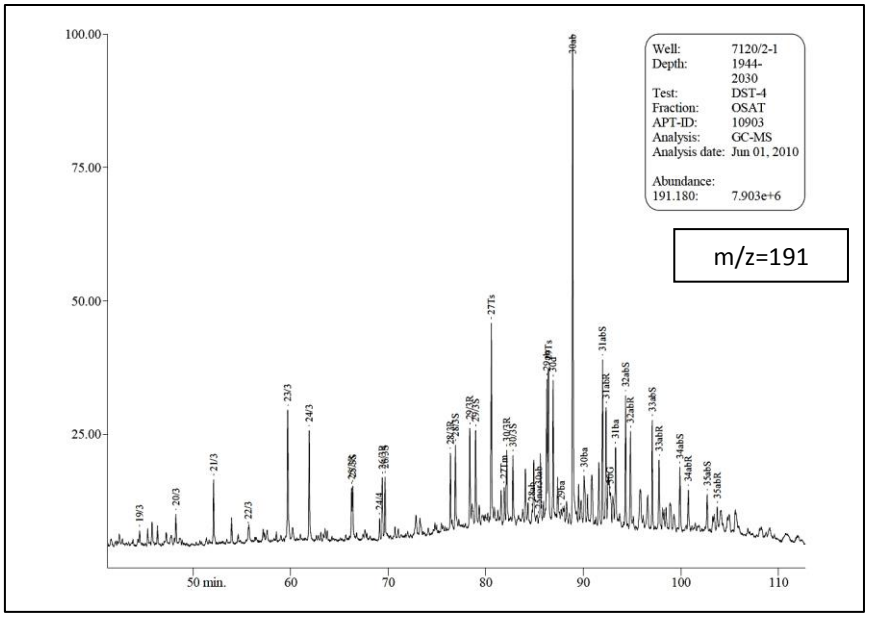

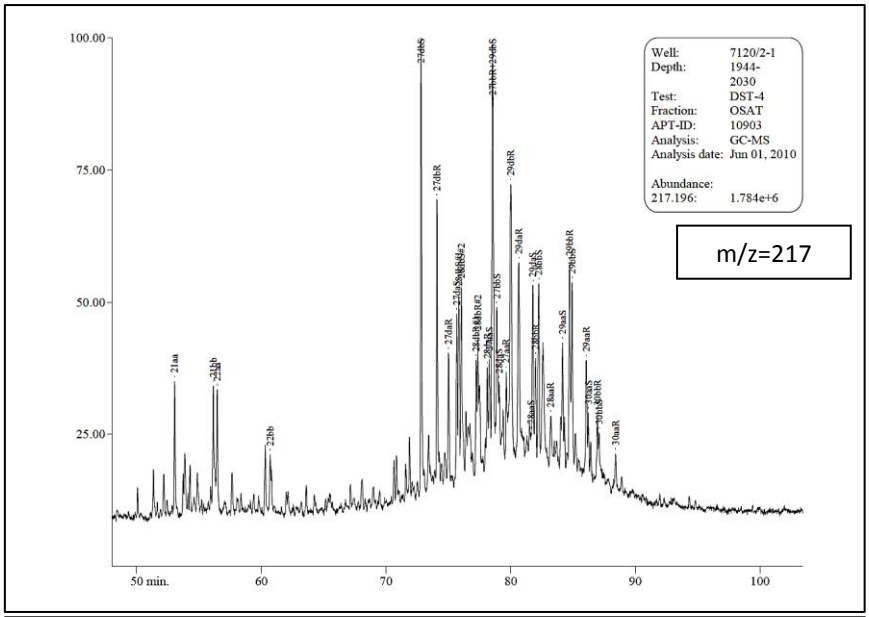
Well: 7120/2-1
Depth: 1944-2030
Test: DST-4
Fraction: OSAT
APT-ID: 10903
Analysis: GC-MS
Analysis date: Jun 01, 2010
Abundance:
217.196: 1.784e+6
m/z=217
100.00
75.00
50.00
25.00
50 min.
60
70
80
90
100

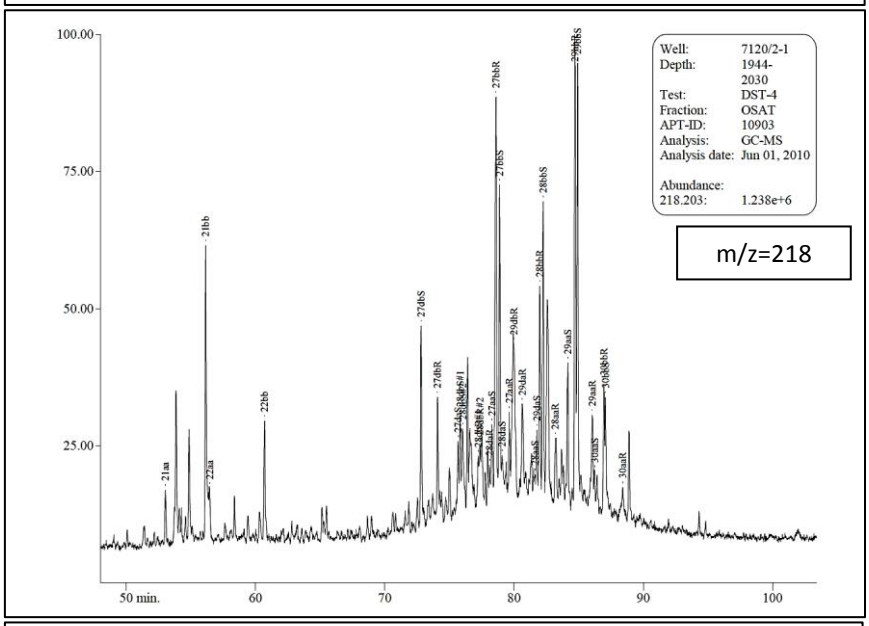
Well: 7120/2-1
Depth: 1944-2030
Test: DST-4
Fraction: OSAT
APT-ID: 10903
Analysis: GC-MS
Analysis date: Jun 01, 2010
Abundance:
218.203: 1.238e+6
m/z=218
100.00
75.00
50.00
25.00
50 min.
60
70
80
90
100

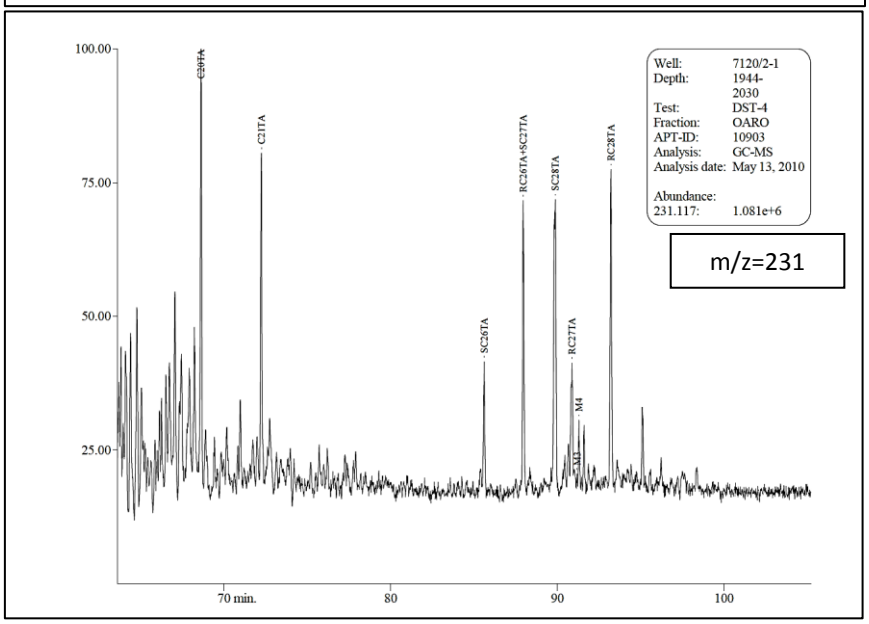
Well: 7120/2-1
Depth: 1944-2030
Test: DST-4
Fraction: OARO
APT-ID: 10903
Analysis: GC-MS
Analysis date: May 13, 2010
Abundance:
231.117: 1.081e+6
m/z=231
100.00
75.00
50.00
25.00
70 min.
80
90
100

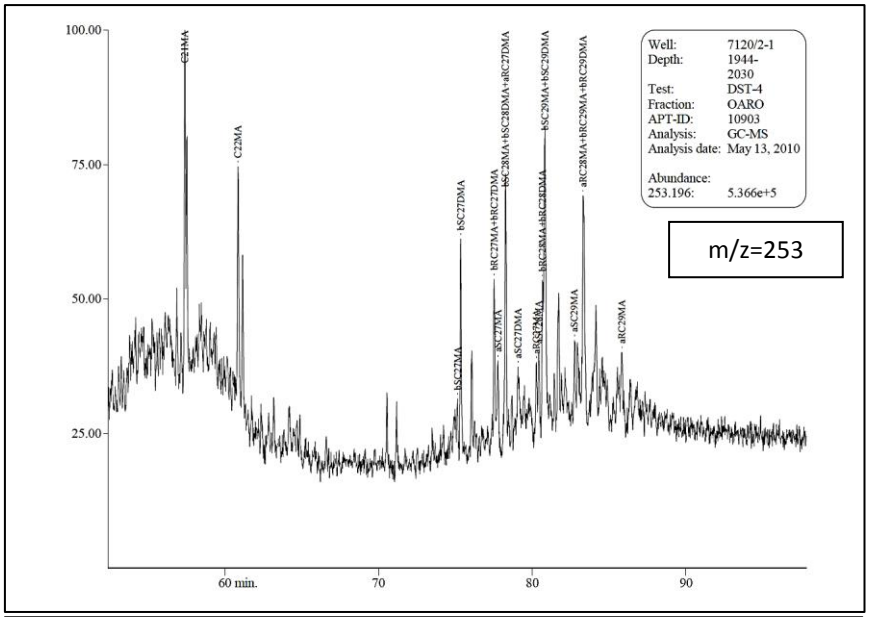
Well: 7120/2-1
Depth: 1944-2030
Test: DST-4
Fraction: OARO
APT-ID: 10903
Analysis: GC-MS
Analysis date: May 13, 2010
Abundance:
253.196: 5.366e+5
m/z=253
C21MA
C22MA
bSC27DMA
bRC27MA+bRC27DMA
bSC28MA+bSC28DMA+aRC27DMA
bSC29MA+bSC29DMA
aRC28MA+bRC29MA+bRC29DMA
aSC27MA
aSC27DMA
aSC29MA
aRC29MA
100.00
75.00
50.00
25.00
60 min.
70
80
90

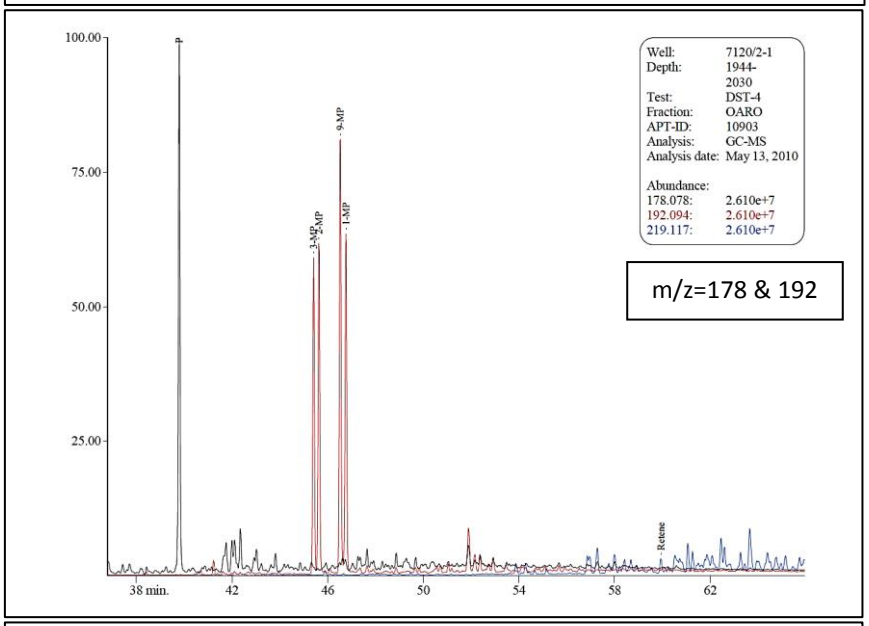
Well: 7120/2-1
Depth: 1944-2030
Test: DST-4
Fraction: OARO
APT-ID: 10903
Analysis: GC-MS
Analysis date: May 13, 2010
Abundance:
178.078: 2.610e+7
192.094: 2.610e+7
219.117: 2.610e+7
m/z=178 & 192
P
3-MP
2-MP
9-MP
1-MP
Retene
100.00
75.00
50.00
25.00
38 min.
42
46
50
54
58
62

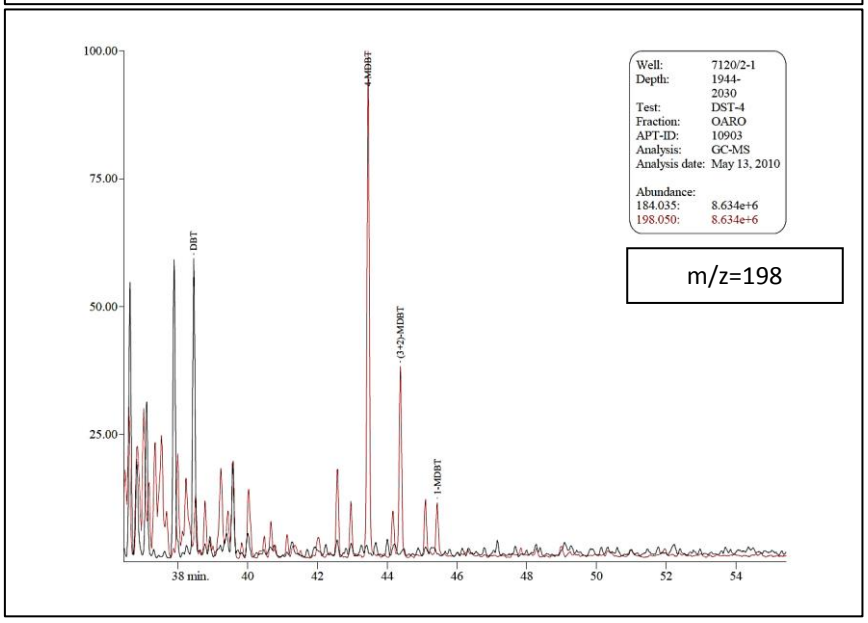
Well: 7120/2-1
Depth: 1944-2030
Test: DST-4
Fraction: OARO
APT-ID: 10903
Analysis: GC-MS
Analysis date: May 13, 2010
Abundance:
184.035: 8.634e+6
198.050: 8.634e+6
m/z=198
4-MDBT
DBT
(3+2)-MDBT
1-MDBT
100.00
75.00
50.00
25.00
38 min.
40
42
44
46
48
50
52
54

GC-FID Chromatogram for oil sample "E1" from well 7120/6-1

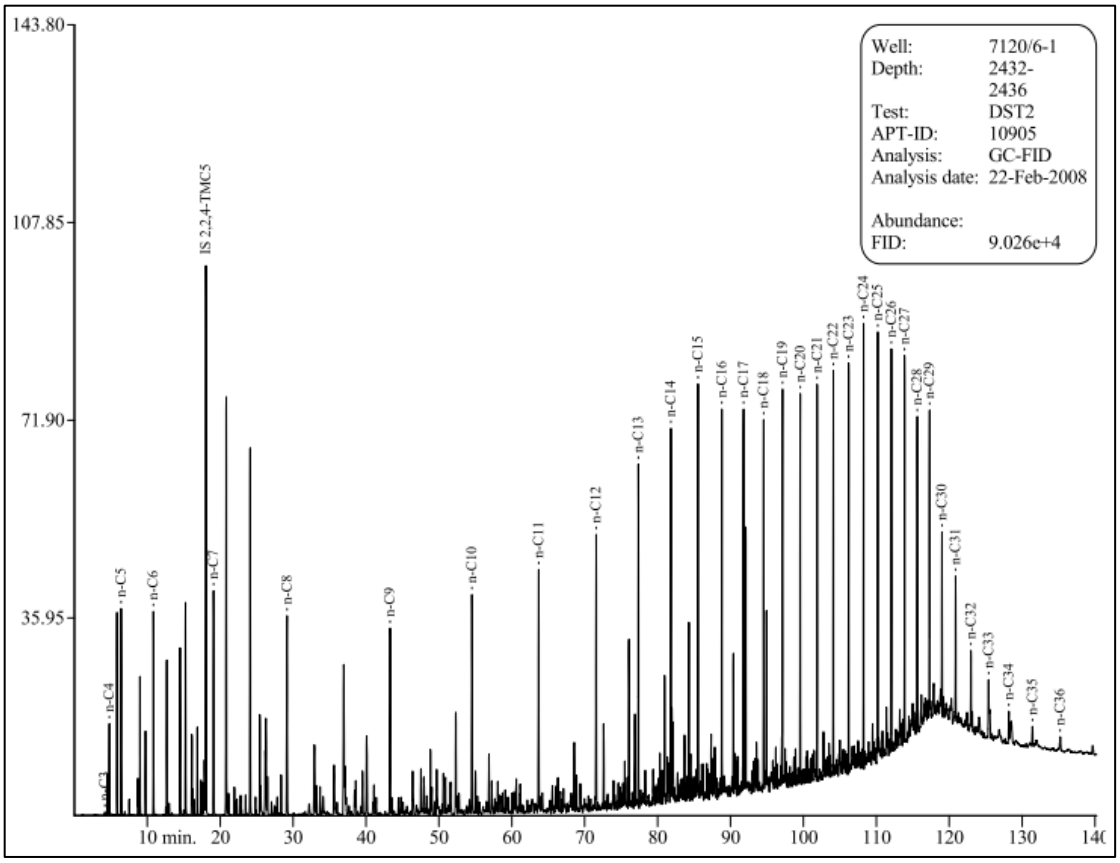

GC-MS Chromatograms for oil sample "E1" from well 7120/6-1

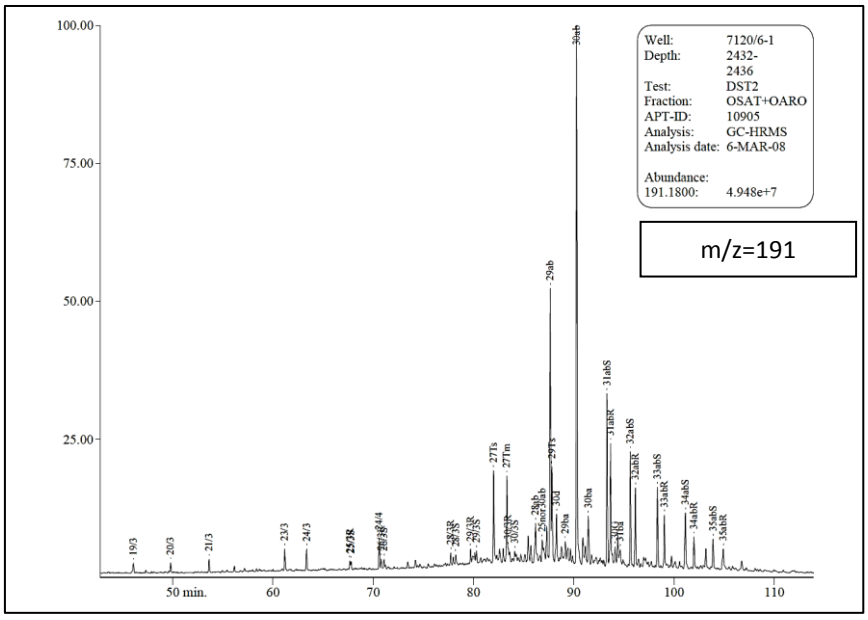

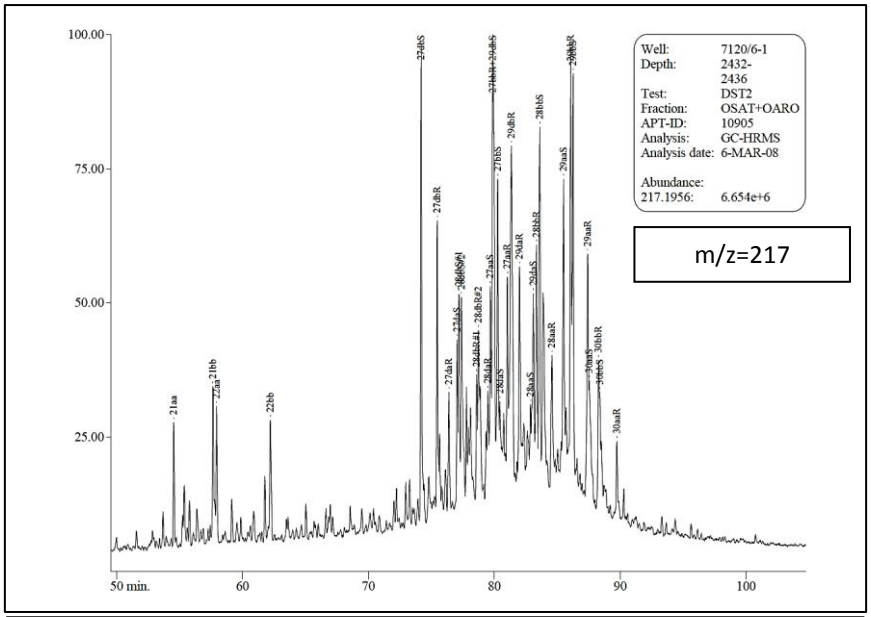
Well: 7120/6-1
Depth: 2432-2436
Test: DST2
Fraction: OSAT+OARO
APT-ID: 10905
Analysis: GC-HRMS
Analysis date: 6-MAR-08
Abundance:
217.1956: 6.654e+6
m/z=217
100.00
75.00
50.00
25.00
50 min.
60
70
80
90
100

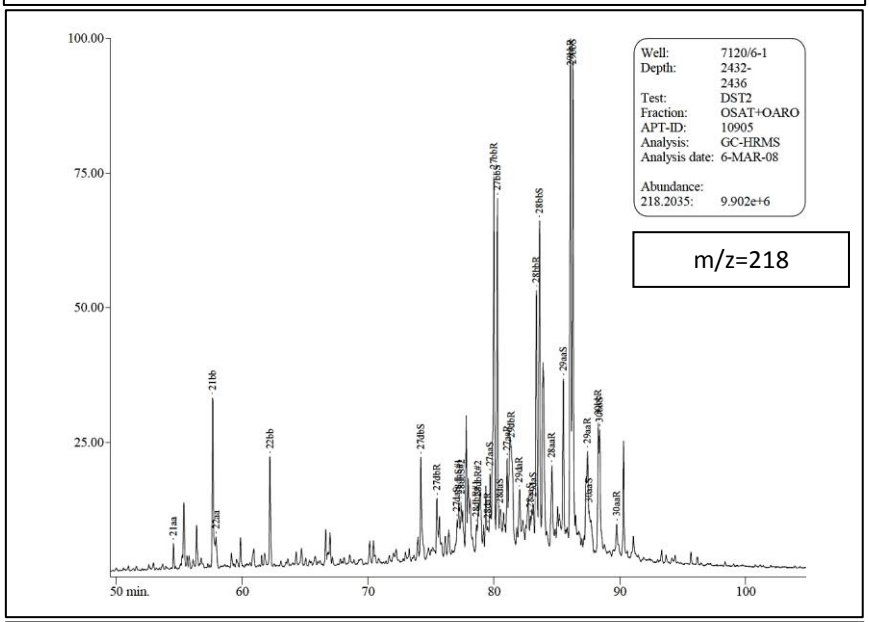
Well: 7120/6-1
Depth: 2432-2436
Test: DST2
Fraction: OSAT+OARO
APT-ID: 10905
Analysis: GC-HRMS
Analysis date: 6-MAR-08
Abundance:
218.2035: 9.902e+6
m/z=218
100.00
75.00
50.00
25.00
50 min.
60
70
80
90
100

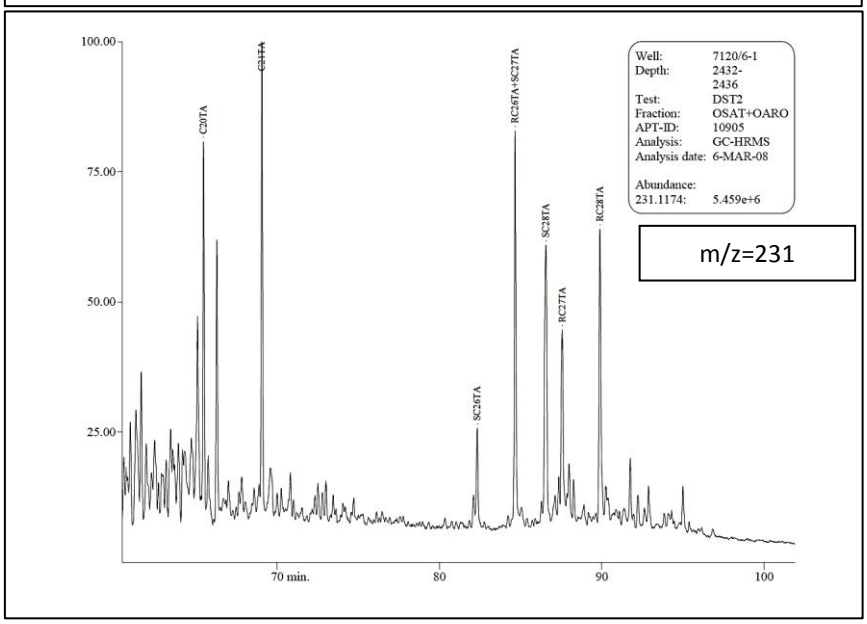
Well: 7120/6-1
Depth: 2432-2436
Test: DST2
Fraction: OSAT+OARO
APT-ID: 10905
Analysis: GC-HRMS
Analysis date: 6-MAR-08
Abundance:
231.1174: 5.459e+6
m/z=231
100.00
75.00
50.00
25.00
70 min.
80
90
100

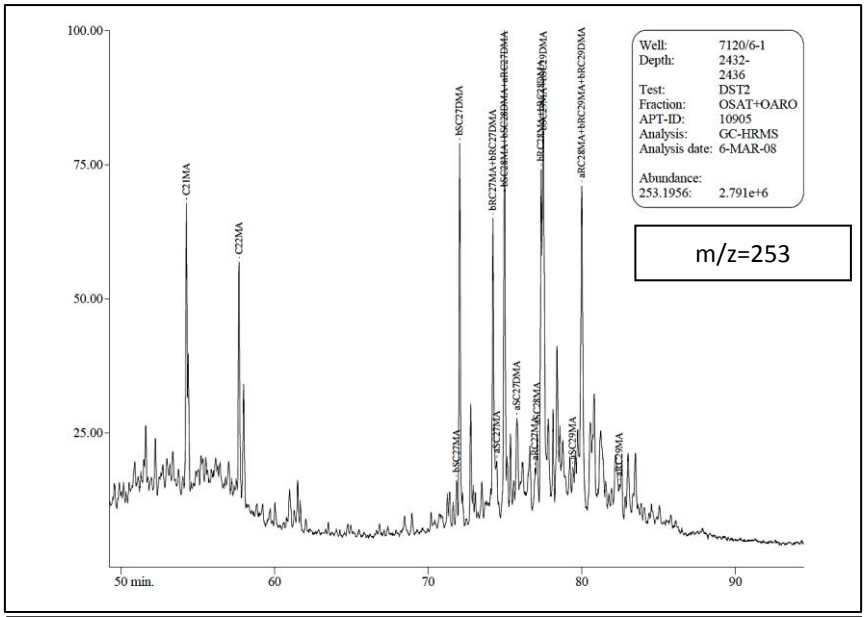
Well: 7120/6-1
Depth: 2432-2436
Test: DST2
Fraction: OSAT+OARO
APT-ID: 10905
Analysis: GC-HRMS
Analysis date: 6-MAR-08
Abundance:
253.1956: 2.791e+6
m/z=253
C1MA
C2MA
bSC27DMA
bRC27MA+bRC27DMA
aSC27DMA
bRC29MA+bRC29DMA
50 min.
60
70
80
90

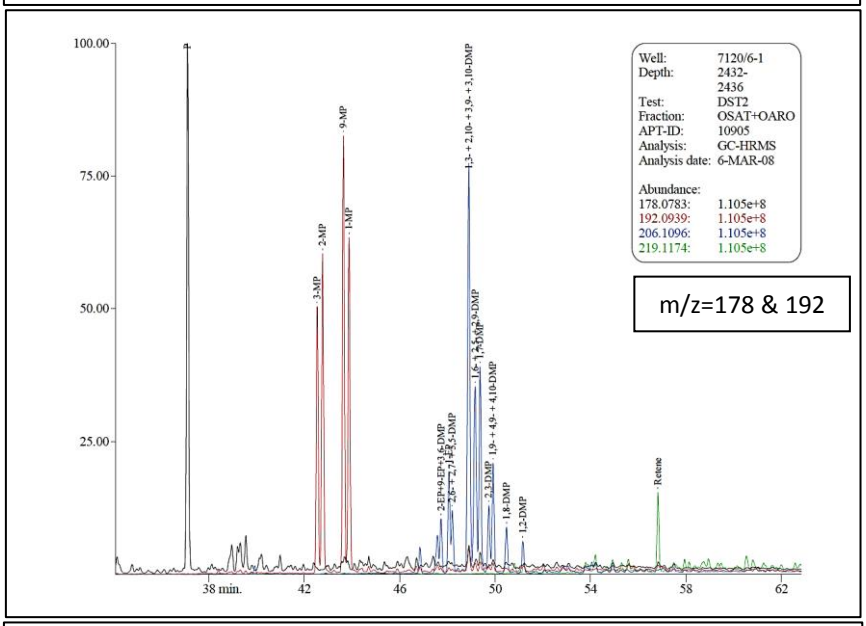
Well: 7120/6-1
Depth: 2432-2436
Test: DST2
Fraction: OSAT+OARO
APT-ID: 10905
Analysis: GC-HRMS
Analysis date: 6-MAR-08
Abundance:
178.0783: 1.105e+8
192.0939: 1.105e+8
206.1096: 1.105e+8
219.1174: 1.105e+8
m/z=178 & 192
3-MP
2-MP
9-MP
1-MP
1,3- + 2,10- + 3,9- + 3,10-DMP
1,6- + 3,5- + 3,9-DMP
1,9- + 4,9- + 4,10-DMP
2,3-DMP
1,8-DMP
1,2-DMP
Retene
38 min.
42
46
50
54
58
62

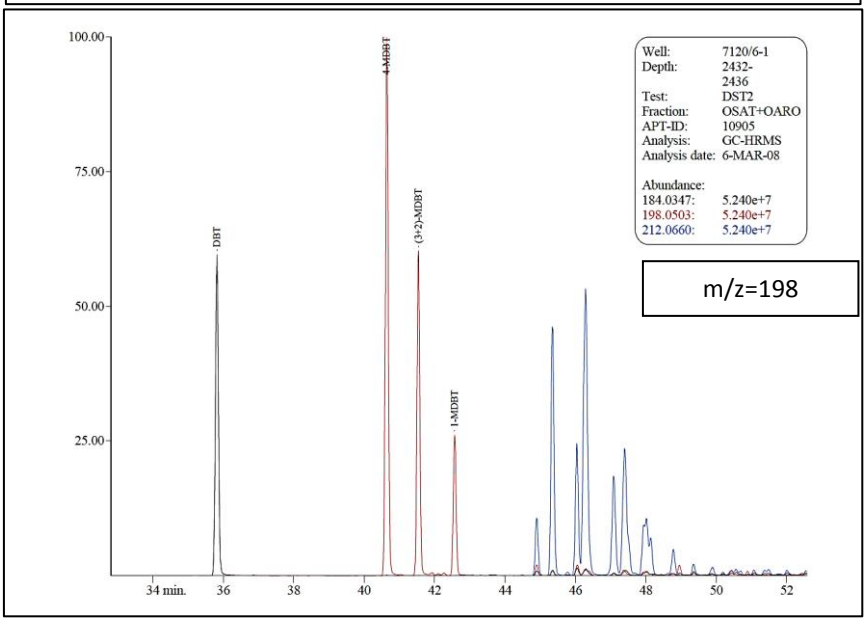
Well: 7120/6-1
Depth: 2432-2436
Test: DST2
Fraction: OSAT+OARO
APT-ID: 10905
Analysis: GC-HRMS
Analysis date: 6-MAR-08
Abundance:
184.0347: 5.240e+7
198.0503: 5.240e+7
212.0660: 5.240e+7
m/z=198
DBT
4-MDBT
(3+2)-MDBT
1-MDBT
34 min.
36
38
40
42
44
46
48
50
52

GC-FID Chromatogram for oil sample "O" from well 7121/5-2

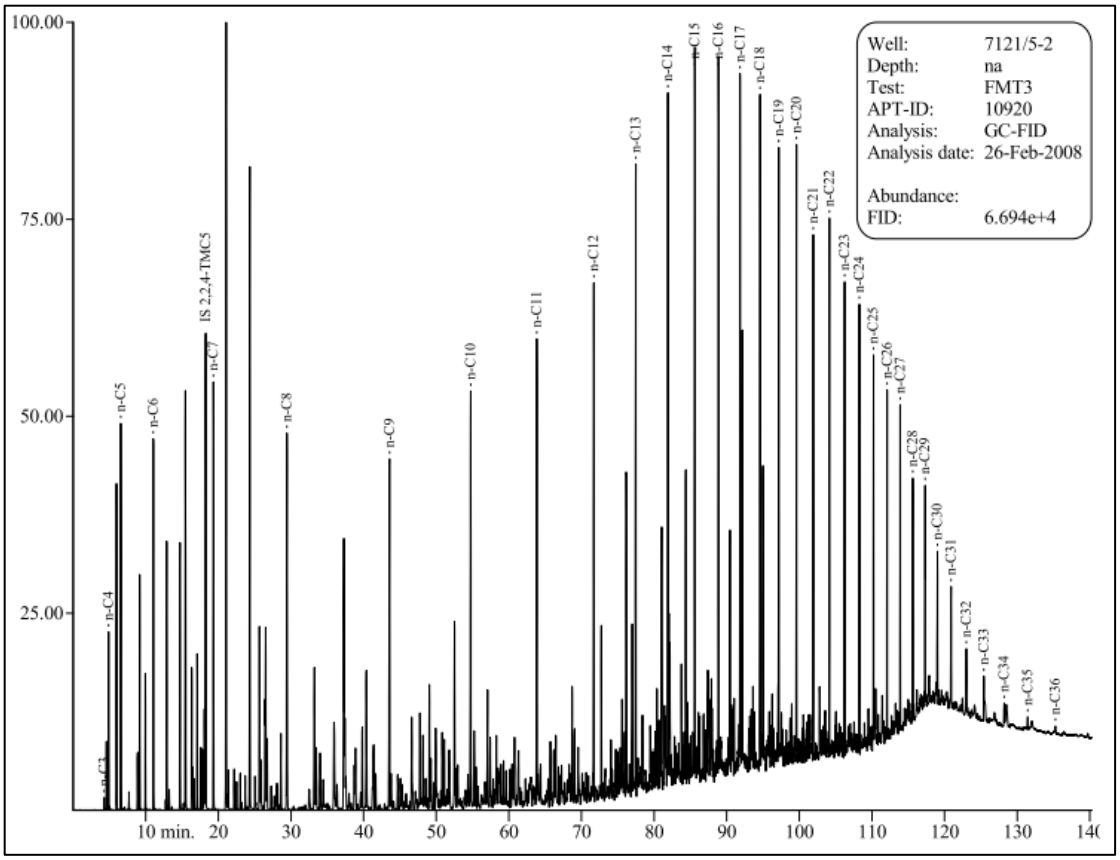

GC-MS Chromatograms for oil sample "O" from well 7121/5-2

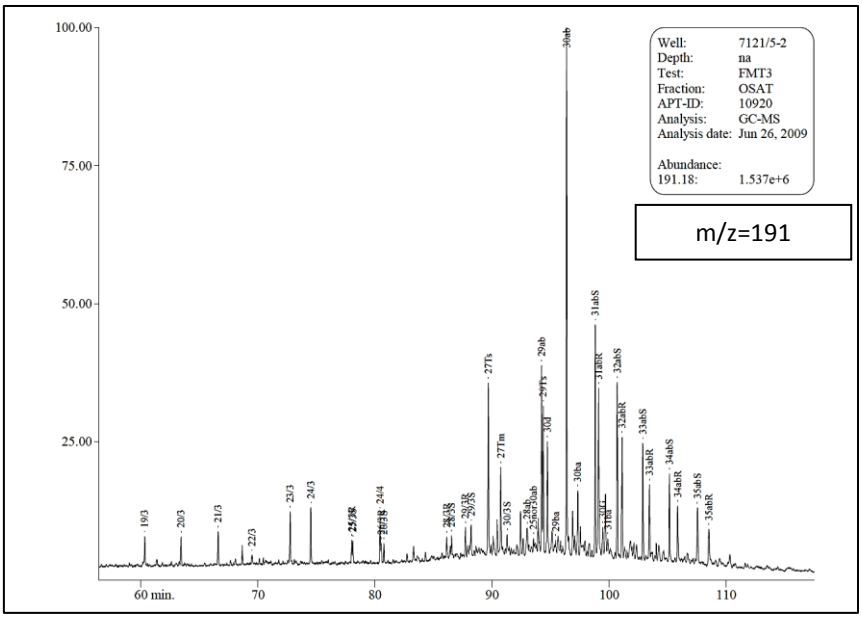

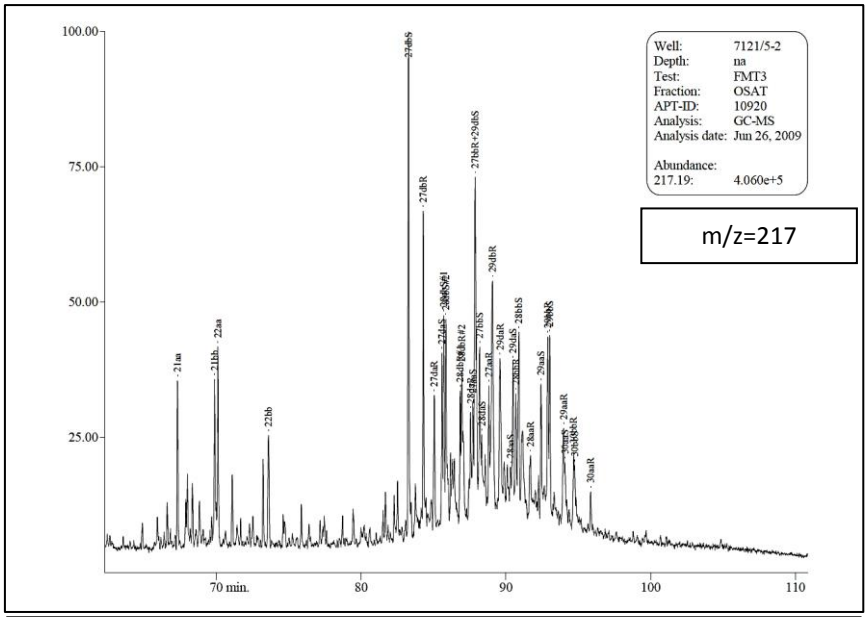
Well: 7121/5-2
Depth: na
Test: FMT3
Fraction: OSAT
APT-ID: 10920
Analysis: GC-MS
Analysis date: Jun 26, 2009
Abundance:
217.19: 4.060e+5
m/z=217
100.00
75.00
50.00
25.00
70 min.
80
90
100
110

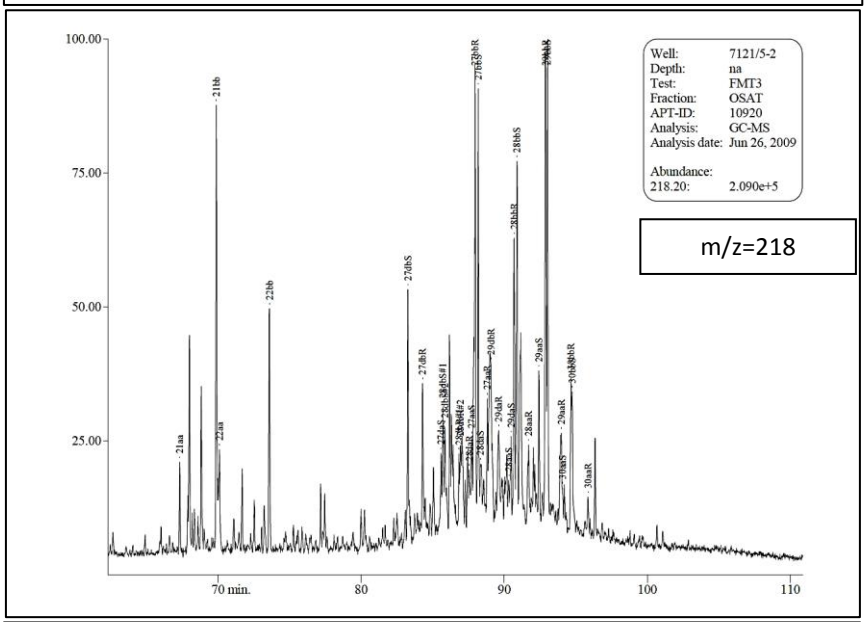
Well: 7121/5-2
Depth: na
Test: FMT3
Fraction: OSAT
APT-ID: 10920
Analysis: GC-MS
Analysis date: Jun 26, 2009
Abundance:
218.20: 2.090e+5
m/z=218
100.00
75.00
50.00
25.00
70 min.
80
90
100
110

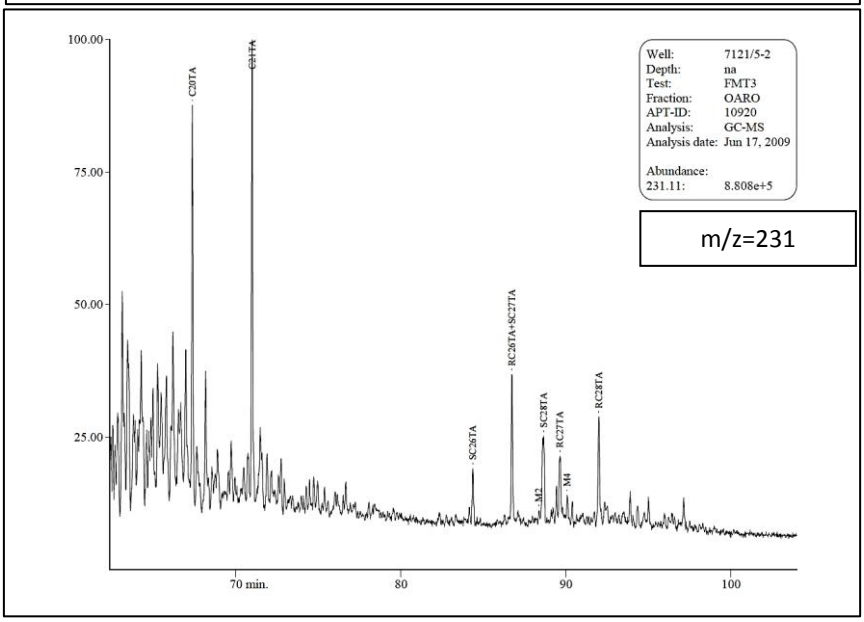
Well: 7121/5-2
Depth: na
Test: FMT3
Fraction: OARO
APT-ID: 10920
Analysis: GC-MS
Analysis date: Jun 17, 2009
Abundance:
231.11: 8.808e+5
m/z=231
100.00
75.00
50.00
25.00
C20TA
C21TA
SC26TA
RC26TA+SC27TA
SC28TA
M2
RC27TA
M4
RC28TA
70 min.
80
90
100

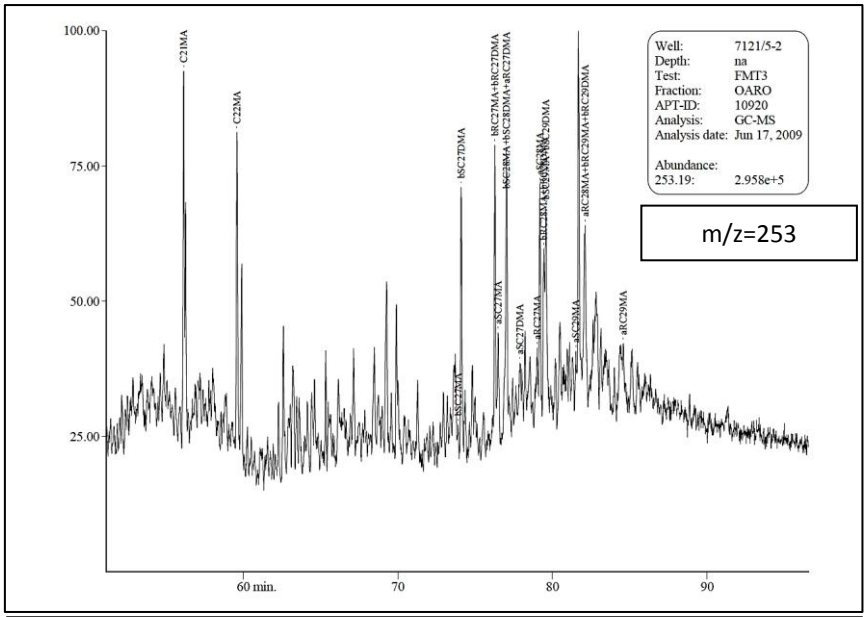
C21MA
C22MA
bSC27DMA
aSC27MA
aSC27DMA
aRC27MA
aSC29MA
aRC29MA
Well: 7121/5-2
Depth: na
Test: FMT3
Fraction: OARO
APT-ID: 10920
Analysis: GC-MS
Analysis date: Jun 17, 2009
Abundance:
253.19: 2.958e+5
m/z=253
60 min.

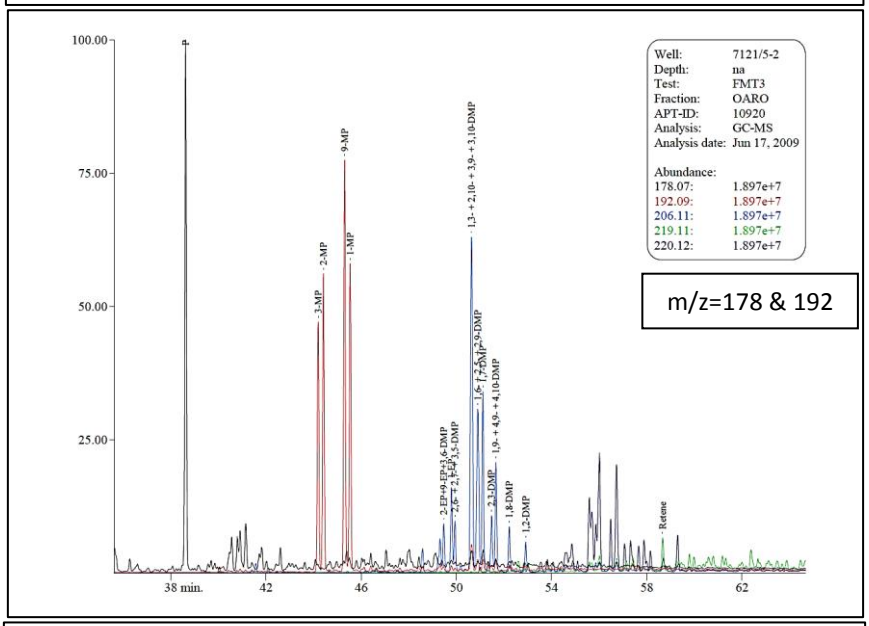
p.
3-MP
2-MP
9-MP
1-MP
1,3- + 2,10- + 3,9- + 3,10-DMP
1,8-DMP
1,2-DMP
Retene
Well: 7121/5-2
Depth: na
Test: FMT3
Fraction: OARO
APT-ID: 10920
Analysis: GC-MS
Analysis date: Jun 17, 2009
Abundance:
178.07: 1.897e+7
192.09: 1.897e+7
206.11: 1.897e+7
219.11: 1.897e+7
220.12: 1.897e+7
m/z=178 & 192
38 min.

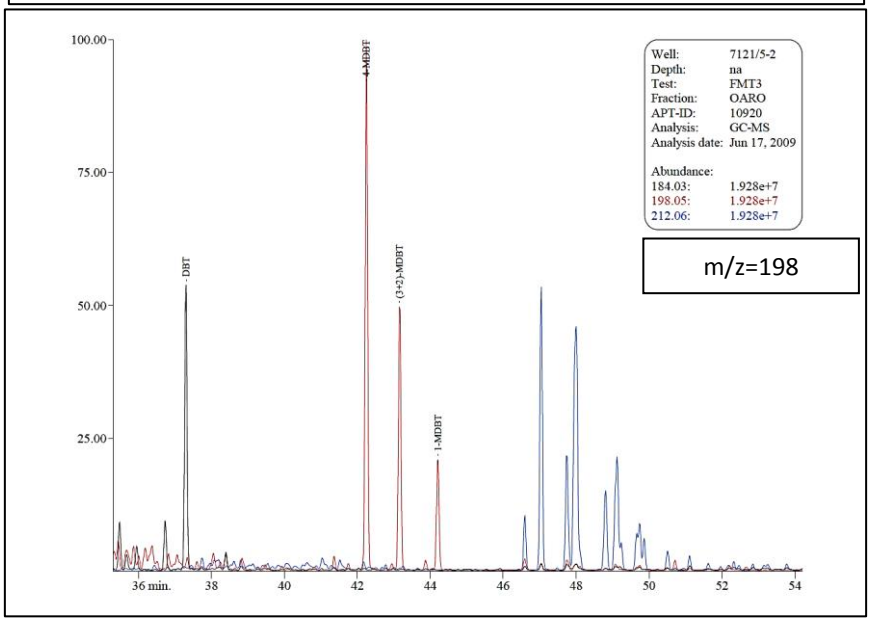
4-MDBT
DBT
(3+2)-MDBT
1-MDBT
Well: 7121/5-2
Depth: na
Test: FMT3
Fraction: OARO
APT-ID: 10920
Analysis: GC-MS
Analysis date: Jun 17, 2009
Abundance:
184.03: 1.928e+7
198.05: 1.928e+7
212.06: 1.928e+7
m/z=198
36 min.

GC-FID Chromatogram for oil sample "T2" from well 7122/7-3

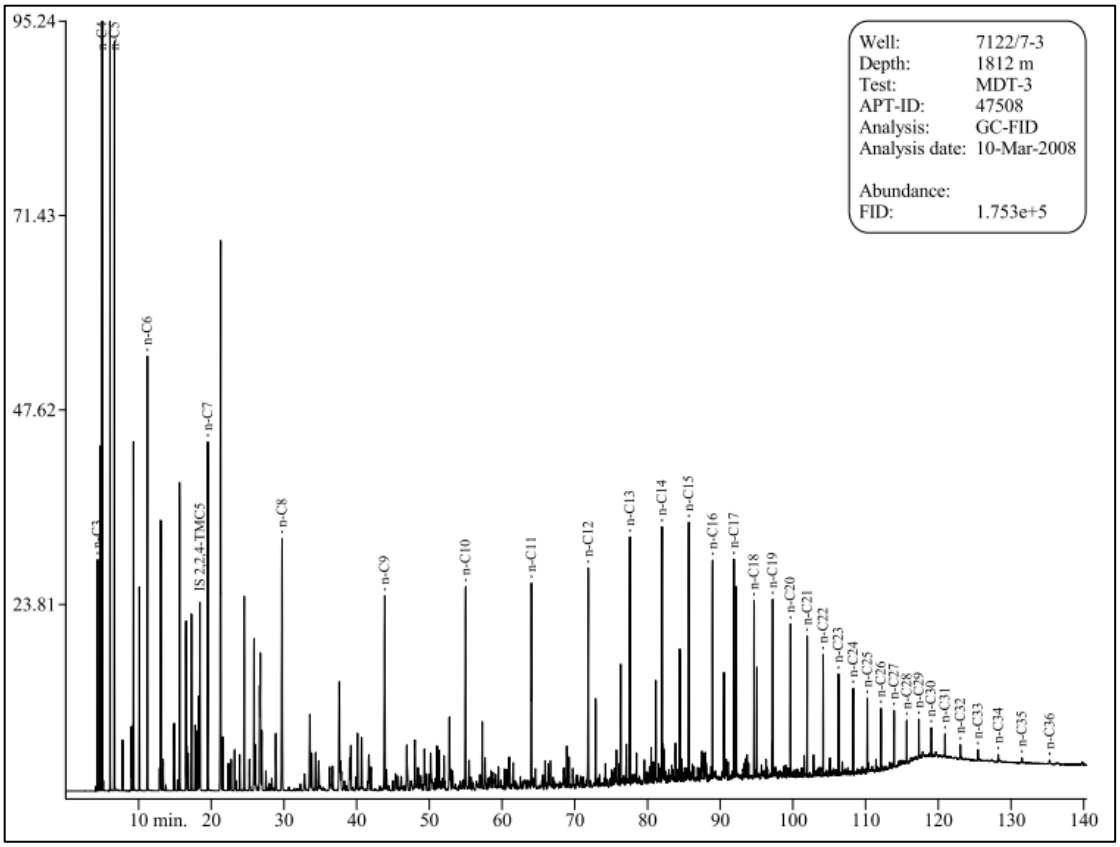

GC-MS Chromatograms for oil sample "T1" from well 7122/7-3

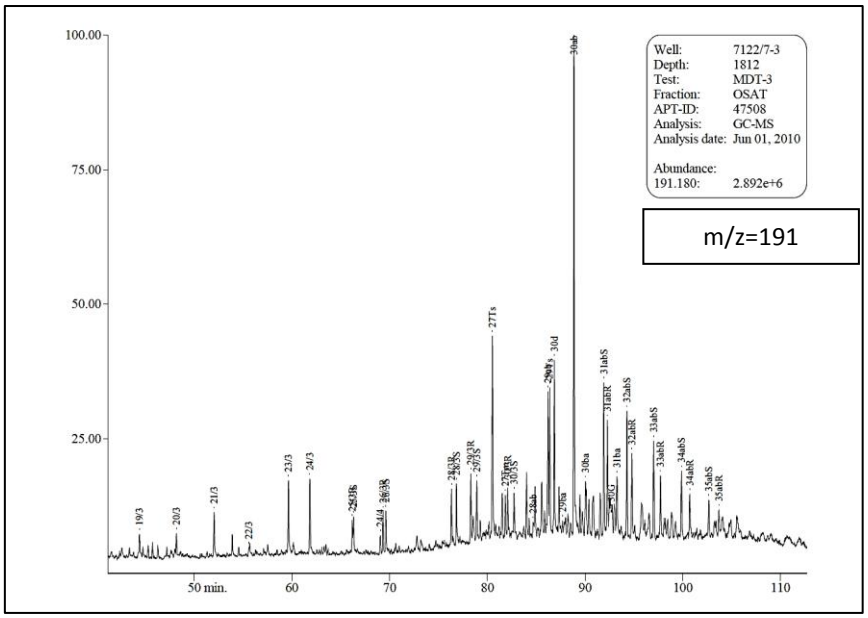

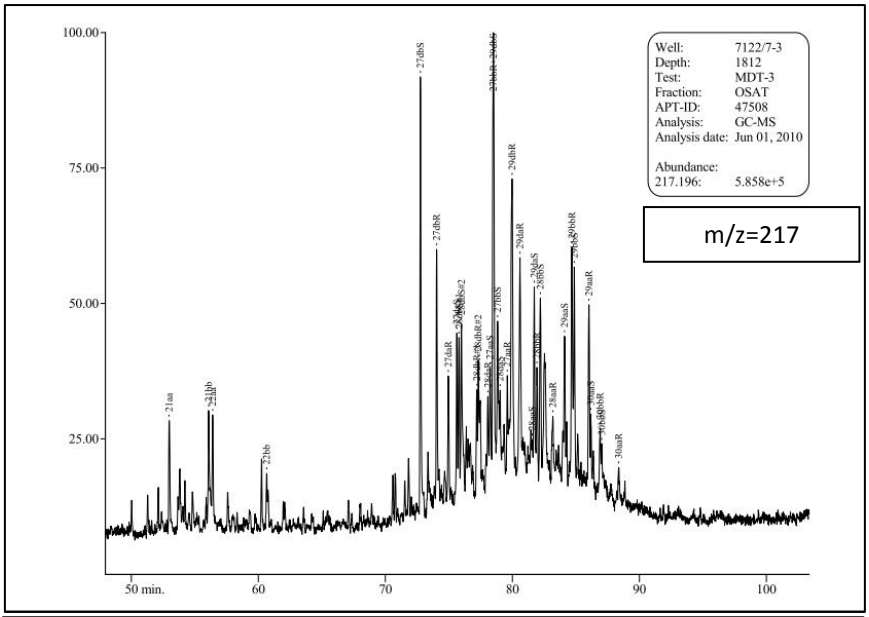
Well: 7122/7-3
Depth: 1812
Test: MDT-3
Fraction: OSAT
APT-ID: 47508
Analysis: GC-MS
Analysis date: Jun 01, 2010
Abundance:
217.196: 5.858e+5
m/z=217

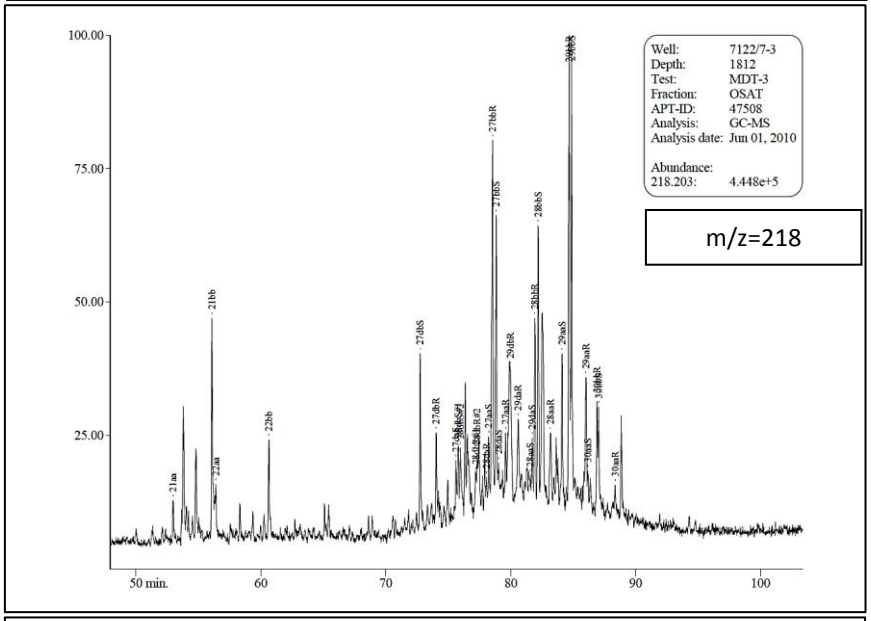
Well: 7122/7-3
Depth: 1812
Test: MDT-3
Fraction: OSAT
APT-ID: 47508
Analysis: GC-MS
Analysis date: Jun 01, 2010
Abundance:
218.203: 4.448e+5
m/z=218

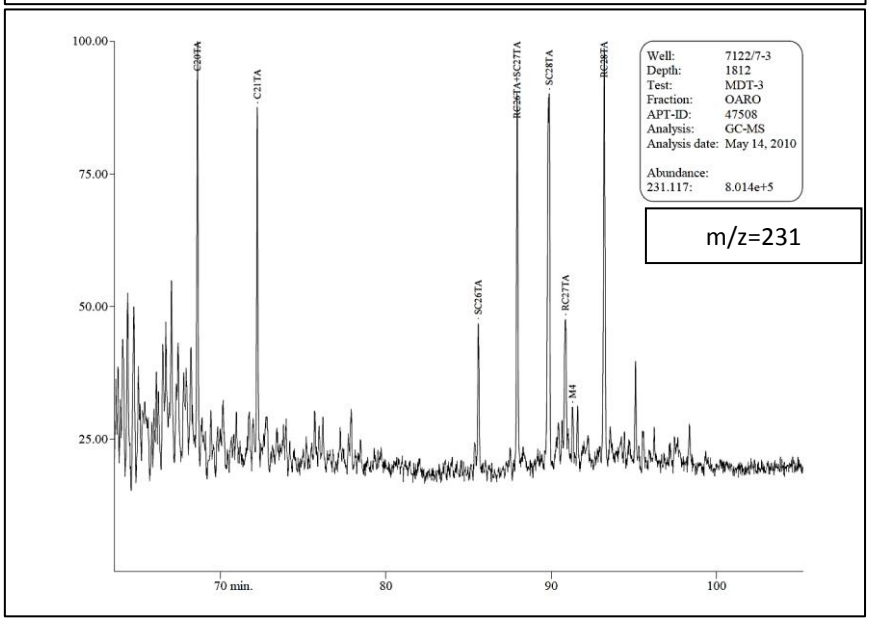
Well: 7122/7-3
Depth: 1812
Test: MDT-3
Fraction: OARO
APT-ID: 47508
Analysis: GC-MS
Analysis date: May 14, 2010
Abundance:
231.117: 8.014e+5
m/z=231

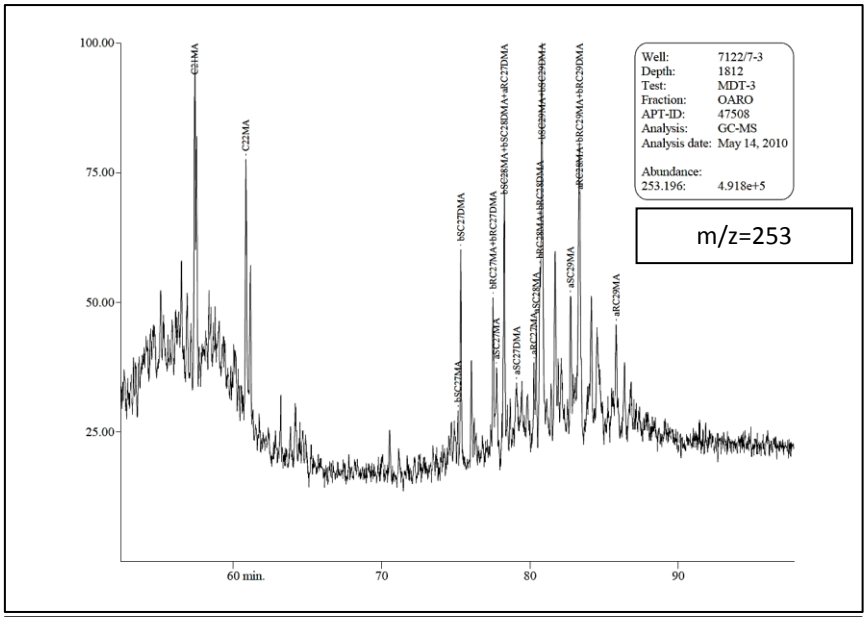
Well: 7122/7-3
Depth: 1812
Test: MDT-3
Fraction: OARO
APT-ID: 47508
Analysis: GC-MS
Analysis date: May 14, 2010
Abundance:
253.196: 4.918e+5
m/z=253
C21MA
C22MA
bSC27DMA
bRC27MA+bRC27DMA
aRC27MA
aSC27DMA
bSC27MA
60 min.

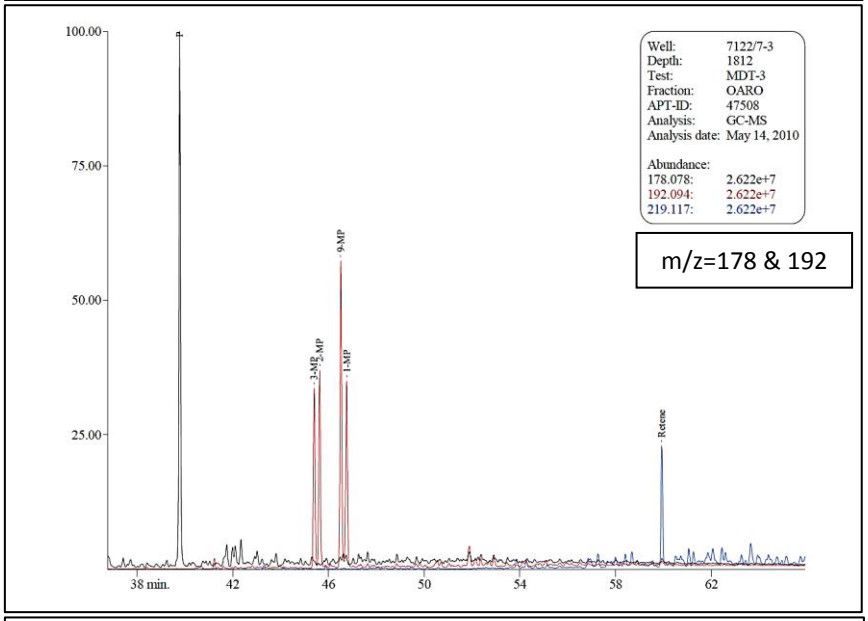
Well: 7122/7-3
Depth: 1812
Test: MDT-3
Fraction: OARO
APT-ID: 47508
Analysis: GC-MS
Analysis date: May 14, 2010
Abundance:
178.078: 2.622e+7
192.094: 2.622e+7
219.117: 2.622e+7
m/z=178 & 192
2-MP
9-MP
1-MP
Rdene
38 min.

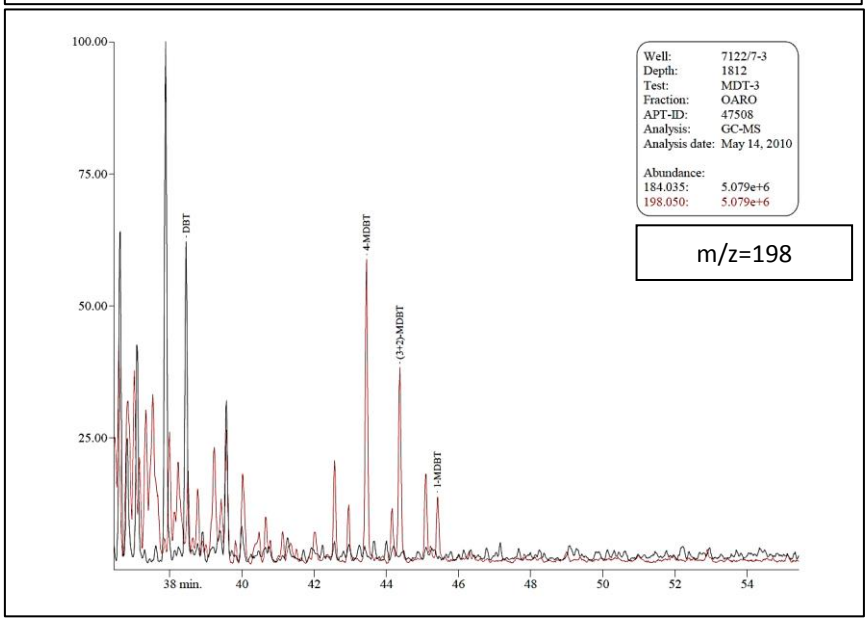
Well: 7122/7-3
Depth: 1812
Test: MDT-3
Fraction: OARO
APT-ID: 47508
Analysis: GC-MS
Analysis date: May 14, 2010
Abundance:
184.035: 5.079e+6
198.050: 5.079e+6
m/z=198
DBT
4-MDBT
(3+2)-MDBT
1-MDBT
38 min.

GC-FID Chromatogram for oil sample "T1" from well 7122/7-3

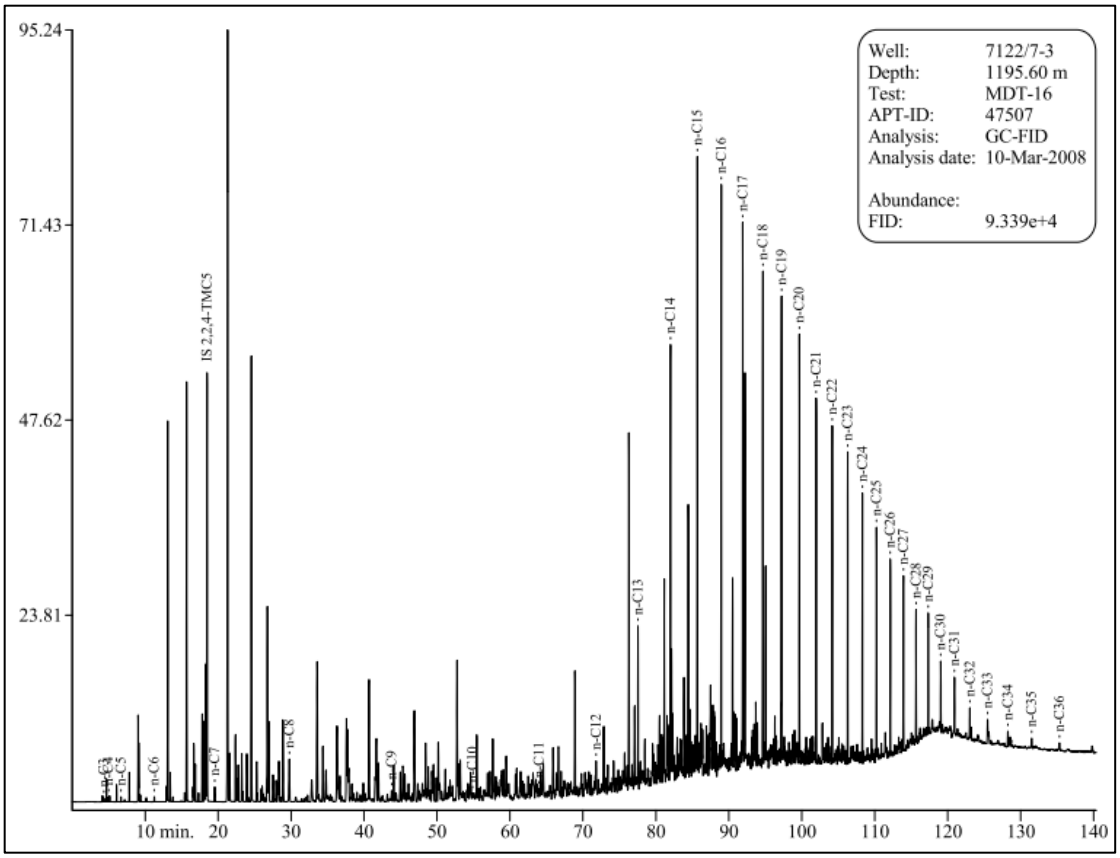

GC-MS Chromatograms for oil sample "T1" from well 7122/7-3

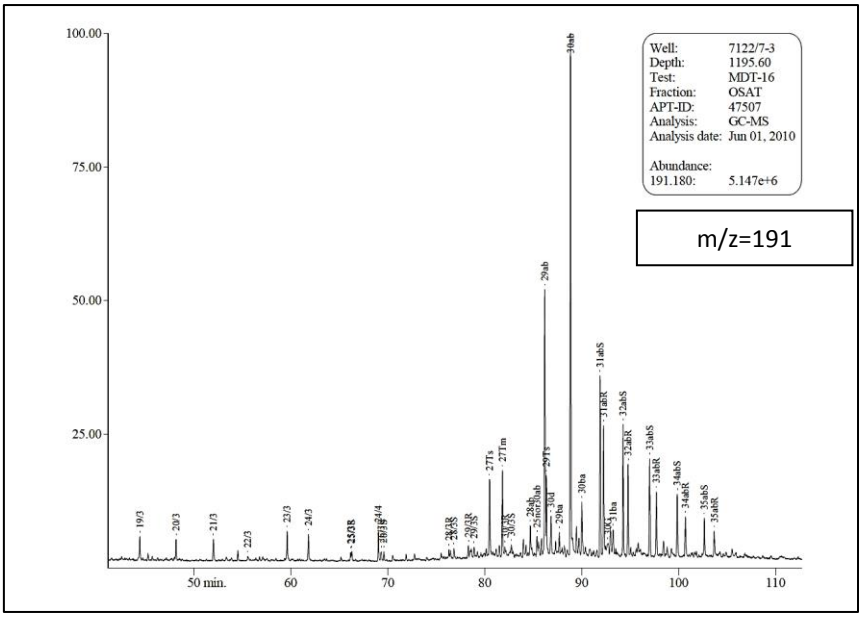

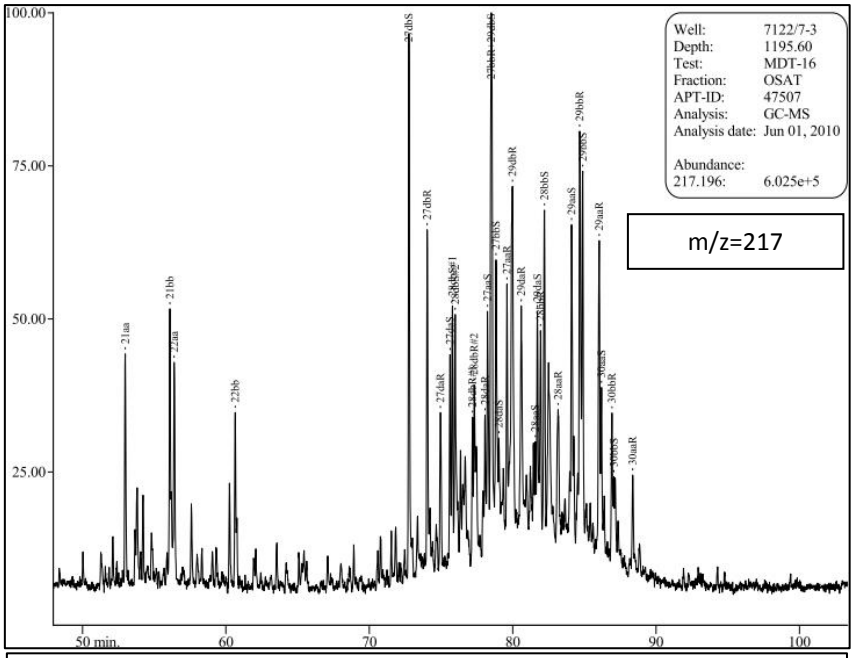
Well: 7122/7-3
Depth: 1195.60
Test: MDT-16
Fraction: OSAT
APT-ID: 47507
Analysis: GC-MS
Analysis date: Jun 01, 2010
Abundance:
217.196: 6.025e+5
m/z=217

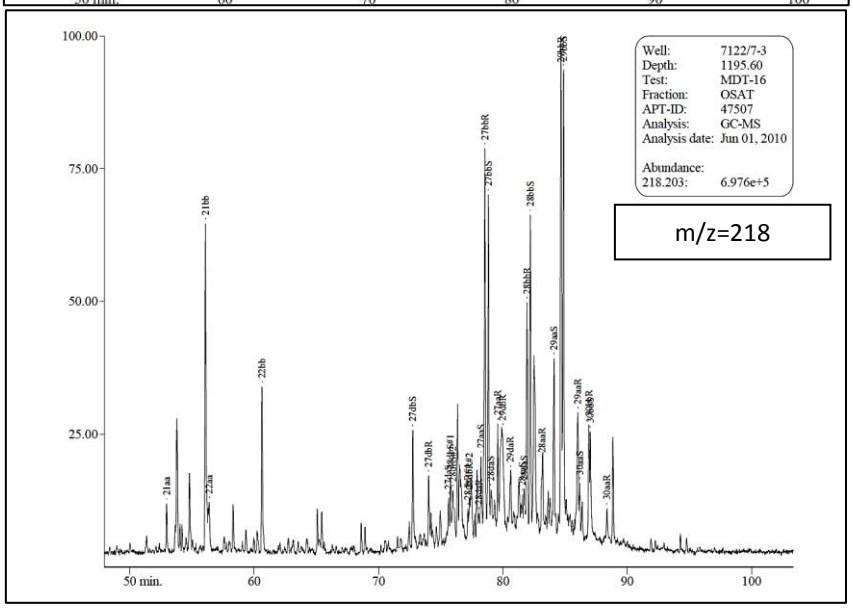
Well: 7122/7-3
Depth: 1195.60
Test: MDT-16
Fraction: OSAT
APT-ID: 47507
Analysis: GC-MS
Analysis date: Jun 01, 2010
Abundance:
218.203: 6.976e+5
m/z=218

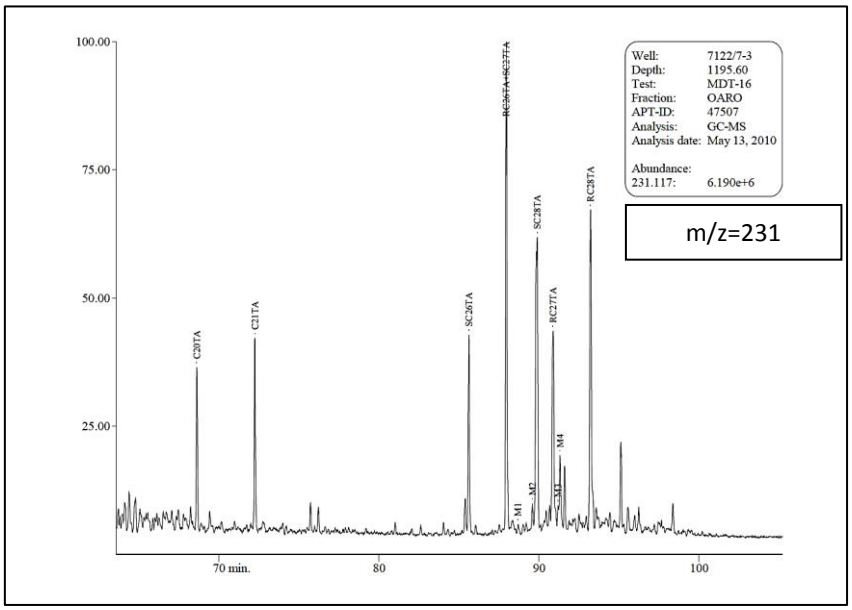
Well: 7122/7-3
Depth: 1195.60
Test: MDT-16
Fraction: OARO
APT-ID: 47507
Analysis: GC-MS
Analysis date: May 13, 2010
Abundance:
231.117: 6.190e+6
m/z=231

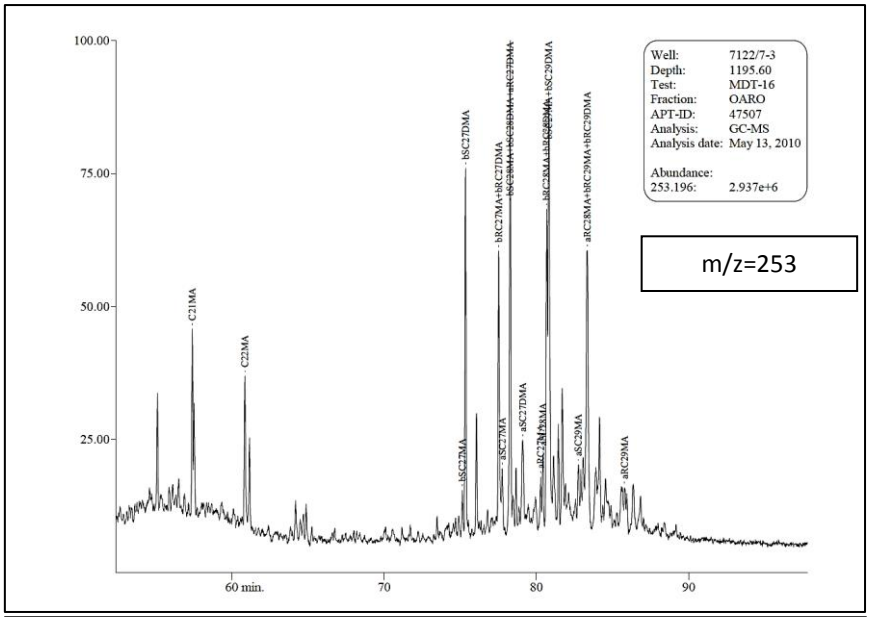
Well: 7122/7-3
Depth: 1195.60
Test: MDT-16
Fraction: OARO
APT-ID: 47507
Analysis: GC-MS
Analysis date: May 13, 2010
Abundance:
253.196: 2.937e+6
m/z=253
C21MA
C22MA
bSC27DMA
bRC27MA+bRC27DMA
aSC27MA
aSC27DMA
aRC29MA
aRC29DMA+bRC29MA+bRC29DMA
60 min.

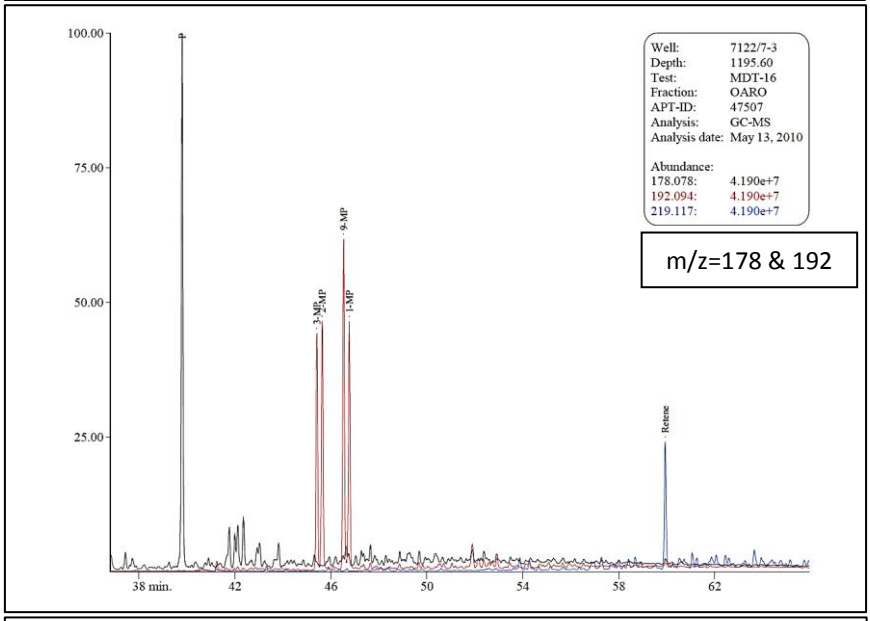
Well: 7122/7-3
Depth: 1195.60
Test: MDT-16
Fraction: OARO
APT-ID: 47507
Analysis: GC-MS
Analysis date: May 13, 2010
Abundance:
178.078: 4.190e+7
192.094: 4.190e+7
219.117: 4.190e+7
m/z=178 & 192
9-MP
3-MP
1-MP
Retene
38 min.

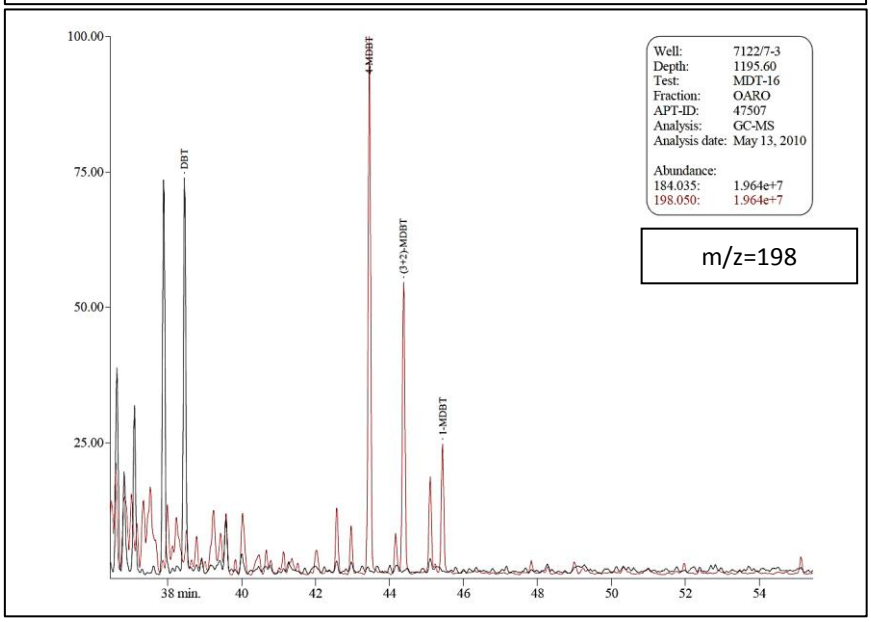
Well: 7122/7-3
Depth: 1195.60
Test: MDT-16
Fraction: OARO
APT-ID: 47507
Analysis: GC-MS
Analysis date: May 13, 2010
Abundance:
184.035: 1.964e+7
198.050: 1.964e+7
m/z=198
DBT
4-MDBT
(3+2)-MDBT
1-MDBT
38 min.

GC-FID Chromatogram for oil sample "V" from well 7123/4-1 A

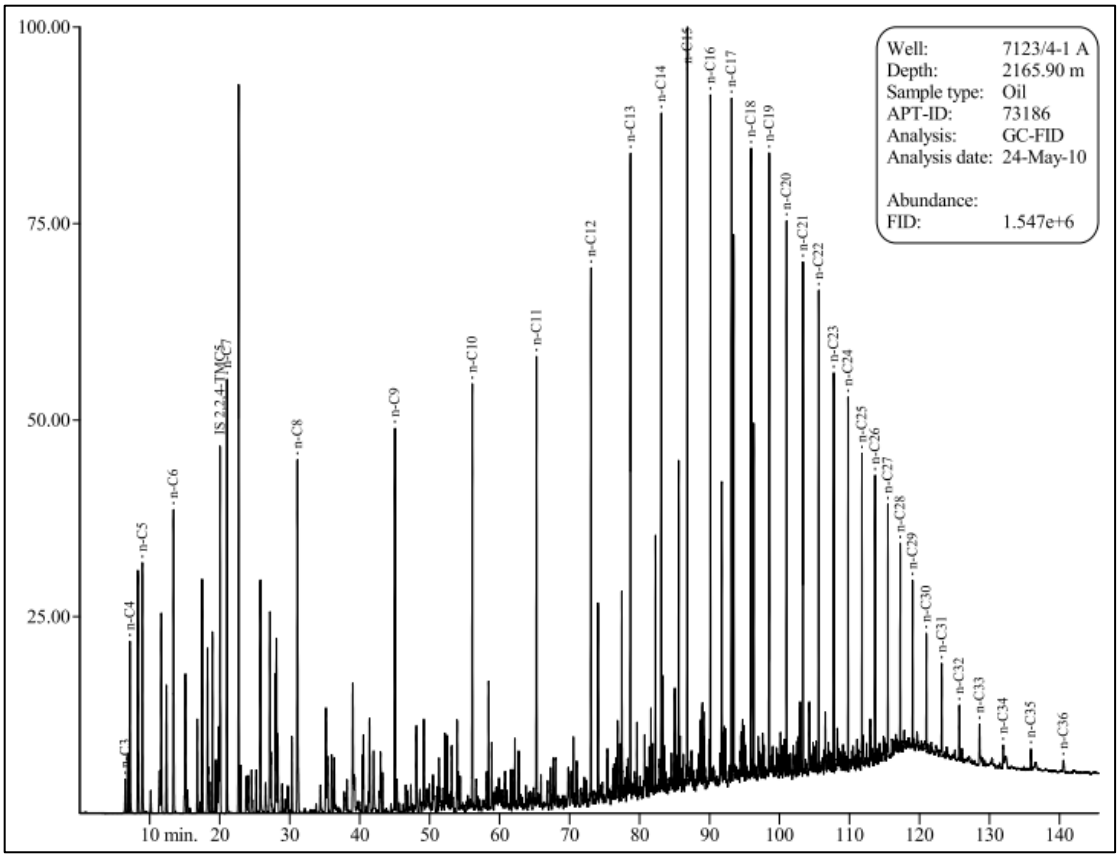

GC-MS Chromatograms for oil sample "V" from well 7123/4-1 A

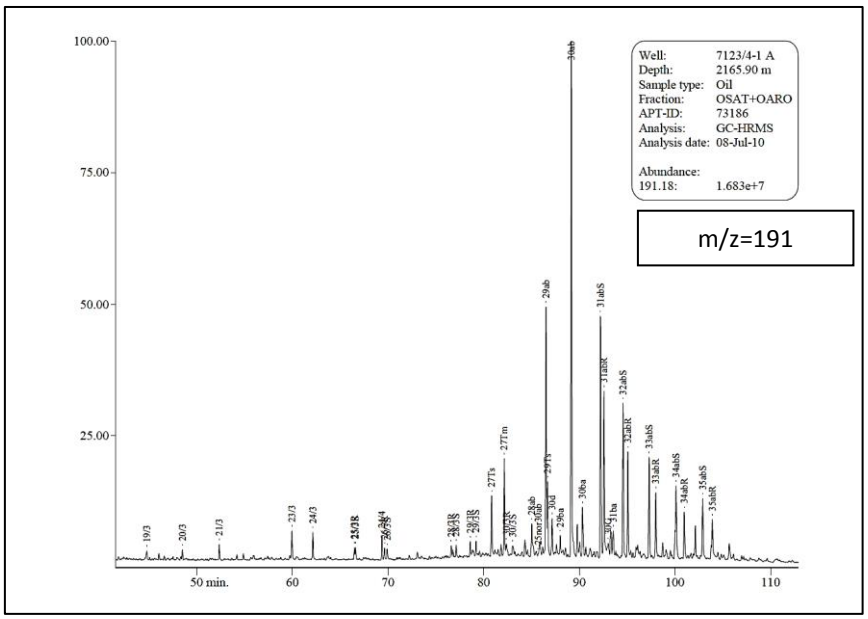

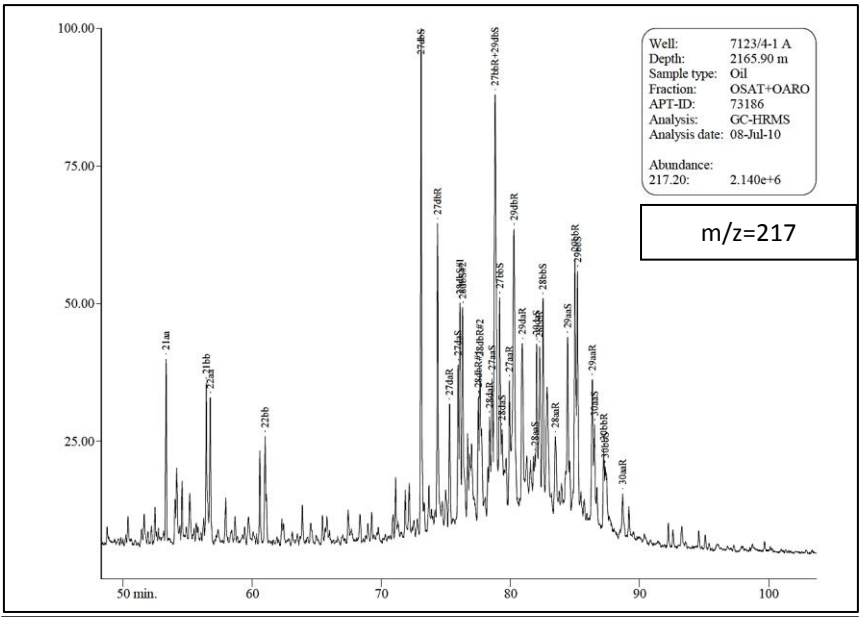
Well: 7123/4-1 A
Depth: 2165.90 m
Sample type: Oil
Fraction: OSAT+OARO
APT-ID: 73186
Analysis: GC-HRMS
Analysis date: 08-Jul-10
Abundance:
217.20: 2.140e+6
m/z=217

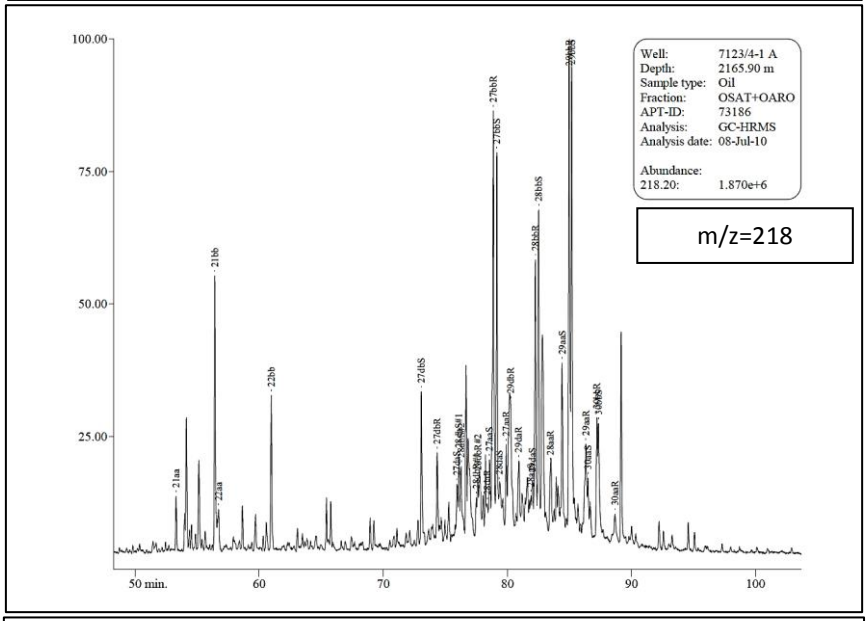
Well: 7123/4-1 A
Depth: 2165.90 m
Sample type: Oil
Fraction: OSAT+OARO
APT-ID: 73186
Analysis: GC-HRMS
Analysis date: 08-Jul-10
Abundance:
218.20: 1.870e+6
m/z=218

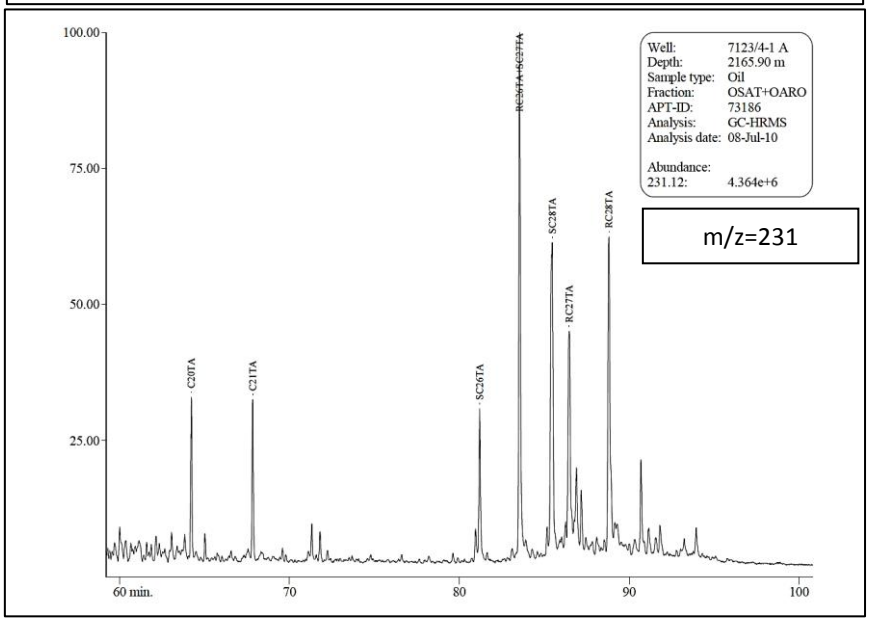
Well: 7123/4-1 A
Depth: 2165.90 m
Sample type: Oil
Fraction: OSAT+OARO
APT-ID: 73186
Analysis: GC-HRMS
Analysis date: 08-Jul-10
Abundance:
231.12: 4.364e+6
m/z=231

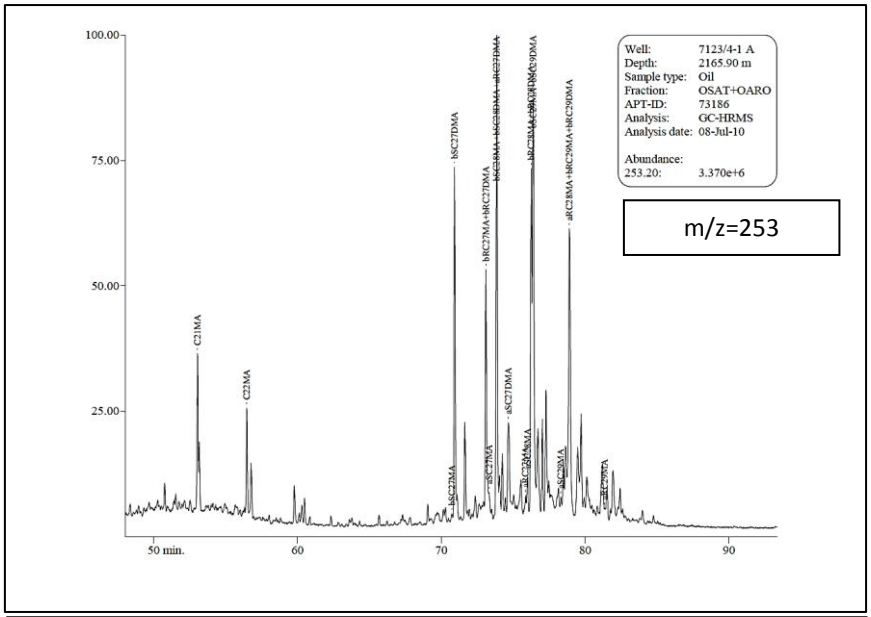
Well: 7123/4-1 A
Depth: 2165.90 m
Sample type: Oil
Fraction: OSAT+OARO
APT-ID: 73186
Analysis: GC-HRMS
Analysis date: 08-Jul-10
Abundance:
253.20: 3.370e+6
m/z=253
C21MA
C22MA
bRC27DMA
bRC27MA+bRC27DMA
aRC27DMA
aRC28MA+bRC29DMA
aRC28MA+bRC29MA+bRC29DMA
50 min.

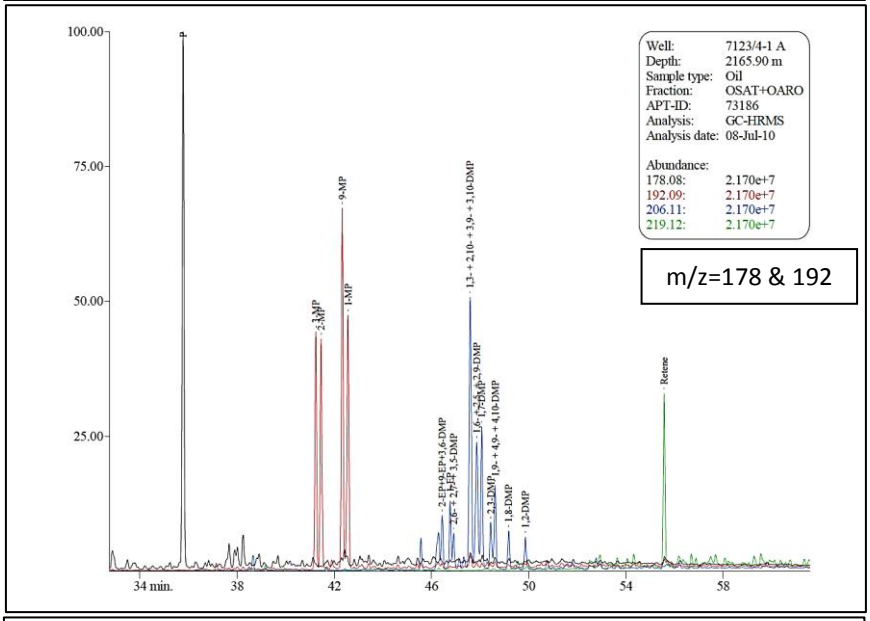
Well: 7123/4-1 A
Depth: 2165.90 m
Sample type: Oil
Fraction: OSAT+OARO
APT-ID: 73186
Analysis: GC-HRMS
Analysis date: 08-Jul-10
Abundance:
178.08: 2.170e+7
192.09: 2.170e+7
206.11: 2.170e+7
219.12: 2.170e+7
m/z=178 & 192
9-MP
1-MP
1,3- + 2,10- + 3,9- + 3,10-DMP
Retene
1,8-DMP
1,2-DMP
34 min.

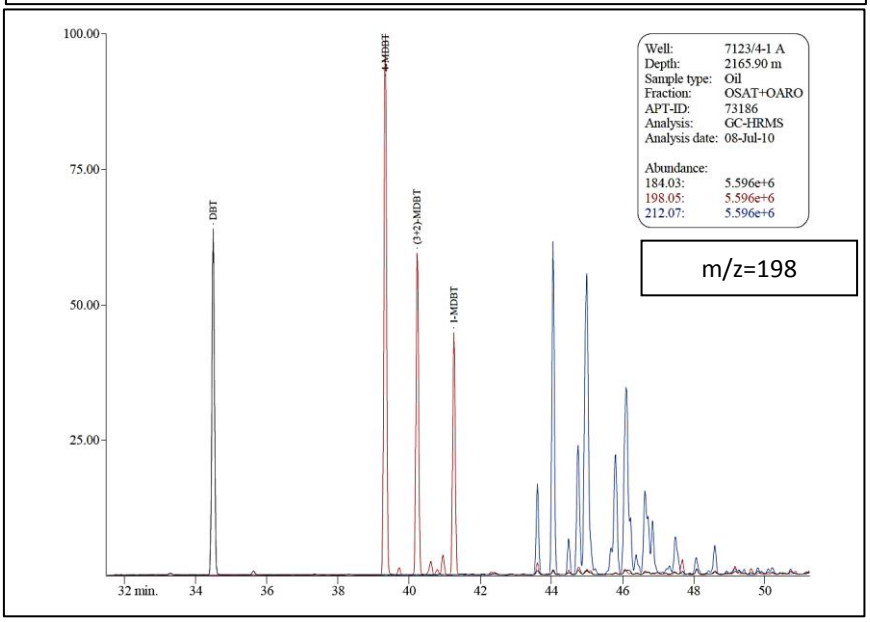
Well: 7123/4-1 A
Depth: 2165.90 m
Sample type: Oil
Fraction: OSAT+OARO
APT-ID: 73186
Analysis: GC-HRMS
Analysis date: 08-Jul-10
Abundance:
184.03: 5.596e+6
198.05: 5.596e+6
212.07: 5.596e+6
m/z=198
DBT
4-MDBT
(3+2)-MDBT
1-MDBT
32 min.

GC-FID Chromatogram for oil sample "W" from well 7124/3-1

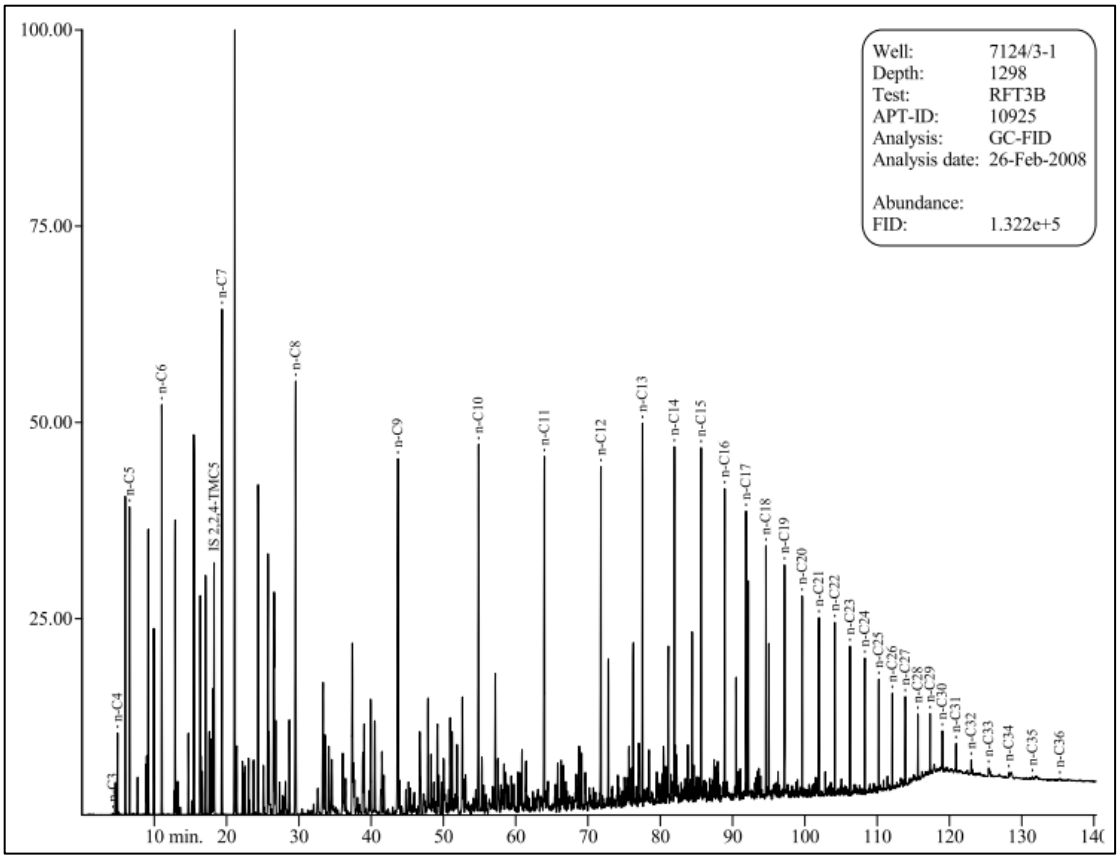

GC-MS Chromatograms for oil sample "W" from well 7124/3-1

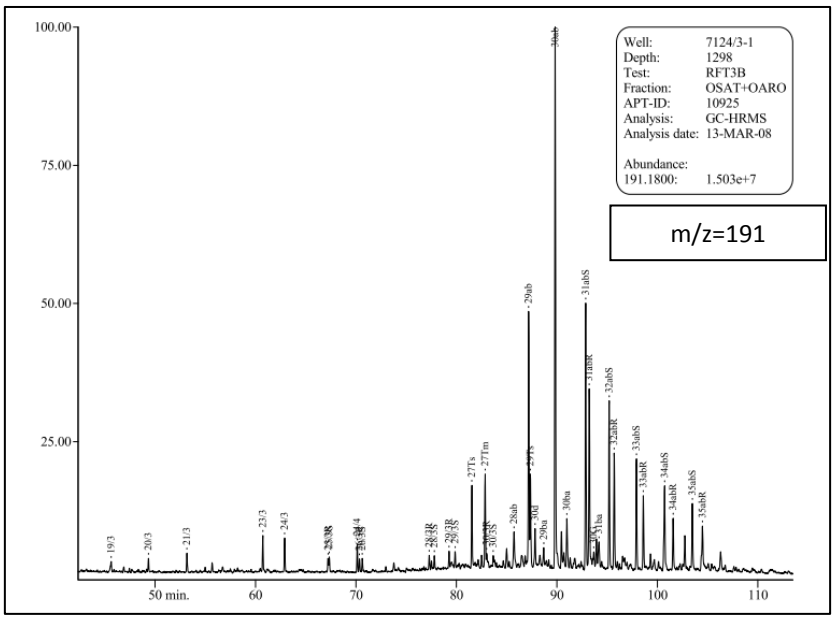

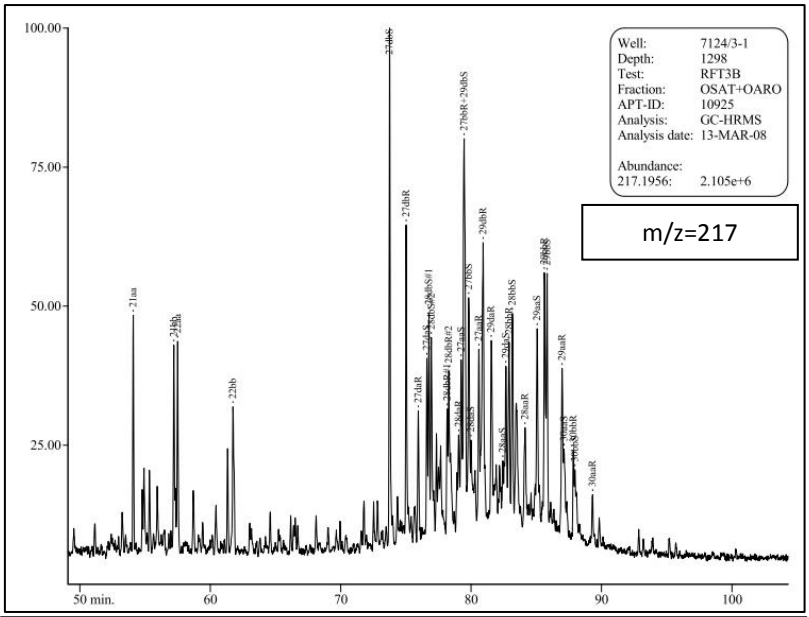
Well: 7124/3-1
Depth: 1298
Test: RFT3B
Fraction: OSAT+OARO
APT-ID: 10925
Analysis: GC-HRMS
Analysis date: 13-MAR-08
Abundance:
217.1956: 2.105e+6
m/z=217
100.00
75.00
50.00
25.00
50 min.
60
70
80
90
100

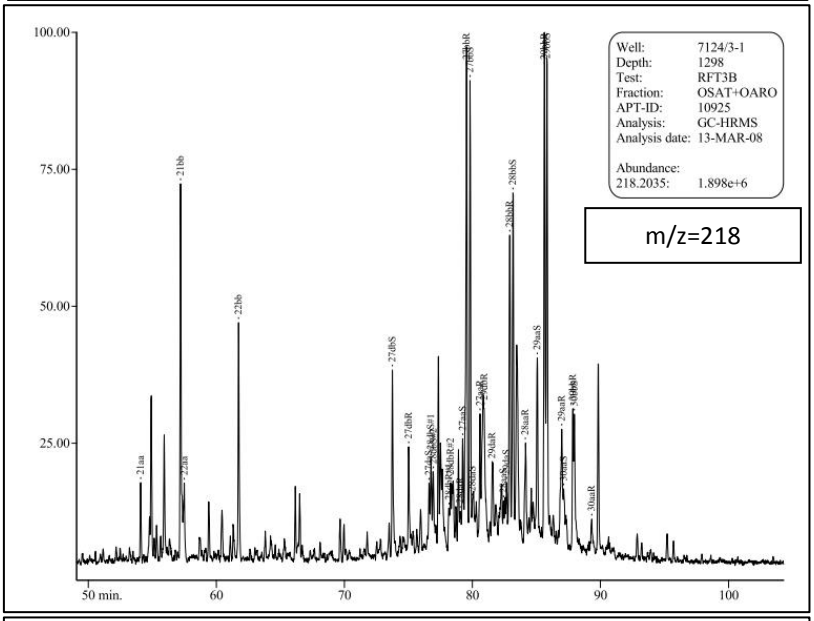
Well: 7124/3-1
Depth: 1298
Test: RFT3B
Fraction: OSAT+OARO
APT-ID: 10925
Analysis: GC-HRMS
Analysis date: 13-MAR-08
Abundance:
218.2035: 1.898e+6
m/z=218
100.00
75.00
50.00
25.00
50 min.
60
70
80
90
100

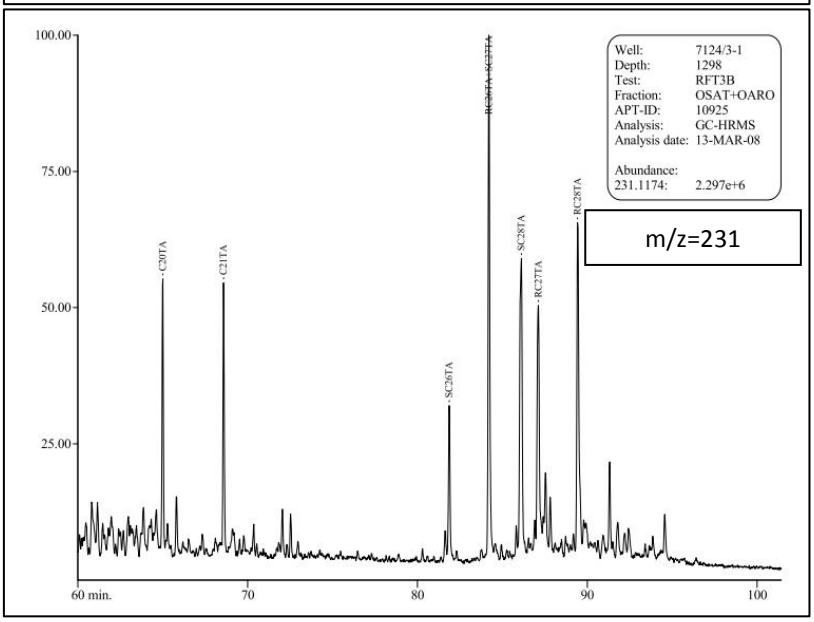
Well: 7124/3-1
Depth: 1298
Test: RFT3B
Fraction: OSAT+OARO
APT-ID: 10925
Analysis: GC-HRMS
Analysis date: 13-MAR-08
Abundance:
231.1174: 2.297e+6
m/z=231
100.00
75.00
50.00
25.00
60 min.
70
80
90
100

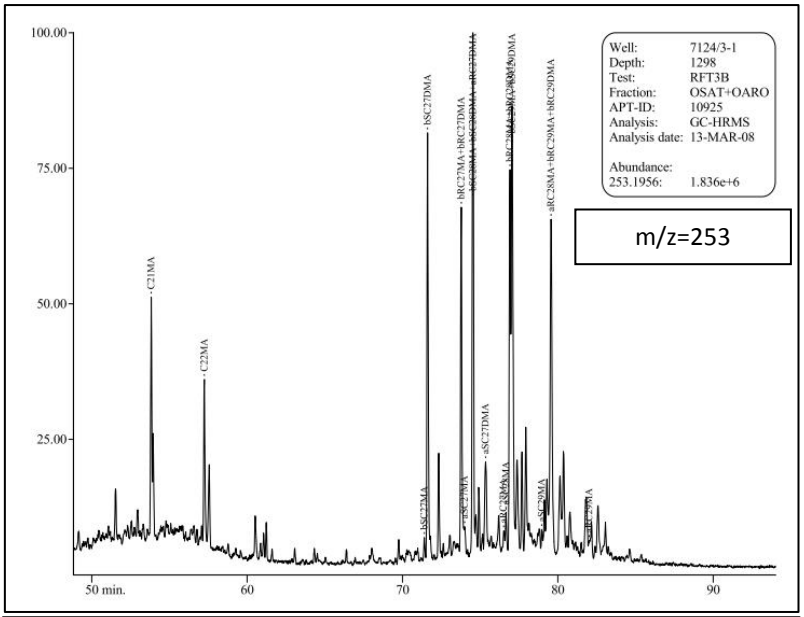
Well: 7124/3-1
Depth: 1298
Test: RFT3B
Fraction: OSAT+OARO
APT-ID: 10925
Analysis: GC-HRMS
Analysis date: 13-MAR-08
Abundance:
253.1956: 1.836e+6
m/z=253
C21MA
C22MA
bSC27DMA
bRC27MA+bRC27DMA
aSC27DMA
aRC28MA+bRC29MA+bRC29DMA
50 min.

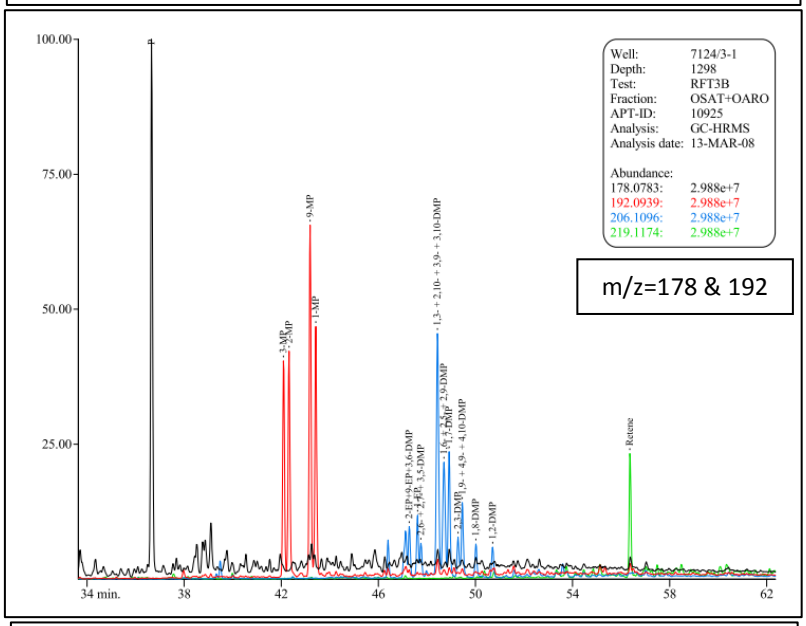
Well: 7124/3-1
Depth: 1298
Test: RFT3B
Fraction: OSAT+OARO
APT-ID: 10925
Analysis: GC-HRMS
Analysis date: 13-MAR-08
Abundance:
178.0783: 2.988e+7
192.0939: 2.988e+7
206.1096: 2.988e+7
219.1174: 2.988e+7
m/z=178 & 192
3-MP
2-MP
9-MP
1-MP
Retene
34 min.

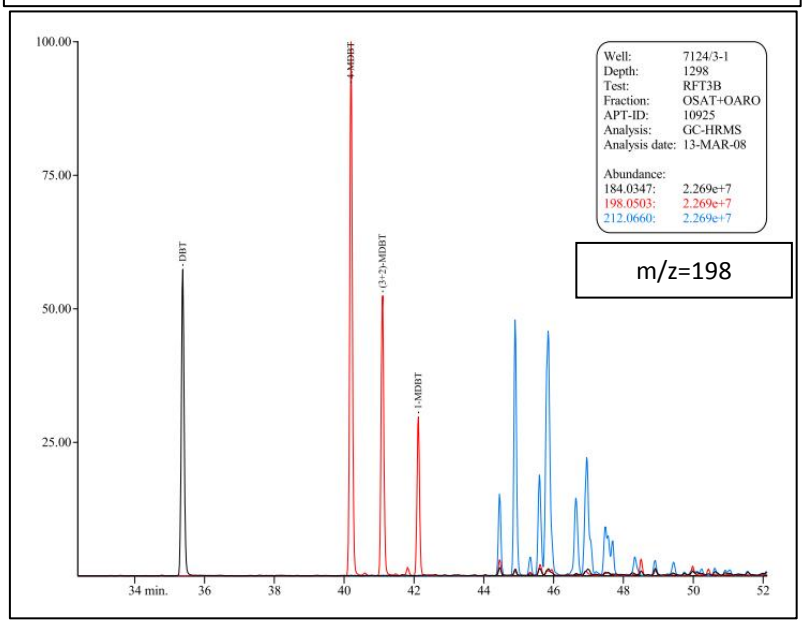
Well: 7124/3-1
Depth: 1298
Test: RFT3B
Fraction: OSAT+OARO
APT-ID: 10925
Analysis: GC-HRMS
Analysis date: 13-MAR-08
Abundance:
184.0347: 2.269e+7
198.0503: 2.269e+7
212.0660: 2.269e+7
m/z=198
DBT
4-MDBT
(3+2)-MDBT
1-MDBT
34 min.

GC-FID Chromatogram for oil sample "X" from well 7125/1-1

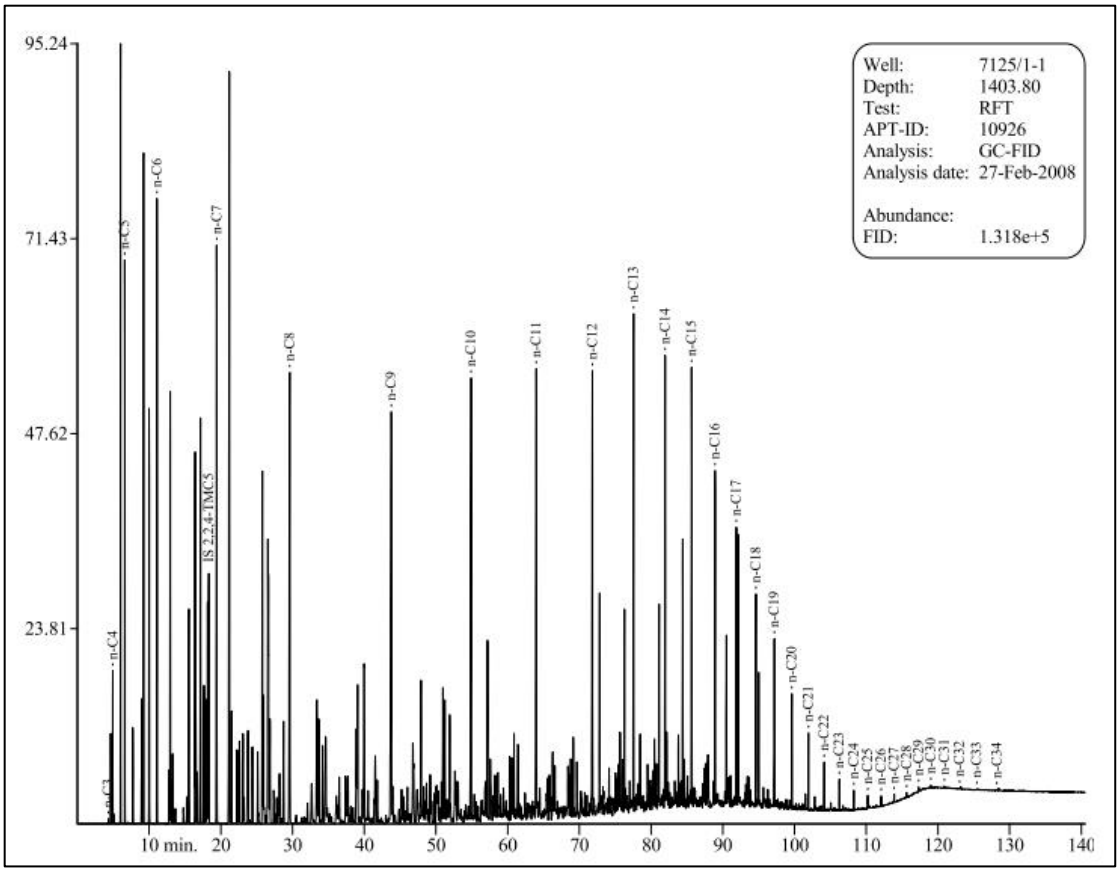

GC-MS Chromatograms for oil sample "X" from well 7125/1-1

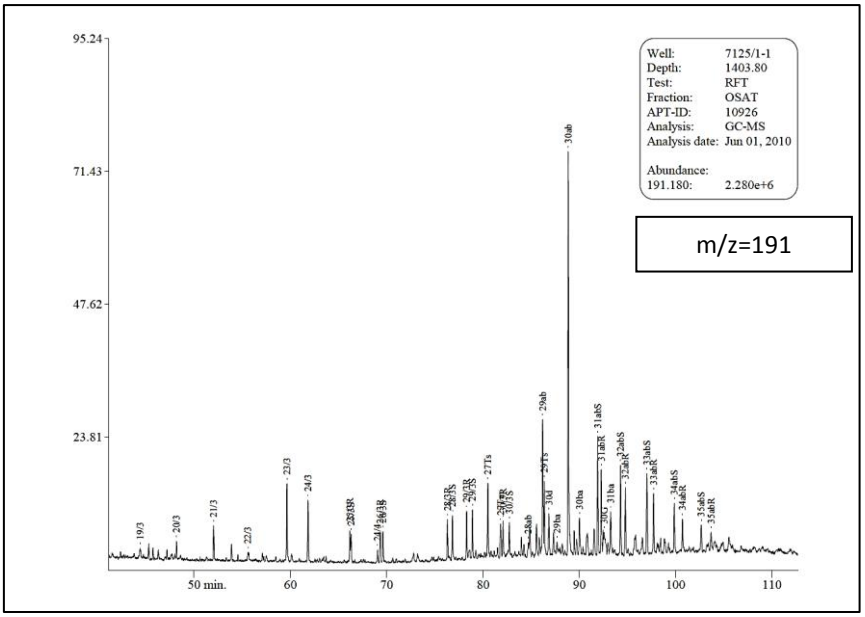

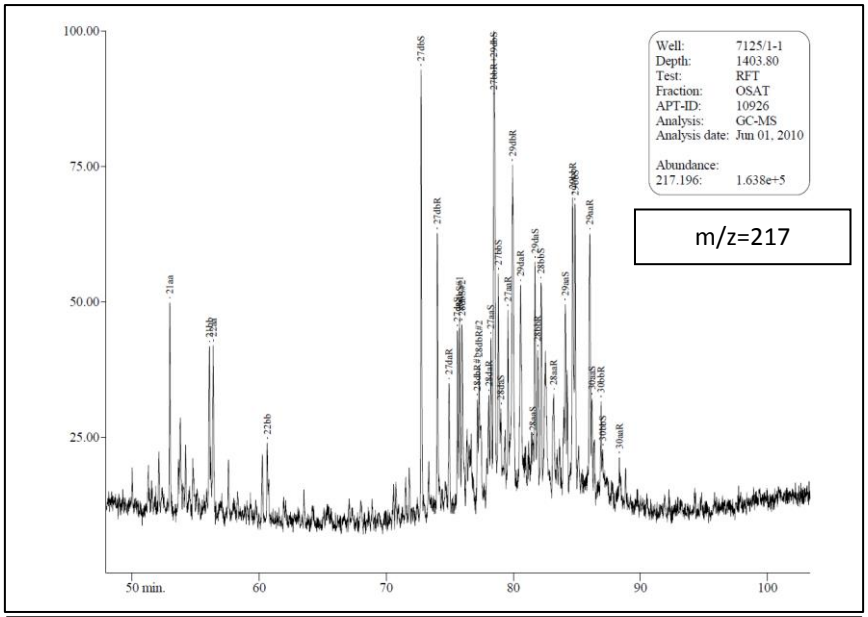
Well: 7125/1-1
Depth: 1403.80
Test: RFT
Fraction: OSAT
APT-ID: 10926
Analysis: GC-MS
Analysis date: Jun 01, 2010
Abundance:
217.196: 1.638e+5
m/z=217
100.00
75.00
50.00
25.00
50 min.
60
70
80
90
100

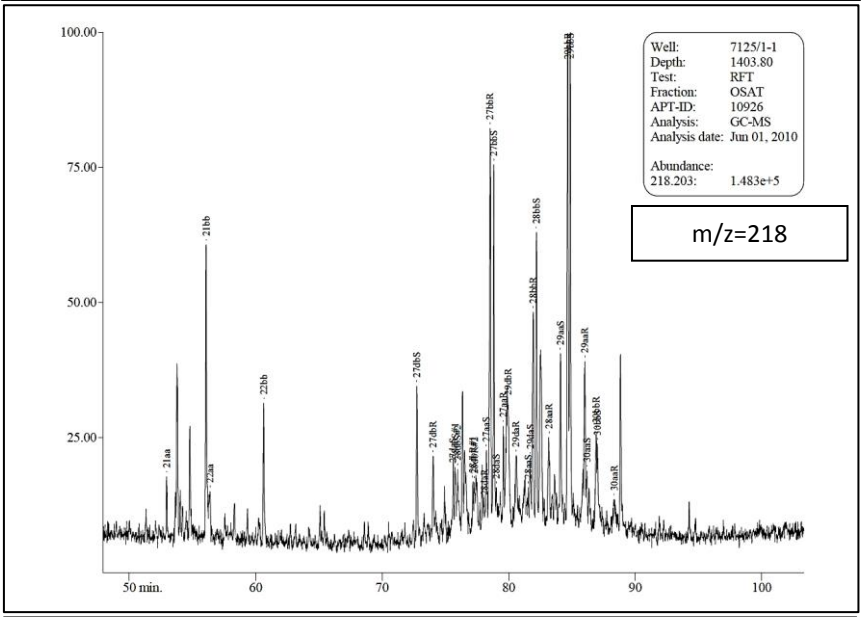
Well: 7125/1-1
Depth: 1403.80
Test: RFT
Fraction: OSAT
APT-ID: 10926
Analysis: GC-MS
Analysis date: Jun 01, 2010
Abundance:
218.203: 1.483e+5
m/z=218
100.00
75.00
50.00
25.00
50 min.
60
70
80
90
100

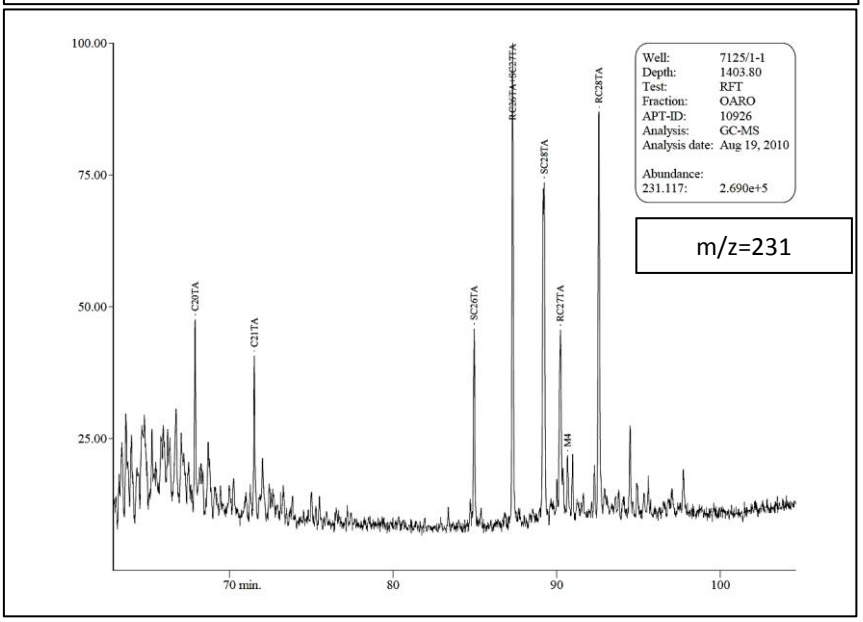
Well: 7125/1-1
Depth: 1403.80
Test: RFT
Fraction: OARO
APT-ID: 10926
Analysis: GC-MS
Analysis date: Aug 19, 2010
Abundance:
231.117: 2.690e+5
m/z=231
100.00
75.00
50.00
25.00
C20TA
C21TA
SC26TA
SC28TA
RC27TA
RC28TA
M4
70 min.
80
90
100

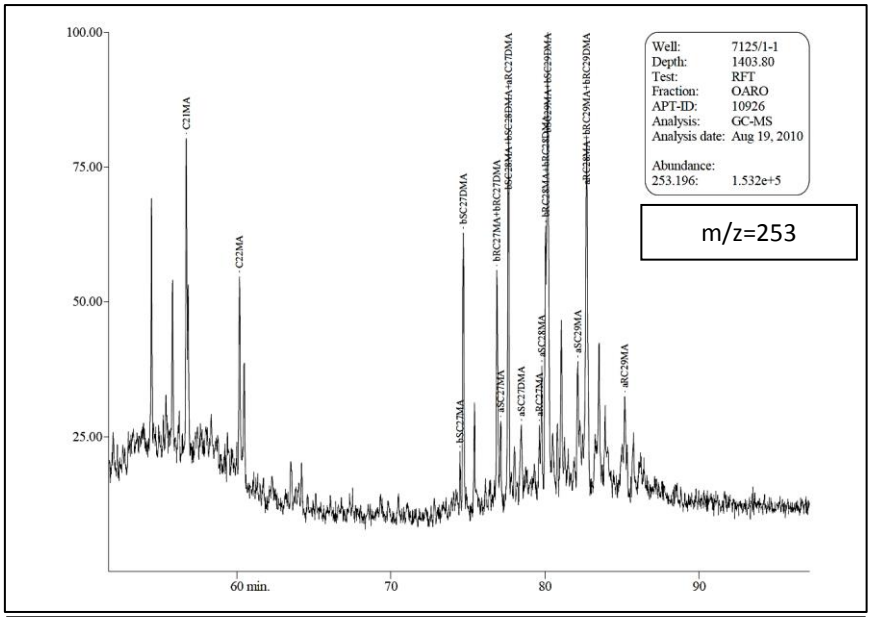
Well: 7125/1-1
Depth: 1403.80
Test: RFT
Fraction: OARO
APT-ID: 10926
Analysis: GC-MS
Analysis date: Aug 19, 2010
Abundance:
253.196: 1.532e+5
m/z=253
C21MA
C22MA
bSC27DMA
bRC27MA+bRC27DMA
aSC27MA
aSC27DMA
aRC27MA
aSC28MA
aSC29MA
aRC29MA
bSC27MA
60 min.
70
80
90

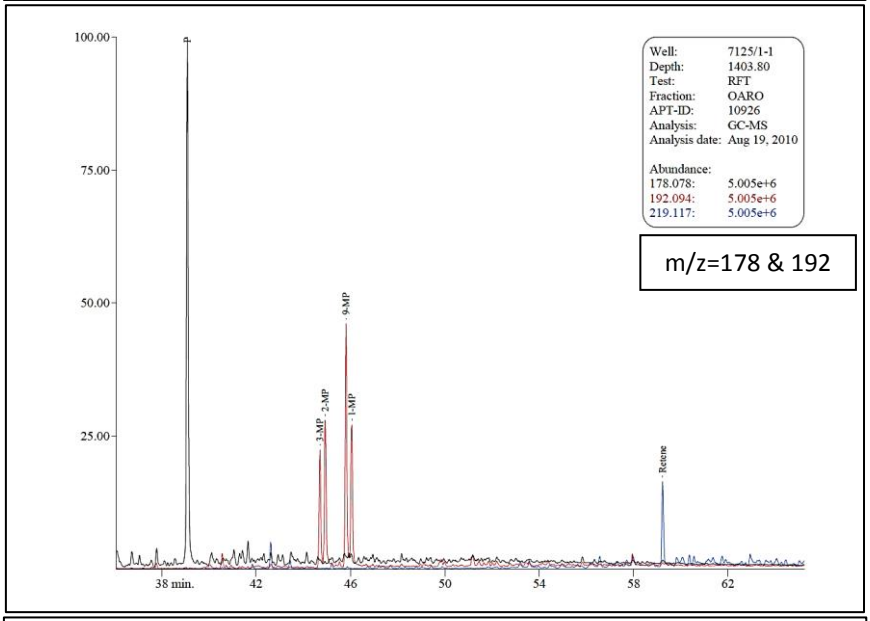
Well: 7125/1-1
Depth: 1403.80
Test: RFT
Fraction: OARO
APT-ID: 10926
Analysis: GC-MS
Analysis date: Aug 19, 2010
Abundance:
178.078: 5.005e+6
192.094: 5.005e+6
219.117: 5.005e+6
m/z=178 & 192
9-MP
2-MP
3-MP
1-MP
Retene
38 min.
42
46
50
54
58
62

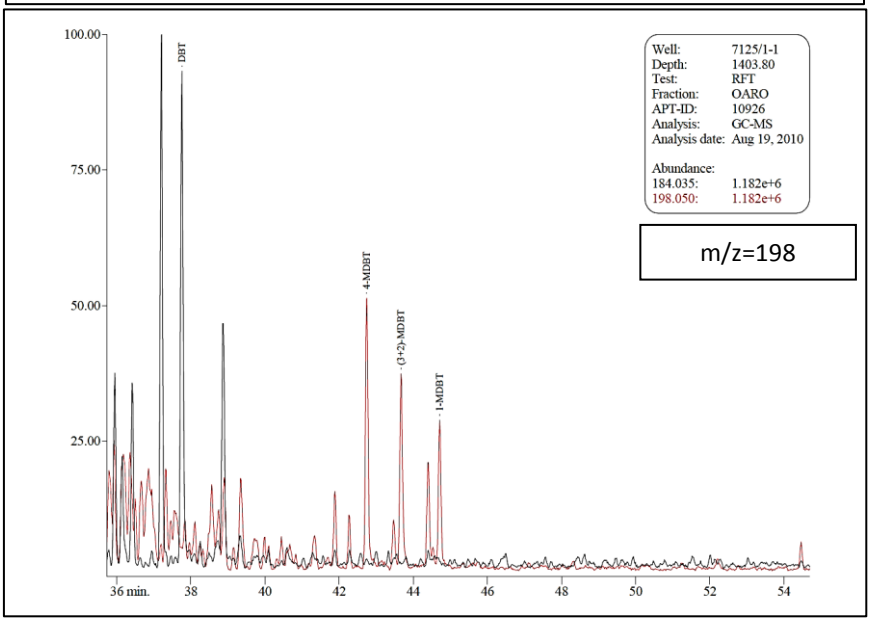
Well: 7125/1-1
Depth: 1403.80
Test: RFT
Fraction: OARO
APT-ID: 10926
Analysis: GC-MS
Analysis date: Aug 19, 2010
Abundance:
184.035: 1.182e+6
198.050: 1.182e+6
m/z=198
DBT
4-MDBT
(3+2)-MDBT
1-MDBT
36 min.
38
40
42
44
46
48
50
52
54

GC-FID Chromatogram for oil sample "Ø" from well 7122/6-1 S

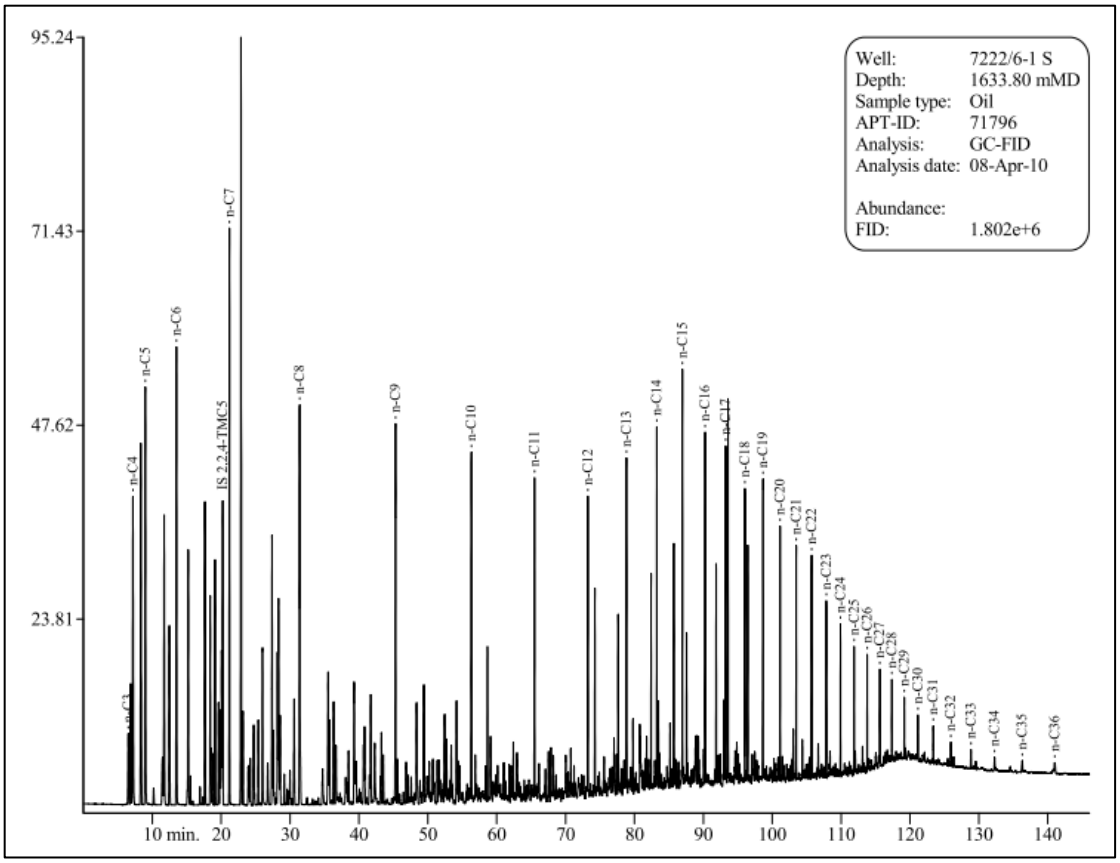

GC-MS Chromatograms for oil sample "Ø" from well 7122/6-1 S

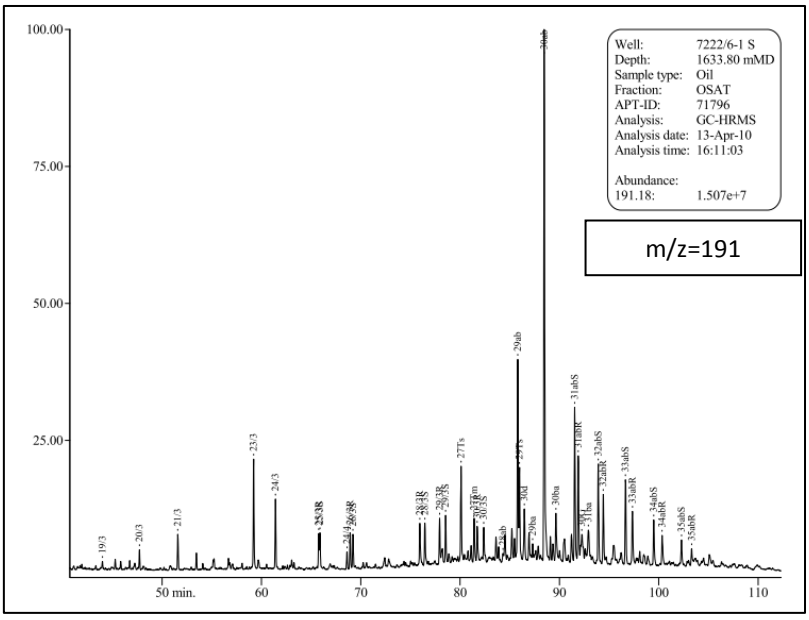

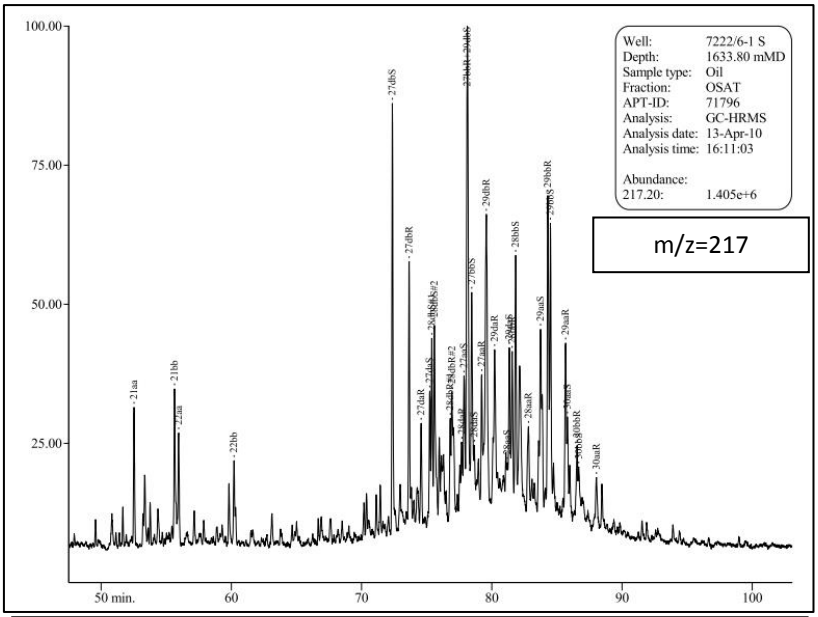
Well: 7222/6-1 S
Depth: 1633.80 mMD
Sample type: Oil
Fraction: OSAT
APT-ID: 71796
Analysis: GC-HRMS
Analysis date: 13-Apr-10
Analysis time: 16:11:03
Abundance:
217.20: 1.405e+6
m/z=217

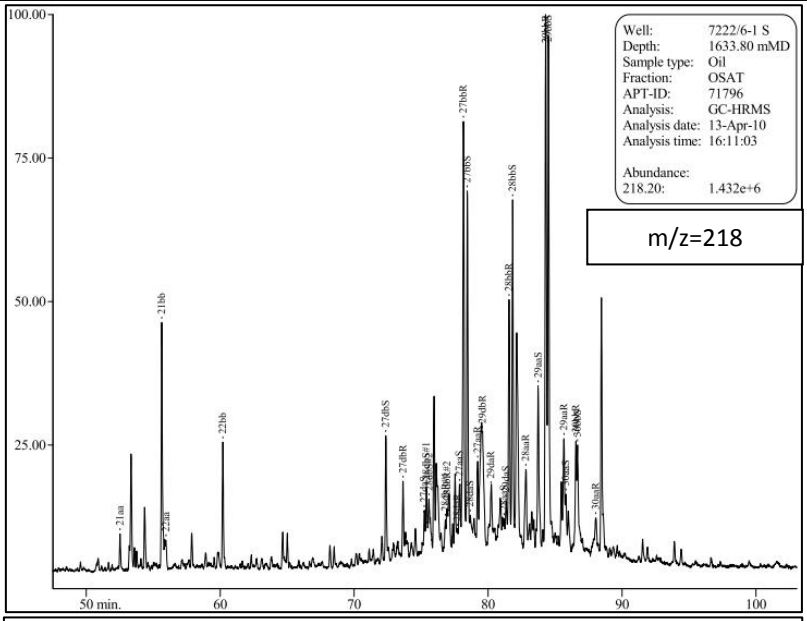
Well: 7222/6-1 S
Depth: 1633.80 mMD
Sample type: Oil
Fraction: OSAT
APT-ID: 71796
Analysis: GC-HRMS
Analysis date: 13-Apr-10
Analysis time: 16:11:03
Abundance:
218.20: 1.432e+6
m/z=218

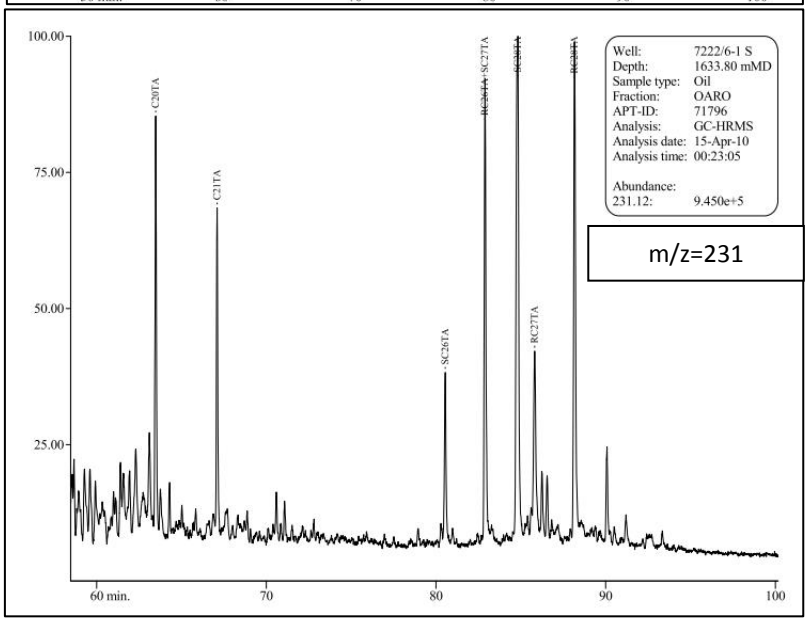
Well: 7222/6-1 S
Depth: 1633.80 mMD
Sample type: Oil
Fraction: OARO
APT-ID: 71796
Analysis: GC-HRMS
Analysis date: 15-Apr-10
Analysis time: 00:23:05
Abundance:
231.12: 9.450e+5
m/z=231

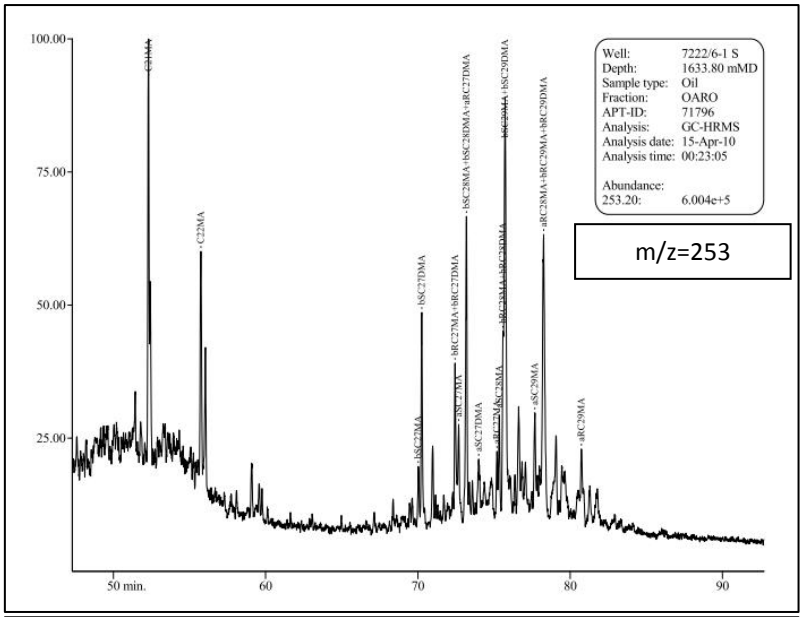
Well: 7222/6-1 S
Depth: 1633.80 mMD
Sample type: Oil
Fraction: OARO
APT-ID: 71796
Analysis: GC-HRMS
Analysis date: 15-Apr-10
Analysis time: 00:23:05
Abundance:
253.20: 6.004e+5
m/z=253
C31MA
C22MA
bSC27DMA
bRC27MA+bRC27DMA
bSC28MA+bSC28DMA+aRC27DMA
bSC29MA
bRC29MA+bRC29DMA
aRC28MA+bRC29MA+bRC29DMA
aSC29MA
aRC29MA
50 min.

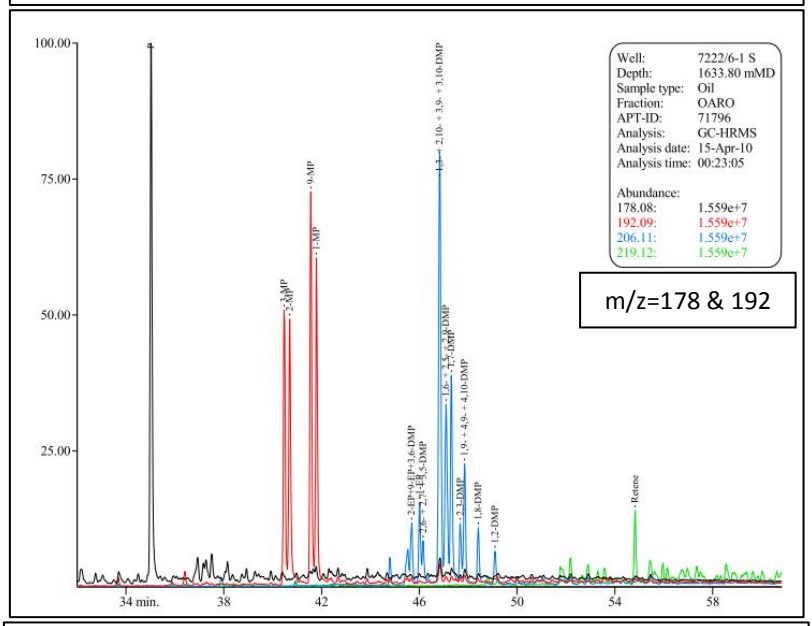
Well: 7222/6-1 S
Depth: 1633.80 mMD
Sample type: Oil
Fraction: OARO
APT-ID: 71796
Analysis: GC-HRMS
Analysis date: 15-Apr-10
Analysis time: 00:23:05
Abundance:
178.08: 1.559e+7
192.09: 1.559e+7
206.11: 1.559e+7
219.12: 1.559e+7
m/z=178 & 192
9-MP
1-MP
2,10- + 3,9- + 3,10-DMP
1,6- + 1,7-DMP
1,9- + 4,9- + 4,10-DMP
1,8-DMP
1,2-DMP
Retene
34 min.

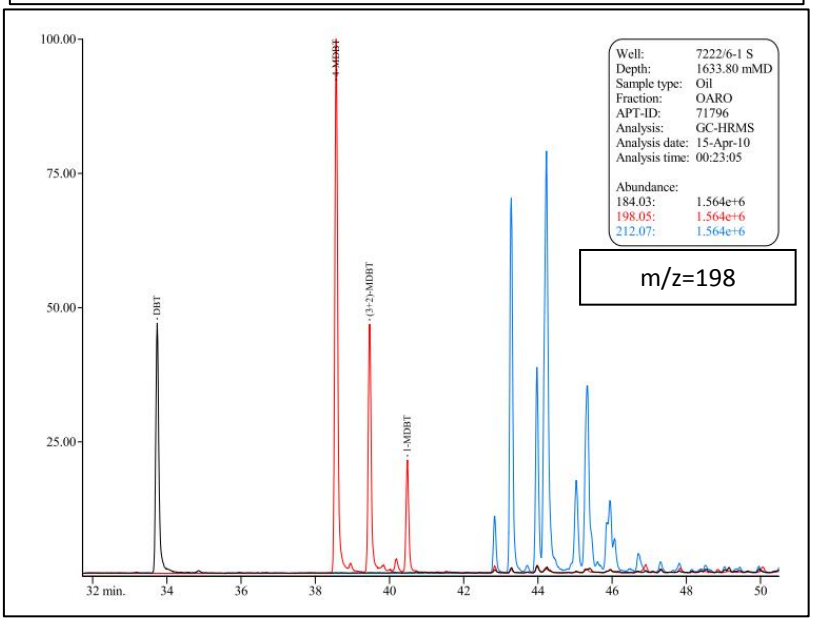
Well: 7222/6-1 S
Depth: 1633.80 mMD
Sample type: Oil
Fraction: OARO
APT-ID: 71796
Analysis: GC-HRMS
Analysis date: 15-Apr-10
Analysis time: 00:23:05
Abundance:
184.03: 1.564e+6
198.05: 1.564e+6
212.07: 1.564e+6
m/z=198
DBT
(3+2)-MDBT
1-MDBT
32 min.

GC-FID Chromatogram for oil sample "AB" from well 7228/7-1A

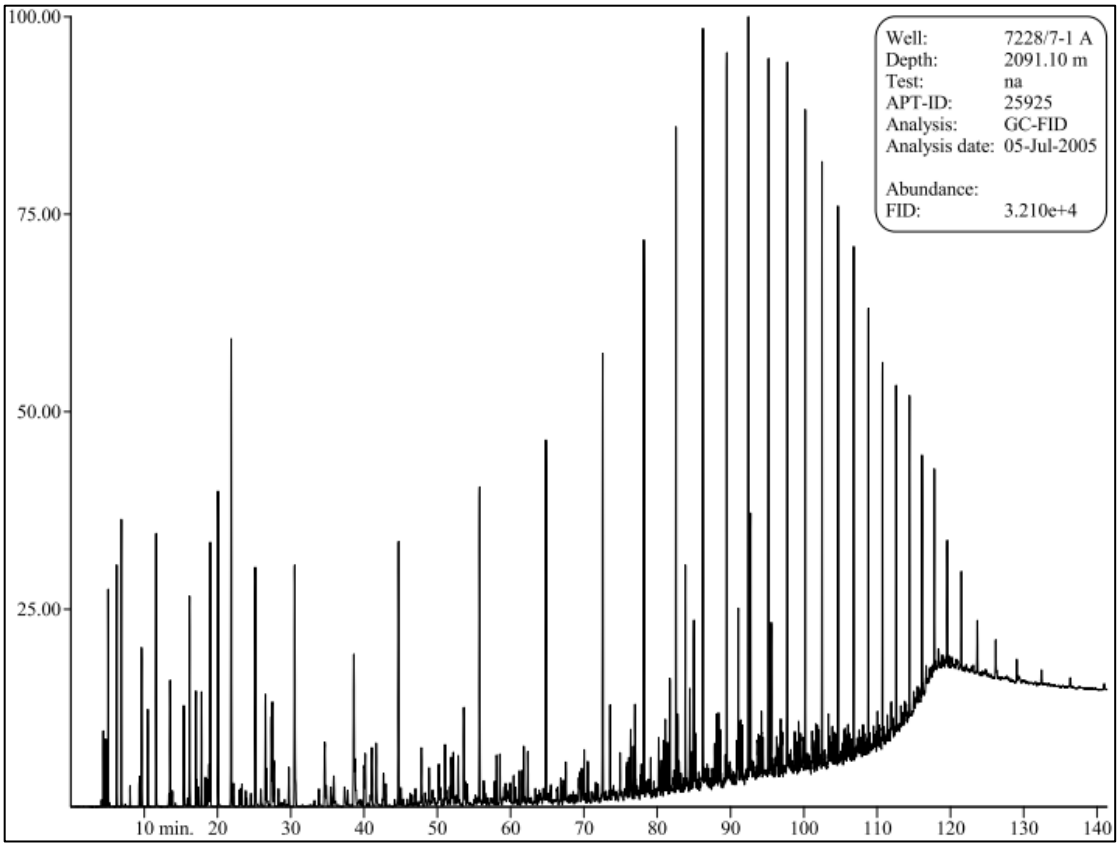

GC-MS Chromatograms for sample "AB" from well 7228/7-1A

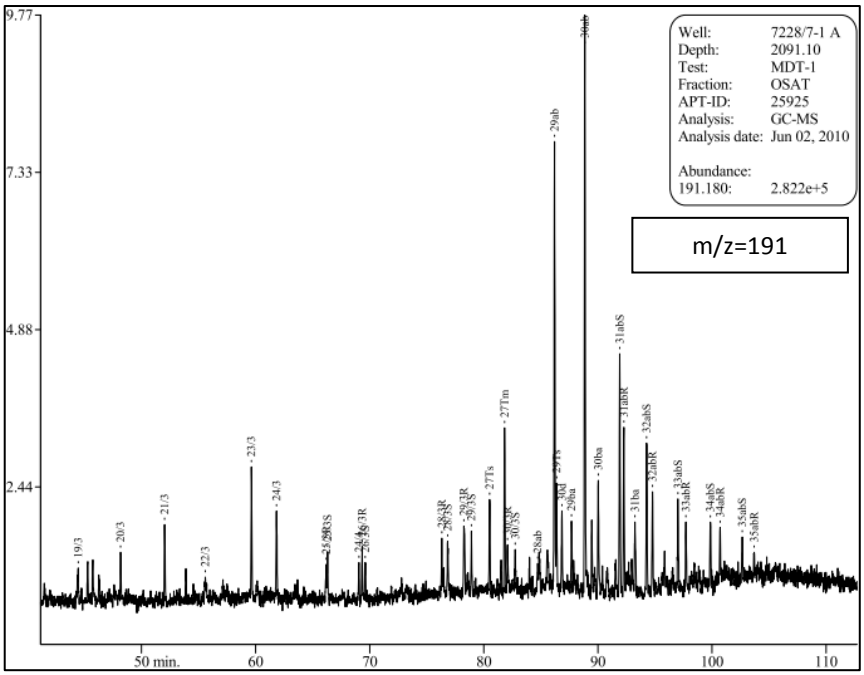

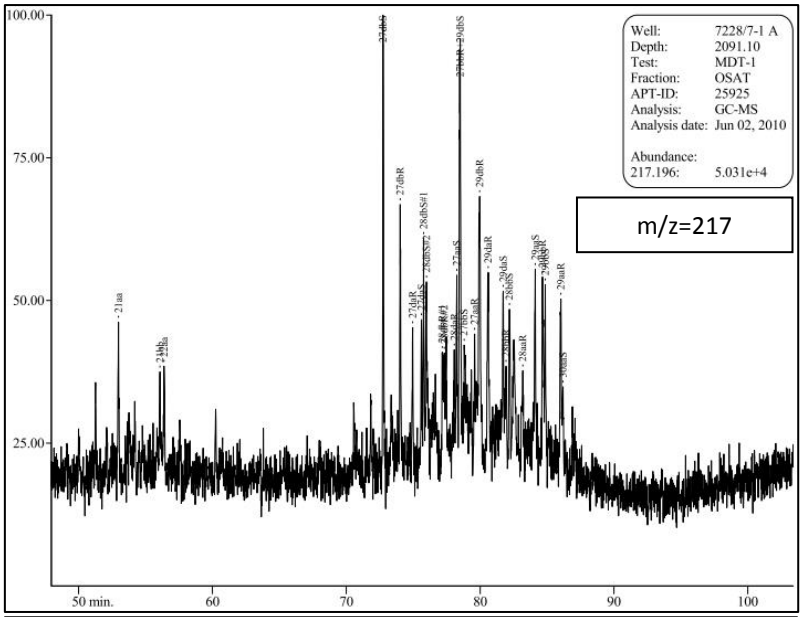
Well: 7228/7-1 A
Depth: 2091.10
Test: MDT-1
Fraction: OSAT
APT-ID: 25925
Analysis: GC-MS
Analysis date: Jun 02, 2010
Abundance:
217.196: 5.031e+4
m/z=217
100.00
75.00
50.00
25.00
50 min.
60
70
80
90
100

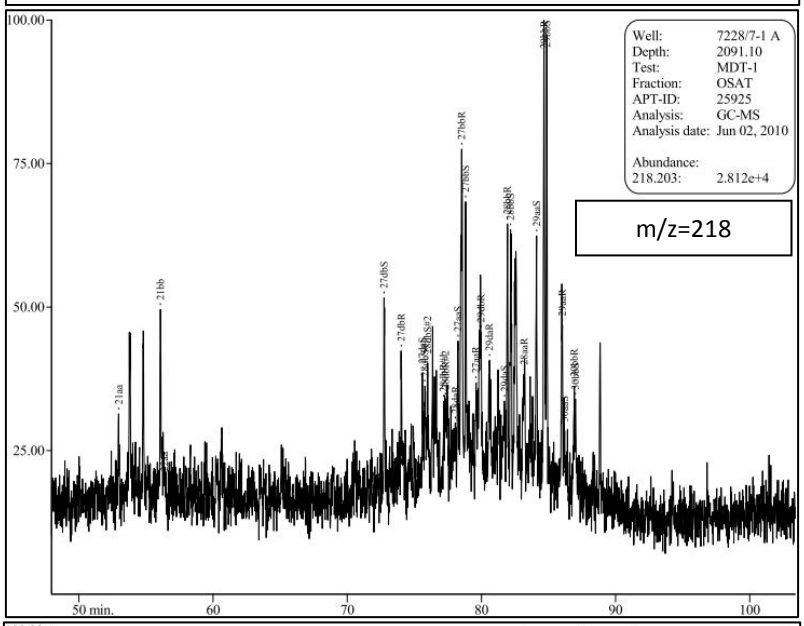
Well: 7228/7-1 A
Depth: 2091.10
Test: MDT-1
Fraction: OSAT
APT-ID: 25925
Analysis: GC-MS
Analysis date: Jun 02, 2010
Abundance:
218.203: 2.812e+4
m/z=218
100.00
75.00
50.00
25.00
50 min.
60
70
80
90
100

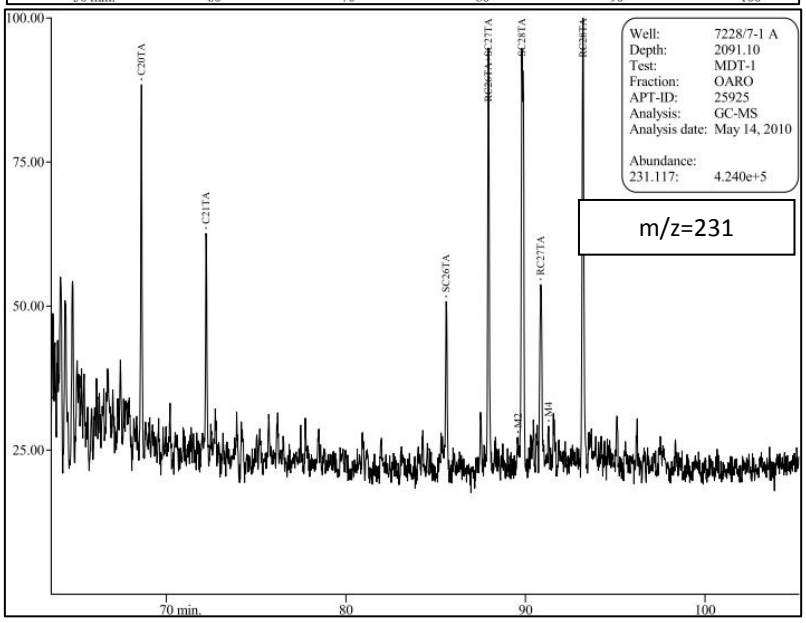
Well: 7228/7-1 A
Depth: 2091.10
Test: MDT-1
Fraction: OARO
APT-ID: 25925
Analysis: GC-MS
Analysis date: May 14, 2010
Abundance:
231.117: 4.240e+5
m/z=231
100.00
75.00
50.00
25.00
70 min.
80
90
100

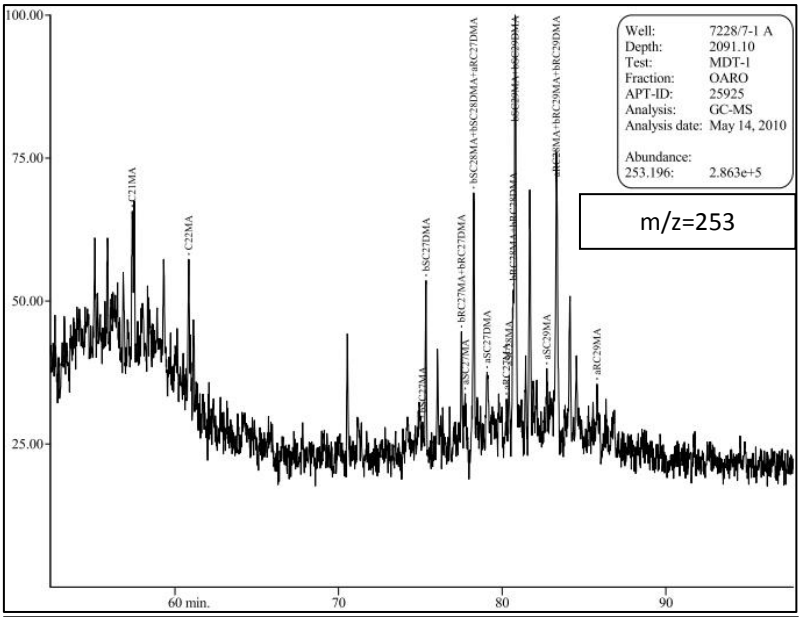
Well: 7228/7-1 A
Depth: 2091.10
Test: MDT-1
Fraction: OARO
APT-ID: 25925
Analysis: GC-MS
Analysis date: May 14, 2010
Abundance:
253.196: 2.863e+5
m/z=253
C21MA
C22MA
bSC27DMA
bRC27MA+bRC27DMA
bSC28MA+bSC28DMA+aRC27DMA
aSC27DMA
aSC29MA
aRC29MA
bRC29MA+bRC29DMA
60 min.

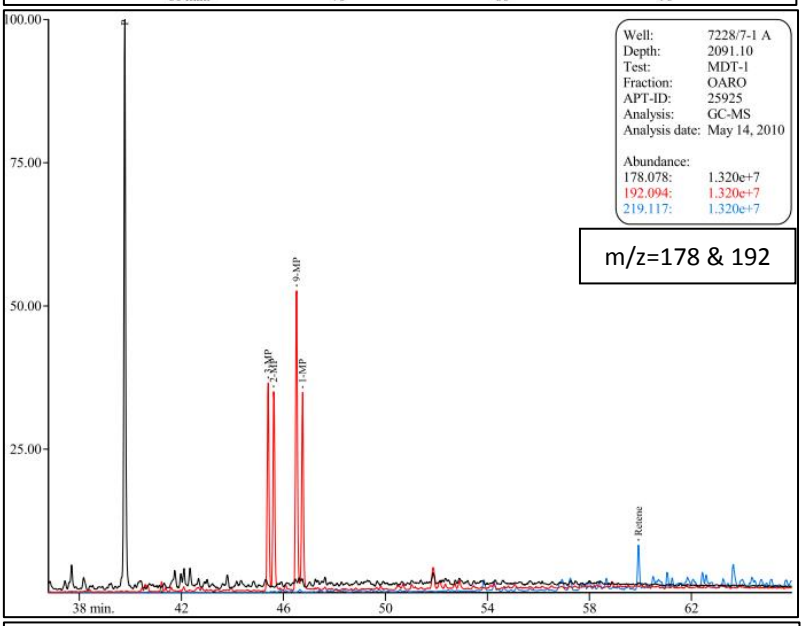
Well: 7228/7-1 A
Depth: 2091.10
Test: MDT-1
Fraction: OARO
APT-ID: 25925
Analysis: GC-MS
Analysis date: May 14, 2010
Abundance:
178.078: 1.320e+7
192.094: 1.320e+7
219.117: 1.320e+7
m/z=178 & 192
2-MP
3-MP
9-MP
1-MP
Retene
38 min.

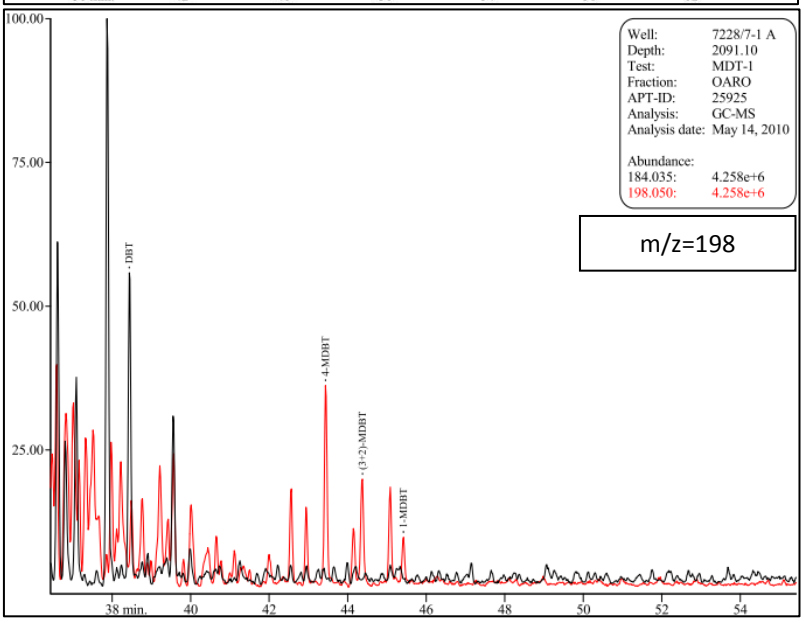
Well: 7228/7-1 A
Depth: 2091.10
Test: MDT-1
Fraction: OARO
APT-ID: 25925
Analysis: GC-MS
Analysis date: May 14, 2010
Abundance:
184.035: 4.258e+6
198.050: 4.258e+6
m/z=198
DBT
4-MDBT
(3+2)-MDBT
1-MDBT
38 min.

GC-FID Chromatogram for S.R sample "S1" from well 7122/6-1

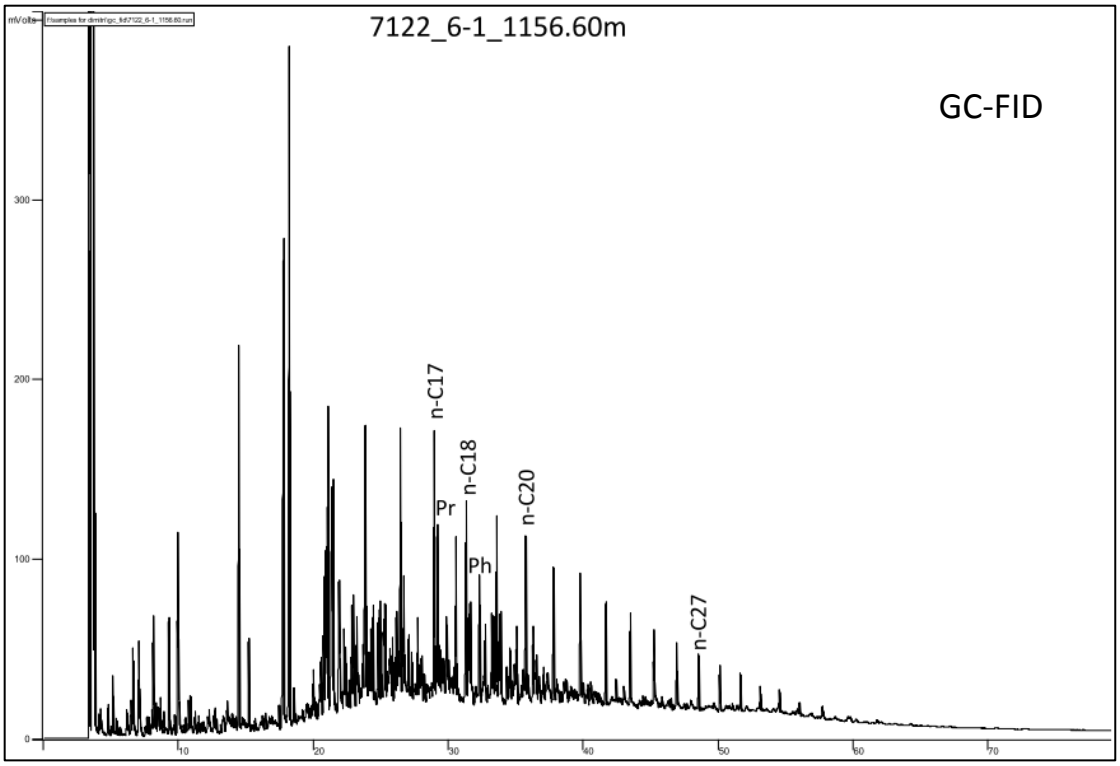

GC-MS Chromatograms for S.R sample "S1" from well 7122/6-1

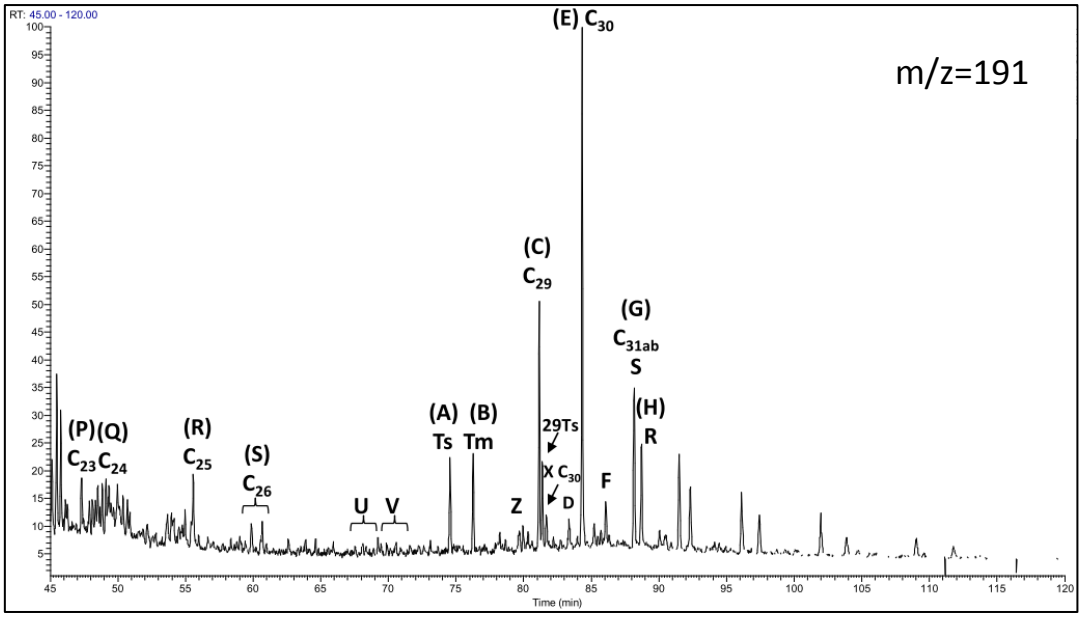

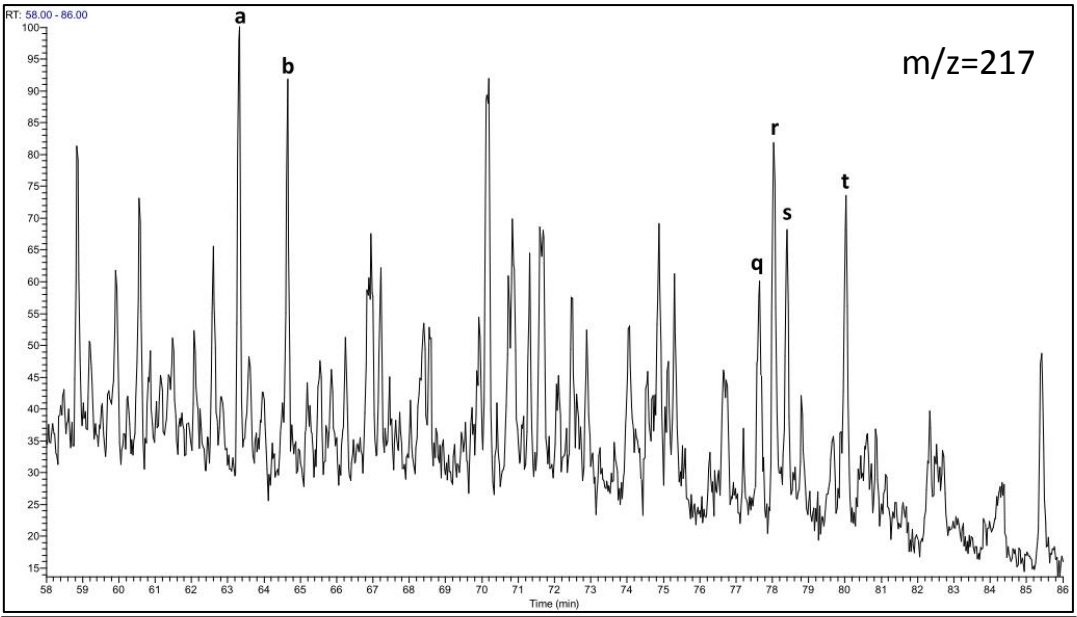
RT: 58.00 - 86.00
m/z=217
a
b
q
r
s
t
Time (min)

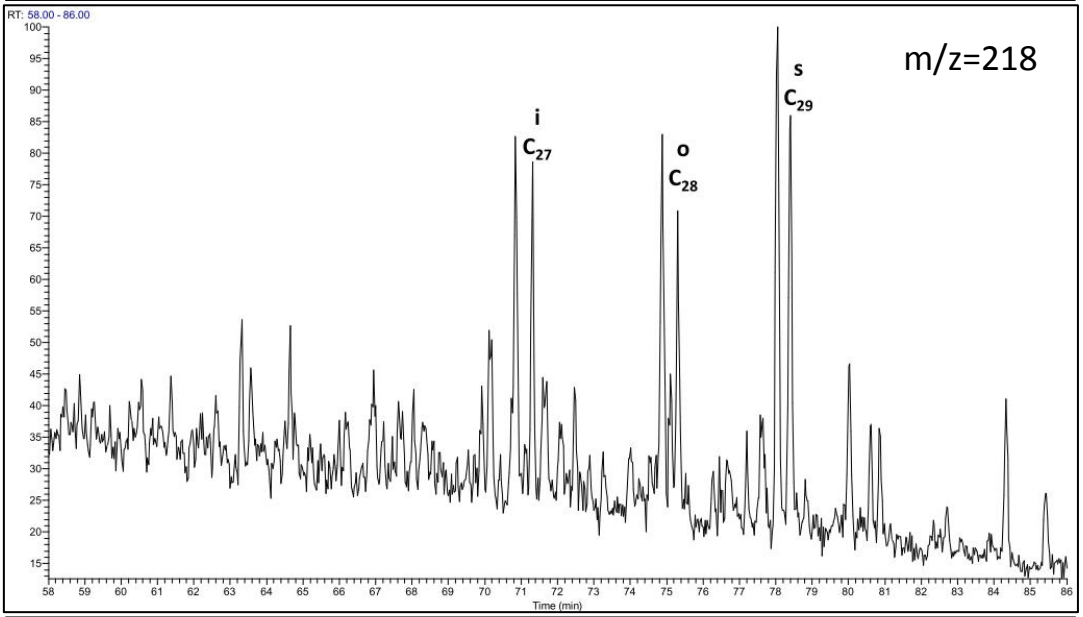
RT: 58.00 - 86.00
m/z=218
i
C27
o
C28
s
C29
Time (min)

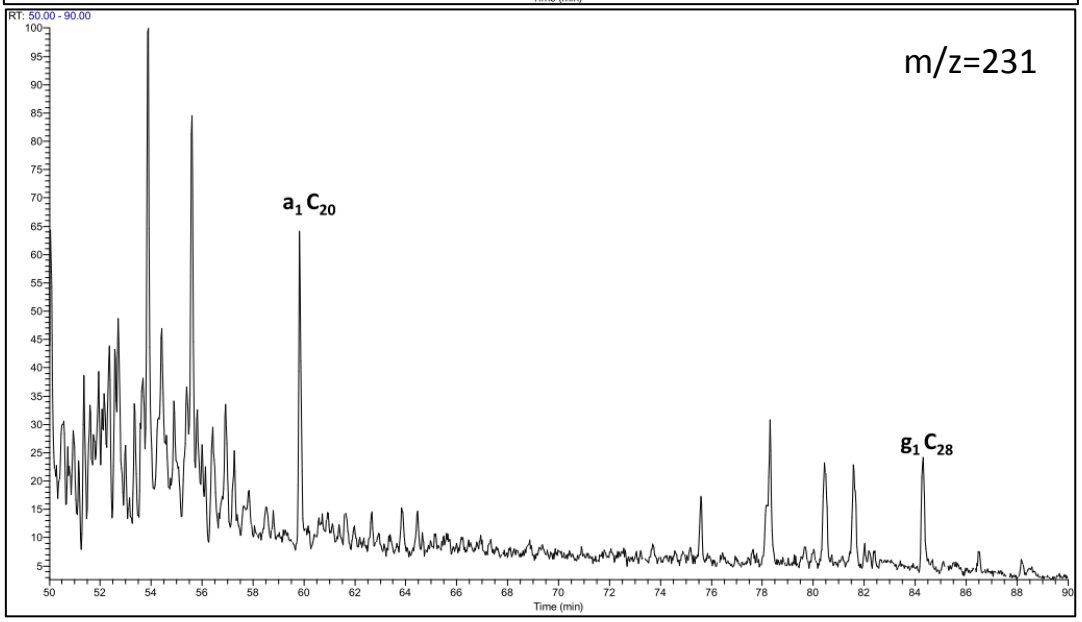
RT: 50.00 - 90.00
m/z=231
a1 C20
g1 C28
Time (min)

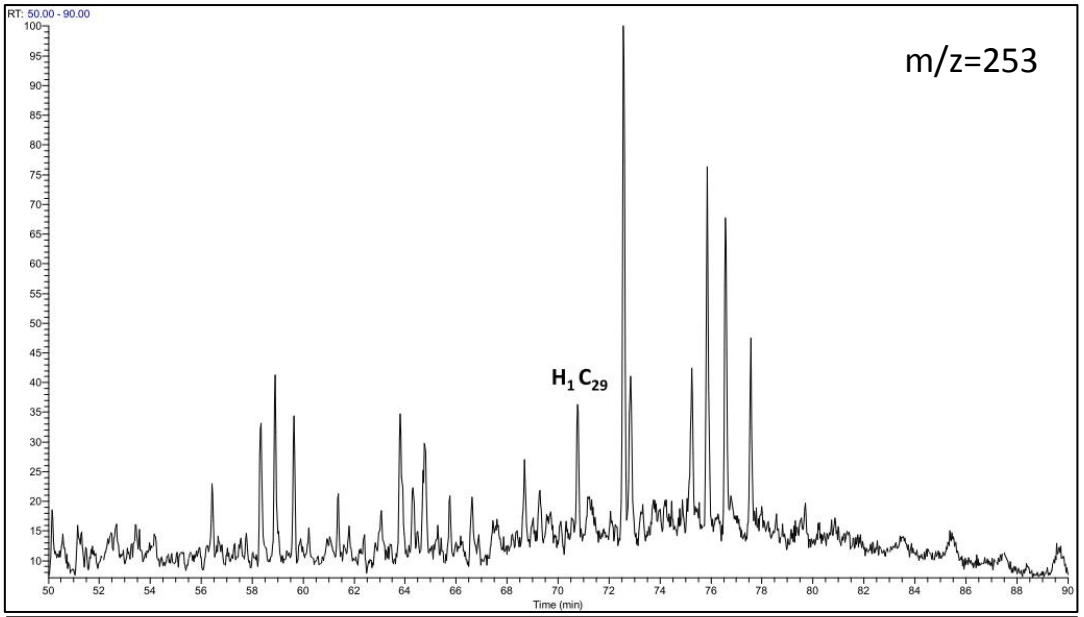
RT: 50.00 - 90.00
m/z=253
H1 C29
Time (min)

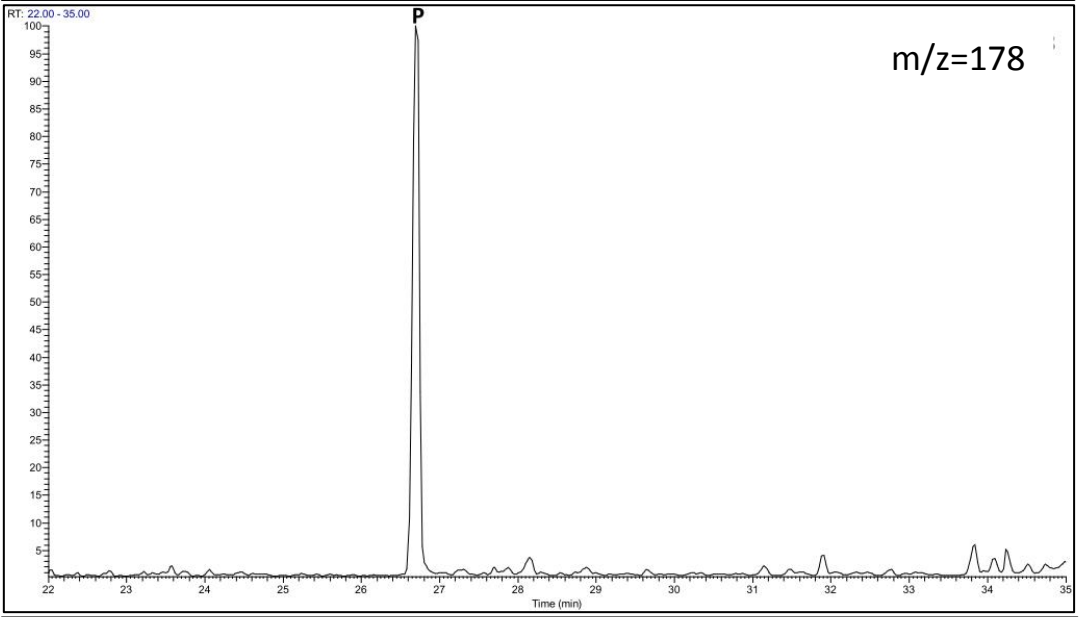
RT: 22.00 - 35.00
P
m/z=178
Time (min)

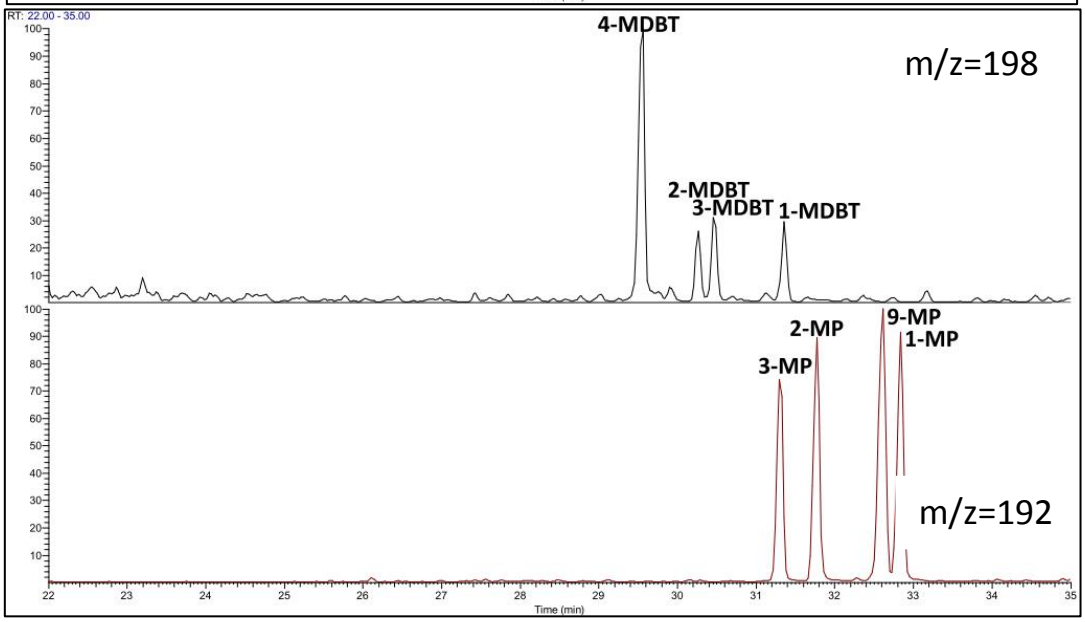
RT: 22.00 - 35.00
4-MDBT
2-MDBT
3-MDBT
1-MDBT
m/z=198
3-MP
2-MP
9-MP
1-MP
m/z=192
Time (min)

GC-FID Chromatogram for S.R sample "S2" from well 7122/6-1

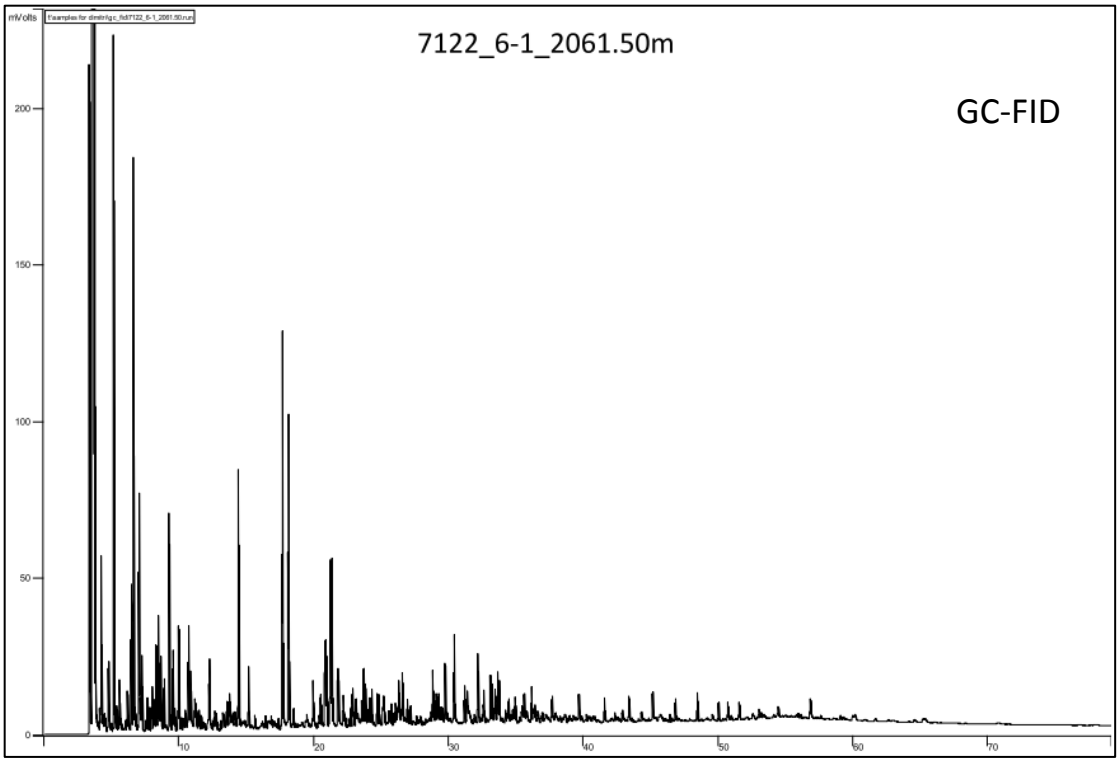

GC-MS Chromatograms for S.R sample "S2" from well 7122/6-1

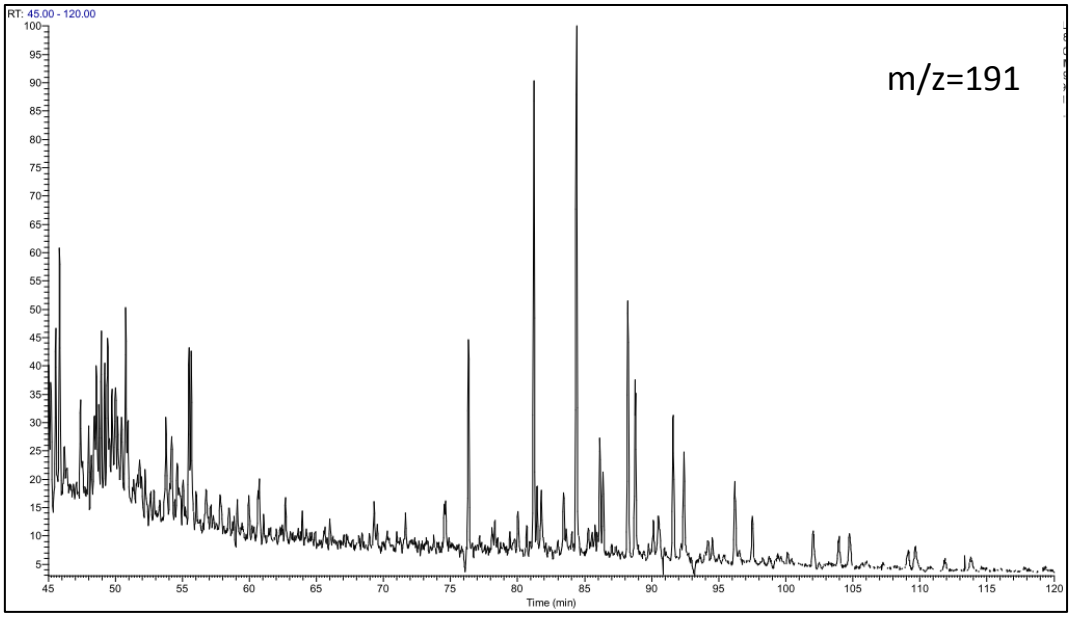

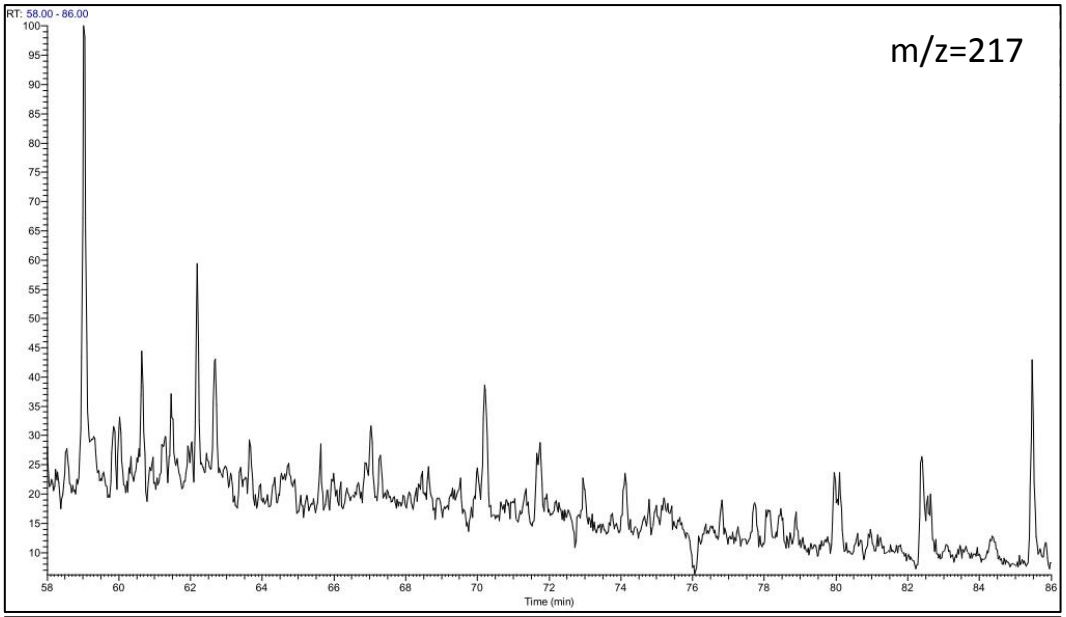
RT: 58.00 - 86.00
m/z=217
Time (min)

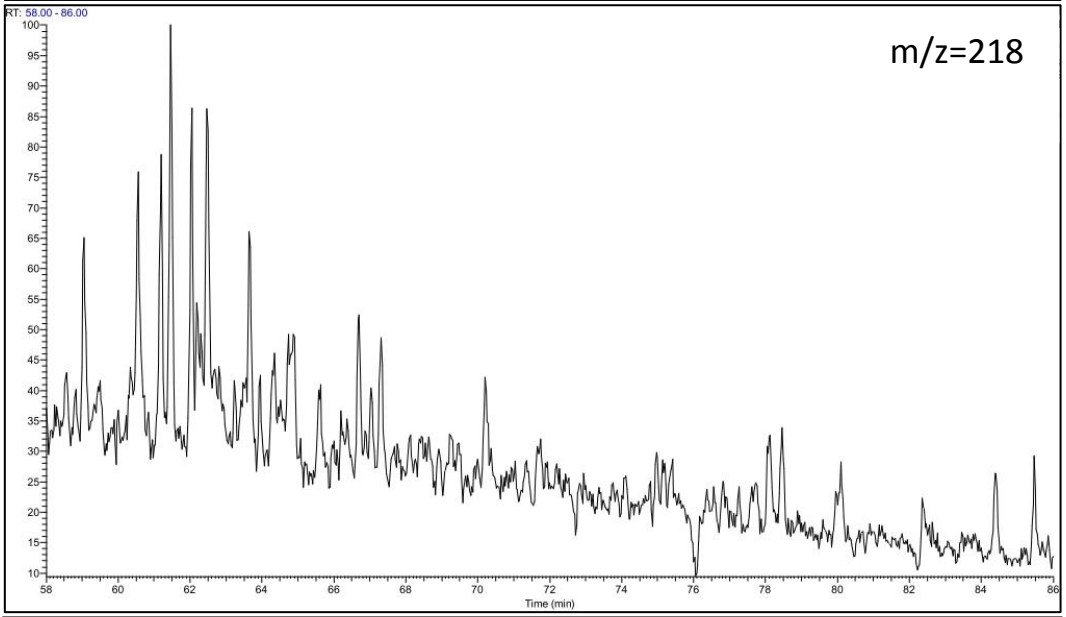
RT: 58.00 - 86.00
m/z=218
Time (min)

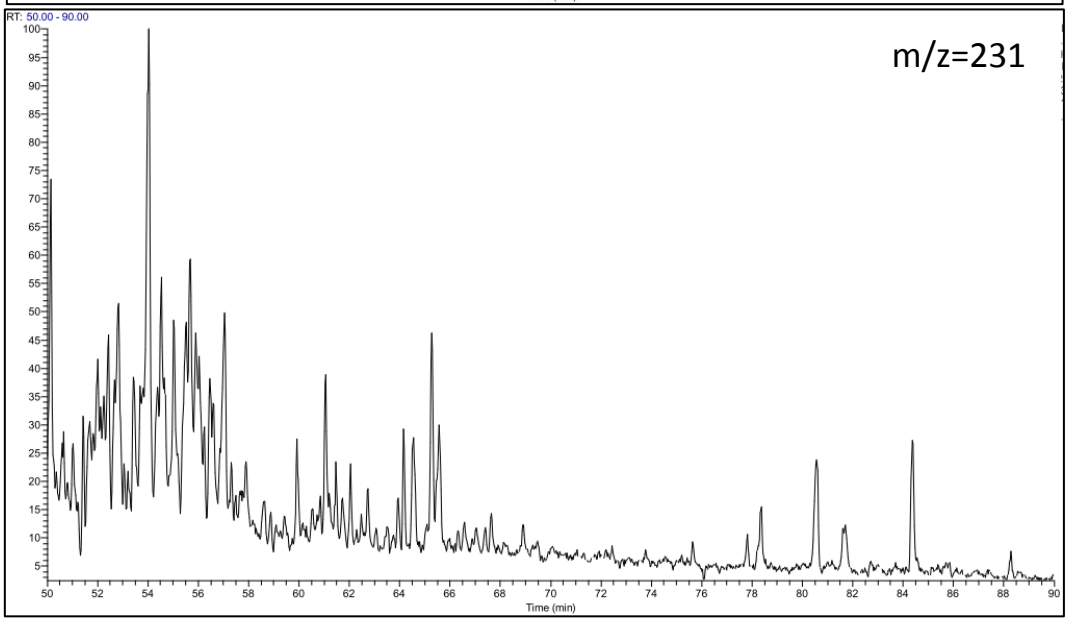
RT: 50.00 - 90.00
m/z=231
Time (min)

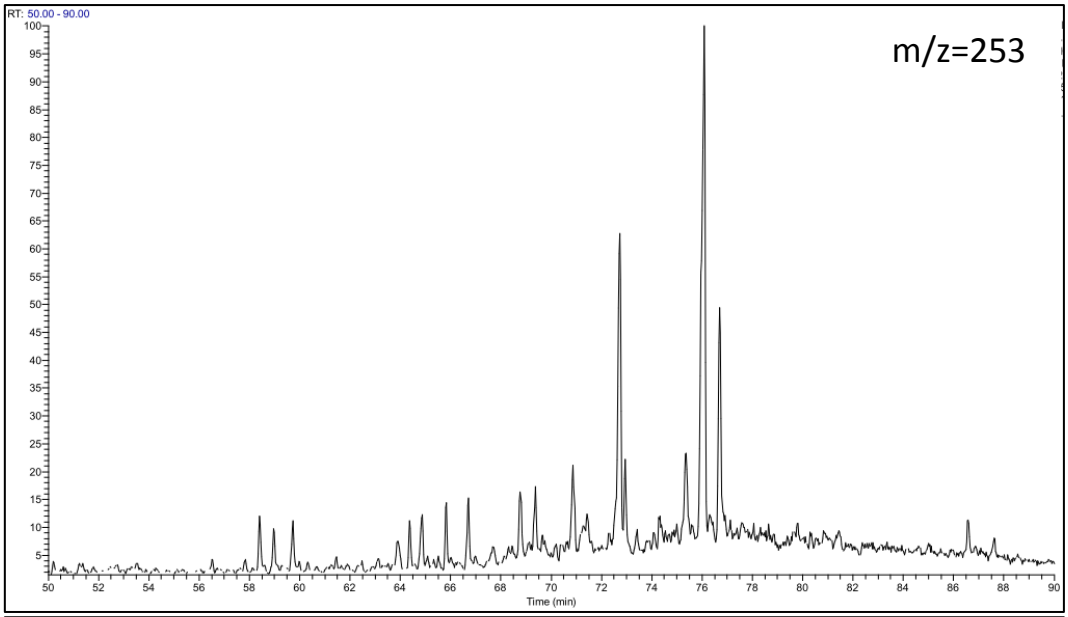
RT: 50.00 - 90.00
m/z=253
Time (min)

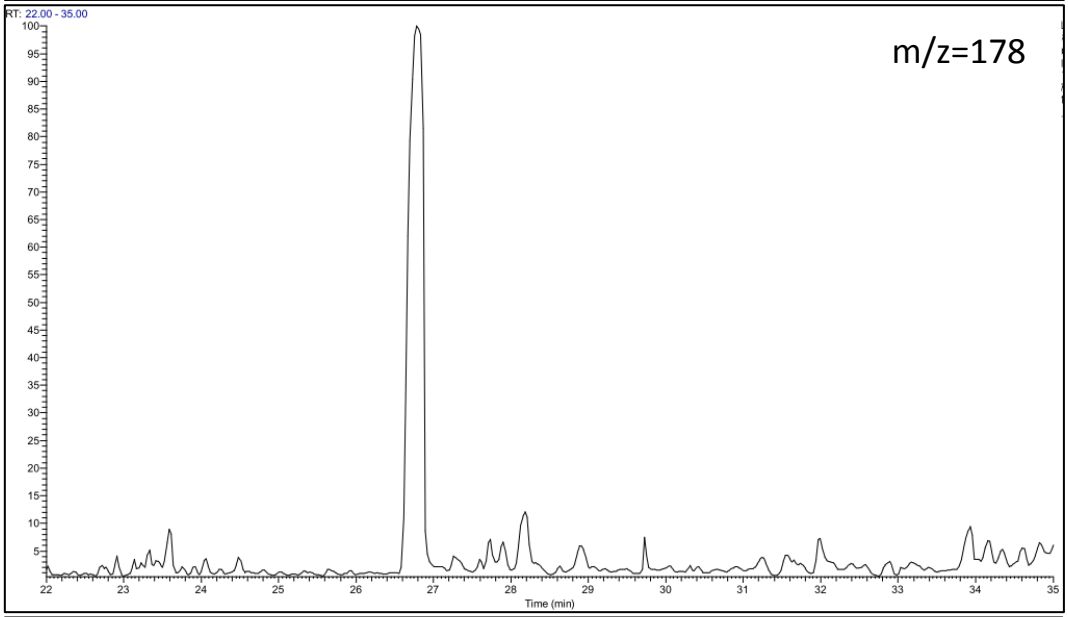
RT: 22.00 - 35.00
m/z=178
Time (min)

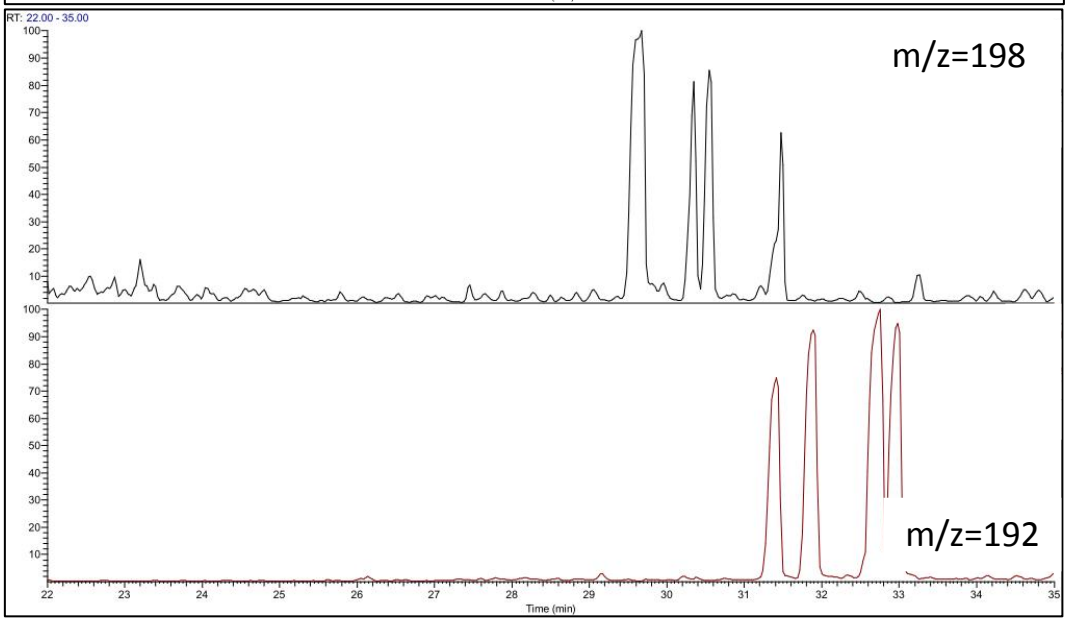
RT: 22.00 - 35.00
m/z=198
m/z=192
Time (min)

GC-FID Chromatogram for S.R sample "S3" from well 7124/3-1

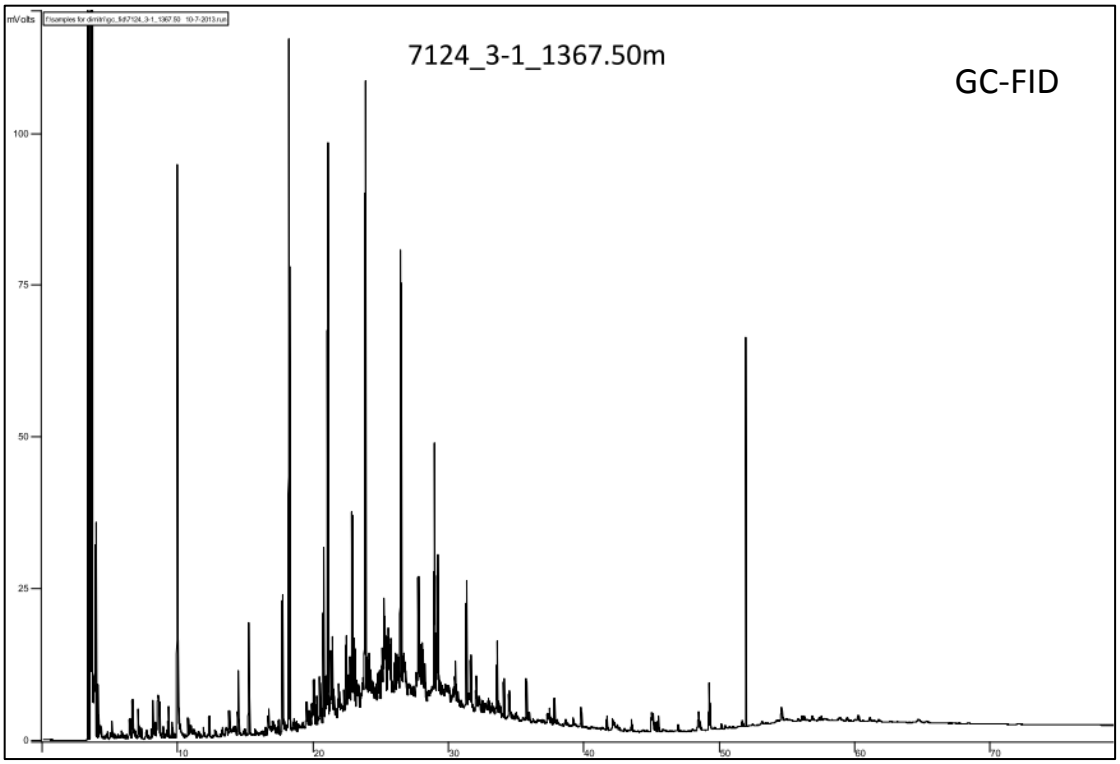

GC-MS Chromatograms for S.R sample "S3" from well 7124/3-1

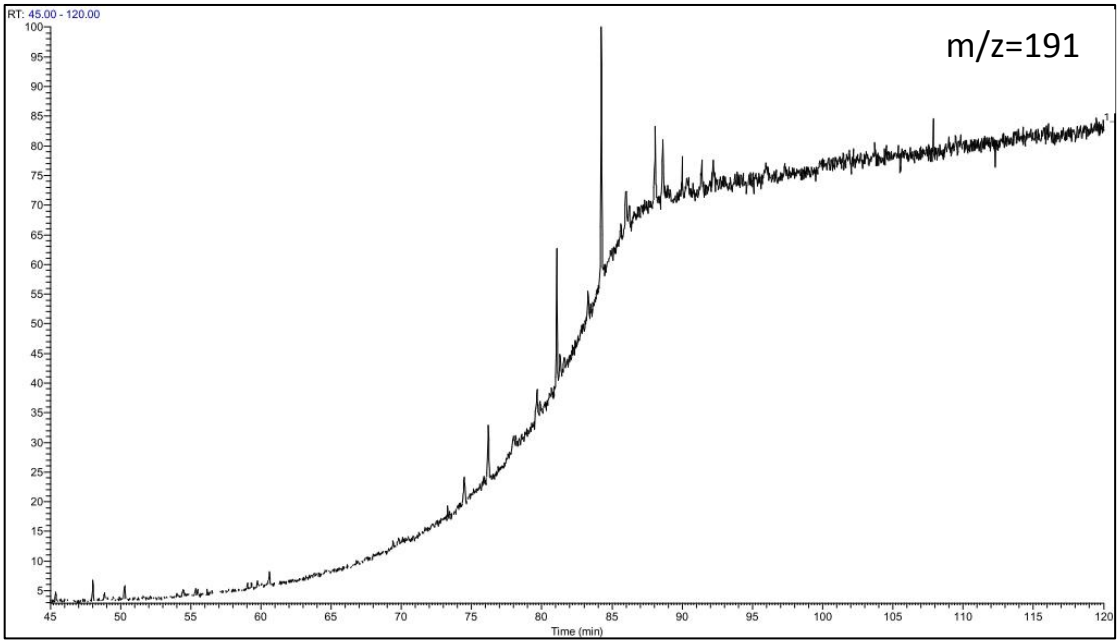

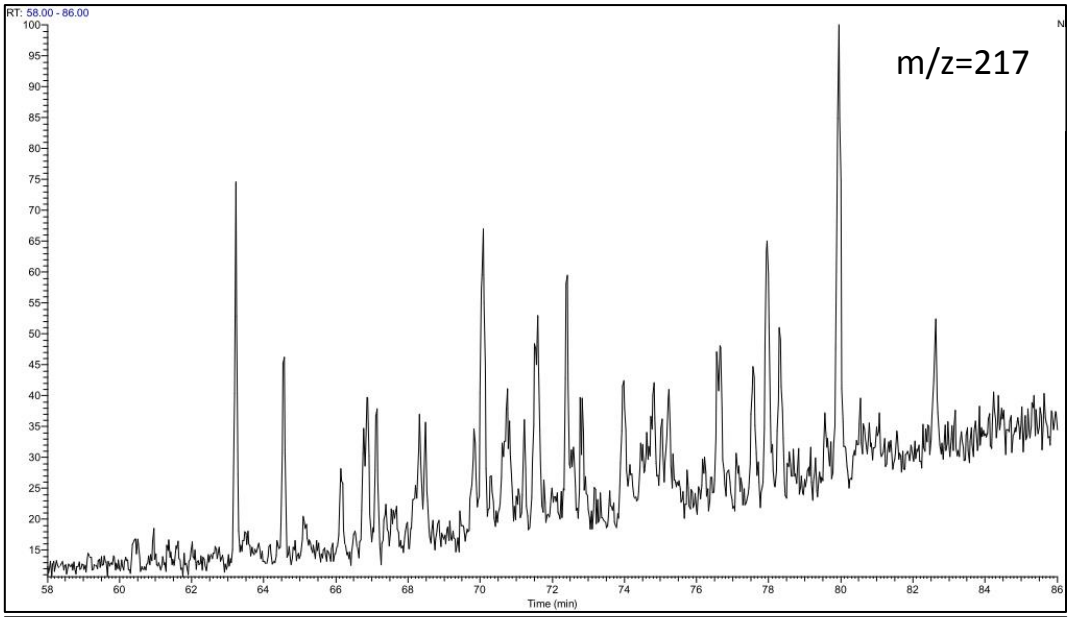
RT: 58.00 - 86.00
m/z=217
Time (min)

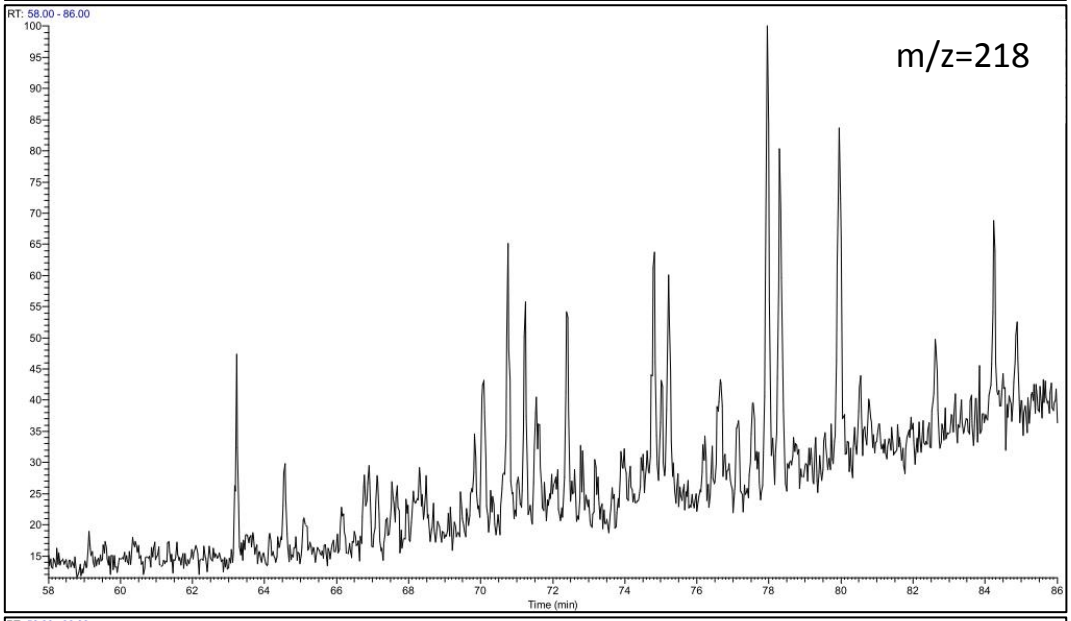
RT: 58.00 - 86.00
m/z=218
Time (min)

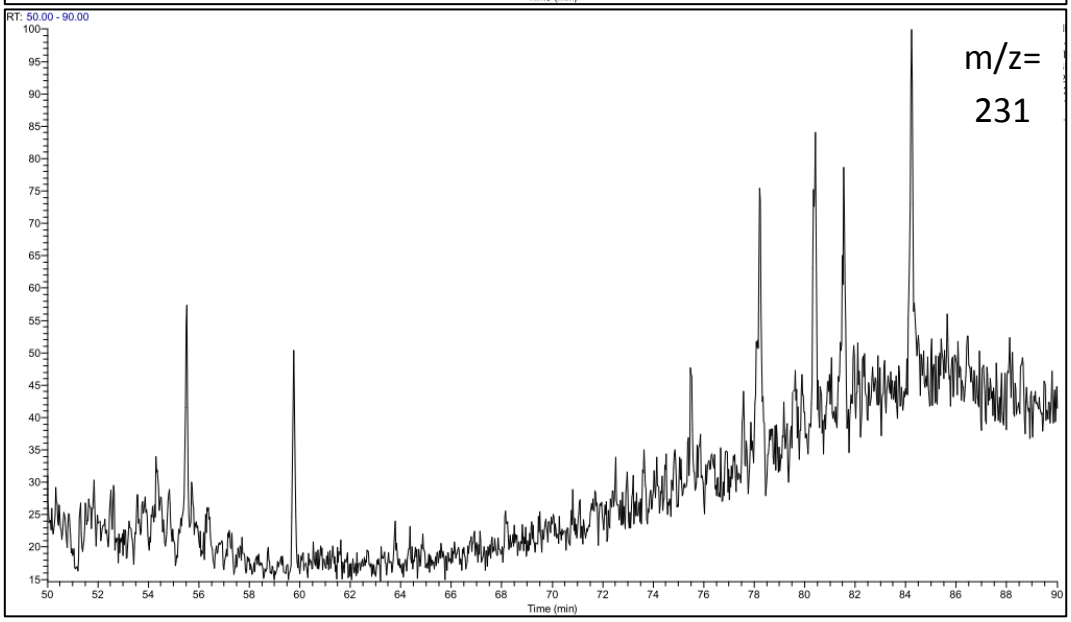
RT: 50.00 - 90.00
m/z=
231
Time (min)

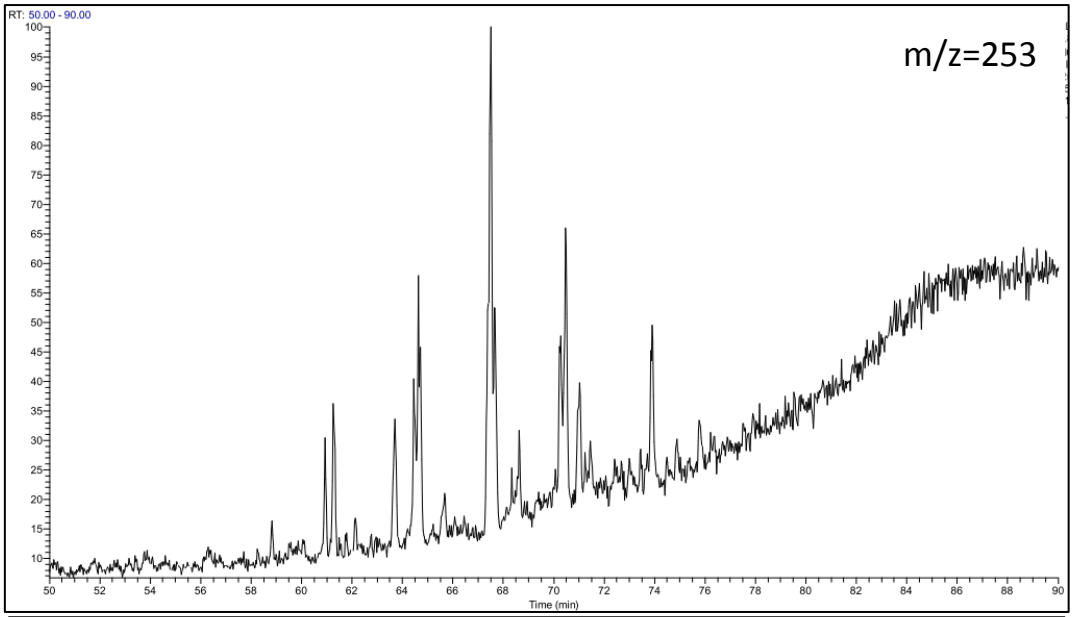
RT: 50.00 - 90.00
m/z=253
Time (min)

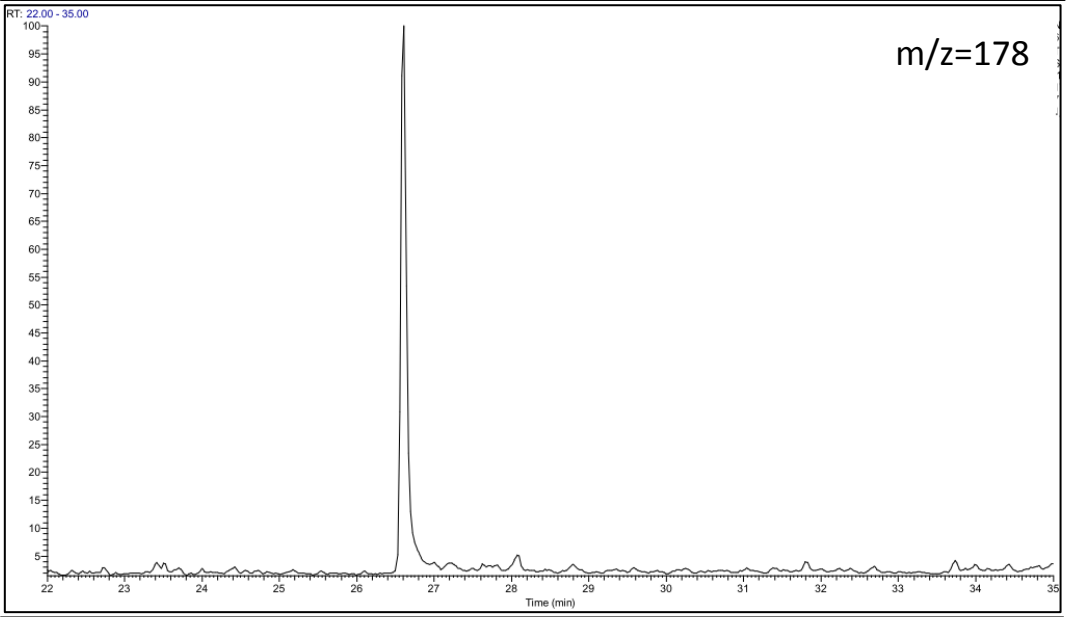
RT: 22.00 - 35.00
m/z=178
Time (min)

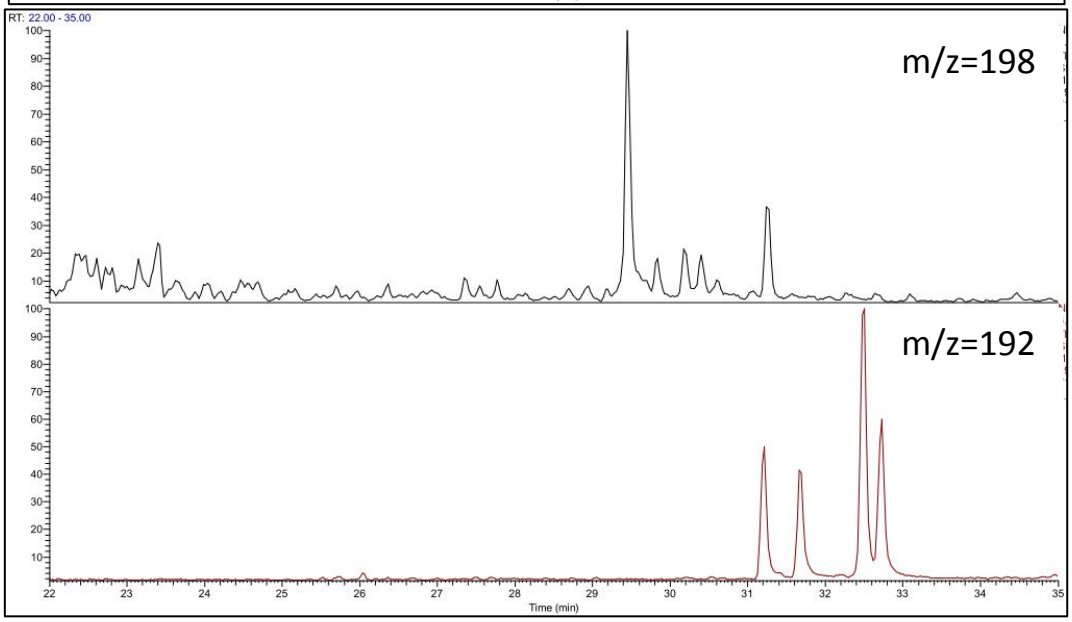
RT: 22.00 - 35.00
m/z=198
m/z=192
Time (min)

GC-FID Chromatogram for S.R sample "S4" from well 7128/6-1

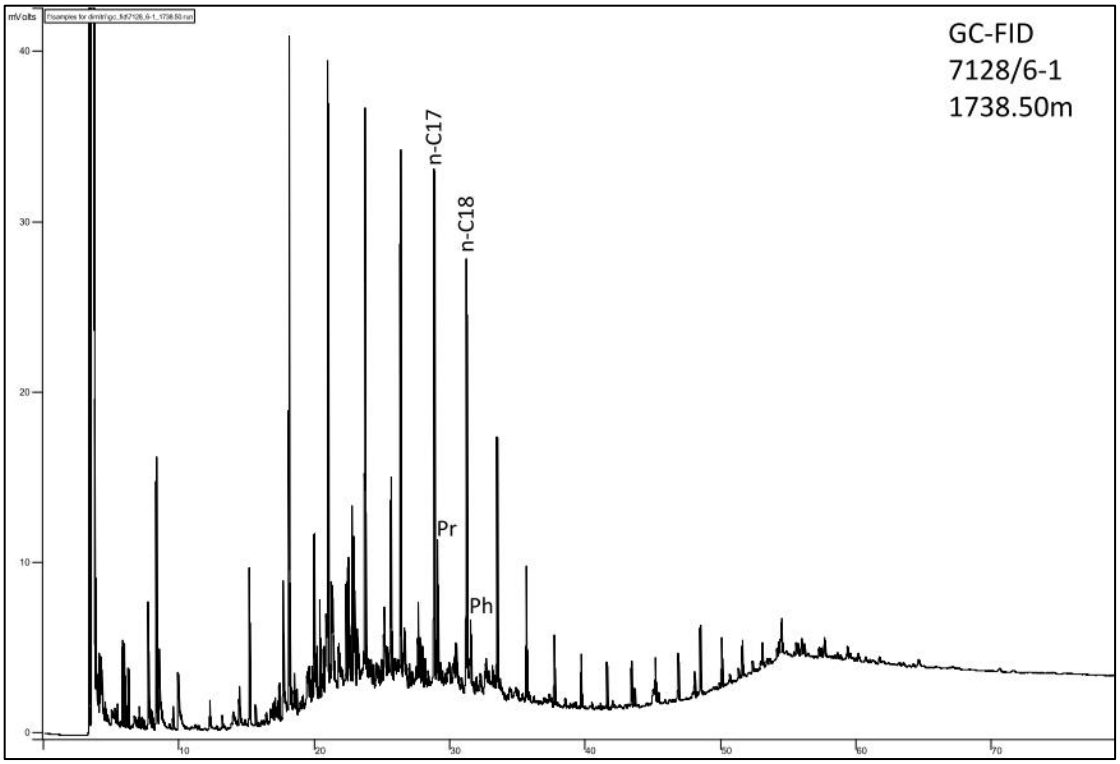

GC-MS Chromatograms for S.R sample "S4" from well 7128/6-1

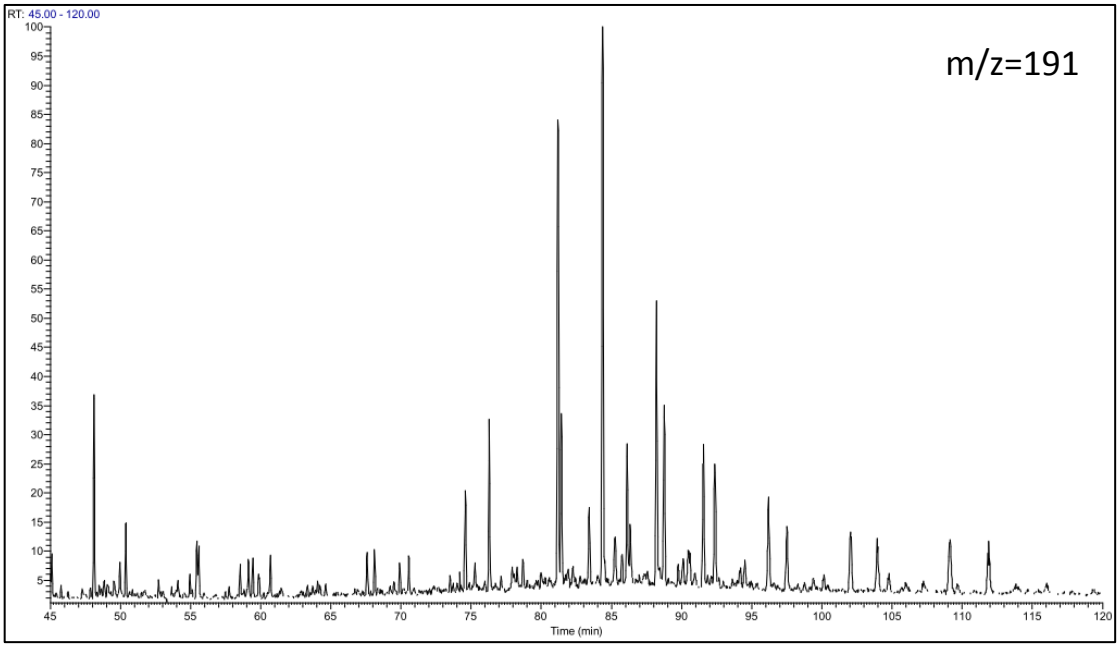

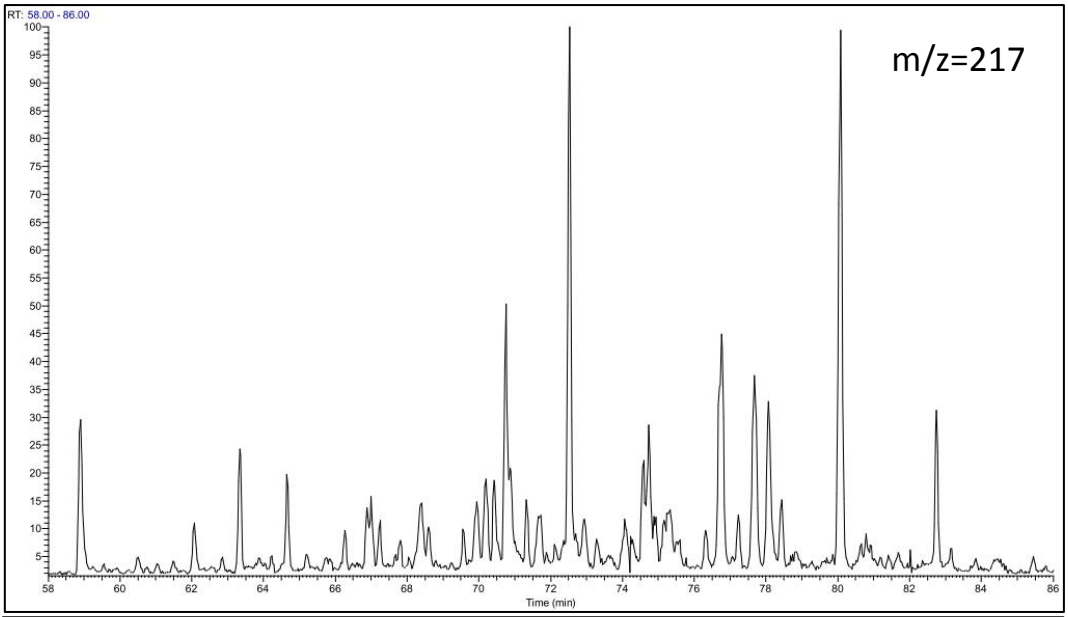
RT: 58.00 - 86.00
m/z=217
Time (min)

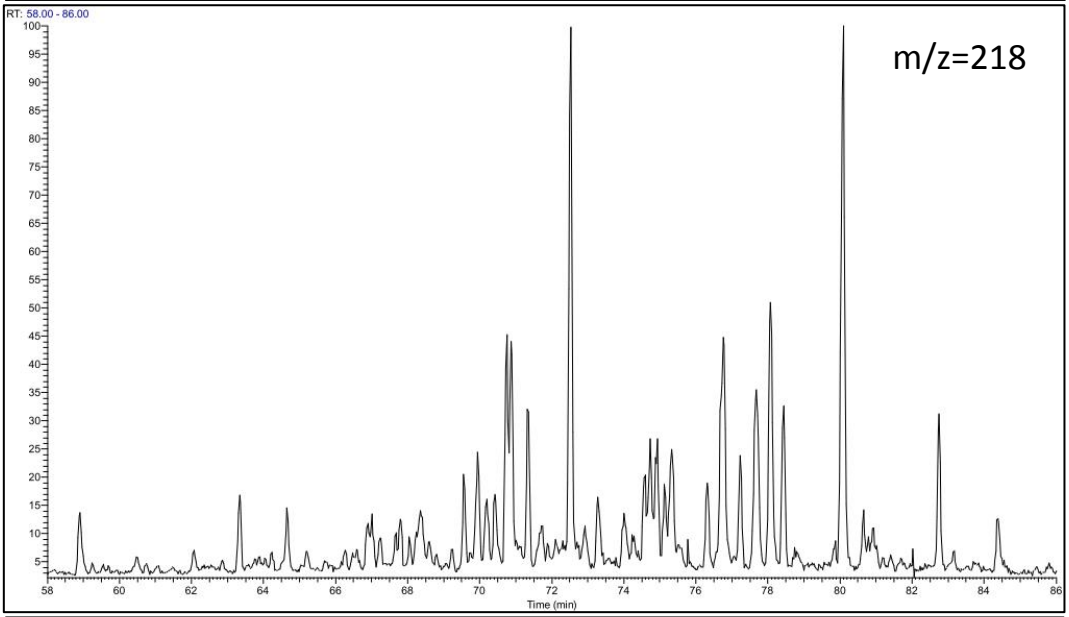
RT: 58.00 - 86.00
m/z=218
Time (min)

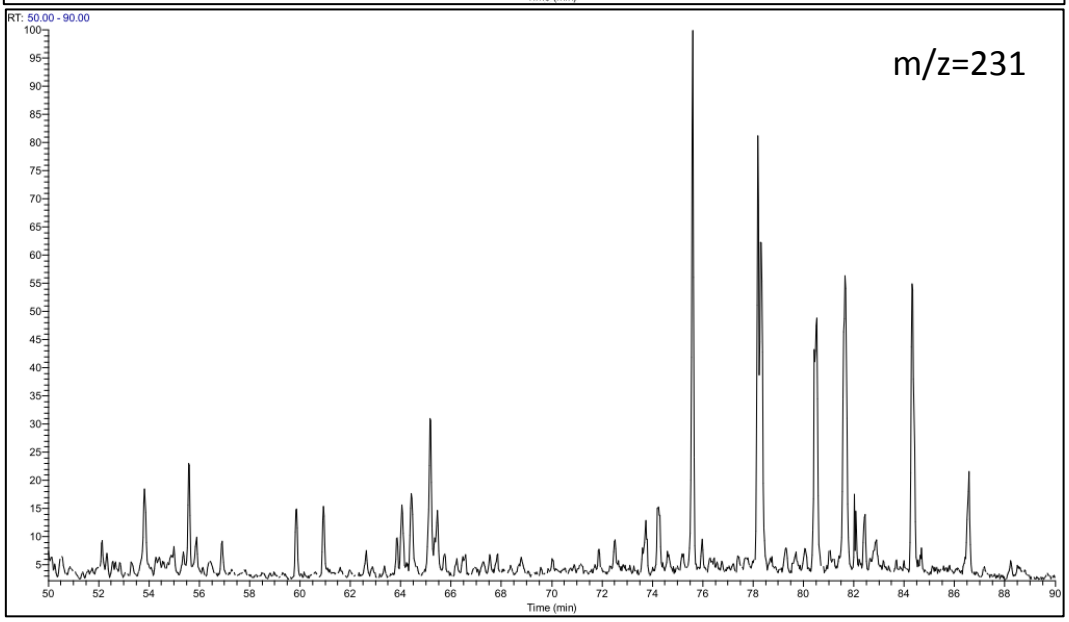
RT: 50.00 - 90.00
m/z=231
Time (min)

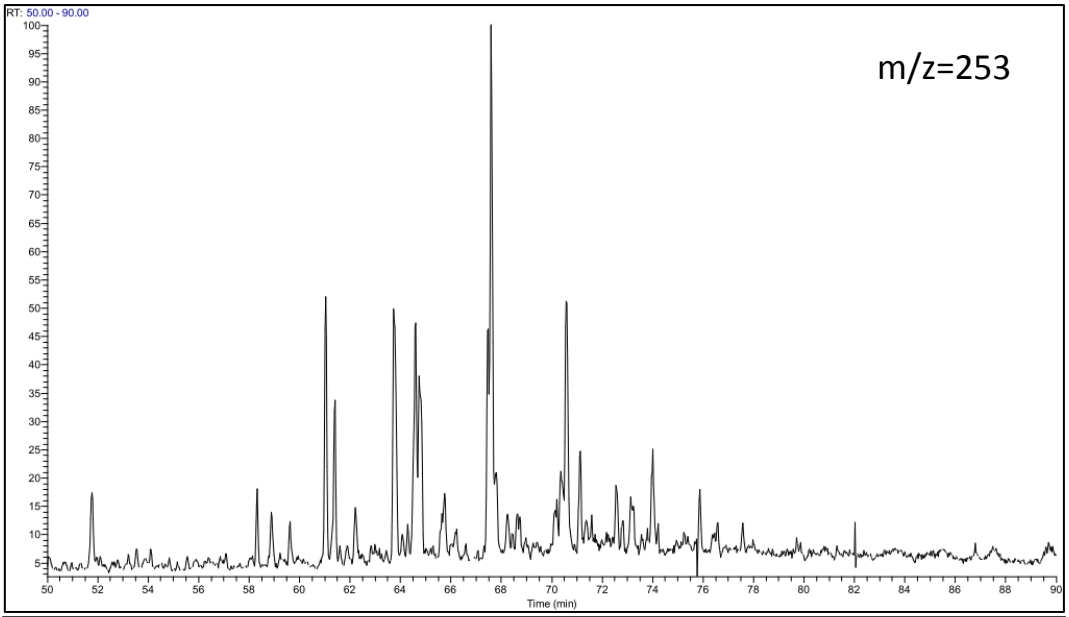
RT: 50.00 - 90.00
m/z=253
Time (min)

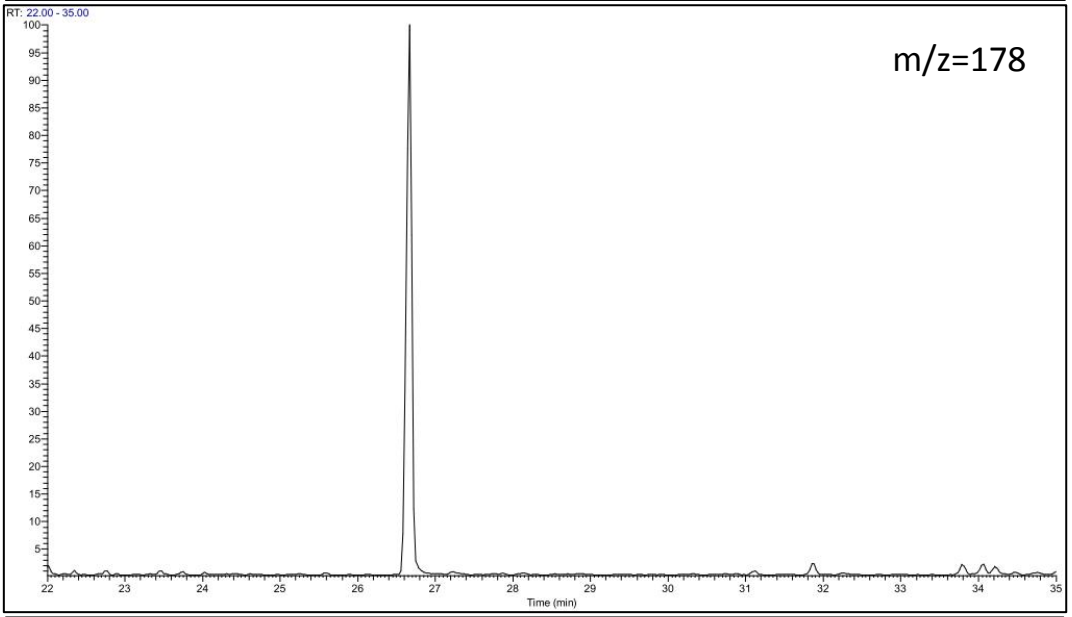
RT: 22.00 - 35.00
m/z=178
Time (min)

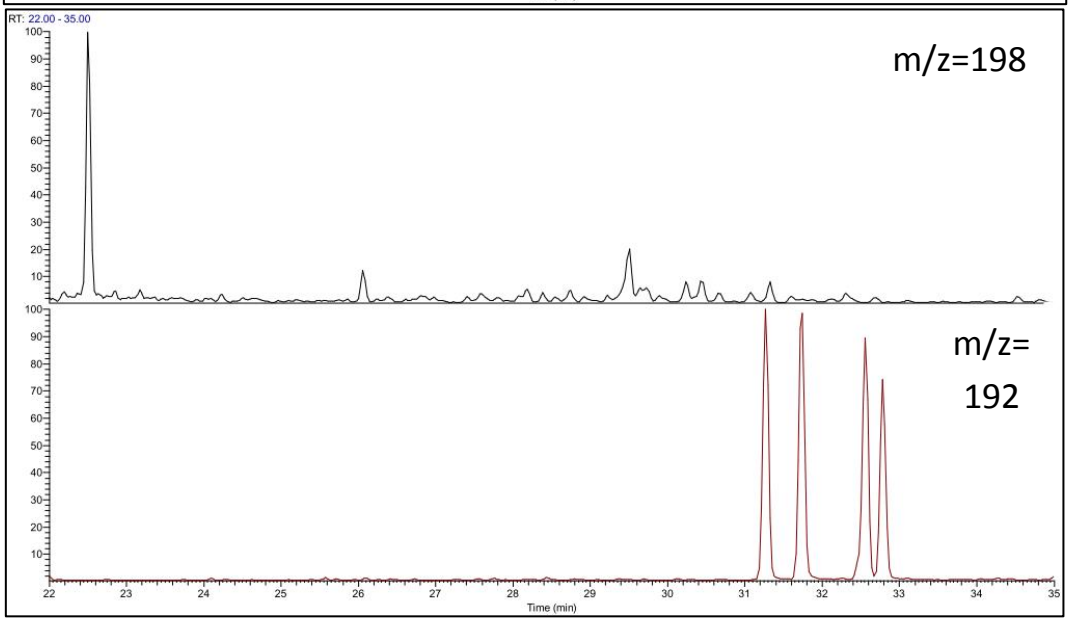
RT: 22.00 - 35.00
m/z=198
m/z=
192
Time (min)

GC-FID Chromatogram for S.R sample "S5" from well 7230/5-U-5

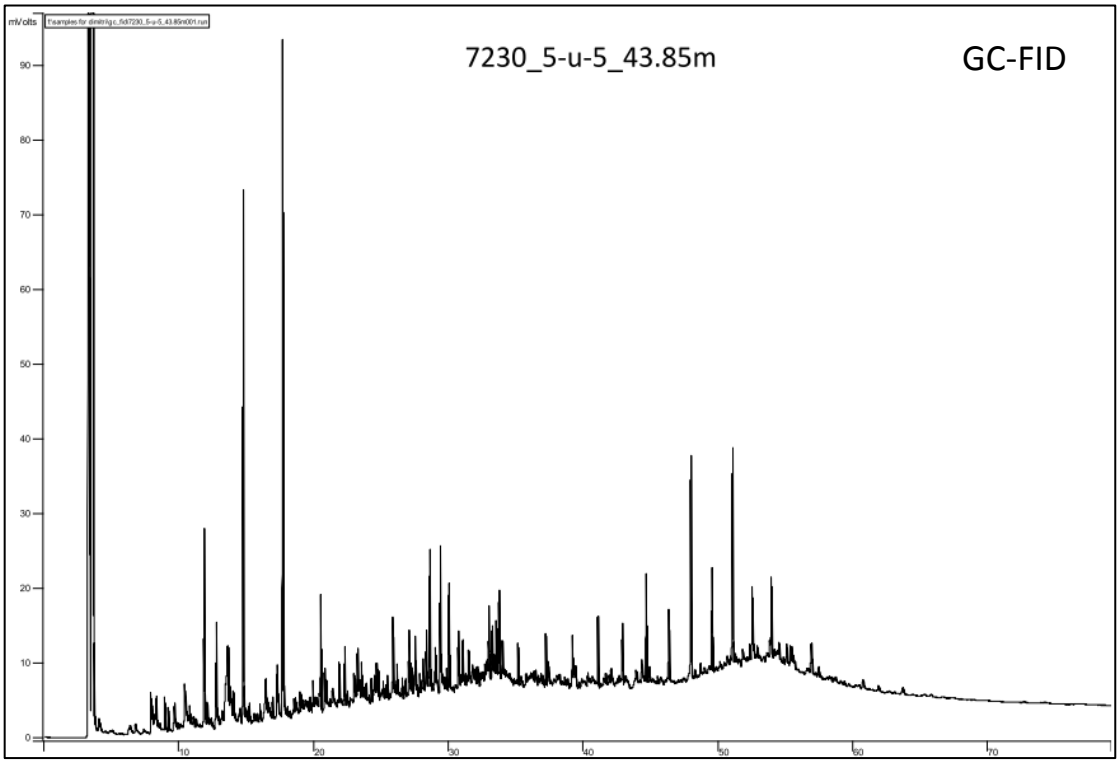

GC-MS Chromatograms for S.R sample "S5" from well 7230/5-U-5

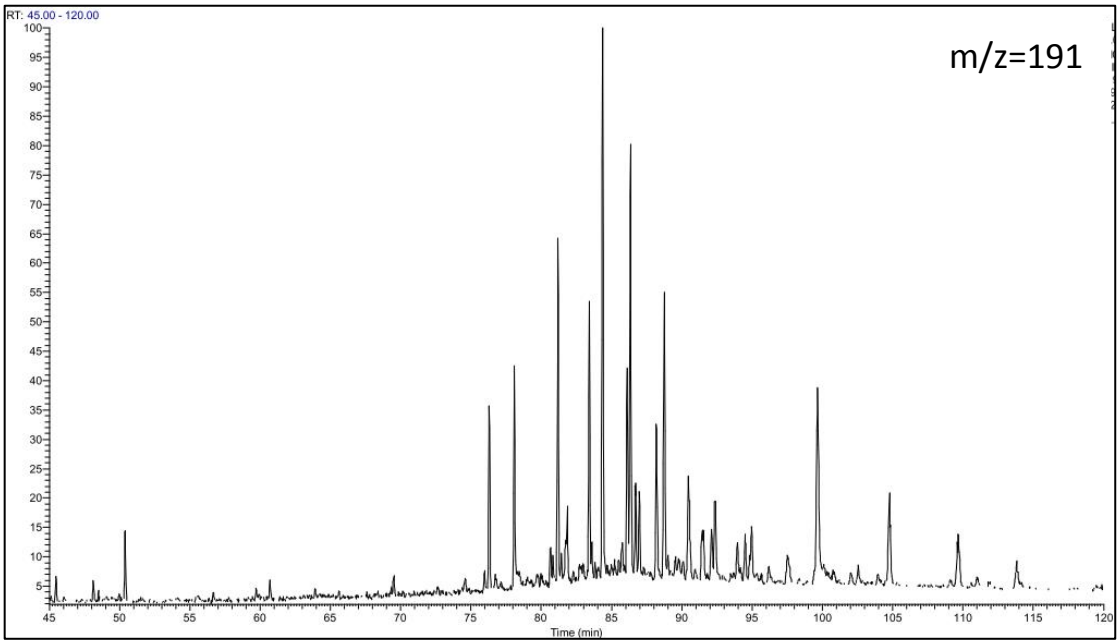

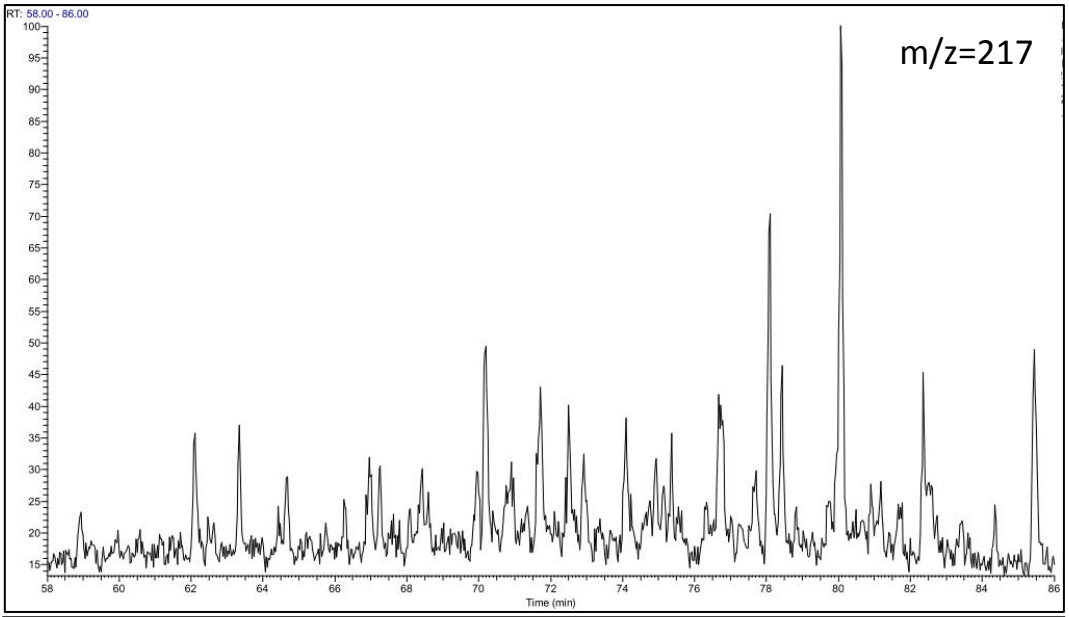
RT: 58.00 - 86.00
m/z=217
Time (min)

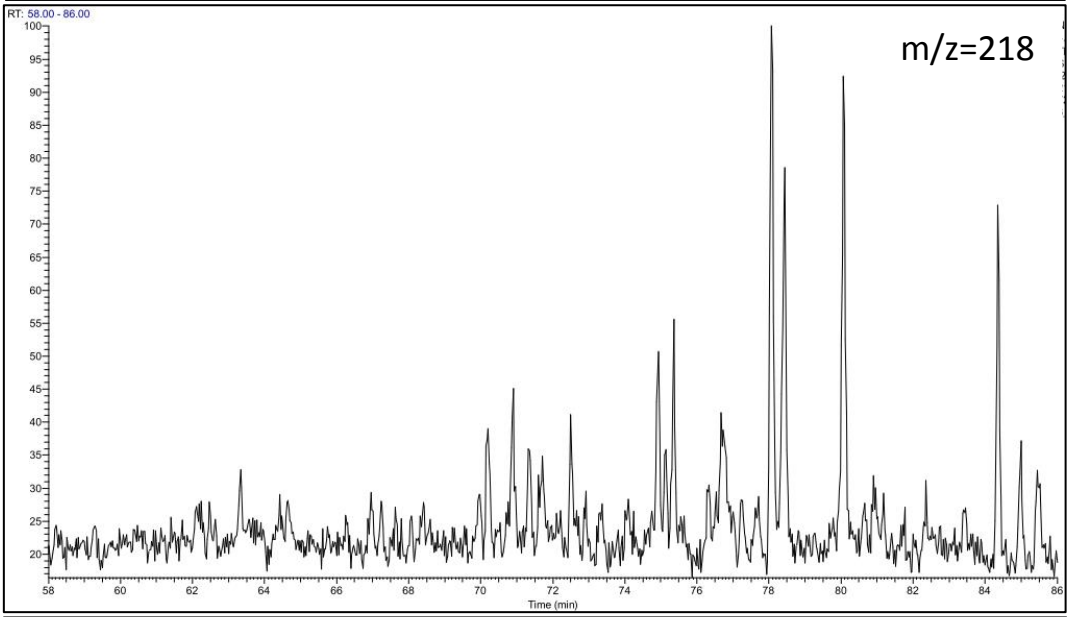
RT: 58.00 - 86.00
m/z=218
Time (min)

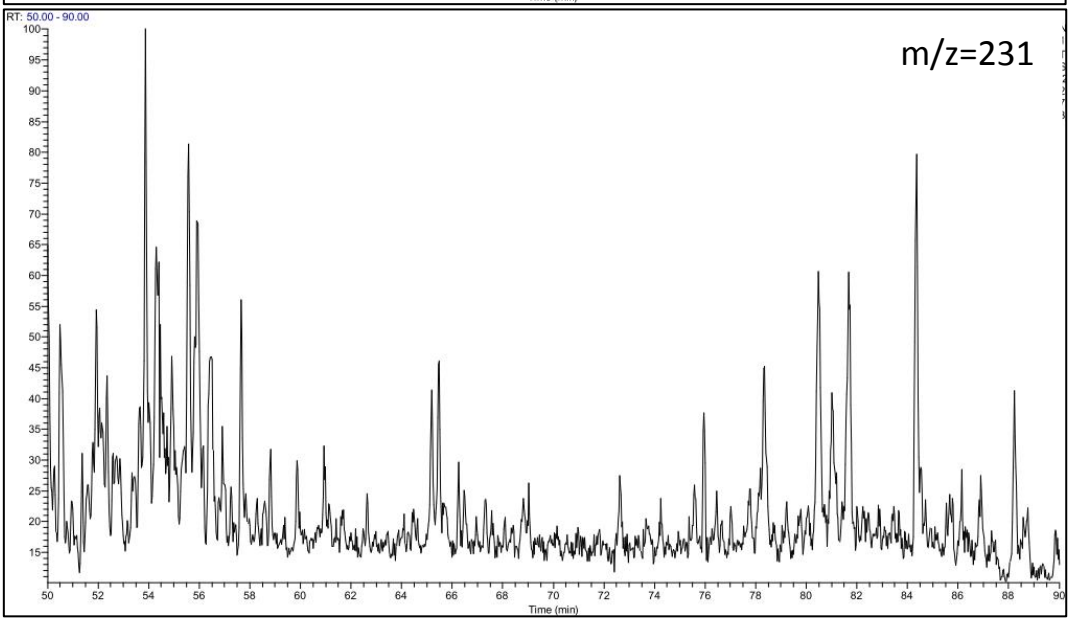
RT: 50.00 - 90.00
m/z=231
Time (min)

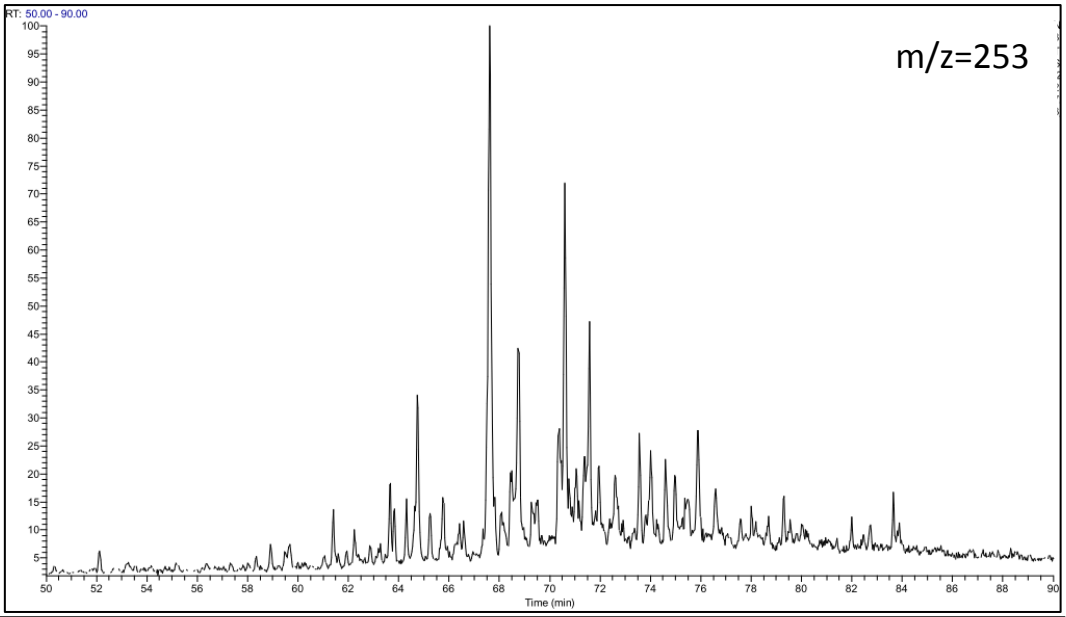
RT: 50.00 - 90.00
m/z=253
Time (min)

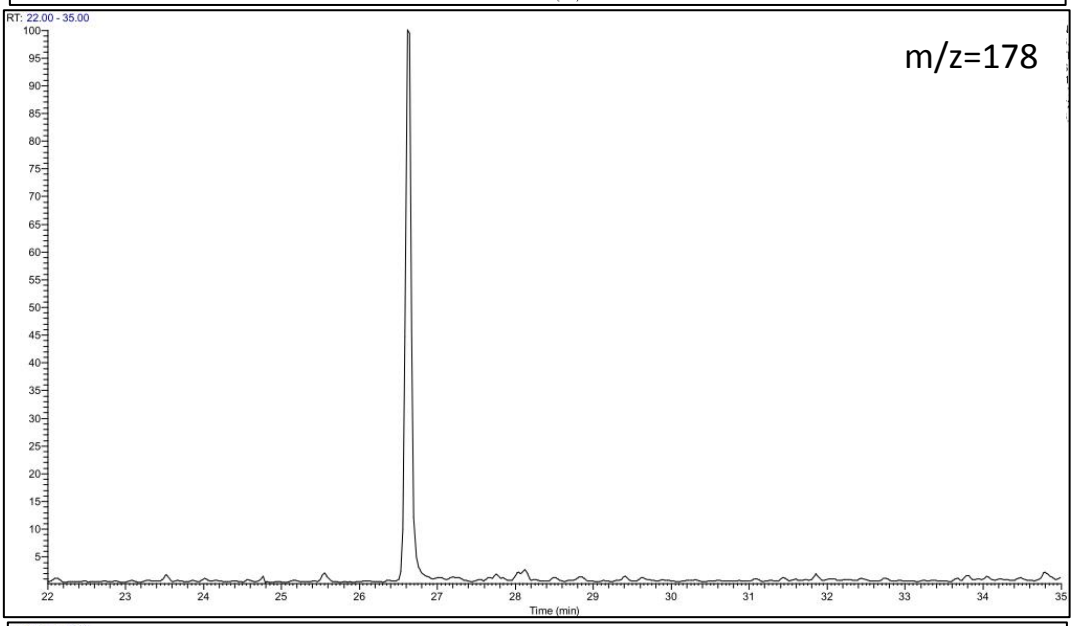
RT: 22.00 - 35.00
m/z=178
Time (min)

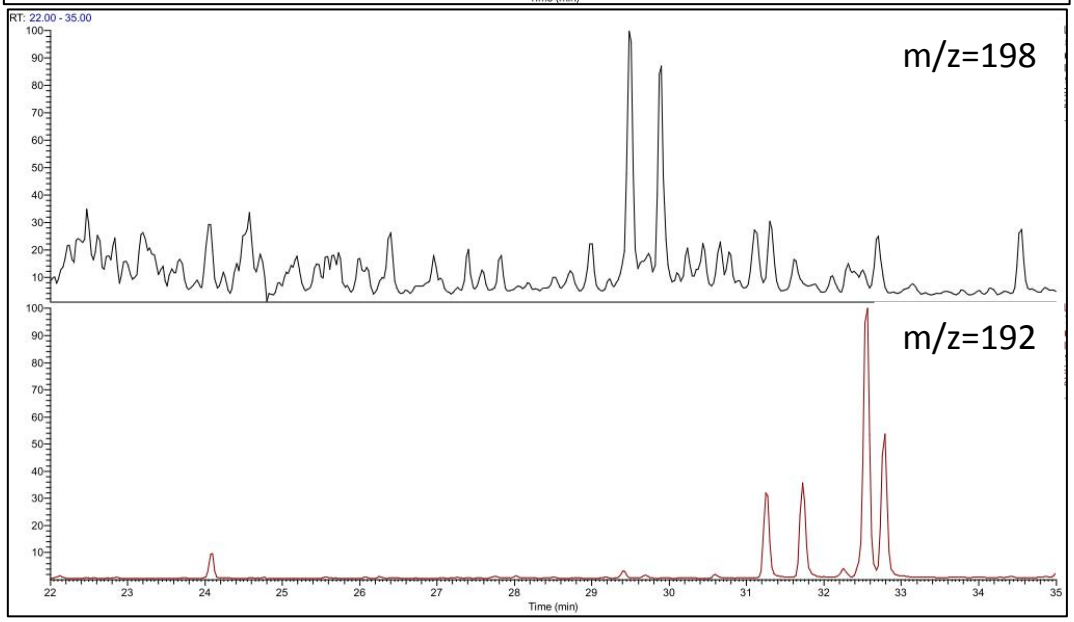
RT: 22.00 - 35.00
m/z=198
m/z=192
Time (min)

GC-FID Chromatogram for S.R sample "S6" from well 7231/1-U-1

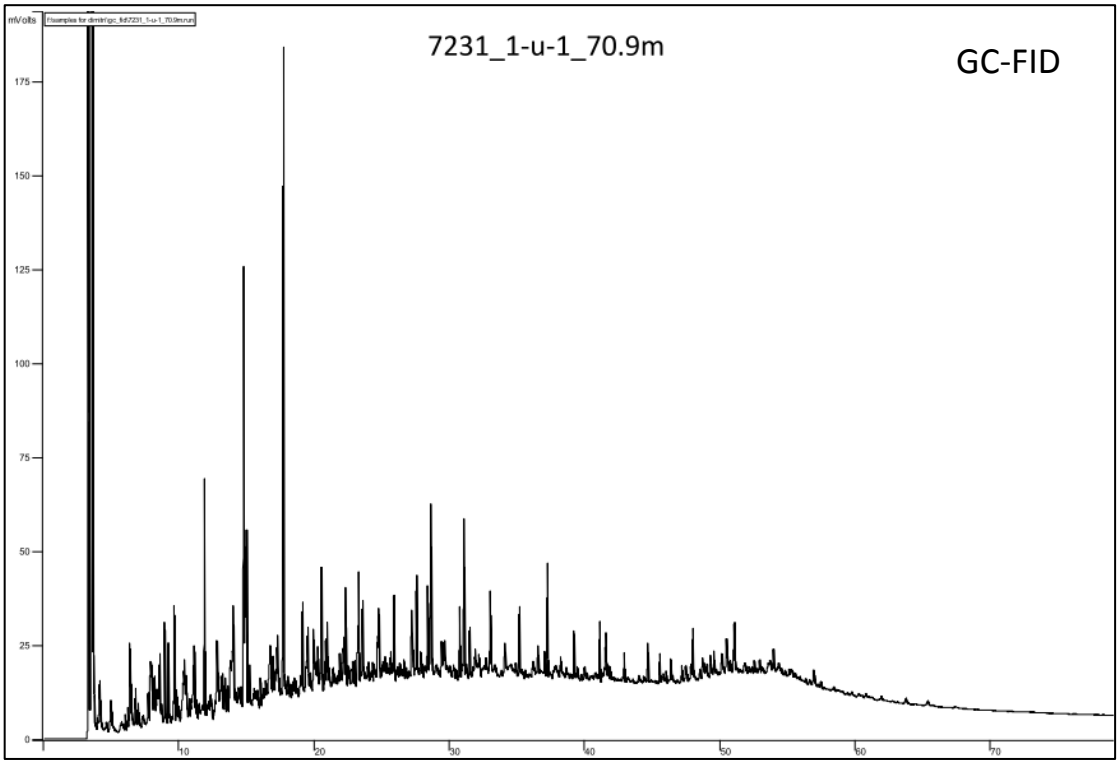

GC-MS Chromatograms for S.R sample "S6" from well 7231/1-U-1

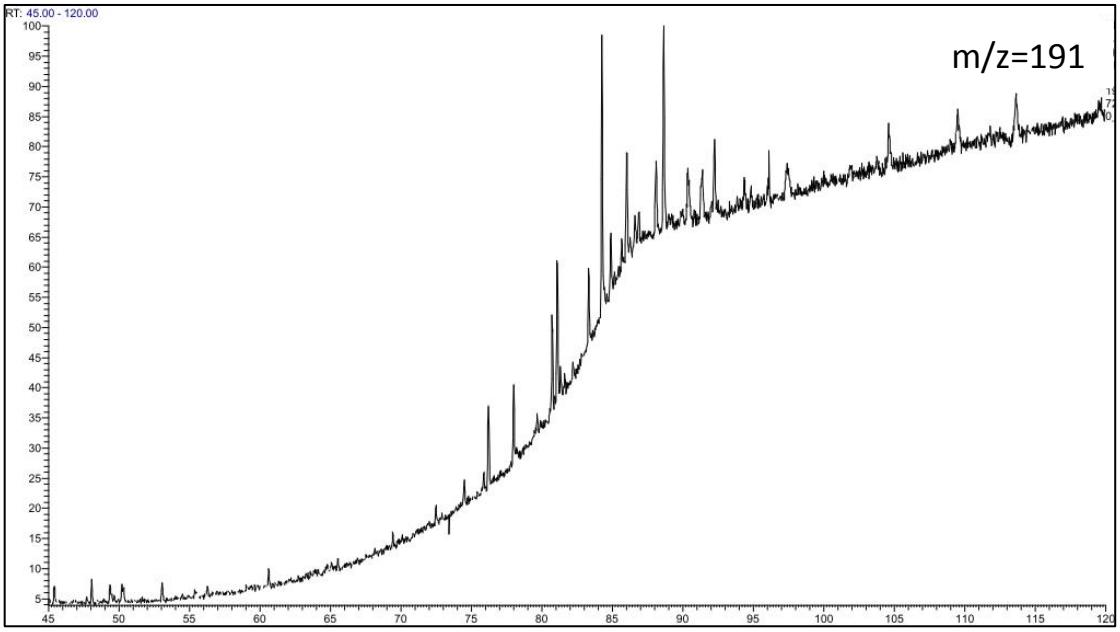

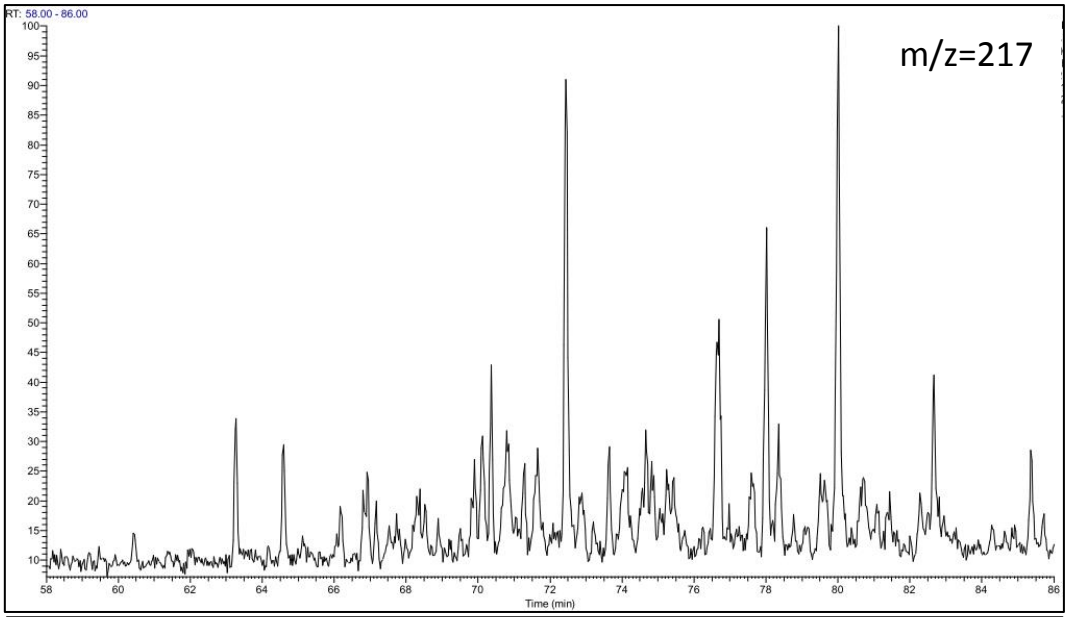
RT: 58.00 - 86.00
m/z=217
Time (min)

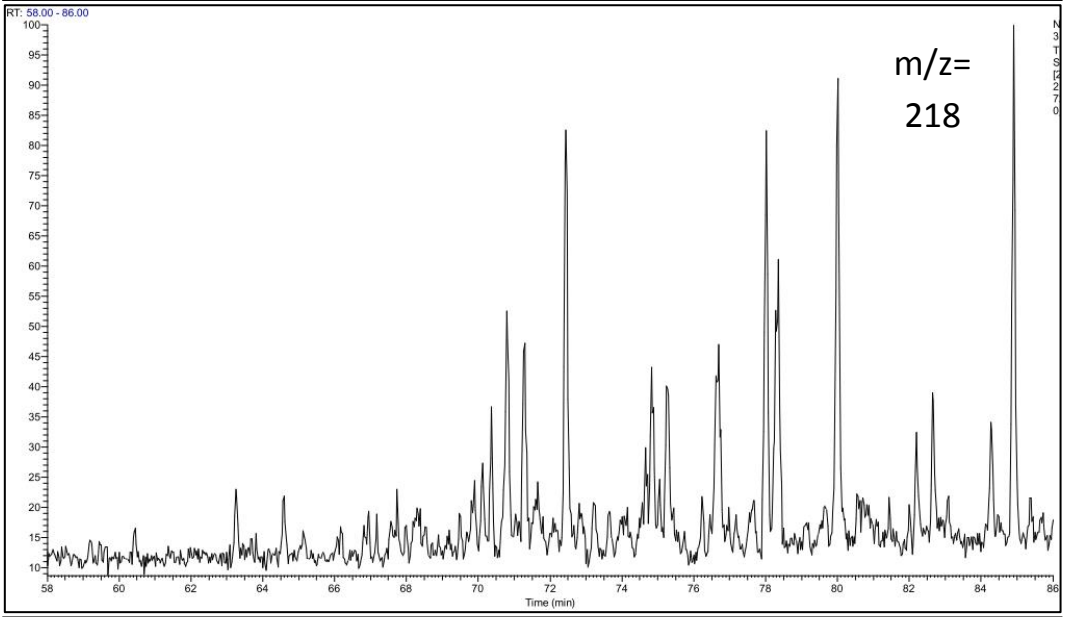
RT: 58.00 - 86.00
m/z=
218
Time (min)

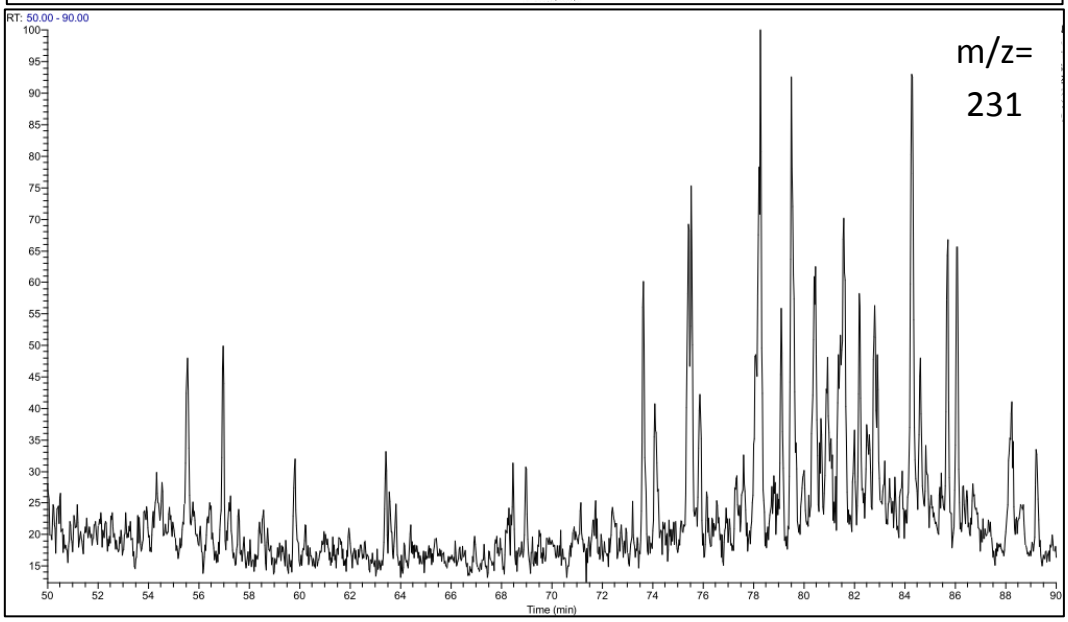
RT: 50.00 - 90.00
m/z=
231
Time (min)

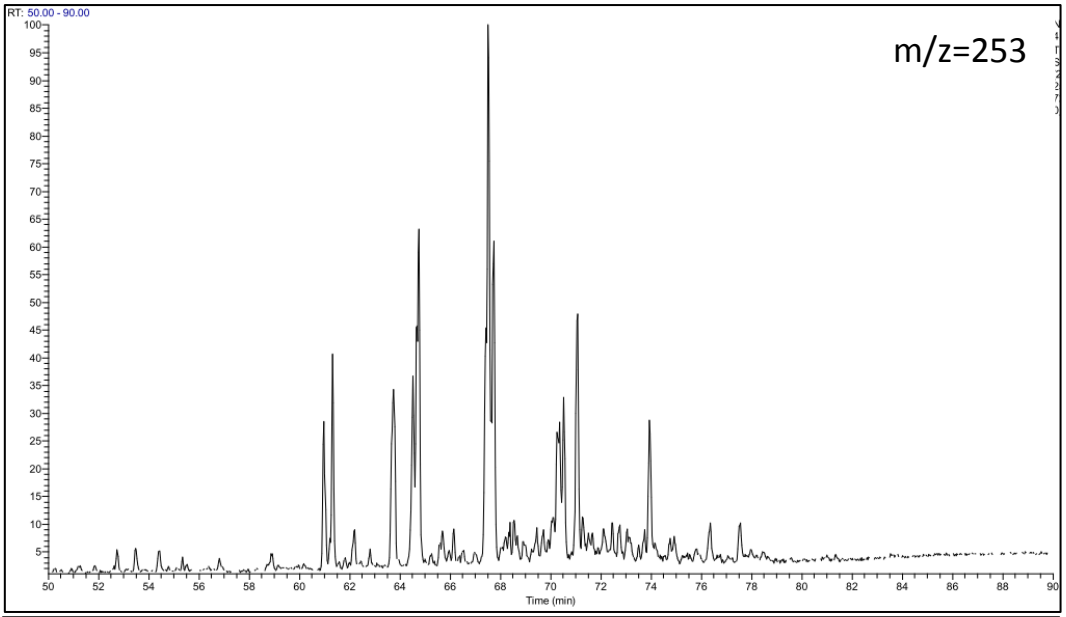
RT: 50.00 - 90.00
m/z=253
Time (min)

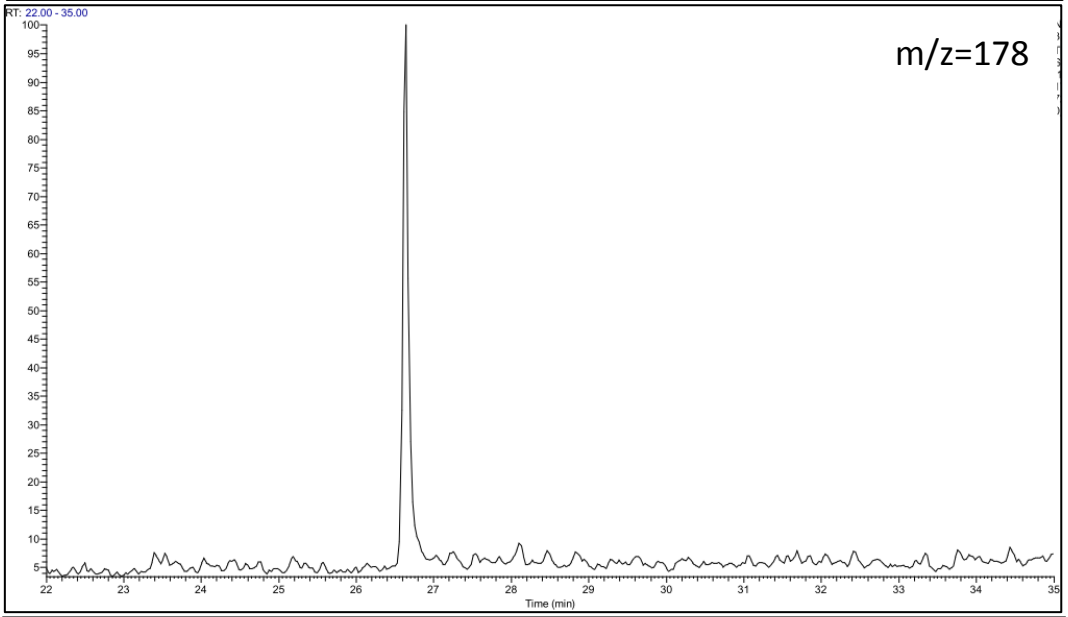
RT: 22.00 - 35.00
m/z=178
Time (min)

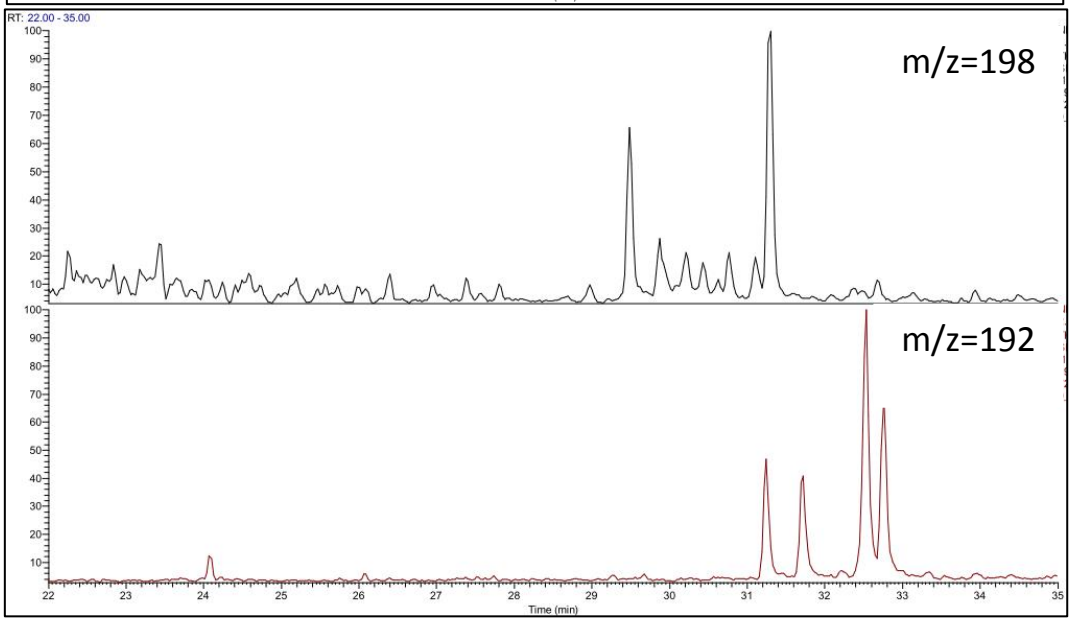
RT: 22.00 - 35.00
m/z=198
m/z=192
Time (min)

GC-FID Chromatogram for S.R sample "S7" from well 7231/1-U-1

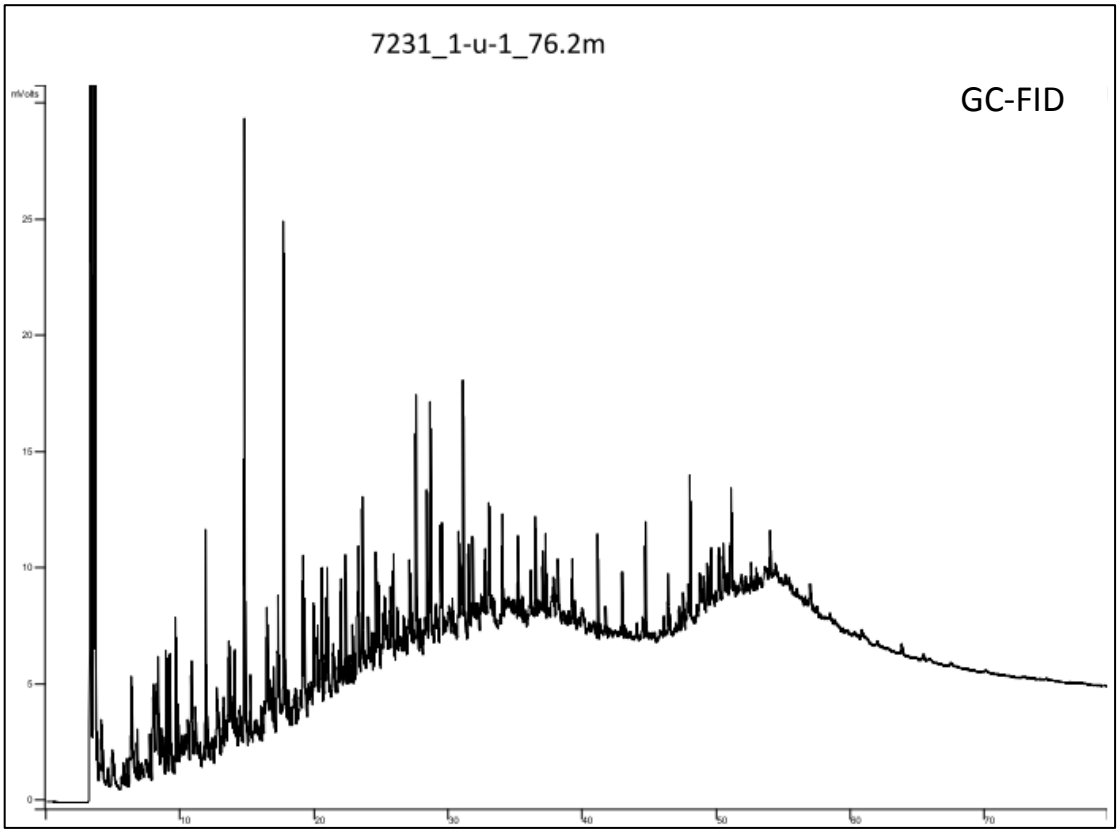

GC-MS Chromatograms for S.R sample "S7" from well 7231/1-U-1

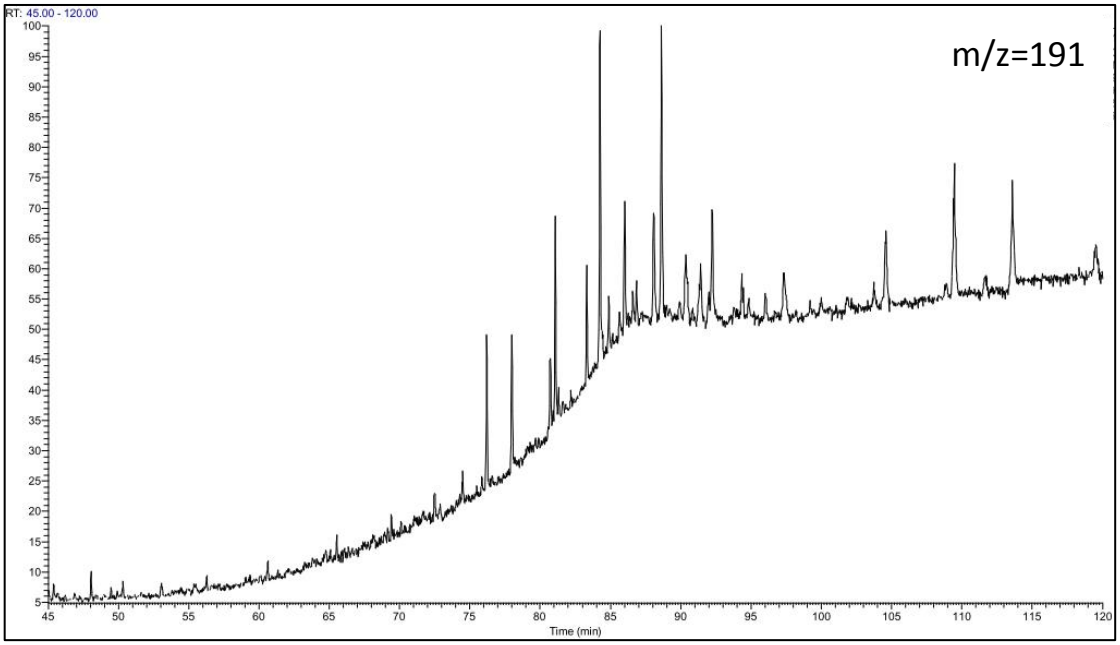

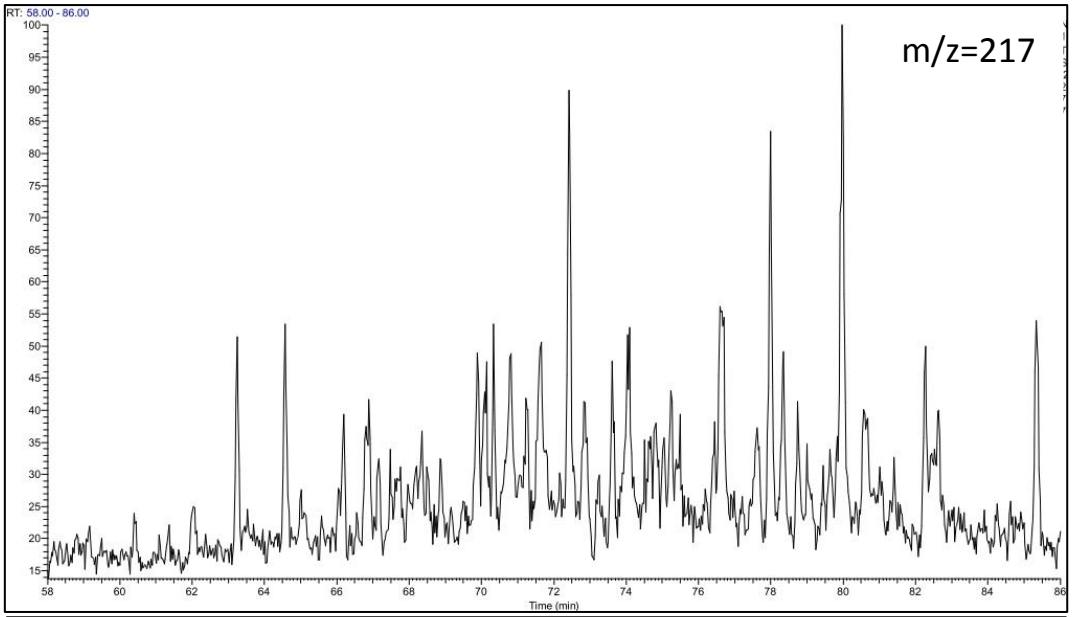
RT: 58.00 - 86.00
m/z=217
Time (min)

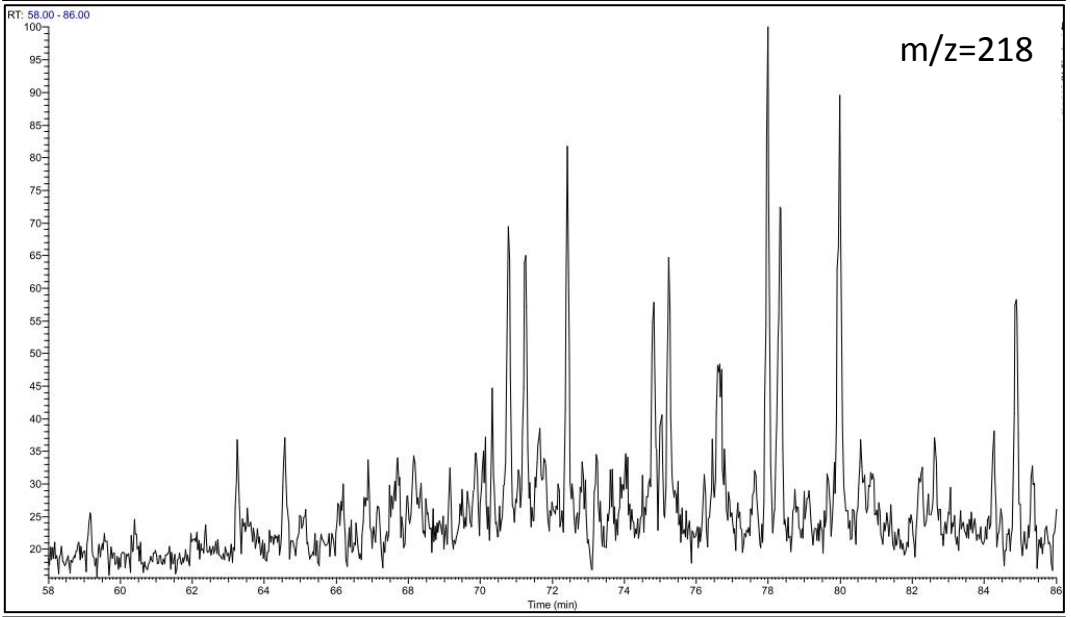
RT: 58.00 - 86.00
m/z=218
Time (min)

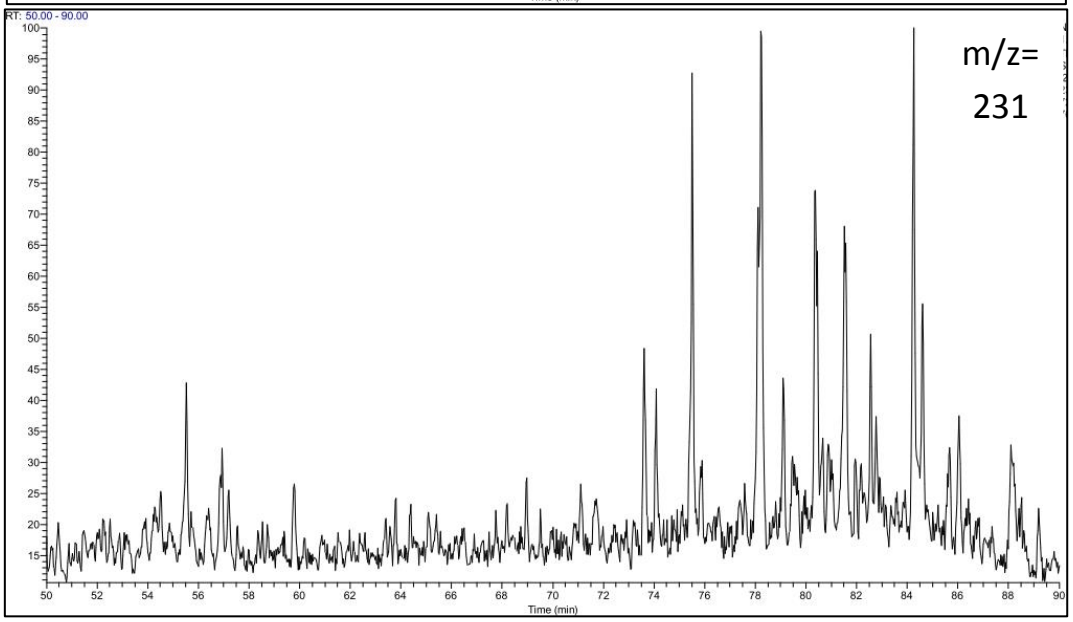
RT: 50.00 - 90.00
m/z=
231
Time (min)

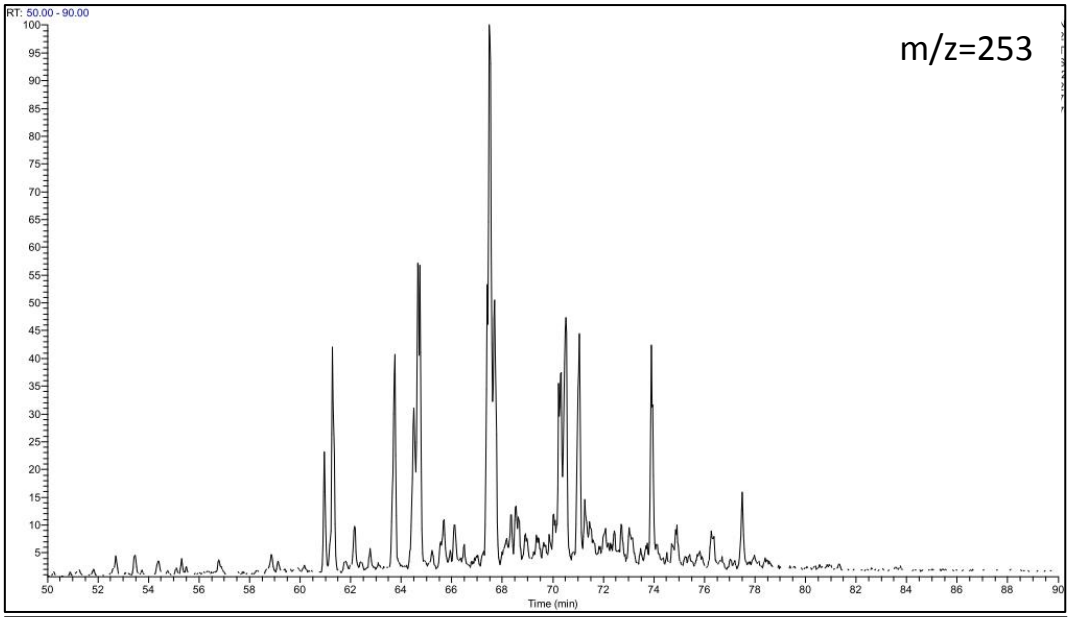
RT: 50.00 - 90.00
m/z=253
Time (min)

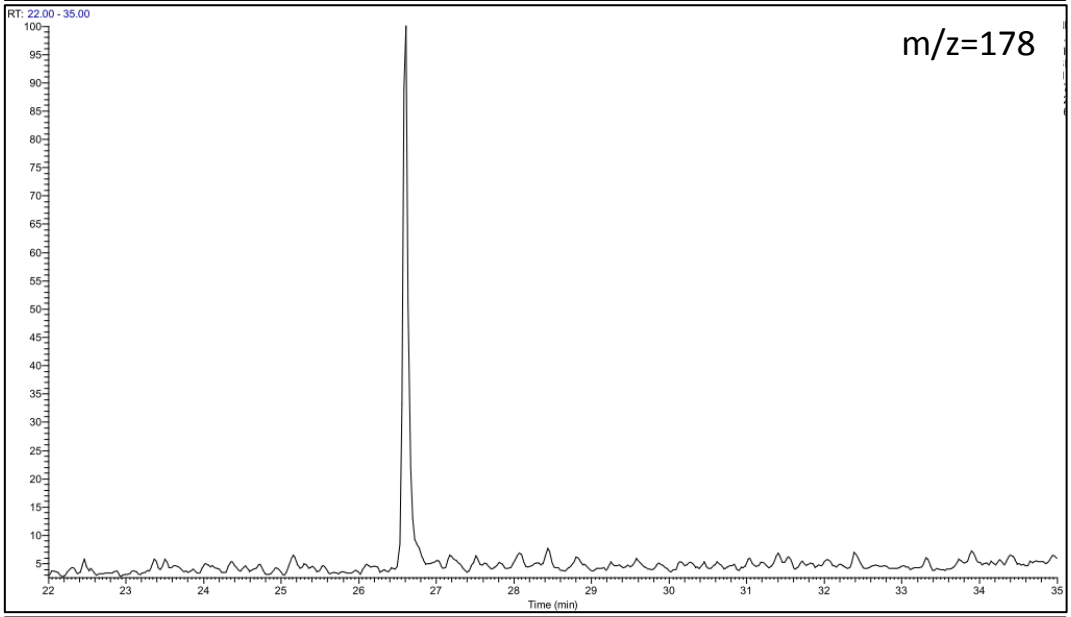
RT: 22.00 - 35.00
m/z=178
Time (min)

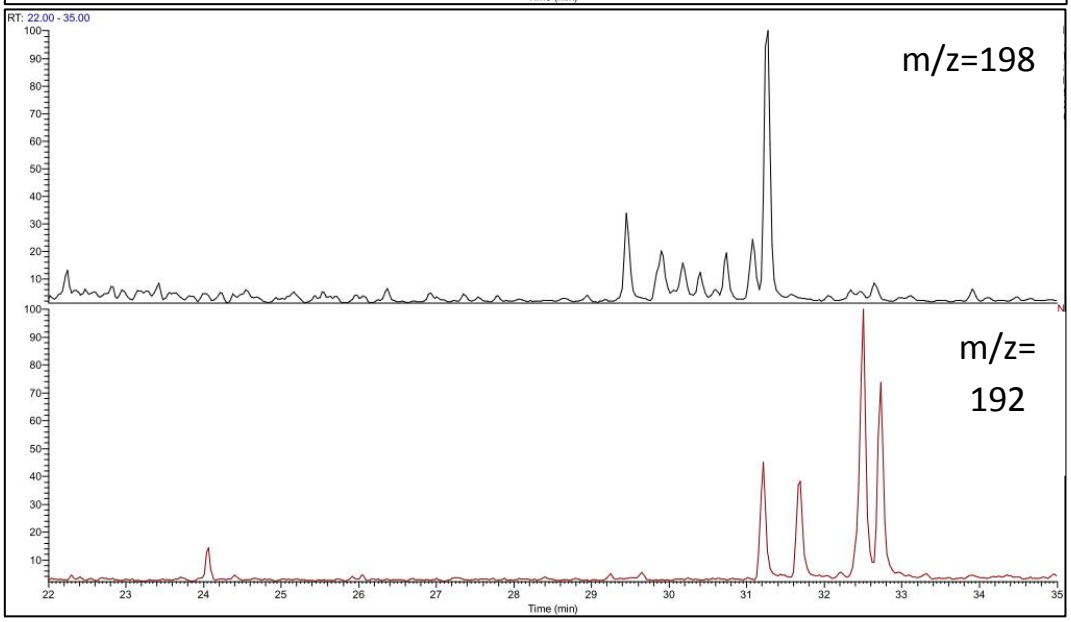
RT: 22.00 - 35.00
m/z=198
m/z=
192
Time (min)

GC-FID Chromatogram for S.R sample "S8" from well 7231/4-U-1

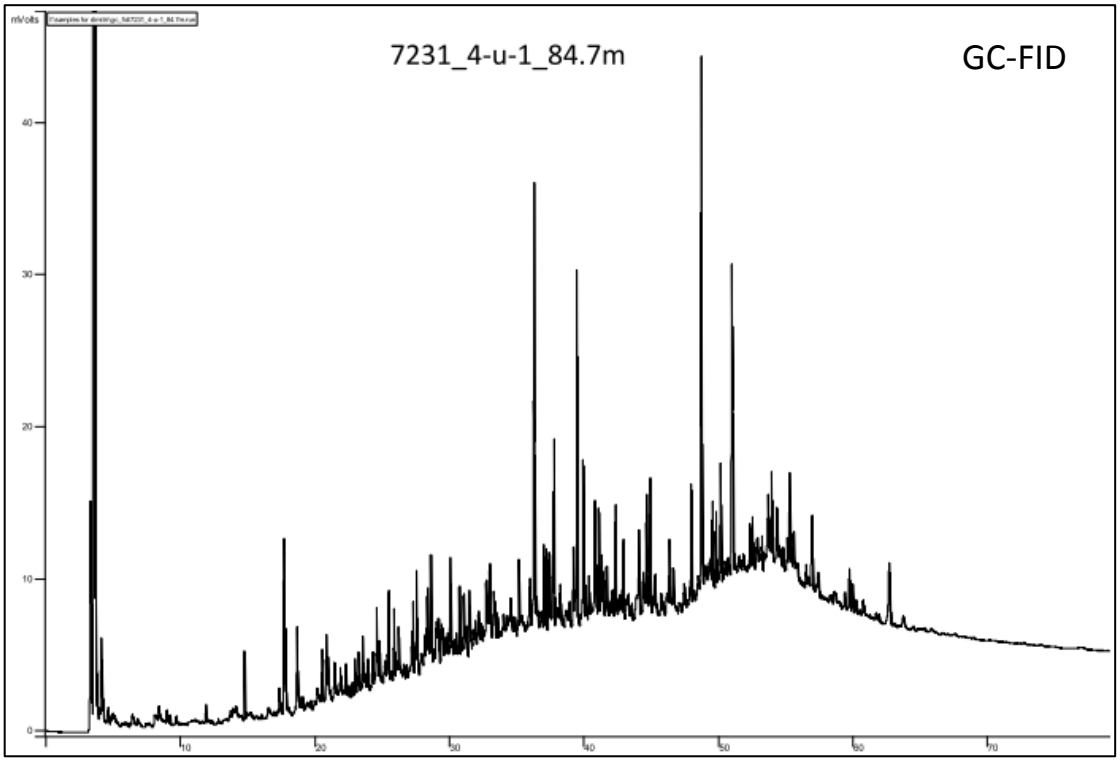

GC-MS Chromatogram for S.R sample "S8" from well 7231/4-U-1

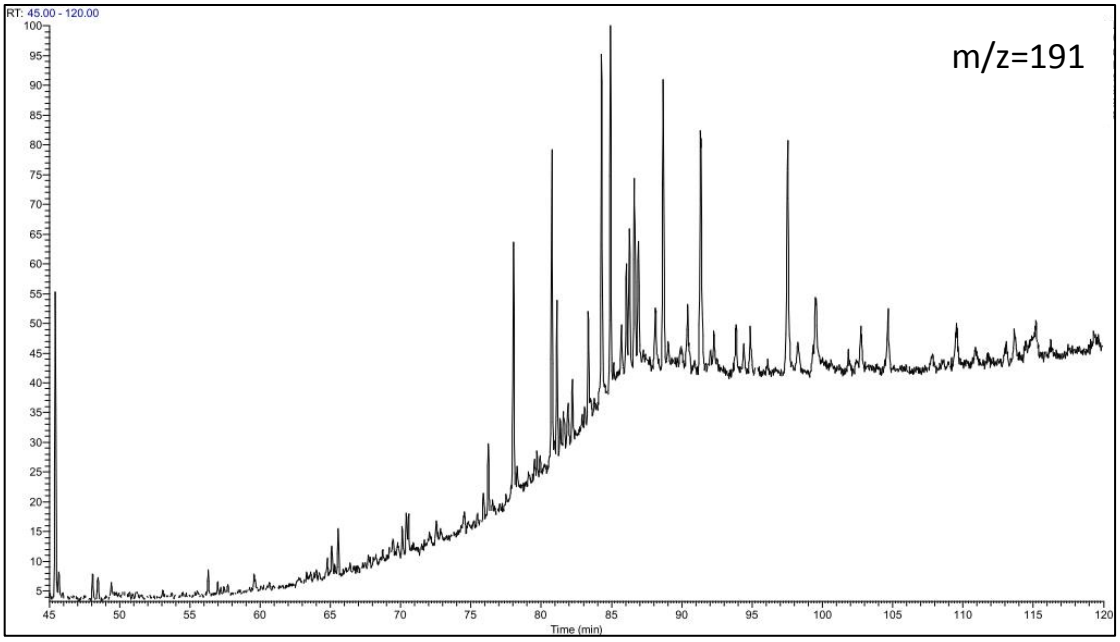

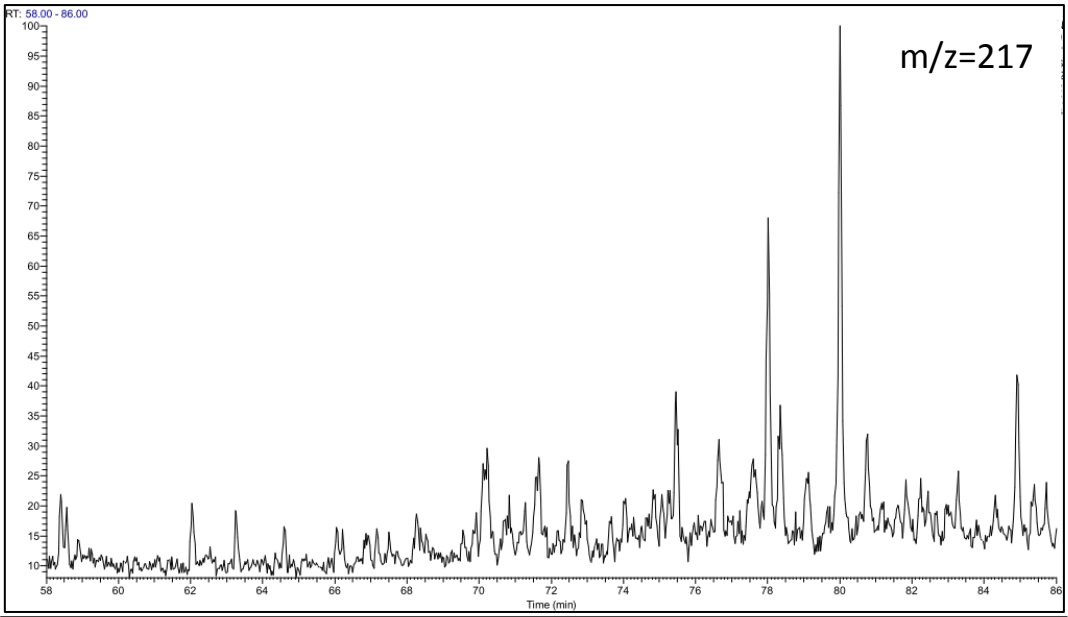
RT: 58.00 - 86.00
m/z=217
Time (min)

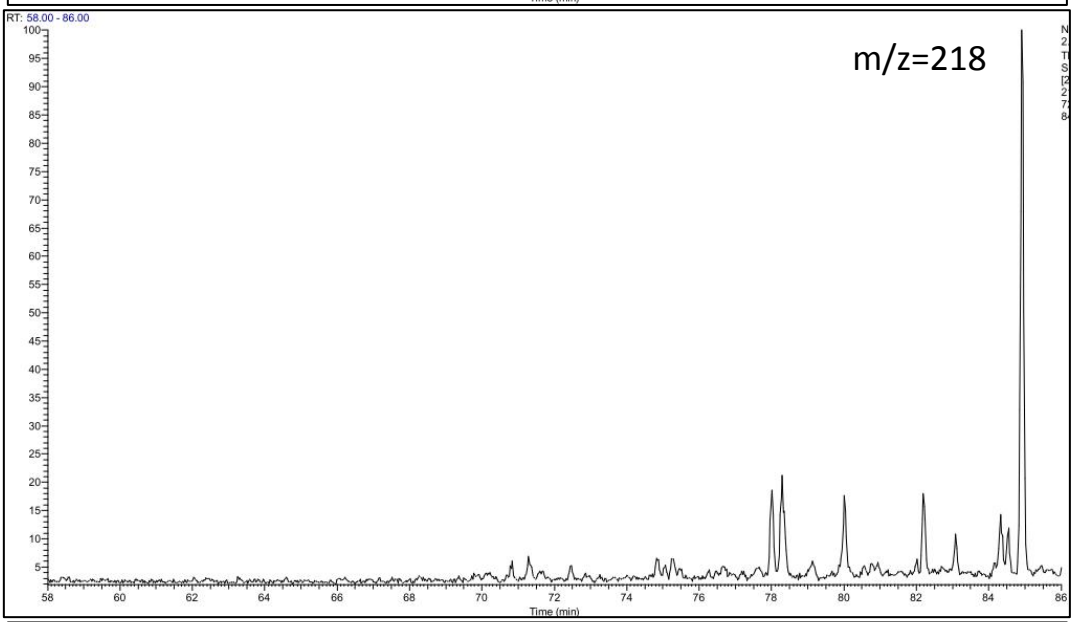
RT: 58.00 - 86.00
m/z=218
Time (min)

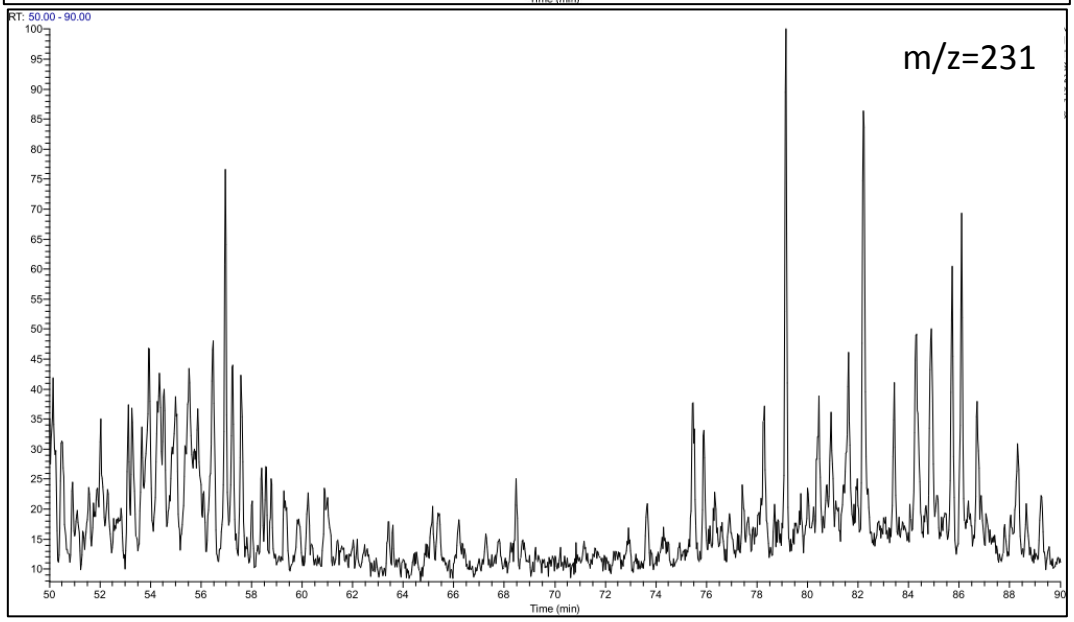
RT: 50.00 - 90.00
m/z=231
Time (min)

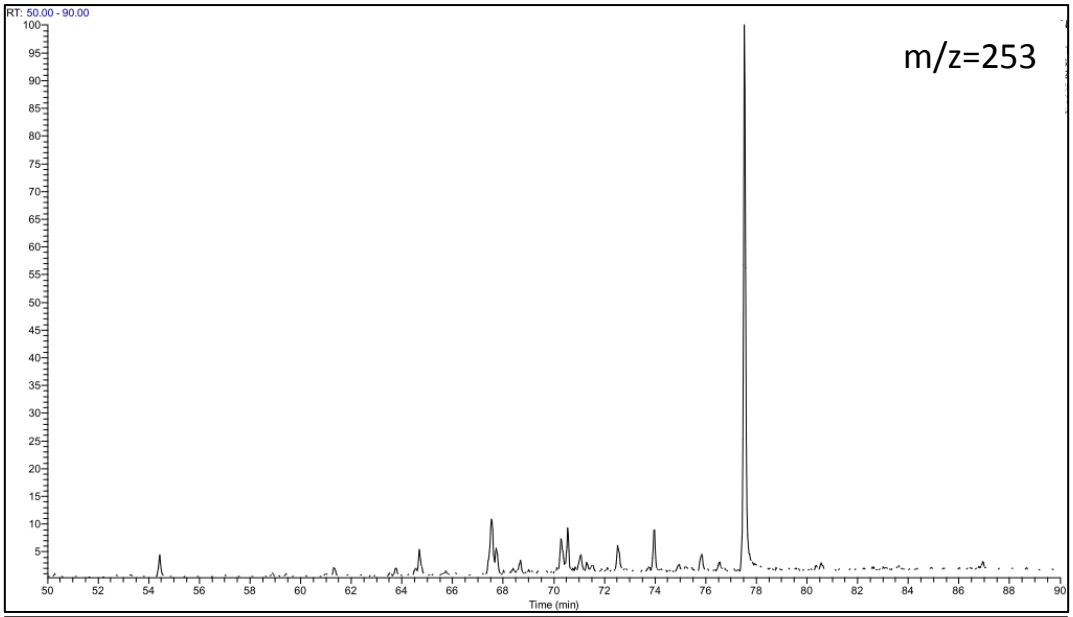
RT: 50.00 - 90.00
m/z=253
Time (min)

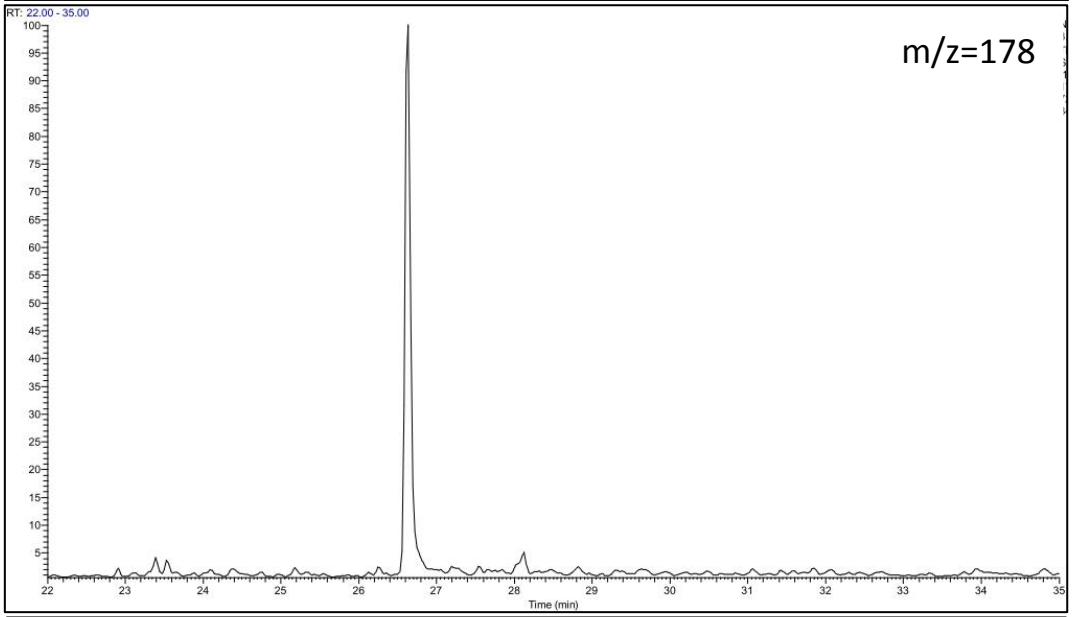
RT: 22.00 - 35.00
m/z=178
Time (min)

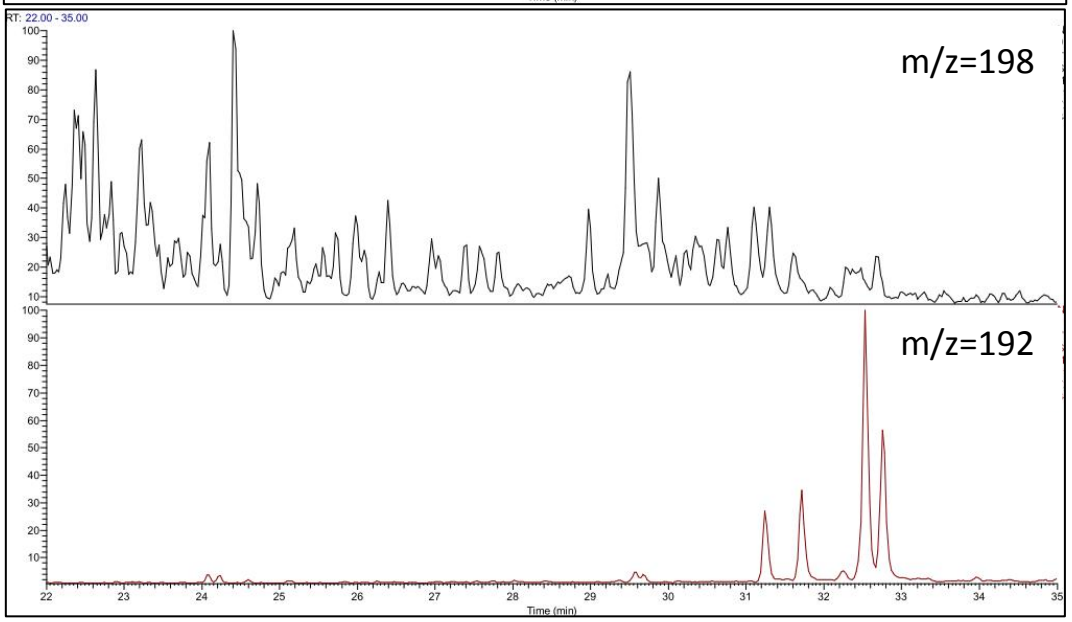
RT: 22.00 - 35.00
m/z=198
m/z=192
Time (min)

GC-FID Chromatogram for S.R sample "S9" from well 7323/7-U-3

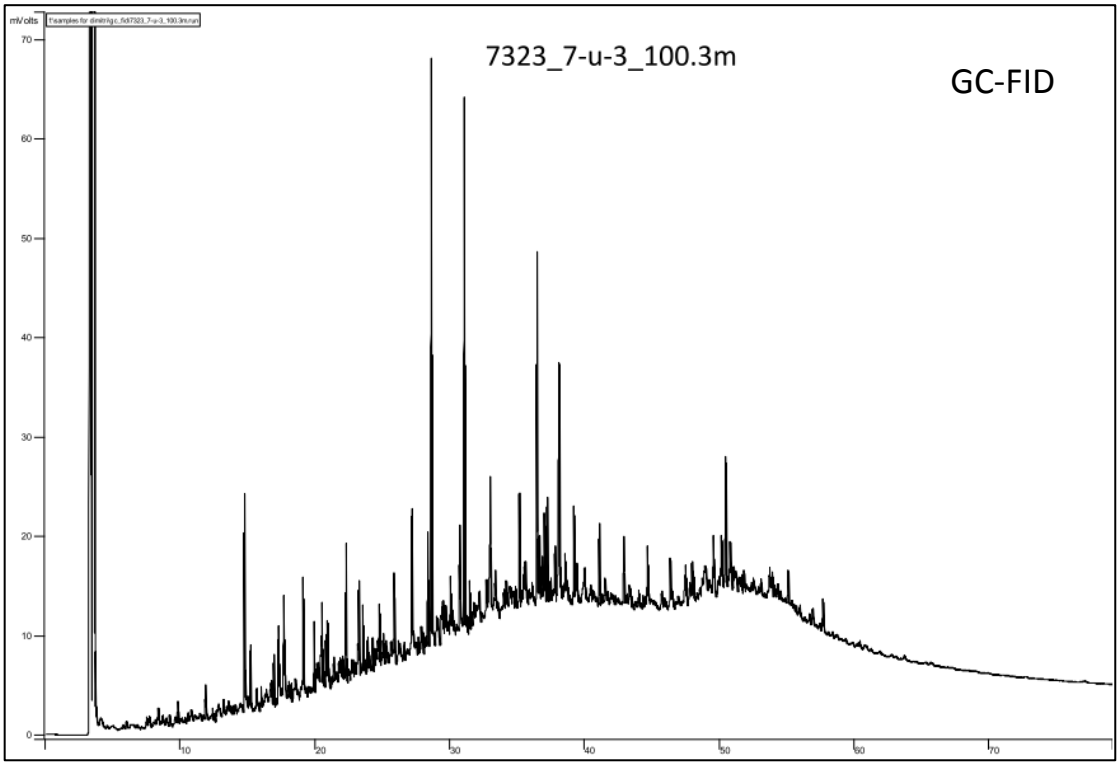

GC-MS Chromatograms for S.R sample "S9" from well 7323/7-U-3

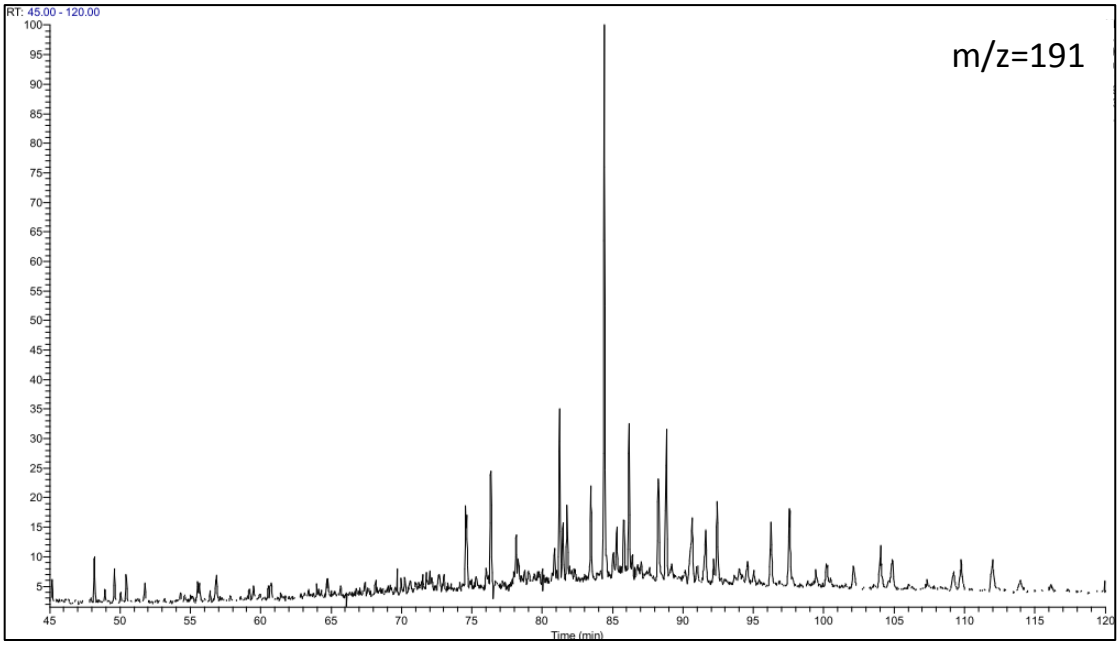

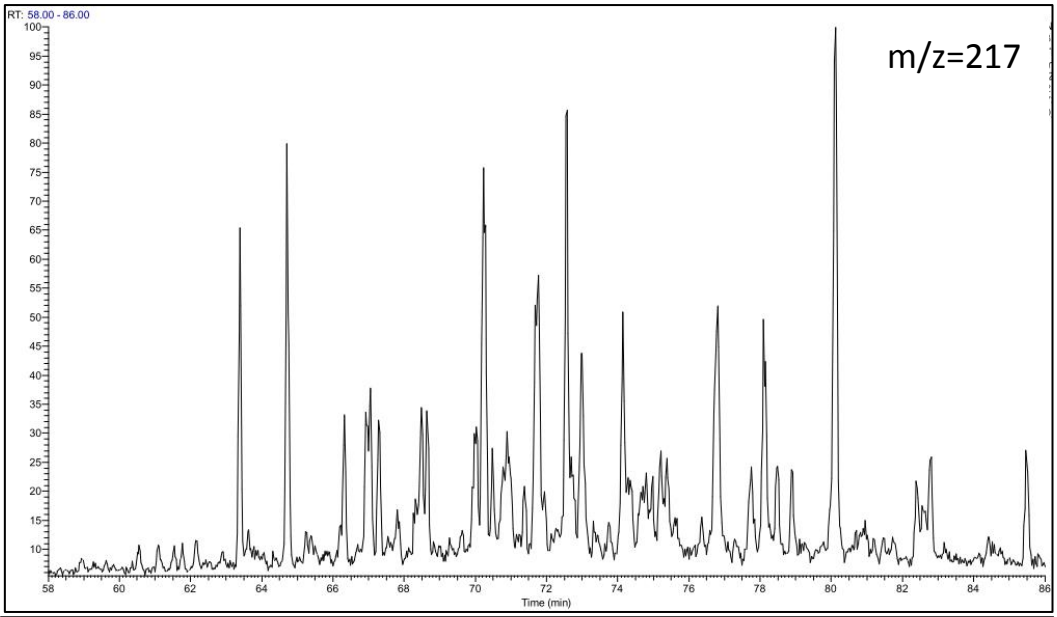
RT: 58.00 - 86.00
m/z=217
Time (min)

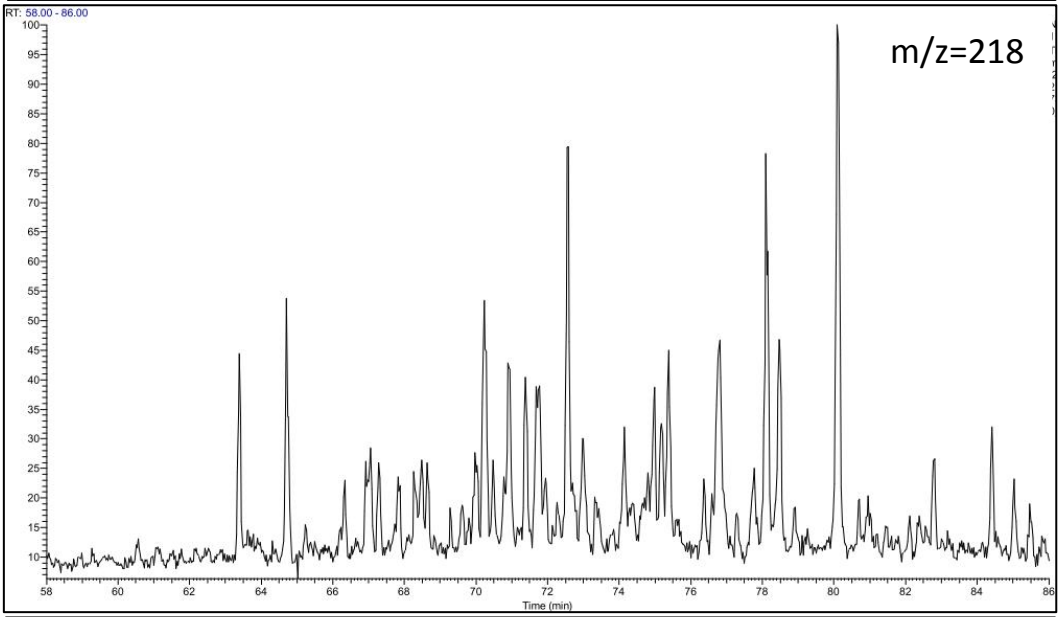
RT: 58.00 - 86.00
m/z=218
Time (min)

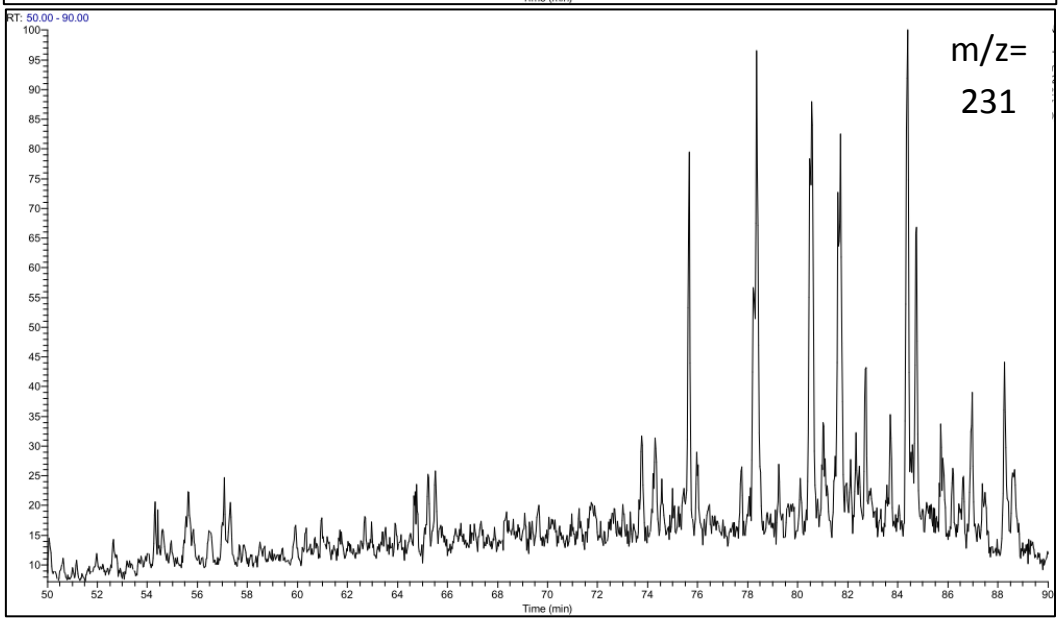
RT: 50.00 - 90.00
m/z=
231
Time (min)

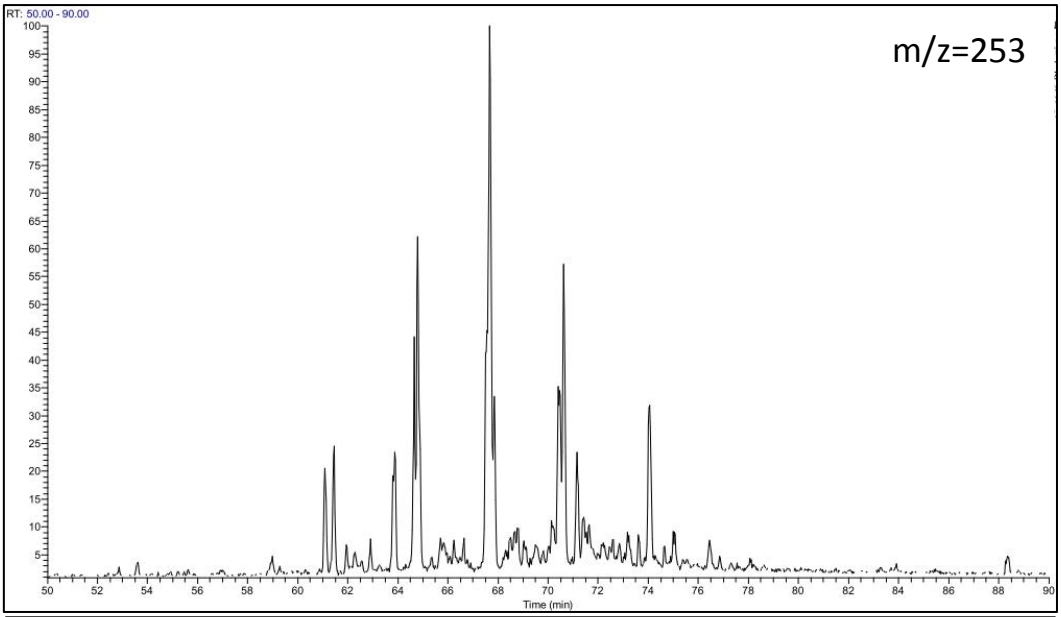
RT: 50.00 - 90.00
m/z=253
Time (min)

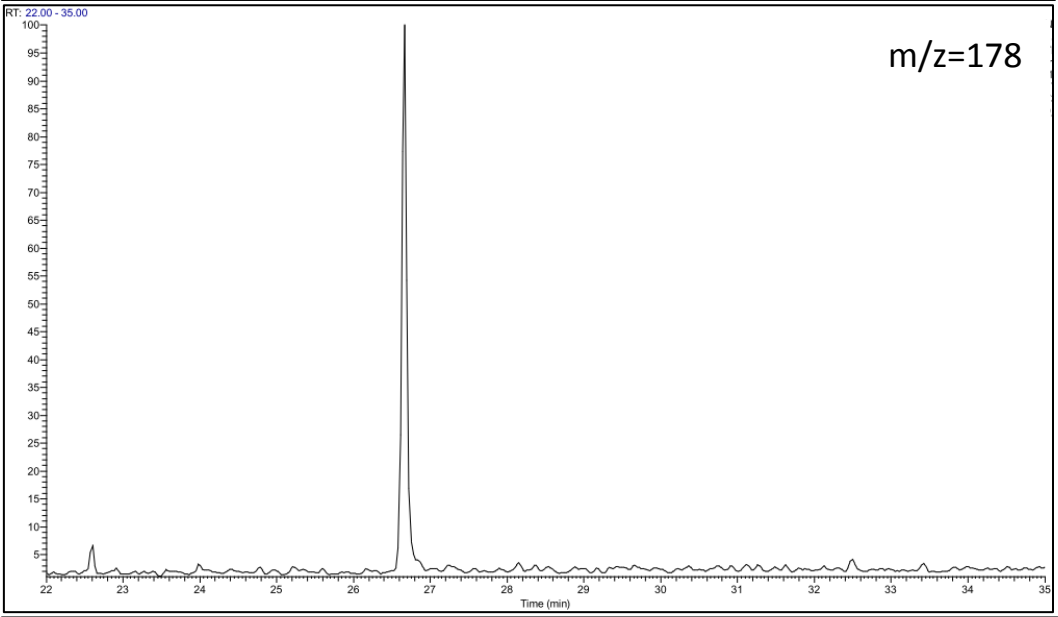
RT: 22.00 - 35.00
m/z=178
Time (min)

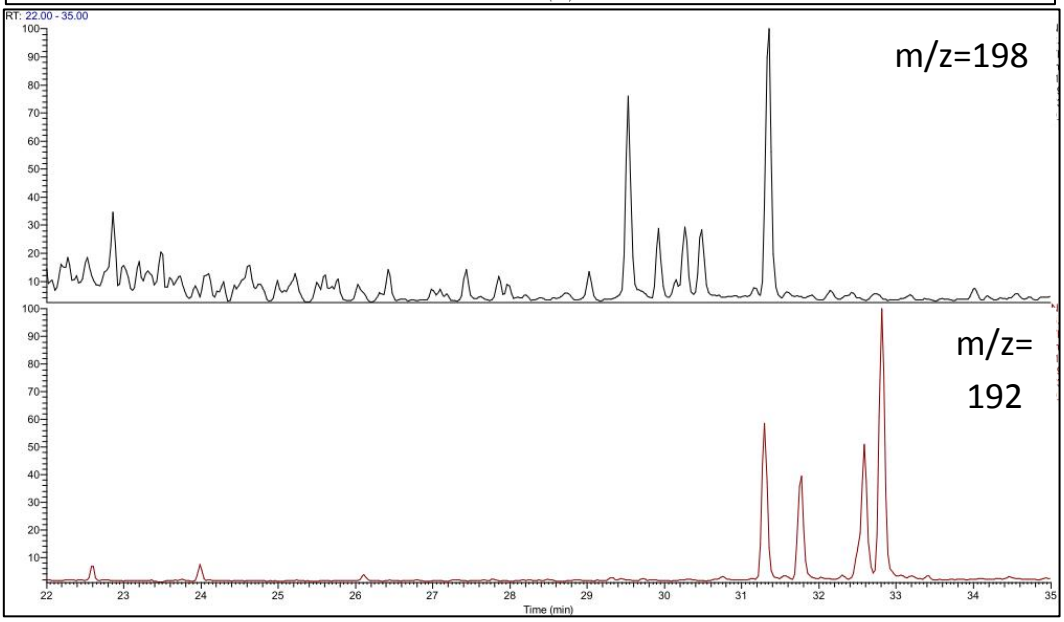
RT: 22.00 - 35.00
m/z=198
m/z=
192
Time (min)

GC-FID Chromatogram for S.R sample "S10" from well 7323/7-U-9

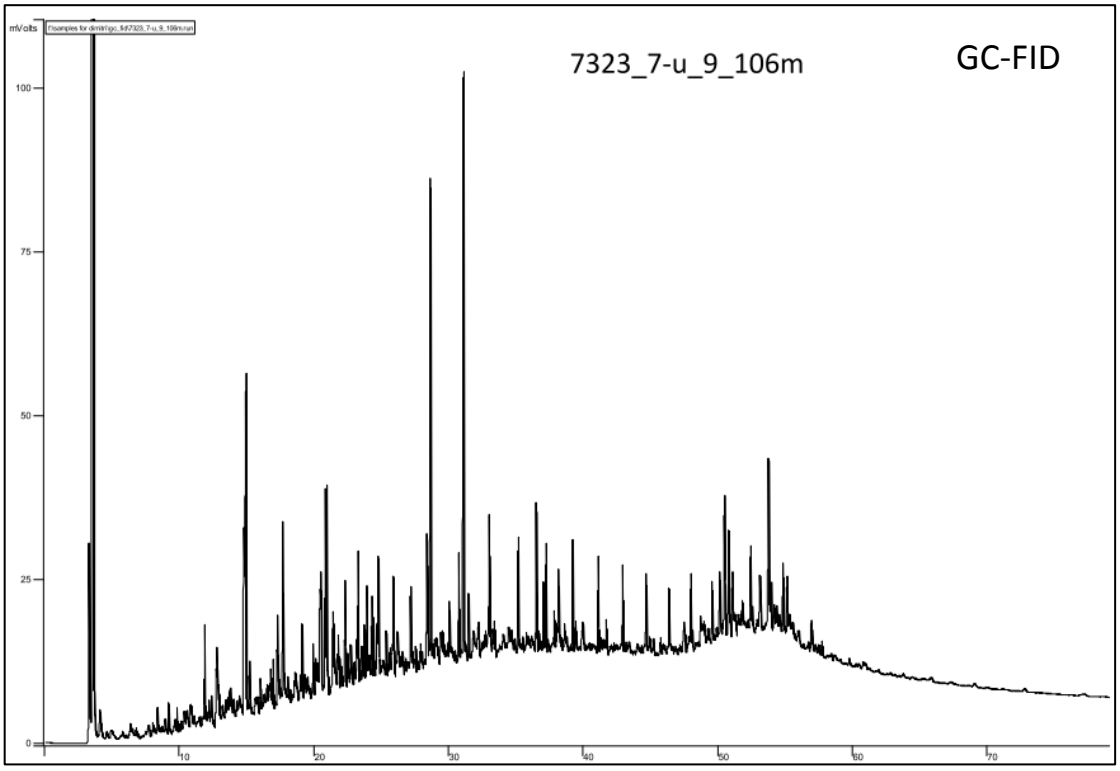

GC-MS Chromatograms for S.R sample "S10" from well 7323/7-U-9

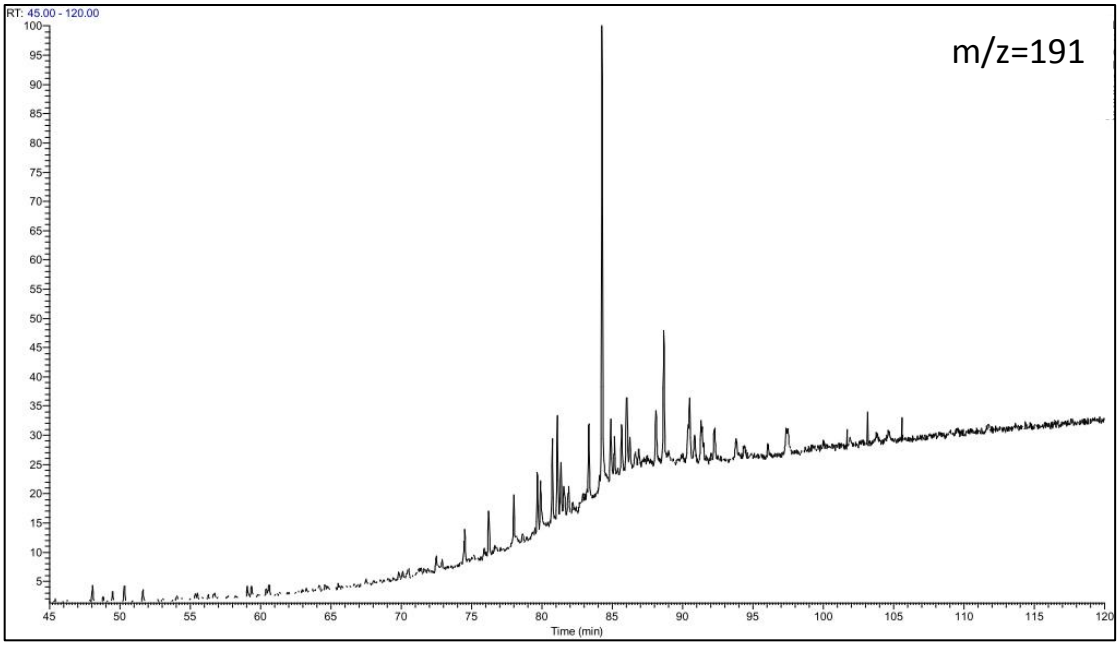

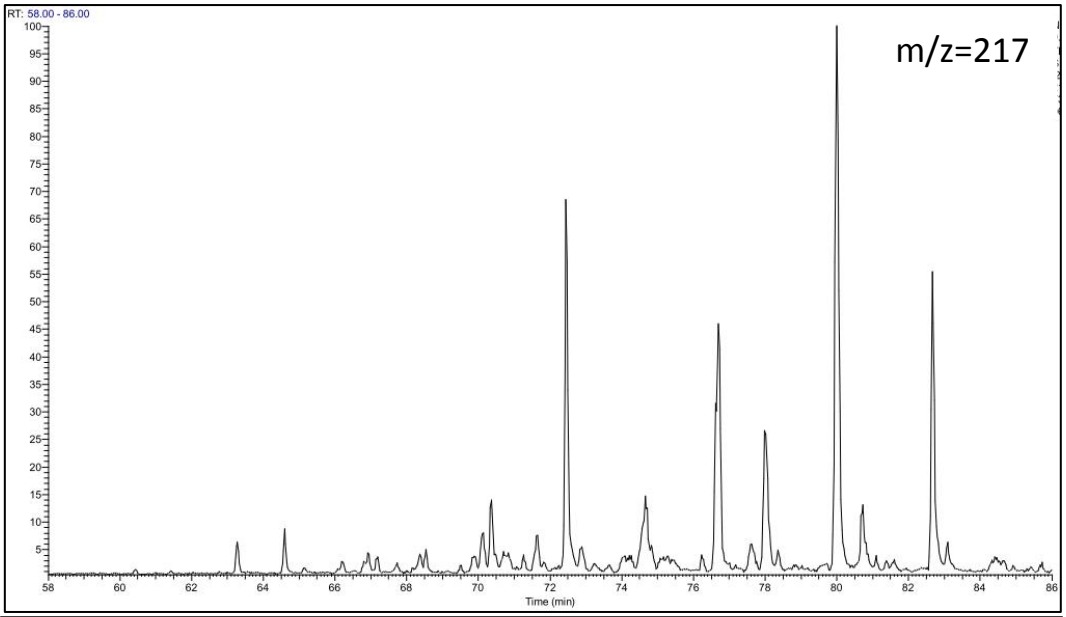
RT: 58.00 - 86.00
m/z=217
Time (min)

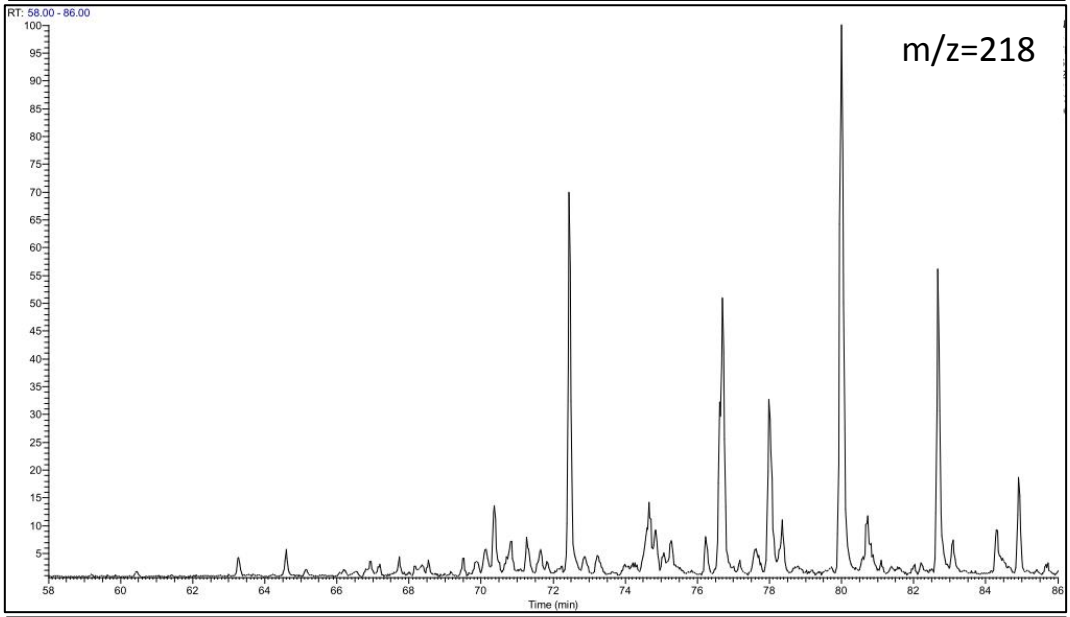
RT: 58.00 - 86.00
m/z=218
Time (min)

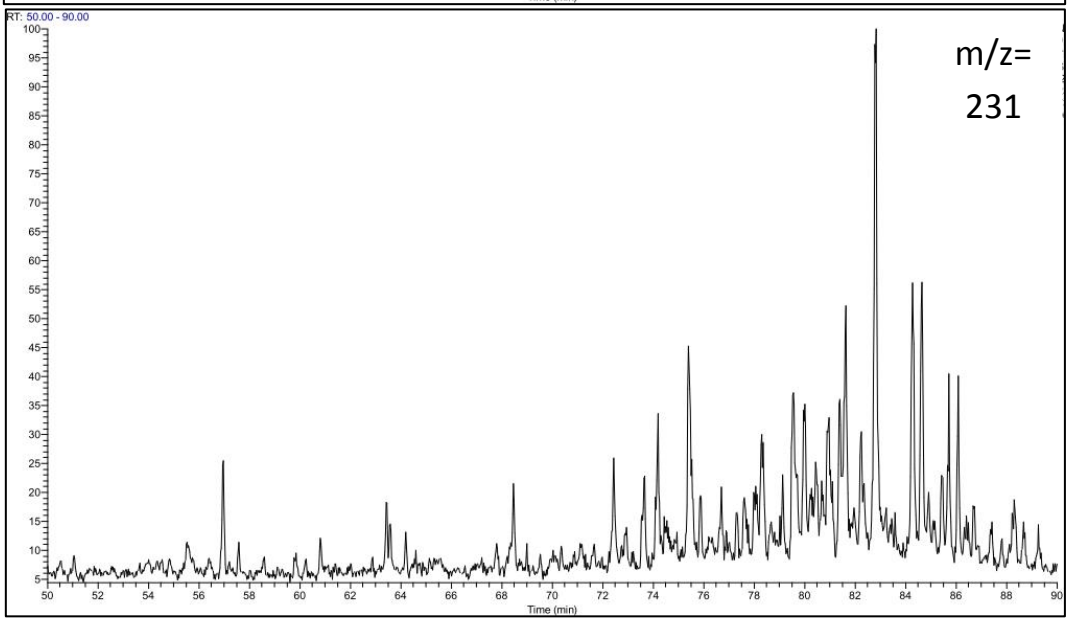
RT: 50.00 - 90.00
m/z=
231
Time (min)

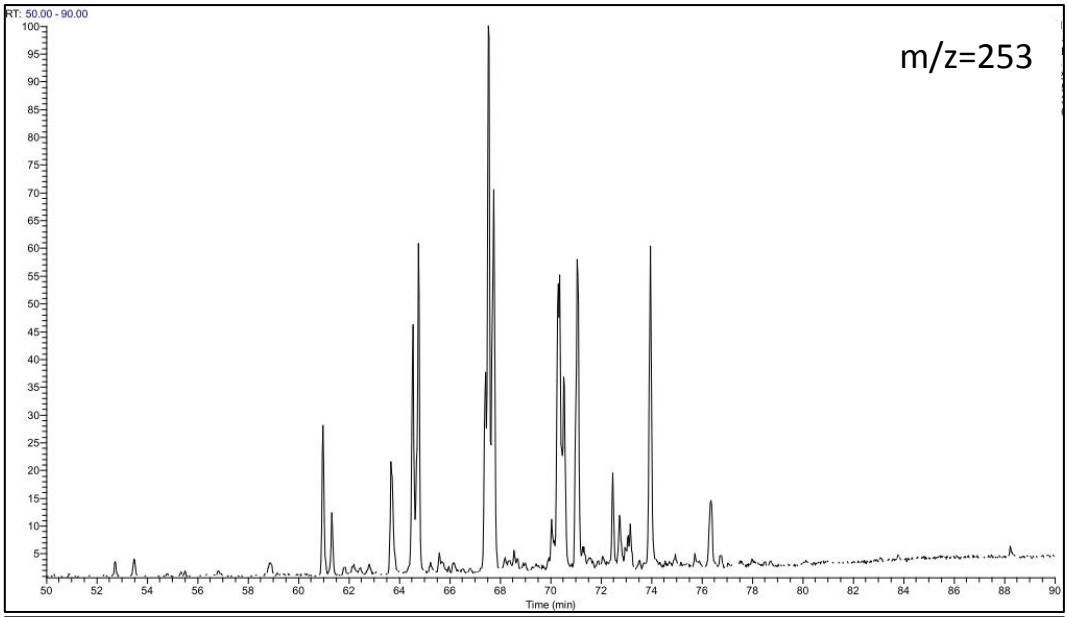
RT: 50.00 - 90.00
m/z=253
Time (min)

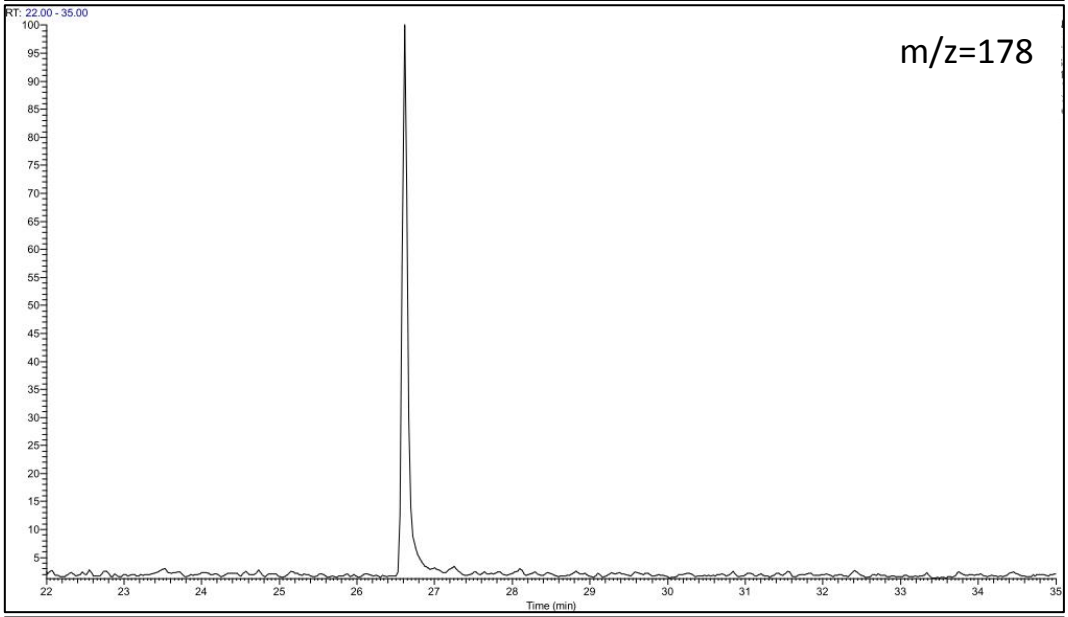
RT: 22.00 - 35.00
m/z=178
Time (min)

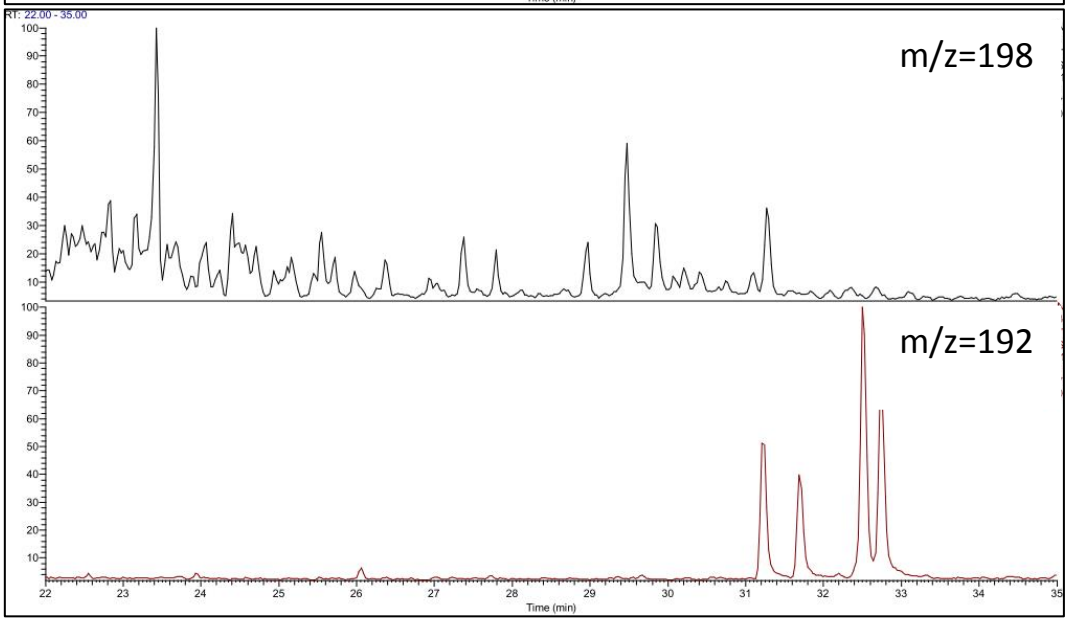
RT: 22.00 - 35.00
m/z=198
m/z=192
Time (min)

GC-FID Chromatogram for S.R sample "S11" from well 7430/7-U-1

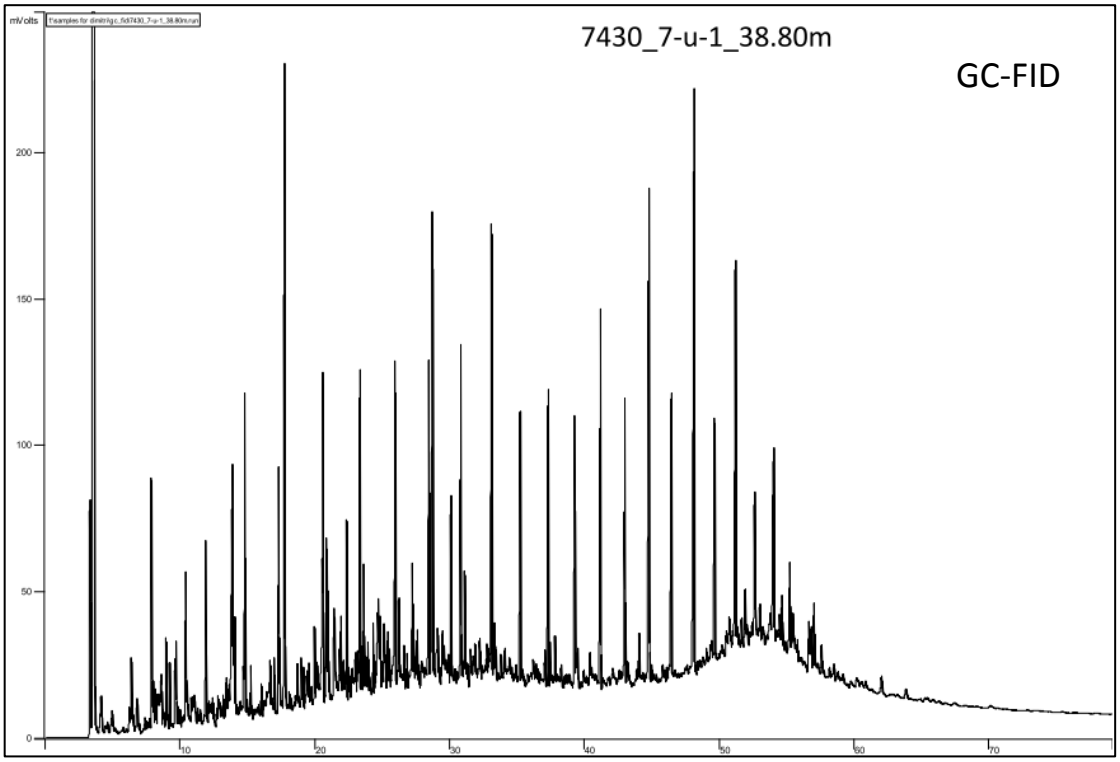

GC-MS Chromatogram for S.R sample "S11" from well 7430/7-U-1

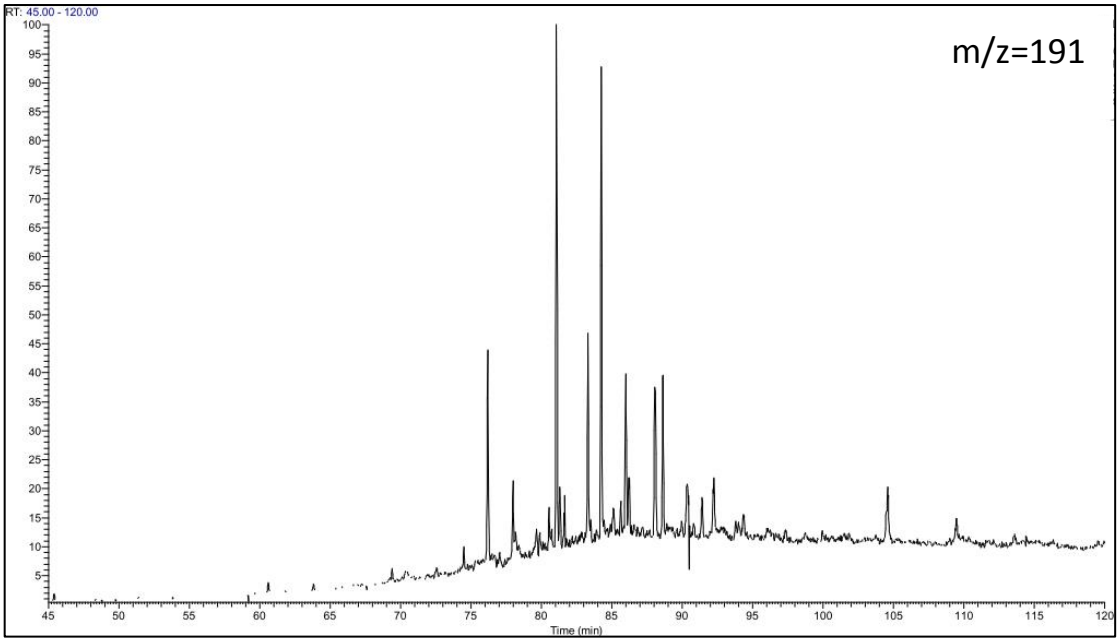

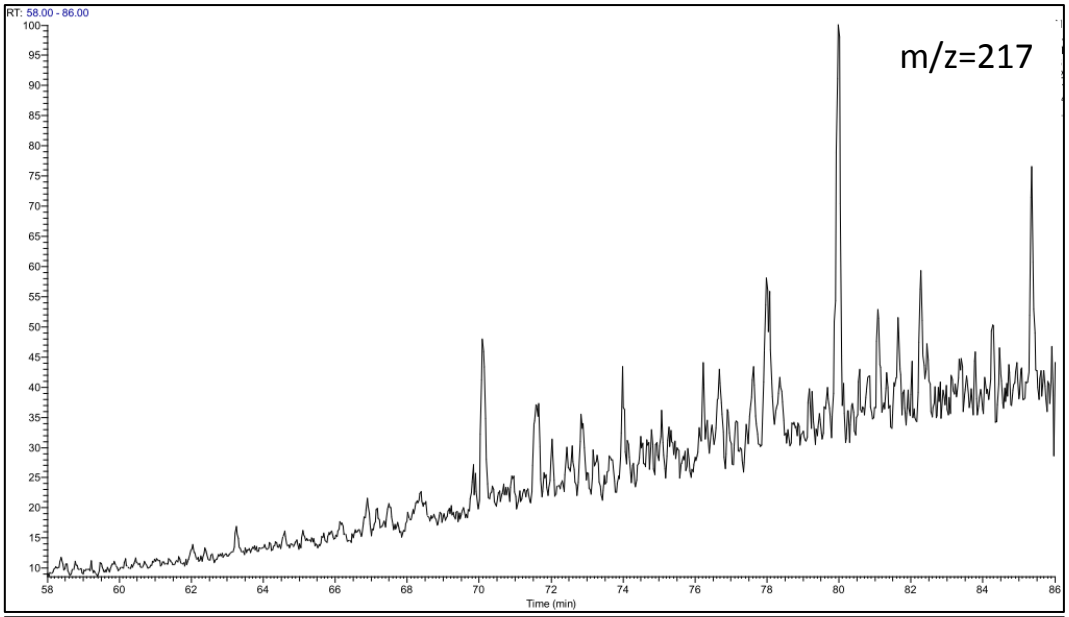
RT: 58.00 - 86.00
m/z=217
Time (min)

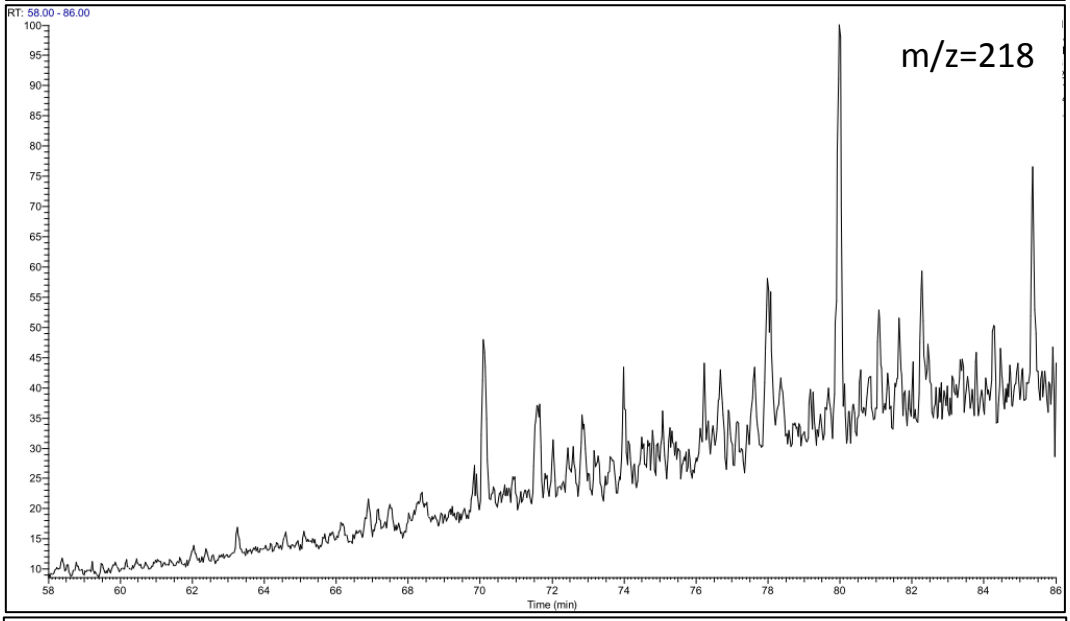
RT: 58.00 - 86.00
m/z=218
Time (min)

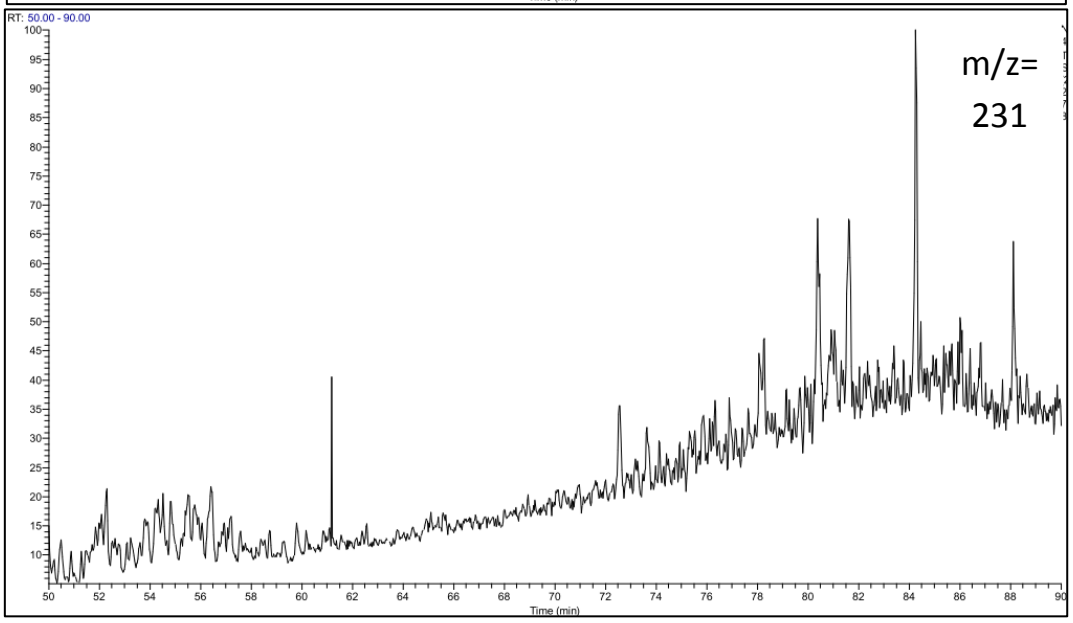
RT: 50.00 - 90.00
m/z=
231
Time (min)

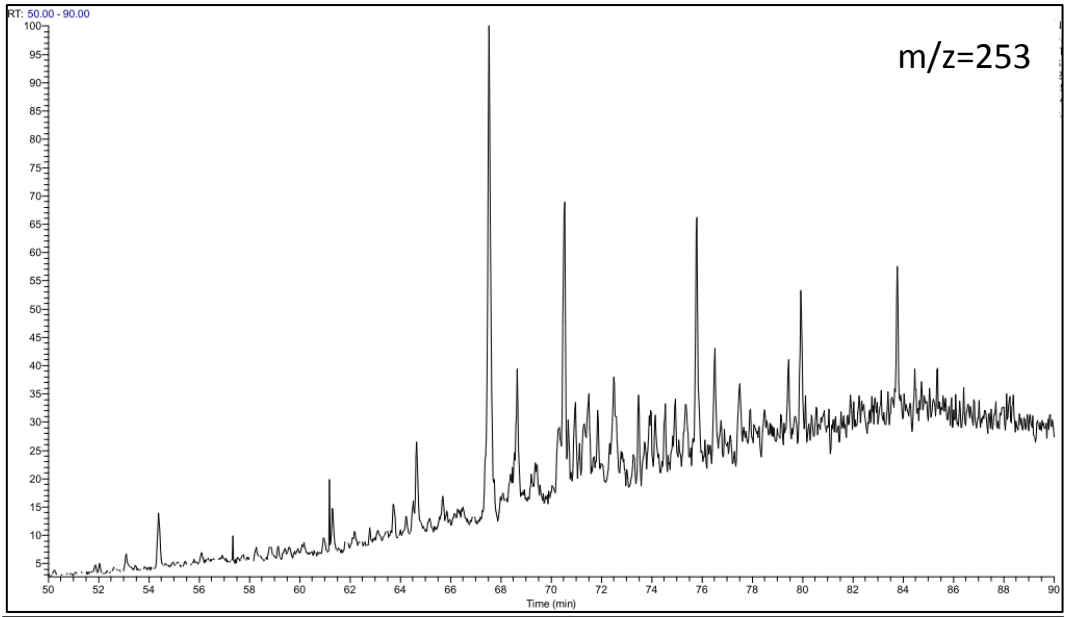
RT: 50.00 - 90.00
m/z=253
Time (min)

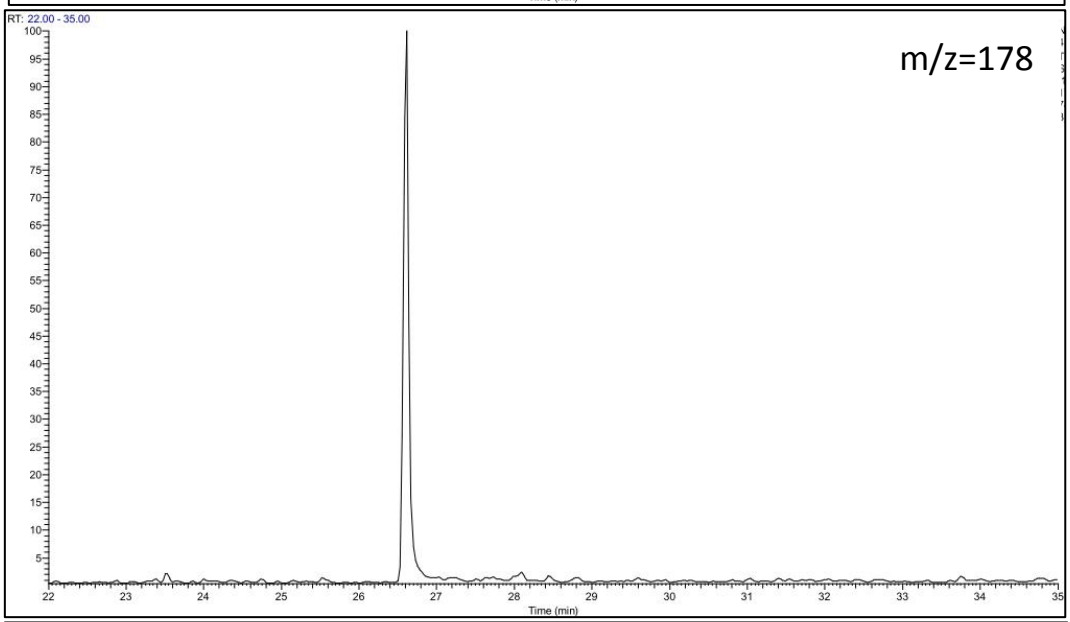
RT: 22.00 - 35.00
m/z=178
Time (min)

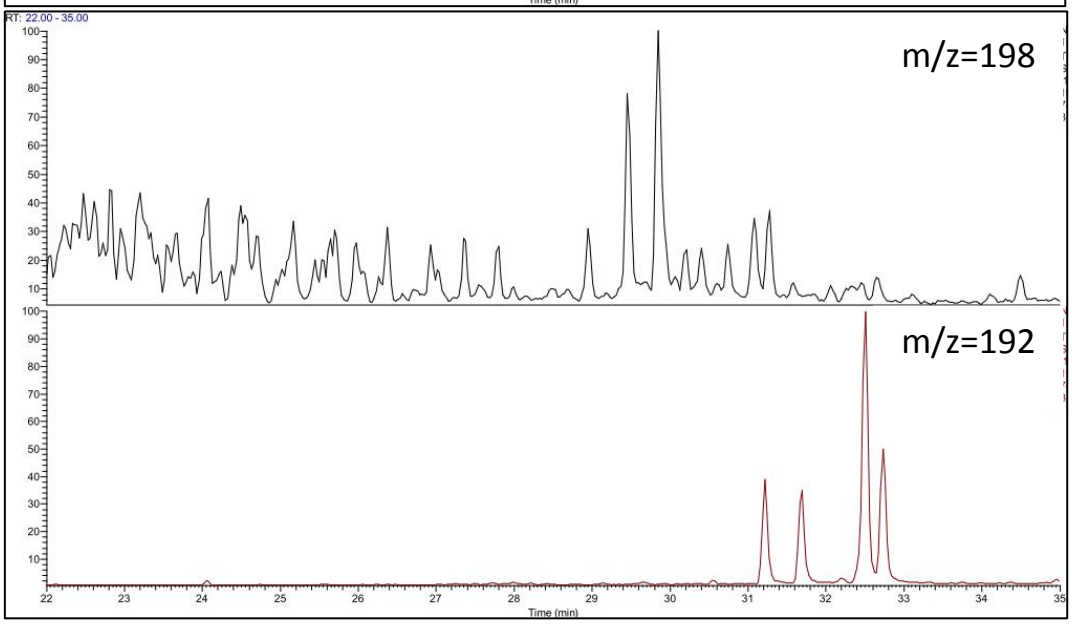
RT: 22.00 - 35.00
m/z=198
m/z=192
Time (min)

GC-FID Chromatogram for S.R sample "S12" from well 7430/7-U-1

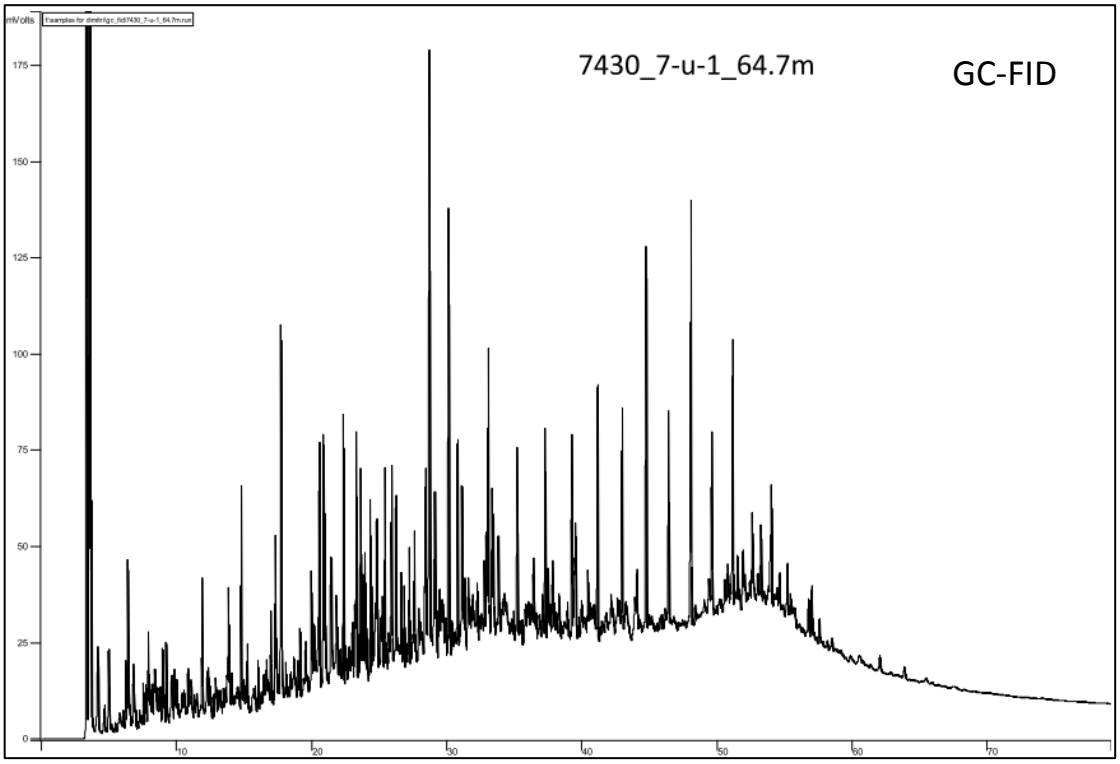

GC-MS Chromatograms for S.R sample "S12" from well 7430/7-U-1

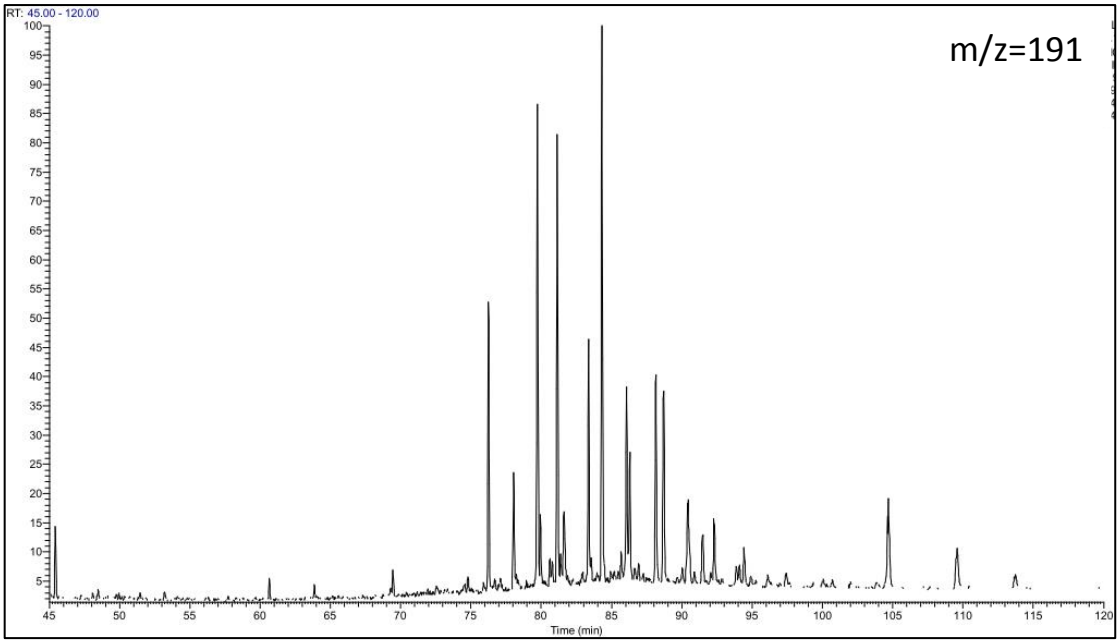

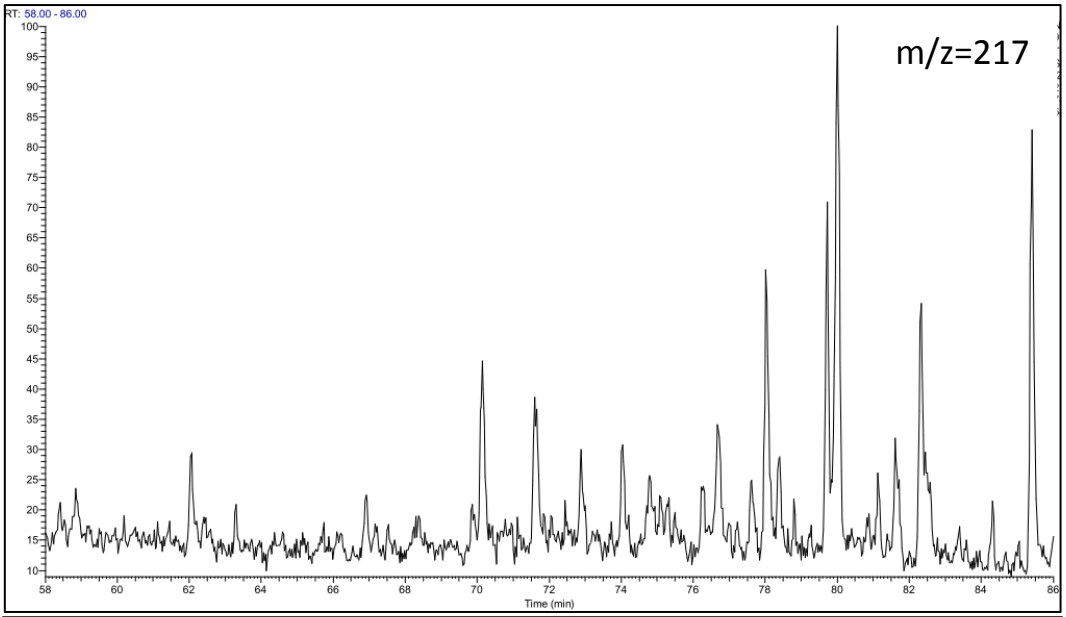
RT: 58.00 - 86.00
m/z=217
Time (min)

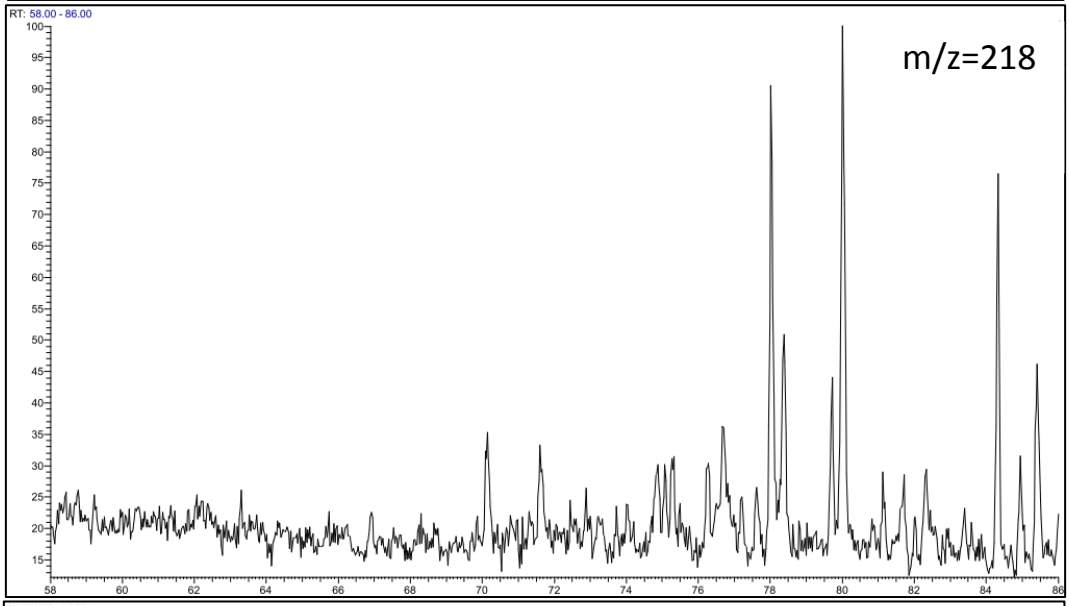
RT: 58.00 - 86.00
m/z=218

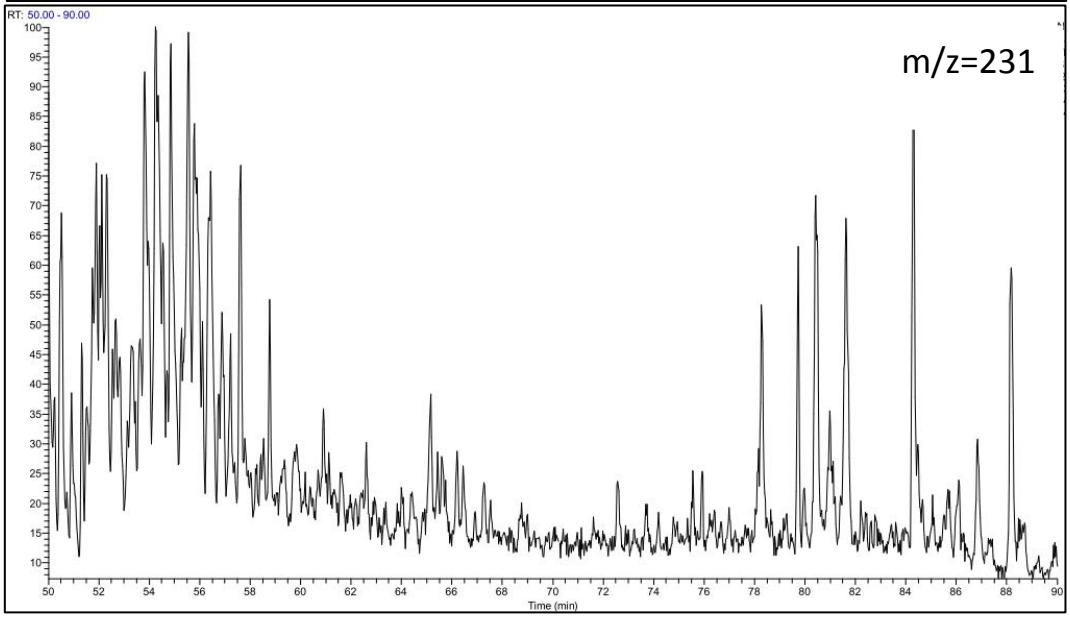
RT: 50.00 - 90.00
m/z=231
Time (min)

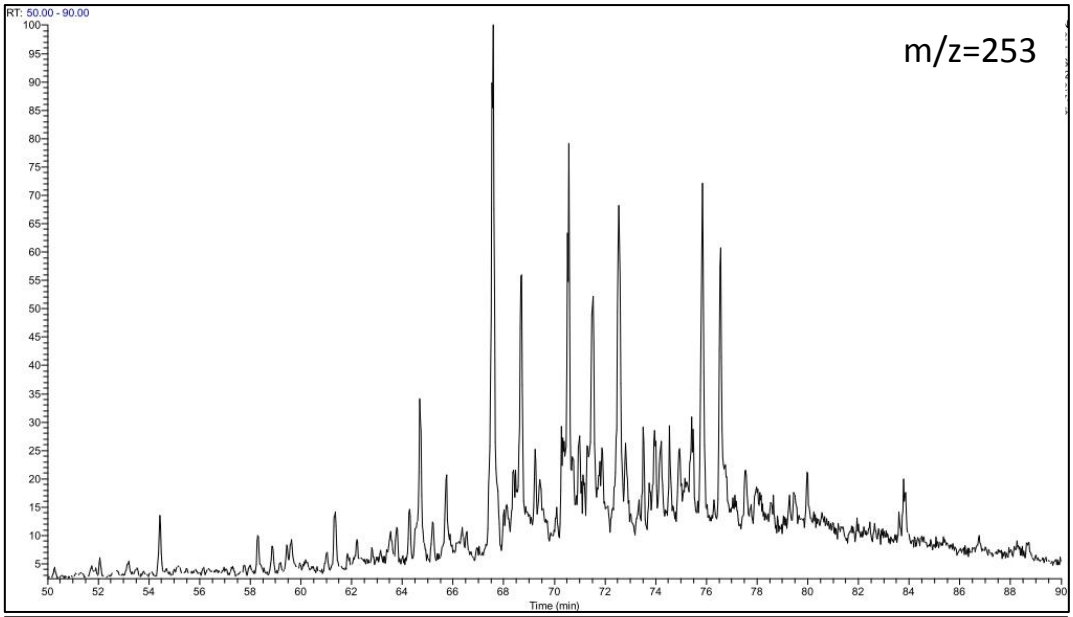
RT: 50.00 - 90.00
m/z=253
Time (min)

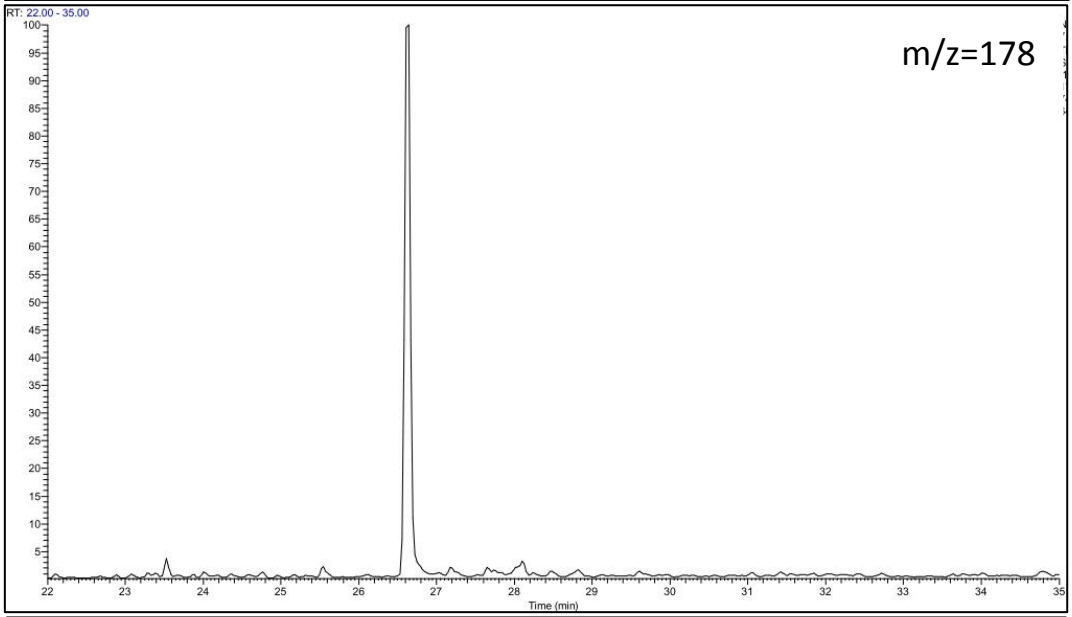
RT: 22.00 - 35.00
m/z=178
Time (min)

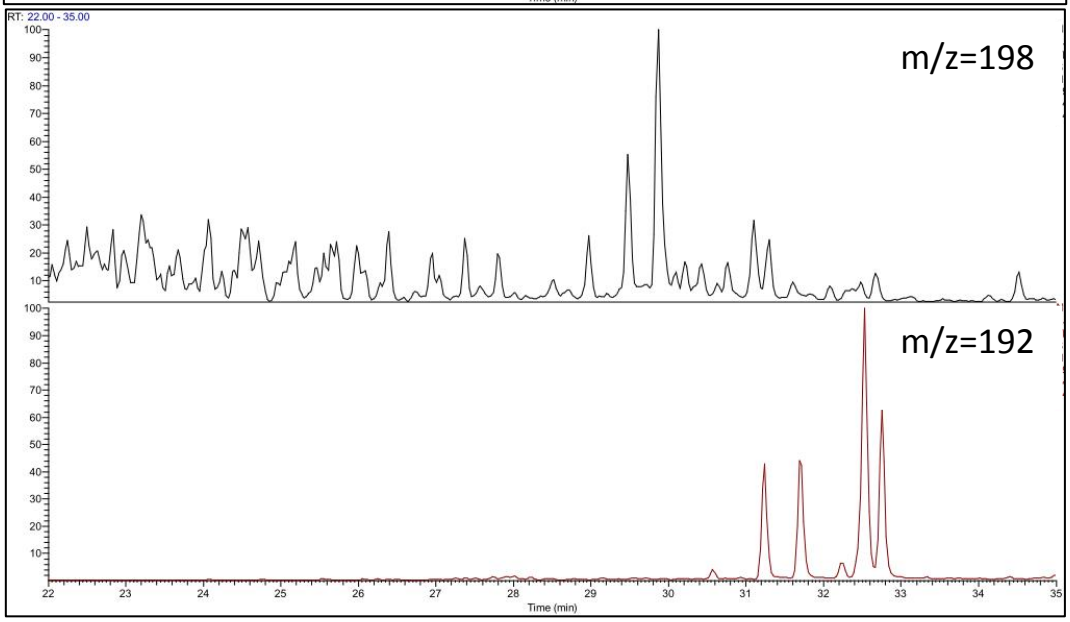
RT: 22.00 - 35.00
m/z=198
m/z=192
Time (min)

GC-FID Chromatogram for outcrop S.R sample "SO-21" from Svalbard

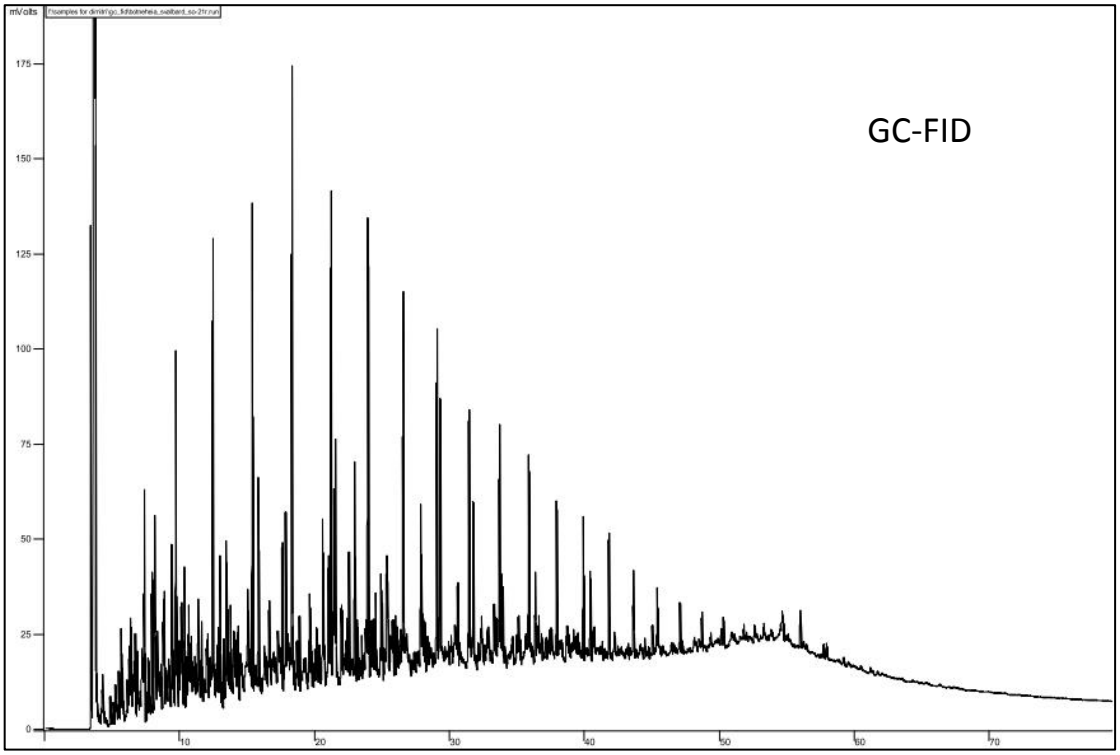

GC-MS Chromatograms for outcrop S.R sample "SO-21" from Svalbard

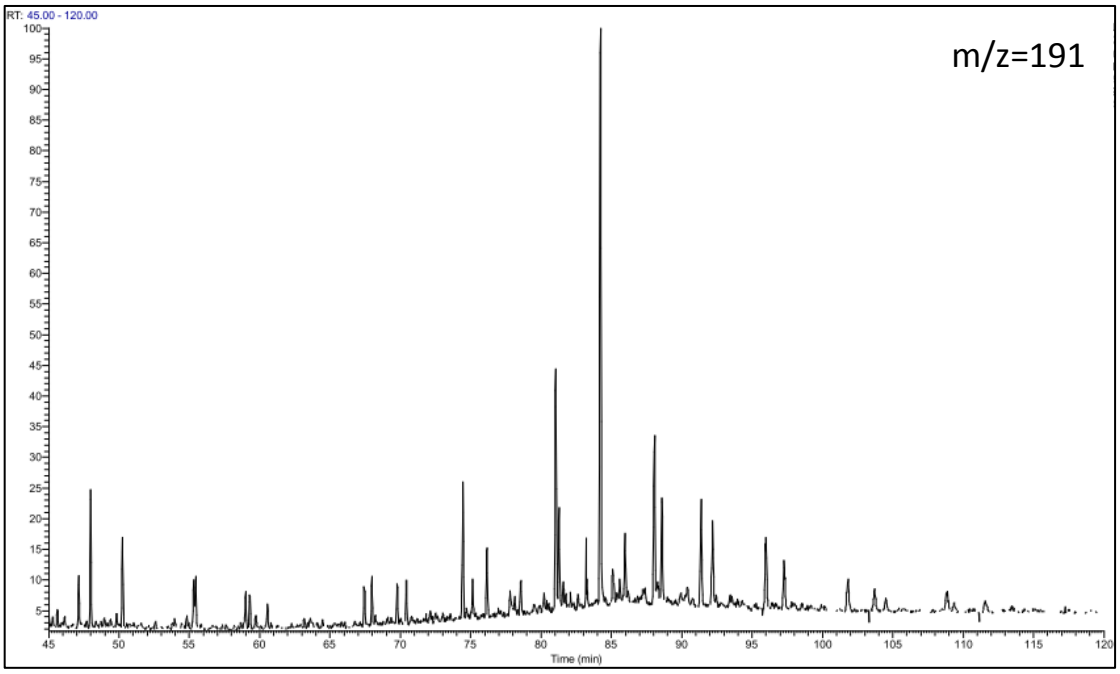

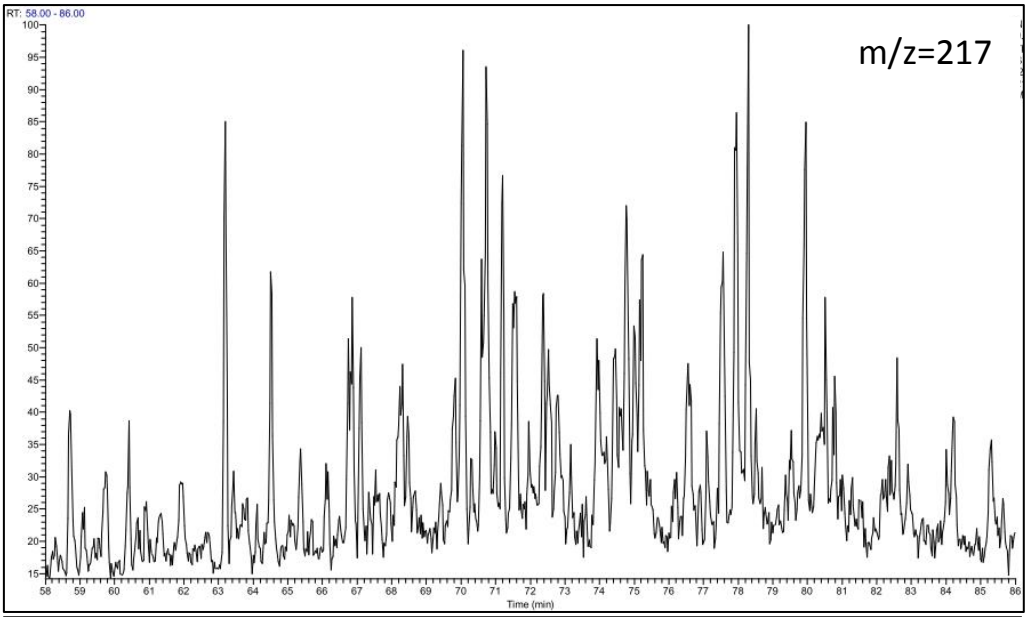
RT: 58.00 - 86.00
m/z=217
Time (min)

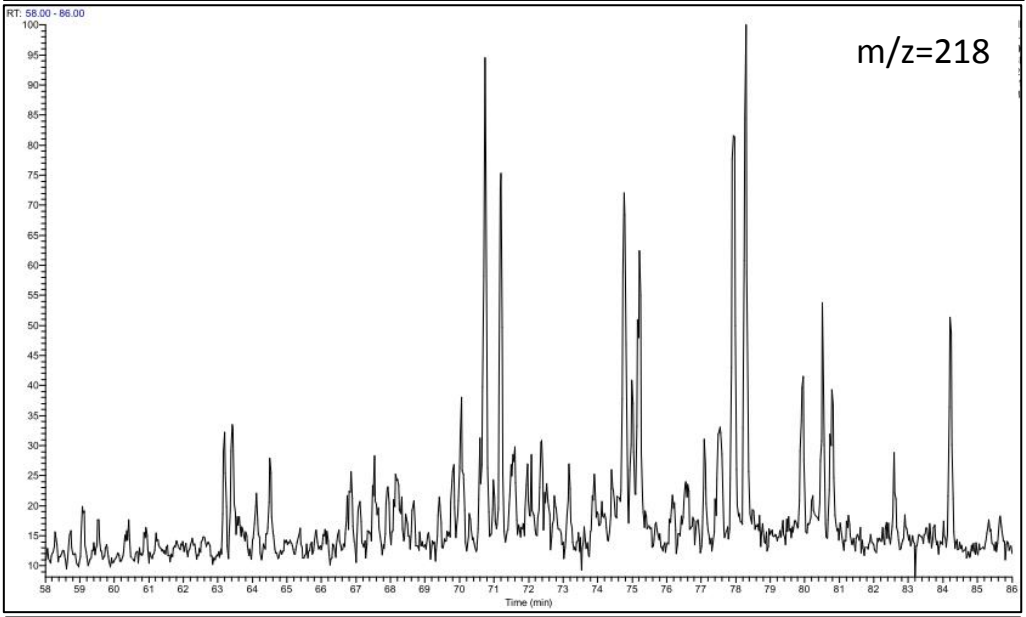
RT: 58.00 - 86.00
m/z=218
Time (min)

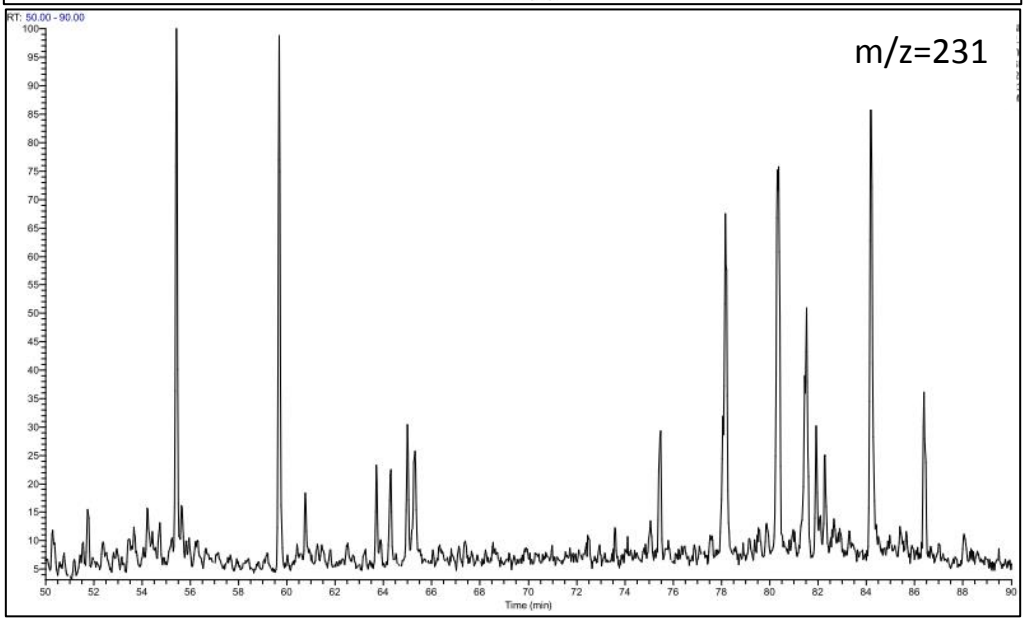
RT: 50.00 - 90.00
m/z=231
Time (min)

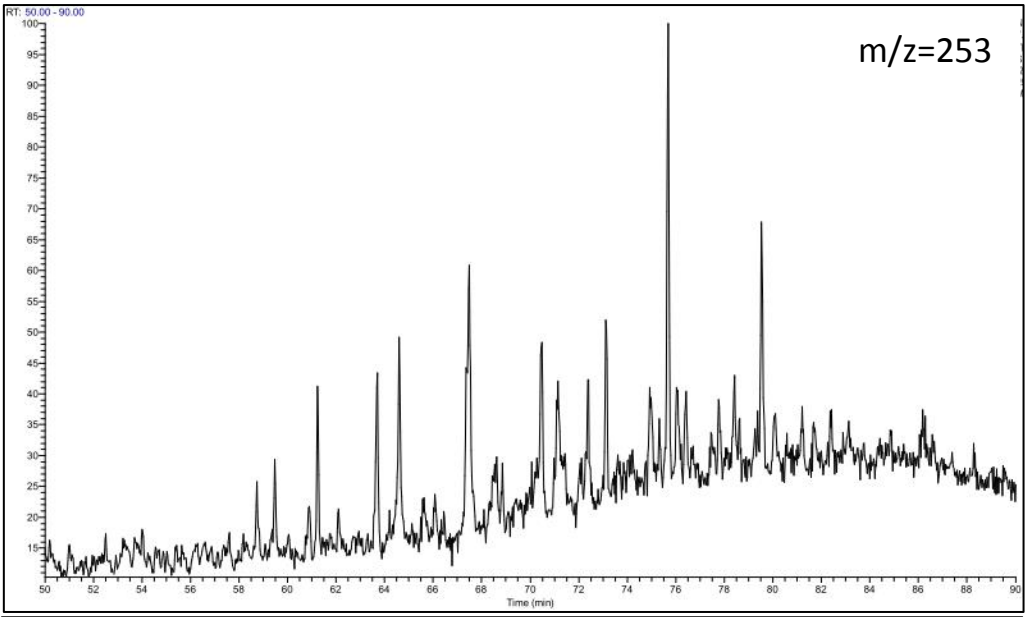
RT: 50.00 - 90.00
m/z=253
Time (min)

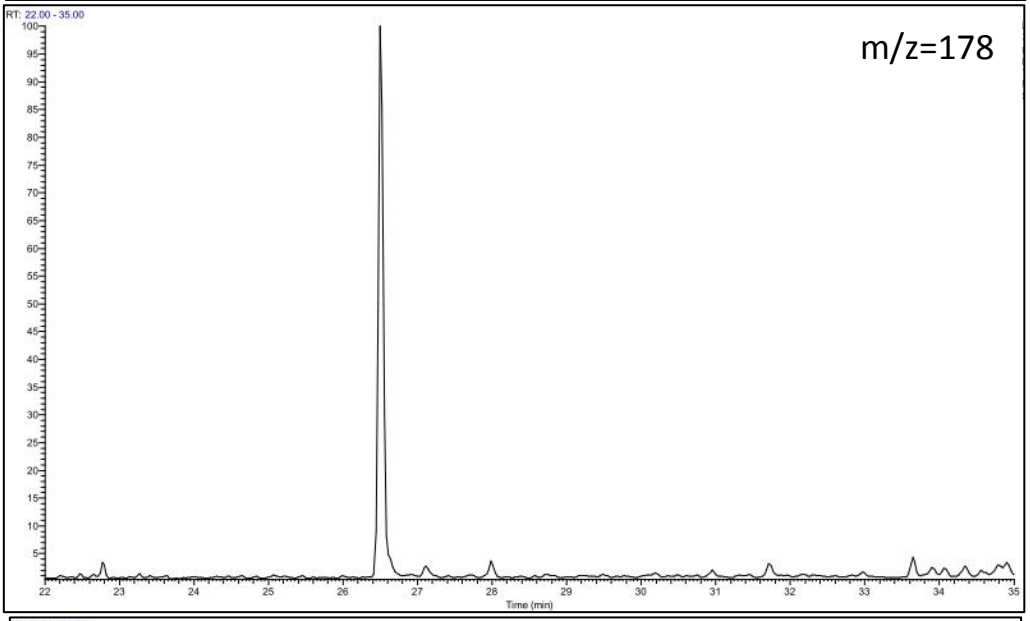
RT: 22.00 - 35.00
m/z=178
Time (min)

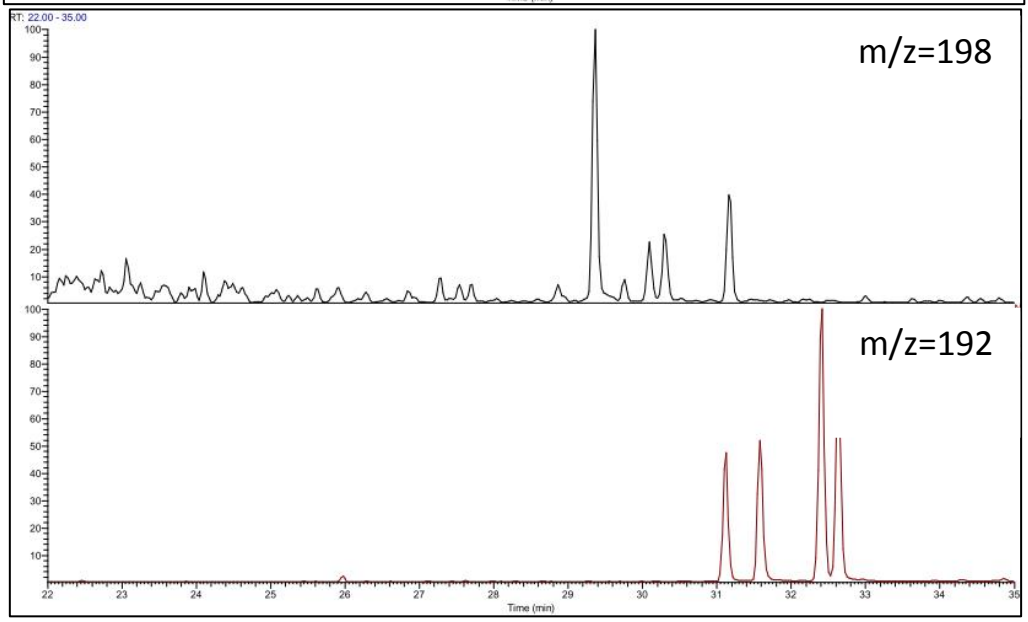
RT: 22.00 - 35.00
m/z=198
m/z=192
Time (min)